

**SYNTHESIS OF ANTIBACTERIAL NATURAL PRODUCTS:  
PRIMIN, CENTROLOBINE, OENOSTACIN AND STUDIES  
ON THE SYNTHESIS OF ALPHA-  
AMINOPHOSPHONATES AND METALLOPNA<sub>s</sub>**

THESIS SUBMITTED TO  
**THE UNIVERSITY OF PUNE**

FOR THE DEGREE OF  
**DOCTOR OF PHILOSOPHY**  
IN  
**CHEMISTRY**

BY  
**TANPREET KAUR**

RESEARCH SUPERVISOR  
**DR. KRISHNA N. GANESH**

RESEARCH CO-SUPERVISOR  
**DR. ASISH K. BHATTACHARYA**

**DIVISION OF ORGANIC CHEMISTRY  
NATIONAL CHEMICAL LABORATORY  
PUNE-411 008, INDIA**

**MAY 2013**



राष्ट्रीय रासायनिक प्रयोगशाला

(वैज्ञानिक तथा औद्योगिक अनुसंधान परिषद)

डॉ. होमी भाभा रोड, पुणे - 411 008. भारत

**NATIONAL CHEMICAL LABORATORY**

(Council of Scientific & Industrial Research)

Dr. Homi Bhabha Road, Pune - 411008. India



## **CERTIFICATE**

This is to certify that the work incorporated in the thesis entitled **“Synthesis of Antibacterial Natural Products: Primin, Centrolobine, Oenostacin and Studies on the Synthesis of Alpha-Aminophosphonates and MetalloPNAs”** submitted by **Ms. Tanpreet Kaur** for the degree of Doctor of Philosophy, was carried out by the candidate under my supervision at the National Chemical Laboratory, Pune, 411 008, India. Such materials, as has been obtained from other sources, have been duly acknowledged in the thesis.

**Prof. Krishna. N. Ganesh, FNA, FNSc.**  
**(Research Supervisor)**  
**Director, IISER Pune**  
**Pune-411 008**

**Dr. Asish K. Bhattacharya**  
**(Research Co-Supervisor)**  
**Division of Organic Chemistry**  
**National Chemical Laboratory,**  
**Pune-411 008**

**J. C. Bose National Fellow**  
**National Chemical Laboratory,**  
**Pune-411 008**

**MAY 2013**



## NATIONAL CHEMICAL LABORATORY

---

# CANDIDATE'S DECLARATION

---

I hereby declare that the thesis entitled “**Synthesis of Antibacterial Natural Products: Primin, Centrolobine, Oenostacin and Studies on the Synthesis of Alpha-Aminophosphonates and MetalloPNAs**” submitted for the Degree of Doctor of Philosophy to the University of Pune, has been carried out by me at the National Chemical Laboratory, Pune. The work is original and has not been submitted in part or full by me for any other degree or diploma to this or any other University.

**MAY 2013**

**PUNE**

**Tanpreet Kaur**

Senior Research Fellow

Division of Organic Chemistry,

National Chemical Laboratory,

Pune-411 008

INDIA



*Dedicated to  
My Parents & My Mentor  
Whose Blessings Always Beckoned  
Me*

### Acknowledgement

First of all, I would like to thank Prof. Krishna N. Ganesh, my research advisor, for showing me the wonderful and exciting world of chemistry. A million thanks to him for his constant guidance and being patient with me during the time of completion of my dissertation. I am thankful to him for introducing me to this field of bio-inorganic chemistry and the freedom he gave me to work and learn new things in this area. This will surely serve as a good platform for my future endeavors.

My special thanks to Dr. Asish K. Bhattacharya, my research co-guide, for his guidance and suggestions. I acknowledge my sincere thanks to the faculty members of IISER-Pune Dr. H. Chakrapani, Dr. R. G. Bhat, Dr. V. G. Anand, Prof. S. K. Kulkarni and Dr. Jaykannan for their support. I am grateful to Dr. Arvind Singh Negi (CIMAP) for his guidance, help and support.

My special vote of thanks to Dr. V. A. Kumar, Dr. Moneesha D'costa, Dr. D. Srinivas, Dr. N. N. Joshi, Dr. G. J. Sanjayan and Prof. D. D. Dhavale (University of Pune) for their help, encouragement and co-operation during my research work. I want to show my gratitude towards Dr. Rahul Banerjee and his group for his support and suggestions in learning crystallization techniques.

I like to thank Mrs. Shantakumari for LCMS work. The kind support from NMR group is greatly acknowledged and thanks to Dr. Rajamohanan, Hilda Davis, Shrikant, Mayur and Snehal for their extra efforts. I also thank Dr. K. D. Deshpande, Mr. Mane and Mr. Javed for solving computer related problems. I also thank organic chemistry office staff- Mrs. Deshpande, Thangaraj, P. V. Iyer, Catherine ma'am, Pooja ma'am, Pawar, Bhumkar and Fernandes for their assistance in many ways throughout my tenure at NCL.

I am grateful to the Directors, Dr. S. Sivaram and Dr. Sourav Pal and Deputy Director, Dr. B. D. Kulkarni for all infrastructural and administrative support and facilities that have been provided during my research period. I am also thankful to Dr. Ganesh Pandey, Head, Division of Organic Chemistry, NCL, Pune for rendering all laboratory facilities to carry out my research work smoothly. My sincere acknowledgement to Dr. P. A. Joy (SAC chairman), Mr. Naveen pavitran, Mrs. A. Puranik, Mrs. Kolthe and Priyanka for helping me during all the times.

## Acknowledgement

---

I express my sincere thanks to my chemistry teachers Asha ma'am (10<sup>th</sup>), Anil Khare sir (12<sup>th</sup>), Dr. Nigam (B. Sc.) and Dr. Naveen khare (M.Sc.) for developing and increasing the interest in chemistry and thankful for their concern and guidance at any step.

I was very lucky to spend my Ph.D time in labs i.e. 346 and 209. In lab no. 346 got an opportunity to work with my helping labmates Late Diallo (Bio), Mujahid, Arvind, Kalpesh, Hemender and Sharmishtha. In Lab no. 209, it got an opportunity to know my educative seniors Dr. Nagendra, Dr. Raman, Dr. Patwa, Dr. Gitali, Dr. Madhuri, Dr. Ashwani, Dr. Roopa, Dr. Manaswini, Dr. Mahesh and Dr. Sreedhar who helped me in learning a lot during my research work. I am thankful to my juniors Deepak, Nitin, Vijay, Satish, Madhan, Shahaji and Prabhakar. My special thanks to Dr. Sreedhar and Madhan who helped in understanding my experimental problems in a novel way.

My colourful friendship with Dr. Rosy, Dr. Gokarneswar, Dr. Panchami, Dr. Reeta, Dr. Anjana, Dr. Arvind, Dr. Smita, Dr. Sivaram, Dr. Rajendra Reddy, Dr. Tanveer, Shobha Kamat ma'am, Sony di, Nidarshana, Vivek, Pitamber, Sujit, Rahul, Harshali, Richa, Mangesh, Kailash (KP), Kishor, Pushpanyali, Anshu, Jaya, Pankaj upreti, Rekha, Bindu, Leena, Abhishek-Jyoti, Reetika-Ambrish, Mayura-Manish, Anusha (Symbiosis), Pradeep (Symbiosis), Sheetal, Himanshu, Tanay (Crystal), Chinmay (Fluorescence), Kaushal, Ghanshyam, Mahesh bhure, Deva, Seema, Namrata, Anjan, Kiran, Venu, Tanaya, Shruti, Divya, Krishanu, Dayanand (DK), Alok ranjan, Vijay B. (Junior), Amit pandya, Gowri, Vijaydas, Priyanka and Roshana.

I must acknowledge the help from students of IISER Pune, specially Keerthi, Neeraj, Paritosh, Kavita, Shweta, Usha, Sumit, Padamshri, Susheel, Ganesh, Abhijeet Chaudhari, Sanjog, Sohini, Arundhati, Biplab (CIF), Hema, Dharma, Satish Malvel, Priyanka, Pramod, Wilbee, Abhigyan, Priya, Sandeep, Krishna (ITC) and Rajkumar (pH meter). My sincere thanks to Smita ma'am (IISER-Physics) for her help. My special thanks to Arvind Gupta for helping me to get one of the most beautiful Palladium crystal.

The support from Swati Dixit (MALDI), Pooja Lunawat (NMR), Archana Jogdand (single crystal X-ray) and Swati Shendage (HRMS) is also acknowledged. Vrushali and Archana for proving purchase support in IISER-Pune. I would like

## Acknowledgement

---

to thank Mr. Amol Patil (Sigma Aldrich) for providing me chemicals timely. I would like to thank office assistants of IISER pune Mr. Manoj Chaudhari, Miss Nayana, Mr. Prabhakar, Mr. Mayuresh and Mr. Anil Jadhav (IISER Hostel) for their support and help whenever needed.

I have spent a significant amount of time there with my dear friends Roshan, Arvind, Roshna, Keerthi, Madhan (Jerry), Neeraj (Tom & White kharghosh) and Kavita who taught me many aspects of science and life. They helped me when I needed them, without asking anything in return. Mere words cannot repay their love, care and support...Thank you my friends from the bottom of my heart!!!

I am indebted to my Father, S. Harjeet Singh and Mother, Smt. Harminder Kaur in my life; whatever I am today is because of them. They've taught me the value of hard work, self-respect, being persistent and independent. Due to their unrelenting love, tremendous patience, support and unwavering belief in me, I was able to complete my long dissertation journey. I would like to place my sincere thanks to my brother, Randeep Singh for his caring, loving and supportive attitude.

I am thankful to my respective elders Dr. R. S. Vyas and his family, Dr. Umesh Gupta, Vinod uncle ji, Yunus uncle ji and Jamal uncle ji in my life who guided me the with lessons of spirituality to make life easier and happier.

I would also like to acknowledge all the staff members of GC, HPLC, IR, NMR, Mass, X-ray analysis, Library, Administration and technical divisions of NCL and IISER for their assistance during the course of my work. I am thankful to all my medical doctors Late Dr. K. B. Grant, Dr. V. S. Shrikanthan, Dr. N. Edul, Dr. Koparkar and Dr. D. Bhide who helped in maintaining good health during tough and frustrating times.

I am grateful to CSIR, New Delhi, Government of India, for awarding research fellowship (CSIR-JRF), and DST-India (Project-SRF from J. C. Bose Fellowship) for further financial support.

This chain of my gratitude can only be completed if I would thank the **Almighty**. My deepest and sincere gratitude for inspiring and guiding this humble being.

**Tanpreet Kaur**

---

**CONTENTS**

---

<b>GENERAL REMARKS</b>	i
<b>ABBREVIATIONS</b>	iii
<b>ABSTRACT</b>	vi
<b>LIST OF FIGURES</b>	xvi
<b>LIST OF SCHEMES</b>	xxi
<b>LIST OF TABLES</b>	xxiv
<b>PUBLICATION / PRESENTATION</b>	xxvi

---

**CHAPTER 1**  
**SYNTHESIS OF ANTIBACTERIAL NATURAL PRODUCTS**

---

<b>Section A</b>	<b>Synthesis of Antibacterial 1,4-Benzoquinone Primin and its Analogs</b>	
1.1	Introduction	02
1.1.2	Previous reports	05
1.2	Present work: Objective and Rationale	07
1.3	Results and Discussion	08
1.4	Conclusion	13
1.5	Experimental	14
1.6	References	34
1.7	Appendix A	37
<b>Section B</b>	<b>Studies Towards Synthesis of Oenostacin</b>	
1.1	Introduction	54

---



---

1.2	Present work: Objective and Rationale	55
1.3	Results and Discussion	56
1.4	Conclusion	63
1.5	Experimental	64
1.6	References	74
1.7	Appendix B	76

---

**Section C**                      **Formal Synthesis of (-)-Centrolobine**

---

1.1	Introduction	96
1.1.2	Previous reports	96
1.2	Present work: Objective and Rationale	105
1.3	Oxidative Kinetic Resolution (OKR)	105
1.4	Results and Discussion	107
1.5	Conclusion	111
1.6	Experimental	112
1.7	References	120
1.8	Appendix C	122

---

**CHAPTER 2**  
**NEW SYNTHETIC METHODOLOGIES**

---

**Section A**                      **Decarboxylative Method for the Synthesis of 2-Styryl Furans/Thiophenes**

2.1	Introduction	132
2.1.1	Previous reports	134
2.2	Present work: Objective and Rationale	135

---

2.3	Results and Discussion	135
2.4	Postulated Mechanism	141
2.5	Conclusion	142
2.6	Experimental	143
2.7	References	158
2.8	Appendix D	160

---

**Section B            Synthesis of Biologically Active Alpha-aminophosphonates**

---

2.1	Introduction	181
2.1.1	Previous reports	183
2.2	Present work: Objective and Rationale	186
2.3	Results and Discussion	187
2.4	Postulated Mechanism	194
2.5	Conclusion	195
2.6	Experimental	196
2.7	References	208
2.8	Appendix E	210

---

**CHAPTER 3  
DESIGN, SYNTHESIS AND METAL COMPLEXATION STUDIES  
OF METALLOPNAS**

---

<b>3.1</b>	<b>Introduction</b>	<b>223</b>
3.1.1	Nucleic acids: chemical structure	224
3.1.2	DNA modifications	226
3.1.3	Peptide nucleic acids (PNAs)	227

---

3.1.4	Metal organic complexes	229
3.1.5	Metallo-DNAs	231
3.1.6	Metallo-PNAs	232
3.1.7	Synthetic methods and characterization of polyamide <i>aeg</i> oligomers	235
3.1.8	Metal binding studies of polyamide <i>aeg</i> oligomers	243
<b>3.2</b>	<b>Present work: Rationale and Objective</b>	246
<b>3.3</b>	<b>Results and Discussion</b>	248
3.3.1	Synthesis of <i>N</i> -Boc-aminoethyl 2-pyridylbenzimidazole (PBI) glycinate	249
3.3.2	Synthesis of <i>N</i> -Boc-aminoethyl- <i>o</i> -phenylenediamine (PDA) glycinate	252
3.3.3	Synthesis of <i>N</i> -Boc-aminoethyl-3,4-dihydroxyphenyl (CAT) glycinate	253
3.3.4	Synthesis of <i>N</i> -Boc-aminoethyl 2-pyridylbenzimidazole (PBI) <sub>2</sub> (glycinate) <sub>2</sub>	255
<b>3.4</b>	<b>Synthesis of the polyamide oligomers</b>	257
3.4.1	Solid phase method followed for polyamide oligomers	257
3.4.2	Cleavage of the oligomers from the solid support	259
<b>3.5</b>	<b>Purification and characterization of the polyamide oligomers</b>	260
3.5.1	High Performance Liquid Chromatography (HPLC)	261
3.5.2	Matrix Assisted Laser Desorption Ionization-Time of Flight (MALDI-TOF) characterization	262
<b>3.6</b>	<b>Molar Extinction Coefficients of polyamide oligomers</b>	263
<b>3.7</b>	<b>Determination of <math>pK_a</math> of synthesized oligomers</b>	267
<b>3.8</b>	<b>NMR studies</b>	272
3.8.1	NMR studies on ethyl- <i>N</i> -Boc-aminoethyl-3,4-dihydroxy phenyl (CAT) glycinate, <b>15</b>	272
3.8.2	NMR studies on benzyl <i>N</i> -Boc-aminoethyl-3,4-dihydroxy phenyl (CAT) glycinate, <b>17</b>	273

---

<b>3.9</b>	<b>High Resolution-Mass spectrometry (HR-MS) Studies</b>	
3.9.1	HR-MS studies on ethyl- <i>N</i> -Boc-aminoethyl-2-pyridyl benzimidazole (PBI) glycinate 8	275
3.9.2	HR-MS studies on ethyl- <i>N</i> -Boc-aminoethyl-2-pyridyl benzimidazole (PBI) <sub>2</sub> (glycinate) <sub>2</sub> 21	277
<b>3.10</b>	<b>UV-Vis spectroscopic studies</b>	279
3.10.1	UV-Vis spectrophotometric titrations of (PBI) and (CAT) <i>aeg</i> linked ligand	279
3.10.2	UV-Vis spectrophotometric titrations of (PBI) Dimer	288
3.10.3	UV-Vis spectrophotometric titrations of polyamide <i>homo</i> -oligomers	293
3.10.4	UV-Vis spectrophotometric titrations of polyamide <i>hetero</i> -oligomers	301
<b>3.11</b>	<b>Isothermal Titration Calorimetry (ITC)</b>	314
<b>3.12</b>	<b>Co-ordination chemistry of metal complexes</b>	318
<b>3.13</b>	<b>Binding models</b>	321
<b>3.14</b>	<b>Conclusion</b>	324
<b>3.15</b>	<b>Experimental Section</b>	326
<b>3.16</b>	<b>References</b>	352
<b>3.17</b>	<b>Appendix F</b>	358

---

---

**GENERAL REMARKS**

---

- ✚ <sup>1</sup>H NMR spectra were recorded on Bruker AC-200 MHz, JEOL-400 MHz, MSL-300 MHz, and DRX-500 MHz spectrometer using tetramethylsilane (TMS) as an internal standard. Chemical shifts have been expressed in ppm units downfield from TMS.
- ✚ <sup>13</sup>C NMR spectra were recorded on AC-50 MHz, JEOL-100 MHz, MSL-75 MHz, and DRX-125 MHz spectrometer.
- ✚ ESI-Mass spectra were recorded on API-Q-STAR spectrometer (Applied Biosystems).
- ✚ MALDI analysis were done on MDS-SCIEX 4800 MALDI TOF/TOF instrument (Applied Biosystems).
- ✚ High Resolution Mass Spectrometry (HRMS) was recorded on Waters SYNAPT G2 MS system.
- ✚ Infrared spectra were scanned on Shimadzu IR-470 or Perkin-Elmer Spectra One FT-IR spectrometers with NaCl optics and are measured in cm<sup>-1</sup>.
- ✚ Optical rotations were measured with a JASCO DIP 370 digital polarimeter.
- ✚ Melting points were recorded on Büchi M-560 melting point apparatus in an open capillaries and are uncorrected.
- ✚ All reactions were monitored by Thin Layer Chromatography (TLC) carried out on 0.2 mm Merck silica gel plates (60 F<sub>254</sub>) with UV light, I<sub>2</sub> and anisaldehyde or ninhydrin in ethanol as development reagents.
- ✚ All solvents and reagents were purified and dried according to procedures given in Vogel's Text book of "Practical Organic Chemistry". All reactions were carried out under nitrogen or argon atmosphere with dry, freshly distilled solvents under anhydrous conditions unless otherwise specified. Yields refer to chromatographically and spectroscopically homogeneous materials unless otherwise stated.
- ✚ All evaporations were carried out under reduced pressure on Buchi rotary evaporator below 40 °C.
- ✚ Silica gel (60–120) or (100-200) used for column chromatography was purchased from Merck (India).

- ✚ HPLC purification was done on Dionex ICS-3000 series attached with PDA detector and equipped with SP (single pump).
- ✚ UV-Vis spectrophotometric titrations were done on Perkin Elmer 950 spectrophotometer.

---

**ABBREVIATIONS & SYMBOLS**

---

Ac	Acetyl
AcOH	Acetic acid
Ac <sub>2</sub> O	Acetic anhydride
<i>aeg</i>	aminoethylglycine
ap	antiparallel
Anhyd.	Anhydrous
(Boc) <sub>2</sub> O	Boc anhydride
BnBr	Benzyl bromide
BF <sub>3</sub> .Et <sub>2</sub> O	Boron trifluoride-diethyletherate
<i>n</i> -BuLi	Butyl-lithium
Bu <sub>3</sub> SnH	Tributyltinhydride
Cbz	Benzyloxycarbonyl
CD	Circular dichroism
COSY	Correlation spectroscopy
CuSO <sub>4</sub>	Copper sulphate
Cu(NO <sub>3</sub> ) <sub>2</sub>	Copper nitrate
DCC	Dicyclohexylcarbodiimide
DCM	Dichloromethane
DIPEA/DIEA	<i>N, N'</i> -diisopropylethylamine
DMAP	<i>N, N'</i> -dimethyl-4-aminopyridine
DMF	<i>N, N'</i> -dimethylformamide
DNA	2'-deoxyribonucleic acid
<i>ds</i>	Double strand
DMSO	Dimethylsulphoxide
eda	Ethylenediamine
EtOAc	Ethyl acetate
Et <sub>3</sub> N	Triethylamine
EtOH	Ethanol
ESI-MS	Electrospray Ionization-Mass spectroscopy
EA	Ethyl acetate
ΔG	Change in Gibb's free energy

---

---

g	gram
h	Hours
Hz	Hertz
HBTU	2-(1H-Benzotriazole)-1,1',3,3'-tetramethyluronium hexafluorophosphate
HOBt	<i>N</i> -hydroxybenzotriazole
HMBC	Heteronuclear Multiple Bond Coherence
HPLC	High Performance Liquid Chromatography
HSQC	Heteronuclear Single Quantum Coherence
IBX	<i>o</i> -Iodoxybenzoic acid
IR	Infrared
ITC	Isothermal Titration Calorimetry
K <sub>2</sub> CO <sub>3</sub>	Potassium carbonate
K	Kelvin/Kilo/Binding constant
KBrO <sub>3</sub>	Potassium bromate
LC-MS	Liquid Chromatography-Mass Spectrometry
LAH	Lithium aluminium hydride
<i>m</i>	Meta
MeOH	Methanol
M	Molar
MALDI-TOF	Matrix Assisted Laser Desorption Ionisation-Time Of Flight
MBHA	4-Methylbenzhydramine
mg	milligram
MHz	megahertz
Min	minutes
μL	microlitre
μM	micromolar
mL	millilitre
mM	millimolar
mmol	millimoles
m.p	Melting point
MS	Mass spectrometry

---



MsCl	Mesyl chloride
MW	Mol. Wt
NaH	Sodium hydride
NaBH <sub>4</sub>	Sodium borohydride
NMR	Nuclear Magnetic Resonance
NiCl <sub>2</sub> .6H <sub>2</sub> O	Nickel chloride hexahydrate
ORTEP	Oak Ridge Thermal Ellipsoid Plot
<i>o</i>	Ortho
Pd/C	Palladium on charcoal
Pd(OAc) <sub>2</sub>	Palladium acetate
<i>p</i> -TSA	<i>para</i> -toluene sulphonic acid
ppm	Parts per million
PNA	Peptide nucleic acid
<i>p</i>	Para
PE	Pet-ether
R	Rectus
rt	Room temperature
RT	Retention time
R <sub>f</sub>	Retention factor
SPPS	Solid Phase Peptide Synthesis
TMB	Trimethyl borate
<i>t</i> -Boc	<i>tert</i> -butoxy carbonyl
TEA/Et <sub>3</sub> N	Triethylamine
TFA	Trifluoroacetic acid
TFMSA	Trifluoromethanesulphonic acid
TsCl	<i>p</i> -toluenesulphonyl chloride
UV-Vis	Ultraviolet-Visible

---

**ABSTRACT**

---

**Research Student:** Tanpreet Kaur**Research Guide:** Prof. Krishna N. Ganesh**Research Co-Guide:** Dr. Asish K. Bhattacharya

---

The thesis entitled “**Synthesis of Antibacterial Natural Products: Primin, Centrolobine, Oenostacin and Studies on the Synthesis of Alpha-Aminophosphonates and MetalloPNAs**” comprises syntheses of antibacterial agents *i.e.* primin and its analogs, synthetic efforts for the synthesis of oenostacin; formal synthesis of (-)-centrolobine. It includes development of new synthetic routes for the synthesis of 2-styryl-furans/thiophenes and  $\alpha$ -aminophosphonates. The synthesis and metal complexation studies of novel aminoethyl glyceryl (*aeg*) linked ligands are discussed. The thesis has been divided into three chapters.

**Chapter-1:** The first chapter gives an overview on background literature for undertaking the research work. It consists of a brief review of recent literature on synthesis of antibacterial agents followed by the present work on the synthesis of antibacterial agents; primin and primin acid; oenostacin and (-)-centrolobine.

**Chapter-2:** This chapter discusses a brief review of recent literature and synthetic efforts for the development of novel synthetic routes towards the 2-styryl-furans/thiophenes and  $\alpha$ -aminophosphonates (AAPs).

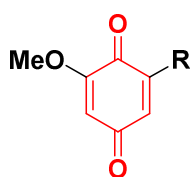
**Chapter-3:** This chapter gives an overview on background literature for undertaking the research work with a brief review of the metallo-DNA/PNA literature. Following which design, synthesis and metal-complexation studies of novel aminoethyl glyceryl (*aeg*) linked ligands monomers, dimer and oligomers.

---

## Chapter 1. Synthesis of Antibacterial Natural Products

### Section (A). Synthesis of Antibacterial 1,4-Benzoquinone Primin, and its Analogs

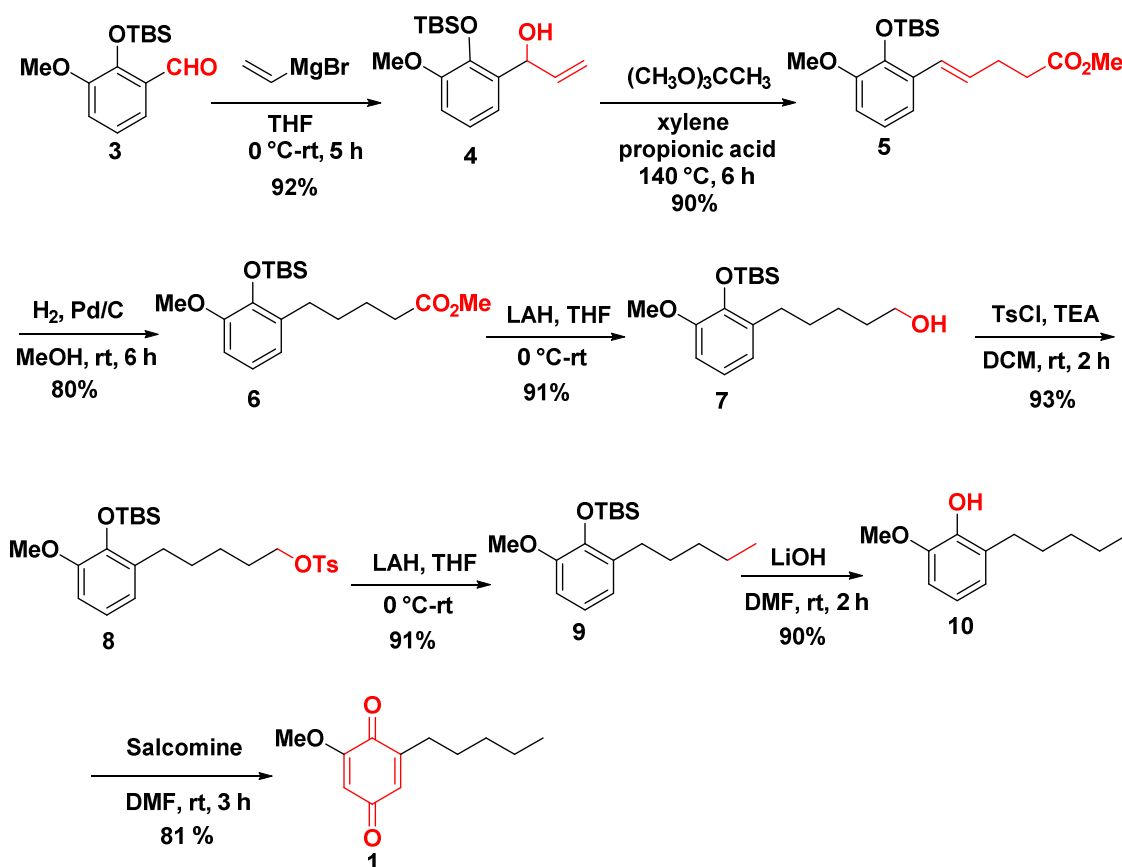
This section discusses previous literature protocols about the synthesis of 1,4-benzoquinone derivatives. Primin **1** (Figure 1), has been isolated from variety of plants including *Primula obconica* (primrose),<sup>1</sup> *Miconia* (*M. eriodonta* DC) (Melastomaceae)<sup>2</sup> and *Iris* (*I. sibirica*, *I. pseudacorus*, *I. missouriensis*) (Iridaceae) species<sup>3</sup> and broth extract of endophytic fungus *Botryosphaeria mamane* PSU-M76.<sup>4</sup>



- (1) R = (C<sub>4</sub>H<sub>9</sub>) CH<sub>3</sub>, Primin  
 (2) R = (C<sub>4</sub>H<sub>9</sub>) CO<sub>2</sub>H, Primin acid

Figure 1. Structure of primin **1** and its analogues.

It involves utilization of well known synthetic protocols *e.g.* Grignard reaction and Johnson's Claisen rearrangement for synthesizing 1,4-benzoquinones (Scheme 1).



Scheme 1. Synthesis of 2-methoxy-6-pentyl-1,4-benzoquinone, Primin **1**.

The synthesis of Primin **1** was started with the protected *o*-vanillin **3**, which was subjected to Grignard reaction<sup>5</sup> and Johnson-Claisen rearrangement<sup>6</sup> conditions to compound **4**. Further synthetic manipulations resulted in the formation of compound **9**. The TBS group was deprotected in compound **9** using LiOH/DMF to furnish the compound **10**, which on oxidation with salcomine afforded the title compound, primin **1** in 81% yield. In conclusion, an efficient syntheses<sup>7</sup> of antibacterial benzoquinones **1** and its analogues has been achieved from *o*-vanillin.

### Section (B). Studies Towards Synthesis of Oenostacin

The plant *Oenothera biennis* (Family: Onagraceae) commonly known as Evening Primrose is a genus of herbs and shrubs. The bioactive component oenostacin **1** was isolated from the roots of the plant *O. biennis*<sup>8</sup> in the year 1999 (Figure 2).

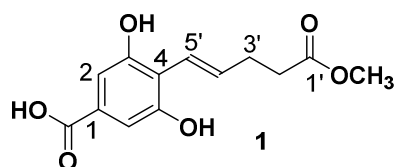
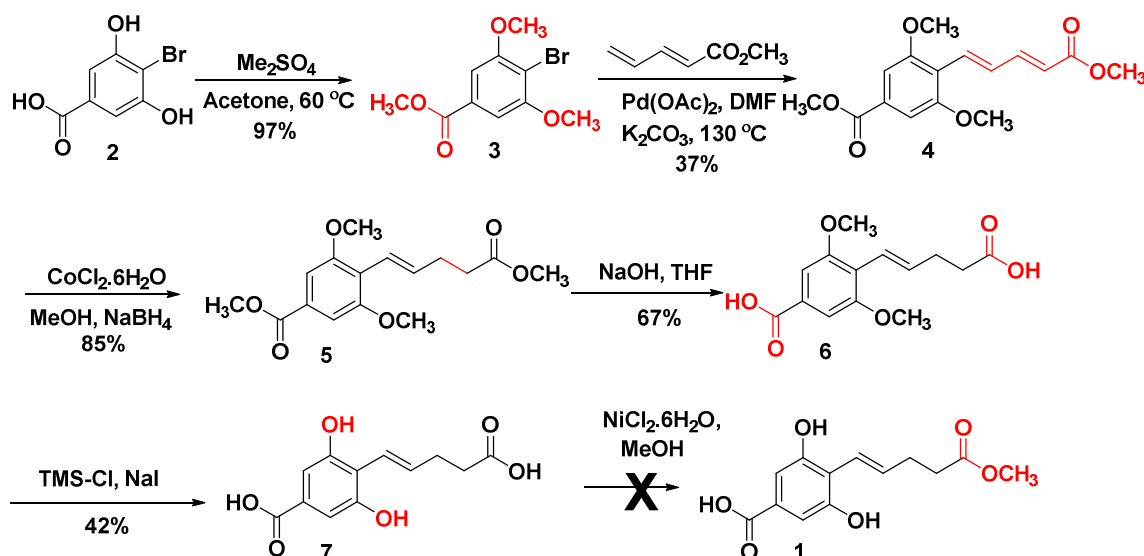


Figure 2. Structure of antibacterial agent Oenostacin, **1**.

This section deals with the synthetic efforts tried towards the first total synthesis of antibacterial natural product, oenostacin. It involves utilization of synthetic protocols for example extended Heck reaction and Chelation control selective reduction for synthesizing this natural product (Scheme 2).



Scheme 2. Synthetic efforts towards the synthesis of antibacterial agent, Oenostacin, **1**.

4-bromo-3,5-dihydroxy benzoic acid **2** was protected as methoxy and methyl ester, respectively. The Heck reaction on the compound **3** furnished the desired  $\alpha,\beta,\gamma,\delta$ -conjugated diene ester **4** in 37% yield.<sup>9</sup> The reduction using sodium borohydride and cobalt chloride hexahydrate as a catalyst was utilized for the product **5**, in 85% yield.<sup>10</sup> To synthesize compound **7**, compound **5** was subjected to TMS-Cl/NaI conditions to furnish deprotected analogue **7**.<sup>11</sup> Few methods reported in the literature were tried for the selective esterification of compound **7**. However, none of the methods could furnish the desired product. In conclusion, synthetic route was explored towards the synthesis of antibacterial agent oenostacin, **1**.

### Section (C). Formal Synthesis of (-)-Centrolobine

(-)-Centrolobine **1** is a crystalline substance isolated from the heartwood of *Centrolobium robustum* and from the stem of *Brosimum potabile* (Figure 3).<sup>12</sup>

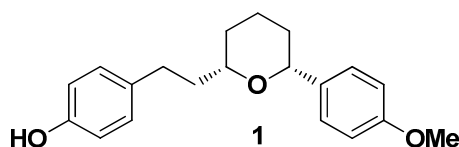
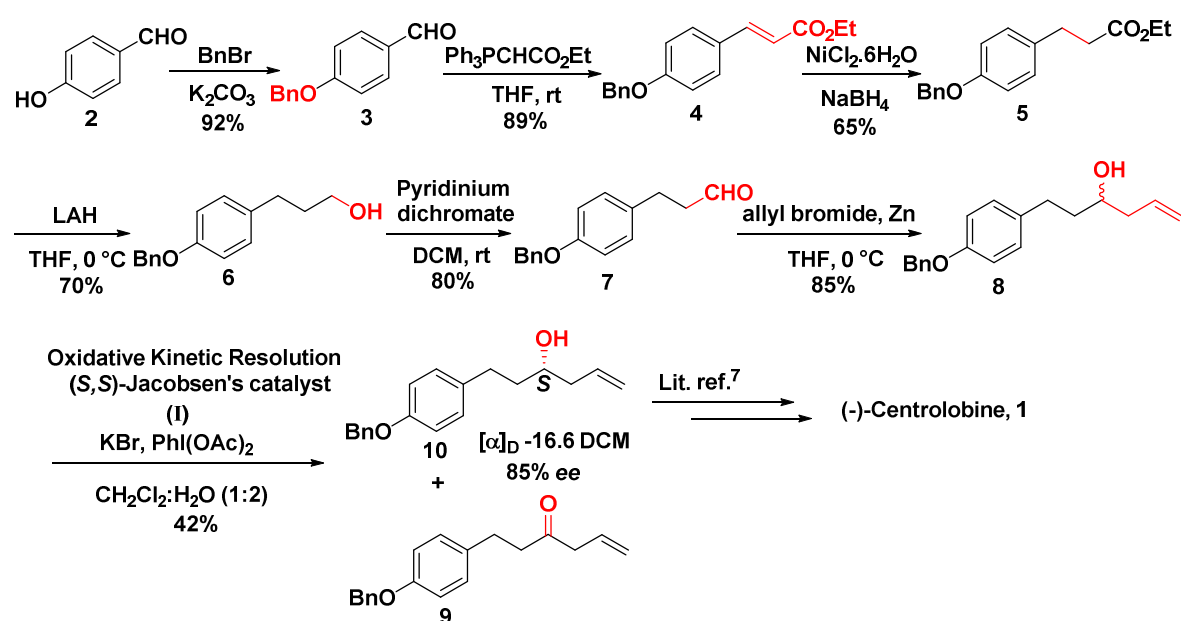


Figure 3. Structure of (-)-centrolobine, **1**.

It involves utilization of well known synthetic protocols for example extended Oxidative Kinetic Resolution (OKR) and Barbier reaction towards formal synthesis of this natural product (Scheme 5).



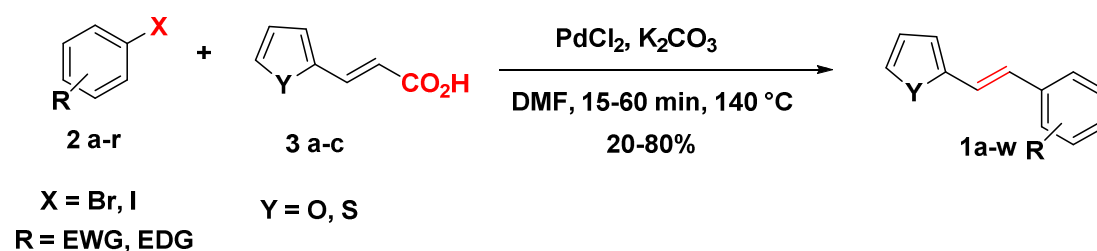
Scheme 5. Formal synthesis of (-)-centrolobine, **1**.

The synthesis of key intermediate, homo-allylic alcohol **10**, was achieved by utilizing oxidative kinetic resolution (OKR). The compound **10** could be transformed into the title compound **1** by following reported methods.<sup>7</sup> In conclusion, we have accomplished a formal synthesis of (-)-centrolobine **1**.

## Chapter 2. New Synthetic Methodologies

### Section (A). Decarboxylative Method for the Synthesis of 2-Styryl Furans/Thiophenes

2-styryl furans/thiophenes could be useful in the synthesis of various useful analogues, but in the literature very few reports are there for its synthesis (Scheme 6).<sup>13</sup>



**Scheme 6.** Synthesis of 2-(*E*-styryl)furan **1** *via* decarboxylative cross-coupling reaction.

In summary, an efficient decarboxylative cross-coupling reaction for preparing 2-styryl furans/thiophenes has been developed which is useful for wide range of electron donating and electron withdrawing groups.

### Section (B). Synthesis of Biologically Active Alpha-Aminophosphonates

$\alpha$ -Aminophosphonates can act as enzyme inhibitors,<sup>14</sup> peptide mimics,<sup>15</sup> antibiotics and pharmacologic agents,<sup>16</sup> herbicidal and haptens of catalytic antibodies (Figure 5).<sup>17</sup>

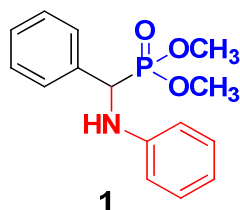
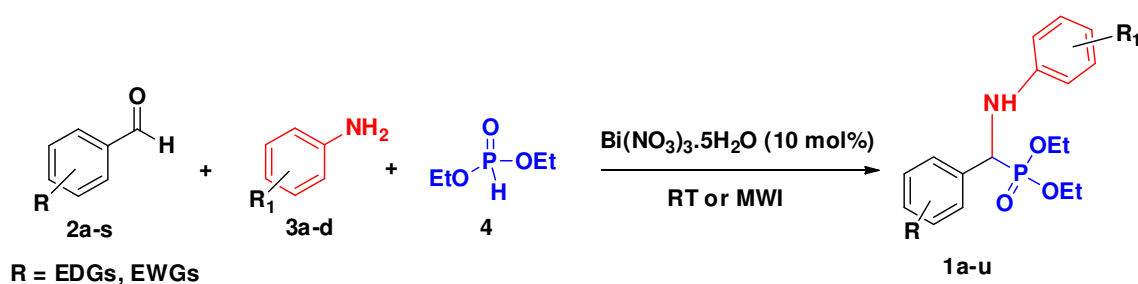


**Figure 5.** Structure of  $\alpha$ -aminophosphonate (AAP) derivative, **1**.

$\text{Bi}(\text{NO}_3)_3 \cdot 5\text{H}_2\text{O}$  is relatively less toxic, cheaply available<sup>18</sup> and utilized in the one-pot synthesis of structurally diverse  $\alpha$ -aminophosphonates from carbonyl compounds, amines and diethylphosphite was developed.



**Scheme 7.** Bismuth nitrate catalyzed synthesis of  $\alpha$ -aminophosphonates.

In summary, Bismuth (III) nitrate pentahydrate<sup>19</sup> was proved to be an efficient catalyst for three-component (3CR) one-pot reaction for the synthesis of  $\alpha$ -aminophosphonates.

### Chapter 3. Design, Synthesis and Metal Complexation Studies of MetalloPNAs

Peptide nucleic acid (PNA), a DNA mimic resulting from the replacement of sugar-phosphate backbone by a pseudopeptide backbone, was introduced by Nielsen *et al.*<sup>20</sup> in 1991. Even though PNA does not have sugar and phosphate linkages, it mimics the behavior of DNA in many respects, and in some applications demonstrates superior properties.<sup>21</sup> Shionoya *et al.*<sup>22</sup> replaced natural DNA base pairs with unnatural base pairs that can be coordinated with metal ions. In order to construct molecular wires, similar idea was utilized by replacing natural base pairs of PNA with unnatural ones (Figure 6).

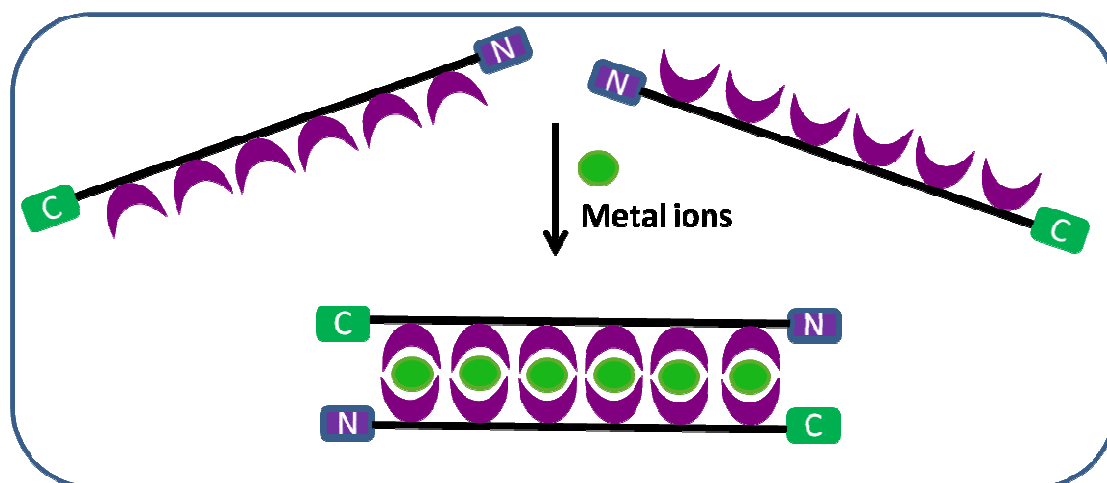


**Figure 6.** Metal mediated duplex formation in modified-PNA strands.

With the requisites of above mentioned characteristics in mind, 2-pyridyl benzimidazole (PBI) **1**, *o*-phenylenediamine (PDA) **2**, catechol (CAT) **3** were chosen

as metal chelating ligands for incorporation of metal ions to aminoethyl glyceryl (*aeg*) backbone (Figure 7). The (PBI) **1**, (PDA) **2** and (CAT) **3** monomers were synthesized successfully. These were incorporated using solid phase peptide synthesis on MBHA resin, using *Boc* chemistry to the *homo*-oligomers (PBI)<sub>6</sub> **4**, (PDA)<sub>6</sub> **5**, (CAT)<sub>6</sub> **6** as well as *hetero*-oligomers (PBI)<sub>3</sub>-(PDA)<sub>3</sub> **7**, (PBI-PDA)<sub>3</sub> **8**, (PBI)<sub>3</sub>-(CAT)<sub>3</sub> **9**, (PBI-CAT)<sub>3</sub> **10**.

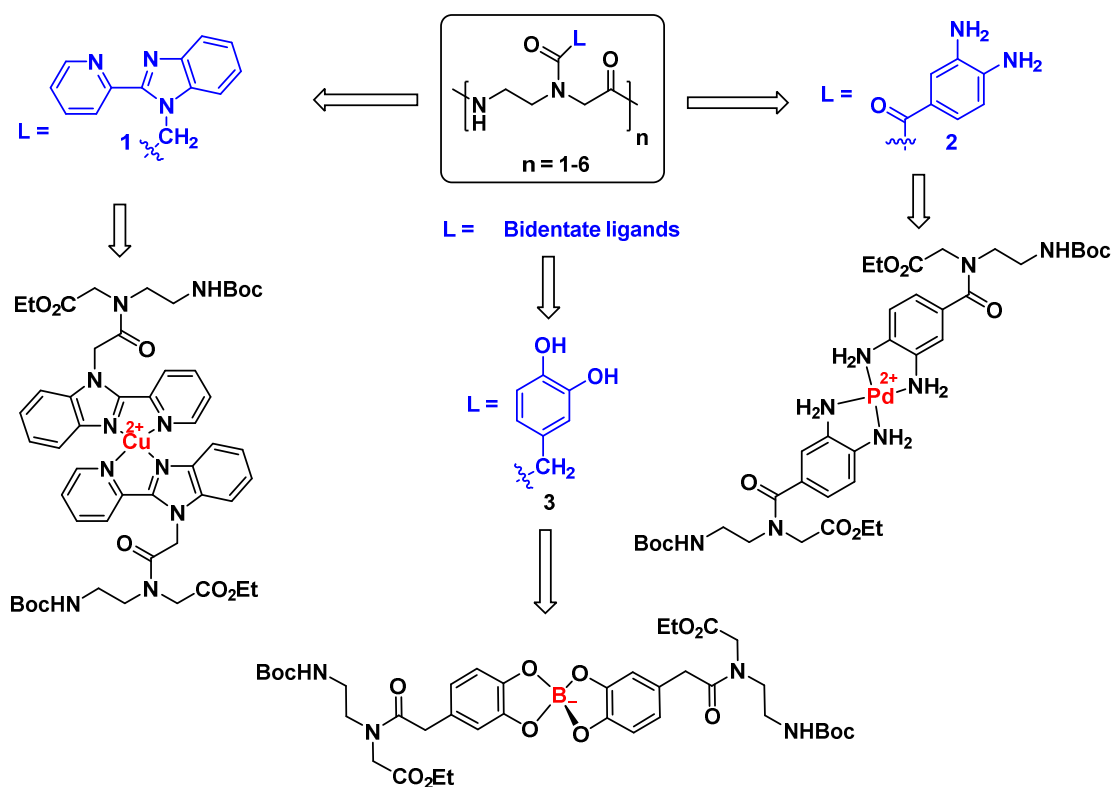


**Figure 7.** Designed novel *aeg* linked ligands and their metal complexation.

These polyamide oligomers were subsequently purified by reverse phase-HPLC on a preparative column and their purity was confirmed by MALDI-TOF mass spectrometric analysis. Molar Extinction Coefficients ( $\epsilon$ ) and  $pK_a$  were determined for all polyamide oligomers and represented in Table 3.

**Table 3.** Molar Extinction Coefficients ( $\epsilon$ ) and  $pK_a$  for the synthesized oligomers

Oligomer	Molar Extinction	
	Coefficient ( $\epsilon$ ) ( $M^{-1} cm^{-1}$ )	$pK_a$
(PBI) <sub>6</sub> <b>4</b>	53.9	5.7
(PDA) <sub>6</sub> <b>5</b>	7.7	5.4
(CAT) <sub>6</sub> <b>6</b>	16.7	5.7
(PBI) <sub>3</sub> -(PDA) <sub>3</sub> <b>7</b>	27.6	5.6
(PBI-PDA) <sub>3</sub> <b>8</b>	46.9	5.1
(PBI) <sub>3</sub> -(CAT) <sub>3</sub> <b>9</b>	32.0	4.8
(PBI-CAT) <sub>3</sub> <b>10</b>	25.0	4.1



Metal binding studies were done on the *aeg* linked ligands and polyamide oligomers using HRMS, UV-Vis spectroscopy, Isothermal Titration Calorimetry and NMR. UV-Vis titrations were performed using methanolic/water solutions with known concentrations of *aeg* linked ligands or oligomers with different metal salts *i.e.* copper nitrate, nickel nitrate, palladium nitrate, lead nitrate, iron nitrate, zinc nitrate, cobalt nitrate, ruthenium trichloride, silver nitrate, gold chloride (Table 4) *etc.* These designed *aeg* linked ligands and polyamide oligomers were shown appreciable binding with selected metal salts. Finally, binding constants were determined by employing UV-Vis and ITC analysis.

**Table 4.** Summary of UV-Vis spectrophotometric titrations

Ligands	Metal salts			
	CuNO <sub>3</sub>	NiNO <sub>3</sub>	AuCl <sub>3</sub>	ZnCl <sub>2</sub>
(PBI) <b>1</b>	Binding	Binding	Weak binding	No binding
(CAT) <b>3</b>	Weak binding	No binding	Binding	No binding
(PBI) <sub>6</sub> <b>4</b>	Binding	Binding	Binding	No binding
(PDA) <sub>6</sub> <b>5</b>	No binding	No binding	No binding	Weak binding
(CAT) <sub>6</sub> <b>6</b>	No binding	No binding	No binding	No binding
(PBI) <sub>3</sub> - (PDA) <sub>3</sub> <b>7</b>	Binding	Binding	Weak binding	No binding
(PBI-PDA) <sub>3</sub> <b>8</b>	Binding	Binding	Weak binding	No binding
(PBI) <sub>3</sub> - (CAT) <sub>3</sub> <b>9</b>	Binding	Binding	Weak binding	No binding
(PBI-CAT) <sub>3</sub> <b>10</b>	Binding	Binding	Weak binding	No binding

Some of the advantages of these metal arrays are that they are likely to impart rigidity and specific geometry to the structures while generating interesting chemical and physical properties. Also, changes in metal dependent functions such as redox and photochemical catalysis can be expected in these polyamide oligomers. In summary, these metal complexes could be useful in developing metal wires, molecular devices and catalysis.

---

**References**

1. (a) Schildknecht, H.; Schmidt, H. *Z. Naturforsch.* **1967**, *22b*, 287; (b) Bloch, B.; Karrer, P. *Vjschr. naturforsch. Ges. Zürich* **1927**, *72*, 1; *Chem. Abstr.* **1928**, *22*, 2784.
2. (a) Marini-Bettolo, G. B.; Monache, F. D.; da Lima, O. G.; Coelho, S. B. *Gazz. Chim. Ital.* **1971**, *101*, 41-43; (b) Bernays, E.; Lupi, A.; Bettolo, R. M.; Mastrofrancesco, C.; Tagliatesta, P. *Experientia* **1984**, *40*, 1010-1012.
3. Darwish, F. M. M.; Abdallah, O. M.; El-Emary, N. A.; Ali, A. A. *Bull. Pharm. Sci.* **1995**, *18*, 45.
4. Ongcharoen, W. P.; Ukachaisirikul, V. R.; Hongpaichit, S. P. *Chem. Pharm. Bull.* **2007**, *55*, 1404.
5. Lauchli, R.; Shea, K. J. *Org. Lett.* **2006**, *8*, 5287.
6. Meza-Aviña, M. E.; Ordoñez, M.; Fernández-Zertuche, M.; Rodríguez-Fragoso, L.; Reyes-Esparza, J.; Ríos-Corsino, A. A. M. de los *Bioorg. Med. Chem.* **2005**, *13*, 6521.
7. Bhattacharya, A. K.; Kaur, T.; Ganesh, K. N. *Synthesis*, **2010**, *7*, 1141.
8. (a) Shukla, Y. N.; Srivastava, A.; Santhakumar, T. R.; Khanuja, S. P. S.; Kumar, S. *Indian Drugs*, **2000**, *37*, 60; (b) Shukla, Y. N.; Srivastava, A.; Kumar, S. *Indian J. Chem.*, **1999**, *38B*, 705.
9. Botella, L.; Na, C. *J. Org. Chem.* **2005**, 4360; (b) Alacid, E.; Nájera, C. *J. Org. Chem.* **2009**, *74*, 2321.
10. (a) Ranu, B. C.; Samanta, S. *J. Org. Chem.* **2003**, *68*, 7130; (b) Ranu, B. C.; Dutta, J.; Guchhait, S. K. *Org. Lett.* **2001**, *3*, 2603.
11. Olah, G.; Narang, S. C.; Gupta, B. G. B.; Malhotra, R. *J. Org. Chem.* **1979**, *44*, 1247.
12. De Albuquerque, I. L.; Galeffi, C.; Casinovi, C. G.; Marini-Bettòlo, G. B. *Gazz. Chim. Ital.* **1964**, *94*, 287.
13. Allen, M. C.; Fuhrer, W.; Tuck, B.; Wade, R.; Wood, J. M. *J. Med. Chem.* **1989**, *32*, 1652.
14. R. Hildebrand. *The role of Phosphonates in Living system*; CRC Press: Boca Raton, **1983**.
15. Atherton, F. R.; Hassal, C. H.; Lambert, R. W. *J. Med. Chem.* **1986**, *29*, 29.

- 
16. Hirschmann, R.; Smith III, A. B.; Taylor, C. M.; Benkovic, P. A.; Taylor, S. D.; Yager, K. M.; Sprengler, P. A.; Venkovic, S. J. *Science* **1994**, 265, 234.
  17. Srivastava, N.; Banik, B. K. *J. Org. Chem.* **2003**, 68, 2109.
  18. Bhattacharya, A.; Kaur, T. *Synlett* **2007**, 745.
  19. Nielsen, P. E.; Egholm, M.; Berg, R. H.; Buchardt, O. *Science* **1991**, 254, 1497-1500.
  20. (a) D'Costa, M.; Kumar, V. A.; Ganesh, K. N.; *Org. Lett.* **1999**, 1, 1513-1516; (b) Govindaraju, T.; Kumar, V. A.; Ganesh, K. N. *Chem. Commun.* **2004**, 860-861.
  21. (a) Shionoya, M.; Tanaka, K. *Bull. Chem. Soc. Jpn.* **2000**, 73, 1945-1954; (b) Shionoya, M.; Tanaka, K. *Chemistry Letters*, **2006**, 35, 694-699.
  22. (a) Molecules, H. A.; Hiraoka, S.; Harano, K.; Nakamura, T.; Shiro, M.; Shionoya, M. *Angew. Chem. Int. Ed.* **2009**, 48, 7006-7009; (b) Clever, G. H.; Tashiro, S.; Shionoya, M. *Angew. Chem. Int. Ed.* **2009**, 48, 7010-7012.

## List of Figures

Figure No.	Chapter 1 Section A	Page No.
Figure 1	Structure of Doxorubicin <b>1</b>	2
Figure 2	Structure of Lettowiquinone <b>2</b>	3
Figure 3	Structure of Belamcandaquinones (J) <b>3a</b> , (K) <b>3b</b> , (L) <b>3c</b> and (M) <b>3d</b>	3
Figure 4	Structure of Taiwaniaquinones A ( <b>4a</b> ), D ( <b>4b</b> ), H ( <b>4c</b> ) and dichroanal ( <b>4d</b> )	4
Figure 5	Structure of 3-Hydroxythymoquinone <b>5</b>	4
Figure 6	Structure of Primin <b>8</b> and its analogues	5
Figure 7	ORTEP diagram of 2-methoxy-6-propyl-1,4-benzoquinone, <b>6</b>	9
Figure 8	ORTEP diagram of compound <b>34</b>	12
<b>Section B</b>		
Figure 1	Structure of antibacterial agent Oenostacin, <b>1</b>	54
<b>Section C</b>		
Figure 1	Structure of (-)-Centrolobine, <b>1</b>	96
Figure 2	Structure of Jacobsen's catalysts	106
<b>Chapter 2</b> <b>Section A</b>		
Figure 1	Structure of few useful biaryl derivatives synthesized <i>via</i> Suzuki-Miyaura cross-coupling reactions	132
Figure 2	Previous reports for the synthesis of biaryl derivatives	133
Figure 3	ORTEP diagram of derivatives <b>21e</b> and <b>21u</b>	141
<b>Section B</b>		
Figure 1	Structure of naturally occurring 2-aminoethanephosphonic acid (AEP) derivatives	181
Figure 2	Structure of synthetic $\alpha$ -aminophosphonic acid derivatives	182
Figure 3	ORTEP diagram of $\alpha$ -aminophosphonate derivative, <b>22t</b>	194
<b>Chapter 3</b>		
Figure 1	Structure of DNA duplex and nucleobases	224
Figure 2	Hydrogen-bonding interactions between (A) A-T and (B) G-C base pairs	225
Figure 3	Chemical modifications in the development of oligonucleotides	226
Figure 4	Structure of (A) PNA structure and (B) DNA	227
Figure 5	Modified nucleobases used in the synthesis of PNA oligomers	228
Figure 6	Naphthyridine-pyrimidine metallofoldamer reported by Lehn	230
Figure 7	Pyridine-hydrazone metallofoldamer exhibited binding to Pb <sup>2+</sup>	230

<b>Figure 8</b>	Cu <sup>2+</sup> -mediated duplex formation between two artificial DNA strands in which hydroxypyridone nucleobases replace natural base pairs	231
<b>Figure 9</b>	Metal binding ligands instead of A/T/G/C nucleobases used in DNA oligomers	232
<b>Figure 10</b>	Synthesized cobaltocene peptides having lysines and guanidines	233
<b>Figure 11</b>	Structures of metal binding ligands attached to PNA backbone	234
<b>Figure 12</b>	Proposed approach for metal binding of Zn-dpa probes to oligonucleotides	235
<b>Figure 13</b>	Representation of isosbestic point in UV-Vis spectroscopy	244
<b>Figure 14</b>	Representation of maxima and minima in Job's plot	244
<b>Figure 15</b>	Metal complexes with designed ligands linked to <i>aeg</i> backbone	246
<b>Figure 16</b>	Designed novel <i>aeg</i> linked bidentate ligands	247
<b>Figure 17</b>	Metal mediated duplex formation in modified ligand aminoethyl glycine ( <i>aeg</i> ) strands	248
<b>Figure 18</b>	ORTEP diagram of <i>N</i> -Boc-aminoethyl--2-pyridylbenzimidazole (PBI) glycinate <b>8</b> and <b>Pd</b> complex	251
<b>Figure 19</b>	ORTEP diagram of compound <b>15</b>	254
<b>Figure 20</b>	Structure of polyamide <i>homo</i> -oligomers (PBI) <sub>6</sub> <b>22</b> , (PDA) <sub>6</sub> <b>23</b> , (CAT) <sub>6</sub> <b>24</b>	259
<b>Figure 21</b>	Structure of polyamide <i>hetero</i> -oligomers (PBI) <sub>3</sub> -(PDA) <sub>3</sub> <b>25</b> , (PBI-PDA) <sub>3</sub> <b>26</b> , (PBI) <sub>3</sub> -(CAT) <sub>3</sub> <b>27</b> and (PBI-CAT) <sub>3</sub> <b>28</b>	260
<b>Figure 22</b>	HPLC of polyamide oligomers (A) (PBI) <sub>6</sub> <b>22</b> , (B) (PDA) <sub>6</sub> <b>23</b>	261
<b>Figure 23</b>	MALDI-TOF of polyamide oligomers (A) (PBI) <sub>6</sub> <b>22</b> , (B) (PDA) <sub>6</sub> <b>23</b> , (C) (CAT) <sub>6</sub> <b>24</b> and (D) (PBI) <sub>3</sub> -(PDA) <sub>3</sub> <b>25</b> .	262
<b>Figure 24</b>	Concentration vs absorbance plots for calculating molar extinction coefficient ( $\epsilon$ ) for polyamide oligomer (A) (PBI) <sub>6</sub> <b>22</b> (B) (PDA) <sub>6</sub> <b>23</b> (C) (CAT) <sub>6</sub> <b>24</b>	264
<b>Figure 25</b>	Concentration vs absorbance plots for calculating molar extinction coefficient ( $\epsilon$ ) for polyamide oligomer (D) (PBI) <sub>3</sub> -(PDA) <sub>3</sub> <b>25</b> , (E) (PBI-PDA) <sub>3</sub> <b>26</b> (F) (PBI) <sub>3</sub> -(CAT) <sub>3</sub> <b>27</b>	265
<b>Figure 26</b>	Concentration vs absorbance for calculating molar extinction coefficient ( $\epsilon$ ) for polyamide oligomer (G) (PBI-CAT) <sub>3</sub> <b>28</b>	266
<b>Figure 27</b>	pH titration of polyamide oligomers with NaOH (0.5 M) (A) (PBI) <sub>6</sub> <b>22</b> , (B) (PDA) <sub>6</sub> <b>23</b> , (C) (CAT) <sub>6</sub> <b>24</b> , (D) (PBI) <sub>3</sub> -(PDA) <sub>3</sub> <b>25</b> , (E) (PBI-PDA) <sub>3</sub> <b>26</b> , (F) (PBI) <sub>3</sub> -(CAT) <sub>3</sub> <b>27</b> , (G) (PBI-CAT) <sub>3</sub> <b>28</b>	268
<b>Figure 28</b>	Acid base equilibria of (PBI) <sub>6</sub> polyamide oligomer <b>22</b>	269
<b>Figure 29</b>	Acid base equilibria of (PDA) <sub>6</sub> polyamide oligomers <b>23</b>	270
<b>Figure 30</b>	Acid base equilibria of (CAT) <sub>6</sub> polyamide oligomers <b>24</b>	270
<b>Figure 31</b>	NMR studies of ethyl- <i>N</i> -Boc-aminoethyl-3,4-dihydroxyphenyl (CAT) glycinate <b>15</b> and trimethyl borate	273
<b>Figure 32</b>	<sup>1</sup> H NMR studies of benzyl- <i>N</i> -Boc-aminoethyl-3,4-dihydroxyphenyl (CAT) glycinate <b>17</b> and trimethyl borate in DMSO-d <sub>6</sub>	274
<b>Figure 33</b>	Pictorial representation of ethyl and benzyl- <i>N</i> -Boc-aminoethyl-3,4-dihydroxyphenyl (CAT) glycinate <b>15</b> and <b>17</b> with boron ion.	274
<b>Figure 34</b>	Structures of complexes of ethyl- <i>N</i> -Boc-aminoethyl-2-pyridylbenzimidazole (PBI) glycinate <b>8</b> with various metal salts.	275
<b>Figure 35</b>	HR-MS spectra for ethyl- <i>N</i> -Boc-aminoethyl-2-pyridylbenzimidazole (PBI) glycinate <b>8</b> with (A) copper chloride (B) copper nitrate (C) copper perchlorate (D)	276

	nickel chloride	
<b>Figure 36</b>	Schematic representation of <i>aeg</i> linked ethyl- <i>N</i> -Boc-aminoethyl-2-pyridylbenzimidazole (PBI) glycinate <b>8</b> with copper and nickel metal salts	277
<b>Figure 37</b>	Structure of <i>N</i> -Boc-aminoethyl (PBI) <sub>2</sub> (glycinate) <sub>2</sub> <b>21</b> and copper chloride complex	277
<b>Figure 38</b>	HR-MS spectra of <i>N</i> -Boc-aminoethyl (PBI) <sub>2</sub> (glycinate) <sub>2</sub> <b>21</b> with copper chloride	278
<b>Figure 39</b>	Schematic representation of <i>N</i> -Boc-aminoethyl (PBI) <sub>2</sub> (glycinate) <sub>2</sub> <b>21</b> with copper chloride	278
<b>Figure 40</b>	Changes in the absorption spectra of the <i>N</i> -Boc-aminoethyl-2-pyridylbenzimidazole (PBI) glycinate <b>8</b> (25 μM) in methanol upon the addition of copper and nickel nitrates	280
<b>Figure 41</b>	Changes in the absorption spectra of the <i>N</i> -Boc-aminoethyl-2-pyridylbenzimidazole (PBI) glycinate <b>8</b> (25 μM) in methanol upon the addition of AuCl <sub>3</sub>	281
<b>Figure 42</b>	Job's plot of <i>N</i> -Boc-aminoethyl-2-pyridylbenzimidazole (PBI) glycinate <b>8</b> with Cu(NO <sub>3</sub> ) <sub>2</sub> and Ni(NO <sub>3</sub> ) <sub>2</sub>	283
<b>Figure 43</b>	Benesi Hildebrand's plots of <i>N</i> -Boc-aminoethyl-2-pyridylbenzimidazole (PBI) glycinate <b>8</b> with Cu(NO <sub>3</sub> ) <sub>2</sub> and Ni(NO <sub>3</sub> ) <sub>2</sub>	284
<b>Figure 44</b>	Proposed model of <i>N</i> -Boc-aminoethyl-2-pyridylbenzimidazole (PBI) glycinate <b>8</b> with copper and nickel nitrates	284
<b>Figure 45</b>	Changes in the absorption spectra of <i>N</i> -Boc-aminoethyl-catechol (CAT) glycinate <b>17</b> (50 μM) upon the addition of phenylboronic acid (2.5 mM)	285
<b>Figure 46</b>	Changes in the absorption spectra of <i>N</i> -Boc-aminoethyl-catechol (CAT) glycinate <b>17</b> (50 μM) in methanol upon the addition of metal salts (A) Cu(NO <sub>3</sub> ) <sub>2</sub> (B) Ni(NO <sub>3</sub> ) <sub>2</sub> . (C) ZnNO <sub>3</sub> ) <sub>2</sub> (D) RuCl <sub>3</sub>	286
<b>Figure 47</b>	Changes in the absorption spectra of <i>N</i> -Boc-aminoethyl-catechol (CAT) glycinate <b>17</b> (50 μM) in methanol upon the addition of metal salts (A) AgNO <sub>3</sub> (B) AuCl <sub>3</sub>	287
<b>Figure 48</b>	Changes in the absorption spectra of <i>N</i> -Boc-aminoethyl 2-pyridylbenzimidazole (PBI) <sub>2</sub> (glycinate) <sub>2</sub> <b>21</b> (10 μM) in water upon the addition of Cu(NO <sub>3</sub> ) <sub>2</sub> . And Ni(NO <sub>3</sub> ) <sub>2</sub>	289
<b>Figure 49</b>	Job's plot of <i>N</i> -Boc-aminoethyl 2-pyridylbenzimidazole (PBI) <sub>2</sub> (glycinate) <sub>2</sub> <b>21</b> with Cu(NO <sub>3</sub> ) <sub>2</sub> and Ni(NO <sub>3</sub> ) <sub>2</sub>	290
<b>Figure 50</b>	Benesi Hildebrand's plots of <i>N</i> -Boc-aminoethyl 2-pyridylbenzimidazole (PBI) <sub>2</sub> (glycinate) <sub>2</sub> <b>21</b> with Cu(NO <sub>3</sub> ) <sub>2</sub> and Ni(NO <sub>3</sub> ) <sub>2</sub>	291
<b>Figure 51</b>	Proposed model for <i>N</i> -Boc-aminoethyl 2-pyridylbenzimidazole (PBI) <sub>2</sub> (glycinate) <sub>2</sub> <b>21</b> (A) with Cu(NO <sub>3</sub> ) <sub>2</sub> and (B) Ni(NO <sub>3</sub> ) <sub>2</sub>	292
<b>Figure 52</b>	Structure of 2-pyridylbenzimidazole (PBI) <sub>6</sub> oligomer <b>22</b>	293
<b>Figure 53</b>	Changes in the absorption spectra of 2-pyridylbenzimidazole (PBI) <sub>6</sub> oligomer <b>22</b> (8-10 μM) in water upon the addition of metal salts (A) Cu(NO <sub>3</sub> ) <sub>2</sub> . (C) Ni(NO <sub>3</sub> ) <sub>2</sub>	294
<b>Figure 54</b>	Changes in the absorption spectra of 2-pyridylbenzimidazole (PBI) <sub>6</sub> oligomer <b>22</b> (8-10 μM) in water upon the addition of AuCl <sub>3</sub>	294
<b>Figure 55</b>	Job's plot of 2-pyridylbenzimidazole (PBI) <sub>6</sub> oligomer <b>22</b> with Cu(NO <sub>3</sub> ) <sub>2</sub> and Ni(NO <sub>3</sub> ) <sub>2</sub>	296
<b>Figure 56</b>	Benesi Hildebrand's plots of 2-pyridylbenzimidazole (PBI) <sub>6</sub> oligomer <b>22</b> with	296

	Cu(NO <sub>3</sub> ) <sub>2</sub> and Ni(NO <sub>3</sub> ) <sub>2</sub>	
<b>Figure 57</b>	Structure of <i>o</i> -phenylenediamine oligomer (PDA) <sub>6</sub> <b>23</b>	297
<b>Figure 58</b>	Changes in the absorption spectra of <i>o</i> -phenylenediamine oligomer (PDA) <sub>6</sub> <b>23</b> (8-10 μM) in water upon the addition of metal salts (A) Cu(NO <sub>3</sub> ) <sub>2</sub> (B) Ni(NO <sub>3</sub> ) <sub>2</sub> (C) AuCl <sub>3</sub>	298
<b>Figure 59</b>	Changes in the absorption spectra of <i>o</i> -phenylenediamine oligomer (PDA) <sub>6</sub> <b>23</b> (8-10 μM) in water upon the addition of metal salts. (A) Pd(NO <sub>3</sub> ) <sub>2</sub> (B) Zn(NO <sub>3</sub> ) <sub>2</sub> (C) Cd(NO <sub>3</sub> ) <sub>2</sub> (D) Hg(ClO <sub>4</sub> ) <sub>2</sub>	299
<b>Figure 60</b>	Changes in the absorption spectra of <i>o</i> -phenylenediamine oligomer (PDA) <sub>6</sub> <b>23</b> (8-10 μM) in water upon the addition of metal salts followed by NaOH (0.5 M) (A) Cu(NO <sub>3</sub> ) <sub>2</sub> . (B) Ni(NO <sub>3</sub> ) <sub>2</sub>	299
<b>Figure 61</b>	Structure of catechol (CAT) <sub>6</sub> oligomer <b>24</b>	300
<b>Figure 62</b>	Changes in the absorption spectra of catechol (CAT) <sub>6</sub> oligomer <b>24</b> (8-10 μM) in water upon the addition of metal salts (A) Cu(NO <sub>3</sub> ) <sub>2</sub> . (B) Ni(NO <sub>3</sub> ) <sub>2</sub>	300
<b>Figure 63</b>	Changes in the absorption spectra of catechol (CAT) <sub>6</sub> oligomer <b>24</b> (8-10 μM) in water upon the addition of AuCl <sub>3</sub>	301
<b>Figure 64</b>	Structure of (PBI) <sub>3</sub> -(PDA) <sub>3</sub> oligomer <b>25</b>	301
<b>Figure 65</b>	Changes in the absorption spectra of (PBI) <sub>3</sub> -(PDA) <sub>3</sub> oligomer <b>25</b> (8-10 μM) in water upon the addition of metal salts (A) Cu(NO <sub>3</sub> ) <sub>2</sub> (C) Ni(NO <sub>3</sub> ) <sub>2</sub>	302
<b>Figure 66</b>	Changes in the absorption spectra of (PBI) <sub>3</sub> -(PDA) <sub>3</sub> oligomer <b>25</b> (8-10 μM) in water upon the addition of AuCl <sub>3</sub>	303
<b>Figure 67</b>	Changes in the absorption spectra of (PBI) <sub>6</sub> oligomer <b>22</b> (8-10 μM) in water upon the addition of metal salts (A) Ni(NO <sub>3</sub> ) <sub>2</sub> (7.5 mM)	303
<b>Figure 68</b>	Job's plot of (PBI) <sub>3</sub> -(PDA) <sub>3</sub> oligomer <b>25</b> with Cu(NO <sub>3</sub> ) <sub>2</sub> and Ni(NO <sub>3</sub> ) <sub>2</sub>	304
<b>Figure 69</b>	Benesi Hildebrand's plots of (PBI) <sub>3</sub> -(PDA) <sub>3</sub> oligomer <b>25</b> with Cu(NO <sub>3</sub> ) <sub>2</sub> and Ni(NO <sub>3</sub> ) <sub>2</sub>	305
<b>Figure 70</b>	Structure of (PBI-PDA) <sub>3</sub> oligomer <b>26</b>	305
<b>Figure 71</b>	Changes in absorption spectra of (PBI-PDA) <sub>3</sub> oligomer <b>26</b> (8-10 μM) in water upon the addition of metal salts (A) Cu(NO <sub>3</sub> ) <sub>2</sub> (C) Ni(NO <sub>3</sub> ) <sub>2</sub>	306
<b>Figure 72</b>	Changes in absorption spectra of (PBI-PDA) <sub>3</sub> oligomer <b>26</b> (8-10 μM) in water upon the addition of AuCl <sub>3</sub>	307
<b>Figure 73</b>	Job's plot of (PBI-PDA) <sub>3</sub> oligomer <b>26</b> with Cu(NO <sub>3</sub> ) <sub>2</sub> and Ni(NO <sub>3</sub> ) <sub>2</sub>	308
<b>Figure 74</b>	Benesi Hildebrand's plots of (PBI-PDA) <sub>3</sub> oligomer <b>26</b> with Cu(NO <sub>3</sub> ) <sub>2</sub> and Ni(NO <sub>3</sub> ) <sub>2</sub>	308
<b>Figure 75</b>	Structure of (PBI) <sub>3</sub> -(CAT) <sub>3</sub> oligomer <b>27</b>	309
<b>Figure 76</b>	Changes in the absorption spectra of (PBI) <sub>3</sub> -(CAT) <sub>3</sub> oligomer <b>27</b> (8-10 μM) in water upon the addition of Cu(NO <sub>3</sub> ) <sub>2</sub> and (C) Ni(NO <sub>3</sub> ) <sub>2</sub>	309
<b>Figure 77</b>	Job's plot of (PBI) <sub>3</sub> -(CAT) <sub>3</sub> oligomer <b>27</b> with Cu(NO <sub>3</sub> ) <sub>2</sub> and Ni(NO <sub>3</sub> ) <sub>2</sub>	310
<b>Figure 78</b>	Benesi Hildebrand's plots of (PBI) <sub>3</sub> -(CAT) <sub>3</sub> oligomer <b>27</b> with Cu(NO <sub>3</sub> ) <sub>2</sub> and Ni(NO <sub>3</sub> ) <sub>2</sub>	311
<b>Figure 79</b>	Structure of (PBI) <sub>3</sub> -(CAT) <sub>3</sub> oligomer <b>28</b>	311
<b>Figure 80</b>	Changes in the absorption spectra of (PBI) <sub>3</sub> -(CAT) <sub>3</sub> oligomer <b>28</b> (8-10 μM) in water upon the addition of Cu(NO <sub>3</sub> ) <sub>2</sub> (C) Ni(NO <sub>3</sub> ) <sub>2</sub>	312
<b>Figure 81</b>	Job's plot of (PBI) <sub>3</sub> -(CAT) <sub>3</sub> oligomer <b>28</b> with Cu(NO <sub>3</sub> ) <sub>2</sub> and Ni(NO <sub>3</sub> ) <sub>2</sub>	313
<b>Figure 82</b>	Benesi Hildebrand's plots of (PBI) <sub>3</sub> -(CAT) <sub>3</sub> oligomer <b>28</b> with Cu(NO <sub>3</sub> ) <sub>2</sub> and	313

	Ni(NO <sub>3</sub> ) <sub>2</sub>	
<b>Figure 83</b>	Schematic diagram of polyamide oligomers binding with (A) Cu(NO <sub>3</sub> ) <sub>2</sub> and (B) Ni(NO <sub>3</sub> ) <sub>2</sub>	314
<b>Figure 84</b>	ITC figures in water for (PBI) <sub>6</sub> oligomer <b>22</b> with Cu(NO <sub>3</sub> ) <sub>2</sub>	315
<b>Figure 85</b>	ITC figures in water for (A) (PBI) <sub>3</sub> - (PDA) <sub>3</sub> oligomer <b>25</b> with Ni(NO <sub>3</sub> ) <sub>2</sub> , (B) (PBI-PDA) <sub>3</sub> oligomer <b>26</b> with Cu(NO <sub>3</sub> ) <sub>2</sub> , (C) (PBI) <sub>3</sub> -(CAT) <sub>3</sub> oligomer <b>27</b> with Cu(NO <sub>3</sub> ) <sub>2</sub> . (D) (PBI-CAT) <sub>3</sub> <b>28</b> in water with Cu(NO <sub>3</sub> ) <sub>2</sub>	316
<b>Figure 86</b>	Co-ordination geometries of the reported ligands	319
<b>Figure 87</b>	Co-ordination geometries of the synthesized <i>aeg</i> linked ligands	320
<b>Figure 88</b>	Plausible co-ordination geometries of the <i>aeg</i> linked ligands in the formed metal mediated duplexes	321
<b>Figure 89</b>	Pictorial representation of possible binding mode for 2-pyridylbenzimidazole (PBI) monomer <b>8</b> , dimer <b>21</b> and oligomers <b>22</b>	322
<b>Figure 90</b>	Pictorial representation of possible binding mode for (PDA) oligomers <b>23</b>	322
<b>Figure 91</b>	Pictorial representation of possible binding mode for (CAT) monomer <b>17</b> and oligomers <b>24</b>	323
<b>Figure 92</b>	Pictorial representation of possible binding mode for 2-pyridylbenzimidazole (PBI) and <i>o</i> -phenylenediamine (PDA) <i>hetero</i> -oligomers	323
<b>Figure 93</b>	Pictorial representation of possible binding mode for 2-pyridylbenzimidazole (PBI) and catechol (CAT) <i>hetero</i> -oligomers	324
<b>Figure 94</b>	(A) HPLC of oligomers (PBI) <sub>6</sub> <b>22</b> . (B) MALDI-TOF of (PBI) <sub>6</sub> <b>22</b> . (C) HPLC of oligomer (PDA) <sub>6</sub> <b>23</b> . (D) MALDI-TOF of oligomer (PDA) <sub>6</sub> <b>23</b> . (E) HPLC of oligomer (CAT) <sub>6</sub> <b>24</b> . (F) MALDI-TOF of (CAT) <sub>6</sub> <b>24</b>	382
<b>Figure 95</b>	(A) HPLC of oligomer (PBI) <sub>3</sub> -(PDA) <sub>3</sub> <b>25</b> . (B) MALDI-TOF of oligomer (PBI) <sub>3</sub> -(PDA) <sub>3</sub> <b>25</b> . (C) HPLC of oligomer (PBI-PDA) <sub>3</sub> <b>26</b> . (D) MALDI-TOF of (PBI-PDA) <sub>3</sub> <b>26</b> . (E) HPLC of oligomer (PBI) <sub>3</sub> -(CAT) <sub>3</sub> <b>27</b> . (F) MALDI-TOF of oligomer (PBI) <sub>3</sub> -(CAT) <sub>3</sub> <b>27</b> . (G) HPLC of oligomer (PBI-CAT) <sub>3</sub> <b>28</b> (G) MALDI-TOF of oligomer (PBI-CAT) <sub>3</sub> <b>28</b>	383
<b>Figure 96</b>	UV-Vis spectrophotometric titrations of 2-pyridylbenzimidazole (PBI) <i>aeg</i> <b>8</b>	385
<b>Figure 97</b>	UV-Vis spectrophotometric titrations of benzyl-N-Boc-aminoethyl-3,4-dihydroxyphenyl (CAT) glycinate <b>17</b>	385
<b>Figure 98</b>	UV-Vis spectrophotometric titrations of 2-pyridylbenzimidazole (PBI) <sub>6</sub> oligomer <b>22</b>	386
<b>Figure 99</b>	UV-Vis spectrophotometric titrations of 2-pyridylbenzimidazole (PBI) <sub>6</sub> oligomer <b>22</b>	387
<b>Figure 100</b>	UV-Vis spectrophotometric titrations of 2-pyridylbenzimidazole (PBI) <sub>6</sub> oligomer <b>22</b>	388
<b>Figure 101</b>	UV-Vis spectrophotometric titrations of <i>hetero</i> -(PBI) <sub>3</sub> - (PDA) <sub>3</sub> <b>25</b>	389
<b>Figure 102</b>	UV-Vis spectrophotometric titrations of <i>hetero</i> -(PBI) <sub>3</sub> - (PDA) <sub>3</sub> <b>25</b>	390
<b>Figure 103</b>	Isothermal Titration Calorimetry (ITC) analysis of synthesized <i>aeg</i> linked ligands with nickel nitrate	391
<b>Figure 104</b>	Isothermal Titration Calorimetry (ITC) analysis of synthesized <i>aeg</i> linked ligands with nickel nitrate	392



---

## List of Schemes

---

<b>Scheme No.</b>	<b>Chapter 1 Section A</b>	<b>Page No.</b>
<b>Scheme 1</b>	Synthesis of Primin using Schildknecht's approach	6
<b>Scheme 2</b>	Synthesis of Primin using Bieber's approach	6
<b>Scheme 3</b>	Synthesis of Primin using Mabic's approach	6
<b>Scheme 4</b>	Synthesis of Primin using Kingston's approach	7
<b>Scheme 5</b>	Synthesis of Primin using Moody's approach	7
<b>Scheme 6</b>	Retrosynthetic plan for the synthesis of 2-methoxy-6-alkyl-1,4-benzoquinones, (6, 7, 8 and 9)	8
<b>Scheme 7</b>	Synthesis of 2-methoxy-6-propyl-1,4-benzoquinone, 6	9
<b>Scheme 8</b>	Synthesis of 2-methoxy-6-methyl-1,4-benzoquinone, 7	11
<b>Scheme 9</b>	Synthesis of 2-methoxy-6-pentyl-1,4-benzoquinone, Primin 8	12
<b>Scheme 10</b>	Schematic representation of synthesis of Primin acid, 9	13
<b>Section B</b>		
<b>Scheme 1</b>	Retrosynthetic strategy for the synthesis of antibacterial agent, Oenostacin 1	55
<b>Scheme 2</b>	Successful Heck reaction conditions on the analog 12	58
<b>Scheme 3</b>	Optimized conditions for the selective hydrogenation on derivative 3	58
<b>Scheme 4</b>	Optimized reduction reaction conditions on the analog 3	59
<b>Scheme 5</b>	Synthetic efforts towards the synthesis of antibacterial agent Oenostacin, 1	59
<b>Scheme 6</b>	Retrosynthetic strategy for the synthesis of antibacterial agent, Oenostacin 1	60
<b>Scheme 7</b>	Synthetic efforts towards antibacterial agent, oenostacin 1	61
<b>Scheme 8</b>	Synthetic efforts carried out for the oxidation of benzylic alcohol 16	62
<b>Scheme 9</b>	Synthesis of aldehydic compound 23	62
<b>Scheme 10</b>	Synthetic efforts for the oxidation of aldehyde 23 into acid 22	63
<b>Section C</b>		
<b>Scheme 1</b>	Synthesis of (-)-Centrolobine using Solladie's approach	97
<b>Scheme 2</b>	Synthesis of (-)-Centrolobine using Rychnovsky's approach	97
<b>Scheme 3</b>	Synthesis of (-)-Centrolobine using Evan's approach	98
<b>Scheme 4</b>	Synthesis of (-)-Centrolobine using Boulard's approach	98
<b>Scheme 5</b>	Synthesis of (-)-Centrolobine using Clark's approach	99
<b>Scheme 6</b>	Synthesis of (-)-Centrolobine using Loh's approach	100
<b>Scheme 7</b>	Synthesis of (-)-Centrolobine using Chandarshekhar's approach	100
<b>Scheme 8</b>	Synthesis of (-)-Centrolobine using Jenning's approach	101
<b>Scheme 9</b>	Synthesis of (-)-Centrolobine using Blechert's approach	101
<b>Scheme 10</b>	Synthesis of (-)-Centrolobine using Prasad's approach	102
<b>Scheme 11</b>	Synthesis of (-)-Centrolobine using Hasimoto's approach	103
<b>Scheme 12</b>	Synthesis of (-)-Centrolobine using Furman's approach	104

<b>Scheme 13</b>	Synthesis of (-)-Centrolobine using Spilling's approach	104
<b>Scheme 14</b>	Retrosynthetic route for the synthesis of (-)-Centrolobine, <b>1</b>	105
<b>Scheme 15</b>	Postulated mechanism for the oxidative kinetic resolution (OKR)	107
<b>Scheme 16</b>	Synthesis of compound <b>57</b> utilizing Wittig reaction	107
<b>Scheme 17</b>	Synthesis of compound <b>59</b> utilizing Wittig reaction	108
<b>Scheme 18</b>	Formal synthesis of (-)-Centrolobine, <b>1</b>	109
<b>Scheme 19</b>	Alternative route towards the formal synthesis of (-)-Centrolobine, <b>1</b>	110
<b>Scheme 20</b>	Derivatization of alcohol to ester using Moscher's method	110
<b>Scheme 21</b>	Postulated mechanism for the synthesis of compound <b>63</b>	111

## Chapter 2

### Section A

<b>Scheme 1</b>	Optimization of the reaction conditions for the synthesis of 2-styryl furans	134
<b>Scheme 2</b>	Synthesis of 2-( <i>Z</i> -styryl)furan <i>via</i> Negishi cross-coupling reaction	134
<b>Scheme 3</b>	Synthesis of 2-( <i>E</i> -styryl)furan <i>via</i> Wittig reaction	134
<b>Scheme 4</b>	Synthesis of 2-( <i>E</i> -styryl)furan <i>via</i> dehydrogenative cross-coupling	135
<b>Scheme 5</b>	Optimization of reaction conditions for the Synthesis of 2-( <i>E</i> -styryl)furan	135
<b>Scheme 6</b>	Postulated mechanism for the synthesis of ( <i>E</i> )-3-(furan-2-yl)-acrylic acid <b>20a</b> or ( <i>E</i> )-3-(thiophene-2-yl)-acrylic acid <b>20b</b>	142

### Section B

<b>Scheme 1</b>	Synthetic routes to $\alpha$ -aminophosphonates	183
<b>Scheme 2</b>	Synthesis of iso-quinoline phosphonates using $\alpha$ - heterofunctionalization	184
<b>Scheme 3</b>	Catalytic hydrogenation method for the synthesis of $\alpha$ -aminophosphonates	185
<b>Scheme 4</b>	Enantioselective Michael addition to synthesize $\alpha$ -aminophosphonates	185
<b>Scheme 5</b>	Synthesis of $\alpha$ -aminophosphonates using alkylation method	186
<b>Scheme 6</b>	Synthesis of $\alpha$ -aminophosphonates using hydrophosphonylation	186
<b>Scheme 7</b>	One pot synthesis of $\alpha$ -aminophosphonates	188
<b>Scheme 8</b>	Bismuth nitrate catalyzed synthesis of $\alpha$ -aminophosphonates	189
<b>Scheme 9</b>	Postulated mechanism for the synthesis of $\alpha$ -aminophosphonates	195

## Chapter 3

<b>Scheme 1</b>	General protocols for the synthesis of peptides <i>via</i> <i>Boc</i> (left) and <i>Fmoc</i> - groups (right).	238
<b>Scheme 2</b>	General strategies for <i>Boc</i> and <i>Fmoc</i> protecting groups	239
<b>Scheme 3</b>	Proposed mechanism for Ninhydrin test	239
<b>Scheme 4</b>	Proposed mechanism for chloranil's test	240
<b>Scheme 5</b>	Retrosynthetic pathways towards the synthesis of target <i>aeg</i> linked ligands.	249
<b>Scheme 6</b>	Synthesis of <i>N</i> -Boc-aminoethyl-2-pyridylbenzimidazole (PBI) glycinate <b>1</b>	250
<b>Scheme 7</b>	Synthesis of <i>N</i> -Boc-aminoethyl- <i>o</i> -phenylenediamine (PDA) glycinate <b>13</b>	252
<b>Scheme 8</b>	Synthesis of <i>N</i> -Boc-aminoethyl-3,4-dihydroxyphenyl (CAT) glycinate <b>3</b>	253
<b>Scheme 9</b>	Revised synthetic scheme for the synthesis of (CAT) <sub>6</sub> oligomer	254
<b>Scheme 10</b>	Synthesis of <i>Mocdene</i> protected- <i>N</i> -Boc-aminoethyl-3,4-dihydroxyphenyl (CAT)	255

	glycinate <b>19</b> .	
<b>Scheme 11</b>	Synthesis of <i>N</i> -Boc-aminoethyl 2-pyridyl benzimidazole (PBI) <sub>2</sub> (glycinate) <sub>2</sub> <b>21</b>	256
<b>Scheme 12</b>	Schematic representation of Solid Phase Peptide Synthesis (SPPS)	258
<b>Scheme 13</b>	Postulated mechanism of catechol (CAT) linked <i>ae</i> g ligands with triemethyl borate.	272
<b>Scheme 14</b>	Metal Complexation of the <i>N</i> -Boc-aminoethyl-2-pyridyl benzimidazole (PBI) glycinate <b>8</b> .	279
<b>Scheme 15</b>	Metal complexation of <i>N</i> -Boc-aminoethyl-catechol (CAT) glycinate <b>17</b> .	285
<b>Scheme 16</b>	Schematic representation Metal Complexation of the <i>N</i> -Boc-aminoethyl 2-pyridylbenzimidazole (PBI) <sub>2</sub> (glycinate) <sub>2</sub> <b>21</b> .	288

---

## List of Tables

Table No.	Chapter 1 Section A	Page No.
<b>Table 1</b>	Crystal data and structure refinement for compound <b>6</b>	30
<b>Table 2</b>	Crystal data and structure refinement for compound <b>34</b>	31
<b>Section B</b>		
<b>Table 1</b>	Standardization of Heck cross-coupling reaction conditions	56
<b>Table 2</b>	Attempted reaction conditions tried for the selective esterification	60
<b>Chapter 2 Section A</b>		
<b>Table 1</b>	Optimization of reaction conditions	136
<b>Table 2</b>	Synthesis of 2-( <i>E</i> -styryl)furan/thiophenes <i>via</i> decarboxylative cross coupling	137
<b>Table 3</b>	Crystal data and structure refinement for compound <b>21e</b>	155
<b>Table 4</b>	Crystal data and structure refinement for compound <b>21u</b>	157
<b>Section B</b>		
<b>Table 1</b>	One-pot synthesis of $\alpha$ -aminophosphonates catalyzed by $\text{Bi}(\text{NO}_3)_3 \cdot 5\text{H}_2\text{O}$	188
<b>Table 2</b>	Crystal data and structure refinement for compound <b>22t</b>	206
<b>Chapter 3</b>		
<b>Table 1</b>	Solid Phase Peptide Synthesis (SPPS) vs Solution Phase Peptide Synthesis	235
<b>Table 2</b>	Resins Used for Solid Phase Peptide Synthesis	236
<b>Table 3</b>	HPLC retention time and MALDI-TOF mass spectral analysis of oligomers	261
<b>Table 4</b>	Conc. vs absorbance plot at 302 nm for $(\text{PBI})_6$ <b>22</b>	264
<b>Table 5</b>	Conc. vs absorbance plot at 269 nm for $(\text{PDA})_6$ <b>23</b>	264
<b>Table 6</b>	Conc. vs absorbance plot at 281 nm for $(\text{CAT})_6$ <b>24</b>	264
<b>Table 7</b>	Conc. vs absorbance plot at 302 nm for $(\text{PBI})_3$ - $(\text{PDA})_3$ <b>25</b>	265
<b>Table 8</b>	Conc. vs absorbance plot at 302 nm for $(\text{PBI-PDA})_3$ <b>26</b>	265
<b>Table 9</b>	Conc. vs absorbance plot at 302 nm for $(\text{PBI})_3$ - $(\text{CAT})_3$ <b>27</b>	265
<b>Table 10</b>	Conc. vs absorbance plot at 302 nm for $(\text{PBI-CAT})_3$ <b>28</b>	266
<b>Table 11</b>	Molar Extinction Coefficients ( $\epsilon$ ) for the polyamide oligomers	266
<b>Table 12</b>	$pK_a$ for the synthesized polyamide oligomers and reported derivatives	269
<b>Table 13</b>	Summary of UV-Vis titrations for the <i>N</i> -Boc-aminoethyl-2-	282

	pyridylbenzimidazole (PBI) glycinate <b>8</b>	
<b>Table 14</b>	Summary of UV-Vis titrations for the <i>N</i> -Boc-aminoethyl-catechol (CAT) glycinate <b>17</b>	287
<b>Table 15</b>	Summary of UV-Vis titration for the <i>N</i> -Boc-aminoethyl 2-pyridylbenzimidazole (PBI) <sub>2</sub> (glycinate) <sub>2</sub> <b>21</b>	289
<b>Table 16</b>	Calculation of binding constants for (PBI) <sub>2</sub> (glycinate) <sub>2</sub> <b>21</b> using UV-Vis spectroscopy	291
<b>Table 17</b>	Summary of UV-Vis titration results for the 2-pyridylbenzimidazole (PBI) <sub>6</sub> oligomer <b>22</b>	295
<b>Table 18</b>	Summary of UV-Vis titrations for the (PBI) <sub>3</sub> -(PDA) <sub>3</sub> oligomer <b>25</b>	304
<b>Table 19</b>	Summary of UV-Vis titration for the (PBI-PDA) <sub>3</sub> oligomer <b>26</b>	307
<b>Table 20</b>	Summary of UV-Vis titration for the (PBI) <sub>3</sub> -(CAT) <sub>3</sub> oligomer <b>27</b>	311
<b>Table 21</b>	Summary of UV-Vis titration for the (PBI) <sub>3</sub> -(CAT) <sub>3</sub> oligomer <b>28</b>	312
<b>Table 22</b>	ITC thermodynamic parameters describing interaction of oligomers with metal salts	317
<b>Table 23</b>	Comparison of binding constants based on UV-Vis and ITC	318
<b>Table 24</b>	Crystal data and structure refinement for compound <b>15</b>	346
<b>Table 25</b>	Crystal data and structure refinement for compound <b>8</b>	347
<b>Table 26</b>	Crystal data and structure refinement for compound <b>8-Pd</b>	348
<b>Table 27</b>	Calculation of binding constants using Benesi-Hildebrand equation	350

---

---

---

## PUBLICATIONS

---

---

1. Nazarov Reagent: A Novel Reagent for the Synthesis of Natural Products. **Tanpreet Kaur**. *Synlett*, **2006**, *17*, 2853-2854.
2. An Effective One Pot Synthesis of Alpha Aminophosphonates using Bismuth Nitrate Pentahydrate as a Lewis Catalyst. Asish K. Bhattacharya, **Tanpreet Kaur**. *Synlett*, **2007**, *05*, 745-748.
3. Synthesis of the Antibacterial Benzoquinone Primin and its Water-Soluble Analogue, Primin Acid. Asish K. Bhattacharya, **Tanpreet Kaur**, Krishna N. Ganesh. *Synthesis*, **2010**, *07*, 1141-1144.
4. Synthesis and Metal Complexation Studies of aminoethyl glycyl (*aeg*) linked ligands. **Tanpreet Kaur**, Krishna N. Ganesh. (Manuscript under preparation).

---

---

## SYMPOSIA ATTENDED/ POSTER PRESENTED

---

---

### ❖ Conference and Symposium Attended

1. “4<sup>th</sup> INDO-KOSEF International Joint Symposium in Organic Chemistry” held between at 12<sup>th</sup> and 13<sup>th</sup> Jan, 2009 at National Chemical Laboratory, Pune, Maharashtra, India.
2. 59<sup>th</sup> Meetings of Nobel Laureates and Students (28<sup>th</sup> June-3 July 2009), Lindau, Germany.
3. “RSC-CSIR Chemical Sciences Innovation Symposium” held on 30<sup>th</sup> Nov, 2009 at National Chemical Laboratory, Pune, Maharashtra-India.
4. “3<sup>rd</sup> Indian Peptide Symposium” held between 24<sup>th</sup> and 25<sup>th</sup> Feb, 2011 at Yashada, Pune, Maharashtra, India.

❖ **Posters Presented:**

1. **Kaur, T.;** Bhattacharya, A. K.; Ganesh, K. N., **First Total Synthesis of Oenostacin, an Antibacterial Agent from the plant *Oenothera biennis***; “11<sup>th</sup> CRSI National Symposium in Chemistry” held between 6<sup>th</sup> and 8<sup>th</sup> Feb, 2009 held at National Chemical Laboratory, Pune, Maharashtra, India.
2. **Kaur, T.;** Ganesh, K. N., **Programmable self-assembly of metal ions in modified Peptide Nucleic Acids (PNAs)**; “1<sup>st</sup> CRSI Zonal Meeting and National Symposium in Chemistry” held between 13<sup>th</sup> and 14<sup>th</sup> May, 2011 at National Chemical Laboratory, Pune, Maharashtra, India.

# *Chapter 1*

## **Synthesis of Antibacterial Natural Products**

---

### *Section A*

#### **Synthesis of Antibacterial 1,4- Benzoquinone Primin and its Analog**

---

This study deals with the synthesis of antibacterial natural product; Primin and its water soluble analog, Primin acid. It also discusses previous literature protocols and advancements about the synthesis of 1,4-benzoquinone derivatives. It involves utilization of well known synthetic protocols for example Grignard reaction and Johnson's Claisen rearrangement for synthesizing this class of compounds.



## 1.1 Introduction

Nature, produces hundreds of compounds through a variety of biogenetic pathways and quite a few of them have attracted the synthetic organic chemist's attention due to their remarkable structural features and/or the conferred specific bioactivity. Synthesis of bioactive molecules is in the forefront of synthetic organic chemistry. Most of such biologically active compounds were isolated from plants, animals, fungi, and microorganisms like bacteria.<sup>1</sup> Total synthesis is playing a pivotal role in the drug discovery process because it allows exploration and development of chemical biology through molecular design and mechanistic study.<sup>2</sup>

Quinones, mainly terpenoid benzoquinones are abundant in nature,<sup>3</sup> and play a crucial role in many life processes. Natural pigments are coloured due to presence of the quinone skeleton. Quinones exhibit major role in various redox processes. For example, the ubiquinones are important electron transfer agents in the respiratory chain and pyrroloquinolinequinone (PQQ) is a redox cofactor. 1,4-Benzoquinone scaffolds have gained prominence recently owing to their excellent biological properties. This unit is present in several biologically important natural products, for example, doxorubicin **1** (Figure 1) which is used in front-line cancer chemotherapy treatment. Quinone motif is interesting fundamental  $\pi$ -electron system having two interesting qualities of high electron affinity and photoreactivity.<sup>4,5</sup>

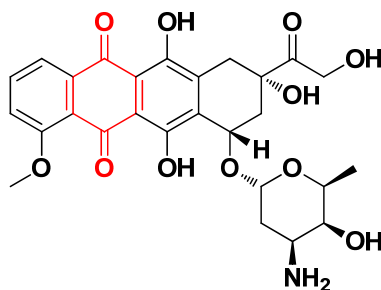


**Figure 1.** Structure of Doxorubicin **1**.

Lettowiquinone **2**<sup>6</sup> (Figure 2) was isolated from ripe and unripe fruits of *Lettowianthus stellatus* by Nkunya and co-workers in 2010. This natural product belongs to the class of geranylbenzoquinoid and exhibits mild *in vitro* activity against *Plasmodium falciparum*, malarial parasite ( $IC_{50} = 20 \mu\text{g mL}^{-1}$ ).

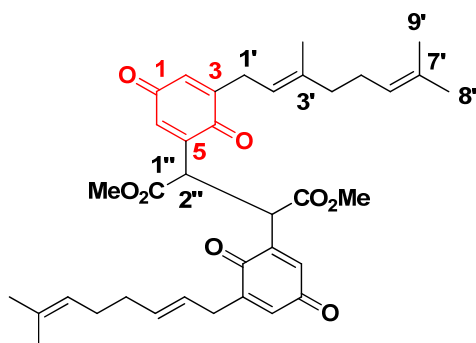


**Figure 2.** Structure of Lettowiquinone 2.

Belamcandaquinones (J) **3a**, belamcandaquinones (K) **3b**, belamcandaquinones (L) **3c**, belamcandaquinones (M) **3d** (Figure 3) are novel 1,4-benzoquinones, which were isolated from the rhizome of *Ardisia gigantifolia*. These compounds were tested for their anticancer activity against cancer cell lines PC-3, EMT6, A549, HeLa, RM-1 and SGC7901. However, they did not exhibit any cytotoxic activity.<sup>7</sup>

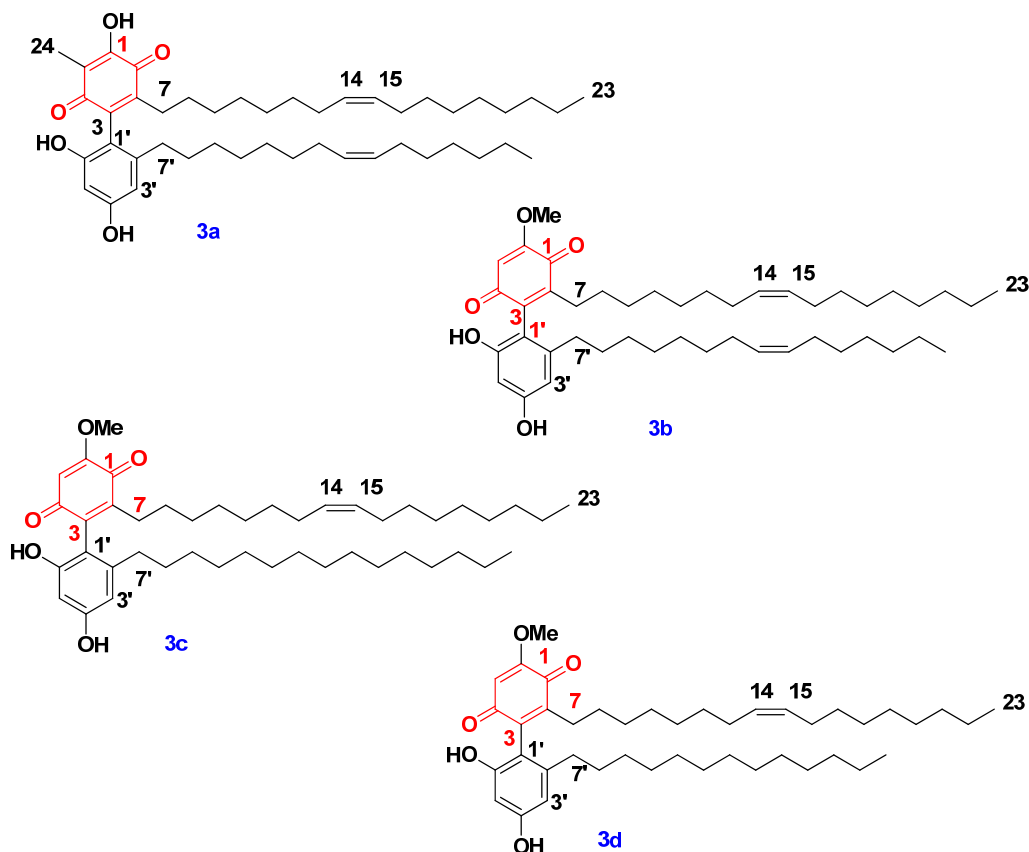


**Figure 3.** Structure of Belamcandaquinones (J) **3a**, (K) **3b**, (L) **3c** and (M) **3d**.

Taiwaniaquinones (A) **4a**,<sup>8</sup> Taiwaniaquinones (D) **4b**,<sup>9</sup> Taiwaniaquinones (H) **4c** and dichroanal (B)<sup>10</sup> **4d** (Figure 4) were isolated from *Taiwania cryptomeria*. Compound **4a** and **4b** have shown potent cytotoxic activity against KB epidermoid carcinoma cancer cells.

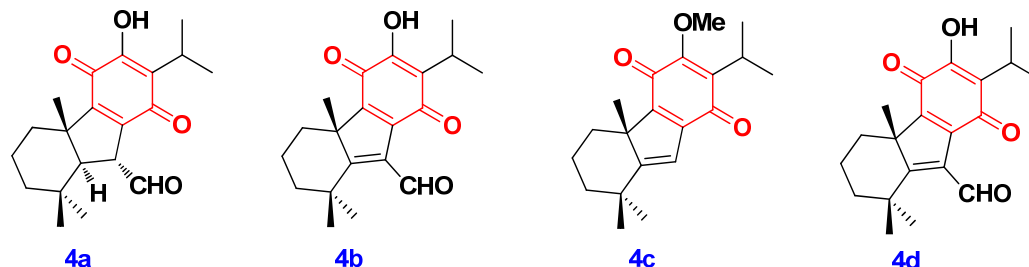


**Figure 4.** Structure of Taiwaniaquinones A (**4a**), D (**4b**), H (**4c**) and dichroanal (**4d**).

3-Hydroxythymoquinone **5**<sup>11</sup> (Figure 5) was isolated from the leaves of the plant *Laggera durrens* (vahl.) and shown phytotoxic activity. Compound **5** inhibited growth and germination of the grass weed *Agrostis capillaris* utilizing 250  $\mu$ M concentration. The mode of action of compound has not yet been deciphered.

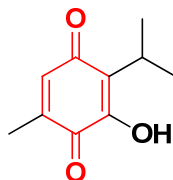


**Figure 5.** Structure of 3-Hydroxythymoquinone **5**.

These 1,4-benzoquinone derivatives possess a wide variety of biological activities. These compounds act as agricultural fungal pathogen control against *Collectotrichum sp.*<sup>12</sup> antibacterial activities against *Staphylococcus aureus* and *Streptococcus pyrogenes*<sup>13</sup> subtermite activity against *Coptotermes formosanus*.<sup>14</sup>

2-Methoxy-6-propyl-1,4-benzoquinone **6** and 2-methoxy-6-methyl-1,4-benzoquinone **7**, antibiotic compounds, have been isolated from the fungus *Carmarops microspora*.<sup>15</sup> Compound **7** was first synthesized by Gras *et al.*<sup>16</sup> on protected guaiacol albeit in low yield. Compound **6** was first synthesized by Claisen *et al.*<sup>17</sup> followed by Dean *et al.*<sup>18</sup>, and by König *et al.*<sup>19</sup> Primin (2-methoxy-6-pentyl-1,4-benzoquinone) **8** was isolated by Bloch *et al.* in 1927 from plant *Primula obconica*.<sup>20</sup> Primin, 2-methoxy-6-pentylbenzoquinone **8** (Figure 6), has been reported to occur in

a variety of plants including *Primula obconica* (primrose), *Miconia* (*M. eriodonta* DC) (Melastomaceae)<sup>21</sup> and *Iris* (*I. sibirica*, *I. pseudacorus*, *I. missouriensis*) (Iridaceae) *species*.<sup>22</sup>



**Figure 6.** Structure of Primin **8** and its analogues.

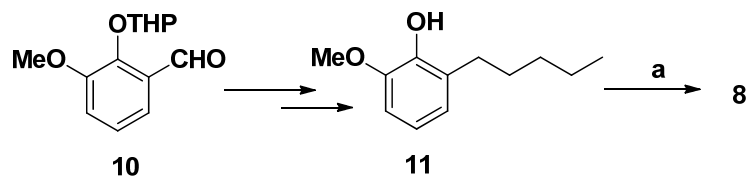
Interestingly, it has also been isolated from the broth extract of endophytic fungus, *Botryosphaeria mamane* PSU-M76<sup>23</sup> and has shown antibacterial activity against *Staphylococcus aureus* ATCC 25923 and methicillin-resistant *S. aureus* SK1 with equal MIC values of 8 µg/mL.

Primin has exhibited potential anticancer activity against M109 tumor cell lines (IC<sub>50</sub> 10 µg/mL) and A2780 cell lines (IC<sub>50</sub> 10 µg/mL).<sup>24</sup> It has also been shown potent antiprotozoal activity against *Trypanosoma brucei rhodesiense* (IC<sub>50</sub> 0.14 µM) and *Leishmania donovani* (IC<sub>50</sub> 0.71 µM).<sup>25</sup> To increase the water solubility of primin (LogP 2.99), its water soluble analog primin acid, **9** (LogP 0.96, *i.e.* about 100 times more hydrophilic) has been designed.<sup>26</sup> The allergenic effect of these *p*-benzoquinones is believed to be mediated from the Michael addition of the nucleophilic protein residues.

### 1.1.1 Previous reports

#### 1.1.1a Schildknecht's approach (1967)

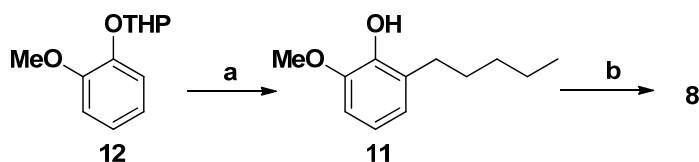
First total synthesis of **8** was reported by H. Schildknecht and co-workers in 1967.<sup>27</sup> Compound **8** was prepared in a five step sequence and in 23% overall yield, starting from *o*-vanillin (Scheme 1).



**Scheme 1.** Synthesis of Primin using Schildknecht's approach; *Reagents and conditions:* (a) Fremy's salt (potassium nitrosodisulfonate), aq. acetone, 21%.

### 1.1.1b Bieber's approach (1990)

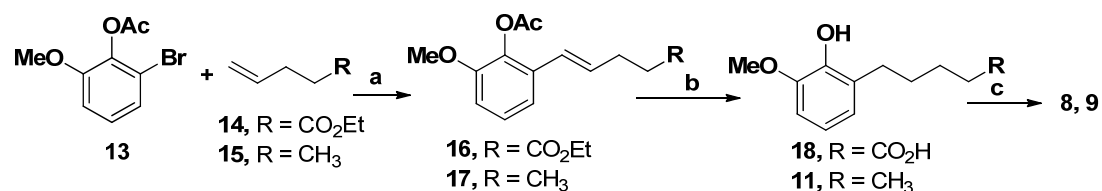
Bieber *et al.*<sup>28</sup> reported the improved synthesis of primin **8** (Scheme 2). In their synthetic protocol, they have used protected guaiacol **12** as a starting material, further treatment with *n*-butyl lithium and quenching with pentyl bromide yielded the phenolic derivative **11**. Subsequently, oxidation of phenolic derivative **11** using salcomine furnished primin **8**.



**Scheme 2.** Synthesis of Primin using Bieber's approach; *Reagents and conditions:* (a) *n*-BuLi, pentylbromide, THF, 80%; (b) *N,N'*-Bis(salicyclidene)ethylenediaminocobalt (II) (Salcomine), DMF, O<sub>2</sub>, 86%.

### 1.1.1c Mabic's approach (1999)

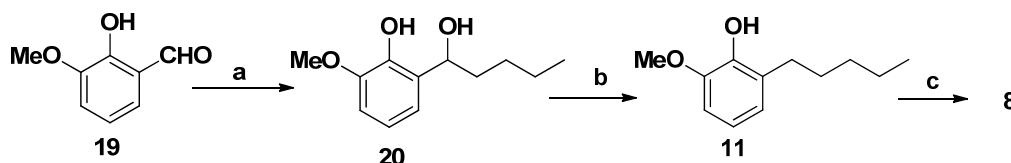
Mabic's *et al.*<sup>26</sup> started the synthesis of **8** (Scheme 3) using acetate protected bromo guaiacol **13** which was treated with alkenes **14**, **15**, respectively under Heck reaction conditions to get the olefins **16**, **17**. The double bonds of alkenes **16**, **17** were reduced and protecting group was removed to get **18** and **11**, respectively. Both phenols **17** and **11** were oxidized to quinones **8** and **9**, respectively.



**Scheme 3.** Synthesis of Primin using Mabic's approach; *Reagents and conditions:* (a) Pd(OAc)<sub>2</sub>, P(*o*-tol)<sub>3</sub>, TEA, 51%; (b) (i) H<sub>2</sub>, Pd/C, EtOAc; (ii) Ba(OH)<sub>2</sub>, H<sub>2</sub>O, THF, 94%; (c) *N,N'* Bis(salicyclidene)ethylenediaminocobalt (II) (Salcomine), DMF, O<sub>2</sub>, 70%.

### 1.1.1d Kingston's approach (2001)

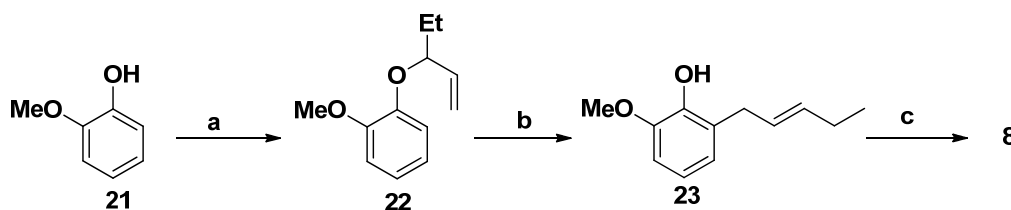
Kingston's *et al.*<sup>24</sup> started the synthesis of primin **8** (Scheme 4) using *o*-vanillin **19**, which was treated with pentyl magnesium bromide to furnish the alcohol **20**. The alcohol **20** was reduced to compound **11** and further oxidized to primin **8** using Fremy's salt.



**Scheme 4.** Synthesis of Primin using Kingston's approach; *Reagents and conditions:* (a) Pentylmagnesiumbromide, THF; (b) H<sub>2</sub>, Pd/C, 2-5 days, MeOH; (c) Fremy's salt (potassium nitrosodisulfonate), aq. acetone, 21%.

### 1.1.1e Moody's approach (2005)

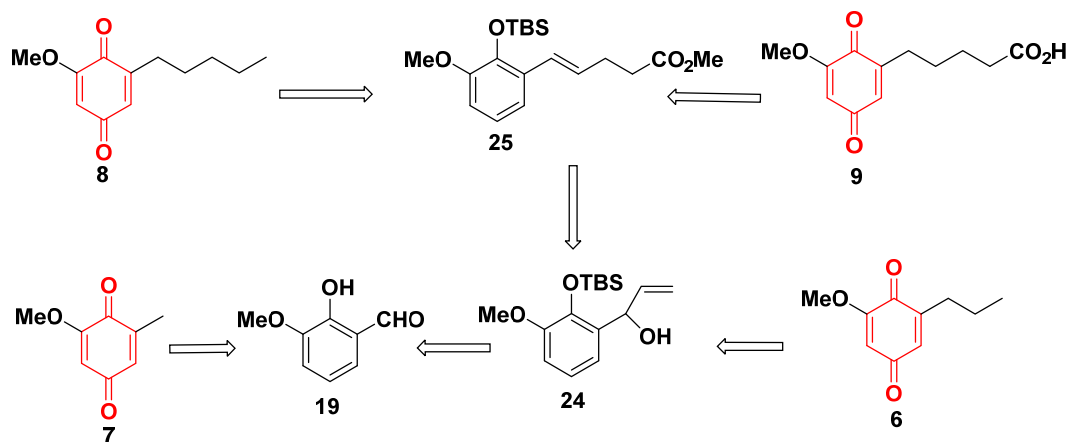
Moody's *et al.*<sup>29</sup> started the synthesis of primin **8** (Scheme 5) using 2-methoxyphenol **21** which was treated with allyl alcohol under Mitsunobu reaction conditions to isolate intermediate ether **22**. The ether **22** was subjected to Claisen rearrangement conditions to furnish the compound **23**. The double bond of compound **23** was reduced and was oxidized to primin **8**.



**Scheme 5.** Synthesis of Primin using Moody's approach; *Reagents and conditions:* (a) TPP, DIAD, allylic alcohol, toluene; (b) DMF,  $\mu$ W (300), 25-60 min; (c) H<sub>2</sub>, Pd/C, EtOAc; (d) Fremy's salt (potassium nitrosodisulfonate), aq. acetone, 43%.

## 1.2 Present work: Objective and Rationale

Our own interest in synthesizing antibacterial bio-active compounds, prompted us to have a look for an efficient synthetic strategy for 1,4-benzoquinones. Due to their diverse biological activities the synthesis of 2-methoxy-6-alkyl-1,4-benzoquinones has been planned. In continuation of our research<sup>30</sup> we were interested in the synthesis of **6**, **7** and **8** and its water-soluble analogue **9**. Flexible scheme was devised and outlined in retrosynthetic plan (Scheme 6).



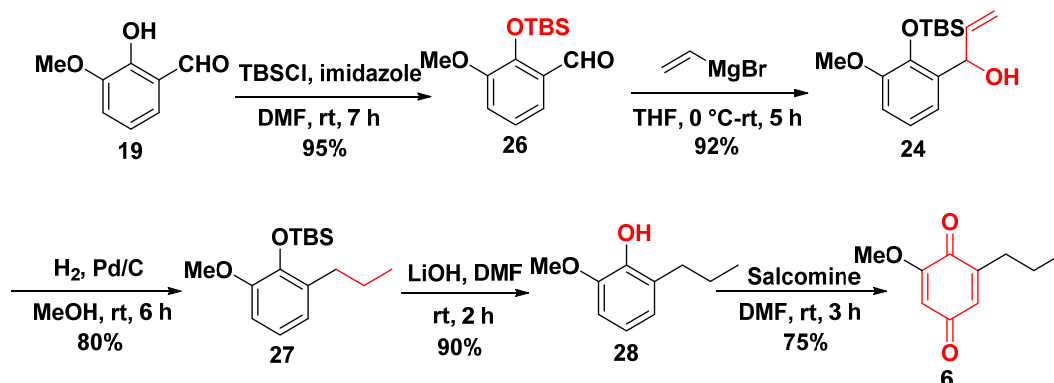
**Scheme 6.** Retrosynthetic plan for the synthesis of 2-methoxy-6-alkyl-1,4-benzo quinones, (**6**, **7**, **8** and **9**).

### 1.3 Results and Discussion

The synthetic approach for the synthesis of primin **8** and its analogs **6**, **7**, and **9** was envisioned *via* the retrosynthetic route as shown in Scheme 6. All the 1,4-substituted-benzoquinones **6**, **7**, **8** and **9** were visualized from common precursor *o*-vanillin. For the synthesis of primin **8** and primin acid **9**, compound **24** could be visualized as a common intermediate. This intermediate **25**, could be obtained from Johnson-Claisen rearrangement of the homoallylic alcohols. Synthesis of 1,4-benzoquinones **6** and **7** were also obtained from *o*-vanillin.

The commercially available material, *o*-vanillin **19** was converted to common intermediate **25**, as illustrated in Scheme 7. Thus, the phenolic group was protected<sup>31</sup> as its TBS ether, using *tert*-butyldimethylsilyl chloride in DMF. The formation of product **26** was confirmed by its spectral analysis. In <sup>1</sup>H NMR spectrum, the TBS proton signals were observed at  $\delta$  0.79 and 0.00 ppm. In <sup>13</sup>C NMR spectrum, the TBS carbon signals were observed at  $\delta$  -4.2, 18.9 and 25.8 ppm. The protected aldehyde **26** was subjected to Grignard reaction<sup>32</sup> conditions using vinylmagnesium bromide (1.0 M in THF) to furnish allylic alcohol **24** in 92% yield. The formation of product **24** was confirmed by its spectral analysis. In <sup>1</sup>H NMR spectrum, the olefinic proton multiplet signals were observed at  $\delta$  6.18-6.01 and 5.40-5.17 ppm. In <sup>13</sup>C NMR spectrum, the terminal olefinic carbon signals were observed at  $\delta$  139.3 and 114.3

ppm. The fully saturated analogue **27** was obtained by the hydrogenation of the olefin **23** at 60 psi in 80% yield.



**Scheme 7.** Synthesis of 2-methoxy-6-propyl-1,4-benzoquinone, **6**.

In the product **27**, absence of olefinic protons in the NMR spectra and appearance of new peaks in  $^1\text{H}$  NMR spectrum, signals at  $\delta$  0.95 (t,  $J = 7.3$  Hz), 1.66-1.55 (m) and 2.60 (t,  $J = 7.9$  Hz) ppm were observed. In  $^{13}\text{C}$  NMR spectrum, the new peaks were appeared at  $\delta$  14.1, 23.3 and 32.6 ppm further confirmed the formation of the saturated analogue **26**. The TBS group was deprotected<sup>32</sup> in compound **27** using LiOH/DMF to furnish the compound **28** which on oxidation with salcomine afforded the title compound, **7** in 75% yield. In  $^1\text{H}$  NMR spectrum, signals of compound **7** at  $\delta$  6.46 (dt,  $J = 2.3$  Hz, 1H) and 5.85 (d,  $J = 2.3$  Hz, 1H) and in  $^{13}\text{C}$  NMR spectrum, signals at  $\delta$  187.6 and 182.1 (C=O) and 107.1 and 133.0 (olefinic bond) ppm characteristic peaks for 1,4-benzoquinone were observed. Compound **6** was crystallized from ethanol/dichloromethane (1:9) and its single crystal X-ray analysis proved the structure (Figure 7).

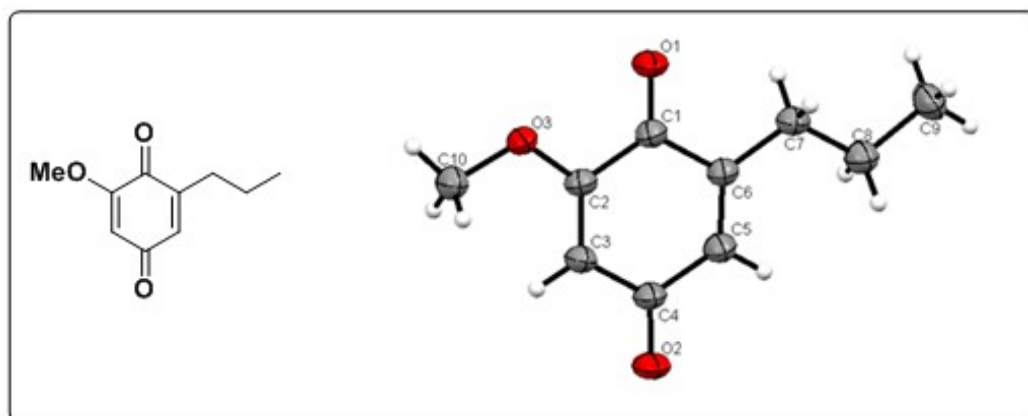
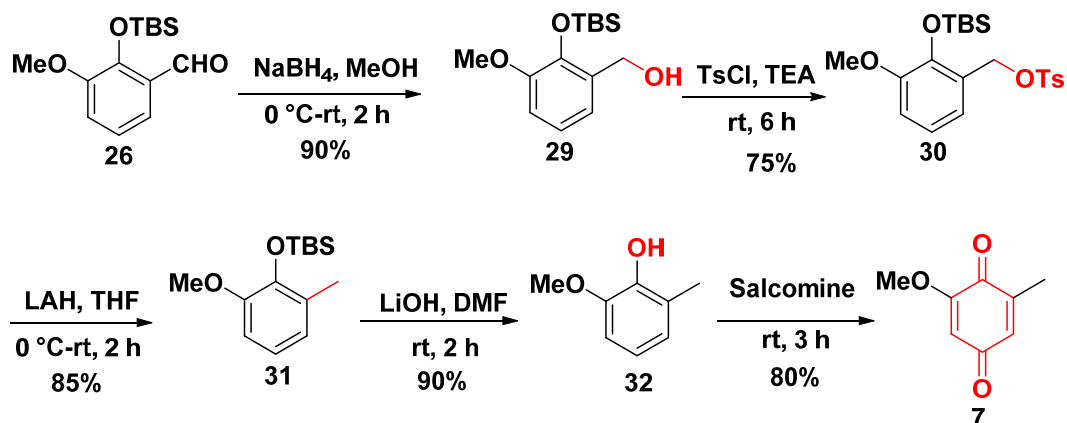


**Figure 7.** ORTEP diagram of 2-methoxy-6-propyl-1,4-benzoquinone, **6**.



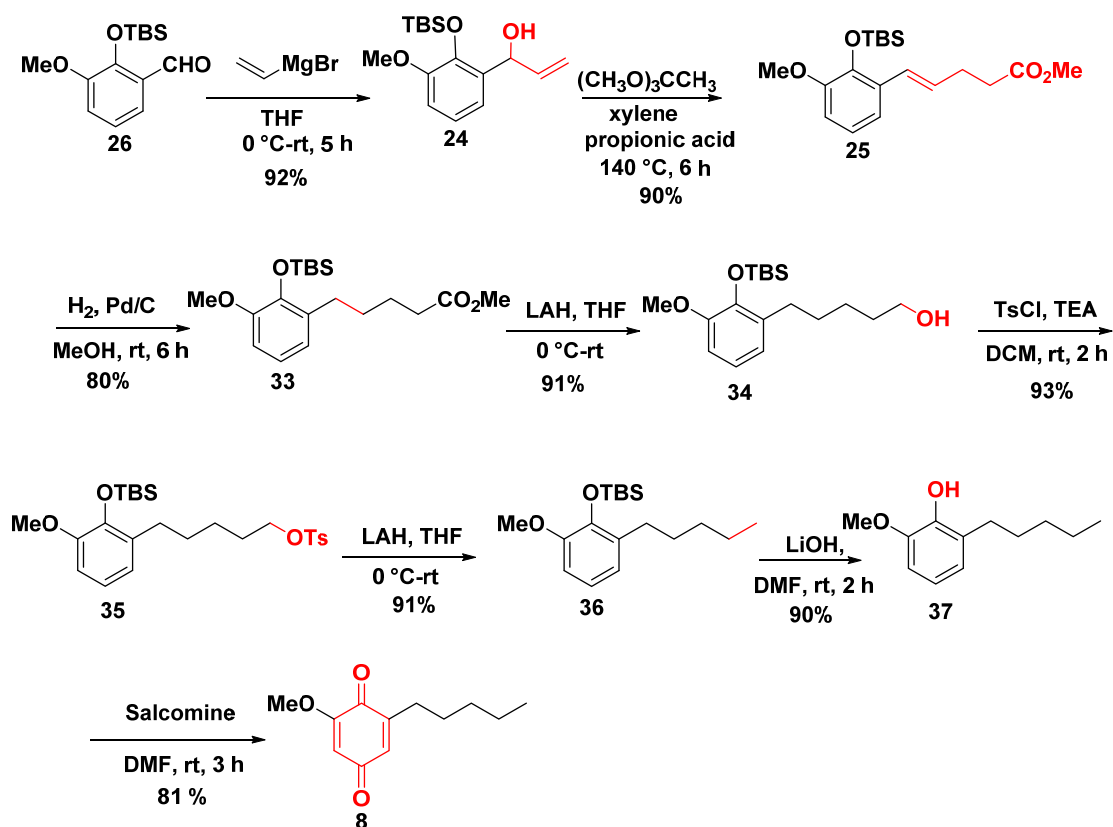
The protected aldehyde **26** was reduced to alcohol **29** in 90% yield. The formation of product **29** was confirmed by NMR analysis. In  $^1\text{H}$  NMR spectrum, signals for the methylene proton at  $\delta$  4.70 ppm and in  $^{13}\text{C}$  NMR spectrum, at  $\delta$  61.8 ppm were observed. The primary alcohol was protected as its tosyl derivative **30** in 75% yield. The formation of product **30** was confirmed by its spectral analysis. In  $^1\text{H}$  NMR spectrum, additional characteristic resonance for the tosyl group were observed as two doublets at  $\delta$  7.92 (d,  $J = 8.5$  Hz), 7.45 (d,  $J = 8.1$  Hz), while the aromatic methyl group appeared as a singlet at  $\delta$  2.48 ppm. In  $^{13}\text{C}$  NMR spectrum, signal for tosyl group (methyl group) resonates at  $\delta$  26.0 ppm. Rest of the spectral data was in full agreement with the assigned structure. The tosylate **30** after reductive removal afforded the compound **31** in 85% yield. The TBS group was deprotected<sup>33</sup> in compound **31** using LiOH/DMF to furnish the compound **32** which on oxidation with salcomine afforded 2-methoxy-6-methyl-1,4-benzoquinone, **7** in 80% yield (Scheme 8). In  $^1\text{H}$  NMR spectrum, signals of compound **7** at  $\delta$  6.51 (dt,  $J = 2.4$  Hz, 1H) and 5.85 (d,  $J = 2.4$  Hz, 1H) and  $^{13}\text{C}$  NMR spectrum, signals at  $\delta$  187.4 and 182.4 ppm (carbonyls) and 107.3 and 133.8 ppm (olefinic bond) characteristics for 1,4-benzoquinone was observed.



**Scheme 8.** Synthesis of 2-methoxy-6-methyl-1,4-benzoquinone, **7**.

The protected aldehyde **26** under Grignard reaction condition using vinylmagnesium bromide furnished allylic alcohol **24** in 92% yield. In  $^1\text{H}$  NMR spectrum, signals for the olefinic proton were observed at  $\delta$  6.18-6.01 and 5.40-5.17 ppm. In  $^{13}\text{C}$  NMR spectrum, signals for the terminal olefinic carbon were observed at

$\delta$  139.3 and 114.3 ppm. The allylic alcohol **24** was subjected to Johnson-Claisen rearrangement<sup>34</sup> using trimethyl-*o*-acetate, xylene and propionic acid in catalytic amount to furnish the product **25** in 90% yield. In <sup>1</sup>H NMR spectrum, signals for the olefinic protons at  $\delta$  6.26-6.13 ppm, aliphatic group protons at  $\delta$  2.75-2.34 ppm and aliphatic ester group protons at  $\delta$  3.75 ppm were observed (Scheme 9). Hydrogenation of the olefinic compound **25** resulted in the formation of compound **33**. The absence of olefinic protons in the NMR confirmed the formation of the product **33**. Compound **32** was reduced with lithium aluminum hydride in THF to furnish the alcohol **34** in 91% yield.



Scheme 9. Synthesis of 2-methoxy-6-pentyl-1,4-benzoquinone, Primin **8**.

This compound **34** was confirmed by absence of ester group protons and presence of methylene protons at  $\delta$  3.6 (t,  $J$  = 6.4 Hz) ppm in <sup>1</sup>H NMR and at  $\delta$  62.8 ppm in <sup>13</sup>C NMR spectra. Compound **34** was crystallized from methanol/dichloromethane (1:9) and its single crystal X-ray analysis proved the structure (Figure 8).

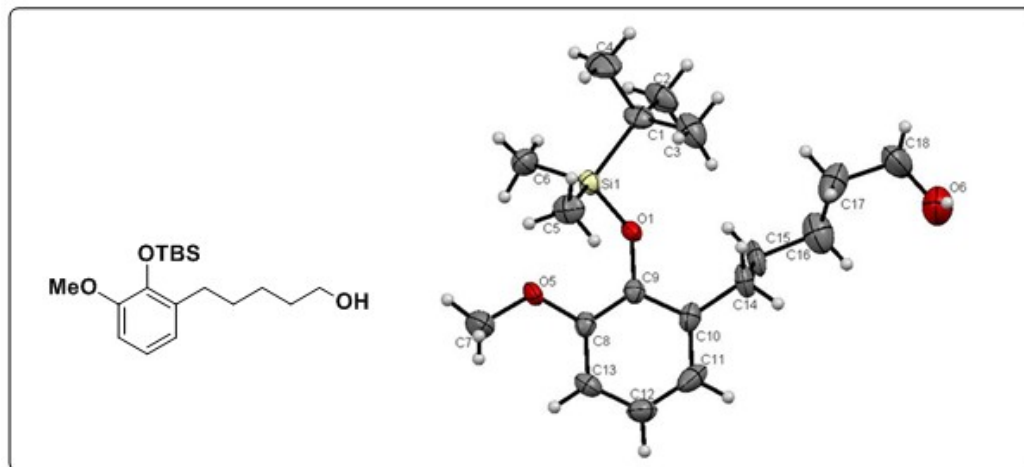
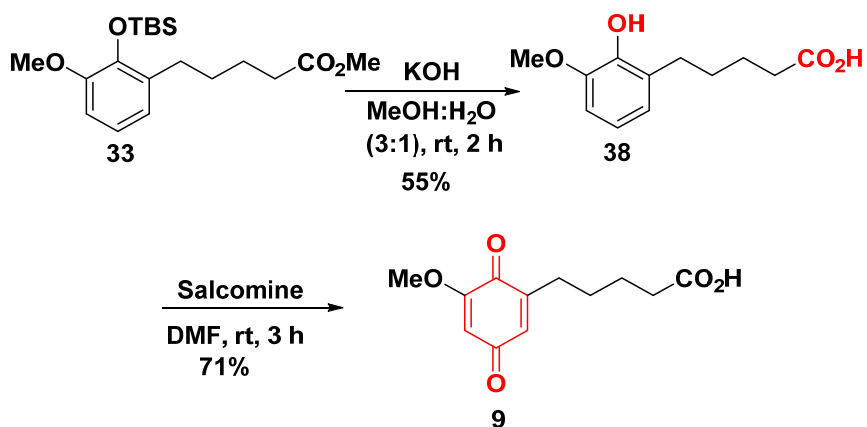


**Figure 8.** ORTEP diagram of compound **34**.

The primary alcohol was protected as its tosyl derivative **35**, 93% yield. The formation of product **35** was confirmed by spectral analysis. In  $^1\text{H}$  NMR spectrum, additional characteristic resonance for the tosyl group were observed as two doublets at  $\delta$  7.79 (d,  $J = 8.2$  Hz), 7.68 (d,  $J = 8.0$  Hz) ppm, while the aromatic methyl group appeared as a singlet at  $\delta$  2.36 ppm. In  $^{13}\text{C}$  NMR spectrum, signals for the tosyl group (methyl) resonates at  $\delta$  21.6 ppm. Compound **35** was subjected to lithium aluminum hydride reduction conditions to furnish compound **36**. In  $^1\text{H}$  NMR spectrum, absence of aromatic ring of tosyl and presence of peak at 0.88 (t,  $J = 8.0$  Hz) confirmed the formation of product **36**. The TBS group was deprotected in compound **36** using LiOH/DMF to furnish the compound **37**, which on oxidation with salcomine afforded the title compound, primin **8** in 81% yield (Scheme 8). In  $^1\text{H}$  NMR spectrum, of compound **8** signals at  $\delta$  6.49 (dt,  $J = 2.3$  Hz, 1H) and 5.88 (d,  $J = 2.3$  Hz, 1H) and  $^{13}\text{C}$  NMR spectrum, signals at  $\delta$  187.7 and 182.1 (carbonyls) and 107.1 and 132.9 (olefinic bond) characteristics for 1,4-benzoquinone were observed.

The deprotection of TBS group and methyl ester of the key intermediate **33** (Scheme 10) which under the similar oxidation conditions employed for the synthesis of primin **8** afforded the water-soluble analog, primin acid **9** in 71% yield. In  $^{13}\text{C}$  NMR spectrum, signals at  $\delta$  187.6 and 182.2 (carbonyls) and 107.2 and 133.3 (olefinic bond) characteristics for 1,4-benzoquinone were observed.

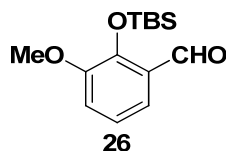


**Scheme 10.** Schematic representation of synthesis of Primin acid, **9**.

## 1.4 Conclusion

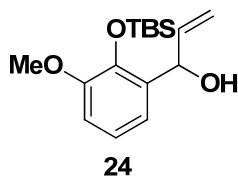
In conclusion, an efficient synthesis<sup>35</sup> of antibacterial benzoquinones, **6**, **7**, **8**, **9** has been achieved from *o*-vanillin in 47, 39, 34, and 25% overall yields, respectively. The key steps were Grignard reaction and Johnson-Claisen rearrangement.

## 1.5 Experimental

2-(*tert*-Butyldimethylsilyloxy)-3-methoxybenzaldehyde (**26**)

To a stirred solution of *o*-vanillin (5.0 g, 32.0 mmol) in anhydrous DMF (10 mL) under nitrogen atmosphere, imidazole (3.3 g, 49.0 mmol) and TBSCl (7.4 g, 49.0 mmol) were added. The reaction was stirred at room temperature for 7 h, water was added and was extracted with EtOAc (3 × 50 mL). The combined organic layer was washed with brine (10 mL), dried over anhydrous Na<sub>2</sub>SO<sub>4</sub> and concentrated under reduced pressure. The crude residue was purified by silica gel column chromatography (PE/EA, 8:2) to afford product **26** (8.3 g).

<b>Yield</b>	8.3 g, 95%; colorless oil; $R_f$ = 0.66 (PE/EA, 7:3).
<b>Mol. Formula</b>	C <sub>14</sub> H <sub>22</sub> O <sub>3</sub> Si
<b>IR</b> (CHCl <sub>3</sub> )	$\nu_{\max}$ (cm <sup>-1</sup> ) = 3034, 2957, 1584, 1481, 1216, 1071.
<b><sup>1</sup>H NMR</b> (CDCl <sub>3</sub> , 200 MHz)	$\delta_H$ (ppm) = 10.30 (s, 1H, CHO), 7.16 (dd, $J$ = 7.7, 7.7 Hz, 1H, CH), 6.85-6.70 (m, 2H, CH), 3.61 (s, 3H, OCH <sub>3</sub> ), 0.79 (s, 9H, CH <sub>3</sub> ), 0.00 (s, 6H, SiCH <sub>3</sub> ).
<b><sup>13</sup>C NMR</b> (CDCl <sub>3</sub> , 50 MHz)	$\delta_C$ (ppm) = 190.3 (CHO), 150.8 (C), 149.2(C), 127.9 (C), 121.2 (CH), 119.1 (CH), 116.9 (CH), 55.1 (OCH <sub>3</sub> ), 25.9 (CH <sub>3</sub> ), 19.0 (C), -4.1(SiCH <sub>3</sub> ).
<b>Elemental analysis</b>	Calcd for C <sub>14</sub> H <sub>22</sub> O <sub>3</sub> Si: C, 63.12; H, 8.32 Found: C, 63.20; H, 8.40.

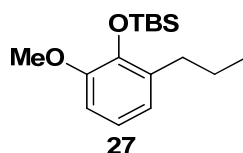
1-[2-(*tert*-Butyldimethylsilyloxy)-3-methoxyphenyl] prop-2-en-1-ol (**24**)

To a 0-5 °C cooled solution of compound **26** (3.9 g, 15.0 mmol) in anhydrous THF (10 mL) vinyl magnesium bromide (15 mL, 15.0 mmol, 1.0 M in THF) was slowly

added. After stirring for 5 h, reaction mixture was quenched with aqueous  $\text{NH}_4\text{Cl}$  solution (2 mL) and extracted with EtOAc ( $3 \times 50$  mL). The combined organic layer was washed with brine (10 mL), dried over anhydrous  $\text{Na}_2\text{SO}_4$  and evaporated under reduced pressure. The crude residue was purified by silica gel column chromatography (PE/EA, 7:3) to give allylic alcohol **24** (4.05 g).

<b>Yield</b>	4.0 g, 95%; colorless oil; $R_f = 0.52$ (PE/EA, 7:3).
<b>Mol. Formula</b>	$\text{C}_{14}\text{H}_{22}\text{O}_3\text{Si}$
<b>IR</b> ( $\text{CHCl}_3$ )	$\nu_{\text{max}} (\text{cm}^{-1}) = 3034, 2957, 1584, 1481, 1216, 1071.$
<b><math>^1\text{H}</math> NMR</b> ( $\text{CDCl}_3$ , 200 MHz)	$\delta_{\text{H}} (\text{ppm}) = 6.94\text{-}6.77$ (m, 3H, CH), 6.18-6.01 (m, 1H, CH), 5.94-5.64 (m, 1H, CH), 5.40-5.17 (m, 2H, CH), 3.79 (s, 3H, $\text{OCH}_3$ ), 1.00 (s, 9H, $\text{CH}_3$ ), 0.21 (s, 6H, $\text{SiCH}_3$ ).
<b><math>^{13}\text{C}</math> NMR</b> ( $\text{CDCl}_3$ , 50 MHz)	$\delta_{\text{C}} (\text{ppm}) = 149.7$ (C), 139.3 (CH), 133.7 (C), 121.2 (CH), 118.9 (CH), 114.3 ( $\text{CH}_2$ ), 110.7 (CH), 68.9 (CH), 60.4 (CHOH), 54.7 ( $\text{OCH}_3$ ), 26.1 ( $\text{CH}_3$ ), 18.9 (C), -3.8 ( $\text{SiCH}_3$ ).
<b>Elemental analysis</b>	Calcd for $\text{C}_{14}\text{H}_{22}\text{O}_3\text{Si}$ : C, 63.12; H, 8.32 Found: C, 63.20; H, 8.40

***tert*-Butyl-(2-methoxy-6-propylphenoxy)-dimethylsilane (**27**)**



To a solution of compound **24** (3.1 g, 10.5 mmol) in anhydrous MeOH (10 mL), 10% Pd/C (0.1 g) was added. The resulting heterogeneous solution was stirred vigorously under  $\text{H}_2$  atm at 60 psi. After stirring for 4 h, the mixture was filtered over celite. The filtrate was evaporated and purified by silica gel column chromatography (PE/EA, 8:2) to furnish pure product **27** (2.36 g).

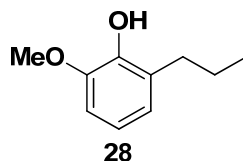
<b>Yield</b>	2.36 g, 80%; colorless oil; $R_f = 0.70$ (PE/EA, 8:2).
<b>Mol. Formula</b>	$\text{C}_{16}\text{H}_{28}\text{O}_2\text{Si}$
<b>IR</b> ( $\text{CHCl}_3$ )	$\nu_{\text{max}} (\text{cm}^{-1}) = 2957, 2931, 2858, 1583, 1481, 1279, 1251, 1228, 1086.$

**<sup>1</sup>H NMR**  
(CDCl<sub>3</sub>, 200 MHz)  $\delta_{\text{H}}$  (ppm) = 6.79-6.72 (m, 3H, CH), 3.78 (s, 3H, OCH<sub>3</sub>), 2.60 (t,  $J$  = 7.9 Hz, 3H, CH<sub>2</sub>), 1.66- 1.55 (m, 2H, CH<sub>2</sub>), 1.01 (s, 9H, CH<sub>3</sub>), 0.95 (t,  $J$  = 7.3 Hz, 3H, CH<sub>3</sub>), 0.19 (s, 6H, SiCH<sub>3</sub>).

**<sup>13</sup>C NMR**  
(CDCl<sub>3</sub>, 50 MHz)  $\delta_{\text{C}}$  (ppm) = 149.8 (C), 142.7 (C), 134.0 (C), 122.0 (CH), 120.4 (CH), 108.9 (CH), 54.7 (OCH<sub>3</sub>), 32.6 (CH<sub>2</sub>), 26.1 (CH<sub>3</sub>), 23.3 (CH<sub>2</sub>), 19.0 (C), 14.1 (CH<sub>3</sub>), -3.8 (SiCH<sub>3</sub>).

**Elemental analysis**  
Calcd for C<sub>16</sub>H<sub>28</sub>O<sub>2</sub>Si: C, 68.52; H, 10.06  
Found: C, 72.38; H, 10.09.

### 2-Methoxy-6-propylphenol (**28**)



To a 0-5 °C cooled solution of compound **27** (0.78 g, 2.74 mmol) in anhydrous DMF (2 mL), LiOH (197 mg, 9.6 mmol) was added. The reaction mixture was stirred at room temperature for 4 h under an argon atmosphere. After completion of reaction, it was extracted with EtOAc (3 × 50 mL). The combined organic layer was washed with brine (10 mL), dried over anhydrous Na<sub>2</sub>SO<sub>4</sub> and evaporated under reduced pressure. The crude residue was purified by silica gel column chromatography (PE/EA, 8:2) to furnish phenol **28** (0.41 g).

**Yield** 0.41 g, 90%; colorless viscous oil;  $R_f$  = 0.48 (PE/EA, 8:2).

**Mol. Formula** C<sub>10</sub>H<sub>14</sub>O<sub>2</sub>

**IR** (CHCl<sub>3</sub>)  $\nu_{\text{max}}$  (cm<sup>-1</sup>) = 3544, 2960, 2870, 1618, 1591, 1478, 1442, 1358, 1268, 1220, 1185, 1080.

**<sup>1</sup>H NMR**  
(CDCl<sub>3</sub>, 200 MHz)  $\delta_{\text{H}}$  (ppm) = 6.78-6.71 (m, 3H, CH), 5.69 (s, 1H, OH), 3.86 (s, 3H, OCH<sub>3</sub>), 2.61 (t,  $J$  = 7.5 Hz, 3H, CH<sub>2</sub>), 1.74- 1.59 (m, 2H, CH<sub>2</sub>), 0.96 (t,  $J$  = 7.3 Hz, 3H, CH<sub>3</sub>).

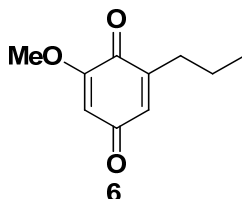
**<sup>13</sup>C NMR**  $\delta_{\text{C}}$  (ppm) = 146.3 (C), 143.3 (C), 128.5 (C), 122.4

(CDCl<sub>3</sub>, 50 MHz) (CH), 119.1 (CH), 108.2 (CH), 55.9 (OCH<sub>3</sub>), 31.8 (CH<sub>2</sub>), 22.9 (CH<sub>2</sub>), 14.0 (CH<sub>3</sub>).

**Elemental analysis**

Calcd for C<sub>10</sub>H<sub>14</sub>O<sub>2</sub>: C, 72.26; H, 8.49

Found: C, 72.38; H, 8.51.

**2-Methoxy-6-propylcyclohexa-2, 5-diene-1, 4-dione (6)**

To a solution of compound **28** (0.3 g, 1.8 mmol) in anhydrous DMF (3 mL), salcomine (59.0 mg, 0.18 mmol) was added. The resulting reaction mixture was stirred vigorously for 6 h. After completion of the reaction, it was extracted with EtOAc (3 × 50 mL). The combined organic layer was washed with brine (10 mL), dried over anhydrous Na<sub>2</sub>SO<sub>4</sub> and evaporated under reduced pressure. The crude residue was purified by silica gel column chromatography (PE/EA, 7:3) to furnish **6** (0.24 g).

**Yield**

0.24 g, 75%; yellow solid; *R<sub>f</sub>* = 0.34 (PE/EA, 7:3).

**Melting point**

76-78°C

**Mol. Formula**

C<sub>10</sub>H<sub>12</sub>O<sub>3</sub>

**IR** (CHCl<sub>3</sub>)

$\nu_{\max}$  (cm<sup>-1</sup>) = 3022, 2966, 2937, 2876, 2847, 1681, 1651, 1603, 1628, 1458, 1317, 1232, 1216.

**<sup>1</sup>H NMR**

(CDCl<sub>3</sub>, 200 MHz)

$\delta_{\text{H}}$  (ppm) = 6.46 (dt, *J* = 2.3 Hz, 1H, CH), 5.85 (d, *J* = 2.3 Hz, 1H, CH), 3.79 (s, 3H, OCH<sub>3</sub>), 2.39 (t, *J* = 6.6 Hz, 3H, CH<sub>2</sub>), 1.58- 1.46 (m, 2H, CH<sub>2</sub>), 0.94 (t, *J* = 7.2 Hz, 3H, CH<sub>3</sub>).

**<sup>13</sup>C NMR**

(CDCl<sub>3</sub>, 50 MHz)

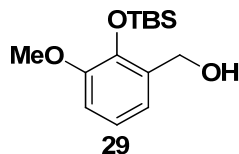
$\delta_{\text{C}}$  (ppm) = 187.6 (C), 182.1 (C), 158.8 (C), 147.2 (C), 133.0 (CH), 107.1 (CH), 56.2 (OCH<sub>3</sub>), 30.6 (CH<sub>2</sub>), 21.0 (CH<sub>2</sub>), 13.7 (CH<sub>3</sub>).

**Elemental analysis**

Calcd for C<sub>10</sub>H<sub>12</sub>O<sub>3</sub>: C, 66.65; H, 6.71

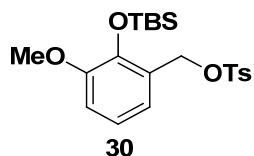
Found: C, 66.72; H, 6.79.



**2-((*tert*-Butyldimethylsilyl)oxy)-3-methoxyphenyl)methanol (29)**

To a cooled solution of compound **26** (2.0 g, 7.49 mmol in anhydrous MeOH (10 mL), sodium borohydride (277 mg, 7.49 mmol) was added. The solution was stirred at room temperature for 2 h under a N<sub>2</sub> atmosphere. After completion of the reaction, methanol was evaporated and was extracted with EtOAc (3 × 50 mL). The combined organic layer was washed with brine (10 mL), dried over anhydrous Na<sub>2</sub>SO<sub>4</sub> and evaporated under reduced pressure. The crude residue was purified by silica gel column chromatography (PE/Ea, 7:3) to give product **29** (1.81 g).

<b>Yield</b>	1.81 g, 90%; colorless viscous oil; $R_f = 0.62$ (PE/Ea, 8:2).
<b>Mol. Formula</b>	C <sub>14</sub> H <sub>24</sub> O <sub>3</sub> Si
<b>IR</b> (CHCl <sub>3</sub> )	$\nu_{\max}$ (cm <sup>-1</sup> ) = 3398, 2929, 1585, 1483, 1277, 1083, 1042.
<b><sup>1</sup>H NMR</b> (CDCl <sub>3</sub> , 200 MHz)	$\delta_H$ (ppm) = 6.92-6.78 (m, 3H, CH), 4.70 (s, 2H, CH <sub>2</sub> ), 3.79 (s, 3H, OCH <sub>3</sub> ), 1.01 (s, 9H, CH <sub>3</sub> ), 0.20 (s, 6H, SiCH <sub>3</sub> ).
<b><sup>13</sup>C NMR</b> (CDCl <sub>3</sub> , 50 MHz)	$\delta_C$ (ppm) = 149.7 (C), 142.6 (C), 132.2 (C), 121.2 (CH), 120.5 (CH), 111.0 (CH), 61.8 (CH <sub>2</sub> OH), 54.8 (OCH <sub>3</sub> ), 26.0 (CH <sub>3</sub> ), 18.8 (C), -4.0 (SiCH <sub>3</sub> ).
<b>Elemental analysis</b>	Calcd for C <sub>14</sub> H <sub>24</sub> O <sub>3</sub> Si: C, 62.64; H, 9.01 Found: C, 62.72; H, 9.09

**2-((*tert*-Butyldimethylsilyl)oxy)-3-methoxybenzyl 4-methylbenzenesulfonate (30)**

To a solution of compound **29** (1.76 g, 6.56 mmol) in anhydrous CH<sub>2</sub>Cl<sub>2</sub> (10 mL), Et<sub>3</sub>N (912  $\mu$ L), TsCl (1.24 g, 6.56 mmol) and DMAP (*cat.*) was added. The resulting

mixture was stirred at room temperature for 2 h. After completion of the reaction (TLC), it was extracted with  $\text{CH}_2\text{Cl}_2$  ( $3 \times 50$  mL). The combined organic layer was washed with brine (10 mL), dried over anhydrous  $\text{Na}_2\text{SO}_4$  and solvent was evaporated under reduced pressure. The crude residue was purified by silica gel column chromatography (PE/EA, 9:1) to furnish product **30** (2.07 g).

**Yield** 2.07 g, 75%; colorless viscous oil;  $R_f = 0.70$  (PE/EA, 9:1).

**Mol. Formula**  $\text{C}_{21}\text{H}_{30}\text{O}_5\text{SSi}$

**IR** ( $\text{CHCl}_3$ )  $\nu_{\text{max}}$  ( $\text{cm}^{-1}$ ) = 3019, 2957, 2931, 2858, 1586, 1595, 1484, 1378, 1288, 1254, 1216, 1174, 1082.

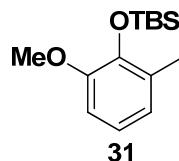
**$^1\text{H}$  NMR** ( $\text{CDCl}_3$ , 200 MHz)  $\delta_{\text{H}}$  (ppm) = 7.92 (d,  $J = 8.5$  Hz, 2H, CH), 7.45 (d,  $J = 8.1$  Hz, 2H, CH), 7.00-6.79 (m, 3H, CH), 4.66 (s, 2H,  $\text{CH}_2$ ), 3.79 (s, 3H,  $\text{OCH}_3$ ), 2.48 (s, 3H,  $\text{CH}_3$ ), 1.03 (s, 9H,  $\text{CH}_3$ ), 0.22 (s, 6H,  $\text{SiCH}_3$ ).

**$^{13}\text{C}$  NMR** ( $\text{CDCl}_3$ , 50 MHz)  $\delta_{\text{C}}$  (ppm) = 149.8 (C), 146.8 (C), 143.1 (C), 141.7 (C), 130.2 (CH), 128.7 (C), 127.0 (CH), 122.3 (C), 121.0 (CH), 111.6 (CH), 54.8 ( $\text{OCH}_3$ ), 41.7 ( $\text{CH}_2\text{OH}$ ), 26.0 ( $\text{CH}_3$ ), 21.8 (C), 18.9 (C), -3.9 ( $\text{SiCH}_3$ ).

**Elemental analysis** Calcd for  $\text{C}_{21}\text{H}_{30}\text{O}_5\text{SSi}$ : C, 59.68; H, 7.16

Found: C, 59.73; H, 7.10

***tert*-Butyl (2-methoxy-6-methylphenoxy)dimethylsilane (31)**



To a 0-5 °C cooled solution of compound **30** (2.76 g, 6.56 mmol) in anhydrous THF (10 mL) LAH (0.24 g, 6.56 mmol) was slowly added. The reaction mixture was stirred at room temperature for 4 h under an argon atmosphere. After completion of the reaction (TLC), it quenched with 1N NaOH (10 mL). The resulting white precipitate was filtered through Celite and the filtrate was dried over anhydrous

## Chapter 1

Na<sub>2</sub>SO<sub>4</sub> and solvent was evaporated to give crude residue which was purified by silica gel column chromatography (PE/EA, 7:3) to furnish product **31** (1.56 g).

**Yield** 1.56 g, 87%; colorless viscous oil;  $R_f = 0.61$  (PE/EA, 9:1).

**Mol. Formula** C<sub>14</sub>H<sub>24</sub>O<sub>2</sub>Si

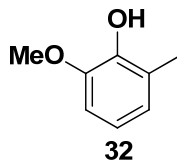
**IR** (CHCl<sub>3</sub>)  $\nu_{\max}$  (cm<sup>-1</sup>) = 3018, 2958, 2931, 2858, 1585, 1487, 1438, 1314, 1279, 1252, 1217, 1085.

**<sup>1</sup>H NMR** (CDCl<sub>3</sub>, 200 MHz)  $\delta_H$  (ppm) = 6.65-6.52 (m, 3H, CH), 3.62 (s, 3H, OCH<sub>3</sub>), 2.09 (s, 3H, CH<sub>3</sub>), 0.86 (s, 9H, CH<sub>3</sub>), 0.02 (s, 6H, SiCH<sub>3</sub>).

**<sup>13</sup>C NMR** (CDCl<sub>3</sub>, 50 MHz)  $\delta_C$  (ppm) = 149.9 (C), 143.1 (C), 129.8 (C), 129.6 (CH), 128.5 (C), 122.8 (C), 120.5 (CH), 109.1 (CH), 54.8 (OCH<sub>3</sub>), 26.1 (CH<sub>3</sub>), 18.8 (C), 17.1 (CH<sub>3</sub>), -3.9 (SiCH<sub>3</sub>).

**Elemental analysis** Calcd for C<sub>14</sub>H<sub>24</sub>O<sub>2</sub>Si: C, 66.61; H, 9.58  
Found: C, 66.71; H, 9.62.

### 2-Methoxy-6-methylphenol (**32**)



To a cooled solution of compound **31** (0.46 g, 2.0 mmol) in anhydrous DMF (2 mL), LiOH (172 mg, 6.0 mmol) was slowly added. The reaction mixture was stirred at room temperature for 4 h under an argon atmosphere. After completion of the reaction (TLC), it was extracted with EtOAc (3 × 50 mL). The combined organic layer was washed with brine (10 mL), dried over anhydrous Na<sub>2</sub>SO<sub>4</sub> and evaporated under reduced pressure. The crude residue was purified by silica gel column chromatography (PE/EA, 9:1) to furnish phenol **32** (0.225 g).

**Yield** 0.23 g, 90%; colorless viscous oil;  $R_f = 0.56$  (PE/EA, 9:1).

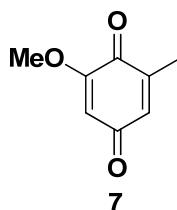
**Mol. Formula** C<sub>8</sub>H<sub>10</sub>O<sub>2</sub>

**IR** (CHCl<sub>3</sub>)  $\nu_{\max}$  (cm<sup>-1</sup>) = 3543, 3020, 2928, 1722, 1602, 1485,

1464, 1357, 1271, 1216, 1091.

**<sup>1</sup>H NMR**(CDCl<sub>3</sub>, 200 MHz) $\delta_{\text{H}}$  (ppm) = 6.73 (m, 3H, CH), 5.68 (s, 2H, OH), 3.87 (s, 3H, OCH<sub>3</sub>), 2.25 (s, 3H, CH<sub>3</sub>).**<sup>13</sup>C NMR**(CDCl<sub>3</sub>, 50 MHz) $\delta_{\text{C}}$  (ppm) = 146.2 (C), 143.7 (C), 123.9 (C), 123.1 (CH), 119.1 (CH), 108.2 (CH), 56.0 (OCH<sub>3</sub>), 15.4 (CH<sub>3</sub>).**Elemental analysis**Calcd for C<sub>8</sub>H<sub>10</sub>O<sub>2</sub>: C, 69.54; H, 7.30

Found: C, 69.50; H, 7.25.

**2-Methoxy-6-methylcyclohexa-2, 5-diene-1, 4-dione (7)**

In a flame-dried flask, phenol **32** (0.214 g, 1.55 mmol) was taken and dissolved in anhydrous DMF (3 mL) and salcomine (50 mg, 0.15 mmol) was added. The resulting reaction mixture was stirred vigorously for 6 h. After completion of the reaction (TLC), it was extracted with EtOAc (3 × 50 mL). The combined organic layer was washed with brine (10 mL), dried over anhydrous Na<sub>2</sub>SO<sub>4</sub> and solvent was evaporated under reduced pressure. The crude residue was purified by silica gel column chromatography (PE/EA, 9:1) to furnish compound **7** (0.19 g).

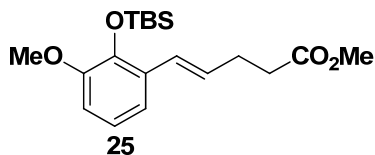
**Yield**0.19 g, 80%; yellow solid;  $R_f$  = 0.13 (PE/EA, 9:1).**Melting Point**

144-6°C

**Mol. Formula**C<sub>8</sub>H<sub>8</sub>O<sub>3</sub>**IR (CHCl<sub>3</sub>)** $\nu_{\text{max}}$  (cm<sup>-1</sup>) = 3423, 3020, 2976, 2927, 2400, 1681, 1652, 1605, 1630, 1524, 1457, 1426, 1314, 1215, 1073.**<sup>1</sup>H NMR**(CDCl<sub>3</sub>, 200 MHz) $\delta_{\text{H}}$  (ppm) = 6.52-6.51 (dt,  $J$  = 2.4 Hz, 1H, CH), 5.85 (d, 1H,  $J$  = 2.4 Hz, CH), 3.79 (s, 3H, OCH<sub>3</sub>), 2.04 (s, 3H, CH<sub>3</sub>).**<sup>13</sup>C NMR**(CDCl<sub>3</sub>, 50 MHz) $\delta_{\text{C}}$  (ppm) = 187.4 (C), 182.4 (C), 158.8 (C), 143.6 (C), 138.6 (CH), 133.8 (CH), 107.3 (CH), 56.3

(OCH<sub>3</sub>), 15.5 (CH<sub>3</sub>).**Elemental analysis**Calcd for C<sub>8</sub>H<sub>8</sub>O<sub>3</sub>: C, 63.15; H, 5.30

Found: C, 63.25; H, 5.24

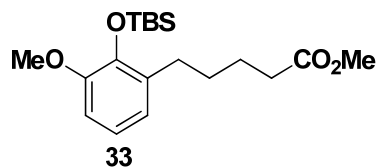
**Methyl-(4*E*)-5-[2-(*tert*-butyldimethylsilyloxy)-3-methoxyphenyl]-pent-4-enoate (25)**

To a solution of compound **24** (4.0 g, 13.6 mmol) in xylene (5 mL), trimethyl-*o*-acetate (9.79 g, 10.2 mL, 8.1 mmol), propionic acid (40 μL) was added in catalytic amount. The resulting mixture was refluxed at 140 °C for 6 h. After completion of the reaction (TLC), the xylene was evaporated under reduced pressure. The crude reaction residue was purified by silica gel column chromatography (PE/EA, 8:2) to afford pure product **25** (4.28 g).

**Yield**4.28 g, 90%; colorless oil;  $R_f$  = 0.60 (PE/EA, 7:3).**Mol. Formula**C<sub>19</sub>H<sub>30</sub>O<sub>4</sub>Si**IR** (CHCl<sub>3</sub>) $\nu_{\max}$  (cm<sup>-1</sup>) = 3021, 2955, 1738, 1480, 1252, 1086.**<sup>1</sup>H NMR**(CDCl<sub>3</sub>, 200 MHz)
 $\delta_H$  (ppm) = 7.32-6.75 (m, 3H, CH), 6.26-6.13 (m, 1H, CH), 3.82 (s, 3H, OCH<sub>3</sub>), 3.75 (s, 3H, OCH<sub>3</sub>), 2.75-2.34 (m, 4H, CH<sub>2</sub>), 1.15 (s, 9H, CH<sub>3</sub>), 0.28 (s, 6H, SiCH<sub>3</sub>).
**<sup>13</sup>C NMR**(CDCl<sub>3</sub>, 50 MHz)
 $\delta_C$  (ppm) = 173.3 (C), 150.6 (C), 142.1 (C), 129.5 (C), 128.3 (CH), 126.4 (CH), 121.0 (CH), 118.0 (CH), 110.1 (CH), 54.8 (OCH<sub>3</sub>), 51.5 (OCH<sub>3</sub>), 33.8 (CH<sub>2</sub>), 28.7 (CH<sub>3</sub>), 26.1 (CH<sub>2</sub>), 18.9 (C), -4.0 (SiCH<sub>3</sub>).
**Elemental analysis**Calcd for C<sub>19</sub>H<sub>30</sub>O<sub>4</sub>Si: C, 65.10; H, 8.63

Found: C, 65.20; H 8.72.

**Methyl 5-(2-(*tert*-butyldimethylsilyloxy)-3-methoxyphenyl)pentanoate (33)**



To a solution of compound **25** (4.5 g, 12.8 mmol) in dry MeOH (10 mL), 10% Pd/C (100 mg) was added. The heterogeneous solution was vigorously stirred for 12 h under H<sub>2</sub> atmosphere. After completion of the reaction (TLC), methanol was evaporated and filtered over celite. The solvent was evaporated and the crude product was purified by silica gel column chromatography (PE/EA, 8:2) to furnish pure product **33** (4.24 g).

**Yield** 4.24 g, 94%; colorless oil;  $R_f$  = 0.51 (PE/EA, 7:3).

**Mol. Formula** C<sub>14</sub>H<sub>22</sub>O<sub>3</sub>Si

**IR** (CHCl<sub>3</sub>)  $\nu_{\max}$  (cm<sup>-1</sup>) = 3033, 2937, 1735, 1475, 1234, 1088.

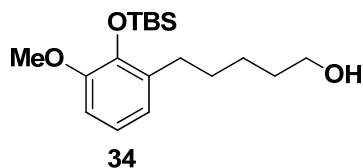
**<sup>1</sup>H NMR** (CDCl<sub>3</sub>, 200 MHz)  $\delta_H$  (ppm) = 6.83-6.72 (m, 3H, CH), 3.77 (s, 3H, OCH<sub>3</sub>), 3.77 (s, 3H, OCH<sub>3</sub>), 2.65 (t,  $J$  = 6.9 Hz, 2H, CH<sub>2</sub>), 2.65 (t,  $J$  = 6.9 Hz, 2H, CH<sub>2</sub>), 2.33-2.27 (m, 2H, CH<sub>2</sub>), 1.74-1.60 (m, 3H, CH<sub>2</sub>), 1.01 (s, 9H, CH<sub>3</sub>), 0.19 (s, 6H, SiCH<sub>3</sub>).

**<sup>13</sup>C NMR** (CDCl<sub>3</sub>, 50 MHz)  $\delta_C$  (ppm) = 174.1 (C), 149.8 (C), 142.6 (C), 133.3 (C), 121.8 (CH), 120.6 (CH), 109.0 (CH), 54.6 (OCH<sub>3</sub>), 51.4 (OCH<sub>3</sub>), 34.0 (CH<sub>2</sub>), 30.1 (CH<sub>2</sub>), 29.5 (CH<sub>2</sub>), 26.1 (CH<sub>3</sub>), 24.8 (CH<sub>2</sub>), 18.9 (C), -3.9 (SiCH<sub>3</sub>).

**Elemental analysis** Calcd for C<sub>14</sub>H<sub>22</sub>O<sub>3</sub>Si: C, 64.73; H, 9.15.

Found: C, 64.81; H, 9.22.

#### 5-[2-(*tert*-Butyldimethylsilyloxy)-3-methoxyphenyl]pentan-1-ol (**34**)



To a cooled solution of compound **33** (4.0 g, 11.0 mmol) in anhydrous THF (10 mL), LAH (0.4 g, 11.0 mmol) was slowly added. The reaction mixture stirred at room

temperature for 4 h under an argon atmosphere. After completion of the reaction (TLC), it was cooled to 0-5°C and quenched with 1N NaOH (10 mL). The resulting white precipitate was filtered through celite and the filtrate was dried over anhydrous Na<sub>2</sub>SO<sub>4</sub> and evaporated. The crude residue was purified by silica gel column chromatography (PE/EA, 7:3) to afford product **34** (3.35 g).

**Yield** 3.35 g, 91%; colorless viscous oil;  $R_f = 0.31$  (PE/EA, 7:3).

**Mol. Formula** C<sub>18</sub>H<sub>32</sub>O<sub>3</sub>Si

**IR** (CHCl<sub>3</sub>)  $\nu_{\max}$  (cm<sup>-1</sup>) = 2953, 2930, 1720, 1465, 1250, 1082.

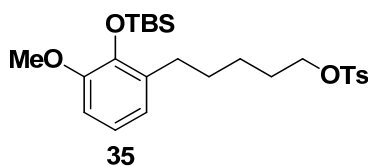
**<sup>1</sup>H NMR** (CDCl<sub>3</sub>, 200 MHz)  $\delta_H$  (ppm) = 6.87-6.68 (m, 3H, CH), 3.77 (s, 3H, OCH<sub>3</sub>), 3.61 (t,  $J = 6.4$  Hz, 2H, CH<sub>2</sub>OH), 2.64 (t,  $J = 7.3$  Hz, 2H, CH<sub>2</sub>), 1.62-1.33 (m, 6H, CH<sub>2</sub>), 1.01 (s, 9H, CH<sub>3</sub>), 0.19 (s, 6H, SiCH<sub>3</sub>).

**<sup>13</sup>C NMR** (CDCl<sub>3</sub>, 50 MHz)  $\delta_C$  (ppm) = 149.8 (C), 142.6 (C), 133.7 (C), 121.8 (CH), 120.5 (CH), 109.0 (CH), 62.8 (CH<sub>2</sub>OH), 54.6 (OCH<sub>3</sub>), 32.7 (CH<sub>2</sub>), 30.4 (CH<sub>2</sub>), 29.8 (CH<sub>2</sub>), 26.0 (CH<sub>3</sub>), 25.7 (CH<sub>2</sub>), 18.8 (C), -3.9 (SiCH<sub>3</sub>).

**Elemental analysis** Calcd for C<sub>18</sub>H<sub>32</sub>O<sub>3</sub>Si: C, 66.62; H, 9.94.

Found: C, 66.73; H, 9.88.

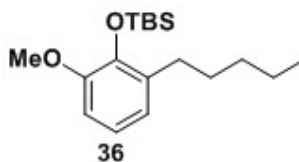
**5-[2-(*tert*-Butyldimethylsilyloxy)-3-methoxyphenyl]pentyl-4-methylbenzene sulfonate (**35**)**



To a solution of compound **34** (3.0 g, 9.2 mmol) in anhydrous CH<sub>2</sub>Cl<sub>2</sub> (10 mL), Et<sub>3</sub>N (1.0 mL), TsCl (1.74 g, 9.2 mmol) and DMAP (cat.) was added. The resulting mixture was stirred at room temperature for 2 h. After completion of the reaction (TLC), it was extracted with CH<sub>2</sub>Cl<sub>2</sub> (3 × 50 mL). The combined organic layer was washed with brine (10 mL), dried over anhydrous Na<sub>2</sub>SO<sub>4</sub> and the solvent was evaporated under reduced pressure. The crude residue was purified by silica gel column chromatography (PE/EA, 9:1) to furnish product **35** (4.11 g).

<b>Yield</b>	4.11 g, 93%; colorless viscous oil; $R_f = 0.50$ (PE/EA, 7:3).
<b>Mol. Formula</b>	$C_{25}H_{38}O_5SSi$
<b>IR</b> ( $CHCl_3$ )	$\nu_{max}$ ( $cm^{-1}$ ) = 3013, 2920, 1720, 1432, 1389, 1208, 1065.
<b><math>^1H</math> NMR</b> ( $CDCl_3$ , 200 MHz)	$\delta_H$ (ppm) = 7.79 (d, $J = 8.2$ Hz, 2H, CH), 7.68 (d, $J = 8.0$ Hz, 2H, CH), 7.30-7.21 (m, 3H, CH), 6.72-6.60 (m, 3H, CH), 3.91 (t, $J = 6.4$ Hz, 2H, $CH_2$ ), 3.66 (s, 3H, $OCH_3$ ), 2.49 (t, $J = 7.6$ Hz, 2H), 2.36 (s, 3H, $CH_3$ ), 1.56-1.24 (m, 6H, $CH_2$ ), 0.90 (s, 9H, $CH_3$ ), 0.09 (s, 6H, $SiCH_3$ ).
<b><math>^{13}C</math> NMR</b> ( $CDCl_3$ , 50 MHz)	$\delta_C$ (ppm) = 149.6 (C), 147.0 (C), 144.5 (C), 142.4 (C), 141.3 (C), 133.1 (C), 132.9 (C), 130.1 (CH), 129.6 (CH), 127.6 (CH), 126.8 (CH), 121.6 (CH), 120.5 (CH), 108.9 (CH), 70.4 ( $CH_2$ ), 54.4 ( $OCH_3$ ), 30.0 ( $CH_2$ ), 29.2 ( $CH_2$ ), 28.5 ( $CH_2$ ), 25.9 ( $CH_3$ ), 25.1 ( $CH_2$ ), 21.6 ( $CH_3$ ), 18.7 (C), -4.02 ( $SiCH_3$ ).
<b>Elemental analysis</b>	Calcd for $C_{25}H_{38}O_5SSi$ : C, 62.72; H, 8.00. Found: C, 62.67; H, 8.12.

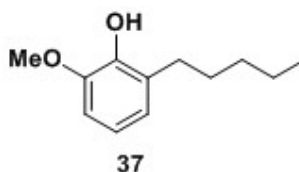
***tert*-Butyl-(2-methoxy-6-pentylphenoxy)dimethylsilane (36)**



To a cooled solution of compound **35** (4.0 g, 8.3 mmol) in anhydrous THF (10 mL), LAH (0.3 g, 8.3 mmol) was slowly added. The reaction mixture was stirred at room temperature for 4 h under an argon atmosphere. After completion of the reaction (TLC), it was quenched with 1N NaOH (10 mL). The resulting white precipitate was filtered over celite and filtrate was evaporated under reduced pressure. The crude residue was purified by silica gel column chromatography (PE/EA, 7:3) to furnish pure product **36** (2.40 g).



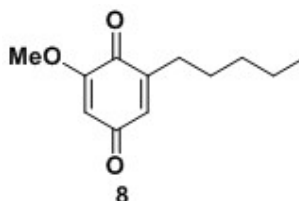
<b>Yield</b>	2.40 g, 95%; colorless viscous oil; $R_f = 0.83$ (PE/EA, 7:3).
<b>Mol. Formula</b>	$C_{18}H_{32}O_2Si$
<b>IR</b> ( $CHCl_3$ )	$\nu_{max} (cm^{-1}) = 3019, 2839, 1585, 1486, 1261, 1099.$
<b><math>^1H</math> NMR</b> ( $CDCl_3$ , 200 MHz)	$\delta_H$ (ppm) = 6.86-6.71 (m, 3H, CH), 3.76 (s, 3H, OCH <sub>3</sub> ), 2.60 (t, $J = 7.8$ Hz, 3H, CH <sub>2</sub> ), 1.61-1.55 (m, 2H, CH <sub>2</sub> ), 1.35-1.32 (m, 2H, CH <sub>2</sub> ), 1.00 (s, 9H, CH <sub>3</sub> ), 0.88 (t, $J = 6.7$ Hz, 3H, CH <sub>3</sub> ), 0.18 (s, 6H SiCH <sub>3</sub> ).
<b><math>^{13}C</math> NMR</b> ( $CDCl_3$ , 50 MHz)	$\delta_C$ (ppm) = 149.8 (C), 142.6 (C), 134.2 (C), 129.8 (CH), 121.8 (CH), 120.5 (CH), 108.9 (CH), 54.7 (OCH <sub>3</sub> ), 32.0 (CH <sub>2</sub> ), 29.9 (CH <sub>2</sub> ), 26.1 (CH <sub>3</sub> ), 22.7 (CH <sub>2</sub> ), 19.0 (C), 14.1 (CH <sub>3</sub> ), -3.9 (SiCH <sub>3</sub> ).
<b>Elemental analysis</b>	Calcd for $C_{18}H_{32}O_2Si$ : C, 70.07; H, 10.45. Found: C, 70.18; H, 10.58.

**2-Methoxy-6-pentylphenol (37)**

To a cooled solution of compound **36** (1.0 g, 3.2 mmol) in anhydrous DMF (2 mL), LiOH (220 mg, 9.6 mmol) was added and the reaction mixture was stirred at room temperature for 4 h under an argon atmosphere. After completion of the reaction (TLC), it was extracted with EtOAc (3 × 50 mL). The combined organic layer was washed with brine (10 mL), dried over anhydrous  $Na_2SO_4$  and the solvent was evaporated under reduced pressure. The crude residue was purified by silica gel column chromatography (PE/EA, 7:3) to furnish phenol **37** (0.5 g).

<b>Yield</b>	0.5 g, 80%; colorless viscous oil; $R_f = 0.45$ (PE/EA, 7:3).
<b>Mol. Formula</b>	$C_{12}H_{18}O_2$
<b>IR</b> ( $CHCl_3$ )	$\nu_{max} (cm^{-1}) = 3500, 2835, 1580, 1483, 1254, 1092.$

<b><sup>1</sup>H NMR</b> (CDCl <sub>3</sub> , 200 MHz)	$\delta_{\text{H}}$ (ppm) = 6.60-6.53 (m, 3H, CH), 5.51 (s, 1H, OH), 3.68 (s, 3H, OCH <sub>3</sub> ), 2.49-2.41 (m, 2H, CH <sub>2</sub> ), 1.44-1.40 (m, 2H, CH <sub>2</sub> ), 1.19-1.08 (m, 3H, CH <sub>2</sub> ), 0.71 (t, $J$ = 6.7 Hz, 3H, CH <sub>3</sub> ).
<b><sup>13</sup>C NMR</b> (CDCl <sub>3</sub> , 50 MHz)	$\delta_{\text{C}}$ (ppm) = 146.2 (C), 143.4 (C), 128.7 (C), 122.4 (CH), 122.3 (CH), 119.1 (CH), 108.9 (CH), 56.0 (OCH <sub>3</sub> ), 31.8 (CH <sub>2</sub> ), 29.6 (CH <sub>2</sub> ), 29.5 (CH <sub>2</sub> ), 26.1 (CH <sub>2</sub> ), 22.6 (CH <sub>2</sub> ), 14.0 (CH <sub>3</sub> ).
<b>Elemental analysis</b>	Calcd for C <sub>12</sub> H <sub>18</sub> O <sub>2</sub> : C, 74.19; H, 9.34. Found: C, 74.23; H, 9.33.

**2-Methoxy-6-pentylcyclohexa-2,5-diene-1,4-dione (Primin) (8)**

To a solution of phenol **37** (0.388 g, 2 mmol) in anhydrous DMF (3 mL), salcomine (64.4 mg, 0.2 mmol) was added. The resulting reaction mixture was stirred vigorously for 6 h. After completion of the reaction (TLC), it was extracted with EtOAc (3 × 50 mL). The combined organic layer was washed with brine (10 mL), dried over anhydrous Na<sub>2</sub>SO<sub>4</sub> and evaporated under reduced pressure. The crude residue was purified by silica gel column chromatography (PE/EA, 6:4) to afford title compound primin **8** (0.33 g).

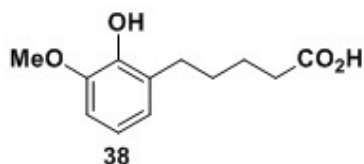
<b>Yield</b>	0.33 g, 81%; yellow solid; $R_f$ = 0.30 (PE/EA, 7:3).
<b>Melting point</b>	62-64°C
<b>Mol. Formula</b>	C <sub>12</sub> H <sub>16</sub> O
<b>IR</b> (CHCl <sub>3</sub> )	$\nu_{\text{max}}$ (cm <sup>-1</sup> ) = 3034, 2912, 1685, 1604, 1432, 1250.
<b><sup>1</sup>H NMR</b> (CDCl <sub>3</sub> , 200 MHz)	$\delta_{\text{H}}$ (ppm) = 6.49 (dt, $J$ = 2.4 Hz, 2H, CH), 5.88 (d, $J$ = 2.3 Hz, 2H, CH), 3.82 (s, 3H, OCH <sub>3</sub> ), 2.47-2.39 (m, 2H, CH <sub>2</sub> ), 1.61-1.29 (m, 6H, CH <sub>2</sub> ), 0.93-0.86 (m, 3H, CH <sub>3</sub> ).
<b><sup>13</sup>C NMR</b>	$\delta_{\text{C}}$ (ppm) = 187.7 (C), 182.1 (C), 158.8 (C), 147.5

(CDCl<sub>3</sub>, 50 MHz) (C), 132.9 (CH), 132.8 (CH), 107.1 (CH), 56.2 (OCH<sub>3</sub>), 31.3 (CH<sub>2</sub>), 28.6 (CH<sub>2</sub>), 27.3 (CH<sub>2</sub>), 22.3 (CH<sub>2</sub>), 13.7 (CH<sub>3</sub>).

**Elemental analysis**

Calcd for C<sub>12</sub>H<sub>16</sub>O: C, 69.21; H, 7.74.

Found: C, 69.26; H, 7.73.

**5-(2-Hydroxy-3-methoxyphenyl) pentanoic acid (38)**

To a solution of ester **37** (0.704 g, 2 mmol) in MeOH (2 mL), 5% KOH in MeOH-H<sub>2</sub>O (12 mL, 3:1) was added and the resulting reaction mixture was heated under reflux for 3 h. The reaction mixture was acidified with 1N HCl (10 mL) and then extracted with EtOAc (3 × 20 mL). The combined organic layer was washed with brine (10 mL), dried over anhydrous Na<sub>2</sub>SO<sub>4</sub> and evaporated under reduced pressure. The crude residue was purified by silica gel column chromatography (PE/EA, 6:4) to furnish acid **38** (0.25 g).

**Yield**

0.25 g, 55%; white solid; *R<sub>f</sub>* = 0.20 (PE/EA, 7:3).

**Mol. Formula**

C<sub>12</sub>H<sub>16</sub>O<sub>4</sub>

**IR (CHCl<sub>3</sub>)**

$\nu_{\max}$  (cm<sup>-1</sup>) = 3400, 2923, 1725, 1338, 1250.

**<sup>1</sup>H NMR**

(CDCl<sub>3</sub>, 200 MHz)

$\delta_{\text{H}}$  (ppm) = 6.47-6.72 (m, 3H, CH), 4.74 (s, 1H, OH), 3.87 (s, 3H, OCH<sub>3</sub>), 2.65 (t, *J* = 7.0 Hz, 2H, CH<sub>2</sub>), 2.38 (t, *J* = 7.0 Hz, 2H, CH<sub>2</sub>), 1.68-1.65 (m, 4H, CH<sub>2</sub>).

**<sup>13</sup>C NMR**

(CDCl<sub>3</sub>, 50 MHz)

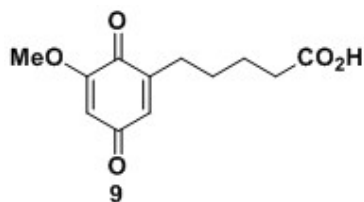
$\delta_{\text{C}}$  (ppm) = 179.2 (C), 146.3 (C), 143.4 (C), 127.8 (C), 122.3 (CH), 119.2 (CH), 108.3 (CH), 55.9 (OCH<sub>3</sub>), 33.8 (CH<sub>2</sub>), 29.2 (CH<sub>2</sub>), 29.1 (CH<sub>2</sub>), 24.4 (CH<sub>2</sub>).

**Elemental analysis**

Calcd for C<sub>12</sub>H<sub>16</sub>O<sub>4</sub>: C, 64.27; H, 7.19.

Found: C, 64.20; H, 7.11.

**5-(5-Methoxy-3,6-dioxocyclohexa-1,4-dienyl)-pentanoic acid (Primin acid) (9)**



In a flame-dried flask, phenol **38** (0.224 g, 1 mmol) was taken and dissolved in anhydrous DMF (3 mL) and stirred for 15 min. Then salcomine (32 mg, 0.1 mmol) was added, and the reaction mixture was stirred vigorously for 7 h (TLC). After completion of the reaction (TLC), it was extracted with EtOAc (3 × 50 mL). The combined organic layer was washed with brine (10 mL), dried over anhydrous Na<sub>2</sub>SO<sub>4</sub> and evaporated under reduced pressure. The crude residue was purified by silica gel column chromatography (PE/Ea, 6:4) gave primin acid **9** (0.17 g).

<b>Yield</b>	0.17 g, 71%; yellow solid; $R_f = 0.14$ (PE/Ea, 7:3).
<b>Melting point</b>	97-98°C
<b>Mol. Formula</b>	C <sub>12</sub> H <sub>14</sub> O <sub>5</sub>
<b>IR</b> (CHCl <sub>3</sub> )	$\nu_{\max}$ (cm <sup>-1</sup> ) = 3390, 1730, 1654, 1602, 1432, 1249.
<b><sup>1</sup>H NMR</b> (CDCl <sub>3</sub> , 200 MHz)	$\delta_H$ (ppm) = 6.47 (dt, $J = 5.7$ Hz, 1H, CH), 5.85 (d, $J = 7.3$ Hz, 2H, CH), 3.77 (s, 3H, OCH <sub>3</sub> ), 3.65 (d, $J = 6.2$ Hz, 1H, CH), 2.54-2.30 (m, 2H, CH <sub>2</sub> ), 1.77-1.55 (m, 4H, CH <sub>2</sub> ).
<b><sup>13</sup>C NMR</b> (CDCl <sub>3</sub> , 50 MHz)	$\delta_C$ (ppm) = 187.6 (C), 182.2 (C), 182.0 (C), 177.5 (C), 158.9 (C), 147.0 (C), 133.3 (CH), 107.2 (CH), 56.4 (OCH <sub>3</sub> ), 30.9 (CH <sub>2</sub> ), 28.4 (CH <sub>2</sub> ), 27.0 (CH <sub>2</sub> ), 25.3 (CH <sub>2</sub> ).
<b>Elemental analysis</b>	Calcd for C <sub>12</sub> H <sub>14</sub> O <sub>5</sub> : C, 60.50; H, 5.92. Found: C, 60.47; H, 5.89.

### X-ray crystal structure determination

X-ray diffraction data for all the crystallized compounds were collected at  $T = 296$  K, on SMART APEX CCD Single Crystal X-ray diffractometer using Mo-K $\alpha$  radiation ( $\lambda = 0.7107$  Å) to a maximum  $\theta$  range of 25.00°. Crystal to detector distance was 6.05 cm, 512 × 512 pixels / frame and other conditions used are oscillation / frame (-0.3°),

maximum detector swing angle ( $-30.0^\circ$ ), beam center (260.2, 252.5) and in plane spot width (1.24). SAINT integration and SADABS correction were also applied. The structures were solved by direct methods using SHELXTL. All the data were corrected for Lorentzian, polarisation and absorption effects. SHELX-97 (ShelxTL)<sup>61</sup> was used for structure solution and full matrix least squares refinement on F<sub>2</sub>. Hydrogen atoms were included in the refinement as per the riding model. The refinements were carried out using SHELXL-97.

### 2-Methoxy-6-propylcyclohexa-2, 5-diene-1,4-dione (6)

Single crystals of the compound were found to grow best in solution mixture of ethanol and dichloromethane by slow evaporation. Colorless needle like crystal of approximate size 320 x 160 x 20 mm<sup>3</sup>, was used for data collection. Multirun data acquisition, total scans (3), total frames (17946), exposure / frame (15.0 sec),  $\theta$  range (2.15 to 29.37°) and completeness to  $\theta$  of 29.37° (98.6 %) were registered. The compound has molecular formula C<sub>10</sub> H<sub>12</sub> O<sub>3</sub> and  $M = 180.20$ . Crystals belong to Triclinic system with P-1 space group with unit cell dimensions as  $a = 10.0123(17)$ ,  $b = 10.2107(18)$ ,  $c = 11.190(3)$  Å. Other parameters like volume 931.3(3) Å<sup>3</sup>,  $Z = 4$ ,  $D_c = 1.285$  Mg/m<sup>3</sup>, absorption coefficient  $\mu$  (Mo-K $\alpha$ ) = 0.094 mm<sup>-1</sup> were also recorded. 11542 reflections measured of which 2874 are unique. The final R indices [ $I > 2\sigma(I)$ ] are  $R1 = 0.0764$ ,  $wR2 = 0.1930$ .

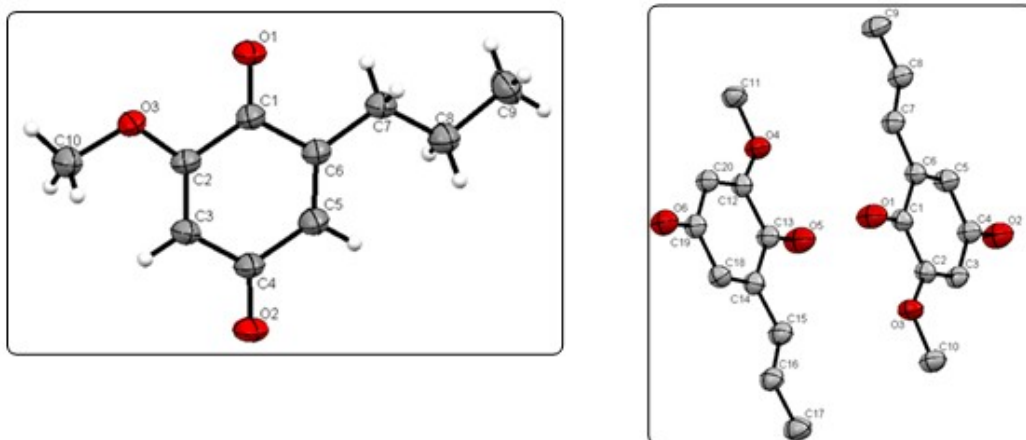


**Table 1.** Crystal data and structure refinement for compound 6.

## Chapter 1

---

Empirical formula	C <sub>10</sub> H <sub>12</sub> O <sub>3</sub>
Formula weight	180.20
Temperature	296(2) K
Wavelength	0.71073 Å
Crystal system	Triclinic
Space group	P-1
Unit cell dimensions	a = 10.0123 (17) Å      α = 98.807(4)° b = 10.2107(18) Å      β = 116.387(3)° c = 11.190(3) Å      γ = 106.241(3)°
Volume	931.3(3) Å <sup>3</sup>
Z	4
Density (Calcd)	1.285 Mg/m <sup>3</sup>
Absorption coefficient	0.094 mm <sup>-1</sup>
F(000)	384
Crystal size	320 x 160 x 20 mm <sup>3</sup>
Theta range for data collection	2.15 to 29.37°
Index ranges	-13<=h<=13, -14<=k<=13, -15<=l<=15
Reflections collected	17946
Independent reflections	5058 [R(int) = 0.0571]
Completeness to theta = 28.28°	98.6 %
Absorption correction	Semi-empirical from equivalents
Refinement method	Full-matrix least-squares on F <sup>2</sup>
Data / restraints / parameters	5058 / 0 / 239
Goodness-of-fit on F <sup>2</sup>	0.966
Final R indices [I>2sigma(I)]	R1 = 0.0764, wR2 = 0.1930
R indices (all data)	R1 = 0.1839, wR2 = 0.2587
Largest diff. peak and hole	0.650 and -0.230 e. Å <sup>-3</sup>

---

### 5-[2-(*tert*-Butyldimethylsilyloxy)-3-methoxyphenyl] pentan-1-ol (34)

Single crystals of the compound were found to grow best in solution mixture of methanol and dichloromethane by slow evaporation. Colorless needle like crystal of approximate size 568 x 223 x 68 mm<sup>3</sup>, was used for data collection. Multirun data acquisition, total scans (3), total frames (40024), exposure / frame (15.0 sec), θ range (0.58 to 28.41°) and completeness to θ of 28.41° (89.6 %) were registered. The compound has molecular formula C<sub>18</sub>H<sub>32</sub>O<sub>3</sub>Si

## Chapter 1

and  $M = 324.53$ . Crystals belong to Triclinic system with P-1 space group with unit cell dimensions as  $a = 7.846(3)$ ,  $b = 14.427(5)$ ,  $c = 35.046(12)$  Å. Other parameters like volume  $3962(2)$  Å<sup>3</sup>,  $Z = 8$ ,  $D_c = 1.088$  Mg/m<sup>3</sup>, absorption coefficient  $\mu$  (Mo-K $\alpha$ ) =  $0.128$  mm<sup>-1</sup> were also recorded. 11542 reflections measured of which 2874 are unique. The final R indices [ $I > 2\sigma(I)$ ] are  $R1 = 0.1706$ ,  $wR2 = 0.4320$ .

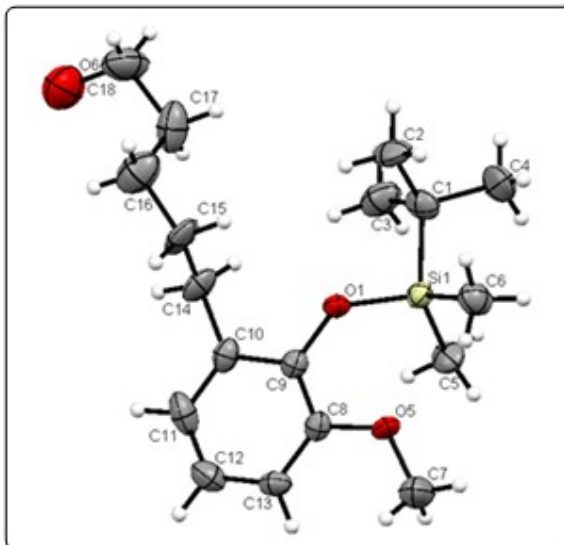


**Table 2.** Crystal data and structure refinement for compound **34**.

Empirical formula	C <sub>18</sub> H <sub>32</sub> O <sub>3</sub> Si	
Formula weight	324.53	
Temperature	296(2) K	
Wavelength	0.71073 Å	
Crystal system	Triclinic	
Space group	P-1	
Unit cell dimensions	$a = 7.846(3)$ Å	$\alpha = 90.044(6)^\circ$ .
	$b = 14.427(5)$ Å	$\beta = 93.070(7)^\circ$ .
	$c = 35.046(12)$ Å	$\gamma = 89.989(7)^\circ$ .
Volume	$3962(2)$ Å <sup>3</sup>	
Z	8	
Density (Calcd)	1.088 Mg/m <sup>3</sup>	
Absorption coefficient	$0.128$ mm <sup>-1</sup>	
F(000)	1424	
Crystal size	568 x 223 x 68 mm <sup>3</sup>	
Theta range for data collection	0.58 to 28.41°.	
Index ranges	$-10 \leq h \leq 9$ , $-19 \leq k \leq 19$ , $-46 \leq l \leq 43$	

## Chapter 1

---

---

Reflections collected	17856 [R(int) = 0.1131]
Independent reflections	5058 [R(int) = 0.0571]
Completeness to theta = 28.41°	89.6 %
Absorption correction	Semi-empirical from equivalents
Refinement method	Full-matrix least-squares on F <sup>2</sup>
Data / restraints / parameters	17856 / 0 / 821
Goodness-of-fit on F <sup>2</sup>	1.053
Final R indices [I > 2sigma(I)]	R1 = 0.1706, wR2 = 0.4320
R indices (all data)	R1 = 0.2670, wR2 = 0.4821
Largest diff. peak and hole	0.981 and -0.591 e. Å <sup>-3</sup>

---



### 1.6 References

1. Moving Beyond Natural Products” *C & E News* **2003**, *81*, 104.
2. Nicolaou, K.; Vourloumis, D.; Winssinger, N.; Baran, P. *Angew. Chem. Int. Ed.* **2000**, *39*, 44.
3. Thomson, R. H. Naturally occurring Quinones, 4<sup>th</sup> ed.; Blackie: London, UK, 1997.
4. Bock, H.; Alt, H. *Angew. Chem. Int. Ed.* **1967**, *6*, 941.
5. Foland, L. D.; Karlsson, J. O.; Perri, S. T.; Schwabe, R.; Patil, S. *J. Am. Chem. Soc.* **1989**, *11*, 976.
6. Makangara, J. J.; Nkunya, M. H. H.; Jonker, S. S. *Nat. Prod. Res.* **2010**, *24*, 710.
7. Liu, H.; Zhao, Y.; Yang, R.; Zheng, M.; Wang, M.; Zhang, X.; Qiu, F.; Wang, H.; Zhao, F. *Hel. Chim. Acta* **2010**, *93*, 249.
8. Lin, W.-H.; Fang, J.-M.; Cheng, Y.-S. *Phytochemistry* **1995**, *40*, 871.
9. Lin, W.-H.; Fang, J.-M.; Cheng, Y.-S. *Phytochemistry* **1996**, *42*, 1657.
10. Kawazoe, K.; Yamamoto, M.; Takaishi, Y.; Honda, G.; Fujita, T.; Sezik, E.; Yesilada, E. *Phytochemistry* **1999**, *50*, 493.
11. Puyvelde, V. L.; Bosselaers, J.; Stevens, C.; Kimpe, N. D.; Gestel, J. V.; Damme, P. V. *J. Agric. Food Chem.* **1999**, *47*, 2116.
12. Meazza, G.; Dayan, F. E.; Wedge, D. E. *J. Agric. Food Chem.* **2003**, *51*, 3824.
13. Lana, E. J. L.; Carazza, F.; Takahashi, J. A. *J. Agric. Food Chem.* **2006**, *54*, 2053.
14. Mozaina, K.; Cantrell, C. L.; Mims, A. B.; Lax, A. R.; Tellez, M. R.; Osbrink, W. L. *J. Agric. Food Chem.* **2008**, *56*, 4021.
15. Sood, R. S.; Roy, K.; Reddy, G. C. S.; Reden, J.; Gangdi, B. N. *J. Antibiot.* **1982**, *35*, 985.
16. Gras, J.-L. *Tetrahedron Lett.* **1977**, *18*, 4117.

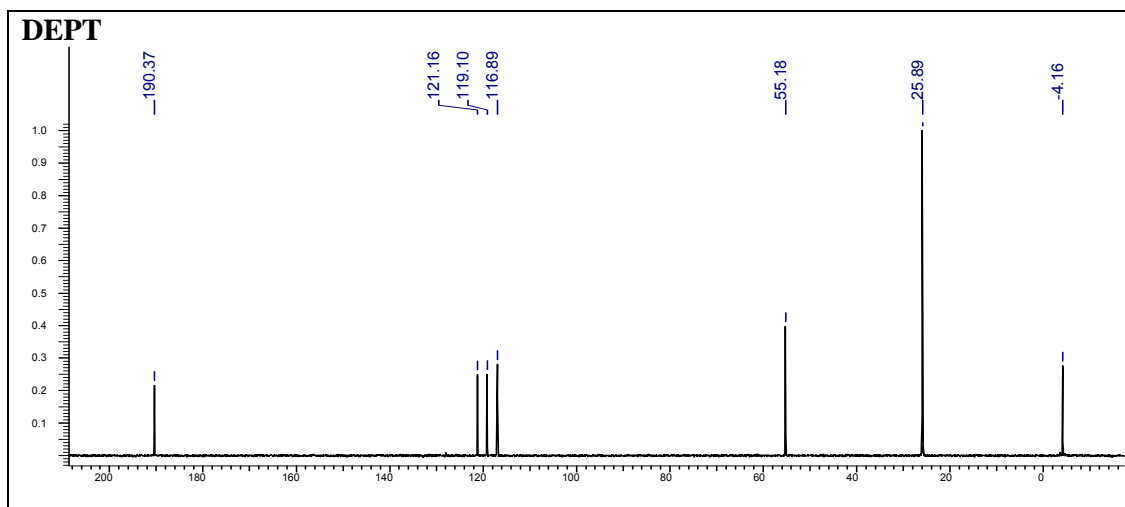
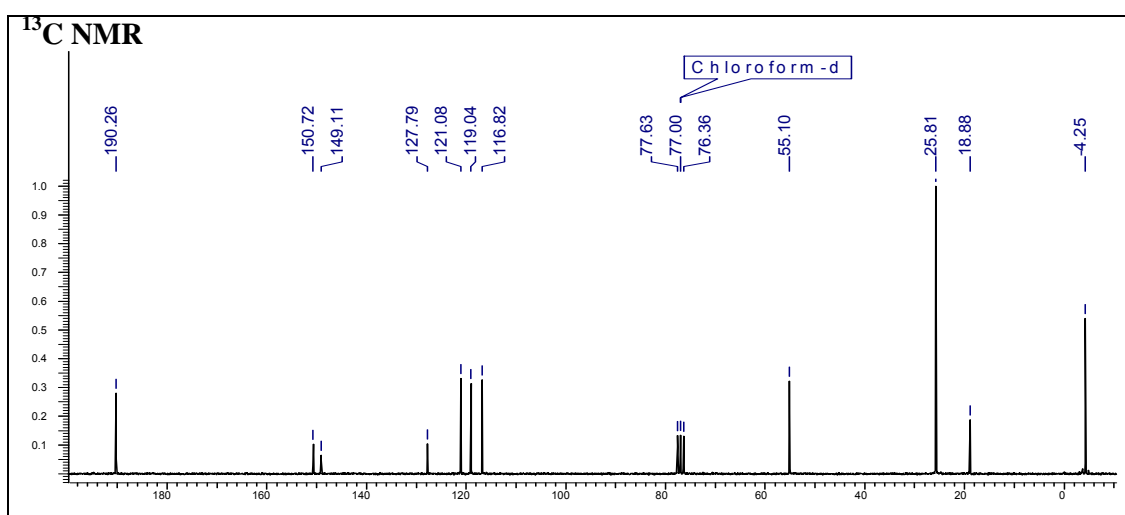
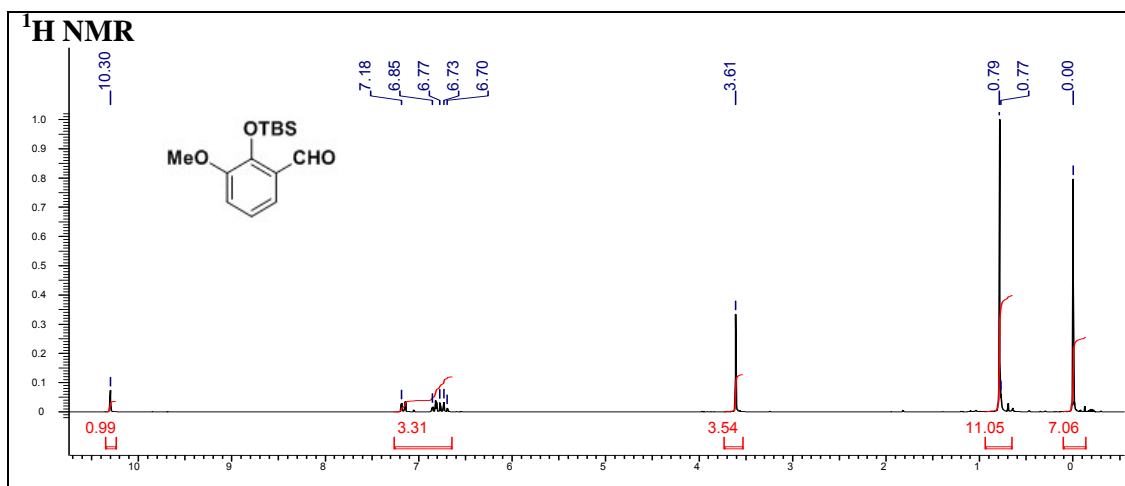
17. Claisen, C. *Ber.*, **1912**, *45*, 3157.
18. Dean, F. M.; Osman, A. M.; Robertson, A. *J. Chem. Soc.* **1955**, 11.
19. König, W. A.; Faasch, H.; Heitsch, H.; Colberg, C.; Hausen, B. M. *Z. Naturforsch. (B)* **1993**, *48*, 387.
20. (a) Schildknecht, H.; Schmidt, H. *Z. Naturforsch.* **1967**, *22b*, 287; (b) Bloch, B.; Karrer, P. *Vjschr. Naturforsch. Ges. Zürich* **1927**, *72*, 1; *Chem. Abstr.* **1928**, *22*, 2784.
21. (a) Marini-Bettolo, G. B.; Monache, F. D.; da Lima, O. G.; Coelho, S. B. *Gazz. Chim. Ital.* **1971**, *101*, 41; (b) Bernays, E.; Lupi, A.; Bettolo, R. M.; Mastrofrancesco, C.; Tagliatesta, P. *Experientia* **1984**, *40*, 1010.
22. Darwish, F. M. M.; Abdallah, O. M.; El-Emary, N. A.; Ali, A. A. *Bull. Pharm. Sci.* **1995**, *18*, 45.
23. Pongcharoen, W.; Rukachaisirikul, V.; Phongpaichit, S. *Chem. Pharm. Bull.* **2007**, *55*, 1404.
24. Gunatilaka, A. A. L.; Berger, J. M.; Evans, R.; Miller, J. S.; Wisse, J. H.; Neddermann, K. M.; Bursuker, I.; Kingston, D. G. I. *J. Nat. Prod.* **2001**, *64*, 2.
25. Tasdemir, D.; Brun, R.; Yardley, V.; Franzblau, S. G.; Rüedi, P. *Chem. Biodiversity* **2006**, *3*, 1230.
26. Mabic, S.; Vaysse, L.; Benezra, C.; Lepoittevin, J.-P. *Synthesis* **1999**, *7*, 1127.
27. Schildknecht, H.; Bayer, I.; Schmidt, H. *Z. Natureforsch., Teil B*, **1967**, *22*, 36.
28. Bieber, L. W.; Chiappeta, A. D. A.; Souza, M. A. M.; Generino, M.; Neto, P. *R. J. Nat. Prod.* **1990**, *53*, 706.
29. (a) Davis, C. J.; Hurst, T. E.; Jacob, A. M.; Moody, C. J. *J. Org. Chem.* **2005**, *70*, 4414. (b) Jacob, A. M.; Moody, C. J. *Tetrahedron Lett.* **2005**, *46*, 8823.
30. (a) Bhattacharya, A. K.; Sharma, R. P. *Heterocycles* **1999**, *51*, 1681; (b) Bhattacharya, A. K.; Jain, D. C.; Sharma, R. P.; Roy, R.; McPhail, A. T. *Tetrahedron* **1997**, *53*, 14975; (c) Bhattacharya, A. K.; Kaur, T. *Synlett* **2007**, 745; and references cited therein; (d) Bhattacharya, A. K.; Rana, K. C.; Mujahid, M.; Sehar, I.; Saxena, A. K. *Bioorg. Med. Chem. Lett.* **2009**, *19*, 5590.
31. Corey, E. J.; Venkateswarlu, A. *J. Am. Chem. Soc.* **1972**, *94*, 6190.
32. Lauchli, R.; Shea, K. *J. Org. Lett.* **2006**, *8*, 5287.
33. Ankala, S. V.; Fenteany, G. *Tetrahedron Lett.* **2002**, *43*, 4729.

- 34.** (a) Johnson, W. S.; Werthemann, L.; Bartlett, W. R.; Brocksom, T. J.; Li, T.-T.; Faulkner, D. J.; Petersen, M. R. *J. Am. Chem. Soc.* **1970**, *92*, 741; (b) Ziegler, F. E. *Chem. Rev.* **1988**, *88*, 1423; (c) Meza-Aviña, M. E.; Ordoñez, M.; Zertuche, M. F.; Fernández, M. -Z.; Fragoso, L. R.; Esparza, J. R.; Ríos-Corsino, A. A. M. *Bioorg. Med. Chem.* **2005**, *13*, 6521.
- 35.** Bhattacharya, A. K.; Kaur, T.; Ganesh, K. N. *Synthesis*, **2010**, *7*, 1141.

## 1.7 Appendix A: Characterization data of synthesized compounds

Compound	Description	Page No.
Compound 26	$^1\text{H}$ NMR, $^{13}\text{C}$ NMR, DEPT-NMR	38
Compound 24	$^1\text{H}$ NMR, $^{13}\text{C}$ NMR, DEPT-NMR	39
Compound 27	$^1\text{H}$ NMR, $^{13}\text{C}$ NMR, DEPT-NMR	40
Compound 28	$^1\text{H}$ NMR, $^{13}\text{C}$ NMR, DEPT-NMR	41
Compound 6	$^1\text{H}$ NMR, $^{13}\text{C}$ NMR, DEPT-NMR	42
Compound 29	$^1\text{H}$ NMR, $^{13}\text{C}$ NMR, DEPT-NMR	43
Compound 30	$^1\text{H}$ NMR, $^{13}\text{C}$ NMR, DEPT-NMR	44
Compound 31	$^1\text{H}$ NMR, $^{13}\text{C}$ NMR, DEPT-NMR	45
Compound 7	$^1\text{H}$ NMR, $^{13}\text{C}$ NMR, DEPT-NMR	46
Compound 33	$^1\text{H}$ NMR, $^{13}\text{C}$ NMR, DEPT-NMR	47
Compound 34	$^1\text{H}$ NMR, $^{13}\text{C}$ NMR, DEPT-NMR	48
Compound 35	$^1\text{H}$ NMR, $^{13}\text{C}$ NMR, DEPT-NMR	49
Compound 36	$^1\text{H}$ NMR, $^{13}\text{C}$ NMR, DEPT-NMR	50
Compound 8	$^1\text{H}$ NMR, $^{13}\text{C}$ NMR, DEPT-NMR	51
Compound 9	$^1\text{H}$ NMR, $^{13}\text{C}$ NMR, DEPT-NMR	52

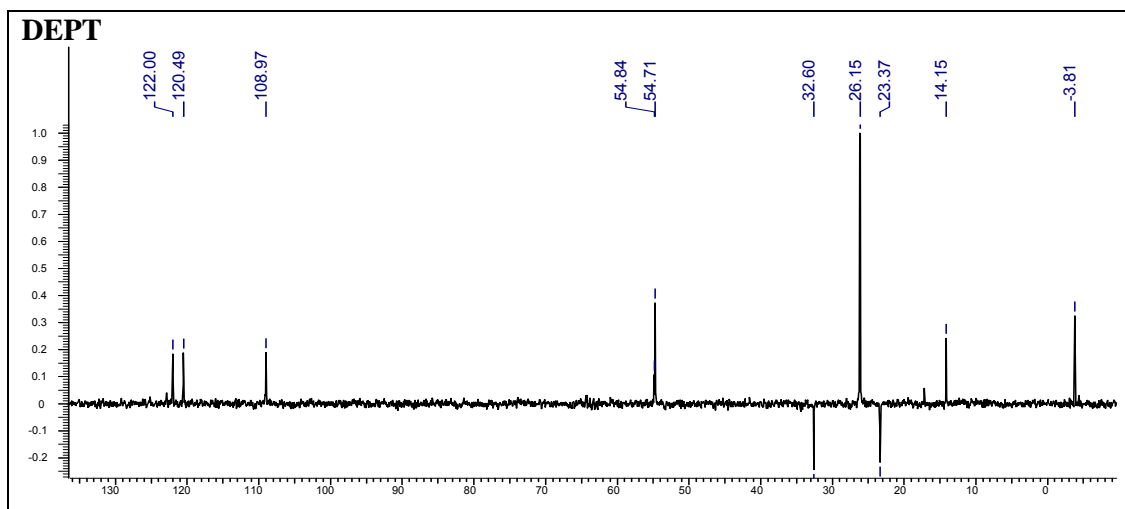
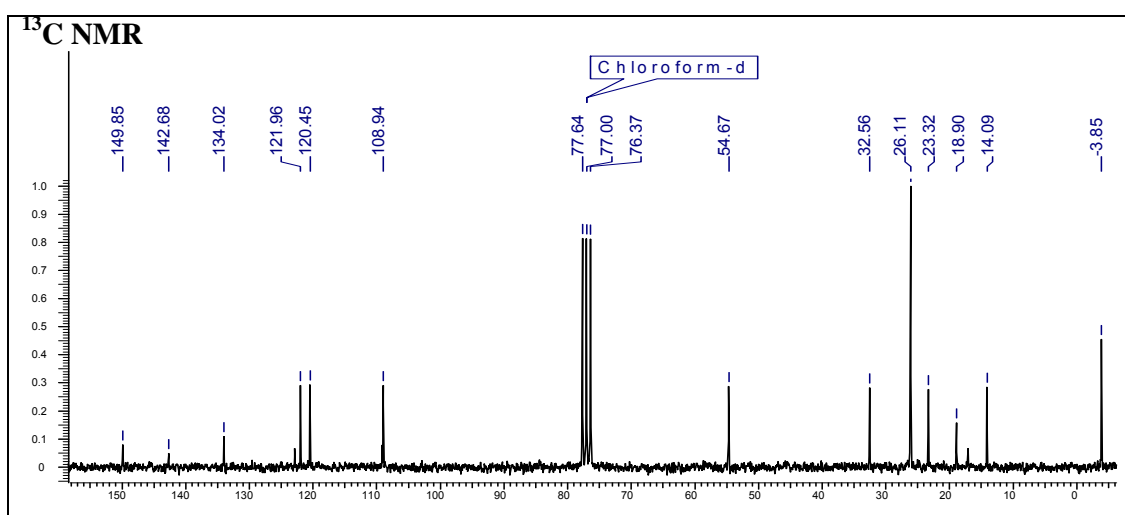
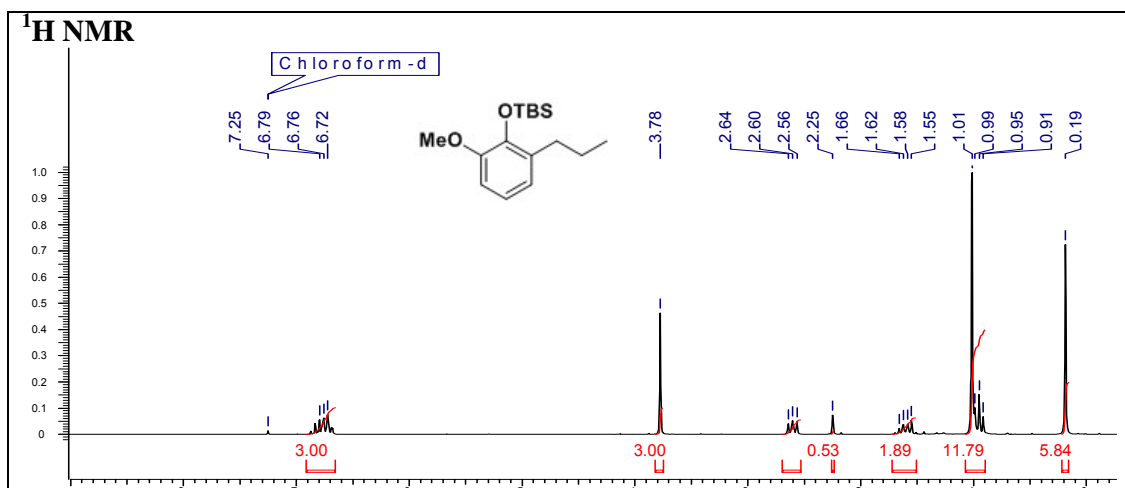
# Chapter 1



**2-(*tert*-Butyldimethylsilyloxy)-3-methoxybenzaldehyde (26)**

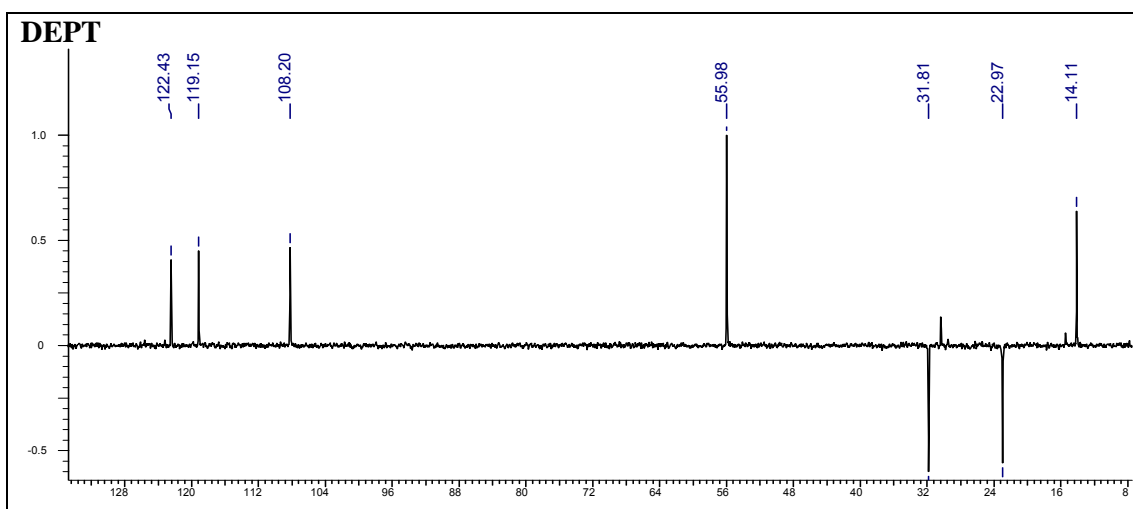
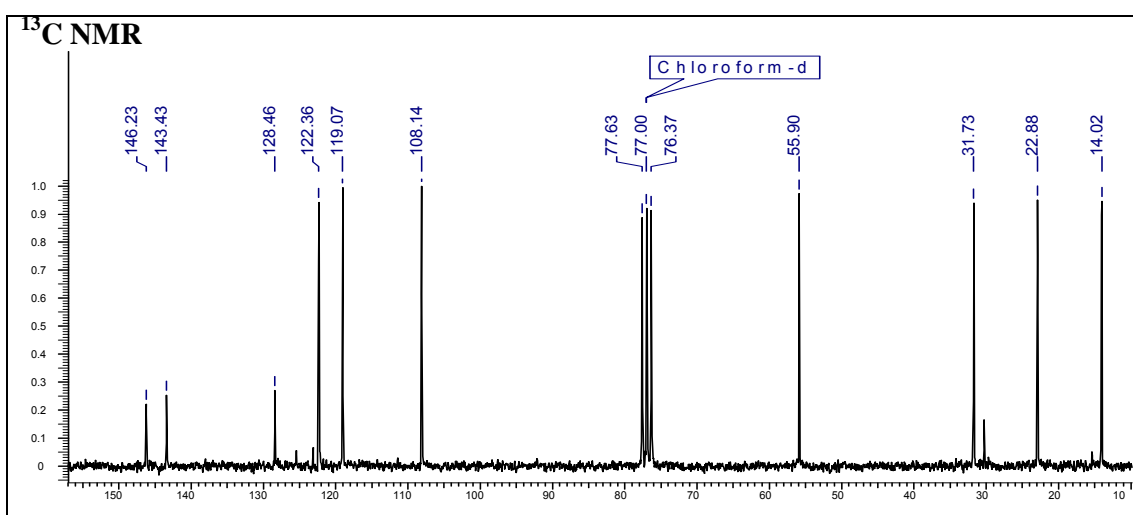
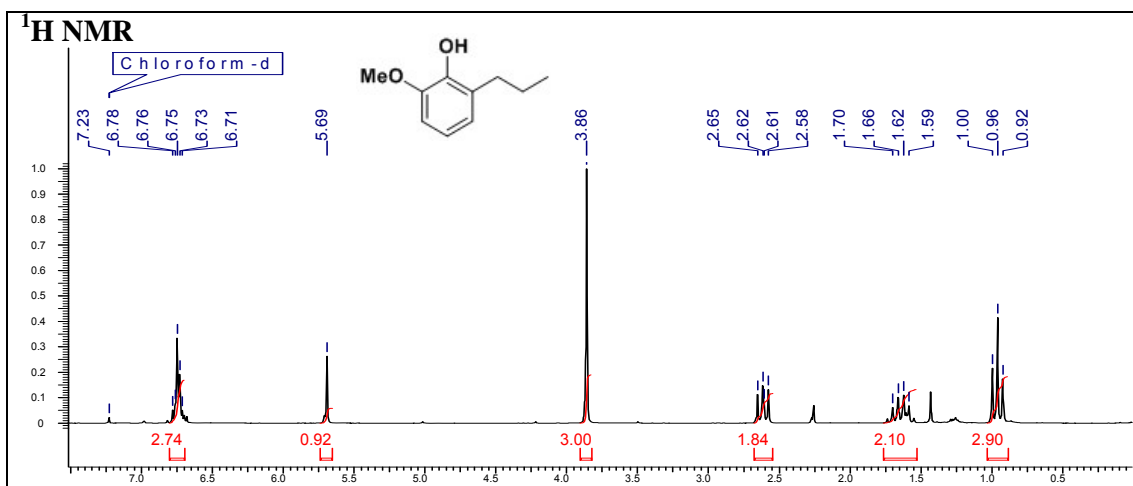


# Chapter 1



***tert*-Butyl-(2-methoxy-6-propylphenoxy)-dimethylsilane (27)**

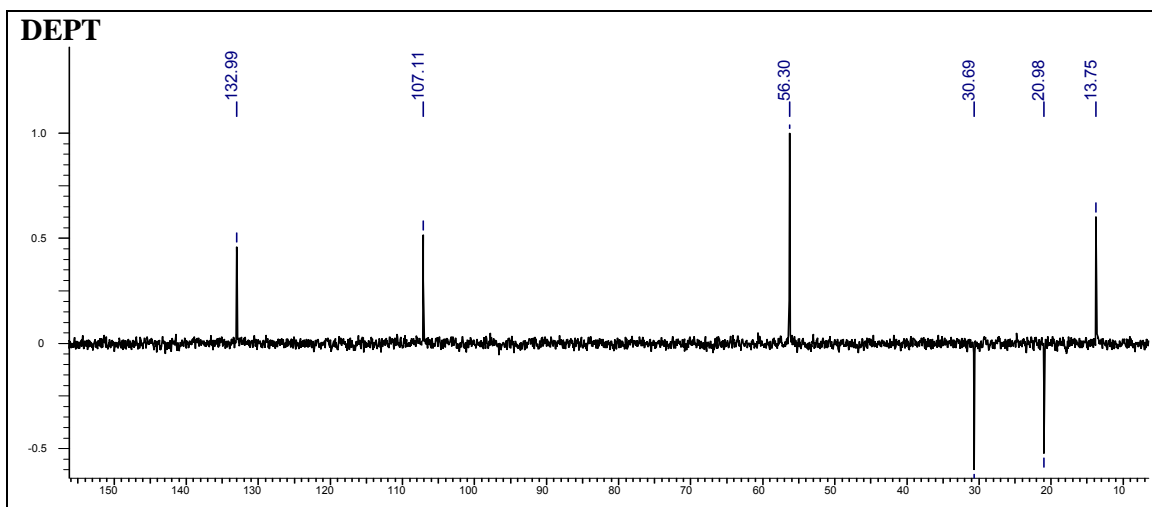
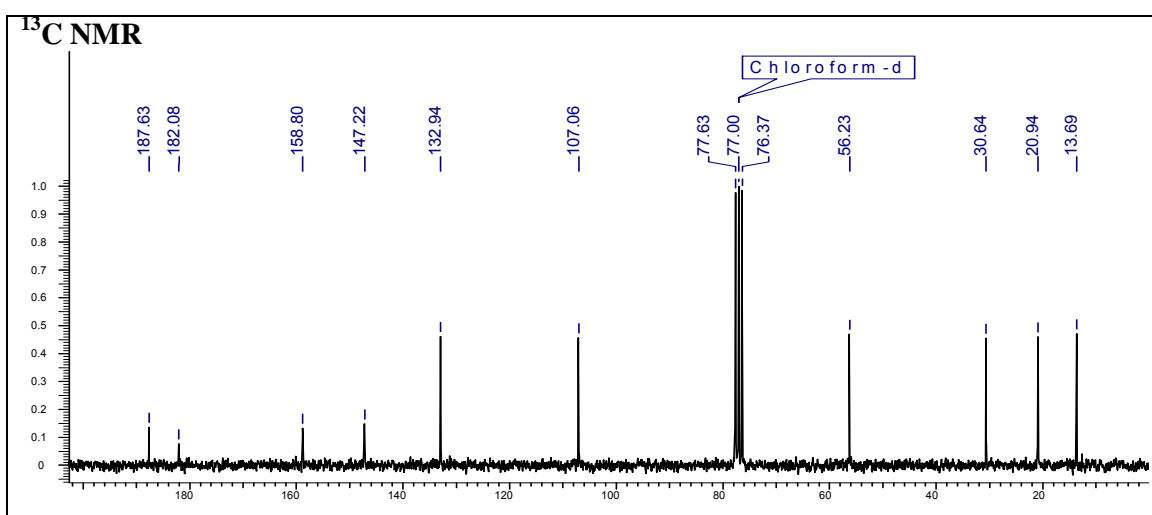
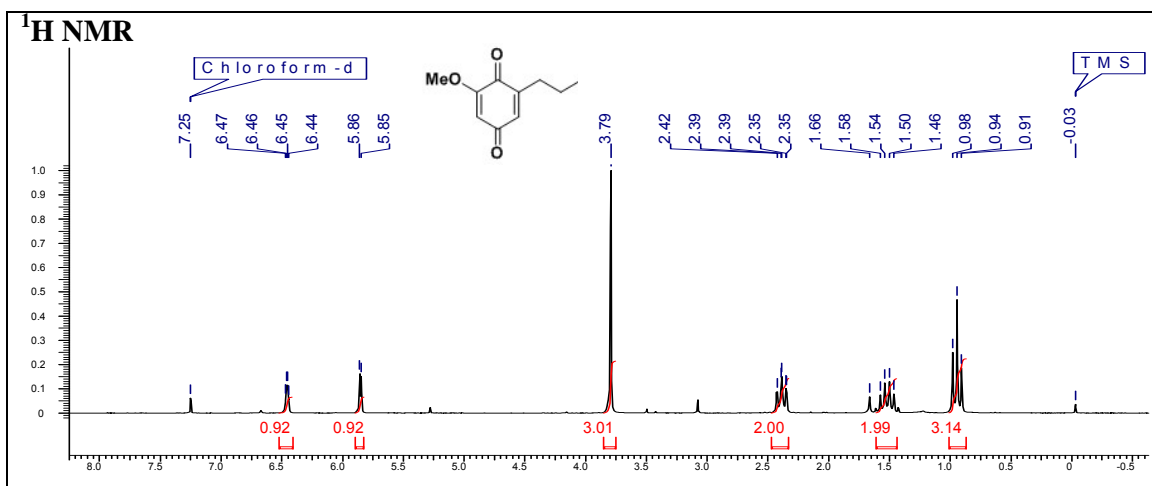
# Chapter 1



**2-Methoxy-6-propylphenol (28)**

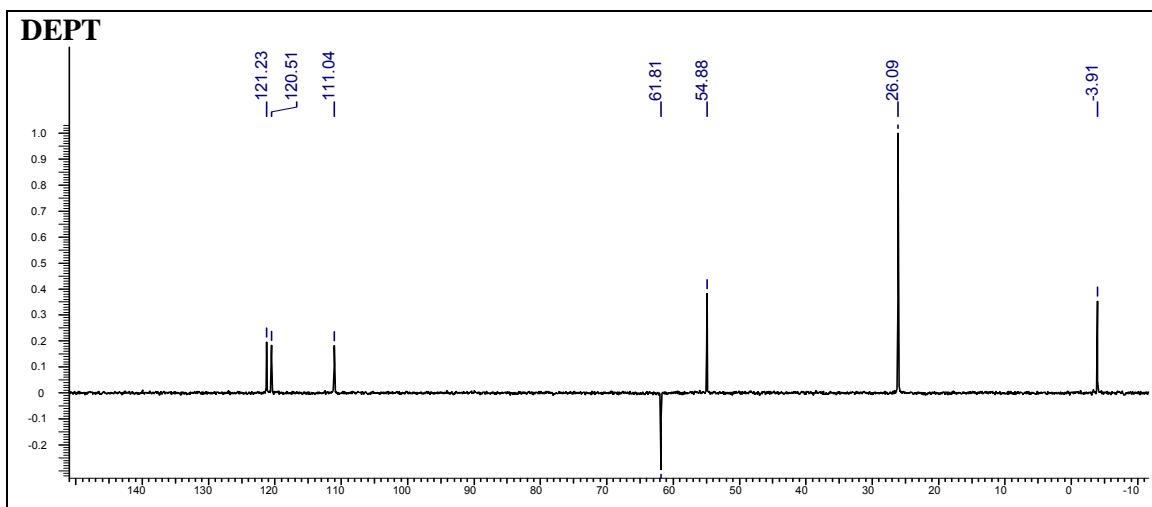
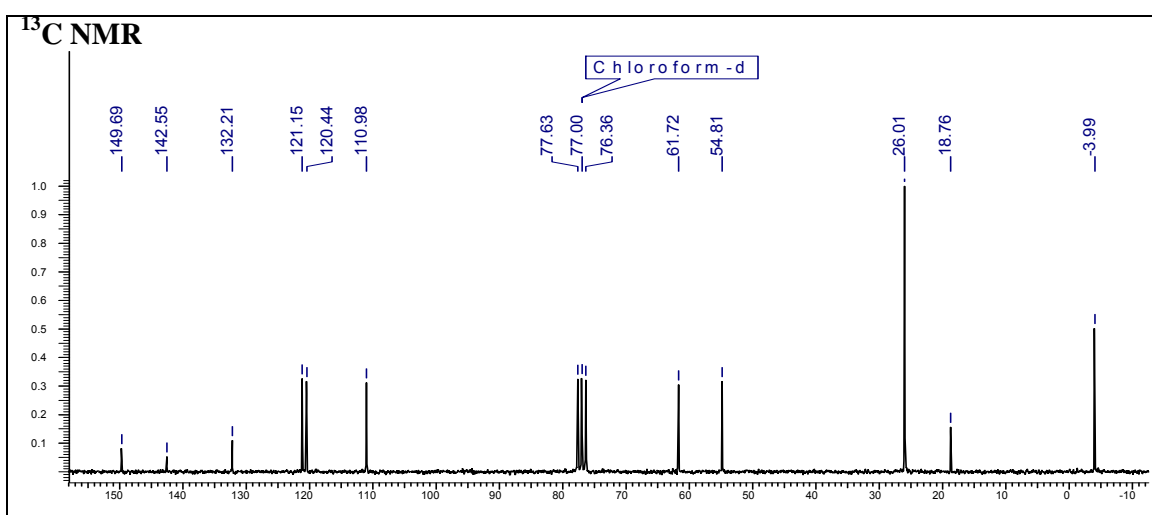
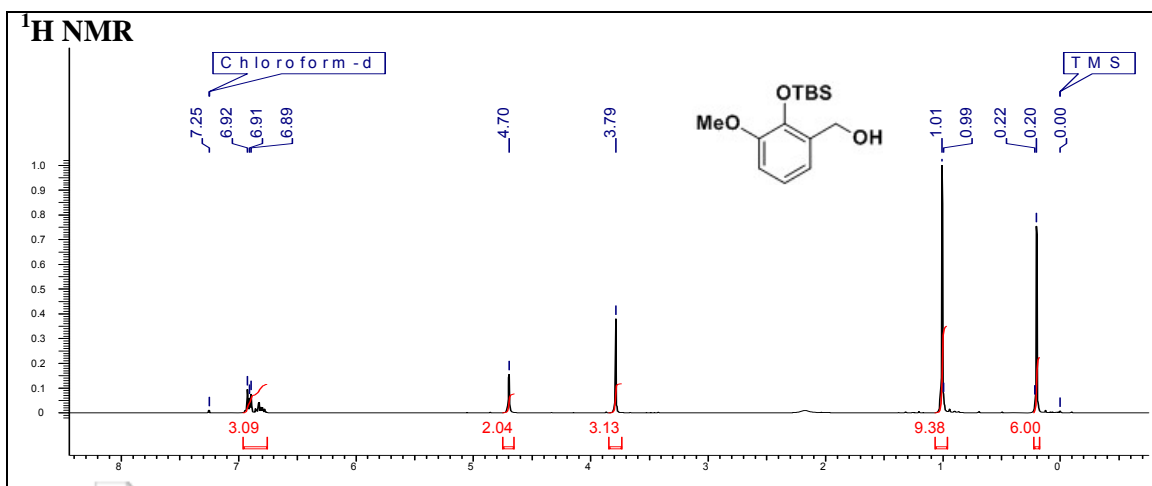


# Chapter 1



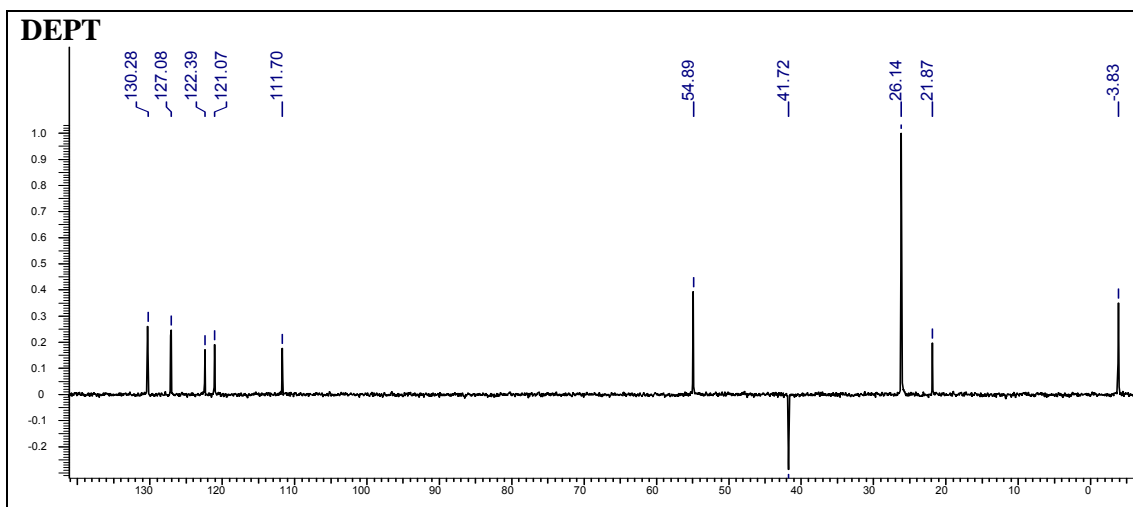
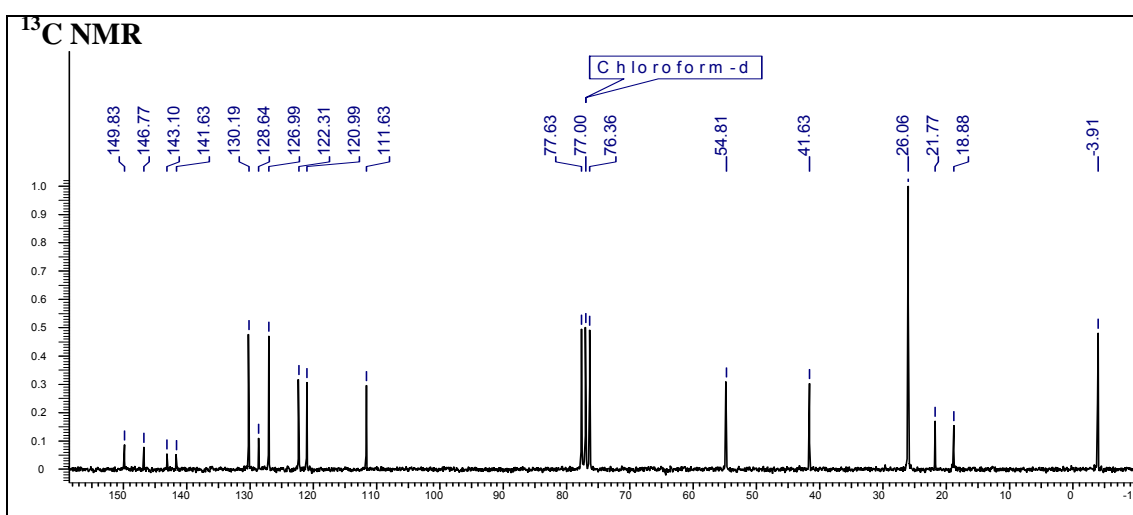
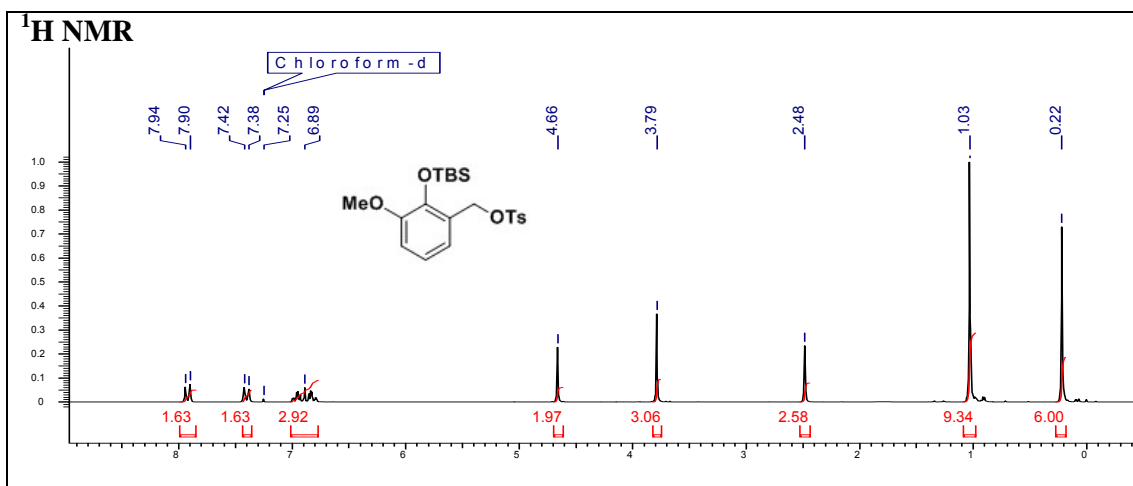
**2-Methoxy-6-propylcyclohexa-2,5-diene-1,4-dione (6)**

# Chapter 1



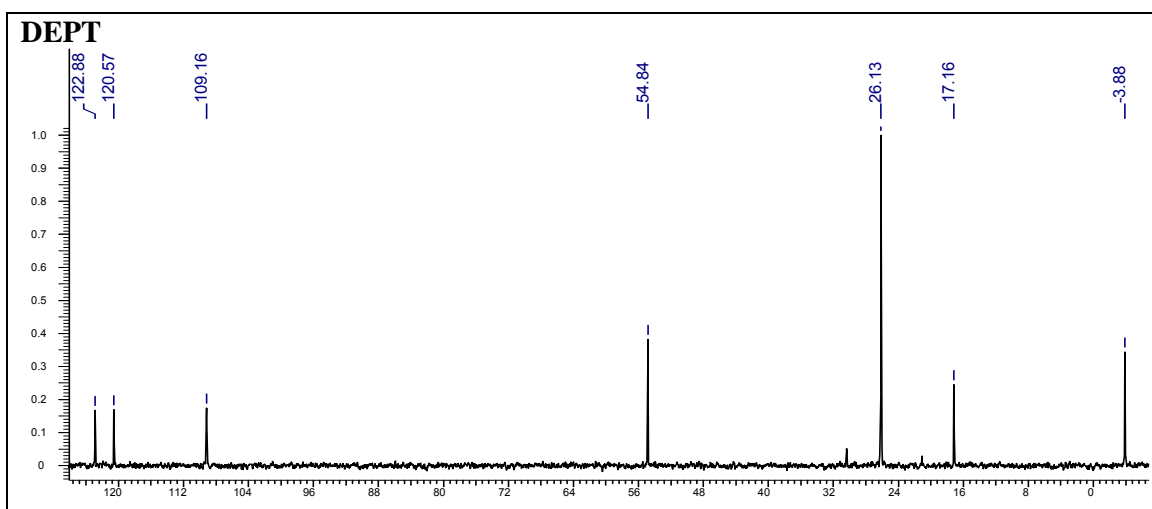
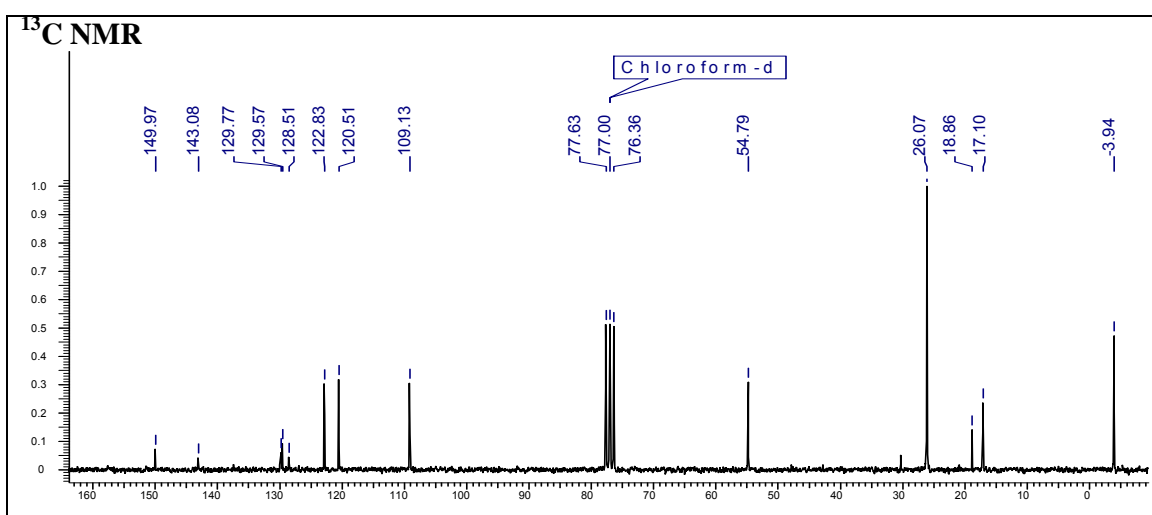
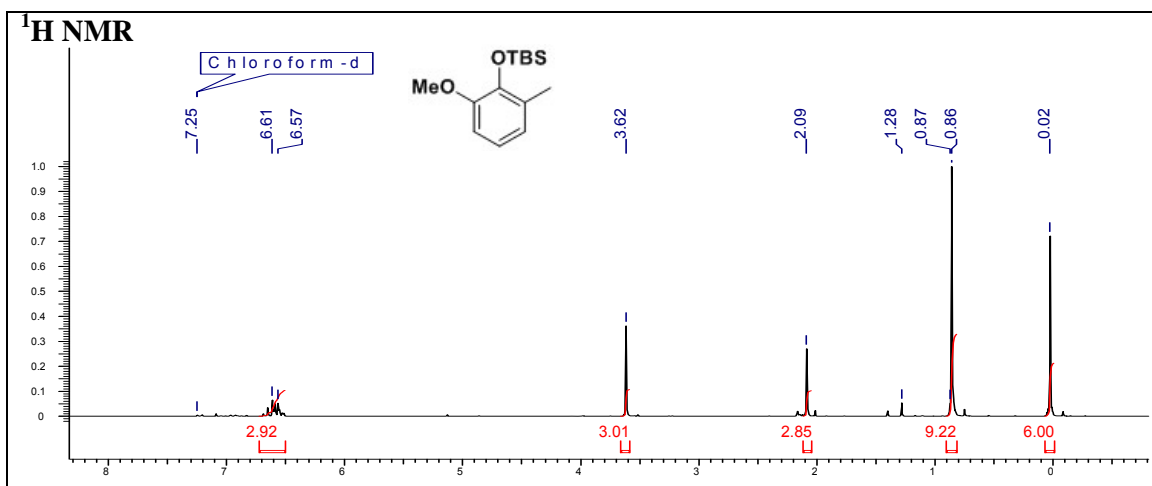
**(2-((*tert*-Butyldimethylsilyloxy)-3-methoxyphenyl)methanol (29)**

# Chapter 1



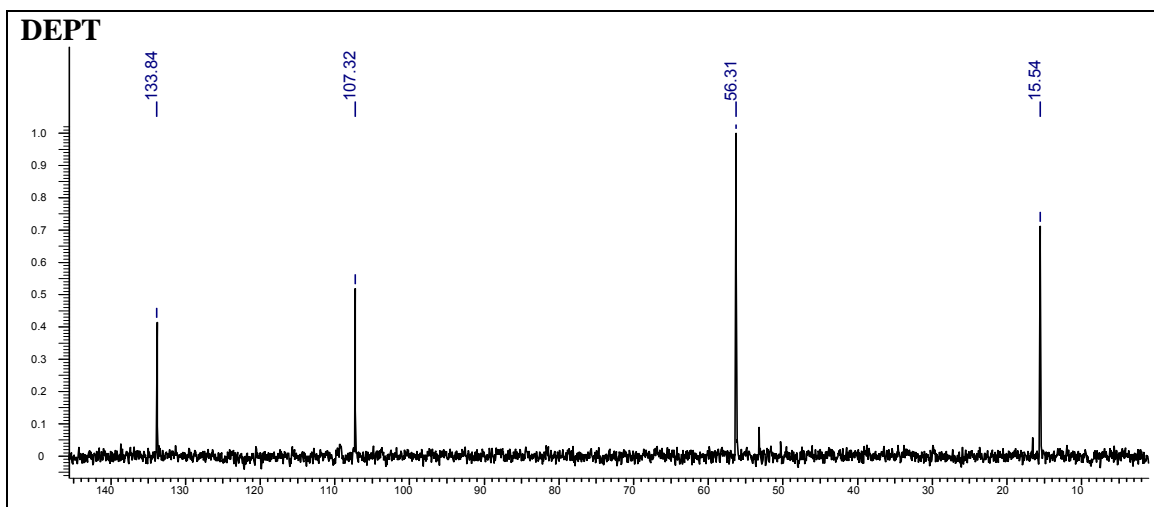
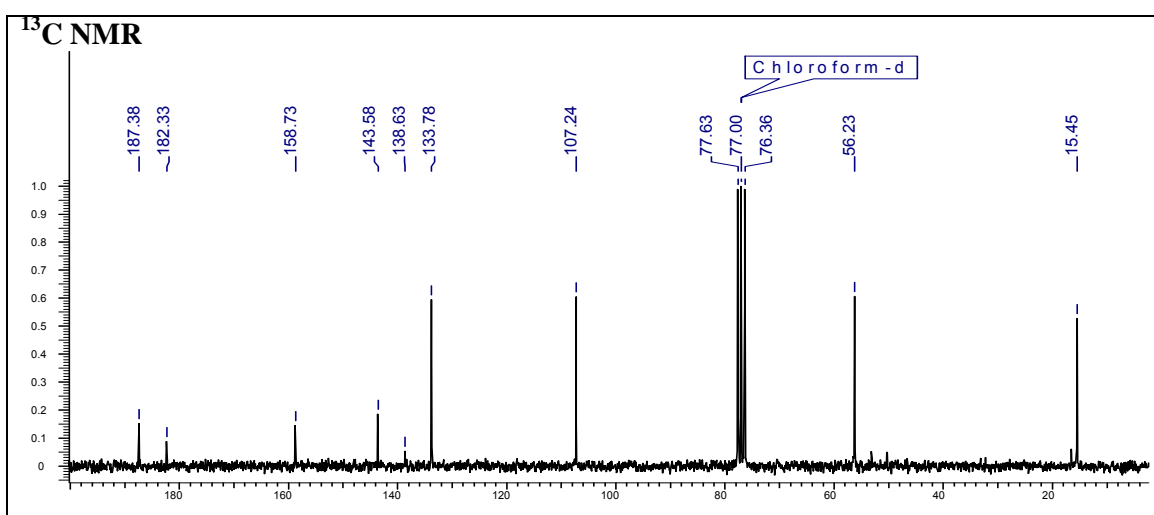
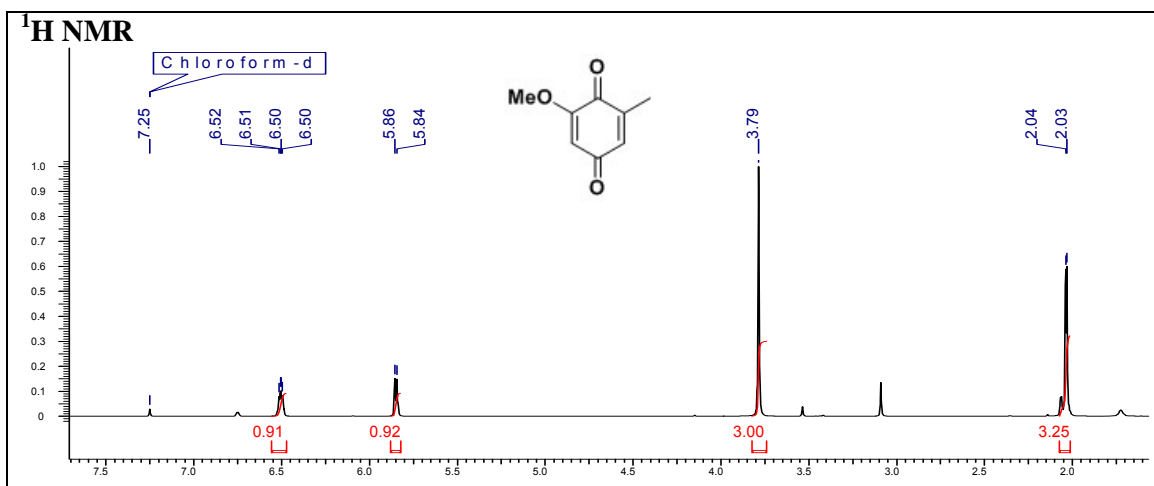
**2-((*tert*-Butyldimethylsilyl)oxy)-3-methoxybenzyl-4-methylbenzenesulfonate (30)**

# Chapter 1



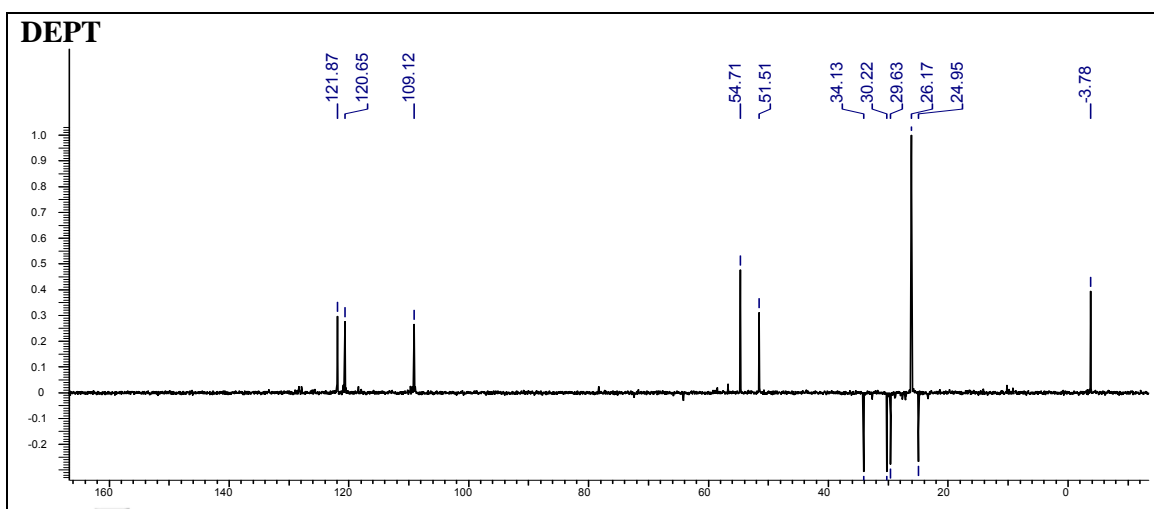
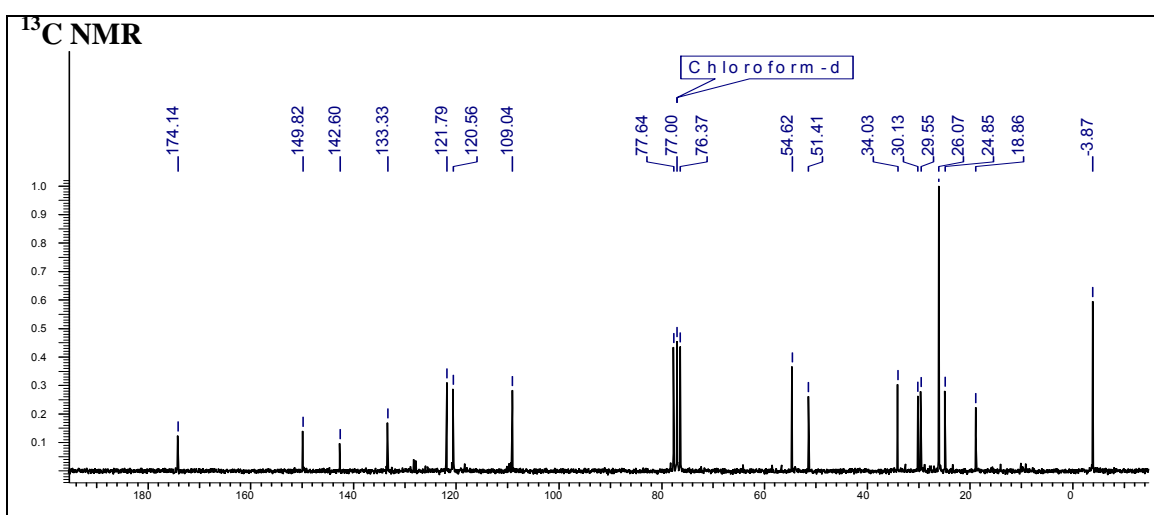
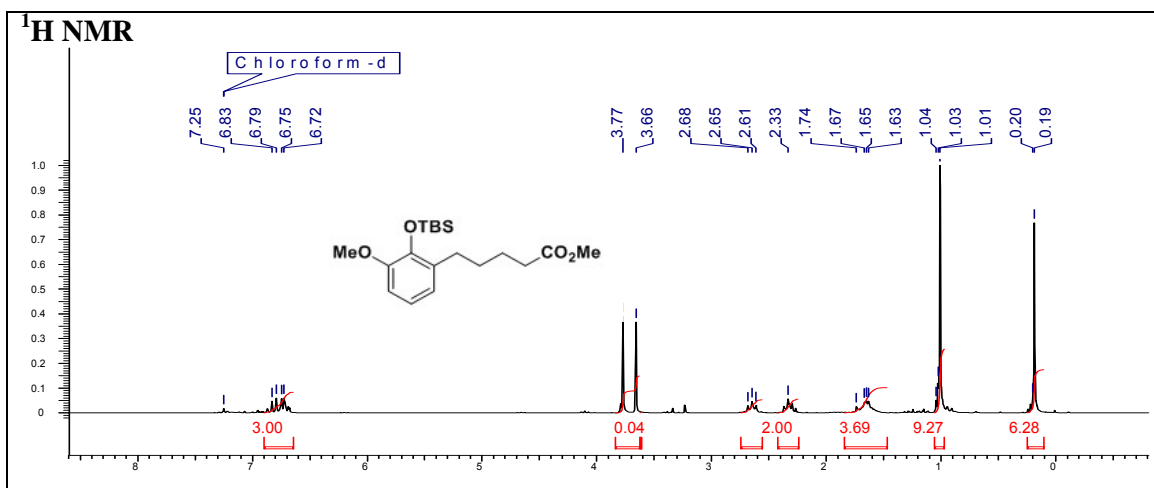
***tert*-Butyl-(2-methoxy-6-methylphenoxy)dimethylsilane (31)**

# Chapter 1



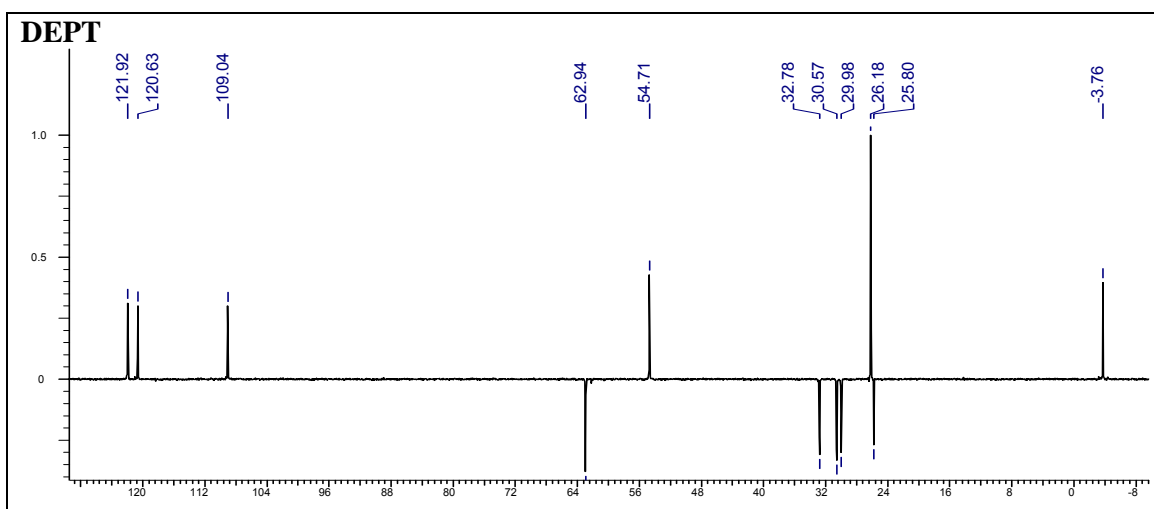
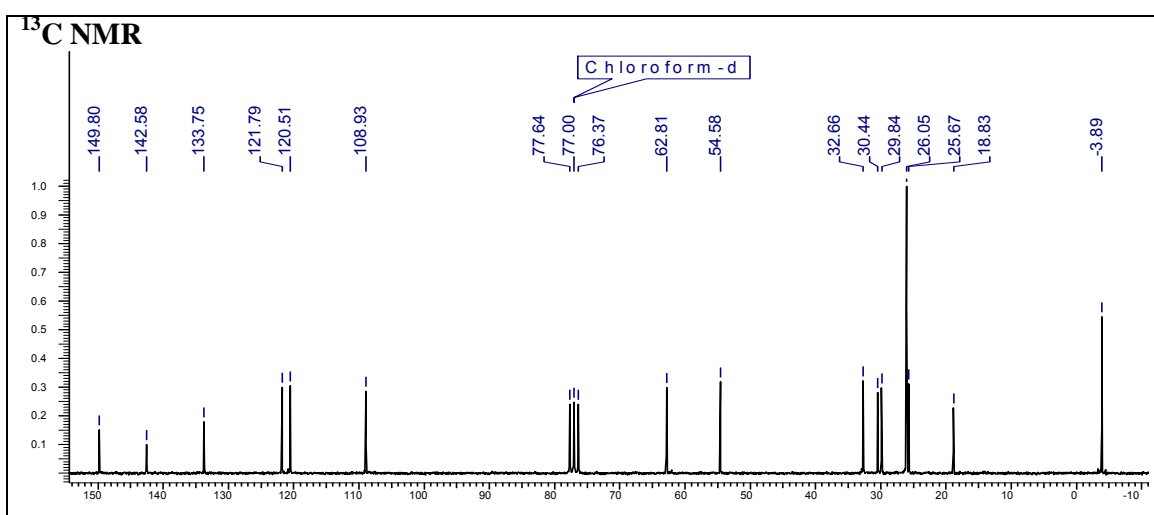
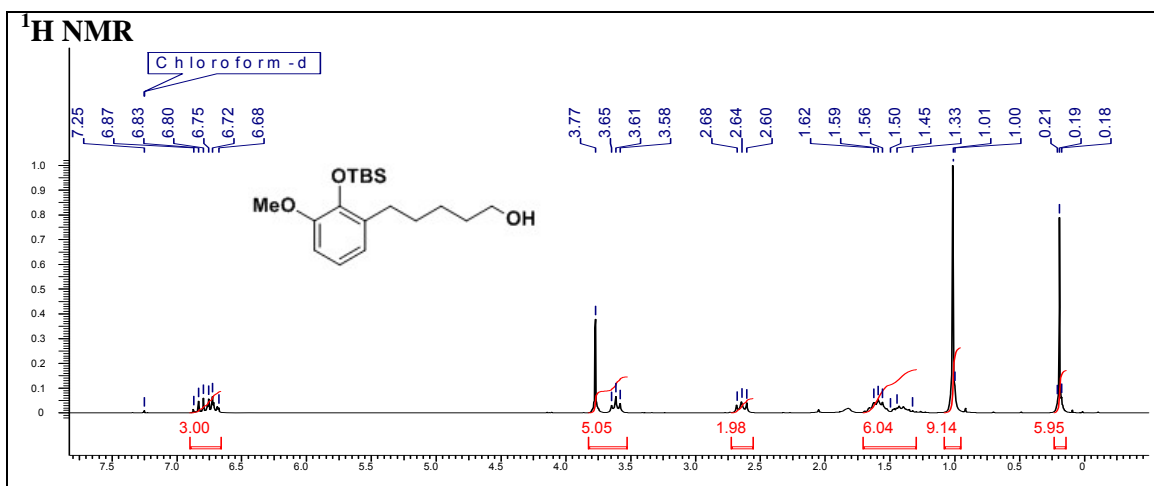
**2-Methoxy-6-methylcyclohexa-2,5-diene-1,4-dione (7)**

# Chapter 1



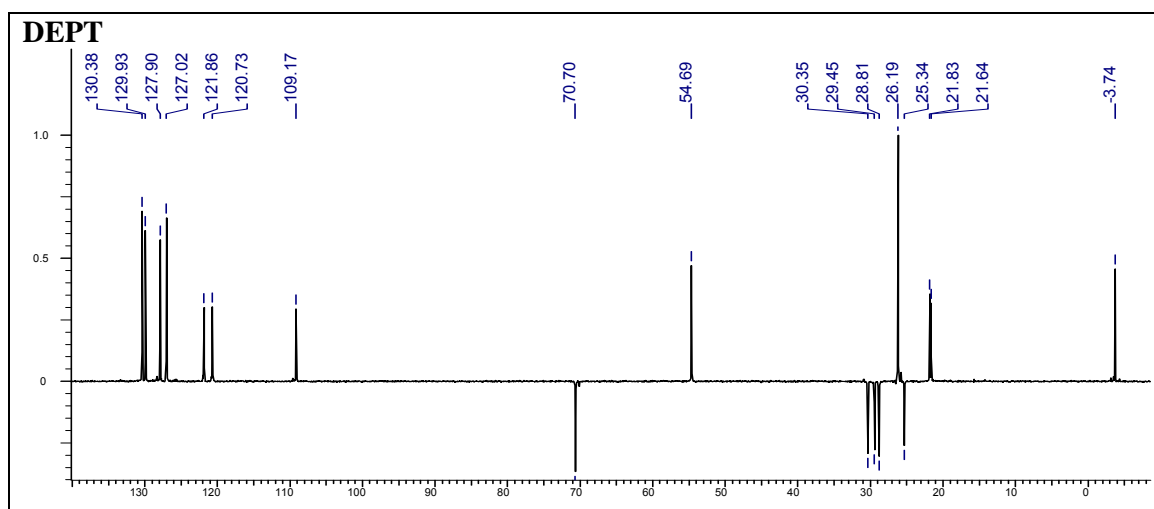
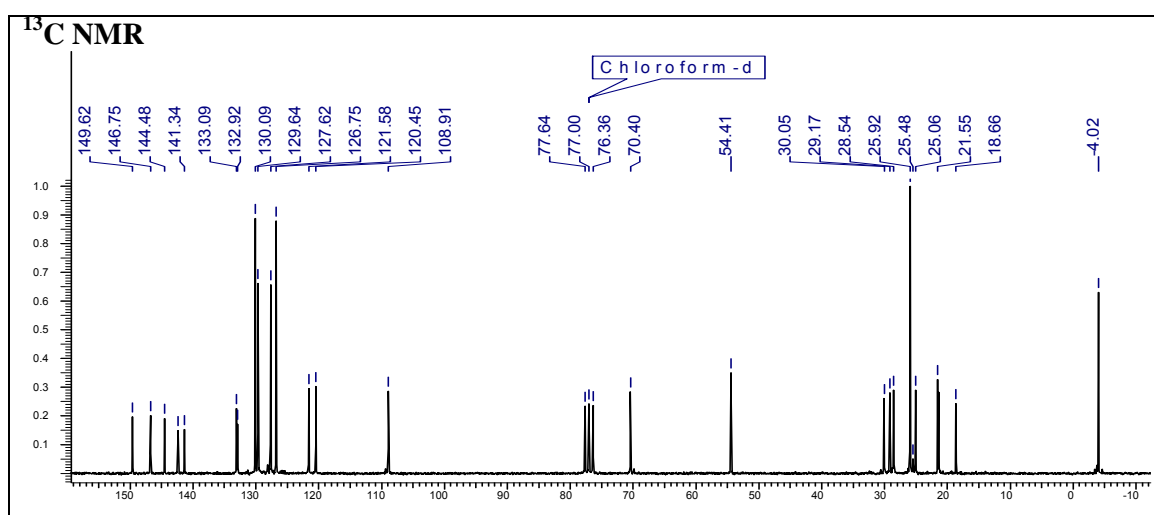
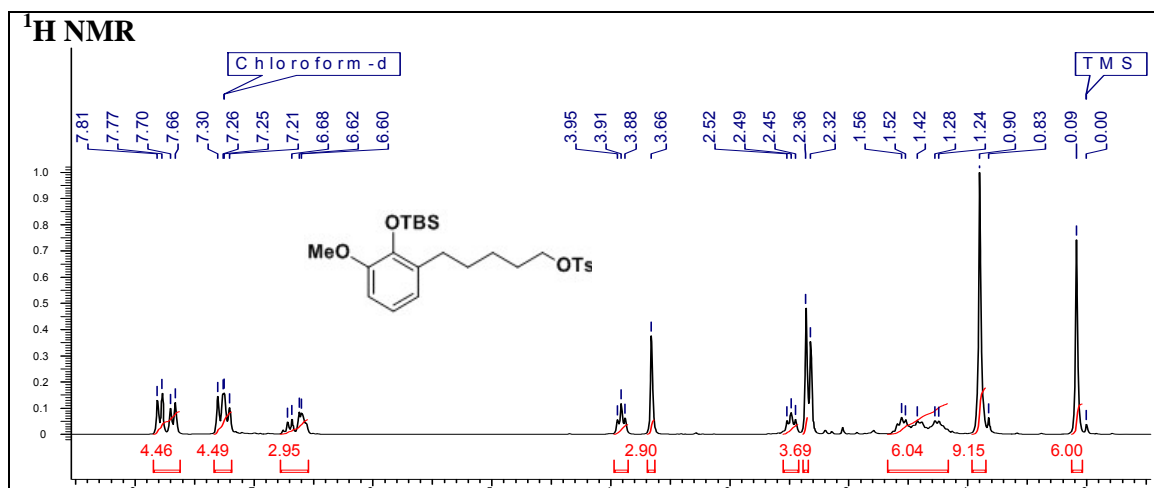
**Methyl 5-(2-(*tert*-butyldimethylsilyloxy)-3-methoxyphenyl)pentanoate (33)**

# Chapter 1



**5-[2-(*tert*-Butyldimethylsilyloxy)-3-methoxyphenyl]pentan-1-ol (34)**

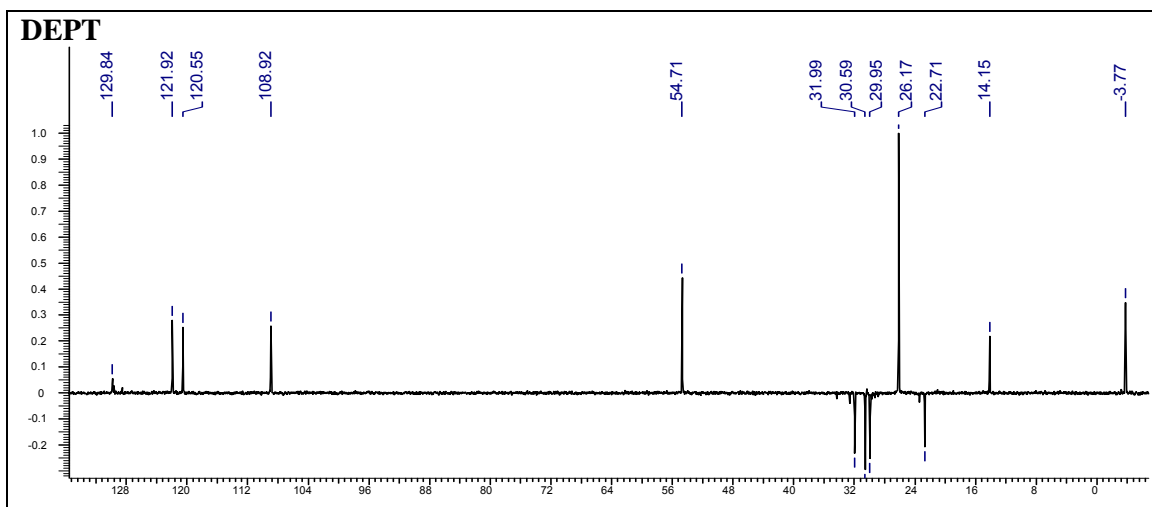
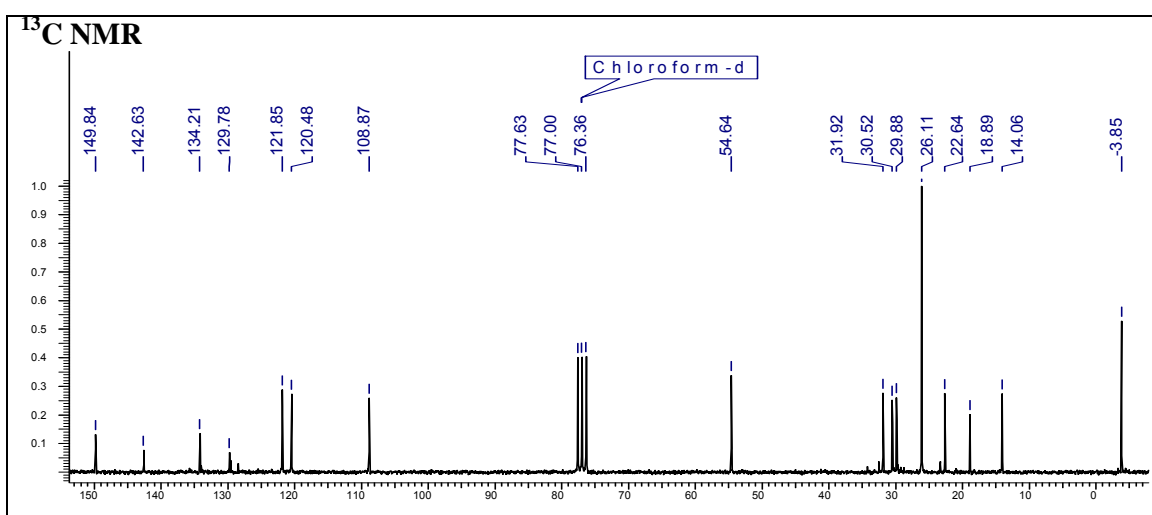
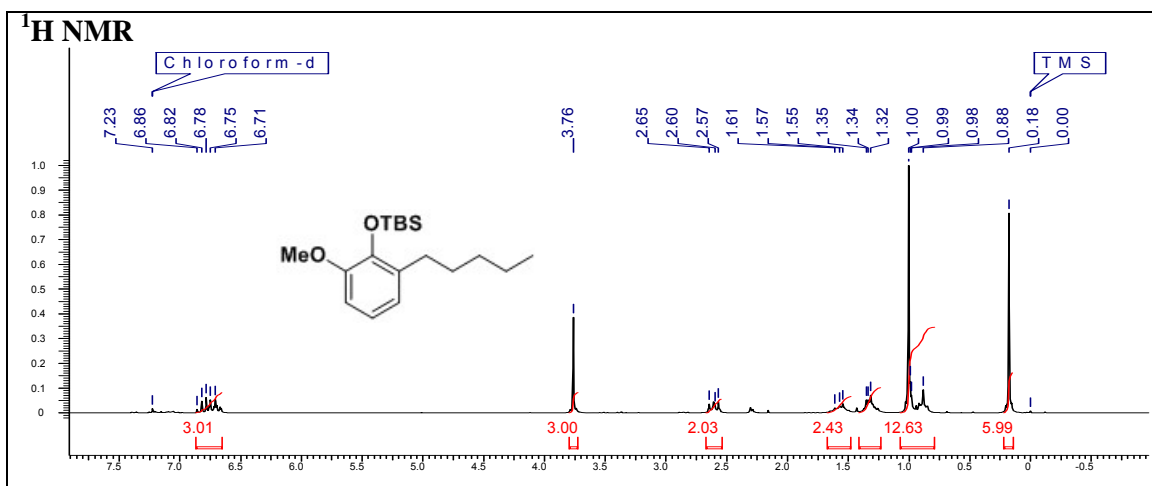
# Chapter 1



**5-[2-(*tert*-Butyldimethylsilyloxy)-3-methoxyphenyl]pentyl-4-methylbenzenesulfonate (35)**

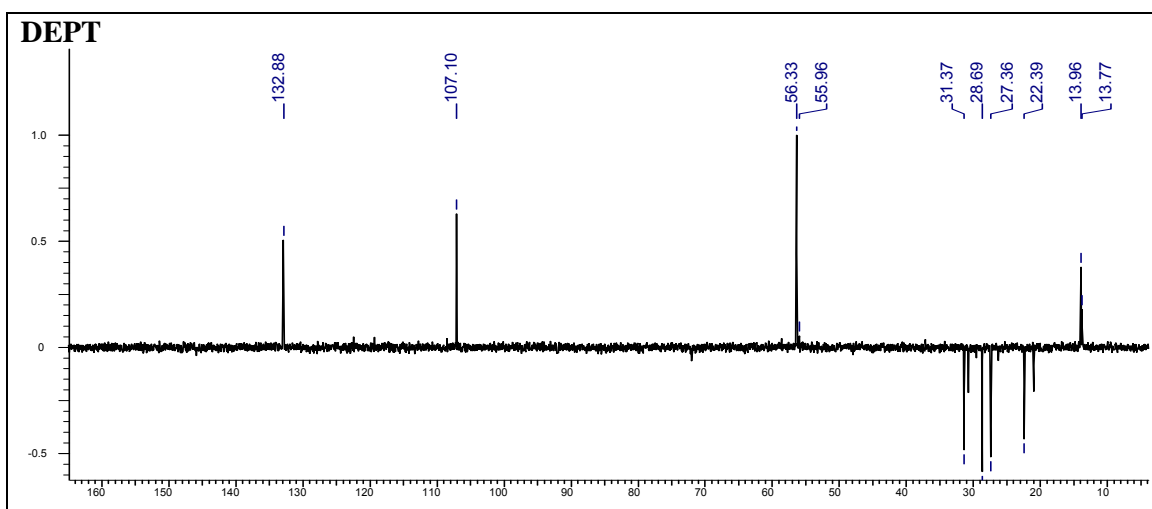
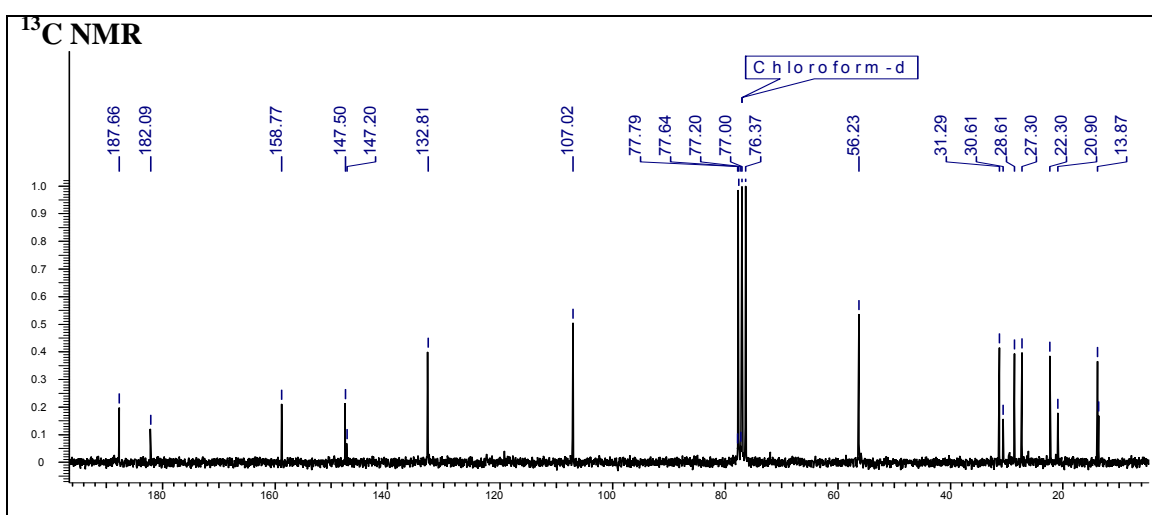
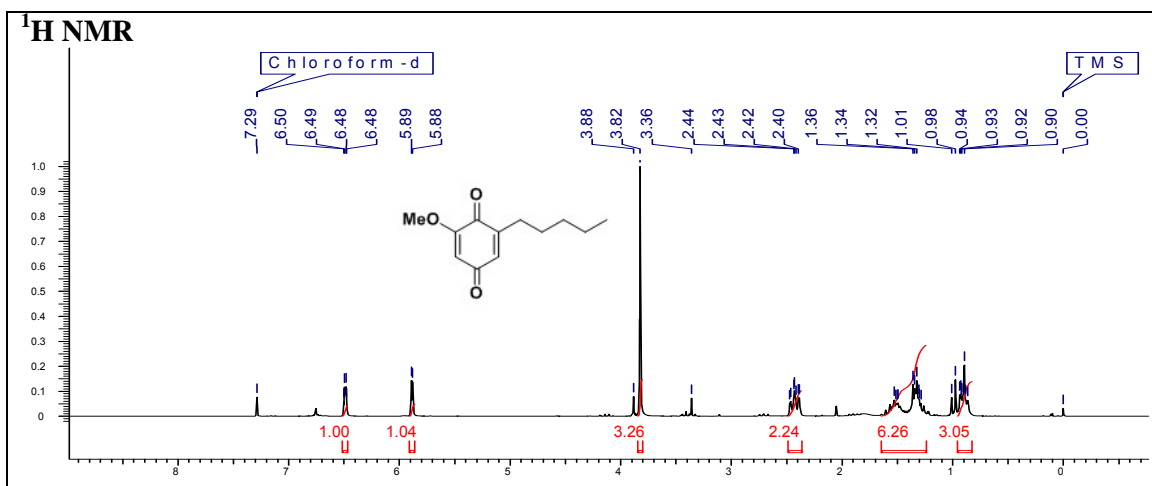


# Chapter 1



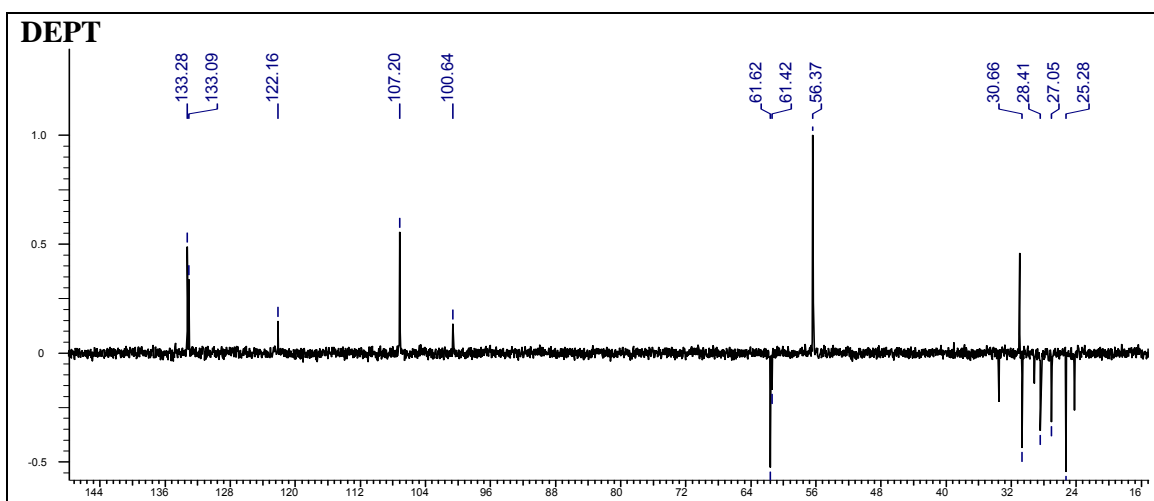
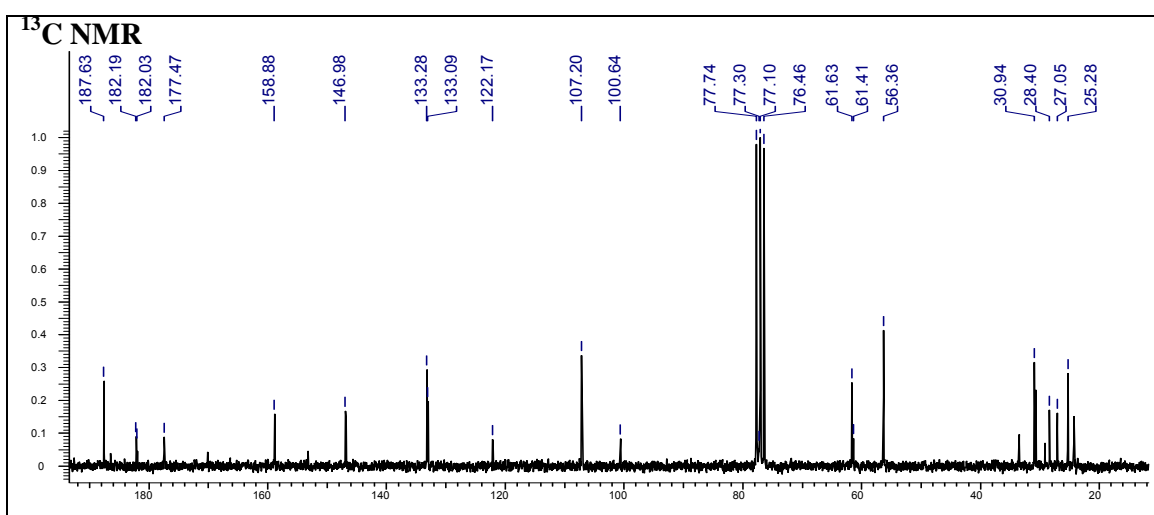
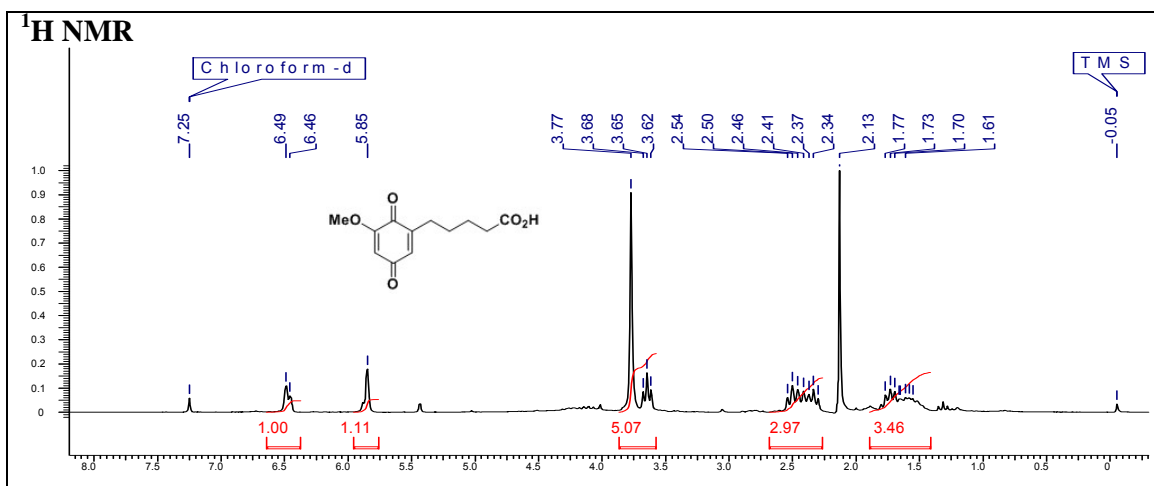
***tert*-Butyl-(2-methoxy-6-pentylphenoxy)dimethylsilane (36)**

# Chapter 1



**2-Methoxy-6-pentylcyclohexa-2,5-diene-1,4-dione (Primin) (8)**

# Chapter 1



**5-(5-Methoxy-3,6-dioxocyclohexa-1,4-dienyl)-pentanoic acid (Primin acid) (9)**

# *Chapter 1*

## **Synthesis of Antibacterial Natural Products**

---

### *Section B*

#### **Studies Towards Synthesis of Oenostacin**

---

This section deals with the synthetic efforts tried towards the first total synthesis of antibacterial natural product, Oenostacin. It also discusses previous literature protocols utilized in the synthesis. It involves utilization of synthetic protocols for example extended Heck reaction and Chelation control selective reduction for synthesizing this natural product.

## 1.1 Introduction

Selman Waksman in 1942 coined the term antibiotic (from Greek αντί - anti, "against" + βιοτικός - biotikos, "fit for life") to describe any substance produced by a micro-organism that is antagonistic to the growth of other micro-organisms in high dilution. The strict definition of "antibiotic" therefore excludes synthetic compounds such as the sulphonamides (which are antimicrobial agents). In modern usage, the term "antibiotic" is more precisely used to refer to any chemotherapeutic or antimicrobial agent with activity against micro-organisms such as bacteria, fungi, or protozoa. Many antibiotic compounds used in modern medicine are produced and isolated from living organisms, such as the penicillin class produced by fungi in the genus penicillin, or streptomycin from bacteria of the genus *Streptomyces*. Although, a plethora of bioactive compounds have been shown to be promising agents against a wide range of micro-organisms, however there is still a strong need felt to develop newer antibiotics since these organisms have been developing resistance against even newly introduced antibiotics.

The plant *Oenothera biennis* (Family: Onagraceae) commonly known as Evening Primrose is a genus of herbs and shrubs; its species are widely distributed in temperate America along with some species found in tropics.<sup>1</sup> Few species of this genus *O. biennis* have been introduced as ornamental plants in India. The seeds contain high  $\gamma$ -linolenic acid content and are useful for the formation of prostaglandins and related hormones. The seeds possess fatty acids<sup>2</sup> and sterols<sup>3</sup> while the leaves show high content of flavonoids<sup>4</sup> and oenothien A.<sup>5-6</sup> The plant possess several bio-active properties e.g. antiarthritic, antitumor and antithrombic properties. The bioactive component oenostacin **1** was isolated from the roots of the plant *O. biennis* in the year 1999 (Figure 1).

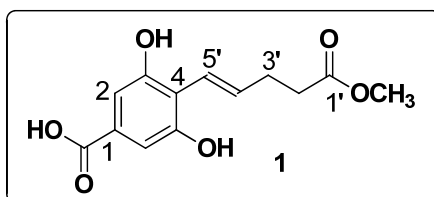


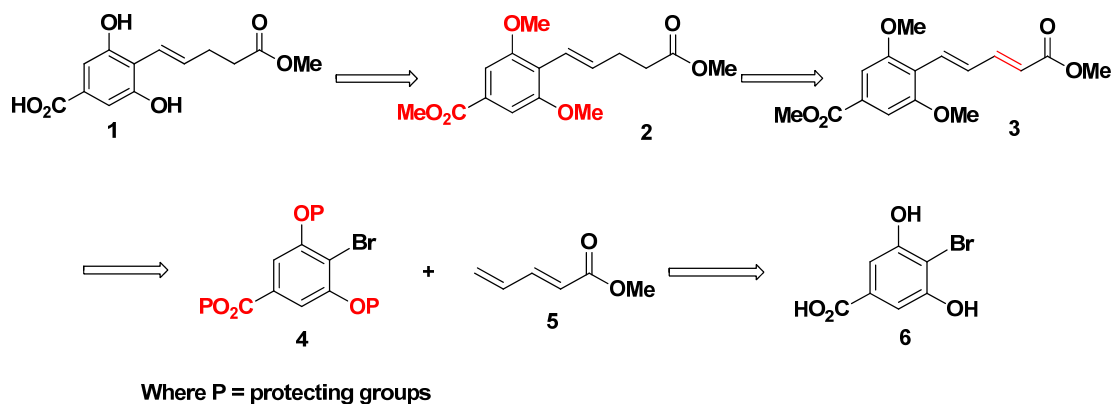
**Figure 1.** Structure of antibacterial agent Oenostacin, **1**.

It has shown to be potent antibacterial agent against *Staphylococcus aureus* and *Staphylococcus epidermidis* having EC<sub>50</sub> 0.12 μM activity. It is known that *S. aureus*, one of the most successful opportunistic human Gram positive pathogens, is responsible for postoperative wound infections, bacteraemia, pneumonia, osteomyelitis, mastitis, acute endocarditis, and deep abscesses in various organs. In contrast to *S. aureus*, infections caused by *S. epidermidis* are less acute in nature. However, *S. epidermidis* is an important human pathogen and is the predominant cause of many nosocomial infections.<sup>1</sup>

Considering, its potent biological activities and low yield from natural sources, it is highly desirable to synthesize this potent antibacterial compound **1**. Oenostacin **1** shows potent activity against *S. aureus* and *S. epidermidis*, respectively and the latter strains has often been found to be resistant to antibiotics such as penicillin, amoxicillin and methicillin.

## 1.2 Present work: Objective and Rationale

However, the bioactive compound **1** is not abundant in nature and no other methods are reported in literature, therefore, synthesis of compound **1** and its analogues for further structural activity relationship (SAR) is highly desirable. The retrosynthetic plan was designed for the antibacterial agent, oenostacin **1**. Flexible scheme was devised and outlined in retrosynthetic plan (Scheme 1).



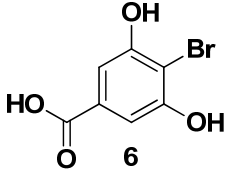
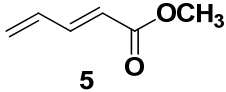
**Scheme 1.** Retrosynthetic strategy for the synthesis of antibacterial agent, Oenostacin **1**.

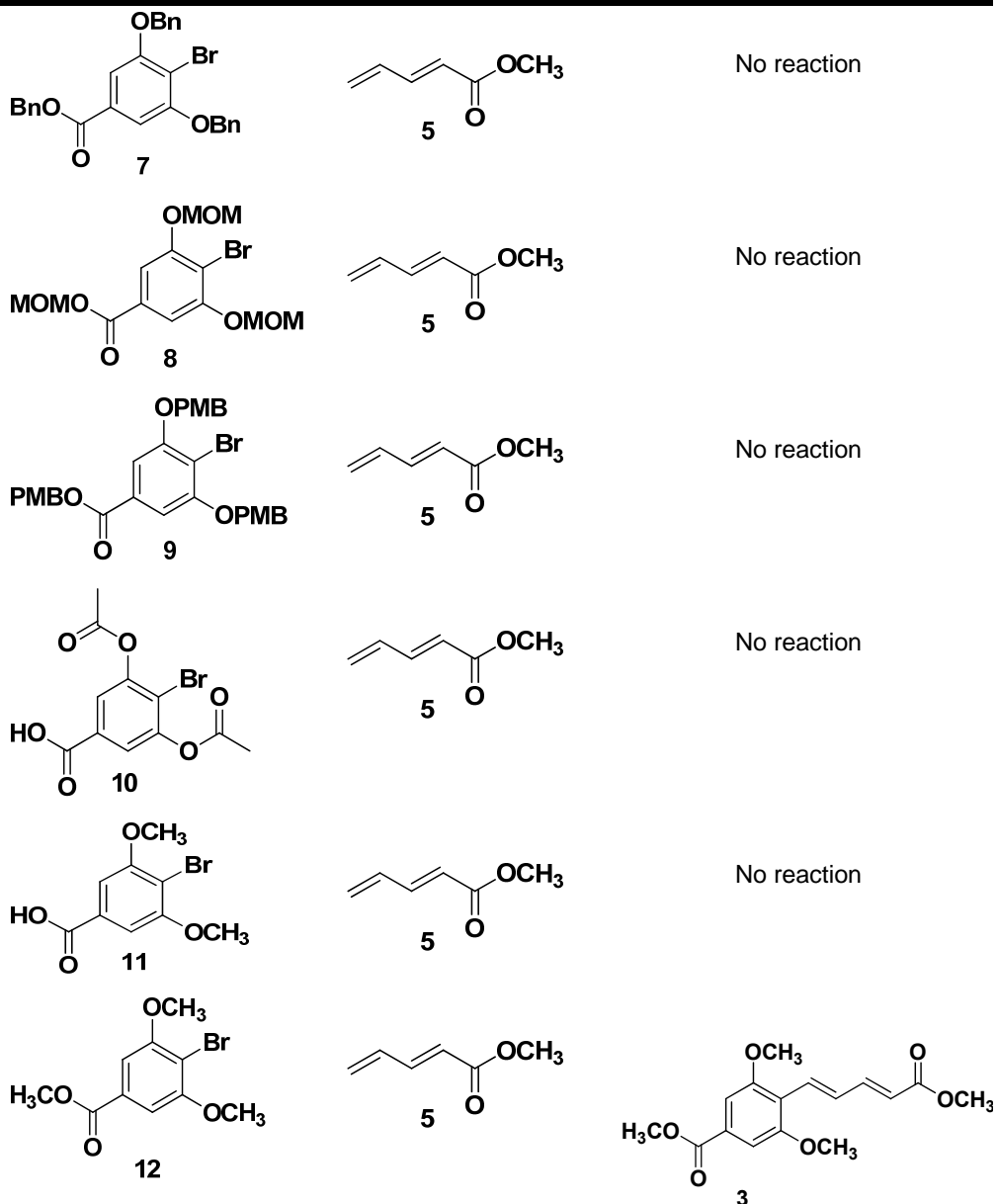
### 1.3 Results and Discussion

Retrosynthetic analysis of oenostacin **1** suggested it could be assessed from the fully methylated analog **2**. This fully protected analog **2** in turn could be synthesized by selective reduction of  $\alpha,\beta$ -double bond of  $\alpha,\beta,\gamma,\delta$ -conjugated diene ester **3**.<sup>7</sup> This diene could be synthesized from the Heck cross-coupling reaction of protected analog **4** and diene **5**. Compound **4** could be easily synthesized by protecting phenolic and carboxylic groups of 4-bromo-3,5-dihydroxy benzoic acid (Scheme 1).

Initially, Heck reaction was tried on 4-bromo-3,5-dihydroxy benzoic acid **6** with (*E*)-methyl-penta-2,4-dienoate **5** using conventional reaction conditions (Table 1).<sup>7</sup> However, unreacted starting materials were recovered. It was then visualized that due to presence of free phenolic and carboxylic acid groups, the coupling reaction was failed to furnish the desired product. So it was mandatory to protect the phenolic and carboxylic acid groups of 4-bromo-3,5-dihydroxy benzoic acid **6**. In order to accomplish this, various protecting groups were screened. To achieve the array of derivatives, 4-bromo-3,5-dihydroxy benzoic acid **6** was treated with benzyl bromide to furnish benzyl derivative **7**, methoxyl methyl bromide to furnish methoxy methyl (MOM) derivative **8**, *p*-methoxy benzyl bromide to furnish *p*-methoxybenzyl (PMB) derivative **9**, and acetyl chloride to furnish acetate derivative **10**, respectively (Table 1). However, Heck reaction of protected 4-bromo-3,5-dihydroxy benzoic acid derivatives **7**, **8**, **9**, **10** with diene compound **5** respectively, did not furnish the desired product.

**Table 1.** Standardization of Heck cross-coupling reaction conditions

Substrates	$\alpha, \beta, \gamma, \delta$ - conjugated-diene	Product
 <b>6</b>	 <b>5</b>	No reaction

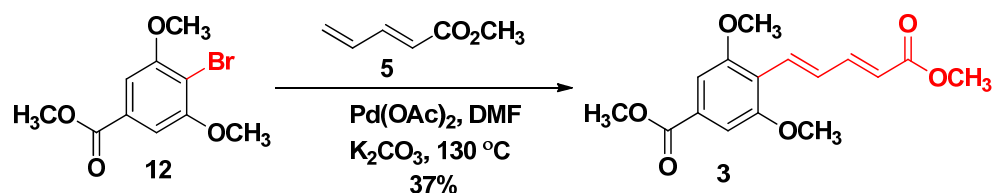


We came to know through literature search that substrates bearing free carboxylic acid group furnishes Heck reaction product in good yields. Hence, we tried our reaction with substrate **11**, however no product formation was observed.<sup>8</sup>

It was then decided to protect the phenolic and carboxylic group of 4-bromo-3,5-dihydroxy benzoic acid **6** as methoxy and methyl ester, respectively and investigate the Heck reaction again. The formation of product **12** was delineated by its

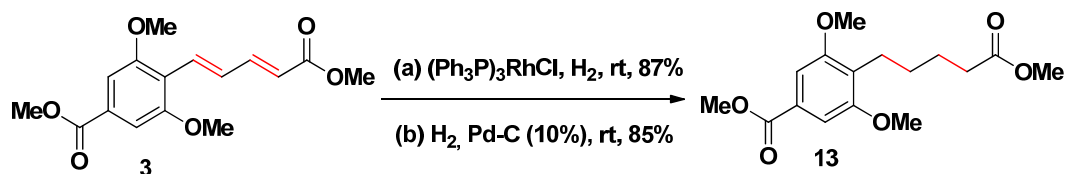


spectral analysis. In  $^1\text{H}$  NMR spectrum, the methoxy proton signals were observed at  $\delta$  3.94 (s) and 3.92 (s) ppm. In  $^{13}\text{C}$  NMR spectrum, the methoxy carbon signals were observed at  $\delta$  56.5 and 52.4 ppm. The classical Heck reaction on the 4-bromo-3,5-dihydroxy benzoic acid **6** with (*E*)-methyl penta-2,4-dienoate **5** and palladium acetate as a catalyst and dicyclohexyl-*N*-methylamine as a base furnished the desired  $\alpha,\beta,\gamma,\delta$ -conjugated diene ester **3** in 37% yield (Scheme 2). The formation of product **3** was confirmed by its spectral analysis. In  $^1\text{H}$  NMR spectrum, the olefinic proton signals were observed at  $\delta$  6.75-6.55 (m) and 7.47-7.32 (m) ppm. In  $^{13}\text{C}$  NMR spectrum, the olefinic carbon signals were observed at  $\delta$  147.3, 131.9, 131.3 and 120.4 ppm.



**Scheme 2.** Successful Heck reaction conditions on the analog **12**.

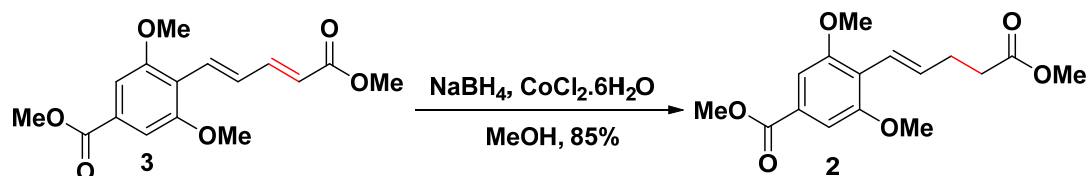
Afterwards, regioselective reduction of  $\alpha,\beta$ -double bond of  $\alpha,\beta,\gamma,\delta$ -conjugated diene ester **3** was attempted under various reduction conditions reported in the literature.<sup>9</sup> Initial attempts for the reduction of **3** with Wilkinson's catalyst or  $\text{H}_2/\text{Pd-C}$  (10%) furnished the tetrahydro compound **13**.<sup>10</sup> The formation of product **13** was confirmed by its spectral analysis. In  $^1\text{H}$  NMR spectrum, the olefinic proton signals were observed at  $\delta$  1.69-1.63 (m) and  $\delta$  2.68 (t,  $J=7.5$  Hz, 2H) and 2.34 (t,  $J=7.8$  Hz, 2H) ppm. In  $^{13}\text{C}$  NMR spectrum, the olefinic carbon signals were observed at  $\delta$  33.9, 30.9, 24.8 and 22.6 ppm (Scheme 3).



**Scheme 3.** Optimized conditions for the selective hydrogenation on derivative **3**.

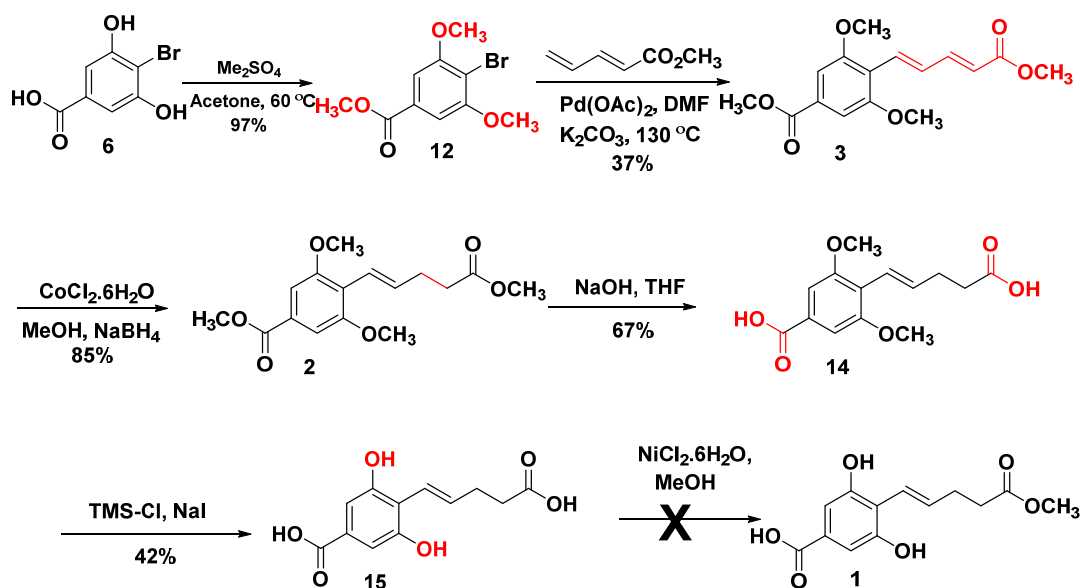
Hence, it was decided to carry out chelation control reduction method using sodium borohydride and cobalt chloride hexahydrate as a catalyst.<sup>11</sup> The formation of product **2** was confirmed by its spectral analysis. In  $^1\text{H}$  NMR spectrum, the olefinic proton signals were observed at  $\delta$  6.18-6.01 (m) and 5.40-5.17 (m) ppm. In  $^{13}\text{C}$  NMR

spectrum, the olefinic carbon signals were observed at  $\delta$  139.3 and 114.3 ppm. The desired product **2** was obtained in 85% yield which was fully characterized by its spectroscopic methods (IR,  $^1\text{H}$ ,  $^{13}\text{C}$  NMR and EI-MS) (Scheme 4).



**Scheme 4.** Optimized reduction reaction conditions on the analog **3**.

To achieve the title compound **1**, protected analogue **2** was first subjected to methyl ester hydrolysis. Afterwards, methoxy groups of compound **14** were deprotected using TMS-Cl/NaI in acetonitrile to furnish deprotected analogue **15** (Scheme 5).<sup>12</sup>



**Scheme 5.** Synthetic efforts towards the synthesis of antibacterial agent Oenostacin, **1**.

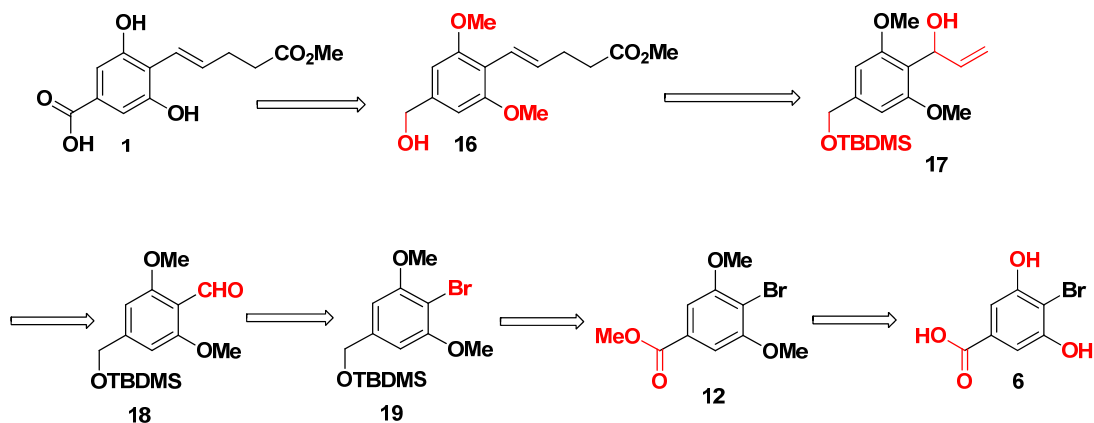
The formation of product **15** was confirmed by its spectral analysis. In  $^1\text{H}$  NMR and  $^{13}\text{C}$  NMR spectrum, absence of proton signals at  $\delta$  3.94 (s), 3.92 (s) and 56.5, 52.4 ppm, respectively confirmed deprotection of all the protecting groups to furnish compound **15**.

There are many reports in the literature to protect aliphatic carboxylic acid group in the presence of aromatic carboxylic group.<sup>13</sup> Few methods reported in the literature were tried for this selective esterification as discussed in Table 2. However, none of the methods could furnish the desired product.

**Table 2.** Attempted reaction conditions tried for the selective esterification

Methods tried	Product
Amberlite-IR 120, MeOH, reflux	Diesterified product
NiCl <sub>2</sub> .6H <sub>2</sub> O, MeOH, reflux	Diesterified product
2N H <sub>2</sub> SO <sub>4</sub> , MeOH, reflux	Decomposition
I <sub>2</sub> /H <sub>2</sub> O, MeOH, reflux	NR

In order to accomplish the synthesis of this natural product in good yield, we thought of alternative strategy (Scheme 6). Alternatively, we visualized that compound **1** could be synthesized by the oxidation of the benzylic acid derivative **16**, which in turn could be obtained from allylic alcohol **17**.

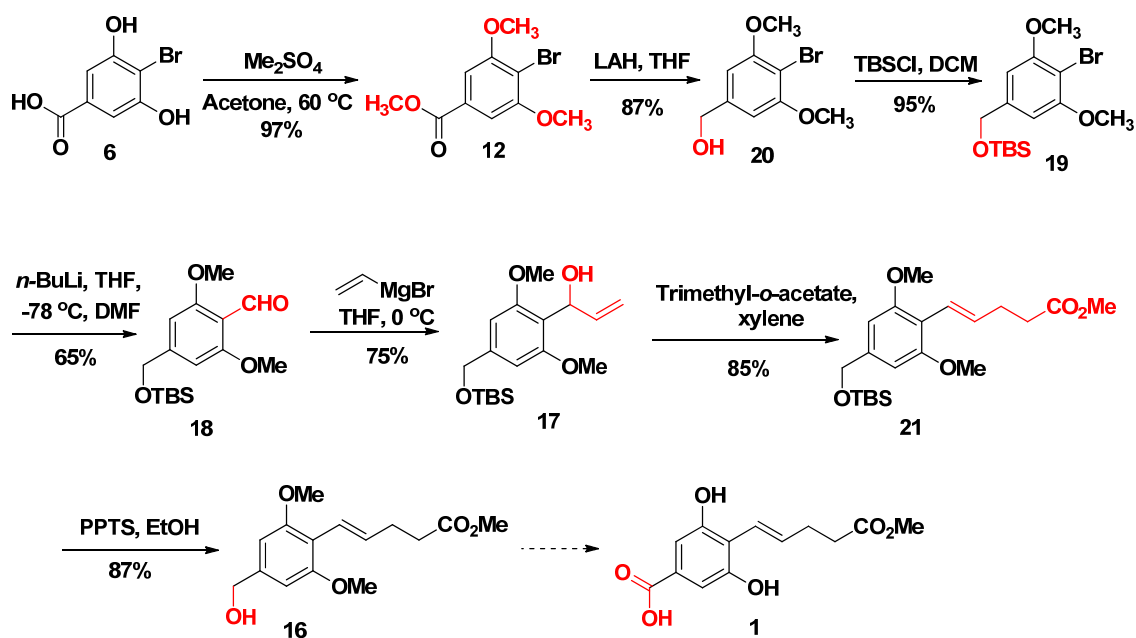


**Scheme 6.** Retrosynthetic strategy for the synthesis of antibacterial agent, Oenostacin **1**.

Compound **17** in turn could be obtained aldehydic compound **18**, which could be easily accessible from bromo derivative **19**. Compound **19** could be synthesized by the reduction of ester **12** and TBS protection of the benzylic alcohol.

First 3,5-dihydroxy-4-bromobenzoic acid **6** was fully protected to furnish compound **12** and further ester group was reduced with LAH/THF to alcohol **20** (Scheme 6). The formation of product **20** was confirmed by its spectral analysis. In <sup>1</sup>H NMR spectrum, the proton signal for benzylic group was observed at δ 4.64 (s) ppm.

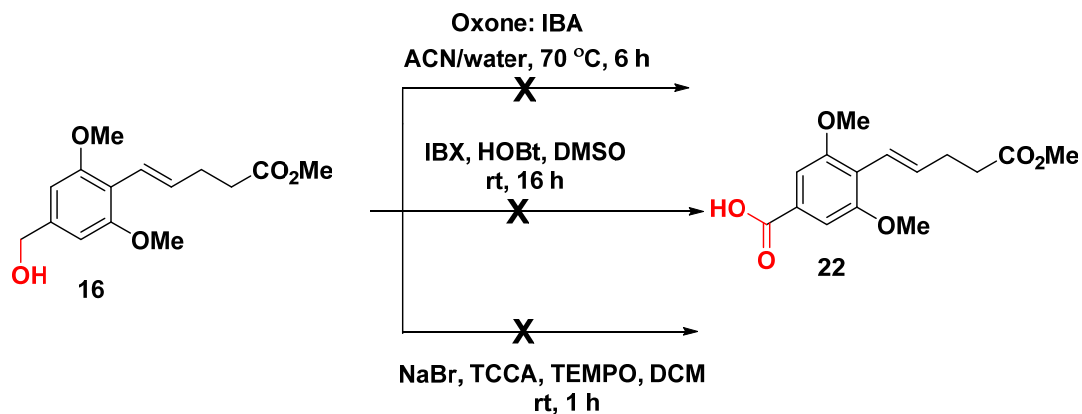
In  $^{13}\text{C}$  NMR spectrum, benzylic carbon signals were observed at  $\delta$  64.7 ppm, thus confirming the formation of the product. The primary alcohol group of compound **20** was then protected as *t*-butyl-dimethylsilyl ether derivative **19**.<sup>14</sup> In  $^1\text{H}$  NMR spectrum, of compound **19** the proton signals for *t*-butyl-dimethylsilyl were observed at  $\delta$  0.94 and 0.10 ppm. In  $^{13}\text{C}$  NMR spectrum, the *t*-butyl-dimethylsilyl carbon signals were observed at  $\delta$  25.89, 18.34 and -5.27 ppm. This bromo compound **19** was subjected to bromo to lithium exchange reaction and quenched with DMF as a nucleophile to furnish aldehydic compound **18**.<sup>15</sup> In  $^1\text{H}$  NMR spectrum, the proton signal for compound **18** aldehydic group was observed at  $\delta$  10.38 ppm. In  $^{13}\text{C}$  NMR spectrum, aldehydic carbon signal was observed at  $\delta$  188.8 ppm.



**Scheme 7.** Synthetic efforts towards antibacterial agent, Oenostacin **1**.

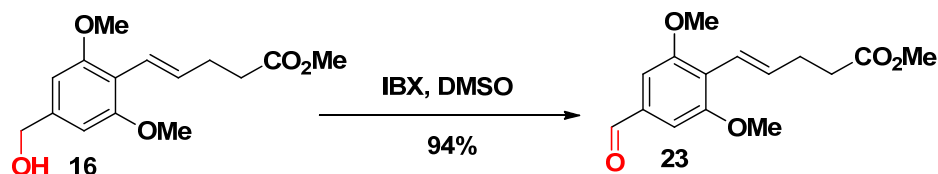
Compound **18** was treated with vinyl magnesium bromide (1.0M) to generate the allylic alcohol **17** in 75% yield.<sup>16</sup> In  $^1\text{H}$  NMR spectrum, the proton signals for compound **17** allylic group were observed at  $\delta$  6.50-6.06 (m), 5.15-5.14 (m) and 4.99-4.94 (m) ppm. In  $^{13}\text{C}$  NMR spectrum, allylic carbon signals were observed at  $\delta$  140.2, 68.4 and 113.2 ppm. This allylic compound **17** was then subjected to Johnson-Claisen rearrangement<sup>17</sup> to obtain the compound **21**. TBDMS group was deprotected in compound **21** using pyridinium-*p*-toluenesulphonate (PPTS) in 87% yield to furnish alcohol **16**.

First we have tried this with Oxone:iodobenzoic acid (1:2) in acetonitrile and water,<sup>18</sup> but the reaction could not furnish the desired product. It results in the generation of complex mixture which was difficult to purify by silica gel column chromatography.



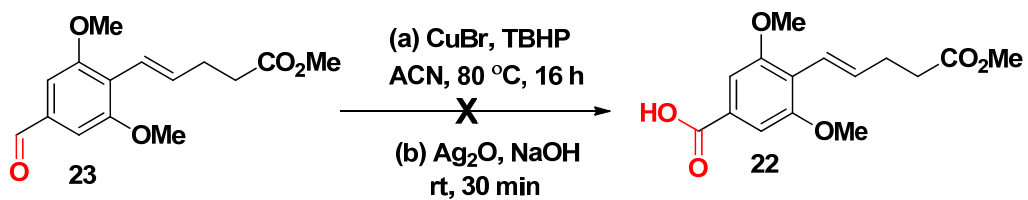
**Scheme 8.** Synthetic efforts carried out for the oxidation of benzylic alcohol **16**.

Again, when the reaction was tried using IBX and HOBT<sup>19</sup> combination, it was unsuccessful. Similarly, when we tried to oxidize alcohol **16** using trichloroisocyanuric acid, TEMPO, sodium bromide, and DCM as a solvent, decomposition of the starting material took place (Scheme 8).<sup>20</sup> However, when we tried to oxidize alcohol **16** using iodoxybenzoic acid (IBX) and DMSO, we could get aldehyde **23** in 94% yield (Scheme 9).



**Scheme 9.** Synthesis of aldehydic compound **23**.

We further tried to oxidize the aldehyde **23** into acid **22** by following methods: (a) CuBr, TBHP (b) Silver Oxide/NaOH.<sup>21</sup> However, none of the methods led to the acid **22** (Scheme 10).

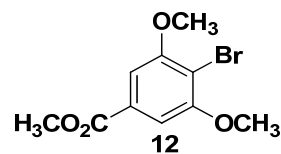


Scheme 10. Synthetic efforts for the oxidation of aldehyde **23** into acid **22**.

## 1.4 Conclusion

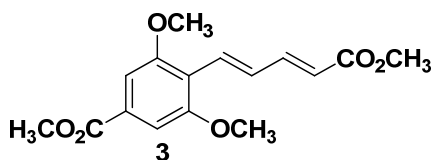
In conclusion, two different synthetic routes were explored towards the synthesis of antibacterial agent oenostacin **1**. Since, the synthesis of target compound **1** could not be accomplished. But we believe that some of the synthesized compounds being close analog of compound **1**, could be useful in deducing valuable structure-activity-relationship (SAR) of bioactive molecules for further studies.

## 1.5 Experimental

Methyl-4-bromo-3,5-dimethoxybenzoate (**12**)

To a stirred suspension of  $K_2CO_3$  (8.91 g, 64.9 mmol) in acetone (20 mL) at room temperature was added 3,5-dihydroxy-4-bromo-benzoic acid (5.0 g, 21.6 mmol). The mixture was stirred for 30 min and then dimethylsulphate (6.15 mL, 64.9 mmol) was added. The reaction mixture was refluxed for 3 h and then filtered through celite. The crude mixture was purified by silica gel column chromatography (PE/EA, 8:2) to isolate product **12** (5.73 g).

<b>Yield</b>	5.73 g, 97%; white solid; $R_f = 0.5$ (PE/EA, 7:3).
<b>Melting Point</b>	122-123°C
<b>Mol. Formula</b>	$C_{10}H_{11}BrO_4$
<b>IR</b> ( $CHCl_3$ )	$\nu_{max}$ ( $cm^{-1}$ ) = 3861, 3860, 3843, 3643, 2936, 2846, 2400, 1741, 1693, 1547, 1515, 1236, 1121.
<b><math>^1H</math> NMR</b> ( $CDCl_3$ , 200 MHz)	$\delta_H$ (ppm) = 7.23 (s, CH, 2H), 3.94 (s, $OCH_3$ , 3H), 3.92 (s, $OCH_3$ , 3H).
<b><math>^{13}C</math> NMR</b> ( $CDCl_3$ , 50 MHz)	$\delta_C$ (ppm) = 166.3 (C), 156.9 (C), 130.1 (CH), 106.5 (CH), 105.4 (CH), 58.5 ( $OCH_3$ ), 56.5 ( $OCH_3$ ), 52.4 ( $OCH_3$ ).
<b>Elemental analysis</b>	Calcd for $C_{10}H_{11}BrO_4$ : C, 43.66; H, 4.03 Found: C, 43.72; H, 4.10.

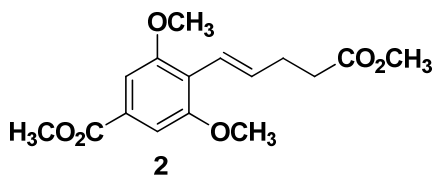
Methyl-3,5-dimethoxy-4-((1E, 3E)-5-methoxy-5-oxopenta-1, 3-dien-1-yl)benzoate (**3**)

To a solution of bromo derivative **12** (2.0 g, 7.32 mmol) in dry DMF (10 ml), potassium carbonate (2.02 g, 14.65 mmol) and palladium acetate (0.82 g, 0.3 mmol) were added and refluxed it at 160 °C for 3 h. The reaction was stirred for 3 h. After

completion it was filtered over celite and filtrate was extracted with EtOAc (3 × 50 mL). The combined organic layer was washed with brine (10 mL), dried over anhydrous Na<sub>2</sub>SO<sub>4</sub> and the solvent was evaporated under reduced pressure. The crude residue was purified by silica gel column chromatography (PE/EA, 9:1) to afford product **3** (0.83 g).

<b>Yield</b>	0.83 g, 37%; yellow solid; $R_f = 0.55$ (PE/EA, 7:3).
<b>Melting Point</b>	104-109°C
<b>Mol. Formula</b>	C <sub>16</sub> H <sub>18</sub> O <sub>6</sub>
<b>IR</b> (CHCl <sub>3</sub> )	$\nu_{\max}$ (cm <sup>-1</sup> ) = 3893, 3860, 3843, 3829, 2948, 2400, 1718, 1238, 747.
<b><sup>1</sup>H NMR</b> (CDCl <sub>3</sub> , 200 MHz)	$\delta_H$ (ppm) = 7.40-7.21 (m, CH, 5H), 6.75-6.55 (m, CH, 1H), 5.96 (d, $J = 14.1$ Hz, CH, 1H), 3.91 (s, OCH <sub>3</sub> , 3H), 3.74 (s, OCH <sub>3</sub> , 3H).
<b><sup>13</sup>C NMR</b> (CDCl <sub>3</sub> , 50 MHz)	$\delta_C$ (ppm) = 167.6 (C), 166.6 (C), 158.7 (C), 147.3 (CH), 131.9 (CH), 131.3 (CH), 130.5 (CH), 120.4 (CH), 117.8 (CH), 104.8 (CH), 55.9 (OCH <sub>3</sub> ), 52.3 (OCH <sub>3</sub> ), 51.4 (OCH <sub>3</sub> ).
<b>Elemental analysis</b>	Calcd for C <sub>16</sub> H <sub>18</sub> O <sub>6</sub> : C, 62.74; H, 5.92 Found: C, 62.81; H, 5.81

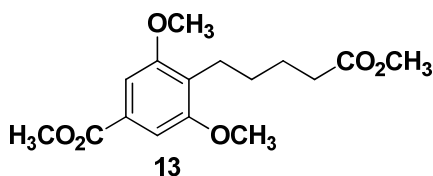
**(E)-Methyl 3,5-dimethoxy-4-(5-methoxy-5-oxopent-1-en-1-yl) benzoate (2)**



To a solution of compound **3** (2.0 g, 6.53 mmol) in anhydrous MeOH (10 mL) and 10% cobalt chloride hexahydrate (190 mg) was added. The resulting solution was cooled at 0 °C for 30 min and slowly NaBH<sub>4</sub> (0.24 g, 6.53 mmol) for 6 h. After completion of the reaction (TLC), MeOH was evaporated and filtrate was extracted with EtOAc (3 × 50 mL). The combined organic layer was washed with brine (10 mL), dried over anhydrous Na<sub>2</sub>SO<sub>4</sub> and the solvent was evaporated under reduced pressure. The crude residue was purified by silica gel column chromatography (PE/EA, 8:2) to furnish pure product **26** (1.71 g).



<b>Yield</b>	1.71 g, 85%; yellow syrupy solid; $R_f = 0.60$ (PE/EA, 8:2).
<b>Mol. Formula</b>	$C_{16}H_{20}O_6$
<b>IR</b> ( $CHCl_3$ )	$\nu_{max}$ ( $cm^{-1}$ ) = 3861, 3843, 3744, 3017, 2950, 1723, 1646, 1578, 1547, 1515, 1458, 1413, 1322, 1238, 1216, 1122.
<b><math>^1H</math> NMR</b> ( $CDCl_3$ , 200 MHz)	$\delta_H$ (ppm) = 7.23 (s, CH, 2H), 3.94 (s, $OCH_3$ , 3H), 3.92 (s, $OCH_3$ , 3H).
<b><math>^{13}C</math> NMR</b> ( $CDCl_3$ , 50 MHz)	$\delta_C$ (ppm) = 166.3 (C), 156.9 (C), 130.1 (CH), 106.5 (CH), 105.4 (CH), 58.5 ( $OCH_3$ ), 56.5 ( $OCH_3$ ), 52.4 ( $OCH_3$ ).
<b>Elemental analysis</b>	Calcd for $C_{16}H_{20}O_6$ : C, 62.33; H, 6.54 Found: C, 62.41; H, 6.62.

**Methyl-3,5-dimethoxy-4-(5-methoxy-5-oxopentyl) benzoate (13)**

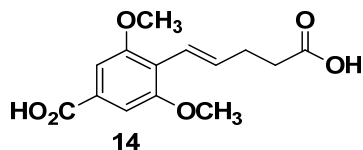
To a solution of compound **3** (0.5 g, 1.612 mmol) in anhydrous MeOH (10 mL), 10% Pd/C (50 mg) was added and the resulting heterogeneous solution was stirred vigorously under  $H_2$  atm for 6 h. After completion of the reaction (TLC), the mixture was filtered over celite. The filtrate was evaporated and purified by silica gel column chromatography (PE/EA, 8:2) to furnish pure product **13** (0.41 mg).

<b>Yield</b>	0.41 g, 80%; syrupy solid; $R_f = 0.62$ (PE/EA, 8:2).
<b>Mol. Formula</b>	$C_{16}H_{22}O_6$
<b>IR</b> ( $CHCl_3$ )	$\nu_{max}$ ( $cm^{-1}$ ) = 3861, 3843, 3019, 2954, 1725, 1582, 1248, 1221, 1130.
<b><math>^1H</math> NMR</b> ( $CDCl_3$ , 200 MHz)	$\delta_H$ (ppm) = 7.23 (s, CH, 2H), 3.91 (s, $OCH_3$ , 3H), 3.85 (s, $OCH_3$ , 3H), 3.66 (s, $OCH_3$ , 3H), 2.68 (t, $J = 7.5$ Hz, 2H), 2.34 (t, $J = 7.8$ Hz, 2H), 1.69-1.61 (m, $CH_2$ , 2H), 1.53-1.49 (m, $CH_2$ , 2H).

**$^{13}\text{C}$  NMR**  $\delta_{\text{C}}$  (ppm) = 174.3 (C), 167.1 (C), 157.9 (C), 128.5 (CH), 124.4 (CH), 104.8 (CH), 55.7 (OCH<sub>3</sub>), 52.1 (OCH<sub>3</sub>), 51.4 (OCH<sub>3</sub>), 33.9 (CH<sub>2</sub>), 30.9 (CH<sub>2</sub>), 24.8 (CH<sub>2</sub>), 22.6 (CH<sub>2</sub>).

**Elemental analysis** Calcd for C<sub>16</sub>H<sub>22</sub>O<sub>6</sub>: C, 61.92; H, 7.15  
Found: C, 61.99; H, 7.23.

**(E)-4-(4-carboxybut-1-en-1-yl)-3,5-dimethoxybenzoic acid (14)**



To a solution of compound **2** (0.5 g, 1.61 mmol) in MeOH-H<sub>2</sub>O (8 mL, 3:1) NaOH was added and the resulting solution was heated at reflux 3 h under an N<sub>2</sub> atmosphere. The reaction mixture was acidified with 1N HCl (10 mL) and then extracted with EtOAc (3 × 20 mL). The crude residue was purified by silica gel column chromatography (PE/EA, 6:4) to give acid **14** (0.30 g).

**Yield** 0.30 g, 67%; white solid;  $R_f$  = 0.20 (PE/EA, 7:3).

**Mol. Formula** C<sub>14</sub>H<sub>16</sub>O<sub>6</sub>

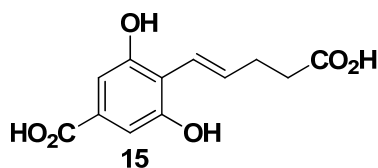
**IR** (CHCl<sub>3</sub>)  $\nu_{\text{max}}$  (cm<sup>-1</sup>) = 3861, 3843, 3019, 2954, 1725, 1582, 1248, 1221, 1130.

**$^1\text{H}$  NMR**  $\delta_{\text{H}}$  (ppm) = 7.26-7.25 (s, CH, 3H), 6.73-6.66 (m, CH, 1H), 3.84 (s, OCH<sub>3</sub>, 3H), 2.69 (t,  $J$  = 7.3 Hz, 2H), 2.30 (t,  $J$  = 7.8 Hz, 2H).

**$^{13}\text{C}$  NMR**  $\delta_{\text{C}}$  (ppm) = 177.9 (C), 170.1 (C), 159.5 (C), 136.5 (CH), 130.7 (C), 125.4 (CH), 122.2 (C), 106.1 (CH), 56.3 (OCH<sub>3</sub>), 34.9 (CH<sub>2</sub>), 29.5 (CH<sub>2</sub>).

**Elemental analysis** Calcd for C<sub>14</sub>H<sub>16</sub>O<sub>6</sub>: C, 59.99; H, 5.75  
Found: C, 60.01; H, 5.82.

**(E)-4-(4-carboxybut-1-en-1-yl)-3,5-dihydroxybenzoic acid (15)**



To a solution of compound **14** (0.282 g, 1.0 mmol) in dry acetonitrile (3.0 mL), chlorotrimethylsilane (0.216 g, 2.0 mmol), sodium iodide (0.45 g, 3.0 mmol) was added and heated at 100 °C under reflux under N<sub>2</sub> atmosphere. The reaction was refluxed for 3 h and acetonitrile was evaporated, acidified with 1N HCl and extracted with EtOAc (3 × 50 mL). The combined organic layer was washed with brine (10 mL), dried over anhydrous Na<sub>2</sub>SO<sub>4</sub> and the solvent was evaporated under reduced pressure. The crude residue was purified by silica gel column chromatography (PE/EA, 8:2) to furnish pure product **26** (0.105 g).

**Yield** 0.105 g, 42%; yellow syrupy solid;  $R_f = 0.2$  (PE/EA, 1:1).

**Mol. Formula** C<sub>12</sub>H<sub>12</sub>O<sub>6</sub>

**IR** (CHCl<sub>3</sub>)  $\nu_{\max}$  (cm<sup>-1</sup>) = 3861, 3843, 3019, 2954, 1725, 1582, 1248, 1221, 1130.

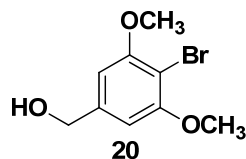
**<sup>1</sup>H NMR** (Acetone-D<sub>6</sub>, 200 MHz)  $\delta_H$  (ppm) = 7.96-7.05 (m, CH, 4H), 3.26 (t,  $J = 8.0$  Hz, 2H), 2.62 (t,  $J = 7.5$  Hz, 2H).

**<sup>13</sup>C NMR** (Acetone-D<sub>6</sub>, 50 MHz)  $\delta_C$  (ppm) = 172.6 (C), 171.8 (C), 151.1 (C), 134.1 (CH), 130.9 (CH), 126.4 (CH), 120.9 (CH), 119.4 (CH), 117.9 (CH), 117.9 (CH), 35.2 (CH<sub>2</sub>), 33.7 (CH<sub>2</sub>).

**Elemental analysis** Calcd for C<sub>12</sub>H<sub>12</sub>O<sub>6</sub>: C, 57.14; H, 4.80

Found: C, 57.23; H, 4.89.

**(4-Bromo-3,5-dimethoxyphenyl) methanol (20)**

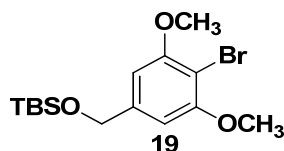


To an ice-cold solution of compound **12** (2.0 g, 7.32 mmol) in anhydrous THF (10 mL), LAH (0.27 g, 7.32 mmol) was added slowly and stirred at room temperature for 4 h under an argon atmosphere. After completion of the reaction, it was cooled to 0-5 °C and quenched with 1N NaOH (10 mL). The resulting white precipitate was filtered through Celite and the filtrate was dried over anhydrous Na<sub>2</sub>SO<sub>4</sub> and evaporated to

give a crude residue which was purified by silica gel column chromatography (PE/EA, 7:3) to furnish product **20** (1.56 g).

<b>Yield</b>	1.56 g, 87%; colorless oil; $R_f$ = 0.61 (PE/EA, 9:1).
<b>Melting Point</b>	98-100°C
<b>Mol. Formula</b>	$C_9H_{11}BrO_3$
<b>IR</b> ( $CHCl_3$ )	$\nu_{max}$ ( $cm^{-1}$ ) = 3894, 3860, 3843, 3643, 2936, 2846, 2401, 1741, 1706, 1693, 1547, 1515, 1236, 1121.
<b><math>^1H</math> NMR</b> ( $CDCl_3$ , 200 MHz)	$\delta_H$ (ppm) = 6.57 (s, CH, 2H), 4.64 (s, $CH_2$ , 2H), 3.89 (s, $OCH_3$ , 3H).
<b><math>^{13}C</math> NMR</b> ( $CDCl_3$ , 50 MHz)	$\delta_C$ (ppm) = 156.8 (C), 141.5 (CH), 102.8 (CH), 99.4 (C), 64.7 ( $CH_2$ ), 56.2 ( $OCH_3$ ).
<b>Elemental analysis</b>	Calcd for $C_9H_{11}BrO_3$ : C, 43.75; H, 4.49 Found: C, 43.82; H, 4.52.

**((4-Bromo-3, 5-dimethoxybenzyl)oxy)(tert-butyl)dimethylsilane (19)**



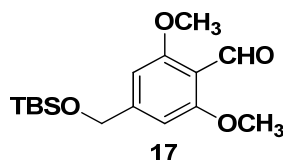
To a solution of compound **20** (3.92 g, 16.0 mmol), in anhydrous DMF (10 mL) imidazole (1.67 g, 24.5 mmol) and TBSCl (3.7 g, 24.5 mmol) was added. The reaction was stirred at room temperature for 7 h. After completion the precipitate, water was added and it was extracted with EtOAc (3 × 50 mL). The combined organic layer was washed with brine (10 mL), dried over anhydrous  $Na_2SO_4$  and the solvent was evaporated under reduced pressure. The crude residue was purified by silica gel column chromatography (PE/EA, 8:2) to afford product **19** (5.47 g).

<b>Yield</b>	5.47 g, 95%; colorless oil; $R_f$ = 0.76 (PE/EA, 7:3).
<b>Mol. Formula</b>	$C_9H_{11}BrO_3Si$
<b>IR</b> ( $CHCl_3$ )	$\nu_{max}$ ( $cm^{-1}$ ) = 3744, 2931, 2890, 2854, 1693, 1547, 1514, 1460, 1415, 1367, 1329, 1255, 1229, 1158.
<b><math>^1H</math> NMR</b> ( $CDCl_3$ , 200 MHz)	$\delta_H$ (ppm) = 6.56 (s, CH, 2H), 4.70 (s, $CH_2$ , 2H), 3.87 (s, $OCH_3$ , 3H), 0.94 (s, $CH_3$ , 9H), 0.10 (s, $Si(CH_3)_2$ , 6H).

**$^{13}\text{C}$  NMR**  $\delta_{\text{C}}$  (ppm) = 156.9 (C), 142.5 (C), 102.2 (CH), 98.8 (CH), 64.6 (CH<sub>2</sub>), 56.3 (OCH<sub>3</sub>), 25.8 (CH<sub>3</sub>)<sub>3</sub>C), 18.3 (CH<sub>3</sub>)<sub>3</sub>C), -5.27 (Si(CH<sub>3</sub>)<sub>2</sub>).

**Elemental analysis** Calcd for C<sub>9</sub>H<sub>11</sub>BrO<sub>3</sub>Si: C, 63.87; H, 8.93  
Found: C, 63.81; H, 8.86.

**4-(((*tert*-Butyldimethylsilyl)oxy)methyl)-2,6-dimethoxybenzaldehyde (17)**



To a -78 °C cooled solution of compound **19** (2.0 g, 5.55 mmol) in anhydrous THF (10 mL) *n*-butyl lithium (5.21 mL, 8.33 mmol, 1.6 M in hexane) was slowly added. The reaction mixture was warmed at 0-5 °C for 0.5 h, again cooled at -78 °C and dimethyl formamide (DMF) (0.65 mL, 8.33 mmol, 1.6 M in hexane) was slowly added at and stirring was continued for another 0.5 h. The reaction mixture was stirred for 1 h, it was quenched with aqueous NH<sub>4</sub>Cl solution (2 mL) and extracted with EtOAc (3 × 50 mL). The combined organic layer was washed with brine (10 mL), dried over anhydrous Na<sub>2</sub>SO<sub>4</sub> and the solvent was evaporated under reduced pressure. The crude residue was purified by silica gel column chromatography (PE/EA, 8:2) to give aldehyde **17** (1.12 g).

**Yield** 1.12 g, 65%; colorless oil;  $R_f$  = 0.30 (PE/EA, 7:3).

**Mol. Formula** C<sub>10</sub>H<sub>26</sub>O<sub>4</sub>Si

**IR** (CHCl<sub>3</sub>)  $\nu_{\text{max}}$  (cm<sup>-1</sup>) = 3743, 3441, 2933, 2855, 1676, 1608, 1576, 1514, 1461, 1409, 1366, 1320, 1229, 1124, 1070.

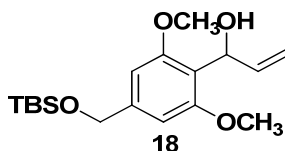
**$^1\text{H}$  NMR**  $\delta_{\text{H}}$  (ppm) = 10.38 (s, CHO, 1H), 6.50 (s, CH, 2H), 4.67 (s, CH<sub>2</sub>, 2H), 3.81 (s, OCH<sub>3</sub>, 3H), 0.89 (s, CH<sub>3</sub>, 9H), 0.05 (s, SiCH<sub>3</sub>, 6H).

**$^{13}\text{C}$  NMR**  $\delta_{\text{C}}$  (ppm) = 188.8 (CHO), 162.1 (C), 150.8 (C), 100.5 (CH), 105.4 (CH), 64.4 (CH<sub>2</sub>), 55.7 (OCH<sub>3</sub>), 25.7 (CH<sub>3</sub>), 18.1 (C), -5.5 (SiCH<sub>3</sub>).

**Elemental analysis** Calcd for C<sub>10</sub>H<sub>26</sub>O<sub>4</sub>Si: C, 61.90; H, 8.44

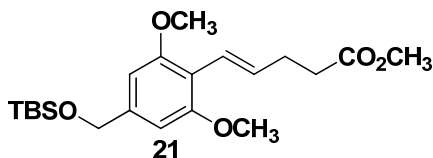
Found: C, 61.98; H, 8.51.

**1-(4-(((*tert*-Butyldimethylsilyl)oxy)methyl)-2,6-dimethoxyphenyl)prop-2-en-1-ol**  
(18)



To a 0-5 °C cooled solution of compound **17** (1.0 g, 3.22 mmol) in anhydrous THF (10 mL), vinyl magnesium bromide (3.22 mL, 3.22 mmol, 1.0 M in THF) was slowly added and stirring was continued for 5 h. After completion of the reaction (TLC), it was quenched with aqueous NH<sub>4</sub>Cl solution (2 mL) and extracted with EtOAc (3 × 50 mL). The combined organic layer was washed with brine (10 mL), dried over anhydrous Na<sub>2</sub>SO<sub>4</sub> and the solvent was evaporated under reduced pressure. The crude residue was purified by silica gel column chromatography (PE/EA, 7:3) to give allylic alcohol **18** (0.82 g).

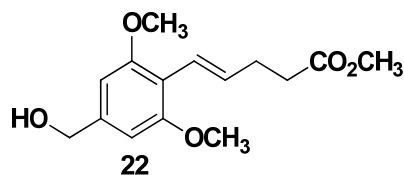
<b>Yield</b>	0.82 g, 75%; yellowish oil; $R_f = 0.25$ (PE/EA, 7:3).
<b>Mol. Formula</b>	C <sub>18</sub> H <sub>30</sub> O <sub>4</sub> Si
<b>IR</b> (CHCl <sub>3</sub> )	$\nu_{\max}$ (cm <sup>-1</sup> ) = 3843, 3744, 3678, 3648, 3619, 3564, 3014, 2932, 2855, 1740, 1693, 1646, 1586, 1515, 1461, 1420, 1367, 1314, 1253, 1216, 1110.
<b><sup>1</sup>H NMR</b> (CDCl <sub>3</sub> , 200 MHz)	$\delta_H$ (ppm) = 6.50 (s, CH, 2H), 6.18-6.01 (m, CH, 1H), 5.61-5.52 (m, CH, 1H), 5.15-4.93 (m, CH <sub>2</sub> , 2H), 4.65 (s, CH <sub>2</sub> , 2H), 3.75 (s, OCH <sub>3</sub> , 3H), 0.89 (s, CH <sub>3</sub> , 9H), 0.04 (s, SiCH <sub>3</sub> , 6H).
<b><sup>13</sup>C NMR</b> (CDCl <sub>3</sub> , 50 MHz)	$\delta_C$ (ppm) = 157.5 (C), 142.7 (C), 140.2 (C), 116.6 (CH <sub>2</sub> ), 113.1 (CH), 101.8 (CH), 105.4 (CH), 68.3 (CH <sub>2</sub> ), 64.8 (CH), 55.7 (OCH <sub>3</sub> ), 25.8 (CH <sub>3</sub> ), 18.3 (C), -5.3 (SiCH <sub>3</sub> ).
<b>Elemental analysis</b>	Calcd for C <sub>18</sub> H <sub>30</sub> O <sub>4</sub> Si: C, 62.74; H, 5.92 Found: C, 62.81; H, 5.81.

**(E)-Methyl-5-(4-(((tert-butyldimethylsilyl)oxy)methyl)-2,6-dimethoxyphenyl)pent-4-enoate (21)**

To a solution of compound **18** (4.0 g, 11.8 mmol) in xylene (5 mL), trimethyl-*o*-acetate (20.2 mL, 16.2 mmol) and propionic acid (40  $\mu$ L) was added in catalytic amount. The resulting mixture was refluxed at 140  $^{\circ}$ C for 6 h. After completion of the reaction (TLC), the xylene was evaporated under reduced pressure. The crude reaction residue was purified by silica gel column chromatography (PE/EA, 8:2) to give pure product **21** (3.5 g).

<b>Yield</b>	3.5 g, 75%; colorless oil; $R_f$ = 0.40 (PE/EA, 7:3).
<b>Mol. Formula</b>	$C_{21}H_{34}O_5Si$
<b>IR</b> ( $CHCl_3$ )	$\nu_{max}$ ( $cm^{-1}$ ) = 3861, 3843, 3829, 3743, 3678, 3648, 3618, 3589, 3557, 3501, 2936, 2850, 1727, 1647, 1609, 1579, 1547, 1514, 1460, 1418, 1366, 1317, 1220, 1124.
<b><math>^1H</math> NMR</b> ( $CDCl_3$ , 200 MHz)	$\delta_H$ (ppm) = 6.94 (d, $J$ = 16.3 Hz, CH, 1H), 6.72-6.64 (m, CH, 2H), 6.53 (d, $J$ = 12.0 Hz, CH, 1H), 4.71 (s, $CH_2$ , 2H), 3.85 (s, $OCH_3$ , 3H), 3.83 (s, $OCH_3$ , 3H), 2.37 (t, $J$ = 7.8 Hz, $CH_2$ , 2H), 1.15 (t, $J$ = 7.5 Hz, $CH_2$ , 2H), 0.09 (s, $CH_3$ , 9H), -0.02 (s, $SiCH_3$ , 6H).
<b><math>^{13}C</math> NMR</b> ( $CDCl_3$ , 50 MHz)	$\delta_C$ (ppm) = 174.5 (C), 158.5 (C), 142.62 (C), 126.2 (CH), 124.6 (CH), 102.2 (CH), 67.0 ( $CH_2$ ), 55.7 ( $OCH_3$ ), 55.6 ( $OCH_3$ ), 34.5 ( $CH_2$ ), 27.7 ( $CH_2$ ), 25.9 ( $CH_3$ ), 18.4 (C), 9.2 ( $SiCH_3$ ).
<b>Elemental analysis</b>	Calcd for $C_{21}H_{34}O_5Si$ : C, 63.92; H, 8.69 Found: C, 63.98; H, 8.75.

**(E)-Methyl 5-(4-(hydroxymethyl)-2,6-dimethoxyphenyl)pent-4-enoate (22)**



To a 0 °C cooled solution of compound **21** (1.0 g, 2.54 mmol) in absolute ethanol (10 mL), pyridinium-*p*-toluene sulphonate (0.64 g, 2.54 mmol) was added and stirred for 6 h. After completion of the reaction, ethanol was evaporated under reduced pressure. The crude reaction residue was purified by silica gel column chromatography (PE/EA, 7:3) to give pure product **22** (0.61 g).

**Yield** 0.61 g, 87%; colorless oil;  $R_f = 0.30$  (PE/EA, 7:3).

**Mol. Formula**  $C_{15}H_{20}O_5$

**IR** ( $CHCl_3$ )  $\nu_{max}$  ( $cm^{-1}$ ) = 3843, 3743, 3678, 3648, 3619, 2932, 2846, 1726, 1647, 1581, 1547, 1515, 1459, 1419, 1314, 1214, 1122.

**$^1H$  NMR** ( $CDCl_3$ , 200 MHz)  $\delta_H$  (ppm) = 6.92 (d,  $J = 16.2$  Hz, CH, 1H), 6.73-6.62 (m, CH, 2H), 6.51 (s, CH, 1H), 4.60 (s,  $CH_2$ , 2H), 3.80 (s,  $OCH_3$ , 3H), 3.79 (s,  $OCH_3$ , 3H), 2.32 (t,  $J = 7.8$  Hz,  $CH_2$ , 2H), 1.13 (t,  $J = 7.6$  Hz,  $CH_2$ , 2H).

**$^{13}C$  NMR** ( $CDCl_3$ , 50 MHz)  $\delta_C$  (ppm) = 174.5 (C), 158.5 (C), 141.9 (C), 126.4 (CH), 124.6 (CH), 112.5 (CH), 101.8 (CH), 64.9 ( $CH_2$ ), 55.5 ( $OCH_3$ ), 55.1 ( $OCH_3$ ), 30.7 ( $CH_2$ ), 29.8 ( $CH_2$ ).

**Elemental analysis** Calcd for  $C_{15}H_{20}O_5$ : C, 64.27; H, 7.19

Found: C, 64.32; H, 7.27.



### 1.6 References

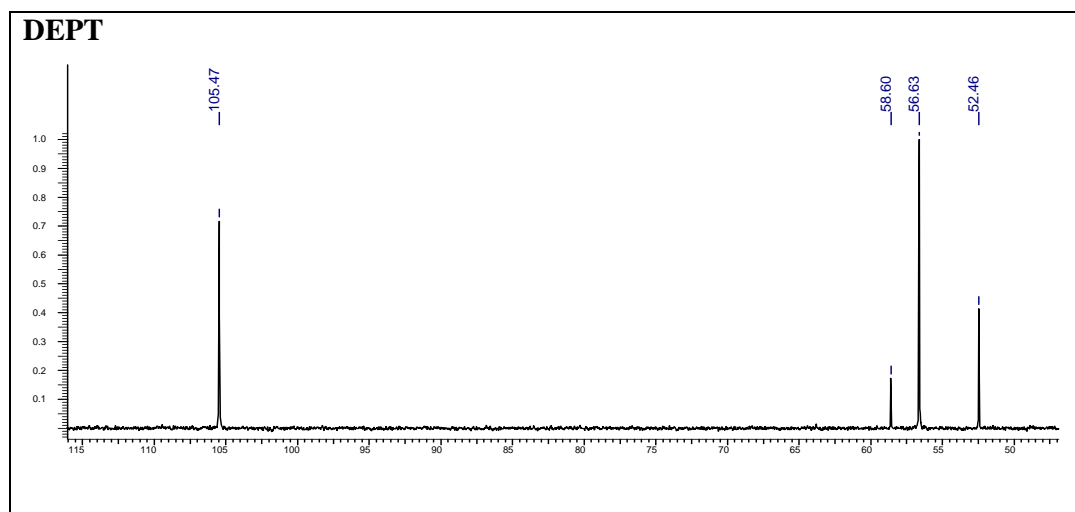
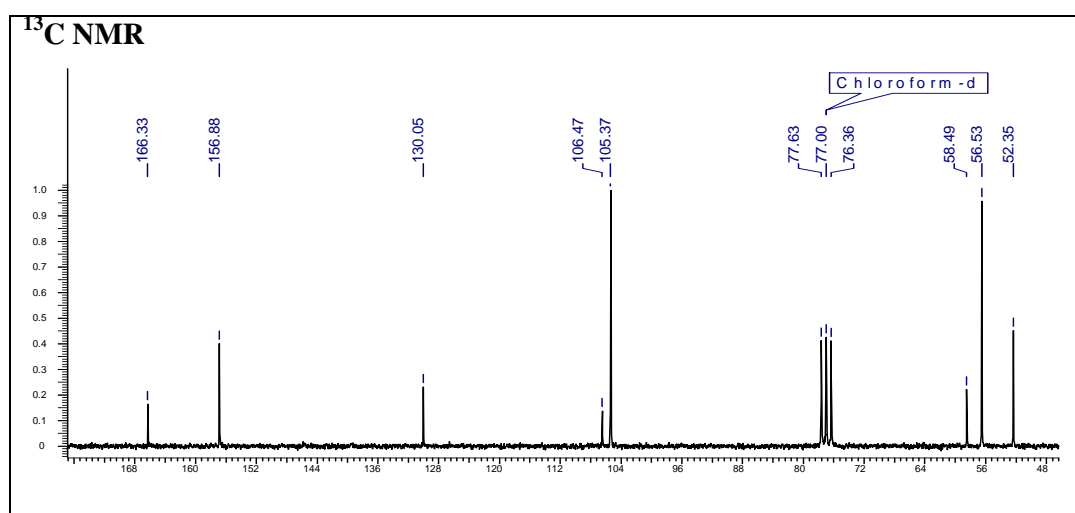
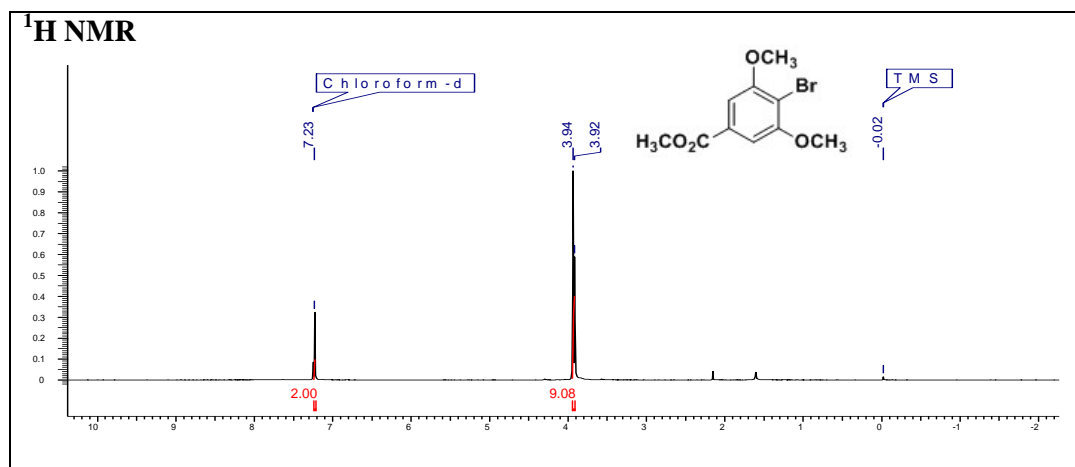
1. (a) Srivastava, V.; Darokar, M. P.; Fatima, A.; Kumar, J. K.; Chowdhury, C.; Saxena, H. O.; Dwivedi, G. R.; Srivastava, K.; Gupta, V.; Chattopadhyay, S. K.; Luqman, S.; Gupta, M. M.; Negi, A. S.; Khanuja, S. P. S. *Bioorg. Med. Chem.* **2007**, *15*, 518; (b) Shukla, Y. N.; Srivastava, A.; Santhakumar, T. R.; Khanuja, S. P. S.; Kumar, S. *Indian Drugs*, **2000**, *37*, 60; (c) Shukla, Y. N.; Srivastava, A.; Kumar, S. *Indian J. Chem.*, **1999**, *38B*, 705.
2. Hudson, B. J. F. *J. Am. Chem. Soc.* **1984**, *61*, 540.
3. Fedeli, E.; Paganuzzi, V.; Tiscorina, E.; *Riv. Ital. Sante Grasse*, **1976**, *53*, 25.
4. Kagan, J. *Phytochemistry*, **1967**, *6*, 317.
5. Yoshida, T.; Chow, T.; Matsuda, M.; Yashuhara, T.; Yazaki, K.; Hatano, T.; Nitta, A.; Okuda, T. *Chem. Pharma. Bull.* **1991**, *39*, 1157.
6. Lesuisse, D.; Berjonneau, J.; Ciot, C.; Devaux, P.; Doucet, B.; Gourvest, J. F.; Khemis, B.; Lang, C.; Legrand, R.; Lowinski, M.; Maquin, P.; Parent, A.; Schoot, B.; Teutsch, G. *J. Nat. Prod.* **1996**, *59*, 490.
7. (a) Botella, L.; Nájera, C. *J. Org. Chem.* **2005**, 4360; (b) Alacid, E.; Nájera, C. *J. Org. Chem.* **2009**, *74*, 2321.
8. Giri, R.; Maugel, N.; Li, J. -J.; Wang, D. -H.; Breazzano, S. P.; Saunders, L. B.; Yu, J.-Q. *J. Am. Chem. Soc.* **2007**, *129*, 3510.
9. (a) Saikia, A.; Barthakur, M. G.; Boruah, R. C. *Synlett* **2005**, 523; (b) Wang, J.; Song, G.; Peng, Y.; Zhu, Y. *Tetrahedron Lett.* **2008**, *49*, 6518.
10. (a) Tonder, J. H. V.; Marais, C.; Cole-Hamilton, D. J.; Bezuidenhoudt, B. C. B. *Synthesis* **2010**, *3*, 421; (b) Blay, G.; Cardona, L.; Pedro, R.; Sa, J. J. *J. Org. Chem.* **1996**, *61*, 3815; (c) Knowles, W. S. *Adv. Synth. Catal.* **2003**, *345*, 3.
11. (a) Jagdale, A. R.; Paraskar, A. S.; Sudalai, A. *Synthesis* **2009**, 660; (b) Jagdale, A. R.; Reddy, R. S.; Sudalai, A. *Org. Lett.* **2009**, *11*, 803; (c) Ranu, B. C.; Samanta, S. *J. Org. Chem.* **2003**, *68*, 7130; (d) Ranu, B. C.; Dutta, J.; Guchhait, S. K. *Org. Lett.* **2001**, *3*, 2603.
12. Olah, G. A.; Narang, S. C.; Gupta, B. G. B.; Malhotra, R. *J. Org. Chem.* **1979**, *44*, 1247.

13. (a) Ram, R. N. *Tetrahedron Lett.* **1997**, *53*, 7335; (b) Ogawa, T.; Hikasa, T.; Ikegami, T.; Ono, N.; Suzuki, H. *J. Chem. Soc. Perkin Trans. 1* **1994**, *1*, 3473; (c) Srinivas, K. V. N. S.; Das, B. *J. Org. Chem.* **2003**, 1165.
14. Corey, E. J.; Venkateswarlu, A. *J. Am. Chem. Soc.* **1972**, *94*, 6190.
15. Nicolaou, K. C.; Sun, Y.-P.; Korman, H.; Sarlah, D. *Angew. Chem. Int. Ed.* **2010**, *49*, 5875.
16. (a) Davis, C. J.; Hurst, T. E.; Jacob, A. M.; Moody, C. J. *J. Org. Chem.* **2005**, *70*, 4414. (b) Jacob, A. M.; Moody, C. J. *Tetrahedron Lett.* **2005**, *46*, 8823.
17. (a) Ziegler, F. E. *Chem. Rev.* **1988**, *88*, 1423; (b) Meza-Aviña, M. E.; Ordoñez, M.; Fernández-Zertuche, M.; Rodríguez-Fragoso, L.; Reyes-Esparza, J.; Ríos-Corsino, A. A. M. de los *Bioorg. Med. Chem.* **2005**, *13*, 6521.
18. Thottumkara, A. P.; Bowsher, M. S.; Vinod, T. K. *Org. Lett.* **2005**, *7*, 2933.
19. Mazitschek, R.; Mülbaier, M.; Giannis, A. *Angew. Chem. Int. Ed.* **2002**, *41*, 4059.
20. (a) Luca, L. D.; Giacomelli, G.; Masala, S.; Porcheddu, A. *J. Org. Chem.* **2003**, *68*, 4999; (b) Luca, L. D.; Giacomelli, G.; Porcheddu, A. *Org. Lett.* **2001**, *3*, 3041.
21. Corey, E. J.; Das, J. *J. Am. Chem. Soc.* **1982**, *104*, 5551.

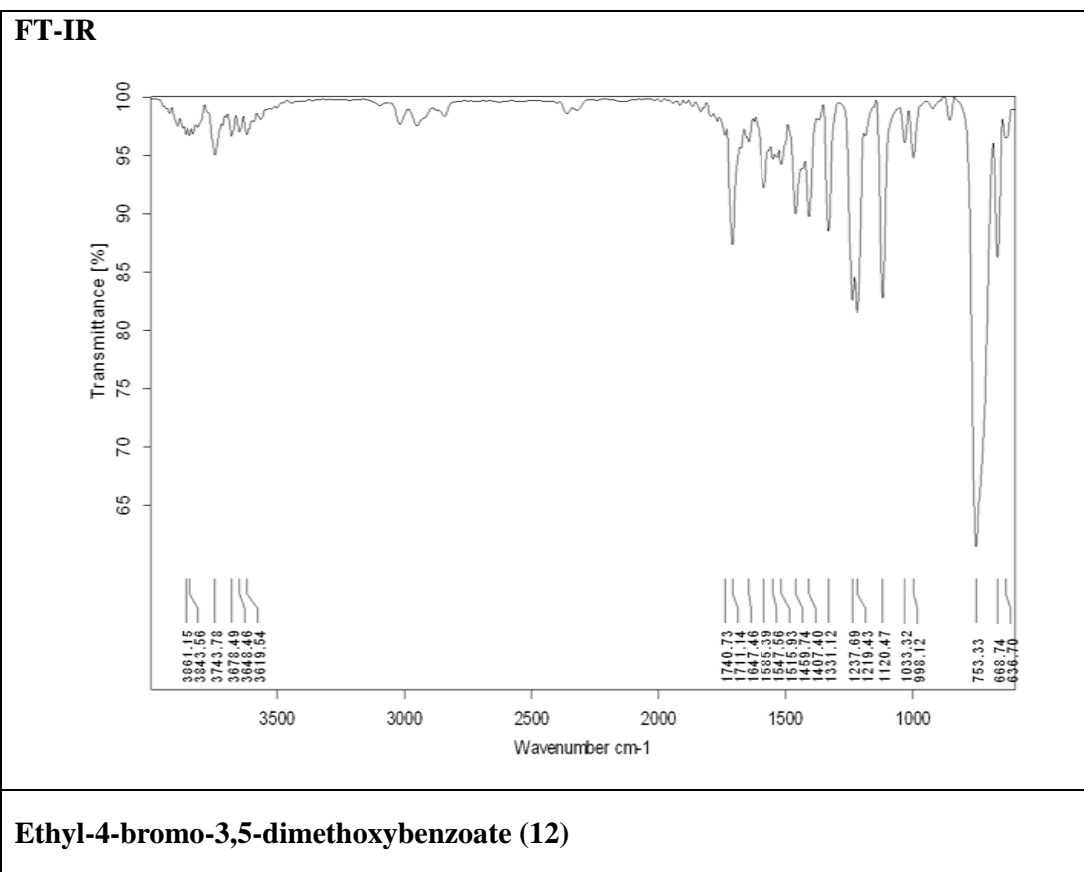
**1.7 Appendix B: Characterization data of synthesized compounds**

Compound	Description	Page No.
Compound 12	<sup>1</sup> H NMR, <sup>13</sup> C NMR, DEPT-NMR, FT-IR	77-78
Compound 3	<sup>1</sup> H NMR, <sup>13</sup> C NMR, DEPT-NMR, FT-IR	79-80
Compound 2	<sup>1</sup> H NMR, <sup>13</sup> C NMR, DEPT-NMR, FT-IR	81-82
Compound 14	<sup>1</sup> H NMR, <sup>13</sup> C NMR, DEPT-NMR	83
Compound 13	<sup>1</sup> H NMR, <sup>13</sup> C NMR, DEPT-NMR	84
Compound 15	<sup>1</sup> H NMR, <sup>13</sup> C NMR, DEPT-NMR	85
Compound 20	<sup>1</sup> H NMR, <sup>13</sup> C NMR, DEPT-NMR, FT-IR	86-87
Compound 19	<sup>1</sup> H NMR, <sup>13</sup> C NMR, DEPT-NMR	88
Compound 17	<sup>1</sup> H NMR, <sup>13</sup> C NMR, DEPT-NMR, FT-IR	89-90
Compound 18	<sup>1</sup> H NMR, <sup>13</sup> C NMR, DEPT-NMR, FT-IR	91-92
Compound 21	<sup>1</sup> H NMR, <sup>13</sup> C NMR, DEPT-NMR	93
Compound 22	<sup>1</sup> H NMR, <sup>13</sup> C NMR, DEPT-NMR	94

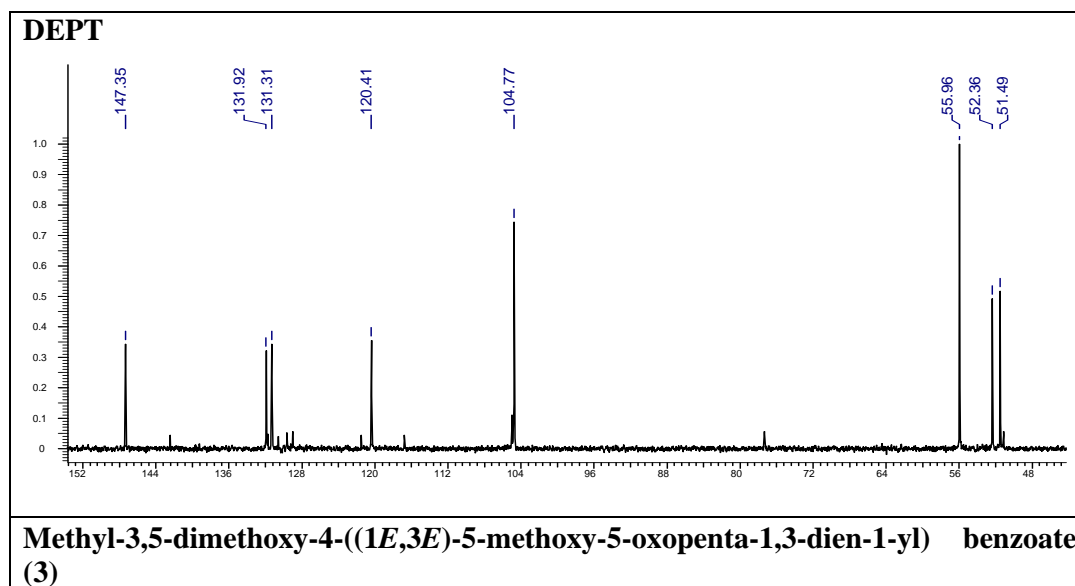
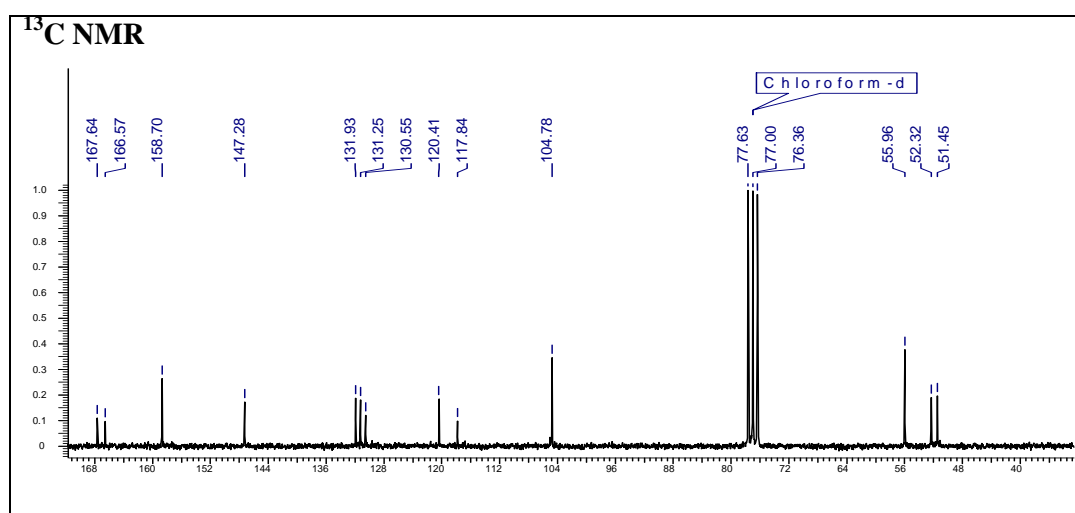
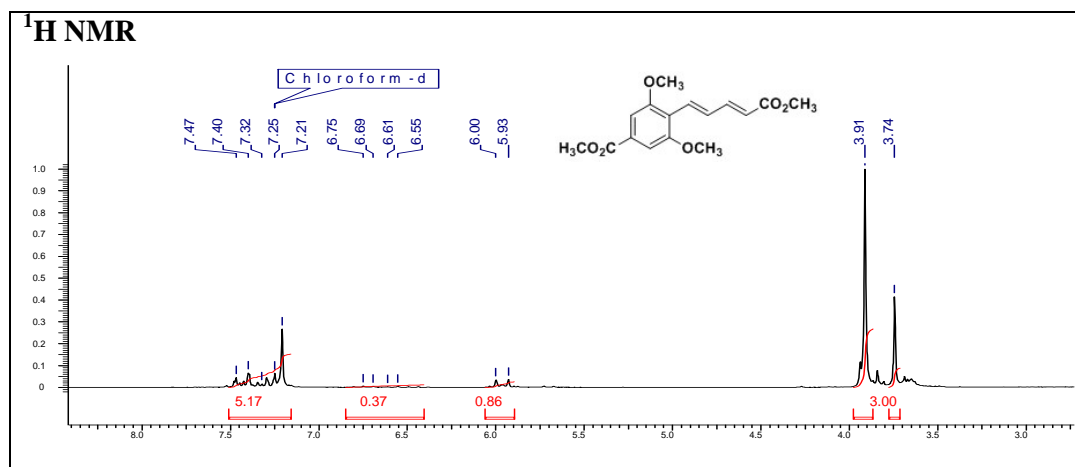
# Chapter 1



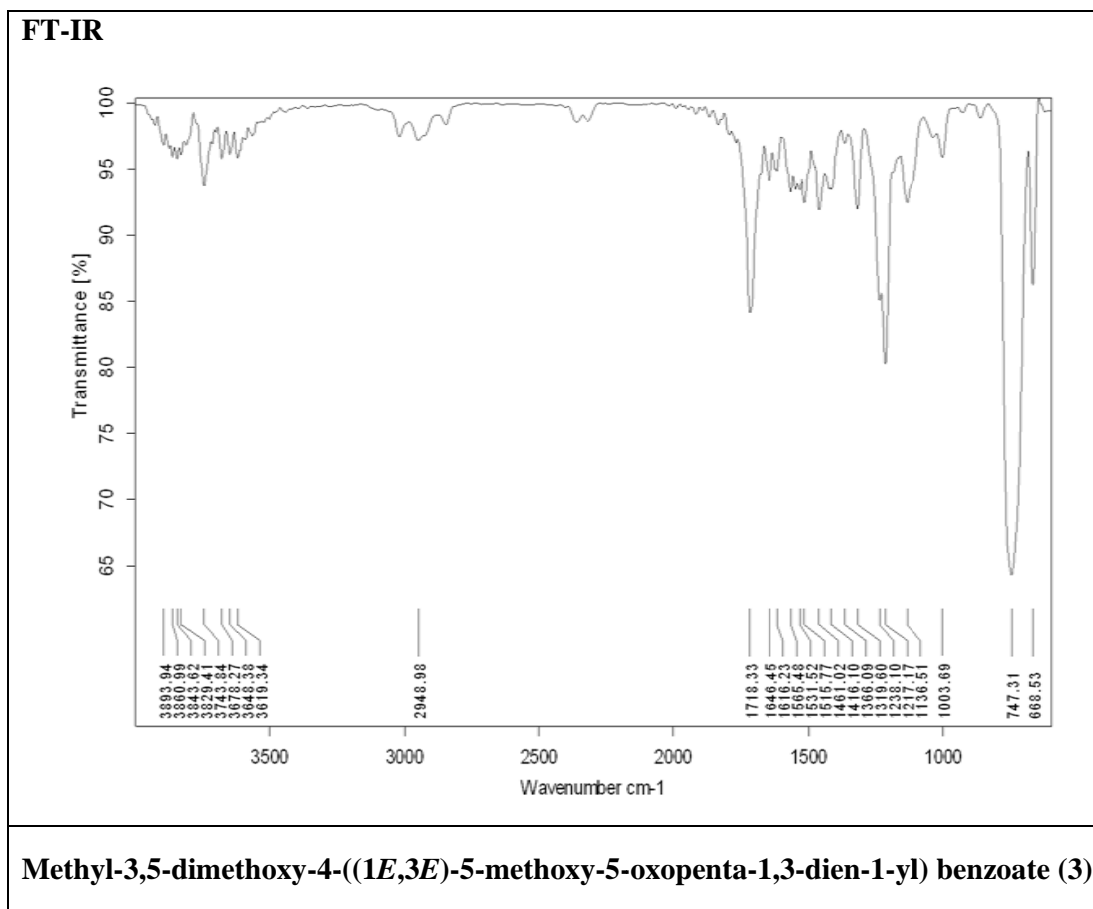
**Ethyl-4-bromo-3,5-dimethoxybenzoate (12)**



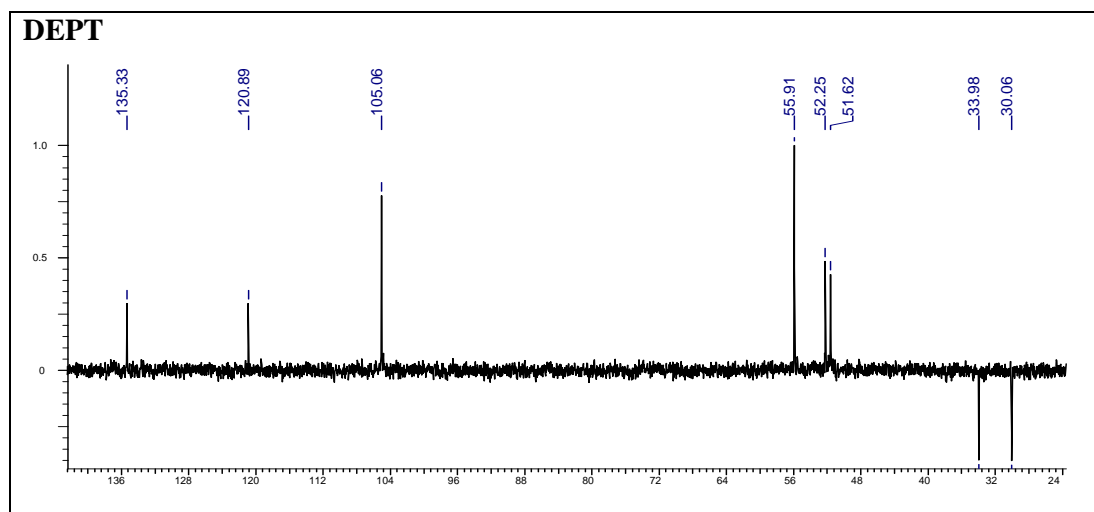
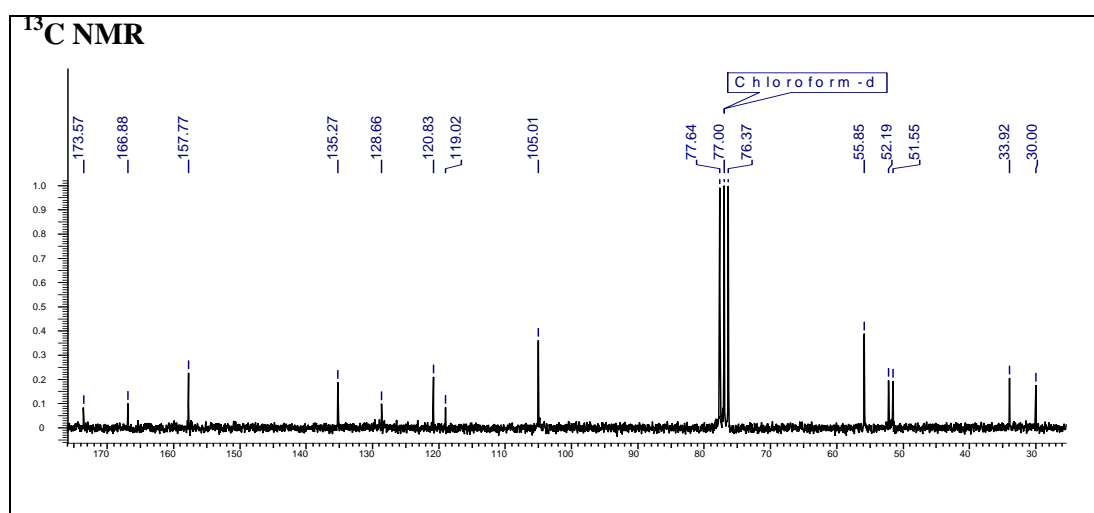
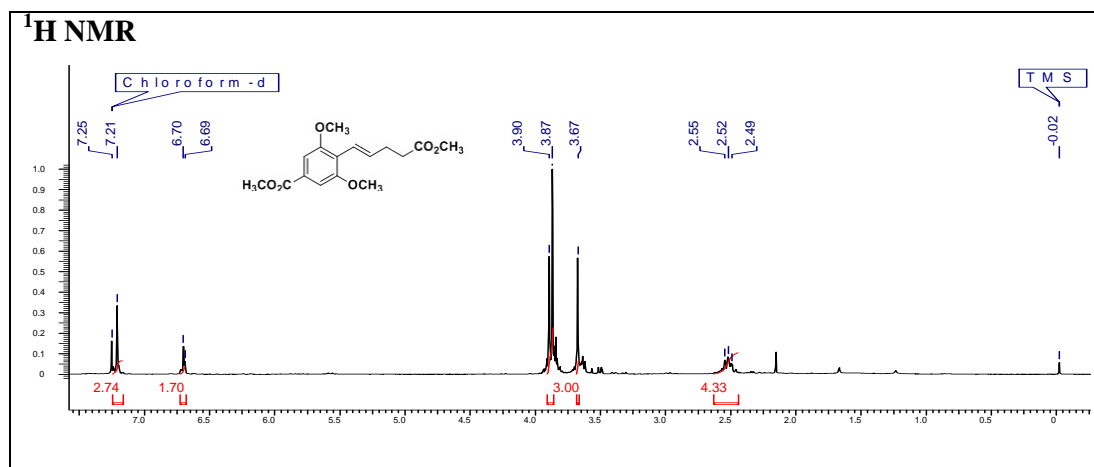
# Chapter 1



**Methyl-3,5-dimethoxy-4-((1E,3E)-5-methoxy-5-oxopenta-1,3-dien-1-yl) benzoate (3)**

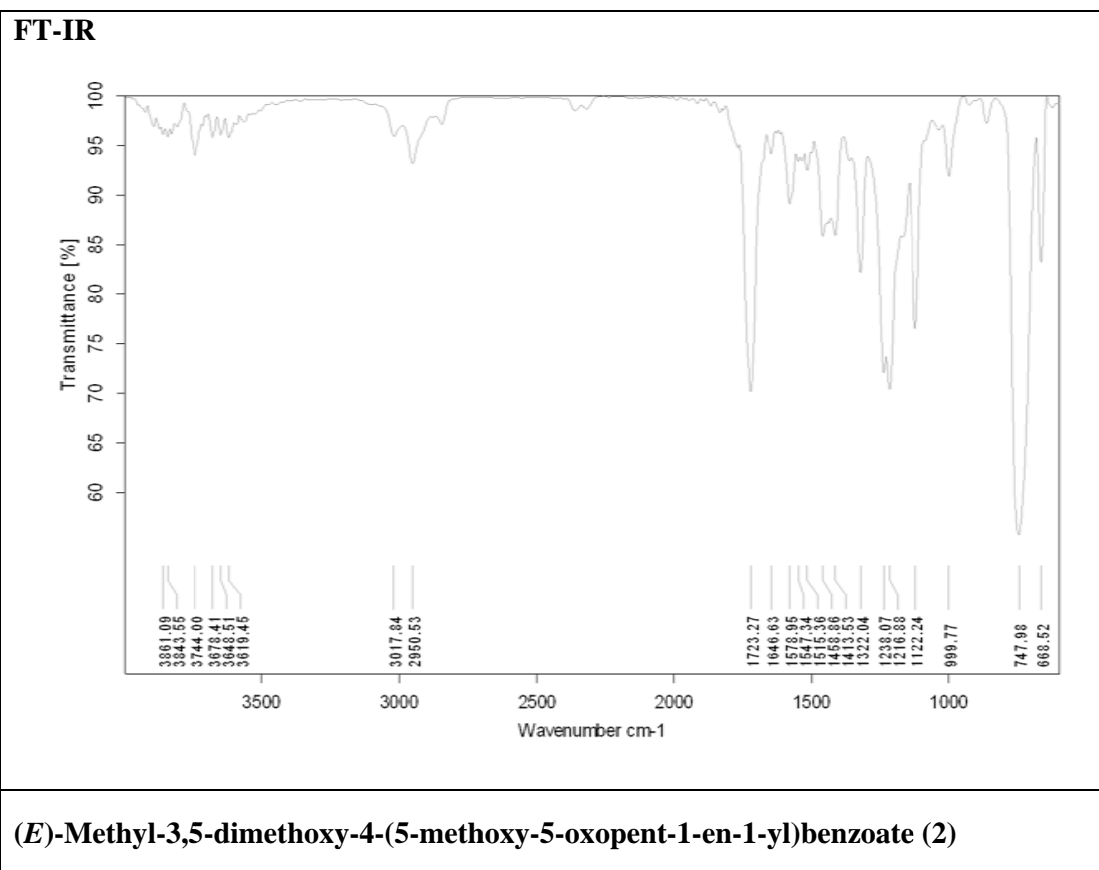


# Chapter 1

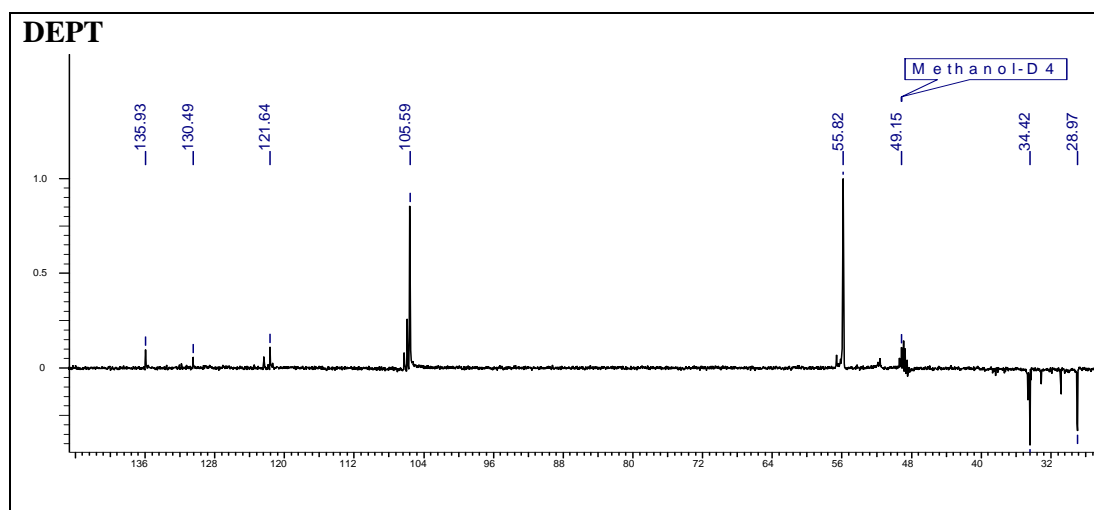
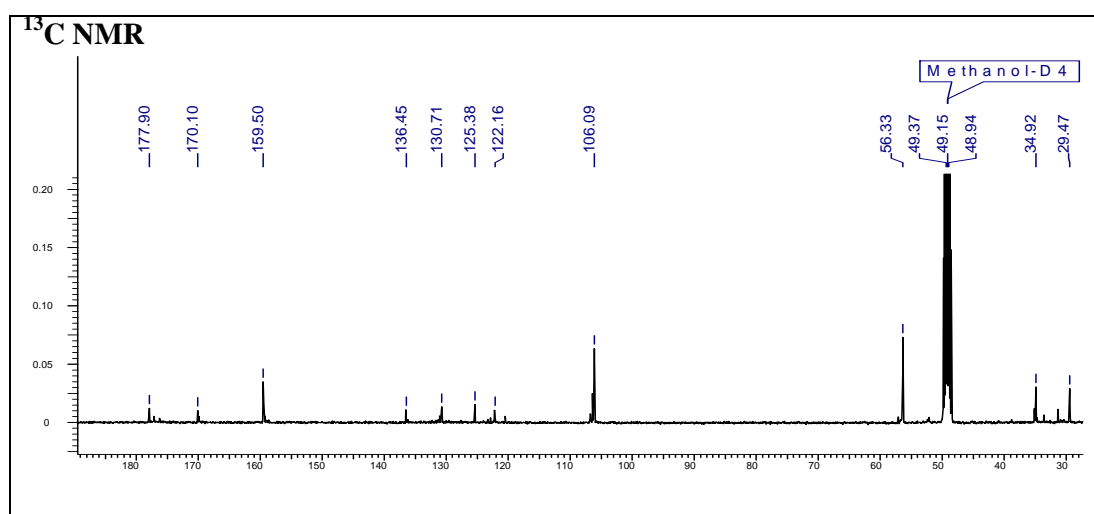
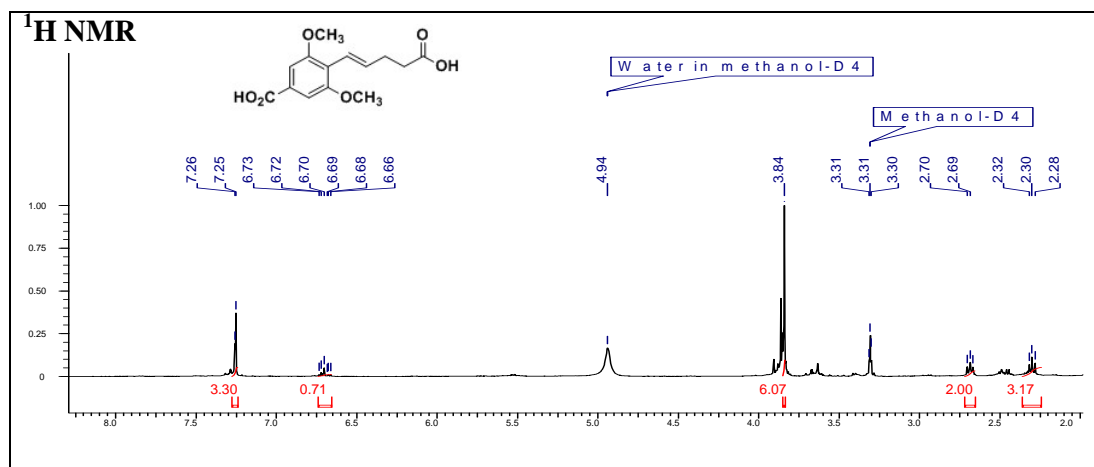


**(E)-Methyl-3,5-dimethoxy-4-(5-methoxy-5-oxopent-1-en-1-yl)benzoate (2)**



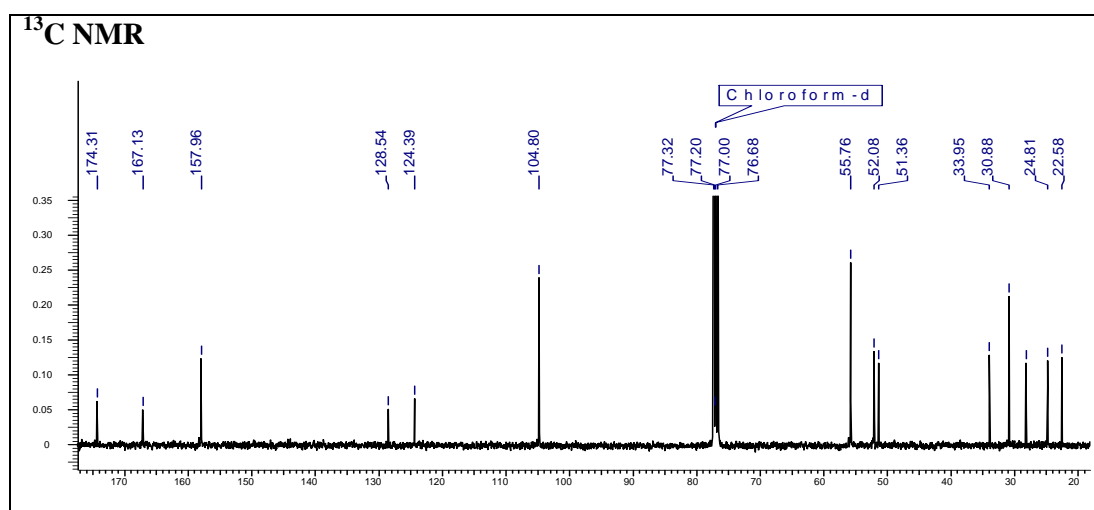
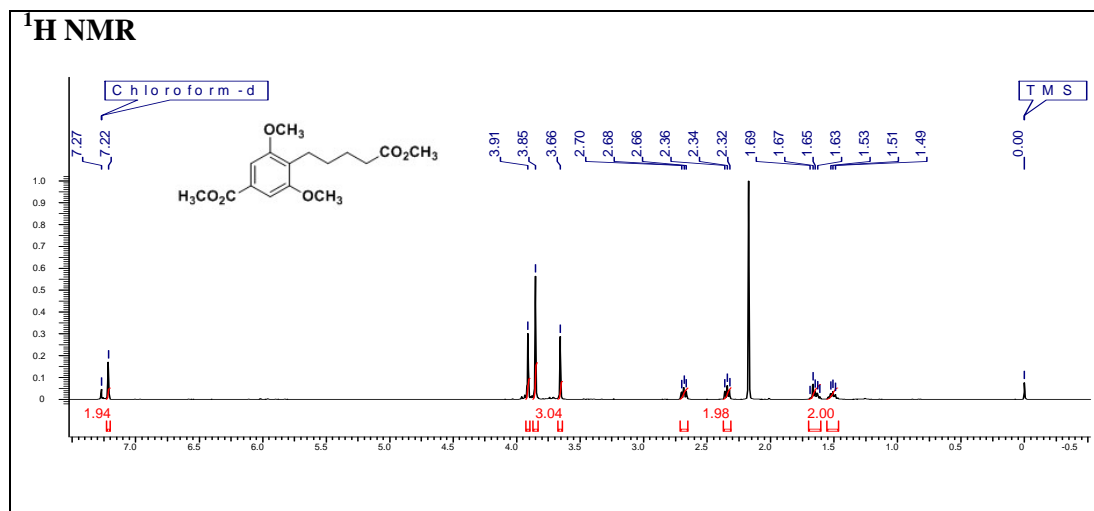


# Chapter 1



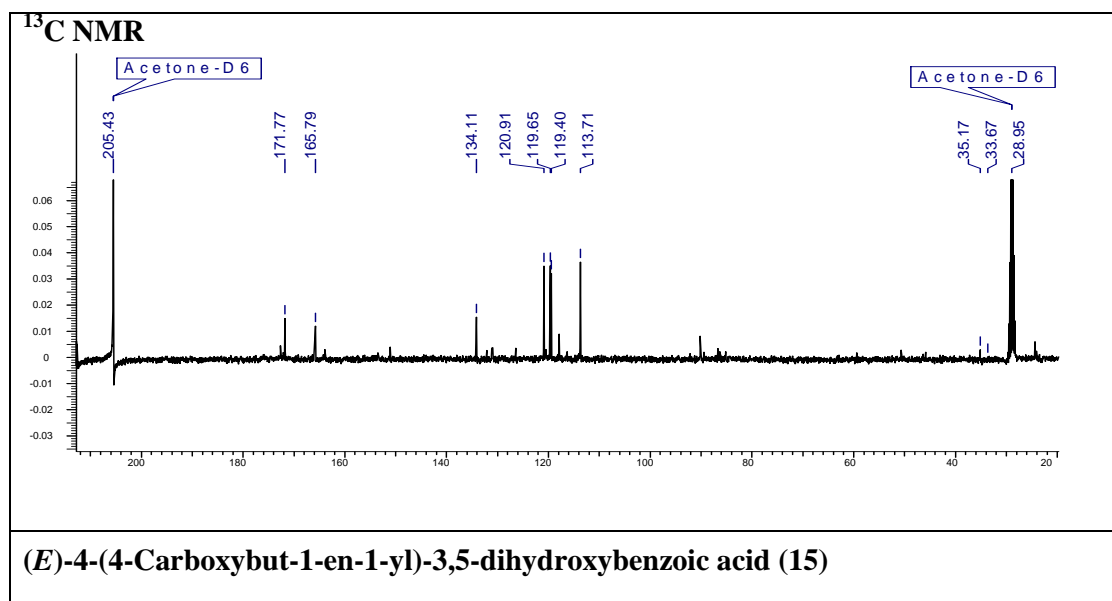
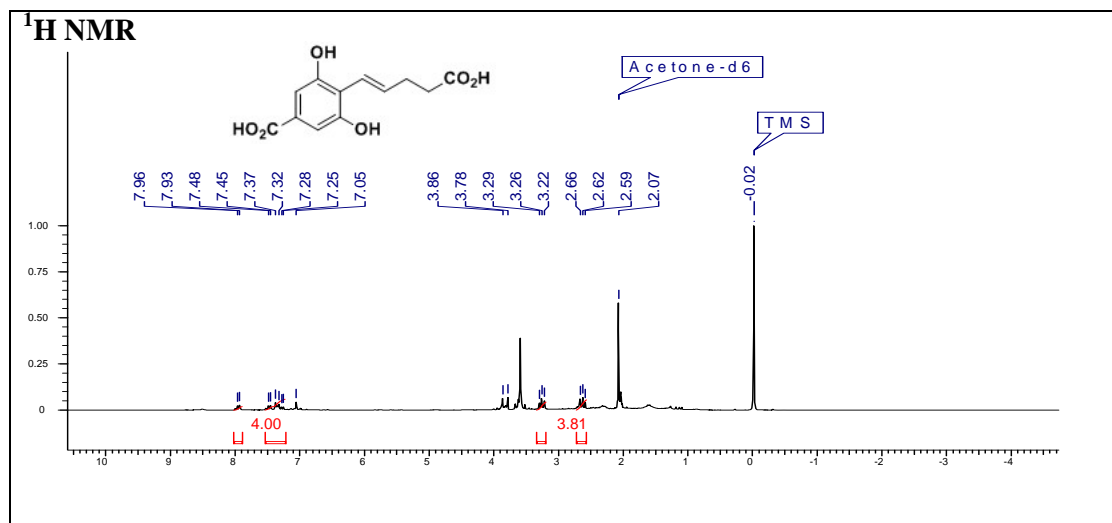
**(E)-4-(4-Carboxybut-1-en-1-yl)-3,5-dimethoxybenzoic acid (14)**

# Chapter 1

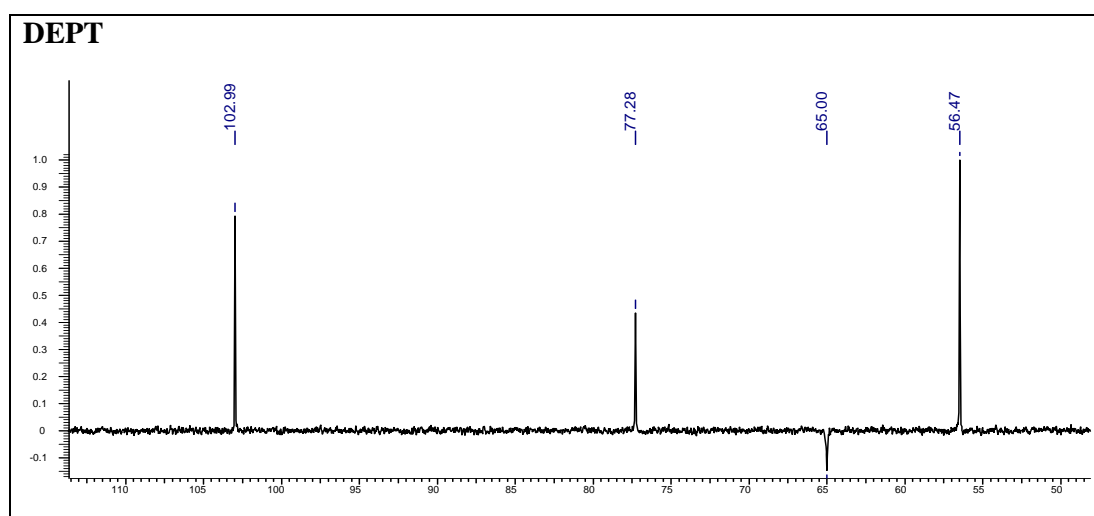
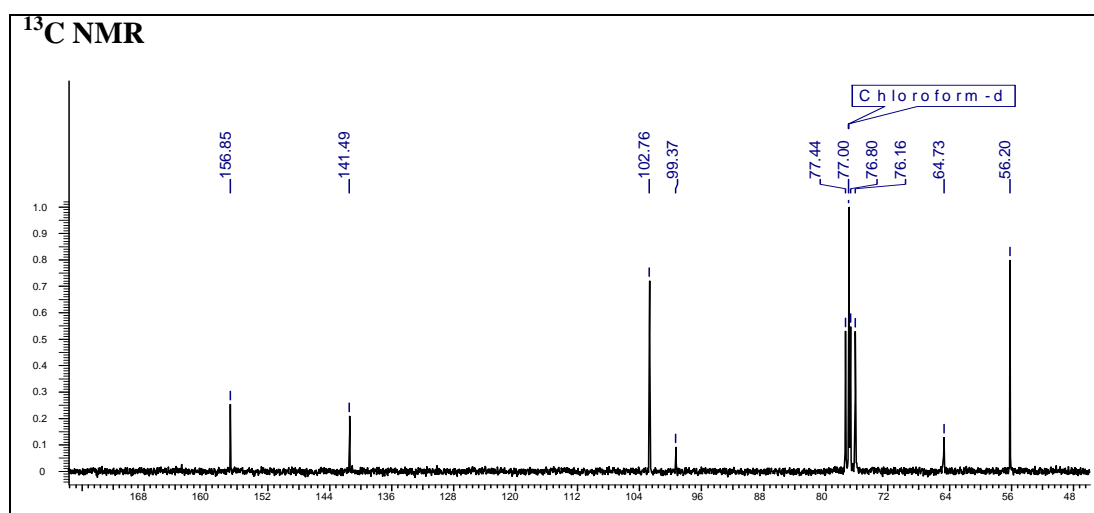
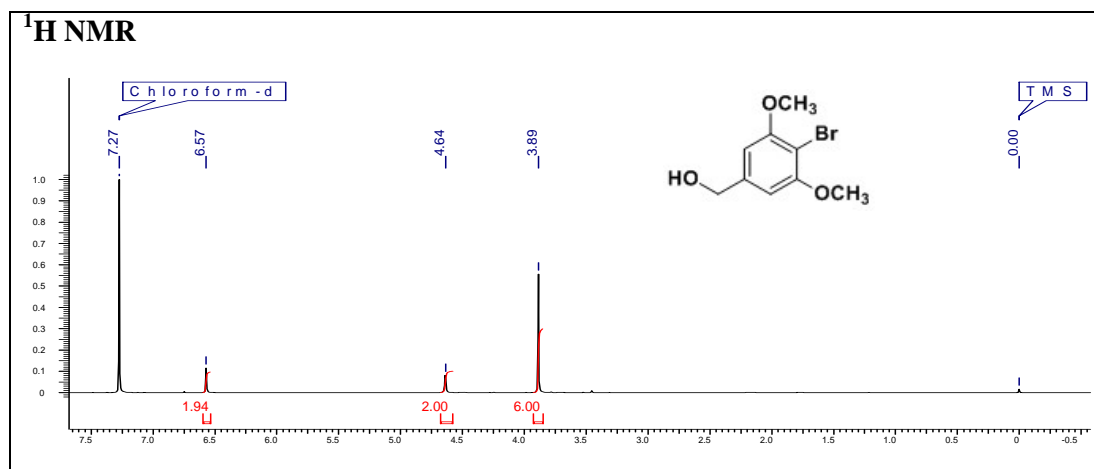


**Methyl-3,5-dimethoxy-4-(5-methoxy-5-oxopentyl)benzoate (13)**

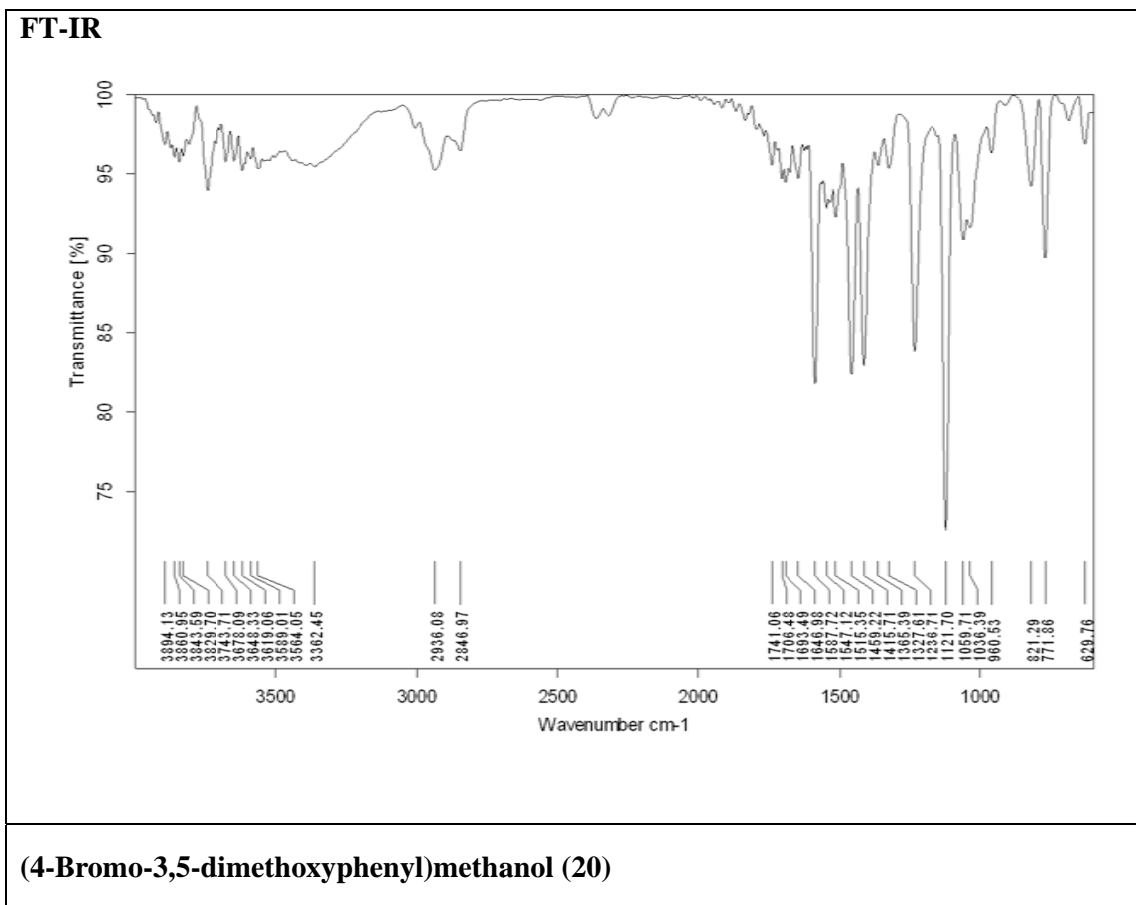
# Chapter 1



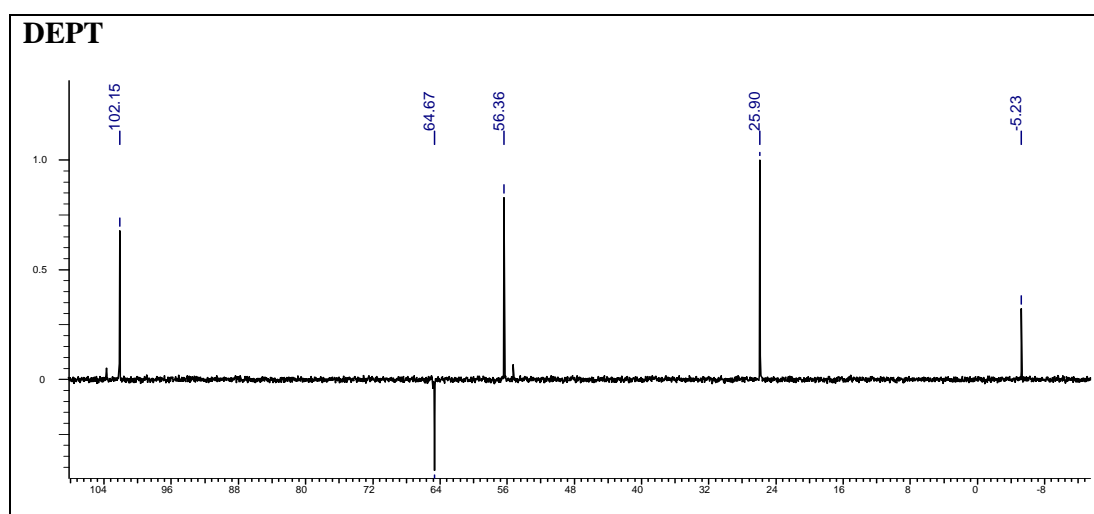
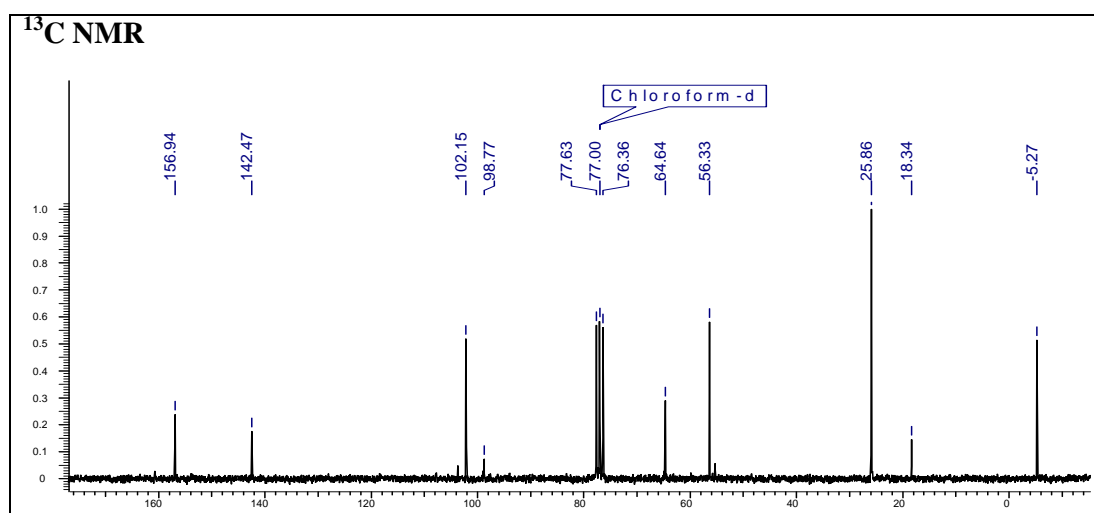
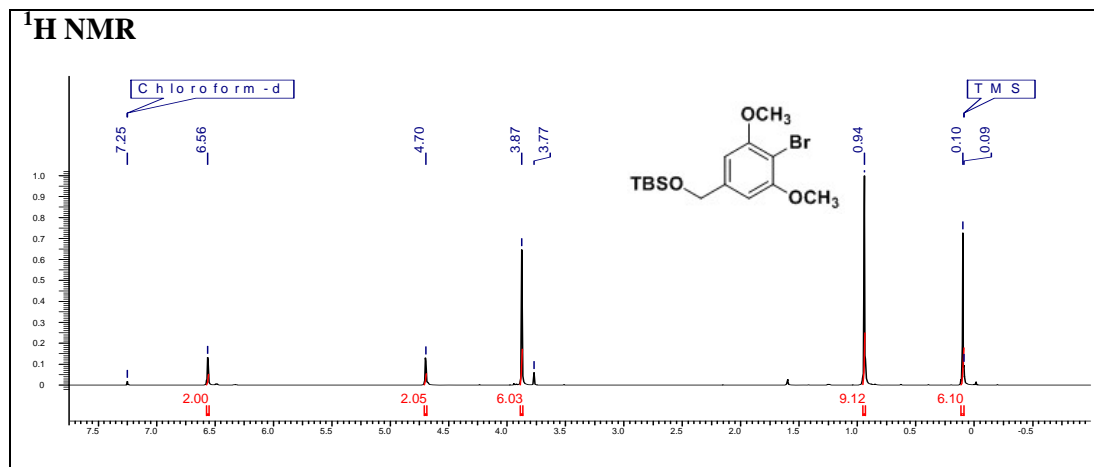
# Chapter 1



**(4-Bromo-3,5-dimethoxyphenyl)methanol (20)**

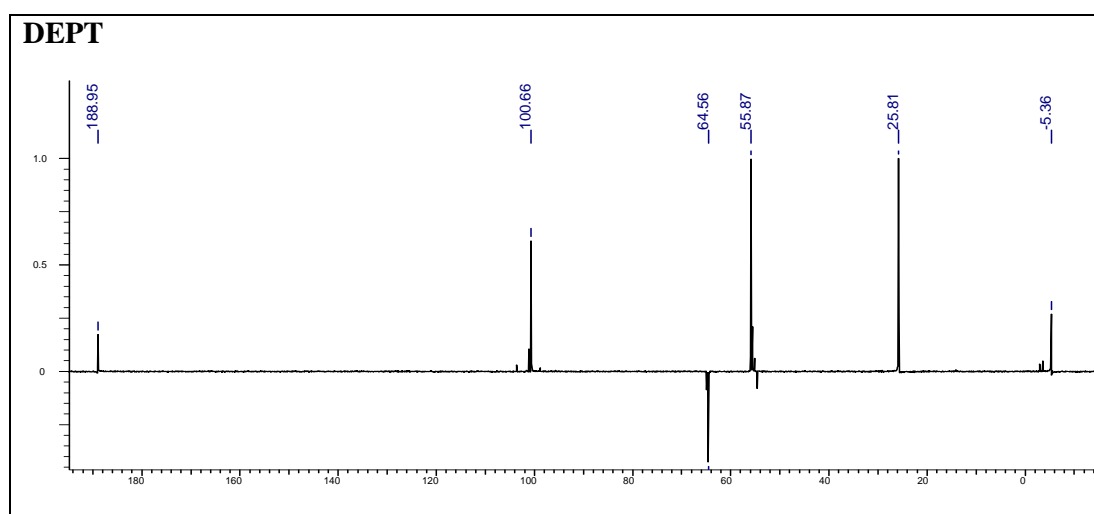
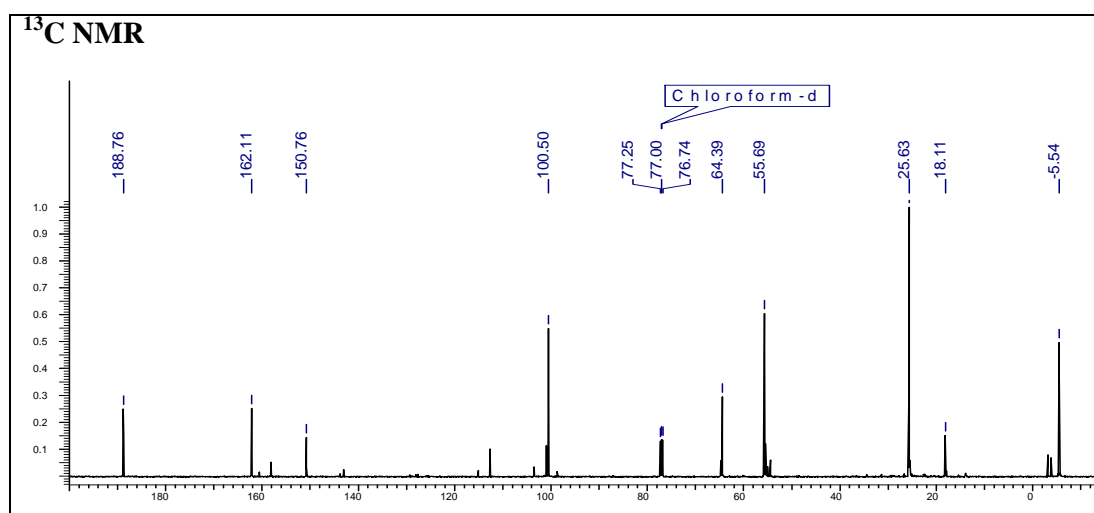
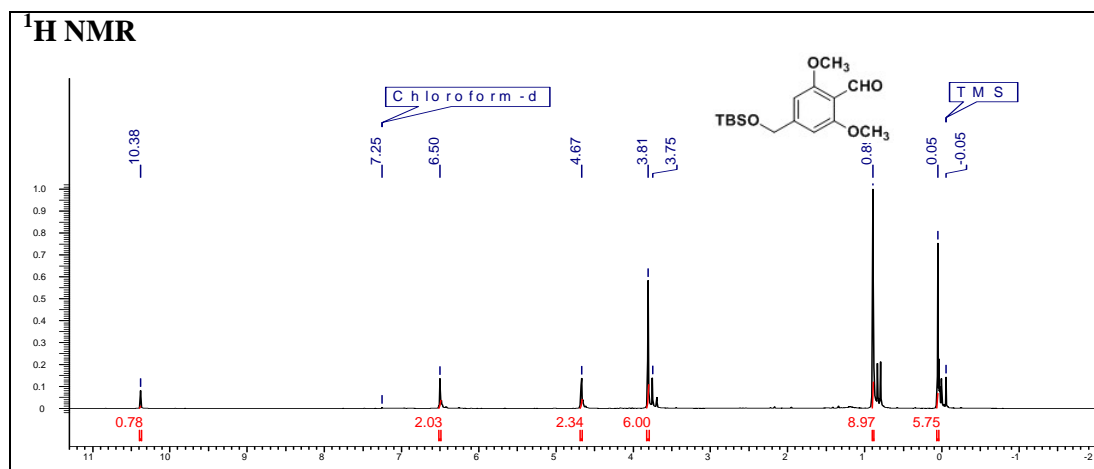


# Chapter 1



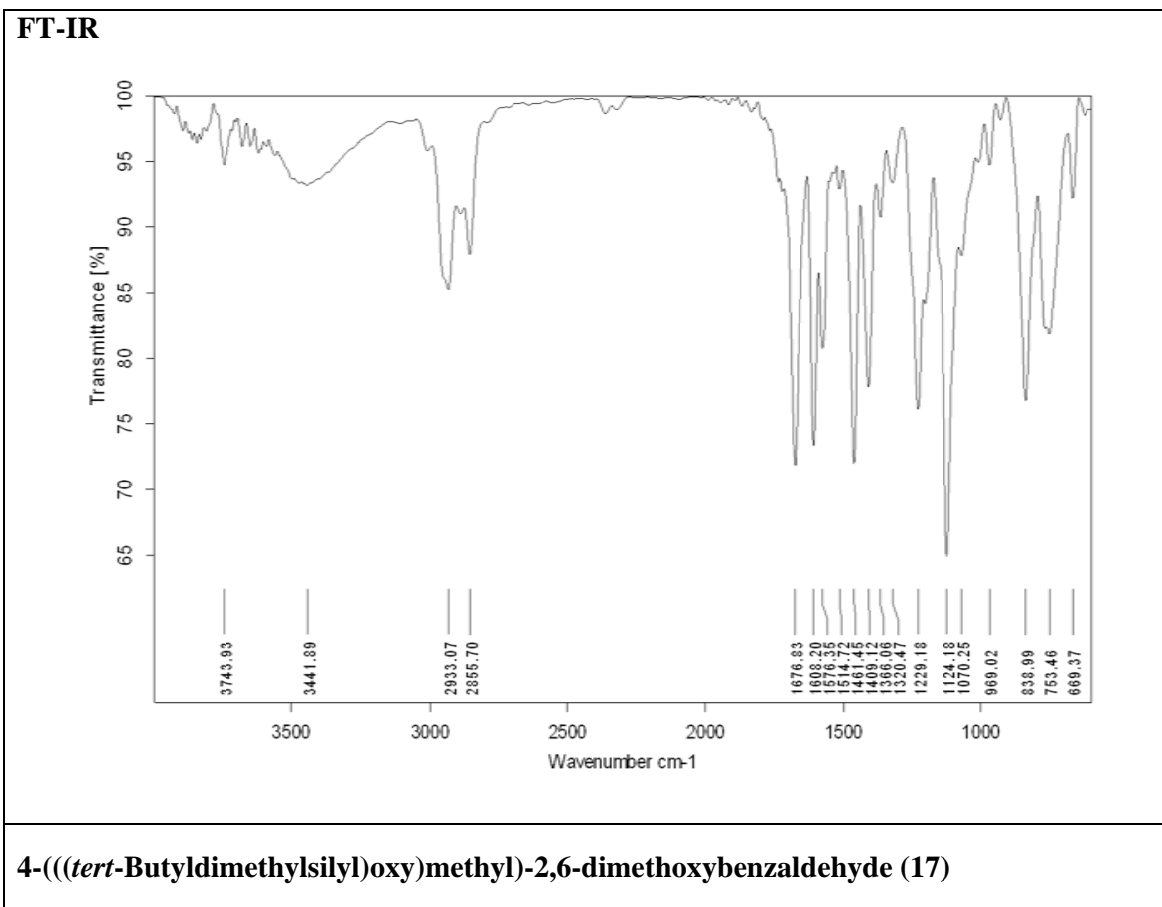
**((4-Bromo-3,5-dimethoxybenzyl)oxy)(*tert*-butyl)dimethylsilane (19)**

# Chapter 1

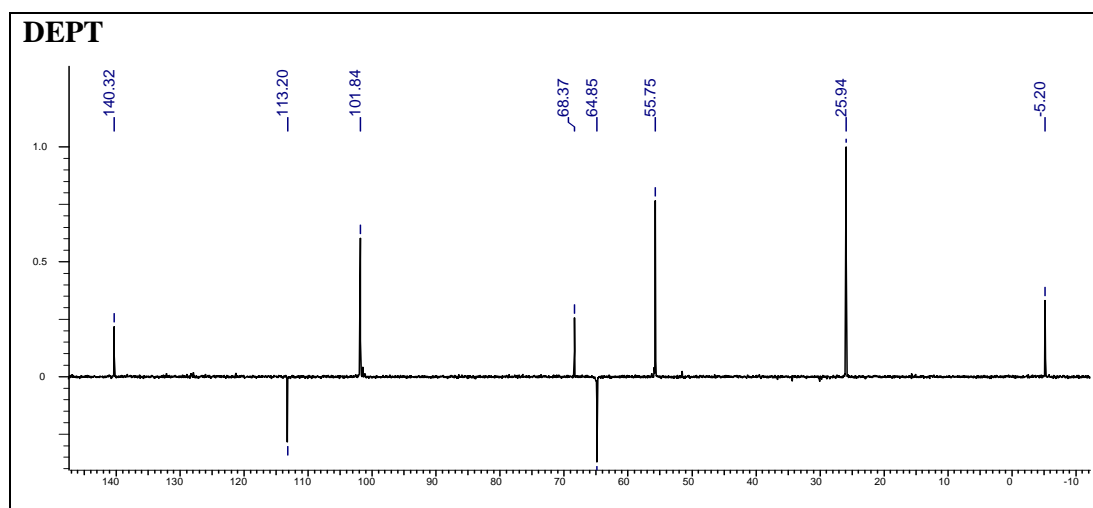
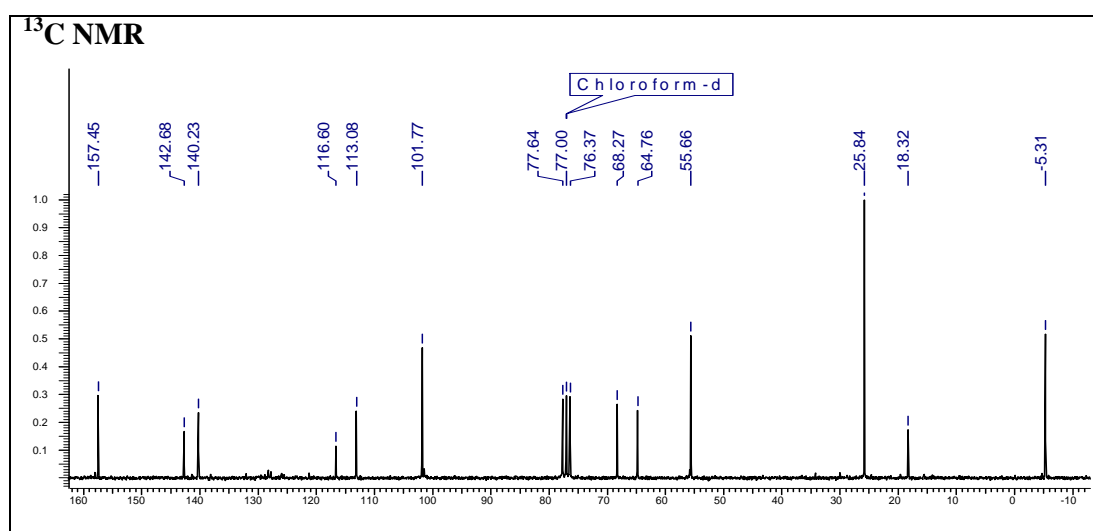
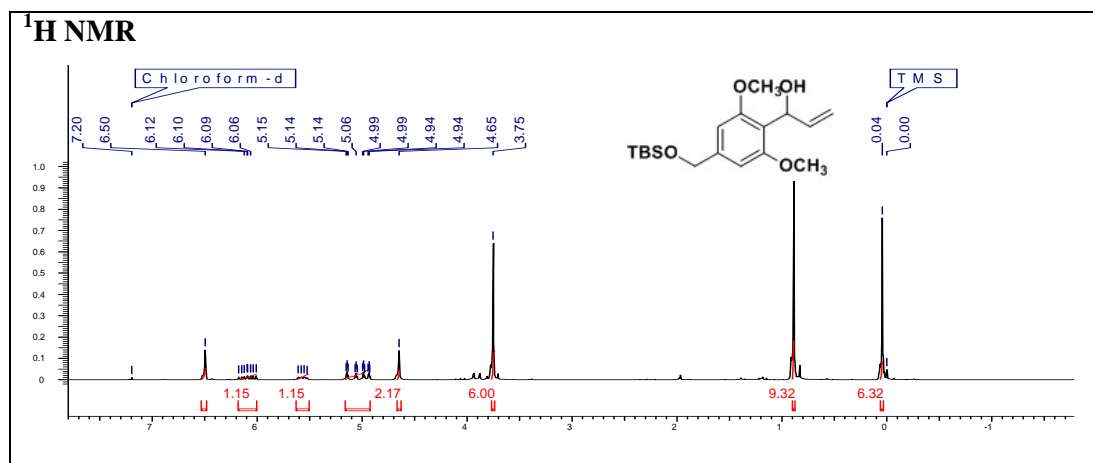


**4-((*tert*-Butyldimethylsilyl)oxy)methyl)-2,6-dimethoxybenzaldehyde (17)**

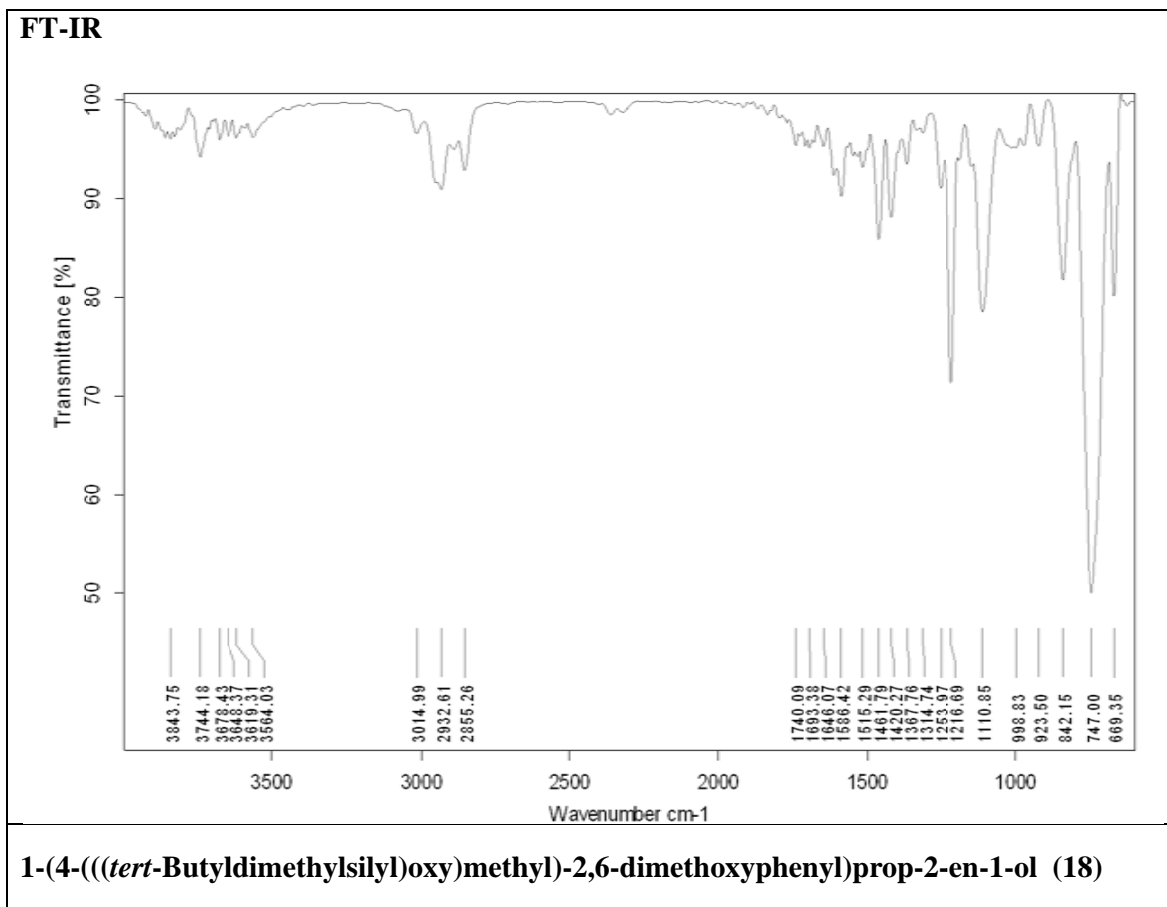




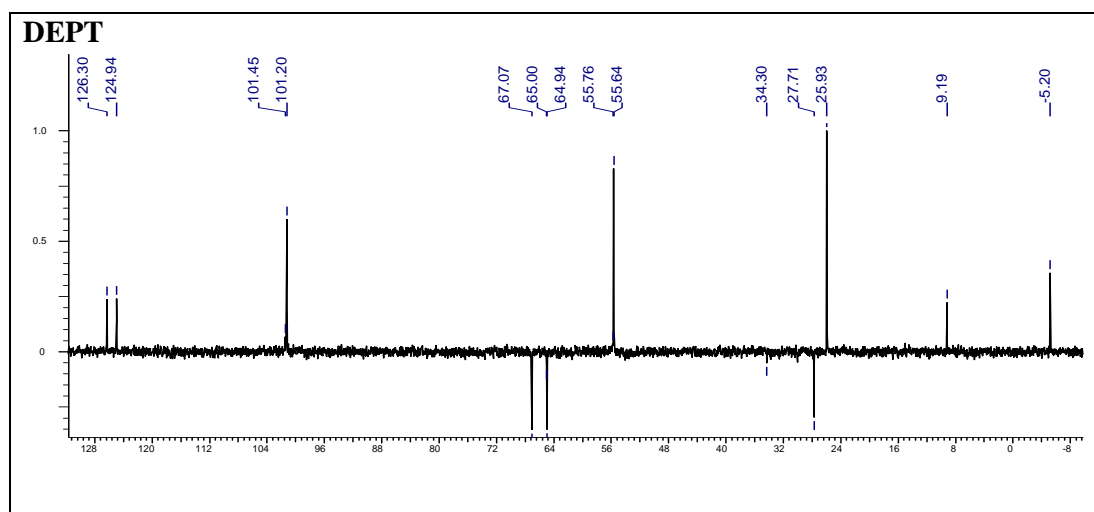
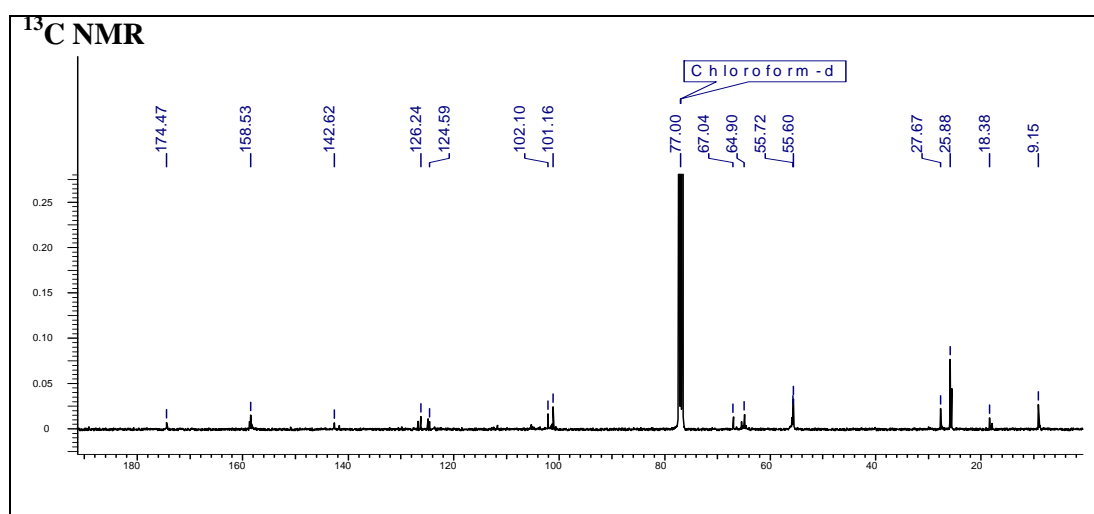
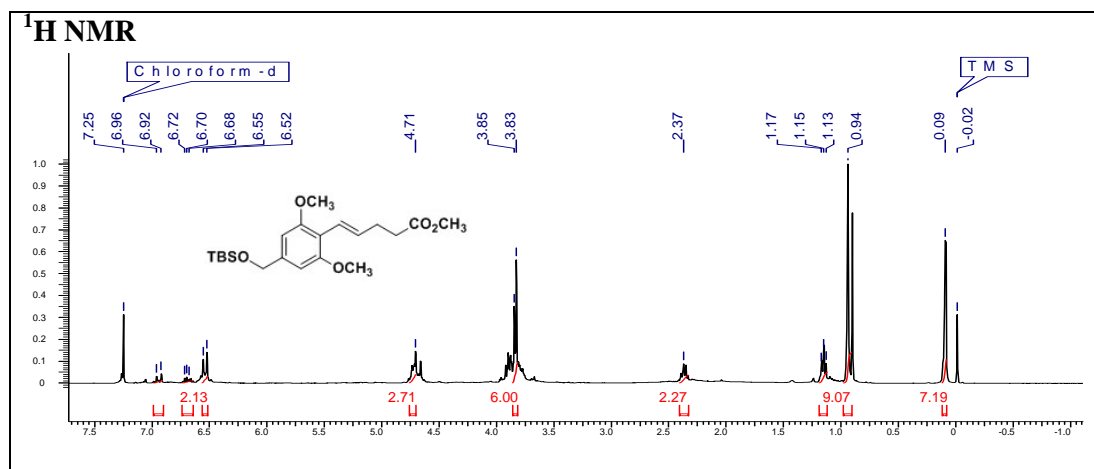
# Chapter 1



**1-(4-(((*tert*-Butyldimethylsilyl)oxy)methyl)-2,6-dimethoxyphenyl)prop-2-en-1-ol (18)**

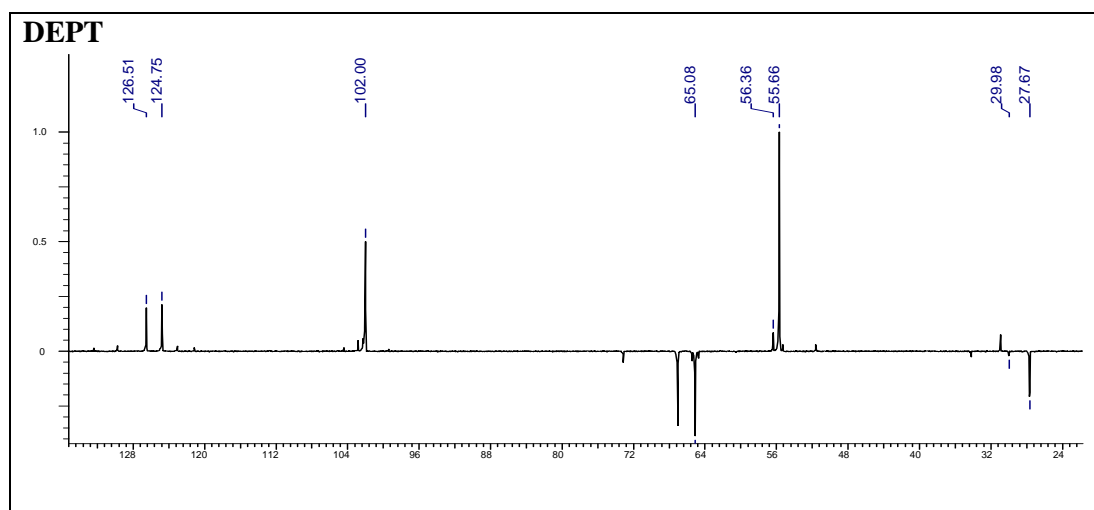
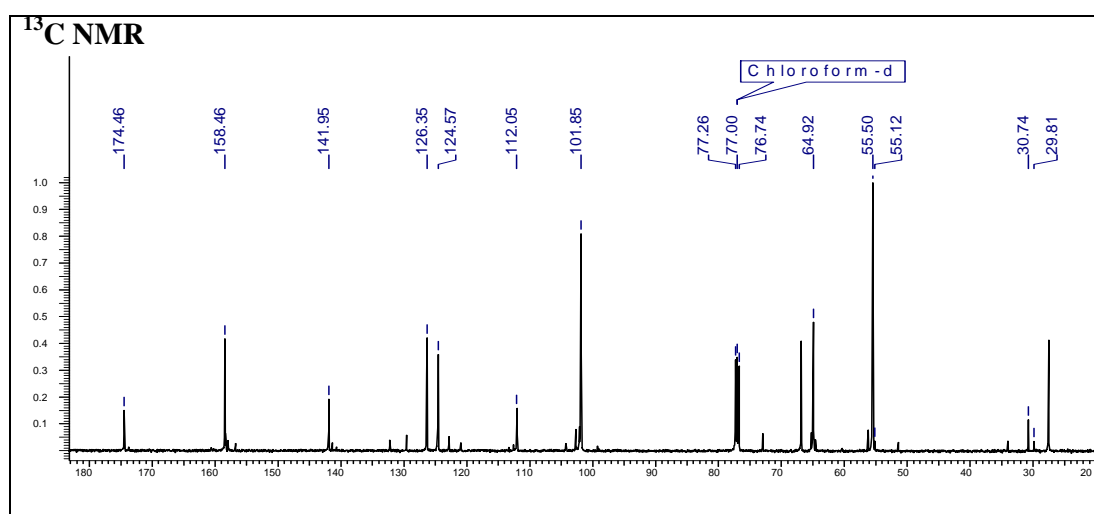
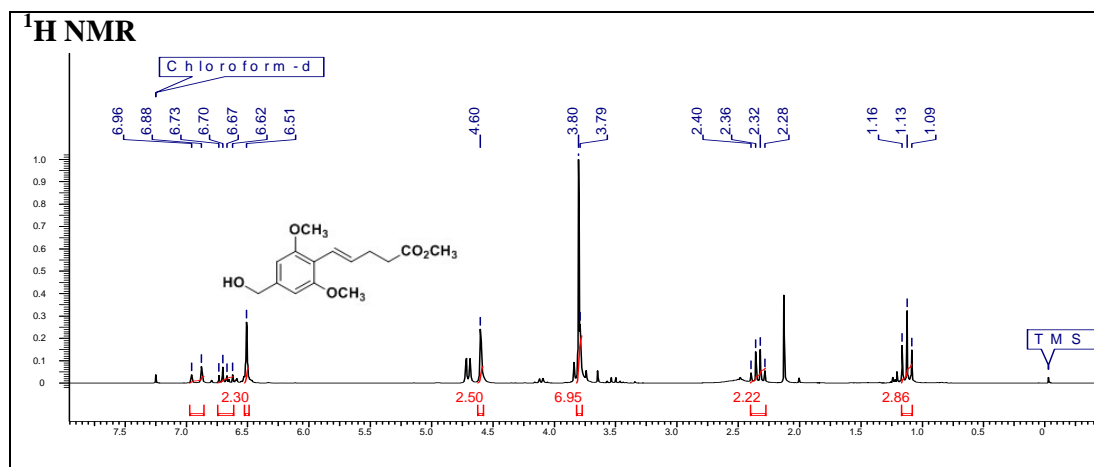


# Chapter 1



**(*E*)-Methyl-5-(4-(((tert-butyl)dimethylsilyloxy)methyl)-2,6-dimethoxyphenyl) pent-4-enoate (21)**

# Chapter 1



**(E)-Methyl-5-(4-(hydroxymethyl)-2,6-dimethoxyphenyl)pent-4-enoate (22)**

# *Chapter 1*

## **Synthesis of Antibacterial Natural Products**

---

### *Section C*

#### **Formal Synthesis of (-)- Centrolobine**

---

This section deals with the formal synthesis of antibacterial natural product, (-)-Centrolobine. It also discusses previous literature protocols utilized in the synthesis. It involves utilization of well known synthetic protocols for example extended Oxidative Kinetic Resolution (OKR) and Barbier reaction towards formal synthesis of this natural product.

## 1.1 Introduction

(-)-Centrolobine **1** is a crystalline substance isolated from the heartwood of *Centrolobium robustum* and from the stem of *Brosimum potabile* growing in the Amazon forest (Figure 3).<sup>1</sup> In 2002, Colobert group accomplished asymmetric total synthesis of compound **1**, confirming its absolute configuration.<sup>2</sup> Three further, asymmetric syntheses followed from the groups of Rychnovsky, Evans and Cossy, respectively.

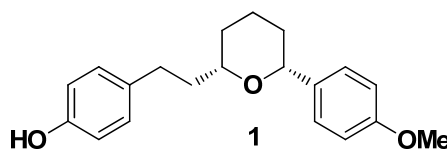


**Figure 1.** Structure of (-)-Centrolobine, **1**.

(-)-Centrolobine **1**, has been reported to be an antibiotic having strong antileishmanial activity with Calculated LD<sub>50</sub> values of 77 nM.

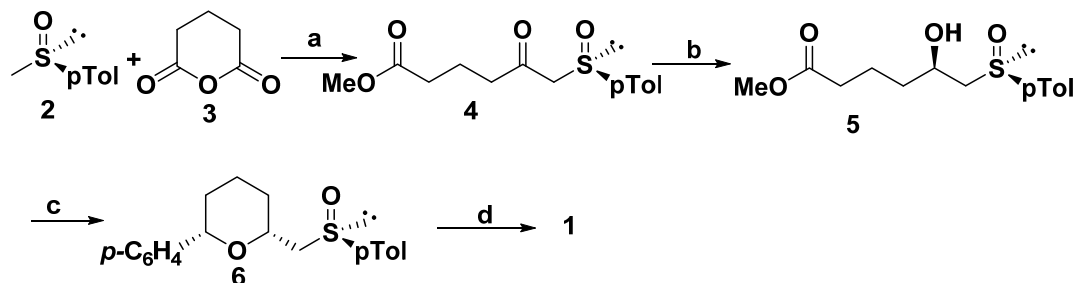
### 1.1.1 Previous reports

Various approaches leading to (-)-centrolobine **1** have been reported. First asymmetric total synthesis of **1** was done by Solladie and co-workers in 2002, which also established the absolute configuration of **1**. Since then, a number of groups have synthesized of **1** in both racemic and optically active forms. A variety of approaches including chiral pool method have been devised to provide access to the *cis*-2,6-disubstituted tetrahydropyran rings. These include Prins and related cyclizations,<sup>2</sup> reductive etherification,<sup>3</sup> one-pot cross metathesis–hydrogenation–lactonization procedure,<sup>5</sup> radical cyclization, nucleophilic addition–stereoselective reduction protocol, intramolecular oxy-Michael reaction, diastereoselective ring rearrangement metathesis–isomerization sequence,<sup>10</sup> FeCl<sub>3</sub>-mediated cyclization of 1,5-diol,<sup>11</sup> and hetero-Diels-Alder reaction.<sup>12</sup>

#### 1.1.1a Solladie's approach (2002)

Solladie *et al.* reported the first enantioselective total synthesis of (-)-centrolobine **1** (Scheme 1). The key reaction was the synthesis of the *cis*-disubstituted tetrahydropyran framework by intramolecular cyclization of the enantiopure

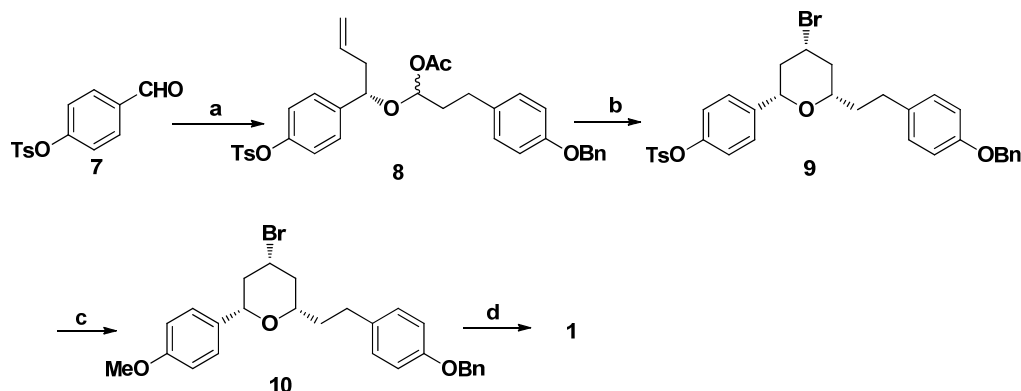
hydroxyketone **5** with  $\text{Et}_3\text{SiH}$  and TMSOTf resulted in the generation of compound **6** which after deprotection of auxiliary and the Wittig reaction on resulting aldehyde, reduction of double bond furnished the compound **1** in 93% yield.<sup>2</sup>



**Scheme 1.** Synthesis of (-)-Centrolobine using Solladie's approach; *Reagents and conditions:* (a) i) LDA, THF,  $-78\text{ }^\circ\text{C}$ ; ii)  $\text{K}_2\text{CO}_3$ , rt, acetone; iii)  $\text{Me}_2\text{SO}_4$ , reflux, 82%; (b) i) DIBAL-H/ $\text{ZnBr}_2$ , THF,  $80\%$ ; ii)  $\text{HCl}\cdot\text{NH}(\text{OMe})_2$ ,  $\text{AlMe}_3$ ,  $\text{CH}_2\text{Cl}_2$ , reflux, 93%; iii)  $p\text{-(OMe)C}_6\text{H}_4\text{MgBr}$ , ether/THF, reflux, 71%; (c) TMSOTf,  $\text{Et}_3\text{SiH}$ ,  $\text{CH}_2\text{Cl}_2$ ,  $0\text{ }^\circ\text{C}$ , 81%; (d) i) TFAA, 2,4,6-collidine, MeCN,  $0\text{ }^\circ\text{C}$ , 82%; ii) 4 benzyloxybenzyltriphenylphosphonium salt,  $n\text{-BuLi}$ ,  $0\text{ }^\circ\text{C}$ , 96%; iii)  $\text{H}_2$ ,  $\text{Pd}/\text{Al}_2\text{O}_3$ , 50 bar, rt, 93%.

### 1.1.1b Rychnovsky's approach (2002)

The synthesis of (-)-centrolobine **1** commenced with a Keck enantioselective allylation of aldehyde **7** to give the homoallylic alcohol (Scheme 2), followed by esterification and reductive acetylation led to the (*R*)-acetoxy ether **8**. The resulting ether derivative **8** was subjected to  $\text{SnBr}_4$  promoted cyclization furnished tetrahydropyran **9**. The tosylate protecting group of compound **9** was transformed to methyl ether by basic hydrolysis and alkylation. Compound **9** was subjected to reduction conditions to furnish (-)-centrolobine **1**.<sup>3</sup>



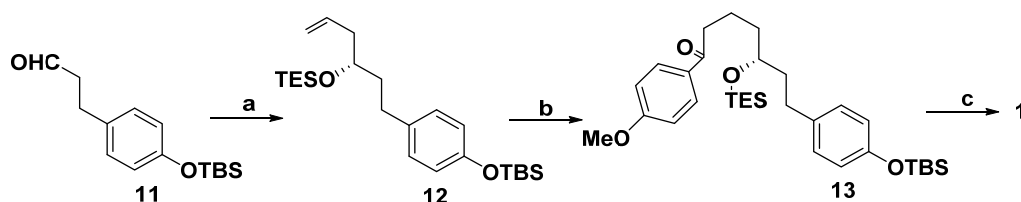
**Scheme 2.** Synthesis of (-)-Centrolobine using Rychnovsky's approach; *Reagents and conditions:* (a) i) (*S*)-BINOL,  $\text{Ti}(\text{O-}i\text{Pr})_4$ , allyl- $\text{SnBu}_3$ , 79%, 94% *ee*; ii) DCC, DMAP, 4-(OBn) $\text{C}_6\text{H}_4\text{CH}_2\text{CH}_2\text{CO}_2\text{H}$ , 94%; iii) (1) DIBAL-H,  $-78\text{ }^\circ\text{C}$ , 96%; (2)  $\text{Ac}_2\text{O}$ , DMAP, pyridine,



93%; (b)  $\text{SnBr}_4$ ,  $\text{CH}_2\text{Cl}_2$ ,  $-78\text{ }^\circ\text{C}$ , 84%; (c) i)  $\text{K}_2\text{CO}_3$ ,  $\text{MeOH}$ , reflux; ii)  $\text{MeI}$ ,  $\text{K}_2\text{CO}_3$ , acetone, 85%; (d) i)  $\text{Bu}_3\text{SnH}$ ,  $\text{AIBN}$  (*cat.*),  $\text{PhCH}_3$ , reflux, 86%; ii)  $\text{H}_2$ , 10%  $\text{Pd/C}$ , 72%.

### 1.1.1c Evans's approach (2003)

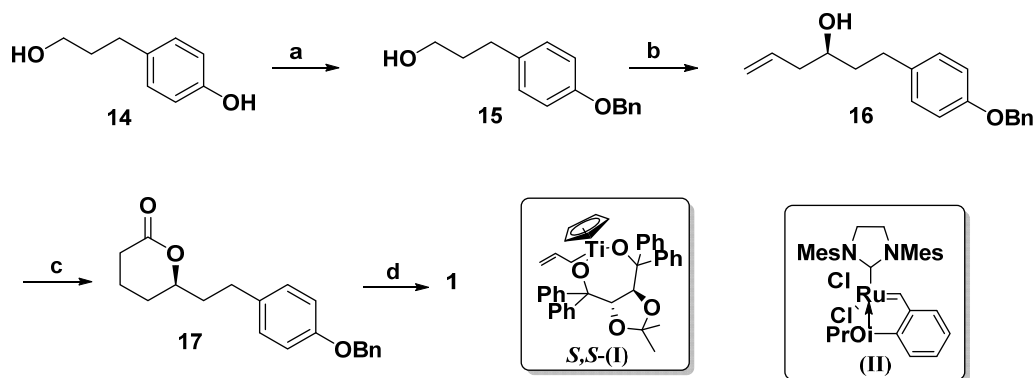
The stereoselective intramolecular reductive etherification of  $\delta$ -trialkylsilyloxy substituted ketones with catalytic bismuth tribromide and triethylsilane was the key step for the synthesis of (-)-centrolobine **1** (Scheme 3). Enantioselective allylation of aldehyde **11** and protection of the resulting secondary alcohol furnished the triethylsilyl ether **12**. The olefinic ether was subjected to cross-metathesis by using the Grubb's 2<sup>nd</sup> generation catalyst to afford the corresponding  $\alpha,\beta$ -unsaturated ketone. Selective hydrogenation of the alkene with Wilkinson's catalyst furnished the aryl ketone **13**. Treatment of the  $\delta$ -triethylsilyloxy aryl ketone **13** with bismuth tribromide and triethylsilane at room temperature followed by *in situ* removal of the *tert*-butyldimethylsilyl group afforded the (-)-centrolobine **1**.<sup>4</sup>



**Scheme 3.** Synthesis of (-)-Centrolobine using Evan's approach; *Reagents and conditions:* (a) i) (*S*)-BINOL,  $\text{Ti}(\text{O}-i\text{Pr})_4$ , allyl- $\text{SnBu}_3$ , 79%, 94% *ee*; ii)  $\text{TESOTf}$ ,  $\text{CH}_2\text{Cl}_2$ , 2,6-lutidine, 77%; (b) i) Grubb's catalyst,  $\text{ArCOCHCH}_2$ ; ii) Wilkinson's catalyst,  $\text{H}_2$ , toluene, 74%; (c) i)  $\text{MeI}$ ,  $\text{K}_2\text{CO}_3$ , acetone, 85%; (d)  $\text{BiBr}_3$ , (10 mol%),  $\text{Et}_3\text{SiH}$ ,  $\text{MeCN}$ , rt, TBAF, 93%.

### 1.1.1d Boulard's approach (2004)

Boulard *et al.* employed the protection on the commercially available alcohol **14**, then protection of free hydroxyl as its benzyl ether **15** and then asymmetric allylation on aldehyde derived from compound **15** by PCC oxidation (Scheme 4).



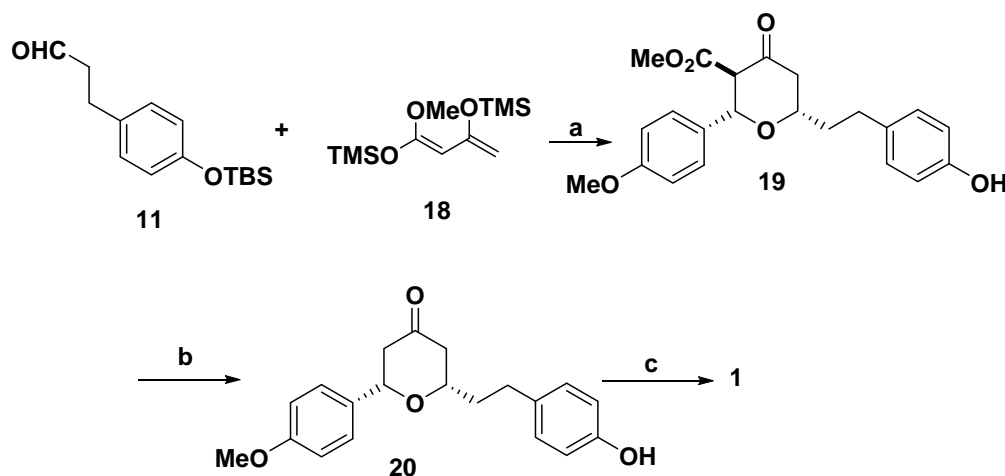
**Scheme 4.** Synthesis of (-)-Centrolobine using Boulard's approach; *Reagents and conditions:* 2013 PhD thesis: T. Kaur, University of Pune

(a) NaH, BnBr, DMF, reflux, 90%; (b) i) PCC, CH<sub>2</sub>Cl<sub>2</sub>, rt, quantitative; ii) *S,S*-**(I)**, ether, -78 °C, 61%; (c) i) Acrylic acid, **(II)**, CH<sub>2</sub>Cl<sub>2</sub>, 2 days, ii) Pd/C, H<sub>2</sub>, 4 days, 56%; (d) i) 4-(OMe)-C<sub>6</sub>H<sub>4</sub>MgBr, THF, -78 °C; ii) TMSOTf, Et<sub>3</sub>SiH, -78 °C to rt, 23%.

The homoallylic alcohol **16** was subjected to following reactions *i.e.* cross metathesis (CM), hydrogenation, lactonization and debenzoylation, respectively to furnish lactone **17**. A one-pot transformation from **17** to **1** was achieved by addition of 4-methoxyphenylmagnesium bromide followed by TMSOTf and Et<sub>3</sub>SiH.<sup>5</sup>

### 1.1.1e Clark's approach (2004)

In the synthesis of centrolobine **1** (Scheme 5), Clark *et al.* carried out one pot three-component Maitland–Japp reaction using Chan's diene **18** and aldehyde **11**, further addition of anisaldehyde furnished tetrahydropyran-4-one **19**. Compound **19** was subjected to ester hydrolysis and subsequent decarboxylation provided keto compound **20**. Finally, reduction of keto group of **20** furnished (-)-centrolobine **1**.<sup>6</sup>

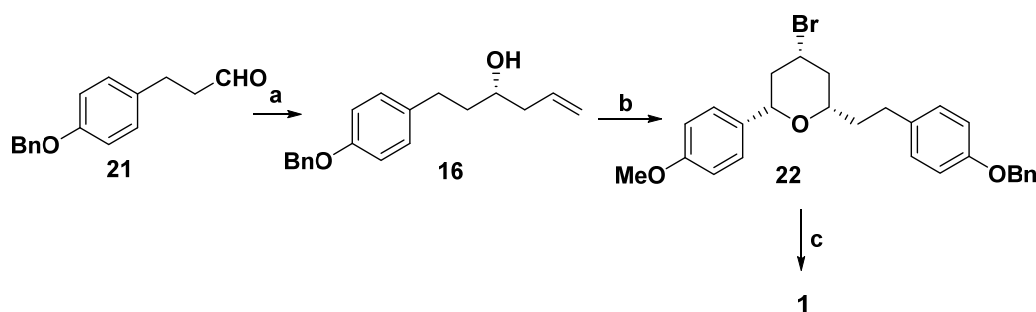


**Scheme 5.** Synthesis of (-)-Centrolobine using Clark's approach; *Reagents and conditions:* (a) Yb(OTf)<sub>3</sub>, anisaldehyde, TFA, -78 °C to rt, 12 h, 92%; (b) H<sub>2</sub>O<sub>2</sub>, LiOH, THF/H<sub>2</sub>O, 70 °C, 60%; (c) i) (CH<sub>2</sub>SH)<sub>2</sub>, BF<sub>3</sub>·Et<sub>2</sub>O, rt, 100%; ii) Raney-Ni, H<sub>2</sub>, EtOH, 100%.

### 1.1.1f Loh's approach (2005)

Loh's approach based on an asymmetric allylation of aldehyde **21** using (*R*)-BINOL indium complex and allyltri-*n*-butyltin as allylating agent. The formation of 4-Bromo THP ring **22** was accomplished *via* catalytic Prin's cyclization using InBr<sub>3</sub>

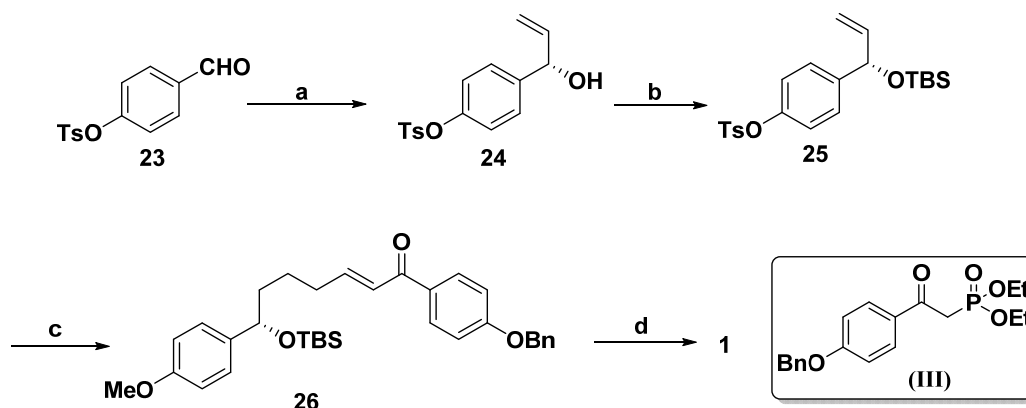
in presence of TMSBr. Finally, dehalogenation and catalytic hydrogenation provided (-)-centrolobine **1** (Scheme 6).<sup>7</sup>



**Scheme 6.** Synthesis of (-)-Centrolobine using Loh's approach; *Reagents and conditions:* (a)  $\text{InCl}_3$ , (*R*)-BINOL, allyl-SnBu<sub>3</sub>,  $\text{CH}_2\text{Cl}_2$ ,  $-78^\circ\text{C}$  to rt, 24 h, 68%, 84% *ee*; (b)  $\text{InBr}_3$ , TMSBr, *p*-anisaldehyde,  $\text{CH}_2\text{Cl}_2$ ,  $-78^\circ\text{C}$ , 83%; (c)  $\text{Bu}_3\text{SnH}$ , 1,1'-azobis(cyclohexane)carbonitrile, reflux, 24 h, 98%; ii) Pd/C,  $\text{H}_2$ , MeOH/EA, 7 h, 71%, 84% *ee*.

### 1.1.1g Chandarshekar's approach (2005)

Chandarshekar *et al.* efficiently utilized Keck allylation on aldehyde **23** (Scheme 7), furnished allylic alcohol **24**. The protection of hydroxyl with TBSCl resulted in compound **25**, which was subjected to the set of functional group manipulations: oxidation, Wittig olefination, reduction of ester as well as double bond, followed by oxidation to aldehyde, then Wittig-Horner olefination with phosphonate (**III**) provided the key intermediate **26**. Compound **26** on exposure to HF-pyridine triggered *in situ* silyl cleavage followed by intramolecular oxy-anion Michael addition to provide substituted pyran, and subsequently benzyl ether cleavage and keto group reduction provided (-)-centrolobine **1**.<sup>8</sup>

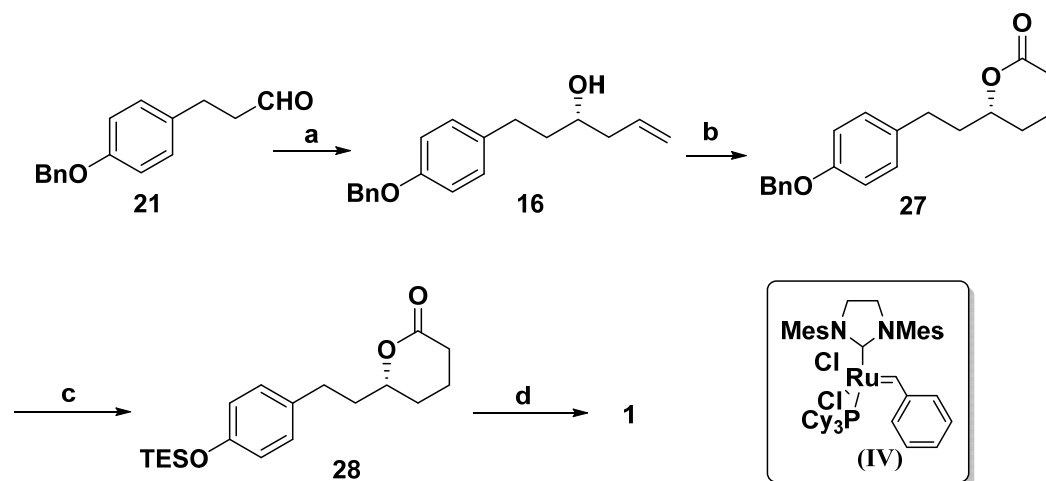


**Scheme 7.** Synthesis of (-)-Centrolobine using Chandarshekar's approach; *Reagents and conditions:* (a) (*R*)-BINOL, allyl-SnBu<sub>3</sub>,  $\text{Ti}(\text{O}-i\text{Pr})_4$ ,  $\text{CH}_2\text{Cl}_2$ ,  $-20^\circ\text{C}$ , 70 h, 73%, 97% *ee*; (b) i) TBSCl,  $\text{CH}_2\text{Cl}_2$ ,  $0^\circ\text{C}$ , 87%; (c) i) Mg/MeOH, rt, 3 h, 85%; ii)  $\text{K}_2\text{CO}_3$ , MeI, acetone,  $0^\circ\text{C}$ , 4 h, 73%; iii)  $\text{O}_3$ ,  $\text{CH}_2\text{Cl}_2$ , 1 h,  $-20^\circ\text{C}$ ; iv)  $\text{Ph}_3\text{PCHCO}_2\text{Et}$ ,  $\text{CH}_2\text{Cl}_2$ , 2 h, 84%; v) Mg/MeOH, rt,

81%; vi) LAH, THF, 0 °C to rt, 76%; vii) IBX, DMSO, rt, 4 h, 80%; viii) (I), Ba(OH)<sub>2</sub>·8H<sub>2</sub>O, THF/H<sub>2</sub>O (4:1), rt, 5 h, 81%; ix) HF-Py, THF, 0 °C to reflux, 4 h, 80%; x) Pd/C, H<sub>2</sub>, EtOH/EA/H<sub>2</sub>O (5:1:1), 10 h, 70%.

### 1.1.1h M. P. Jennings's approach (2005)

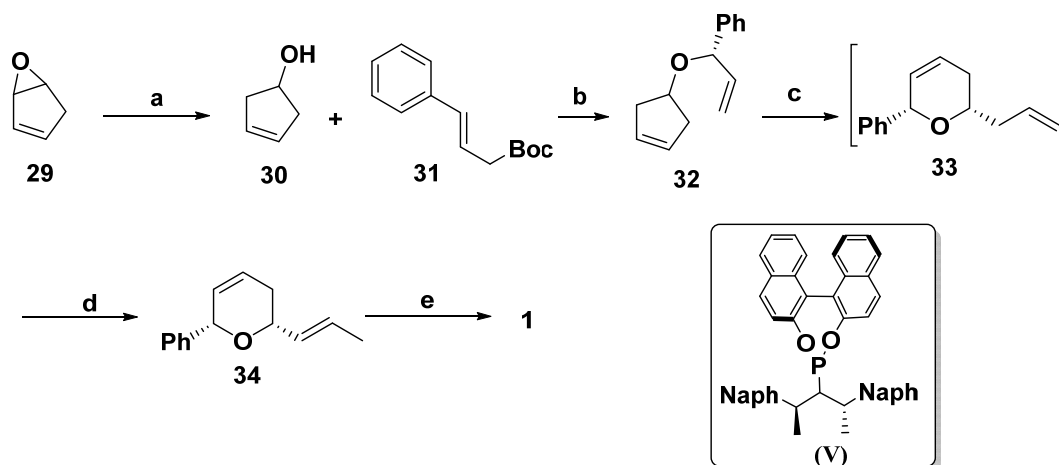
This approach utilized asymmetric allylation of aldehyde **21** to get homoallylic alcohol **16**. Esterification of **16** with acryloyl chloride and subsequent ring closing olefin metathesis with Grubbs' second-generation catalyst (IV) provided compound **27**. Compound **27** was subjected to hydrogenation conditions to furnish compound **28**, which by Grignard reaction and dehydration furnished (-)-centrolobine **1** (Scheme 8).<sup>9</sup>



**Scheme 8.** Synthesis of (-)-Centrolobine using Jennings's approach; *Reagents and conditions:* (a) Allyl-MgBr, THF, -20 °C, 1 h, 84%; (b) acryloyl chloride, Et<sub>3</sub>N, DMAP, CH<sub>2</sub>Cl<sub>2</sub>, 0 °C, 4 h, 86%; ii) Grubb's catalyst (IV), CH<sub>2</sub>Cl<sub>2</sub>, reflux, 5 h, 87%; (c) Pd/C, H<sub>2</sub>, EtOH, rt, 40 h, 84%; ii) TESCl, imidazole, DMF, rt, 87%; (d) *p*-(OMe)-C<sub>6</sub>H<sub>4</sub>MgBr, THF, -78 °C, Et<sub>3</sub>SiH, MeCN, -40 °C, 96%.

### 1.1.1i Blechert's approach (2006)

In Blechert's approach, reductive opening of epoxide **29** with LiAlH<sub>4</sub> (Scheme 9) afforded the alcohol **30**.

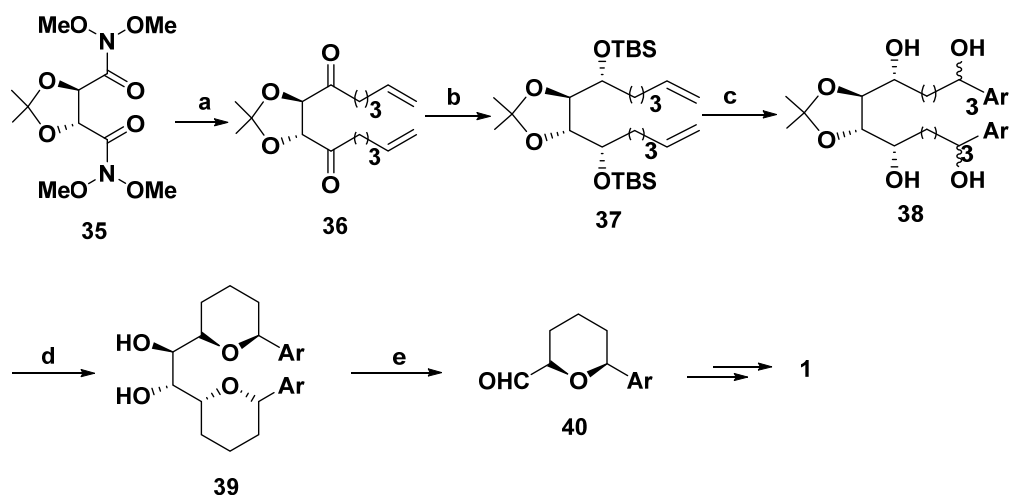


**Scheme 9.** Synthesis of (-)-Centrolobine using Blechert's approach; *Reagents and conditions:* (a) LAH, Et<sub>2</sub>O, -20 °C, 94%; (b) *n*-BuLi, CuI, [Ir(COD)Cl]<sub>2</sub>, (**V**), THF, -20 °C to rt, 87%, 98% *ee*; (c) Grubb's catalyst (**V**), toluene, 50 °C, 6 h; (d) NaBH<sub>4</sub>, 55%; (e) Styrene, Grubb's catalyst, 5 mol% Pd/C, H<sub>2</sub>, 50%.

Transition metal catalyzed asymmetric allylation on **31**, provided ether **32**. Compound **32** was treated with Grubbs' catalyst to furnish compound **33**, which undergoes rearrangement to afford **34**. Compound **34** was subjected to cross metathesis conditions to furnish styrene derivative, which on hydrogenation completed the synthesis of **1**.<sup>10</sup>

### 1.1.1j Prasad's approach (2007)

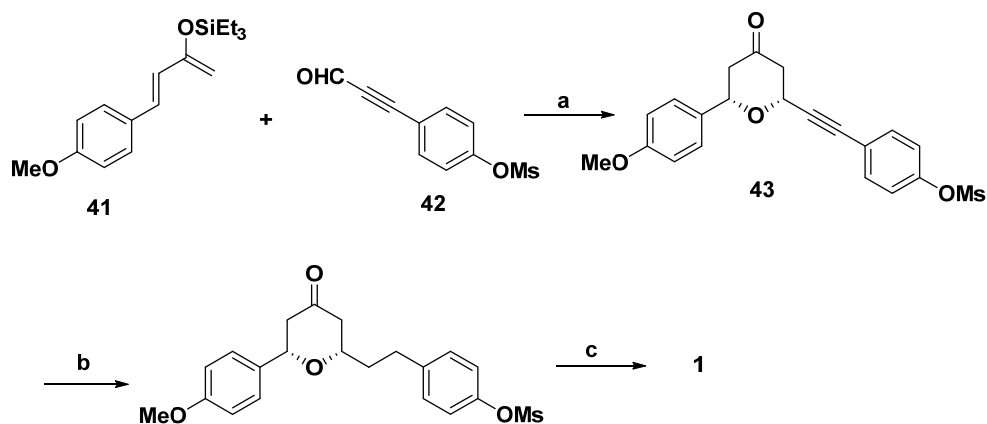
Prasad *et al.* started with *bis*-weinreb amide **35** derived from *L*-(+)-tartaric acid (Scheme 10). *Bis*-Weinreb amide **35** was treated with 4-pentenylmagnesium bromide to furnish 1,4-diketone **36**. Stereoselective reduction of diketo with *L*-selectride, followed by protection with silyl group furnished diene **37**. Ozonolysis followed by Grignard reaction afforded racemic diol, which on desilylation provided compound **38**. FeCl<sub>3</sub> mediated cyclization provided **39**, which on oxidative cleavage was converted to aldehyde **40**, thus completing the formal synthesis of (-)-centrolobine **1**.<sup>11</sup>



**Scheme 10.** Synthesis of (-)-Centrolobine using Prasad's approach; *Reagents and conditions:* (a)  $C_3H_9MgBr$ , THF,  $0\text{ }^\circ\text{C}$ , 1 h, 96%; (b) i) *L*-selectride, THF,  $-78\text{ }^\circ\text{C}$ , 3 h, 94%; ii) TBSCl, imidazole, DMAP, DMF,  $80\text{ }^\circ\text{C}$ , 3 h, 94%; (c) i)  $O_3/O_2$ ,  $Me_2S$ ,  $NaHCO_3$ ,  $CH_2Cl_2$ ,  $MeOH$ ,  $0\text{ }^\circ\text{C}$ , 1 h; ii) *p*-(OMe) $C_6H_4MgBr$ , THF,  $0\text{ }^\circ\text{C}$ , 1 h, 90%; iii) TBAF, THF, rt, 8 h, 89%; (d)  $FeCl_3$ , rt, 30 min, 70%; (e)  $Pb(OAc)_4$ , benzene, rt, 2 h, quantitative yield.

### 1.1.1k Hasimoto's approach (2007)

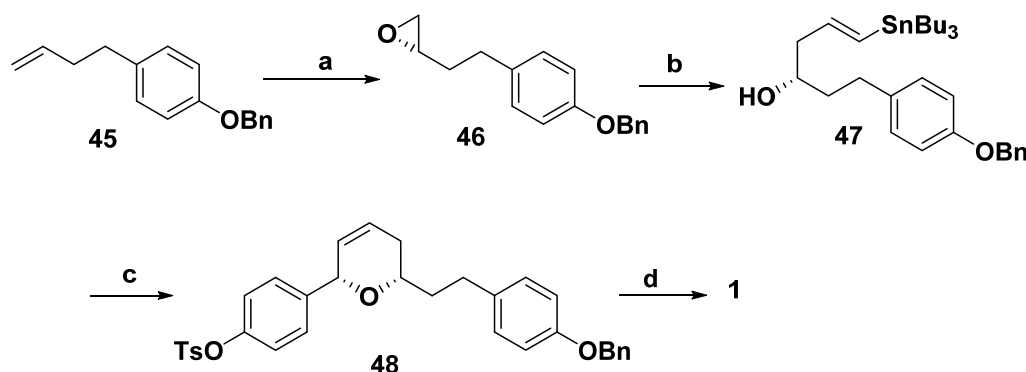
In this synthetic approach, hetero-Diels–Alder (HDA) reaction between 4-aryl-2-silyloxy-1,3-butadiene **41** and phenyl propargyl aldehyde **42** derivative played a key step (Scheme 11). The HDA reaction between **41** and **42** occurred in presence of  $Rh_2(R-BPTPI)_4$ , as a chiral Lewis acid catalyst to provide exclusively *cis*-2,6-disubstituted tetrahydropyran-4-one **43**. The triple bond was reduced by catalytic hydrogenation provided **44**. Keto group reduction and some protecting group manipulation afforded (-)-centrolobine **1**.<sup>12</sup>



**Scheme 11.** Synthesis of (-)-Centrolobine using Hasimoto's approach; *Reagents and conditions:* (a)  $\text{Rh}_2(\text{R-BPTPI})_4$ ,  $\text{CH}_2\text{Cl}_2$ , 87%; (b)  $\text{H}_2$ , 10% Pd/C, EtOAc, 2 h, 94%; (c) i)  $\text{TsNHNH}_2$ , MeOH, reflux, 2 h; ii)  $\text{NaBH}_3\text{CN}$ , TsOH, DMF-sulfolane (1:1), 110 °C, 1 h; ii)  $\text{K}_2\text{CO}_3$ , MeOH, reflux.

### 1.1.1l Furman's approach (2008)

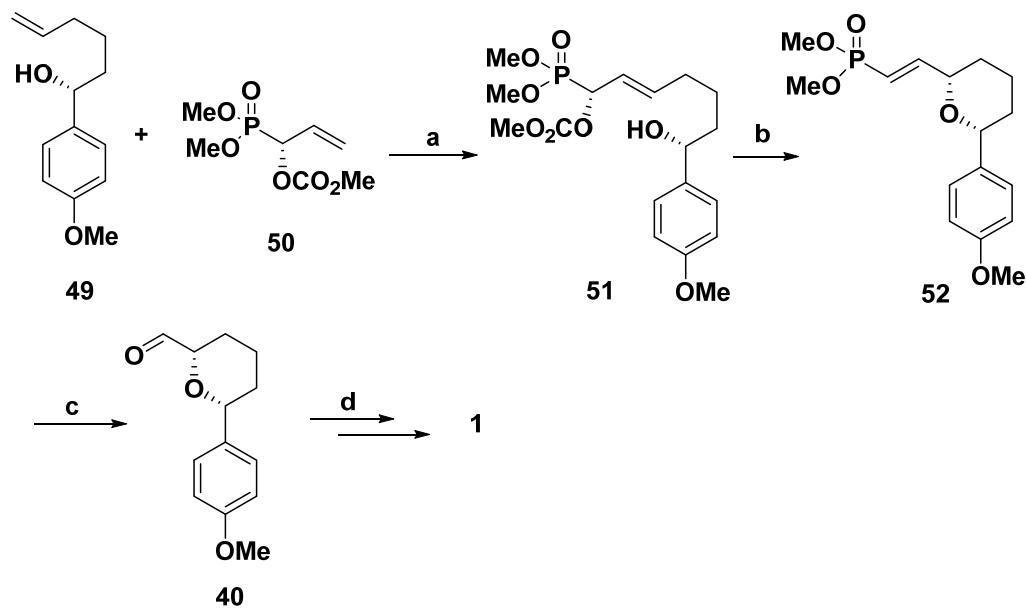
Lewis acid catalyzed intramolecular reactions of oxocarbenium ions with vinylstannanes for the stereoselective construction of 2,6-disubstituted dihydropyrans was used as the key reaction sequence in this current approach (Scheme 12). The starting material epoxide **46** was synthesized from the corresponding olefin **45** via Sharpless asymmetric dihydroxylation followed by tosylation of the primary hydroxyl group and NaOH treatment. The ring opening of epoxide **46** with lithium acetylide-ethylenediamine complex and subsequent hydrostannylation afforded alcohol **47**. The Prin's cyclization of **47** with 4-tosyloxybenzaldehyde in presence of TMSOTf yielded dihydropyran **48**, which on further standard functional group manipulation furnished (-)-centrolobine **1**.<sup>13</sup>



**Scheme 12.** Synthesis of (-)-Centrolobine using Furman's approach; *Reagents and conditions:* (a) i) AD-mix- $\alpha$ ,  $t\text{-BuOH-H}_2\text{O}$ , 0 °C, 90%; ii)  $\text{TsCl}$ , pyridine, 0 °C, 88%; iii)  $\text{NaOH}$ ,  $\text{Et}_2\text{O}$ , 93%; (b) Lithium acetylide, EDTA, DMSO, 0 °C, 83%, 87% ee; ii)  $\text{Bu}_2\text{Sn}(\text{OTf})\text{H}$ ,  $n\text{-BuLi}$ , 72%; (c) Benzaldehyde, TMSOTf,  $\text{Et}_2\text{O}$ , -78 °C, 87%; (d) i) Pd/C,  $\text{H}_2$ , EtOAc, 78%; ii)  $\text{TBSCl}$ , imidazole, 95%; iii)  $\text{Mg}$ , MeOH, 25°C, 50%; iv)  $\text{NaH}$ , MeI, TBAF, THF, 0 °C, 73%.

### 1.1.1m Spilling's approach (2009)

Synthesis of *cis*-tetrahydropyran ring was achieved by cross metathesis reaction of two fragments (*R*)-phosphonate **49** and (*R*)-alkenol **50**, yielding the phosphono-carbonate **51**.



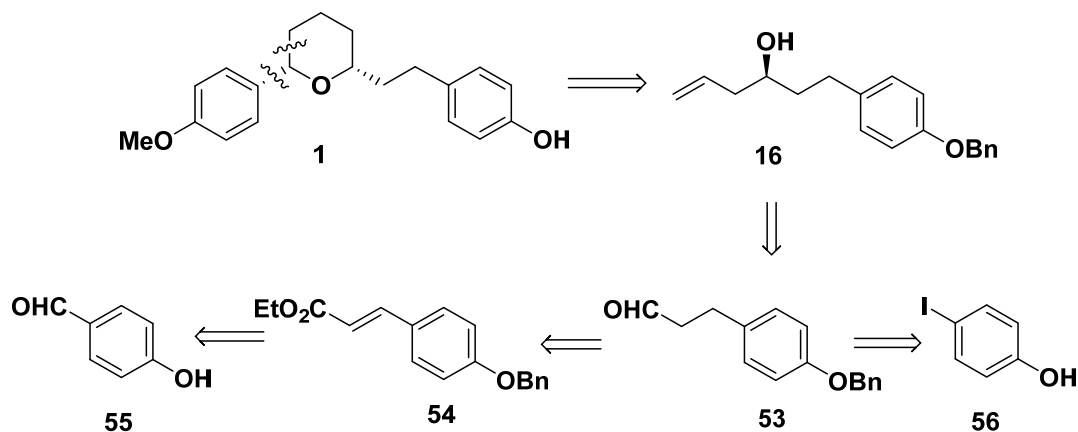
**Scheme 13.** Synthesis of (-)-Centrolobine using Spilling's approach; *Reagents and conditions:* (a) i) Grubb's catalyst, CuI, CH<sub>2</sub>Cl<sub>2</sub>, 0 °C, 60%; (b) Pd<sub>2</sub>(dba)<sub>3</sub>, dppe, *i*-Pr<sub>2</sub>NEt, THF, 60 °C, 85%; (c) O<sub>3</sub>, MeOH, CH<sub>2</sub>Cl<sub>2</sub>, 71%.

The stereospecific palladium catalyzed cyclization furnished *cis*-tetrahydropyran-vinyl phosphonate **52** which after ozonolysis yielded the aldehyde **40**. This aldehyde **40** could be transformed into natural product **1** in two steps (Scheme 13).<sup>14</sup>

## 1.2 Present work: Objective and Rationale

Retro synthetically, synthesis of **1** was visualized from key intermediate homoallylic alcohol **16** (Scheme 14). Compound **16** could be obtained by the Barbier allylation reaction of aldehyde **53**, the resulting racemic homo-allylic alcohol **16** could be resolved by the oxidative kinetic resolution (OKR). This aldehyde **53** in turn could be obtained from (*E*)-ethyl 3-(4-(benzyloxy)phenyl)acrylate **54**, by nickel boride and lithium aluminum hydride (LAH) reduction of double bond and saturated ester, respectively and finally the oxidation of the saturated alcohol with pyridinium dichromate (PDC).

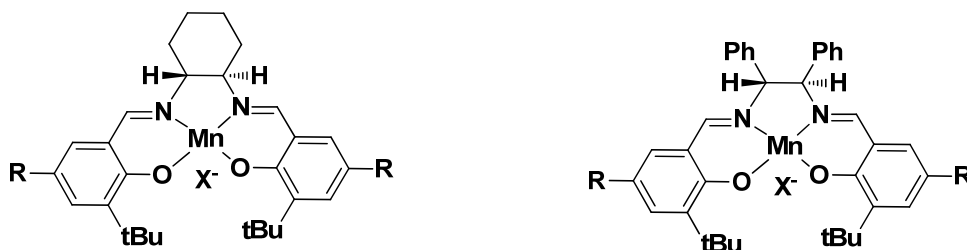




**Scheme 14.** Retrosynthetic route for the synthesis of (-)-Centrolobine, **1**.

### 1.3 Oxidative Kinetic Resolution (OKR)

The oxidative kinetic resolution (OKR) of racemic secondary alcohols plays an important role in the synthesis of various natural products.<sup>15</sup> The enantio-rich alcohols are integral part of several important transformations. Adam *et al.*<sup>16</sup> reported the use of  $[\text{Cr}^{\text{III}}(\text{salen})]$  complexes in the presence of iodosobenzene and  $\text{PhI}(\text{OAc})_2$  as a oxidant for the resolution of racemic secondary alcohols to ketones. Several groups utilized vanadium,<sup>17</sup> cobalt,<sup>18</sup> iridium,<sup>19</sup> palladium catalyzed aerobic oxidative resolution<sup>20</sup> protocols for the resolution of racemic secondary alcohols. Further Xia *et al.*<sup>15</sup> reported the use of  $[\text{Mn}^{\text{III}}(\text{salen})]$  complexes for the resolution of racemic alcohols to optically pure secondary alcohols and ketones. Xia *et al.* modified the protocol, using chiral  $[\text{Mn}^{\text{III}}(\text{salen})]$  complexes as a catalyst, potassium bromide as a phase transfer catalyst and  $\text{PhI}(\text{OAc})_2$  as a co-oxidant (Figure 2).<sup>15</sup>



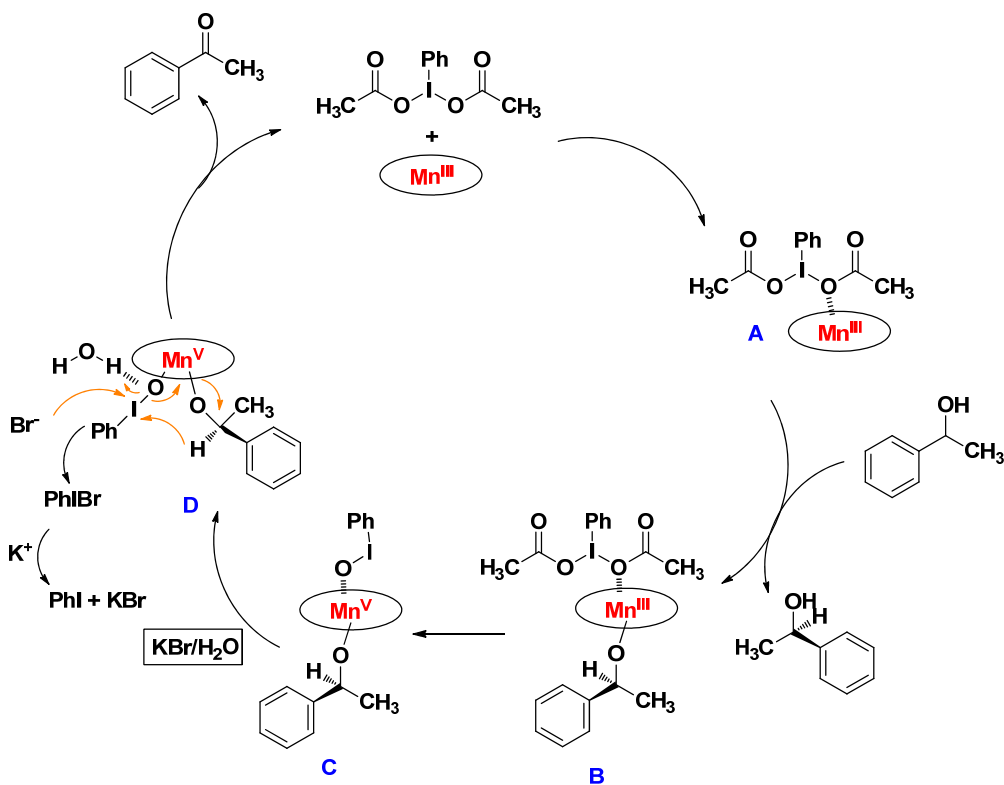
- (VI) a: R = *t*-Bu, X = Cl  
 (VI) a: R = *t*-Bu, X = Br  
 (VI) a: R = *t*-Bu, X = OAc<sup>-</sup>  
 (VI) a: R = *t*-Bu, X = PF<sub>6</sub><sup>-</sup>  
 (VII) a: R = Me, X = PF<sub>6</sub><sup>-</sup>

- (VIII) a: X = Cl  
 (VIII) b: X = PF<sub>6</sub><sup>-</sup>

Figure 2. Structure of Jacobsen's catalysts.

### 1.3a Mechanism for Oxidative Kinetic Resolution (OKR)

First step is the formation of reactive intermediate **A**, which is generated by reaction of iodosobenzenediacetate (IBDA) and Mn(III) complex. This reactive intermediate **A**, reacts selectively with one isomer to form complex **B**. Further electronic reorganization of complex eliminates acetic acid,  $\text{CH}_3(\text{O})\text{C}^\bullet$  radical and high-valent Mn(V) species **C**. This intermediate **C**, in the presence of  $\text{KBr}/\text{H}_2\text{O}$  generates the complex **D**, which results in the generation of ketone and catalyst is generated for next catalytic cycle. This hypothesis has been further corroborated by UV-visible experiments and ESI-MS analysis (Scheme 15).

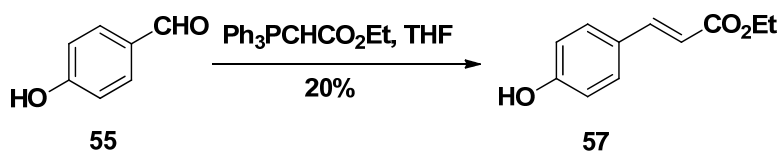


Scheme 15. Postulated mechanism for the oxidative kinetic resolution (OKR).

### 1.4 Results and Discussion

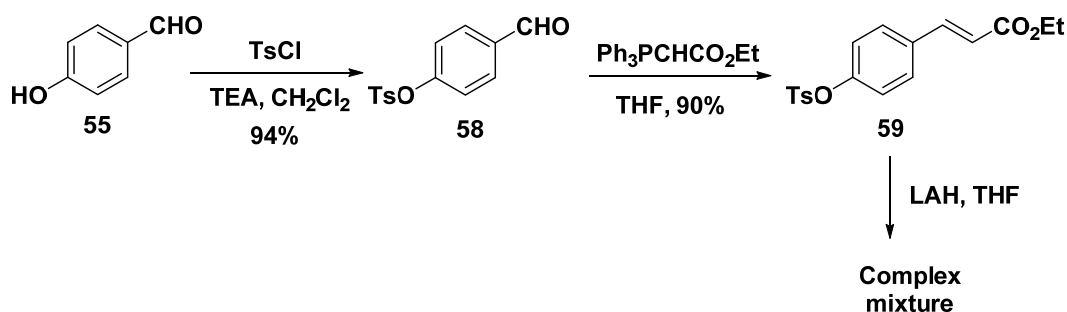
Initially, 4-hydroxybenzaldehyde **55** was taken as a starting material and Wittig reaction was performed on it without protecting phenolic hydroxyl group.  $\alpha,\beta$ -  
2013 PhD thesis: T. Kaur, University of Pune

Unsaturated product **57** was obtained albeit in low yield (Scheme 16). It was assumed that presence of free phenolic group would be responsible for low yield.



**Scheme 16.** Synthesis of compound **57** utilizing Wittig reaction.

Then phenolic hydroxyl group of compound **55** was protected as tosyl **58**, and then Wittig reaction resulted in the generation of  $\alpha,\beta$ -unsaturated ester, **59**. Compound **59** was subjected to lithium aluminum hydride reduction conditions, to furnish the saturated alcohol. This reaction failed to give the desired alcohol and resulting in the generation of complex reaction mixture (Scheme 17).

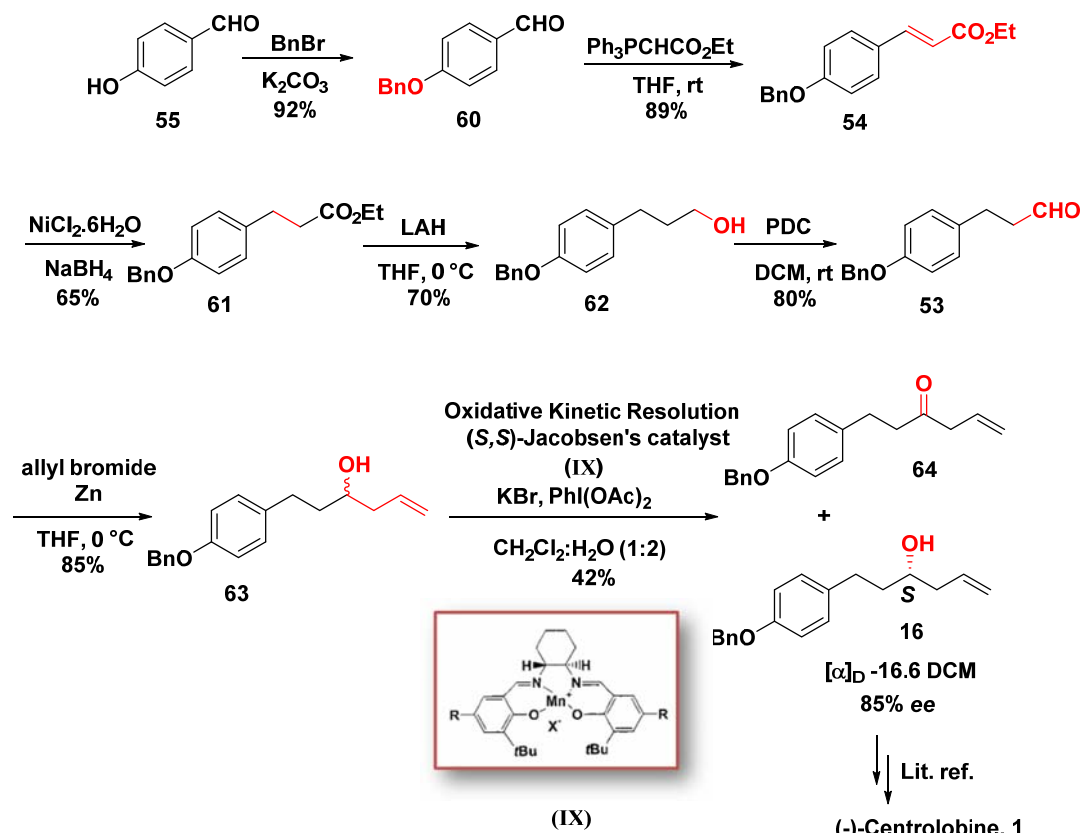


**Scheme 17.** Synthesis of compound **59** utilizing Wittig reaction.

In the next scheme, phenolic group of 4-hydroxybenzaldehyde **55** was protected as benzyl ether to furnish compound **60** (Scheme 18). The protected aldehyde **60** was treated with Wittig salt to form  $\alpha,\beta$ -unsaturated ester **54**.<sup>21</sup> The formation of product **54** was confirmed by its spectral analysis. In  $^1\text{H}$  NMR spectrum, the olefinic proton multiplet signals were observed at  $\delta$  7.64 (d,  $J = 15.9$  Hz, 1H) and 6.30 (d,  $J = 15.9$  Hz, 1H) ppm. In  $^{13}\text{C}$  NMR spectrum, olefinic carbon signals were observed at  $\delta$  144.2 and 115.2 ppm. The double bond reduction was carried out using nickel chloride hexahydrate<sup>22</sup> and sodium borohydride to furnish saturated ester **61**. The formation of product **61** was confirmed by its spectral analysis. In  $^1\text{H}$  NMR spectrum, the olefinic proton multiplet signals were disappeared and new peaks were observed at  $\delta$  2.87 (t,  $J = 8.1$  Hz, 1H) and 2.56 (t,  $J = 7.9$  Hz, 1H) ppm. In  $^{13}\text{C}$  NMR spectrum, carbon signals were observed at  $\delta$  36.1 and 30.0 ppm. Reduction of the

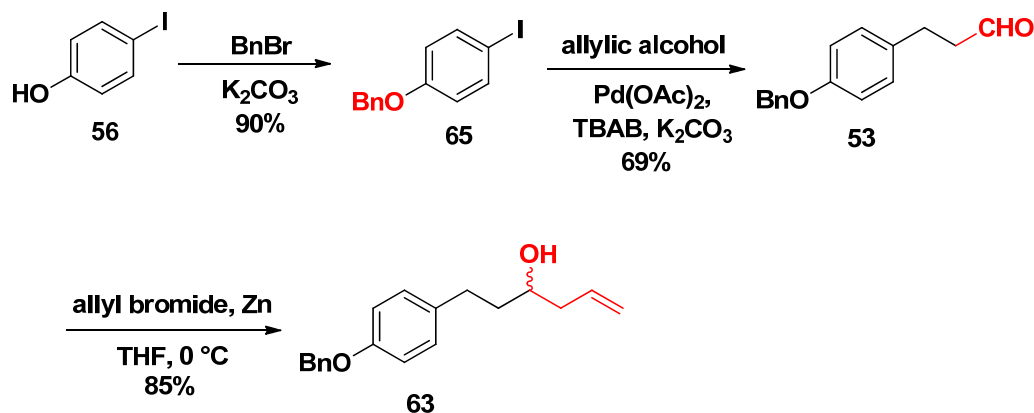
methyl ester **61** with lithium aluminium hydride furnished the alcohol **62** in 70% yield. In  $^1\text{H}$  NMR spectrum, new peak was observed at  $\delta$  3.65 (t,  $J = 6.4$  Hz) in  $^1\text{H}$  and 70.0 ppm in  $^{13}\text{C}$  NMR. The saturated alcohol **62** was oxidized to aldehydic compound **53**. In  $^1\text{H}$  NMR spectrum, the aldehydic proton signals were observed at  $\delta$  9.69 (m) ppm. In  $^{13}\text{C}$  NMR spectrum, carbon signal was observed at  $\delta$  201.4 ppm and in IR spectrum peaks at 2865 and 1720  $\text{cm}^{-1}$ , characteristic of aldehyde were observed. Aldehyde **53** was subjected to Barbier allylation<sup>23</sup> conditions to afford the homoallylic alcohol **54**. In  $^1\text{H}$  NMR spectrum, the olefinic proton signals were appeared at  $\delta$  5.87-5.69 (m, 1H), 5.18-5.14 (m, 1H), 5.11-5.06 (m, 1H), 2.77-2.48 (m, 2H), 2.48-2.11 (m, 2H) ppm. This homoallylic alcohol **63** was oxidized to keto compound **64** and further treated with *R*-alpine borane. The reaction did not yield the desired product. So, we decided to employ Jacobsen's-oxidative kinetic resolution (OKR) method on the racemic homoallylic alcohol **63**.

Finally, we resolved racemic alcohol **63** employing oxidative kinetic resolution (OKR) conditions into enantiomeric pure product **16** and keto derivative **64**. The enantiomeric excess (*ee*) of the resolution was calculated based on the Moscher's ester method and found to be 85%.



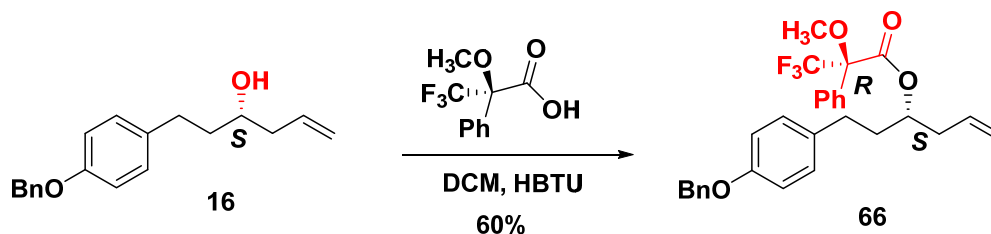
**Scheme 18.** Formal synthesis of (-)-Centrolobine, 1.

In order to improve the yield of the key intermediate, we started with 4-iodophenol **56** for the synthesis of **1**. The phenolic group of compound **56** was protected as benzyl ether to furnish compound **65** (Scheme 19). The protected iodo-compound **65** was treated with allylic alcohol, in the presence of palladium acetate to afford aldehyde **53**.<sup>24</sup> In earlier scheme, the yield of the desired aldehyde **53** was only 29.8% and was synthesized in 5 steps. To improve the yield of desired aldehyde **53** and reduce the number of steps this new method was applied. In this present standardized method we could isolate the aldehyde **53** in 69% yield and in two steps. This aldehyde **53** could be used for Barbier reaction conditions to furnish homoallylic alcohol **63** in 85% yield.



**Scheme 19.** Alternative route towards the formal synthesis of (-)-centrolobine, **1**.

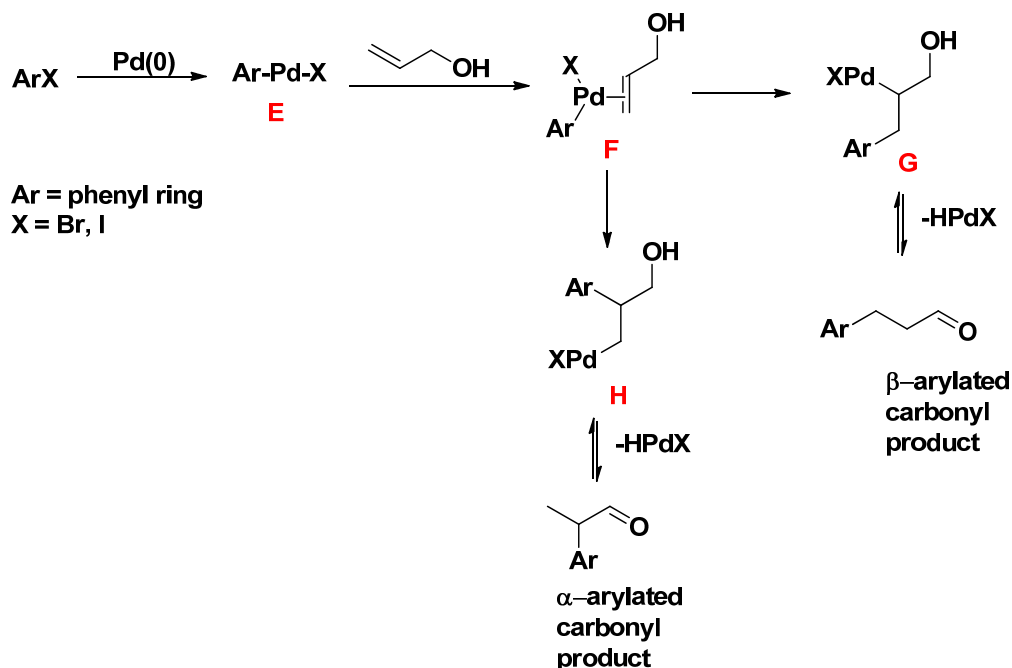
The optical purity of the enantiomeric pure product **16** has been determined using  $^{19}\text{F}$ -NMR spectroscopy.<sup>25</sup> The alcohol **16** coupled with a chiral shift reagent, (*R*)-(+)- $\alpha$ -methoxy- $\alpha$ -(trifluoromethyl)phenylacetic acid in the presence of HBTU and DCM as a solvent, to furnish the optically pure ester **66** in 60% yield (Scheme 20). The enantiomeric excess (*ee*) of the resolution was calculated based on the Moscher's ester method and found to be 85%.



**Scheme 20.** Derivatization of alcohol to ester using Moscher's method.

### **Mechanism for the conversion of iodo-65 to aldehyde-53**

It has been reported in the literature<sup>24</sup> that in the first step palladium (0), subsequently reacts with aromatic halides via oxidative addition to give intermediate (**E**), followed by co-ordination to the  $\pi$ -electron of the allylic alcohol at the  $\beta$ -position to form  $\sigma$ -complex **H** intermediate. Sometimes co-ordination to the  $\pi$ -electron of the allylic alcohol at the  $\alpha$ -position also occurs to form  $\sigma$ -complex **G** intermediate (Scheme 21). Both the intermediates **G** and **H** after syn-elimination yields the  $\alpha/\beta$ -substituted carbonyl compounds.

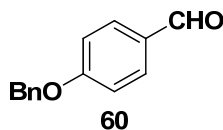


**Scheme 21.** Postulated mechanism for the synthesis of compound **63**.

## 1.5 Conclusion

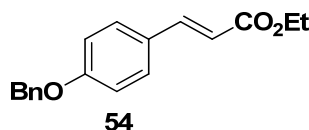
We have accomplished synthesis of the key intermediate, homo-allylic alcohol **16**, by following oxidative kinetic resolution (OKR). Our synthetic route following scheme 18 resulted compound **16** in 8.3% (8 steps). The other route (Scheme 19) furnished compound **16** in 22% overall yields (4 steps). The compound **16** could be transformed into the title compound **1** by following reported methods.<sup>7, 25</sup> In conclusion, we have accomplished a formal synthesis of (-)-centrolobine **1**.

## 1.6 Experimental

4-(Benzyloxy)benzaldehyde (**60**)

To a stirred suspension of  $K_2CO_3$  (10.35 g, 75.0 mmol) in dry DMF (20 mL) at room temperature was added 4-hydroxybenzaldehyde (6.10 g, 50.0 mmol) and TBAI (*cat*). The mixture was stirred for 30 min and then benzyl bromide (8.96 mL, 75.0 mmol) was added. The reaction mixture was stirred at room temperature for 24 h and then quenched with water and extracted with EtOAc (3 x 50 mL). The organic layer was washed with brine, dried over anhydrous  $Na_2SO_4$  and evaporated to give a crude mixture that was purified by silica gel column chromatography (PE/Ea, 8:2) to isolate product **60** (10.0 g).

<b>Yield</b>	10.0 g, 95%; white solid; $R_f = 0.5$ (PE/Ea, 7:3).
<b>Melting Point</b>	78-79°C
<b>Mol. Formula</b>	$C_{14}H_{12}O_2$
<b>IR</b> ( $CHCl_3$ )	$\nu_{max} (cm^{-1}) = 3019, 2725, 1694, 1600, 1509, 1215.$
<b><math>^1H</math> NMR</b> ( $CDCl_3$ , 200 MHz)	$\delta_H$ (ppm) = 9.9 (s, 1H, CHO), 7.83 (d, $J = 8.8$ Hz, 2H, CH), 7.45-7.37 (m, 5H, CH), 7.07 (d, $J = 8.7$ Hz, 2H, CH), 5.14 (s, 2H, $CH_2$ ).
<b><math>^{13}C</math> NMR</b> ( $CDCl_3$ , 50 MHz)	$\delta_C$ (ppm) = 190.8 (CHO), 164.0 (C), 136.0 (C), 132.0 (CH), 130.1 (C), 129.0 (CH), 128.3 (CH), 127.5 (CH), 115.1 (CH), 70.2 ( $CH_2$ ).
<b>Elemental analysis</b>	Calcd for $C_{14}H_{12}O_2$ : C, 79.22; H, 5.70 Found: C, 79.29; H, 5.78
<b>GC/MS (EI)</b>	213 $[M]^+$

*(E)*-Ethyl-3-(4-(benzyloxy)phenyl)acrylate (**54**)

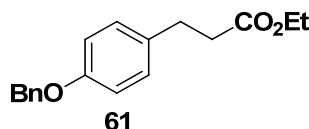


## Chapter 1

In the solution of (ethoxycarbonylmethylene)triphenyl phosphorane (17.4 g, 50.0 mmol) in anhydrous THF (30 mL) was slowly added to a solution of aldehyde **60** (9.54 g, 45.0 mmol) in anhydrous THF (20 mL) and then stirred it at room temperature for 24 h. THF was evaporated and purified by silica gel column chromatography (PE/EA, 8:2) to isolate product **54** (11.4 g).

<b>Yield</b>	11.4 g, 90%; white solid; $R_f = 0.38$ (PE/EA, 8:2).
<b>Melting Point</b>	58.7-58.9°C
<b>Mol. Formula</b>	$C_{18}H_{18}O_3$
<b>IR</b> ( $CHCl_3$ )	$\nu_{max}$ ( $cm^{-1}$ ) = 3019, 2725, 2401, 1698, 1635, 1510, 1216.
<b><math>^1H</math> NMR</b> ( $CDCl_3$ , 200 MHz)	$\delta_H$ (ppm) = 7.64 (d, $J = 15.9$ Hz, 1H, CH), 7.50-7.30 (m, 9H, CH), 6.96 (d, $J = 8.8$ Hz, 2H, CH), 6.30 (d, $J = 15.9$ Hz, 1H, CH), 5.08 (s, 2H, $CH_2$ ), 4.25 (q, $J = 7.1$ Hz, 2H, $CH_2$ ), 1.32 (t, $J = 7.1$ Hz, 3H, $CH_3$ ).
<b><math>^{13}C</math> NMR</b> ( $CDCl_3$ , 50 MHz)	$\delta_C$ (ppm) = 167.3 (C), 160.7 (C), 144.2 (CH), 136.4 (C), 132.0 (C), 129.7 (CH), 128.7 (CH), 128.3 (CH), 128.3 (CH), 127.5 (CH), 115.2 (CH), 70.0 ( $CH_2$ ), 60.3 ( $CH_2$ ), 14.3 ( $CH_3$ ).
<b>Elemental analysis</b>	Calcd for $C_{18}H_{18}O_3$ : C, 76.57; H, 6.43 Found: C, 76.50; H, 6.49.
<b>GC/MS (EI)</b>	282 $[M]^+$

### Ethyl 3-(4-(benzyloxy)phenyl)propanoate (**61**)

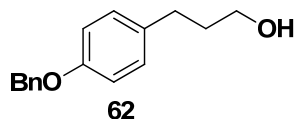


To a cooled solution of compound **54** (5.64 g, 20.0 mmol) in anhydrous MeOH (30 mL),  $NiCl_2 \cdot 6H_2O$  (4.74 g, 20 mmol) was added. To this slowly sodium borohydride (740 mg, 20 mmol) was added and stirred it at room temperature for 4 h. After completion of the reaction, methanol was evaporated, aqueous  $NH_4Cl$  was added (2 mL) and extracted with ethyl acetate (3 x 50 mL). The organic layer was washed with brine, dried over anhydrous  $Na_2SO_4$ , and evaporated to furnish a crude mixture that

was purified by silica gel column chromatography (PE/EA, 8:2) to isolate product **61** (5.05 g).

<b>Yield</b>	5.05 g, 89%; colorless oil; $R_f = 0.4$ (PE/EA, 8:2).
<b>Mol. Formula</b>	$C_{18}H_{20}O_3$
<b>IR</b> ( $CHCl_3$ )	$\nu_{max}$ ( $cm^{-1}$ ) = 3363, 3020, 2400, 1725, 1605, 1511, 1454.
<b><math>^1H</math> NMR</b> ( $CDCl_3$ , 200 MHz)	$\delta_H$ (ppm) = 7.43-7.28 (m, 5H, CH), 7.09 (d, $J = 8.6$ Hz, 2H, CH), 6.88 (d, $J = 8.7$ Hz, 2H, CH), 5.00 (s, 2H, $CH_2$ ), 4.09 (q, $J = 7.1$ Hz, 2H, $CH_2$ ), 2.87 (t, $J = 8.1$ Hz, 2H, $CH_2$ ), 2.56 (t, $J = 7.9$ Hz, 2H, $CH_2$ ), 1.21 (t, $J = 7.1$ Hz, 3H, $CH_3$ ).
<b><math>^{13}C</math> NMR</b> ( $CDCl_3$ , 50 MHz)	$\delta_C$ (ppm) = 172.8 (C), 157.2 (C), 137.0 (C), 132.8 (C), 129.2 (CH), 128.4 (CH), 127.8 (CH), 127.3 (CH), 114.7 (CH), 69.9 ( $CH_2$ ), 60.2 ( $CH_2$ ), 36.1 ( $CH_2$ ), 30.0 ( $CH_2$ ), 14.3 ( $CH_3$ ).
<b>Elemental analysis</b>	Calcd for $C_{18}H_{20}O_3$ : C, 76.03; H, 7.09 Found: C, 76.10; H, 7.16

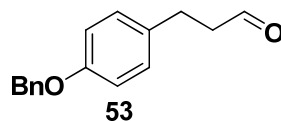
### 3-(4-(Benzyloxy)phenyl)propan-1-ol (**62**)



To a cooled solution of compound **61** (2.84 g, 10.0 mmol) in dry THF (10 mL), LAH (370 mg, 10.0 mmol) was slowly added and stirred at room temperature for 4 h under an atmosphere of argon. After completion of the reaction, it was cooled and quenched with 1N NaOH (10 mL). The white precipitate formed during the reaction was filtered through celite bed and filtrate was dried over anhydrous  $Na_2SO_4$  and the solvent was evaporated to under reduced pressure. The crude was purified by silica gel column chromatography (PE/EA, 7:3) to give product **62** (2.05 g).

<b>Yield</b>	2.05 g, 85%; white solid; $R_f = 0.28$ (PE/EA, 6:4).
<b>Melting Point</b>	46.7-47.9°C
<b>Mol. Formula</b>	$C_{16}H_{18}O_2$
<b>IR</b> ( $CHCl_3$ )	$\nu_{max}$ ( $cm^{-1}$ ) = 3616, 3434, 3018, 2874, 2402, 1611,

	1216.
<b><sup>1</sup>H NMR</b> (CDCl <sub>3</sub> , 200 MHz)	$\delta_{\text{H}}$ (ppm) = 7.47-7.30 (m, 8H, CH), 7.13 (d, $J$ = 8.7 Hz, 2H, CH), 6.92 (d, $J$ = 8.6 Hz, 2H, CH), 5.04 (s, 2H, CH <sub>2</sub> ), 4.68 (s, 1H, OH), 3.65 (t, $J$ = 6.4 Hz, 2H, CH <sub>2</sub> ), 2.65 (t, $J$ = 7.3 Hz, 2H, CH <sub>2</sub> ), 1.85 (m, 2H, CH <sub>2</sub> ).
<b><sup>13</sup>C NMR</b> (CDCl <sub>3</sub> , 50 MHz)	$\delta_{\text{C}}$ (ppm) = 157.0 (C), 140.8 (C), 137.1 (C), 134.1 (C), 129.3 (CH), 128.5 (CH), 127.8 (CH), 127.6 (CH), 127.4 (CH), 126.9 (CH), 114.7 (CH), 70.0 (CH <sub>2</sub> ), 62.2 (CH <sub>2</sub> ), 34.3 (CH <sub>2</sub> ), 31.1 (CH <sub>2</sub> ).
<b>Elemental analysis</b>	Calcd for C <sub>16</sub> H <sub>18</sub> O <sub>2</sub> : C, 79.31; H, 7.49 Found: C, 79.39; H, 7.54
<b>GC/MS (EI)</b>	242 [M] <sup>+</sup>

**3-(4-(Benzyloxy)phenyl)propanal (53)**

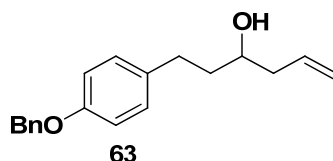
To a solution of the alcohol **62** (2.42 g, 10.0 mmol) in CH<sub>2</sub>Cl<sub>2</sub> (20 mL), trichloroisocyanuric acid (2.32 g, 10.0 mmol) was added and the solution was stirred and maintained at 0°C, followed by addition of TEMPO (0.015 g, 0.1 mmol). After completion of the reaction (TLC), warmed to room temperature and stirred for 15 min and then filtered on Celite, and the organic phase was washed with 15 mL of a saturated solution of Na<sub>2</sub>CO<sub>3</sub>, followed by 1 N HCl and brine, dried over anhydrous Na<sub>2</sub>SO<sub>4</sub>, and evaporated to furnish a crude mixture that was purified by silica gel column chromatography (PE/EA, 7:3) to isolate product **53** (2.20 g).

**Method II:** In a Flame dried RB flask, having magnetic needle was charged with 2.0 g of TBAB, it was refluxed at 130°C until the formation of ionic liquid. Pd(OAc)<sub>2</sub> (5.3 mg, 0.024 mmol), allyl alcohol (272  $\mu$ L, 4.0 mmol), sodium hydrogen carbonate (236 mg, 4.0 mmol) and iodide (620 mg, 2.0 mmol) were refluxed for 3 h. After completion of the reaction (TLC), warmed to room temperature and stirred for 15 min and then filtered on celite, and the organic phase was washed with 1N HCl and brine,

dried over anhydrous  $\text{Na}_2\text{SO}_4$ , and column purified (PE/EA, 7:3) to isolate product **53** (0.33 g, 69%).

<b>Yield</b>	2.2 g, 92%; colorless oil; $R_f = 0.41$ (PE/EA, 8:2).
<b>Mol. Formula</b>	$\text{C}_{16}\text{H}_{16}\text{O}_2$
<b>IR</b> ( $\text{CHCl}_3$ )	$\nu_{\text{max}} (\text{cm}^{-1}) = 3063, 3032, 2865, 1954, 1721, 1601.$
<b><math>^1\text{H}</math> NMR</b> ( $\text{CDCl}_3$ , 200 MHz)	$\delta_{\text{H}}$ (ppm) = 9.69 (m, 1H, CHO), 7.40-7.27 (m, 5H, CH), 7.03 (d, $J = 8.7$ Hz, 2H, CH), 6.86 (d, $J = 8.6$ Hz, 2H, CH), 4.95 (s, 2H, $\text{CH}_2$ ), 2.82 (t, $J = 7.1$ Hz, 2H, $\text{CH}_2$ ), 2.62 (t, $J = 7.9$ Hz, 2H, $\text{CH}_2$ ).
<b><math>^{13}\text{C}</math> NMR</b> ( $\text{CDCl}_3$ , 50 MHz)	$\delta_{\text{C}}$ (ppm) = 201.4 (CHO), 156.9 (C), 136.8 (C), 132.4 (C), 131.7 (CH), 129.0 (CH), 128.3 (CH), 127.6 (CH), 127.2 (CH), 114.6 (CH), 69.6 ( $\text{CH}_2$ ), 45.1 ( $\text{CH}_2$ ), 26.9 ( $\text{CH}_2$ ).
<b>Elemental analysis</b>	Calcd for $\text{C}_{16}\text{H}_{16}\text{O}_2$ : C, 79.97; H, 6.71 Found: C, 79.89; H, 6.65

**1-(4-(Benzyloxy)phenyl)hex-5-en-3-ol (63)**



To a solution of the allyl bromide (1.71 mL, 20 mmol) in THF (10 mL), aldehyde **53** (2.40 g, 10 mmol), saturated aqueous  $\text{NH}_4\text{Cl}$  (5 mL) and zinc metal (3.25 g, 20 mmol) was added. The mixture was stirred at room temperature for 3 h and after completion of the reaction it was filtered to remove excess zinc and precipitated salts, and the organic layer separated. It was extracted with ethyl acetate (3 x 50 mL). The organic layer was washed with brine, dried over anhydrous  $\text{Na}_2\text{SO}_4$ , and evaporated to furnish a crude mixture that was purified by silica gel column chromatography (PE/EA, 7:3) to isolate product **63** (2.50 g).

<b>Yield</b>	2.50 g, 89%; white solid; $R_f = 0.3$ (PE/EA, 7:3).
<b>Melting Point</b>	98-100°C
<b>Mol. Formula</b>	$\text{C}_{19}\text{H}_{22}\text{O}_2$
<b>IR</b> ( $\text{CHCl}_3$ )	$\nu_{\text{max}} (\text{cm}^{-1}) = 3367, 3019, 2935, 2401, 1716, 1610,$

1511, 1454, 1316, 1215.

**<sup>1</sup>H NMR**(CDCl<sub>3</sub>, 200 MHz)

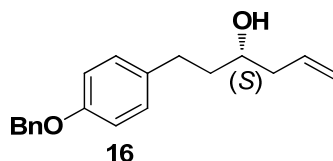
$\delta_{\text{H}}$  (ppm) = 7.44-7.29 (m, 5H, CH), 7.10 (d,  $J = 8.7$  Hz, 2H, CH), 6.89 (d,  $J = 8.7$  Hz, 2H, CH), 5.87-5.69 (m, 1H, CH), 5.18-5.14 (m, 1H, CH), 5.11-5.06 (m, 1H, CH), 5.01 (s, 2H, CH<sub>2</sub>), 3.66-3.57 (m, 1H, CH), 2.77-2.48 (m, 2H, CH<sub>2</sub>), 2.48-2.11 (m, 2H, CH<sub>2</sub>), 1.74 (t,  $J = 7.8$  Hz, 2H, CH<sub>2</sub>).

**<sup>13</sup>C NMR**(CDCl<sub>3</sub>, 50 MHz)

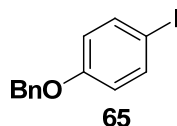
$\delta_{\text{C}}$  (ppm) = 158.1 (C), 156.9 (C), 137.1 (CH), 136.9 (CH), 136.3 (C), 134.6 (C), 134.3 (C), 128.5 (C), 127.9 (CH), 127.8 (CH), 127.4 (CH), 127.0 (CH), 118.1 (CH), 118.0 (CH), 114.7 (CH), 72.9 (CH<sub>2</sub>).

**Elemental analysis**Calcd for C<sub>19</sub>H<sub>22</sub>O<sub>2</sub>: C, 80.82; H, 7.85

Found: C, 80.92; H, 7.95

**(*S*)-1-(4-(Benzyloxy)phenyl)hex-5-en-3-ol (16)**

To a solution of substrate **64** (2.39 g, 8.50 mmol) in CH<sub>2</sub>Cl<sub>2</sub> (5 mL), and water (10 mL) catalyst (*S,S*)-Salen-Mn<sup>III</sup>Cl (0.107 g, 0.16 mmol), additive KBr (0.808 g, 6.80 mmol), was added and stirred for a few minutes at room temperature. The oxidant PhI(OAc)<sub>2</sub> (1.91 g, 5.94 mmol) was added and the mixture was stirred for 30 min until the completion of reaction. The products were extracted by using diethyl ether and purified on silica gel column chromatography giving yields as 43% for (*S*)-**16** (1.02 g,  $R_f = 0.3$ , PE/EA, 7:3) as colorless oil and 46% for **65** (1.30 g).

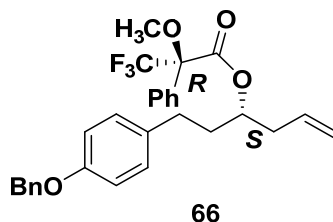
**1-(Benzyloxy)-4-iodobenzene (65)**

To a stirred suspension of K<sub>2</sub>CO<sub>3</sub> (1.88 g, 13.6 mmol) in anhydrous DMF (5 mL) at room temperature was added 4-iodophenol **65** (2.0 g, 9.09 mmol) and TBAI (cat). The mixture was stirred for 20 min and then benzyl bromide (1.3 mL, 10.9 mmol) was

added. The reaction mixture was stirred at room temperature for 10 h and then quenched with water and extracted with EtOAc (3 x 50 mL). The organic layer was washed with brine, dried (anhydrous Na<sub>2</sub>SO<sub>4</sub>) and evaporated to give a crude mixture that was purified by silica gel column chromatography (PE/EA, 8:2) to isolate product **65** (2.62 g).

<b>Yield</b>	2.62 g, 93%; white solid; $R_f = 0.5$ (PE/EA, 6:4).
<b>Melting Point</b>	56.5-58.6°C
<b>Mol. Formula</b>	C <sub>13</sub> H <sub>11</sub> IO
<b>IR</b> (CHCl <sub>3</sub> )	$\nu_{\max}$ (cm <sup>-1</sup> ) = 3362, 3019, 1725, 1614, 1541, 1485, 1454, 1349.
<b><sup>1</sup>H NMR</b> (CDCl <sub>3</sub> , 200 MHz)	$\delta_H$ (ppm) = 7.53 (d, $J = 9.1$ Hz, 2H, CH), 7.43-7.32 (m, 5H, CH), 6.75 (d, $J = 9.0$ Hz, 2H, CH), 5.04 (s, 2H, CH <sub>2</sub> ).
<b><sup>13</sup>C NMR</b> (CDCl <sub>3</sub> , 50 MHz)	$\delta_C$ (ppm) = 158.6 (C), 138.2 (CH), 136.5 (C), 128.6 (CH), 128.1 (CH), 127.4 (CH), 117.3 (CH), 83.0 (C), 70.0 (CH <sub>2</sub> ).
<b>Elemental analysis</b>	Calcd for C <sub>13</sub> H <sub>11</sub> IO: C, 50.35; H, 3.58 Found: C, 50.41; H, 3.65

**(S)-1-(4-(Benzyloxy)phenyl)hex-5-en-3-yl (R)-3,3,3-trifluoro-2-methoxy-2-phenyl propanoate (66)**



To a 0° C cooled solution of substrate **16** (71 mg, 0.25 mmol) in CH<sub>2</sub>Cl<sub>2</sub> (1 mL) and (*R*)-(+)- $\alpha$ -methoxy- $\alpha$ -(trifluoromethyl)phenylacetic acid (58.5 mg, 0.25 mmol), and HBTU (95 mg, 0.25 mmol) was added and stirred for 4 h at that temperature. The products were extracted by using DCM and purified on silica gel column chromatography to furnish product **66** (75.2 mg, 60%).

<b>Yield</b>	75.2 mg, 60%; white solid; $R_f = 0.3$ (PE/EA, 2:8).
<b>Mol. Formula</b>	C <sub>29</sub> H <sub>29</sub> F <sub>3</sub> O <sub>4</sub>

## Chapter 1

---

**$^{19}\text{F}$  NMR**  
( $\text{CDCl}_3$ , 200 MHz)

$\delta_{\text{F}}$  (ppm) = 70.05 (major), 70.02 (minor)

---

## 1.7 References

1. De Albuquerque, I. L.; Galeffi, C.; Casinovi, C. G.; Marini-Bettòlo, G. B. *Gazz. Chim. Ital.* **1964**, *94*, 287; (b) Galeffi, C.; Casinovi, C. G.; Marini-Bettolo, G. B. *Gazz. Chim. Ital.* **1965**, *95*, 95; (c) Craveiro, A. A.; Prado, A. D. C.; Gottlieb, O. R.; Albuquerque, P. C. W. D. *Phytochemistry*, **1970**, *9*, 1869.
2. Colobert, F.; Mazery, R. D.; Solladie, G.; Carreño, M. C. *Org. Lett.* **2002**, *4*, 1723; (b) Carreño, M. C.; Mazery, R. D.; Urbano, A.; Colobert, F.; Solladie, G. *J. Org. Chem.* **2003**, *68*, 7779.
3. Marumoto, S.; Jaber, J. J.; Vitale, J. P.; Rychnovsky, S. D. *Org. Lett.* **2002**, *4*, 3919.
4. Evans, P. A.; Cui, J.; Gharpure, S. J. *Org. Lett.* **2003**, *5*, 3883.
5. Boulard, L.; BouzBouz, S.; Cossy, J.; Franck, X.; Figadère, B. *Tetrahedron Lett.* **2004**, *45*, 6603.
6. Clarke, P. A.; Martin, W. H. C. *Tetrahedron* **2005**, *61*, 5433.
7. (a) Lee, C.-H. A.; Loh, T.-P. *Tetrahedron Lett.* **2006**, *47*, 1641; (b) Zhou, H.; Loh, T.-P. *Tetrahedron Lett.* **2009**, *50*, 4368.
8. Reddy, C.; Madhavi, P.; Chandrasekhar, S. *Synthesis* **2008**, 2939.
9. Jennings, M. P.; Clemens, R. T. *Tetrahedron Lett.* **2005**, *46*, 2021.
10. Böhrsch, V.; Blechert, S. *Chem. Comm.*, **2006**, 1968.
11. Prasad, K. R.; Anbarasan, P. *Tetrahedron* **2007**, *63*, 1089.
12. Washio, T.; Yamaguchi, R.; Abe, T.; Nambu, H.; Anada, M.; Hashimoto, S. *Tetrahedron* **2007**, *63*, 1203.
13. Dziedzic, M.; Furman, B. *Tetrahedron Lett.* **2008**, *49*, 678.
14. He, A.; Sutivisedsak, N.; Spilling, C. D. *Org. Lett.* **2009**, *11*, 3124.
15. (a) Sun, W.; Wang, H.; Xia, C.; Li, J.; Zhao, P. *Angew. Chem. Int. Ed.* **2003**, *42*, 1042;
16. (b) Tripathi, D.; Pandey, S. K.; Kumar, P. *Tetrahedron* **2009**, *65*, 2226.
17. (a) Blanc, A.; Toste, F. D. *Angew. Chem. Int. Ed.* **2006**, *45*, 2096; (b) Radosevich, A. T.; Chan, V. S.; Shih, H.-W.; Toste, F. D. *Angew. Chem. Int. Ed.* **2008**, *47*, 3755.

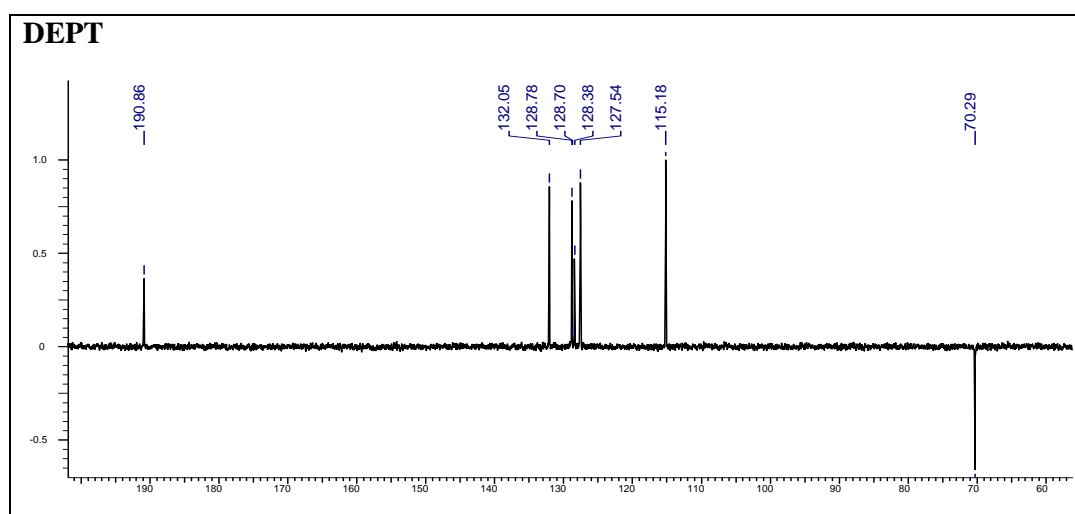
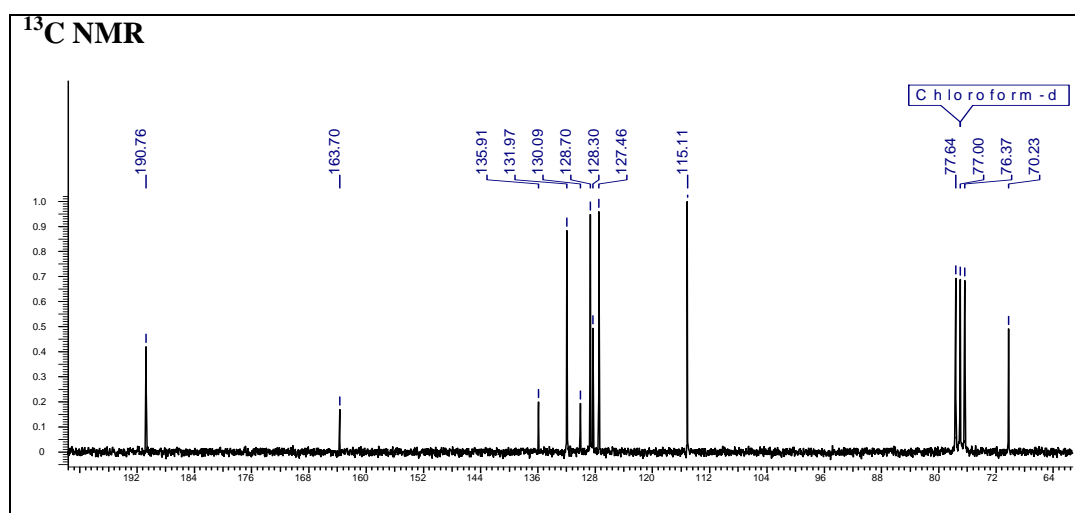
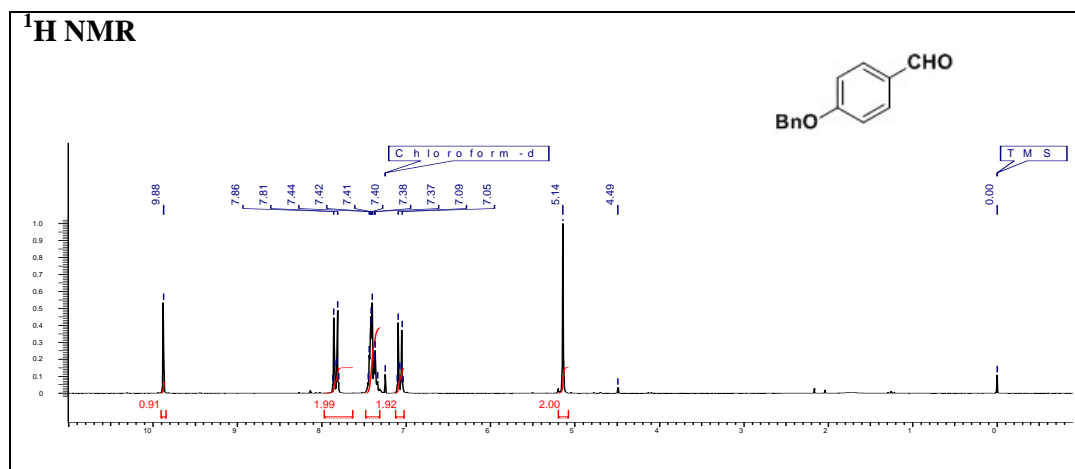


- 18.** (a) Yamada, T.; Higano, S.; Yano, T.; Yamashita, Y. *Chem. Lett.* **2009**, *38*, 40; (b) Alamsetti, S. K.; Muthupandi, P.; Sekar, G. *Chem. Eur. J.* **2009**, *15*, 5424.
- 19.** Arita, S.; Koike, T.; Kayaki, Y.; Ikariya, T. *Angew. Chem. Int. Ed.* **2008**, *47*, 2447.
- 20.** (a) Ebner, D. C.; Trend, R. M.; Genet, C.; McGrath, M. J.; O'Brien, P.; Stoltz, B. M. *Angew. Chem. Int. Ed.* **2008**, *47*, 6367; (b) Bagdanoff, J. T.; Stoltz, B. M. *Angew. Chem. Int. Ed.* **2004**, *43*, 353; (c) Liu, S.-J.; Liu, L.; Shi, M. *App. Org. Chem.* **2009**, *23*, 183; (d) Trend, R. M.; Stoltz, B. M. *J. Am. Chem. Soc.* **2004**, *126*, 4482; (e) Mueller, J. A.; Cowell, A.; Chandler, B. D.; Sigman, M. S. *J. Am. Chem. Soc.* **2005**, *127*, 14817.
- 21.** Fernandes, R. A.; Bodas, M. S.; Kumar, P. *Tetrahedron* **2002**, *58*, 1223.
- 22.** Belisle, C. M.; Yvette, M.; Young, B. S. *Tetrahedron Lett.* **1994**, *35*, 5595.
- 23.** Lago, E.; Marquez, R.; Montoro, R.; Llebearia, A.; Molins, E.; Delgado, A. J. *Org. Chem.* **2002**, *67*, 308.
- 24.** Calò, V.; Nacci, A.; Monopoli, A.; Ferola, V. *J. Org. Chem.* **2007**, *72*, 2596.
- 25.** (a) Dale, J. A.; Mosher, H. S. *J. Am. Chem. Soc.* **1968**, *90*, 3732-3740; (b) Dale, J. A.; Dull, D. L.; Mosher, H. S. *J. Org. Chem.* **1969**, *34*, 2453; (c) Dale, J. A.; Mosher, H. S. *J. Am. Chem. Soc.* **1973**, *95*, 512-519; (d) Sullivan, G. R.; Dale, J. A.; Mosher, H. S. *J. Org. Chem.* **1973**, *38*, 2143.
- 26.** Chan, K. -P.; Loh, T. -P. *Org. Lett.* **2005**, *7*, 4491.

## 1.8 Appendix C: Characterization data of synthesized compounds

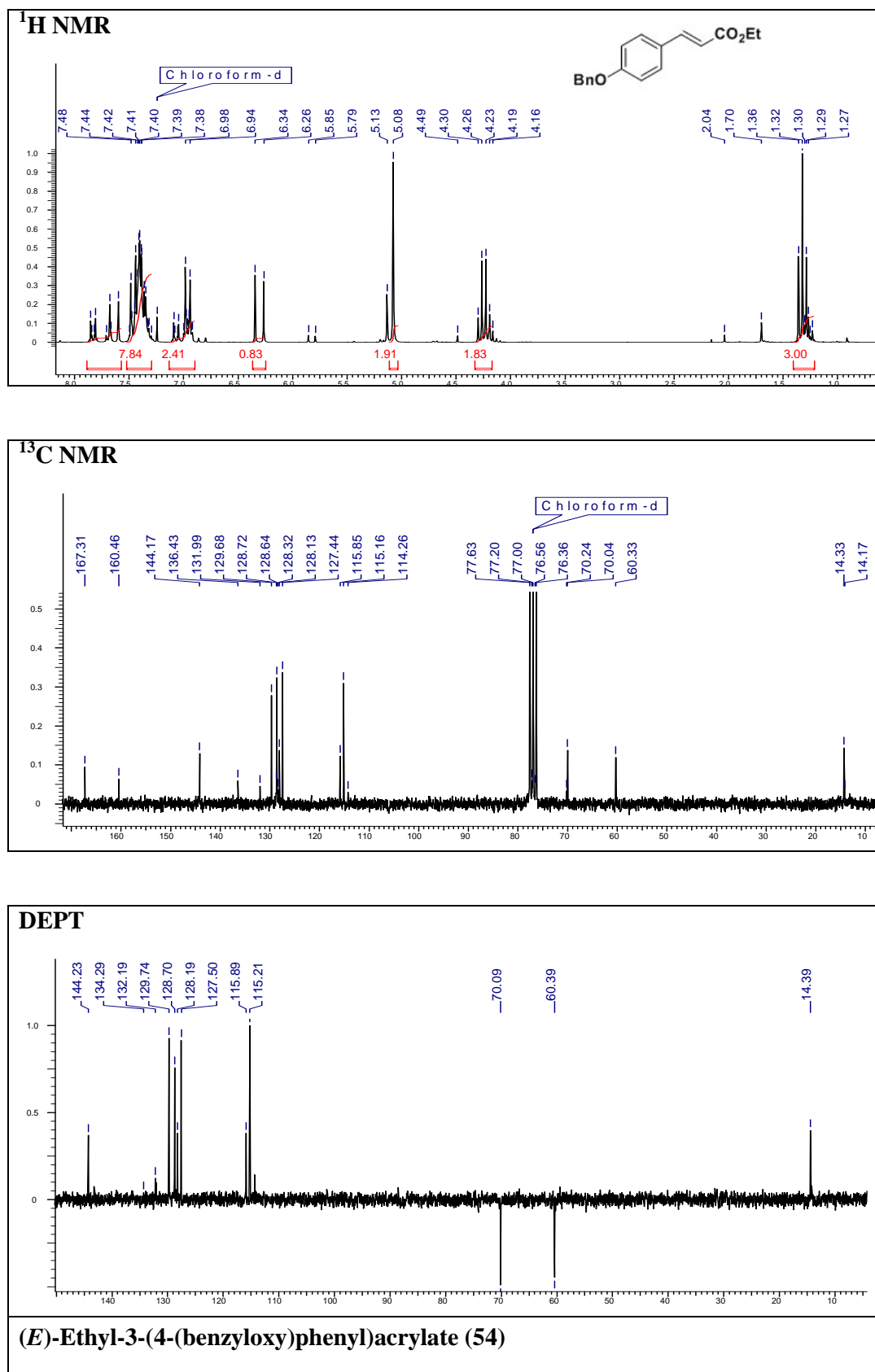
Compound	Description	Page No.
Compound 60	$^1\text{H}$ NMR, $^{13}\text{C}$ NMR, DEPT-NMR	123
Compound 54	$^1\text{H}$ NMR, $^{13}\text{C}$ NMR, DEPT-NMR	124
Compound 61	$^1\text{H}$ NMR, $^{13}\text{C}$ NMR, DEPT-NMR	125
Compound 62	$^1\text{H}$ NMR, $^{13}\text{C}$ NMR, DEPT-NMR	126
Compound 53	$^1\text{H}$ NMR, $^{13}\text{C}$ NMR, DEPT-NMR	127
Compound 63	$^1\text{H}$ NMR, $^{13}\text{C}$ NMR, DEPT-NMR	128
Compound 65	$^1\text{H}$ NMR, $^{13}\text{C}$ NMR, DEPT-NMR	129
Compound 66	$^{19}\text{F}$ NMR	130

# Chapter 1

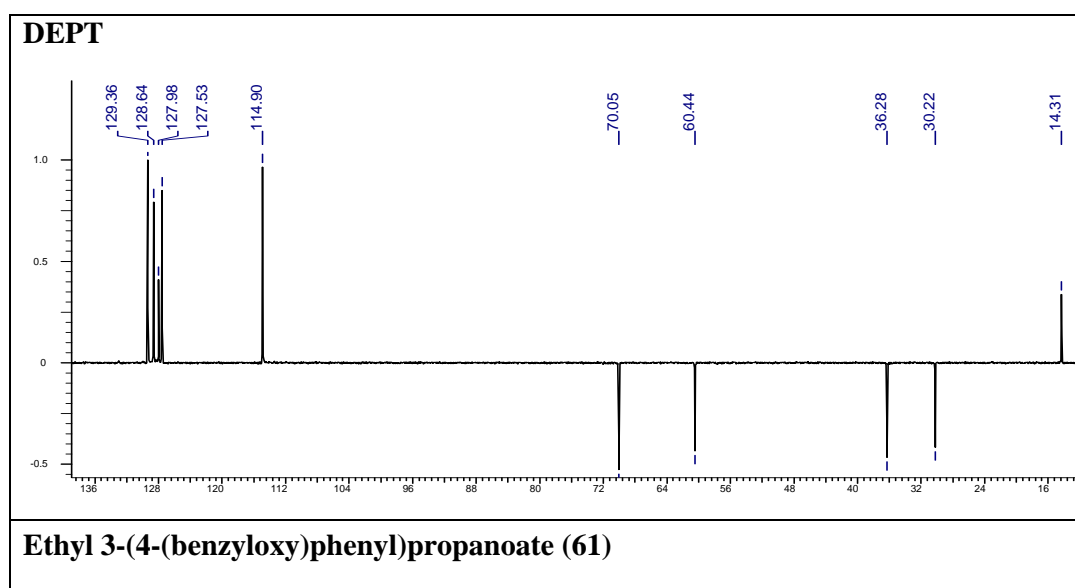
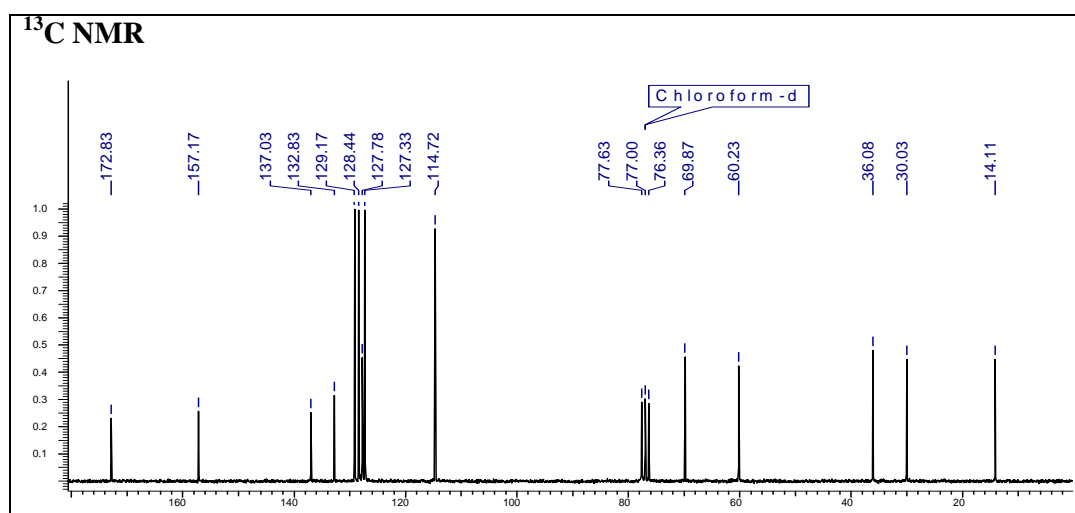
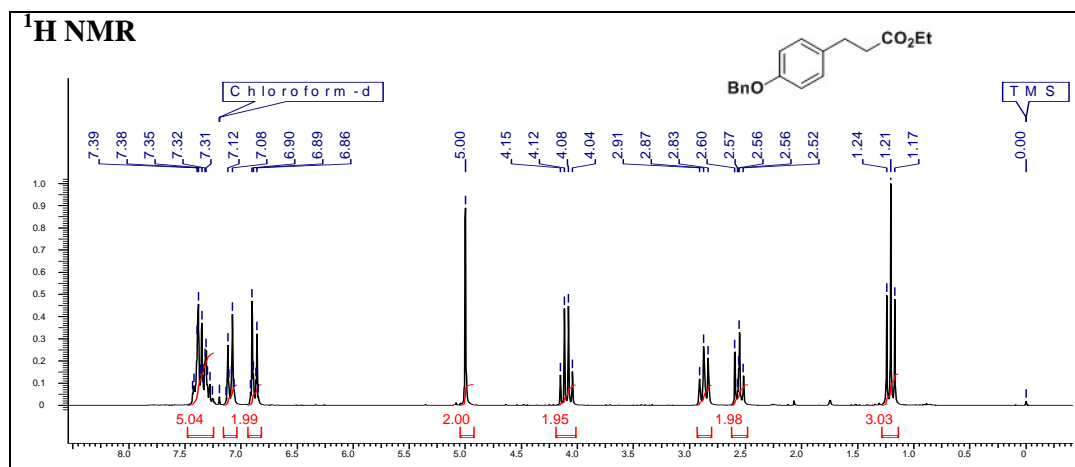


**4-(Benzyloxy)benzaldehyde (60)**

# Chapter 1

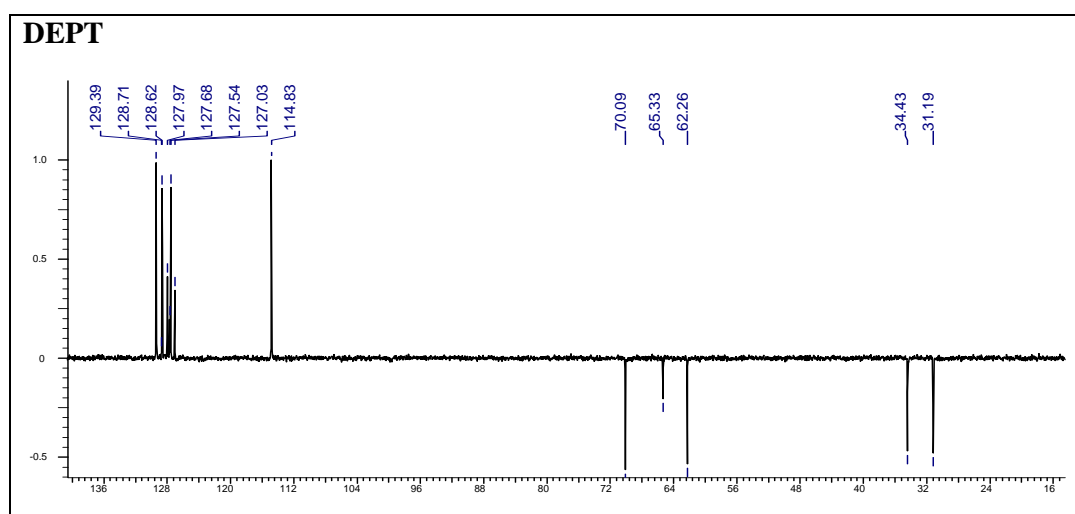
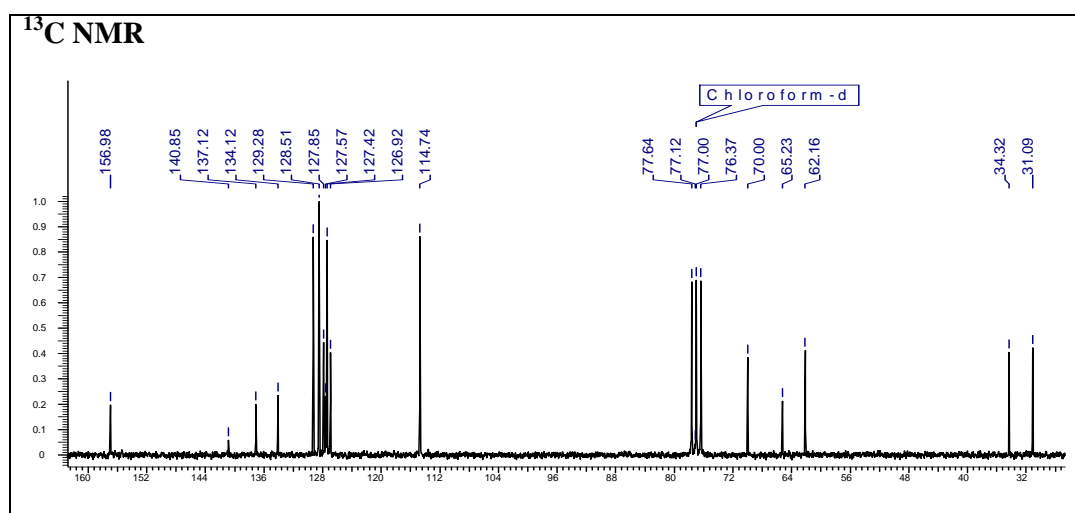
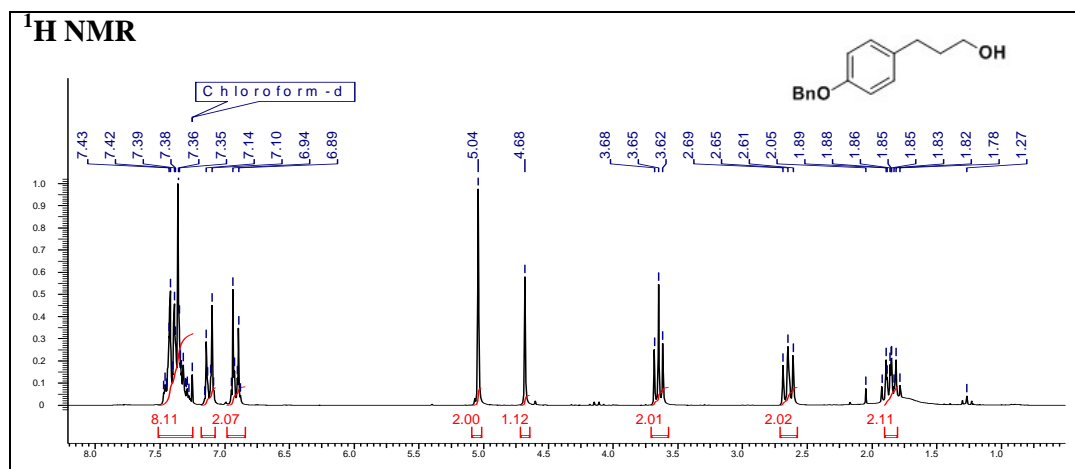


# Chapter 1



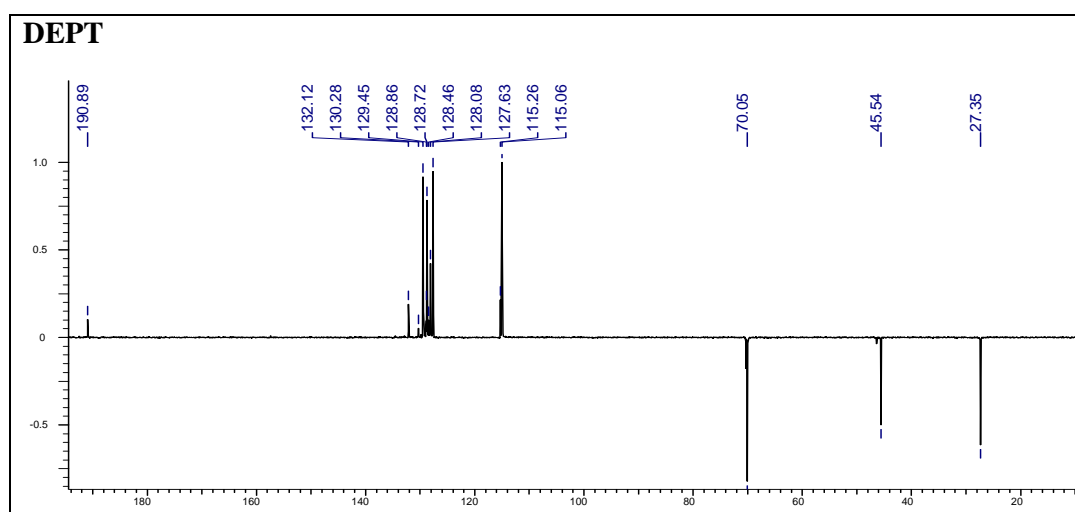
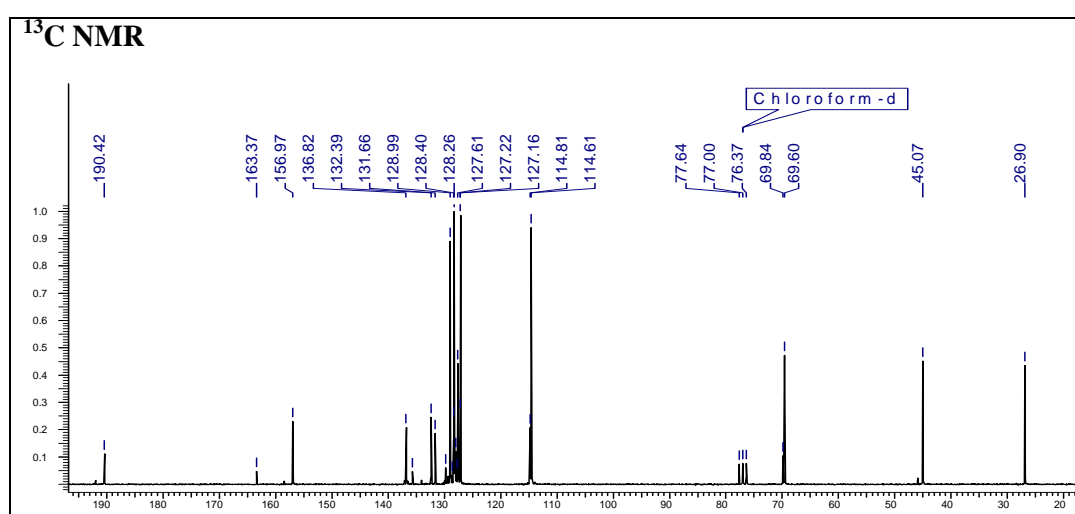
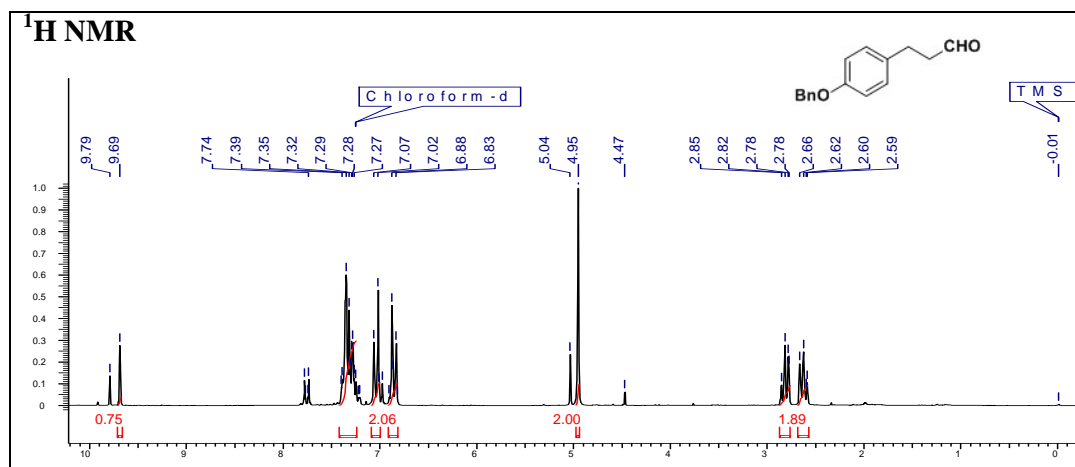
**Ethyl 3-(4-(benzyloxy)phenyl)propanoate (61)**

# Chapter 1



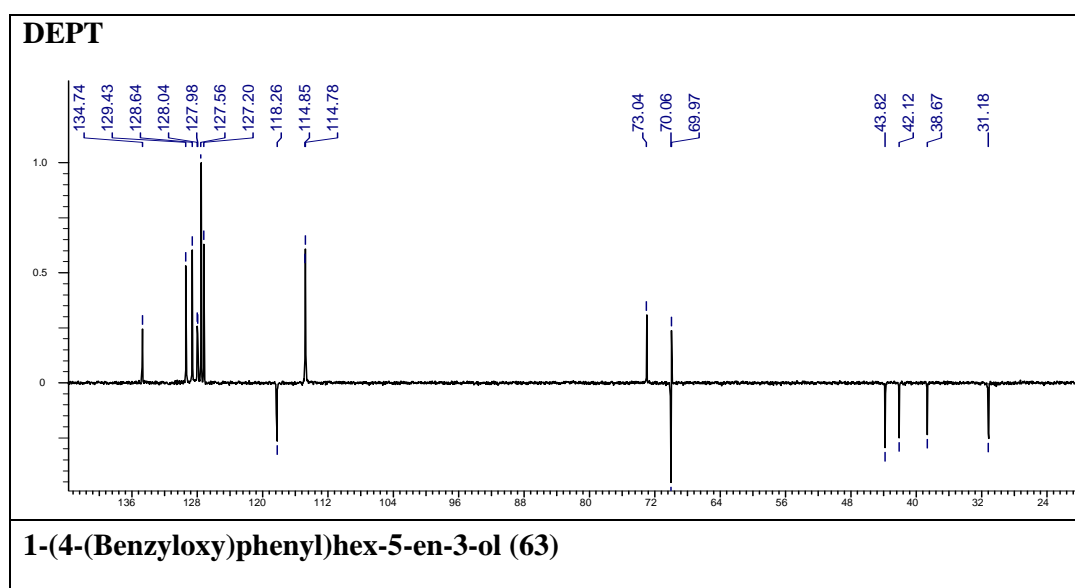
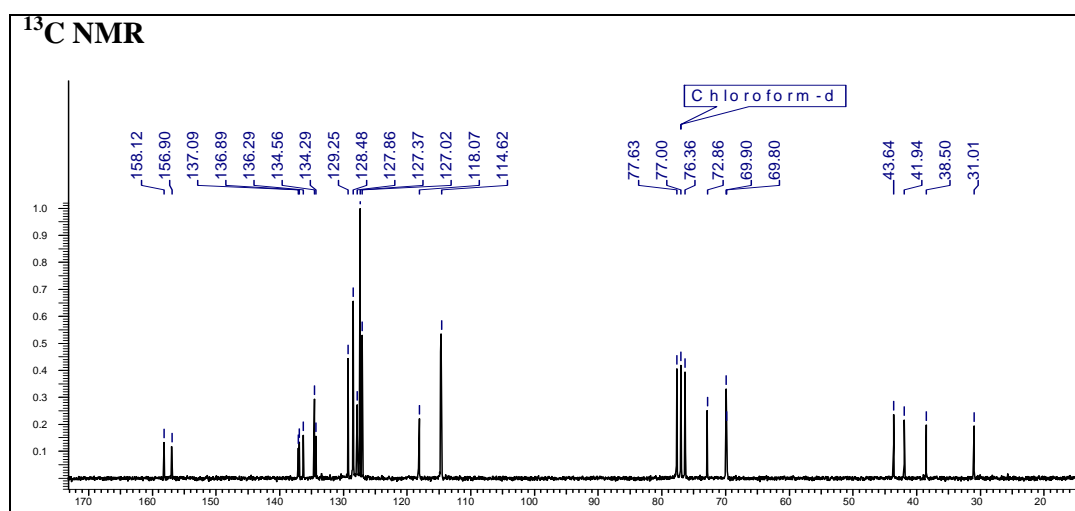
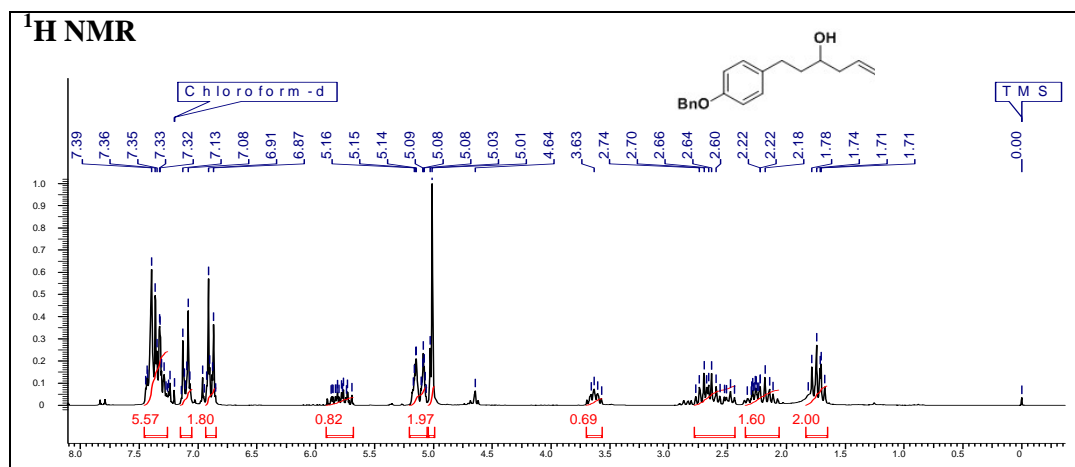
**3-(4-(Benzyloxy)phenyl)propan-1-ol (62)**

# Chapter 1



**3-(4-(Benzyloxy)phenyl)propanal (53)**

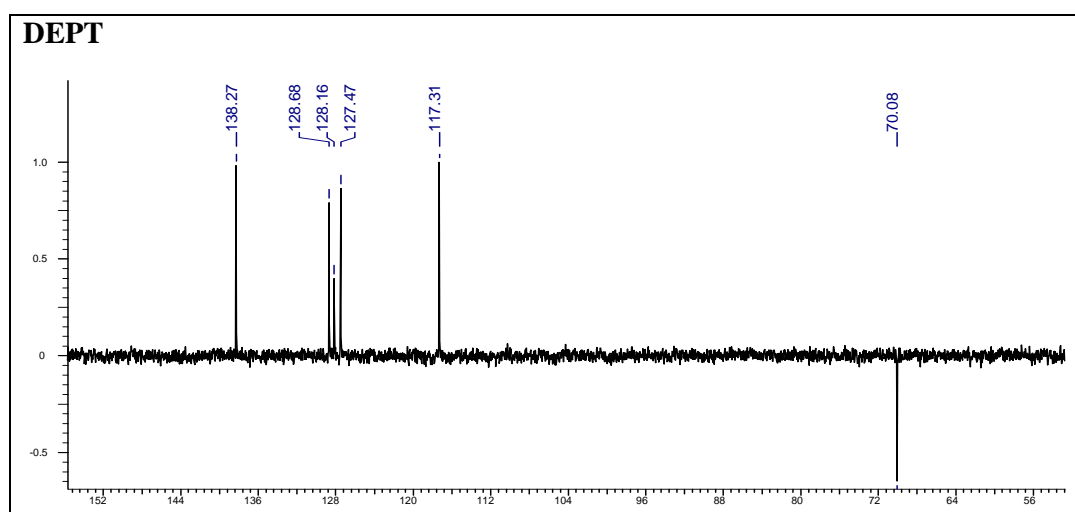
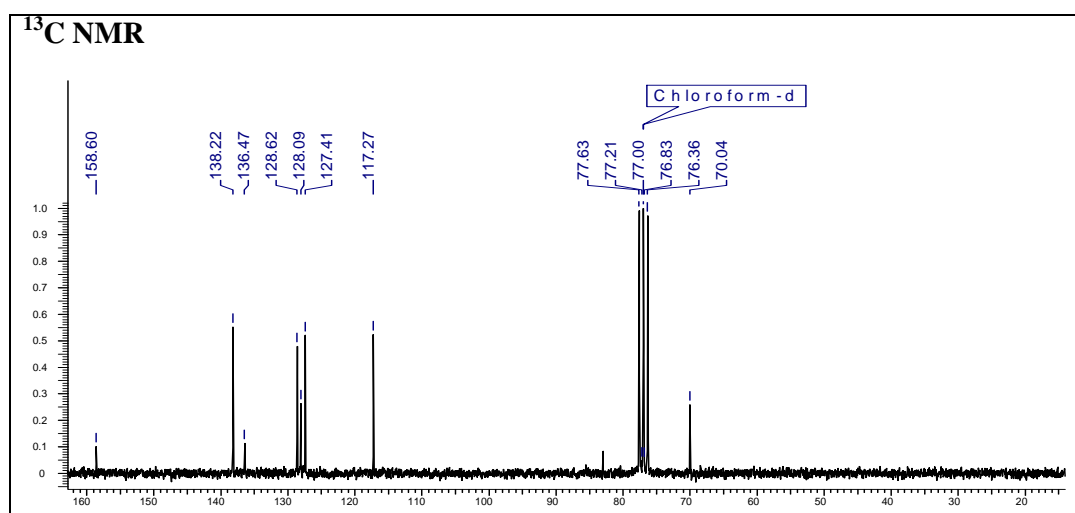
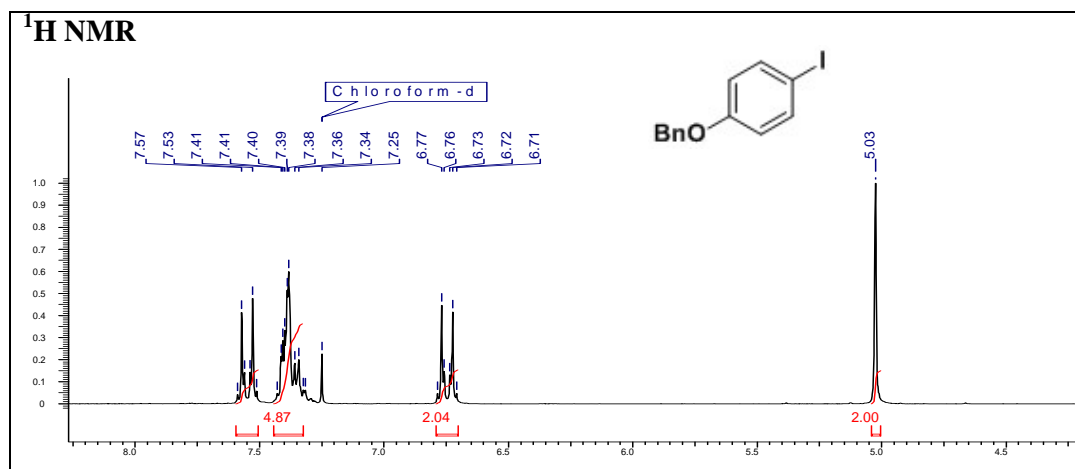
# Chapter 1



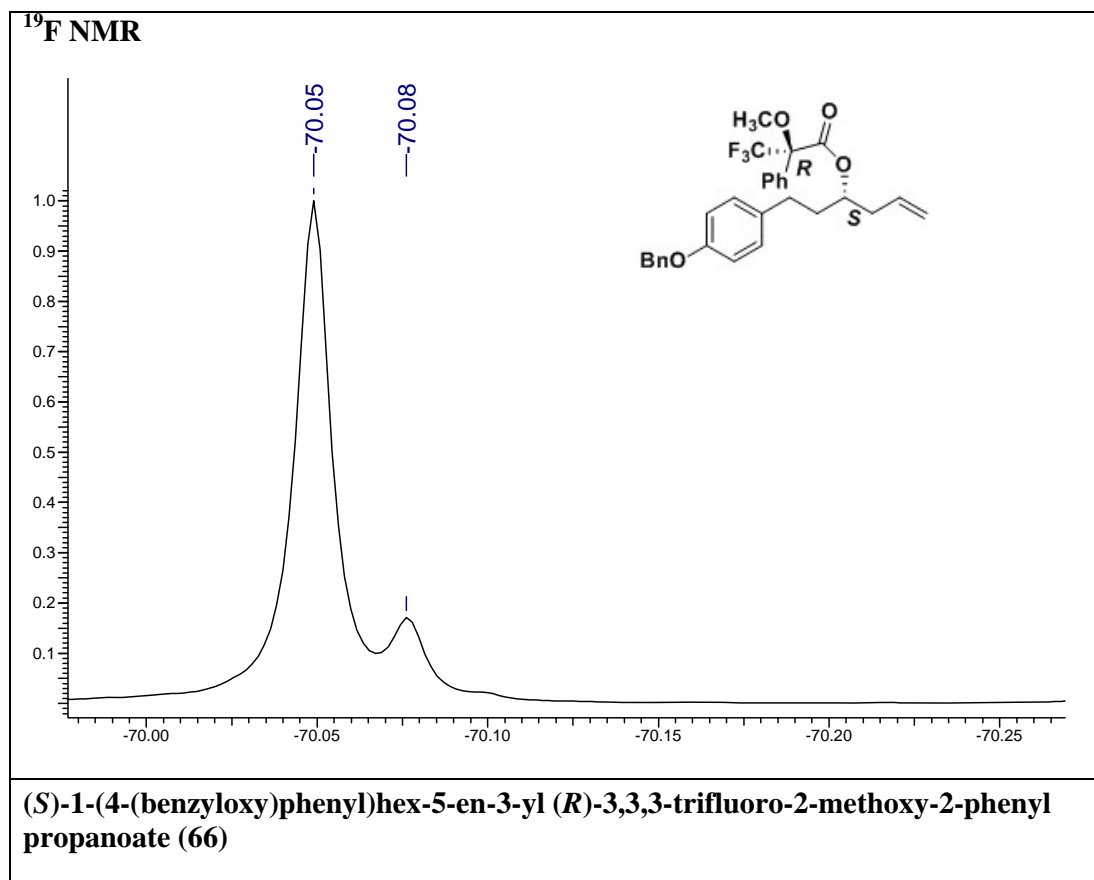
**1-(4-(Benzyloxy)phenyl)hex-5-en-3-ol (63)**



# Chapter 1



**1-(Benzyloxy)-4-iodobenzene (65)**



# *Chapter 2*

## **New Synthetic Methodologies**

---

### *Section A*

#### **Decarboxylative Method for the Synthesis of 2-Styryl Furans/Thiophenes**

---

This section deals with the development of new routes for the synthesis of 2-styryl furans/thiophenes. It also discusses previous literature routes for the synthesis of this class of molecules.

## 2.1 Introduction

The formation of C-C bonds plays an important role in organic synthesis.<sup>1</sup> There are numerous reports for the synthesis of various structural complex motifs *via* the effective use of transition metals. Palladium, which plays pivotal role in the Heck,<sup>2</sup> Stille,<sup>3</sup> and Sonogashira<sup>4</sup> cross-coupling and in various cascade reactions. Palladium catalyzed cross-coupling reactions have emerged as an important tool for the carbon-carbon bond forming reactions. These reactions are better in scope selectivity, regio-specificity and chemo-selectivity as compare to other Fe, Ni, Cu metal catalyzed reactions. Direct cross-coupling between alkenes and aryl halides is well documented in literature.

The development of new carbon-carbon bond forming reactions is essential for the synthesis of important molecules. Over the past decades, Suzuki-Miyaura coupling is the most successful strategy for the synthesis of biaryls.<sup>5</sup> Several biaryl derivatives possess their importance as drug molecules such as Felbinac **1**, Losartan **2**, Imatinib **3** and Boscalid **4** (Figure 1).<sup>6</sup> However, these synthetic methods suffer from few drawbacks as they utilize stoichiometric amounts of organometallic partner.

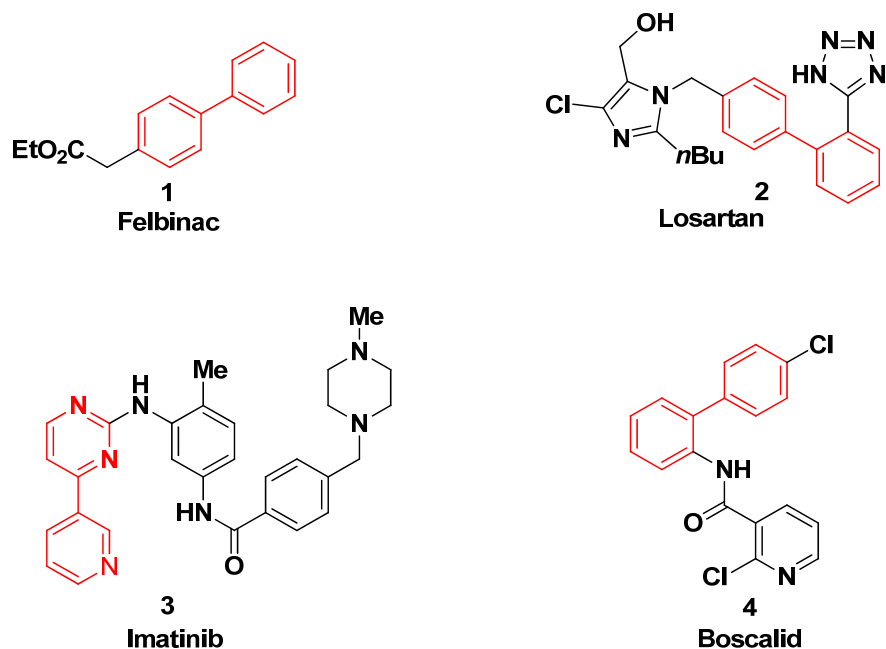


**Figure 1.** Structure of few useful biaryl derivatives synthesized *via* Suzuki-Miyuara cross-coupling reactions.

## Chapter 2

There are few reports for the synthesis of biaryl derivatives. The first method involves conventional cross-coupling reaction between aryl halides and organometallic substrates. However, this method suffers from several drawbacks i.e. low yields and harsh reaction conditions. The second method employs direct arylation, using aryl halides and substrates having active C-H groups. However, C-H activation method has inherent problem of regio-selectivity.<sup>7</sup>

A third and most promising approach consists of decarboxylative cross-coupling between aryl halide and arene carboxylic acid.<sup>8</sup> The carboxylic group ensures regio-selectivity of the reaction and carbon dioxide is a by-product.

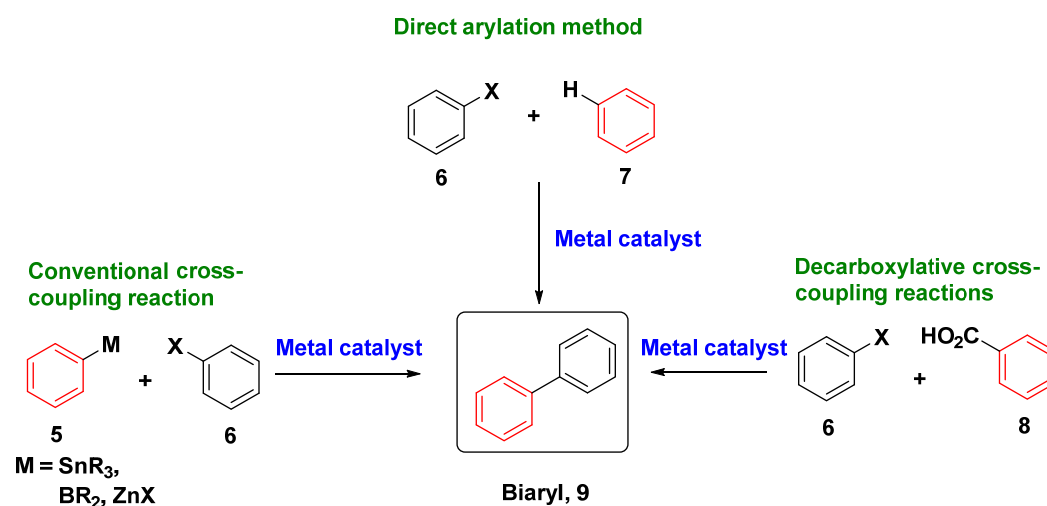
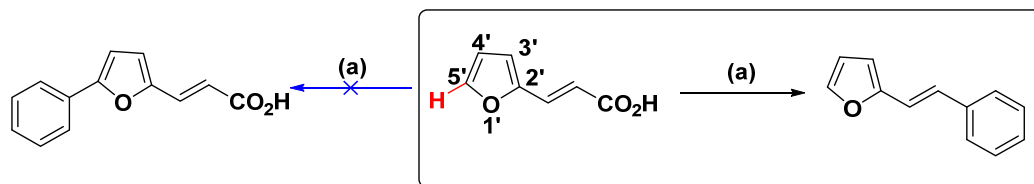


**Figure 2.** Previous reports for the synthesis of biaryl derivatives.

In 1966, Nilsson's *et al.* first reported decarboxylative Ullmann coupling on the aryl iodides.<sup>9</sup> Further advancements in this field came very recently. In 2002, Myers *et al.* carried out Heck type palladium catalyzed decarboxylative coupling between aryl carboxylic acid and olefins.<sup>10</sup> Very recently, Gooßen *et al.*<sup>11</sup> explored palladium catalyzed cross-coupling between heteroaromatic carboxylic acid and aryl halides. These reactions require catalytic amounts of copper or silver salts. Hence, still there exists a need for the development of new synthetic methodologies overcoming some of the short coming of the reported methods.

There are only very few methods in the literature for the synthesis of 2-styryl furans/thiophenes. These 2-styryl furans are highly conjugated analogs and possess

fluorescent properties. While, 2-styryl thiophenes/polythiophenes can be useful in the synthesis of the conjugated polymers, these derivatives are highly sensitive to acidic conditions, hence there is still a need for development of new routes for these cross-coupled products (Scheme 1).



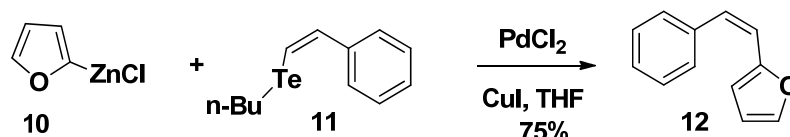
**Scheme 1.** Optimization of the reaction conditions for the synthesis of 2-styryl furans; *Reagent and conditions:* (a) Aryl halide,  $K_2CO_3$ ,  $PdCl_2$ ,  $140\text{ }^\circ C$ ,  $3\text{ \AA}$  molecular sieves, DMF, 15-60 min.

## 2.1.1 Previous reports

There are few reports in the literature for the synthesis of 2-styryl furans. In following section, each one of them has been briefly discussed.

### 2.1.1a Zeni's et al. approach (2004)

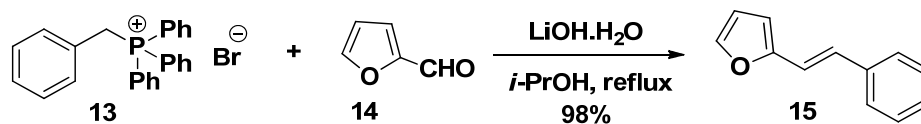
Zeni *et al.*<sup>12</sup> utilized Negishi cross-coupling for the synthesis of 2-(*Z*-styryl)furan. The treatment of 2-furylzinc chloride **10** with *Z*-vinylic tellurides **11** in presence of palladium chloride, and copper iodide resulted in the formation of 2-(*Z*-styryl)furan **12** in 75% yield (Scheme 2).



**Scheme 2.** Synthesis of 2-(*Z*-styryl)furan *via* Negishi cross-coupling reaction.

### 2.1.1b Bonadies's et al. approach (2008)

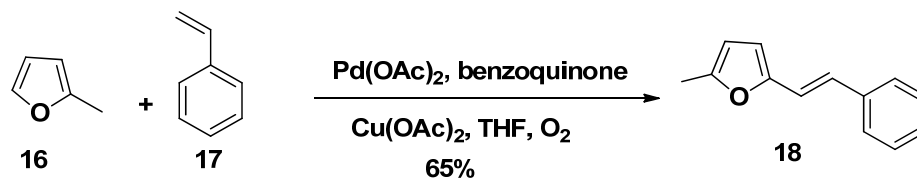
Bonadies *et al.*<sup>13</sup> synthesized 2-styryl-furans **12** *via* the Wittig reaction. In this approach, triphenylbenzyl phosphonium bromide **13** was reacted with furan-2-carboxaldehyde **14** in presence of lithium hydroxide as a base to synthesize 2-(*E*-styryl)furan **15** in 98% yield (Scheme 3).



**Scheme 3.** Synthesis of 2-(*E*-styryl)furan *via* Wittig reaction.

## 2.1.1c Bras's et al. approach (2009)

Bras *et al.*<sup>14</sup> utilized palladium catalyzed dehydrogenative cross-coupling between furan **16** and styrenes **17** to synthesize the 2-(*E*-styryl)furan **18**. This method gave good to excellent yields, and is highly regio- and stereoselective (Scheme 4).



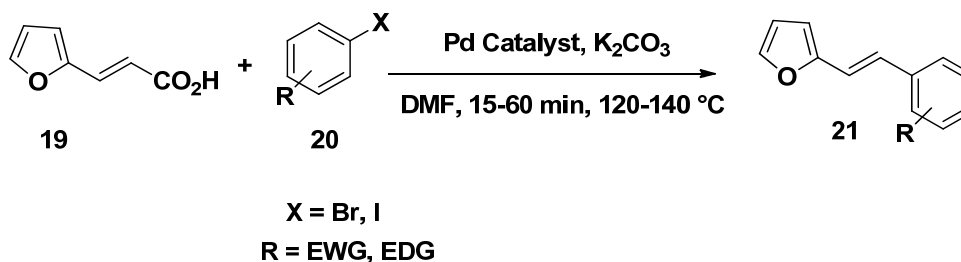
**Scheme 4.** Synthesis of 2-(*E*-styryl)furan *via* dehydrogenative cross-coupling.

## 2.2 Present Work: Objective and Rationale

Although derivatives of 2-styryl furans/thiophenes could be useful in the synthesis of various useful analogs, there are only a few methods in the literature for its synthesis. So, there is a need to develop new routes for the synthesis of these molecules

## 2.3 Results and Discussion

We opined that 2-(*E*-styryl)furan **21** could be synthesized by reacting (*E*)-3-(furan-2-yl)-acrylic acid **19** and aryl halides **20** under palladium catalyzed conditions. An effective strategy for the regiospecific construction of 2-(*E*-styryl)furan **21**, in which (*E*)-3-(furan-2-yl)-acrylic acid **19** undergoes decarboxylation to generate aryl palladium species which further acts as a nucleophilic intermediate in the cross-coupling with aryl halides and triflates. This system allows the coupling of furan carboxylic acids with aryl halides and triflates in the presence of palladium chloride at 140 °C using potassium carbonate as a mild base (Scheme 5).



**Scheme 5.** Optimization of reaction conditions for the Synthesis of 2-(*E*-styryl)furan.

## Chapter 2

The reaction conditions were optimized by heating a mixture of (*E*)-3-(furan-2-yl)acrylic acid and various substituted aryl derivatives at 140 °C in DMF (Table 1). The other coupling substrates studied were boronic acids (entry 11), triflates (entry 10), sulphonyl chloride (entry 12), aromatic chlorides (entry 13), aromatic bromides (entries 2, 4-7) and aromatic iodides. Among all, it was observed that bromides and iodides afforded the desired 2-(*E*-styryl)furan **21** in 60 and 65% yields, respectively (entries 7 and 9). Initially, reactions were carried out at 120 °C, but it was observed that yields are low and prolonged heating were required as compared to reactions carried out at 140 °C. Palladium salts were screened from 0.1 mol % to 5 mol %. The better yields were obtained with 5 mol % of palladium catalysts. The screening of palladium catalysts were carried out under various conditions.

**Table 1.** Optimization of reaction conditions

Entry	X <sup>-</sup>	Palladium catalyst (0.05 eq)	Temp (°C)	Time (min)	Yield (%) <sup>b,c</sup>
1 <sup>a</sup>	Cl	Pd/C	120	30	0 <sup>d</sup>
2 <sup>a</sup>	Br	Pd/C	120	30	0 <sup>d</sup>
3 <sup>a</sup>	I	Pd/C	120	30	10
4 <sup>a</sup>	Br	Pd(PPh <sub>3</sub> ) <sub>4</sub>	140	30	40
5 <sup>a</sup>	Br	Pd(OAc) <sub>2</sub>	120	30	50
6 <sup>a</sup>	Br	Pd(OAc) <sub>2</sub>	140	30	55
7 <sup>a</sup>	Br	PdCl <sub>2</sub>	140	30	60
8 <sup>a</sup>	I	Pd(OAc) <sub>2</sub>	140	30	50
9 <sup>a</sup>	I	PdCl <sub>2</sub>	140	30	65
10 <sup>a</sup>	OTf	Pd/C	120	30	10
11 <sup>a</sup>	B(OH) <sub>2</sub>	PdCl <sub>2</sub>	140	30	42
12 <sup>a</sup>	SO <sub>2</sub> Cl	PdCl <sub>2</sub>	140	30	0 <sup>d</sup>
13 <sup>a</sup>	Cl	PdCl <sub>2</sub>	140	30	0 <sup>d</sup>
14 <sup>a</sup>	OTf	PdCl <sub>2</sub>	140	30	58

<sup>a</sup> Reagent and reaction conditions: (*E*)-3-(furan-2-yl)-acrylic acid (1.0 eq.), K<sub>2</sub>CO<sub>3</sub> (2 eq.), palladium catalyst (0.05 eq.), powdered 3Å molecular sieves (200 mg), dry DMF (10 ml), were added and refluxed at 140 °C for the specified time mentioned in Table 2.

<sup>b</sup> Isolated yields; refers to isolated yields by silica gel column chromatography

<sup>c</sup> *E/Z* ratio are confirmed by <sup>1</sup>H NMR .

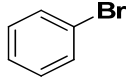
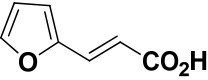
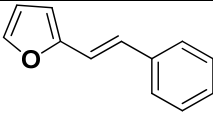
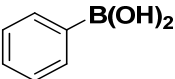
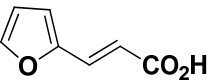
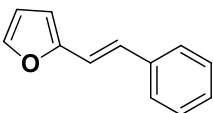
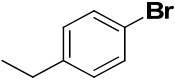
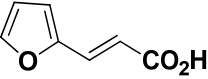
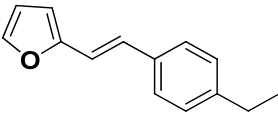
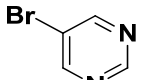
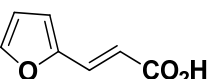
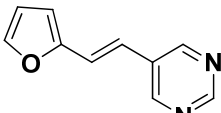
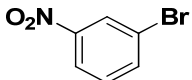
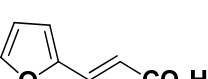
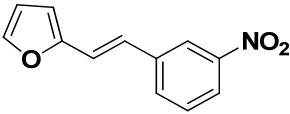
<sup>d</sup> Starting materials were recovered quantitatively.



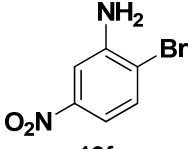
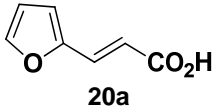
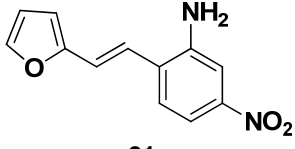
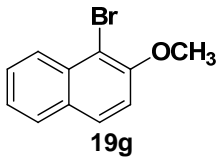
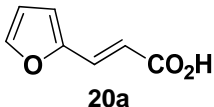
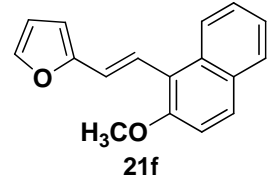
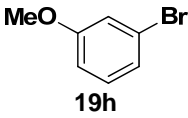
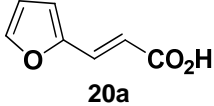
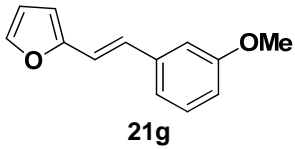
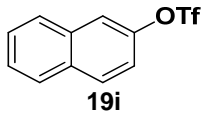
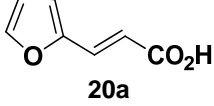
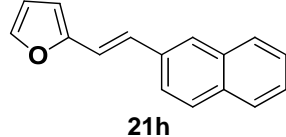
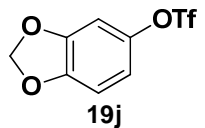
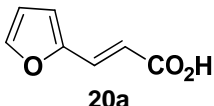
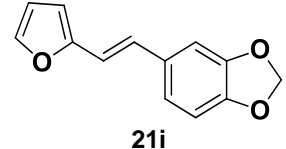
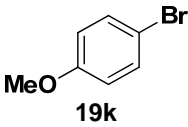
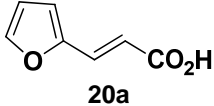
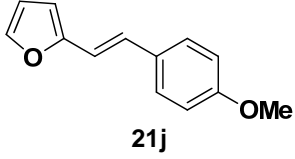
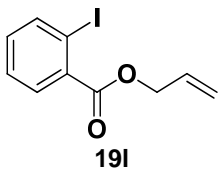
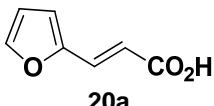
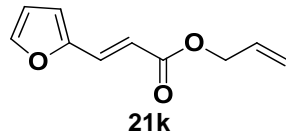
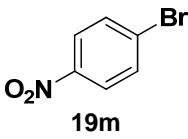
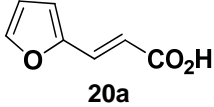
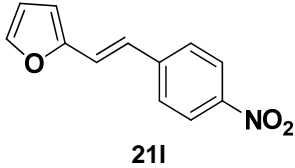
## Chapter 2

Among them, Pd(OAc)<sub>2</sub> (entry 5) afforded slightly lower yield (50%) of the product, while under the same reaction conditions PdCl<sub>2</sub> (entry 7) afforded 60% yield of the product. While, other Pd(0) salts resulted in either no reactions (entries 1-3) or in poor yields (entry 4). Inorganic as well as organic bases both were screened for the current methodology. Both these bases worked equally well under the present reaction conditions. In the present methodology, potassium carbonate was used as a base.

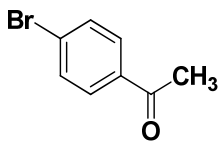
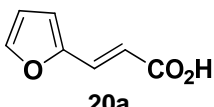
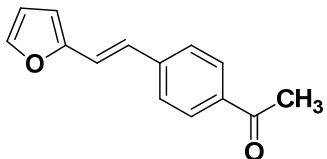
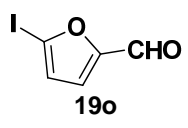
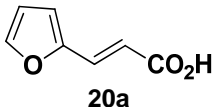
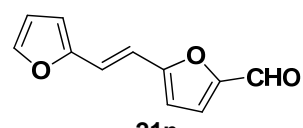
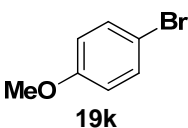
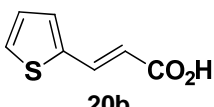
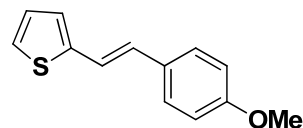
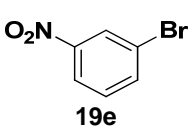
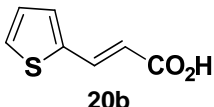
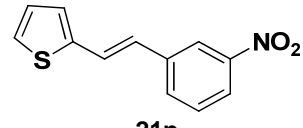
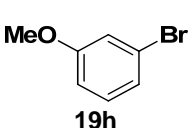
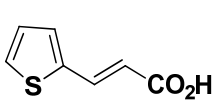
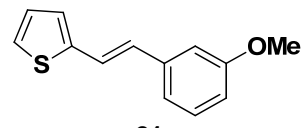
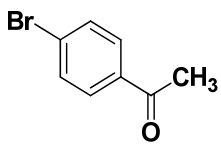
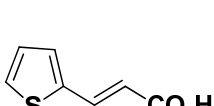
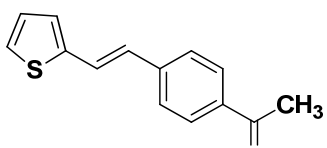
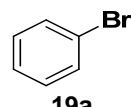
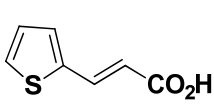
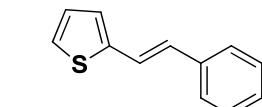
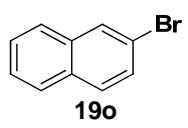
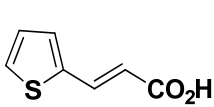
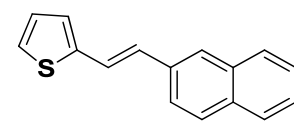
**Table 2:** Synthesis of 2-(*E*-styryl)furan/thiophenes *via* decarboxylative cross coupling.

Entry	Aromatic halides	Carboxylic acid	Product	Time (min)	Yield (%)
1	 19a	 20a	 21a	35	60
2	 19b	 20a	 21a	60	20
3	 19c	 20a	 21b	35	65
4	 19d	 20a	 21c	30	42
5	 19e	 20a	 21d	25	67

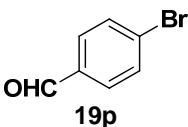
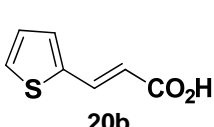
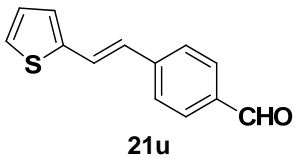
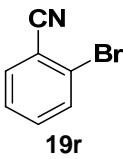
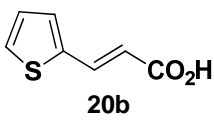
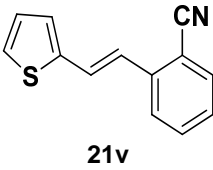
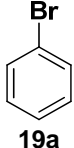
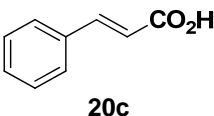
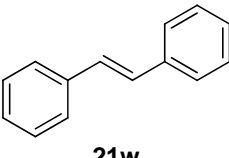
# Chapter 2

6	 19f	 20a	 21e	30	54
7	 19g	 20a	 21f	30	70
8	 19h	 20a	 21g	25	83
9	 19i	 20a	 21h	15	60
10	 19j	 20a	 21i	20	58
11	 19k	 20a	 21j	35	65
12	 19l	 20a	 21k	35	45
13	 19m	 20a	 21l	30	59

## Chapter 2

14	 <b>19n</b>	 <b>20a</b>	 <b>21m</b>	30	53
15	 <b>19o</b>	 <b>20a</b>	 <b>21n</b>	60	40
16	 <b>19k</b>	 <b>20b</b>	 <b>21o</b>	30	78
17	 <b>19e</b>	 <b>20b</b>	 <b>21p</b>	30	80
18	 <b>19h</b>	 <b>20b</b>	 <b>21q</b>	35	72
19	 <b>19n</b>	 <b>20b</b>	 <b>21r</b>	30	60
20	 <b>19a</b>	 <b>20b</b>	 <b>21s</b>	35	50
21	 <b>19o</b>	 <b>20b</b>	 <b>21t</b>	40	70

## Chapter 2

22	 <b>19p</b>	 <b>20b</b>	 <b>21u</b>	40	80
23	 <b>19r</b>	 <b>20b</b>	 <b>21v</b>	35	75
24	 <b>19a</b>	 <b>20c</b>	 <b>21w</b>	45	0

Both electron donating (EDG) and electron withdrawing groups (EWG) were well tolerated under the present reaction conditions. Remarkable functional group tolerability was observed in coupling reaction in the presence of nitro (entries 5, 6, 13, and 17), amino (entry 6), allyl esters (entry 12), methyl ethers (entries 7, 8, 11, 16, and 18), ketone (entries 14, 19), aldehyde (entries 15, 22), methyl ethers (entries 7, 8, 11, 16, and 18), boronic acids (entry 2), triflates (entries 9, 10), bicyclic bromides (entries 7, 9, 10, and 21) and cyano groups (entry 23) on the aromatic ring. Phenyl partners having free hydroxyl groups and *N*-heterocyclic arenes resulted in low yields of the corresponding product (Table 2). In order to prove the utility of (*E*)-3-(furan-2-yl)-acrylic acid **20a**, cinnamic acid **20c** (entry 24) was subjected to present reaction conditions however substrate could not afford the product. It can be concluded that (*E*)-3-(furan-2-yl)-acrylic acid **20a** or (*E*)-3-(thiophene-2-yl)-acrylic acid **20b** are needed for the present cross-coupling reaction. Two of the derivatives **21e** and **21u** were crystallized from methanol/DCM (1:9) and their single crystal X-ray structures of compound **21e** and **21u** are represented in Figure 3.

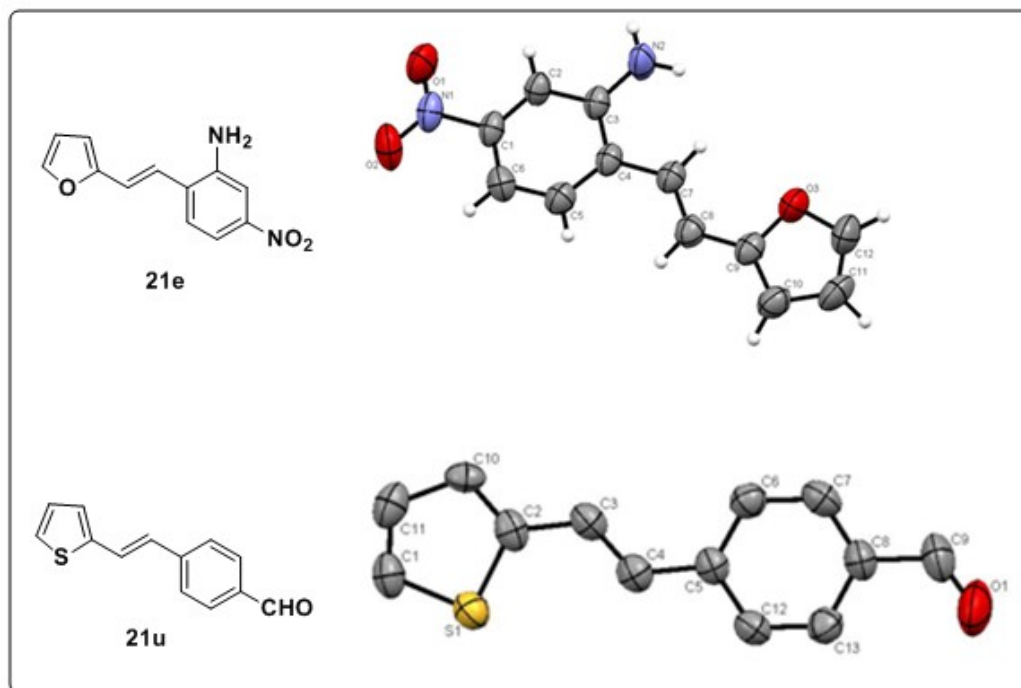


**Figure 3.** ORTEP diagram of derivatives **21e** and **21u**.

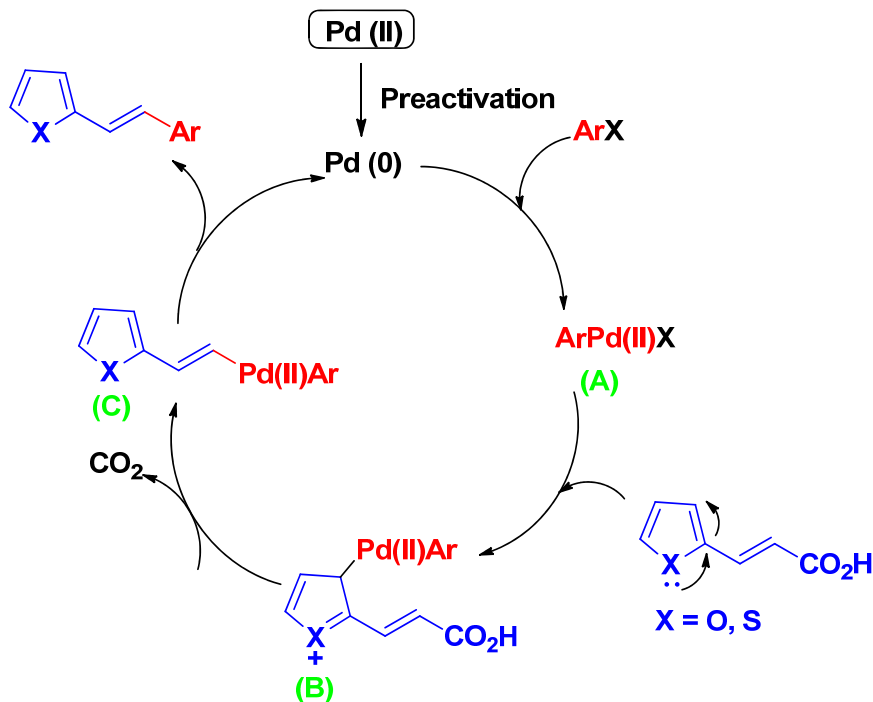
An important distinction between present studies from previously reported methods is that it highlights the ability to selectively perform the reaction in the presence of active C-H bond in an intermolecular fashion. Further, the present protocol is highly regio-specific as acid group directs the coupling. The present method was successfully extended to a variety of substituted aromatic halides having electron donating (EDG) and electron withdrawing groups (EWG) as shown in Table 2 and in all the cases reaction proceeded smoothly to furnish the corresponding product.

## 2.4 Postulated Mechanism

A postulated mechanism has been reported by the Bilodean *et al.*<sup>15</sup> involving (*E*)-3-(furan-2-yl)-acrylic acid **20a** or (*E*)-3-(thiophene-2-yl)-acrylic acid **20b** and aryl bromides **19a**. Since our substrate is similar, we also presumed that our decarboxylative cross-coupling reaction involving (*E*)-3-(furan-2-yl)-acrylic acid **20a** or (*E*)-3-(thiophene-2-yl)-acrylic acid **20b** and aryl bromides **19a** under palladium (0)

## Chapter 2

species should have similar reaction mechanism. In the first step, palladium (0) species formed from the palladium (II) salts.



**Scheme 6.** Postulated mechanism for the synthesis of *(E)*-3-(furan-2-yl)-acrylic acid **20a** or *(E)*-3-(thiophene-2-yl)-acrylic acid **20b**.

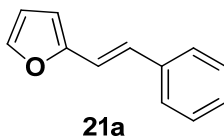
The palladium (0) species then subsequently reacts with aromatic halides *via* oxidative addition to give intermediate (A). Shuffling of electrons from furan ring towards the 3-position of furan ring and attack by palladium yields adduct (B), which on decarboxylation gives intermediate (C), which easily regenerates the original palladium (0) (A) through the reductive elimination and gives the desired 2-styryl furans/thiophenes in good yields (Scheme 6).

### 2.5 Conclusion

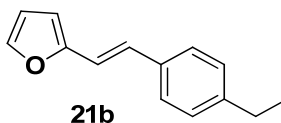
In summary, an efficient decarboxylative cross-coupling reaction for preparing 2-styryl furans/thiophenes from *(E)*-3-(furan-2-yl)-acrylic acid **20a** or *(E)*-3-(thiophene-2-yl)-acrylic acid **20b** has been developed.

## 2.6 Experimental

(*E*)-3-(Furan-2-yl) acrylic acid (276 mg), aryl halide (1.0 eq.), potassium carbonate (551 mg, 2.0 eq.), palladium chloride (17.7 mg, 0.05 eq.), 3 Å molecular sieves (200 mg), and dry DMF (10 mL) were added and refluxed at 140 °C for the appropriate time (see Table 1). After cooling, reaction mixture was filtered over celite and the filtrate was extracted three times with ethyl acetate. The combined organic layers were washed sequentially with water and brine, and then dried over anhydrous Na<sub>2</sub>SO<sub>4</sub>. After removal of the solvent, the crude oil was passed through silica gel column chromatography (elution with PE/EA 90:10-70:30) to give corresponding product (20-80% yield).

**(*E*)-2-Styrylfuran (21a)****Yield**60%; colorless oil;  $R_f = 0.60$  (PE/EA, 7:3).**Mol. Formula**C<sub>12</sub>H<sub>10</sub>O**IR** (CHCl<sub>3</sub>) $\nu_{max}$  (cm<sup>-1</sup>) = 3020, 2400, 1532, 1352, 1215.**<sup>1</sup>H NMR**(CDCl<sub>3</sub>, 200 MHz) $\delta_H$  (ppm) = 7.75-6.83 (m, 8H, CH), 6.41-6.31 (m, 1H, CH).**<sup>13</sup>C NMR**(CDCl<sub>3</sub>, 50 MHz) $\delta_C$  (ppm) = 153.2 (CH), 142.1(CH), 136.9 (C), 128.6 (CH), 127.5 (CH), 127.1 (CH), 126.3 (CH), 123.8 (CH), 116.5 (CH), 111.6 (CH), 108.5 (CH).**Elemental analysis**Calcd for C<sub>12</sub>H<sub>10</sub>O: C, 84.68; H, 5.92

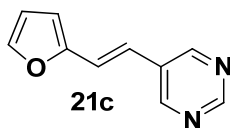
Found: C, 84.50; H, 6.01.

**(*E*)-2-(4-Ethyl)-styryl-furan (21b)****Yield**65%; colorless oil,  $R_f = 0.66$  (PE/EA, 7:3).

## Chapter 2

<b>Mol. Formula</b>	C <sub>14</sub> H <sub>14</sub> O
<b>IR</b> (CHCl <sub>3</sub> )	$\nu_{max}$ (cm <sup>-1</sup> ) = 3019, 2932, 2400, 1777, 1604, 1418, 1215.
<b><sup>1</sup>H NMR</b> (CDCl <sub>3</sub> , 200 MHz)	$\delta_H$ (ppm) = 7.40-6.32 (m, 9H, CH), 2.58 (q, $J$ = 7.6 Hz, 2H, CH <sub>2</sub> ), 1.20 (t, $J$ = 7.6 Hz, 3H, CH <sub>3</sub> ).
<b><sup>13</sup>C NMR</b> (CDCl <sub>3</sub> , 50 MHz)	$\delta_C$ (ppm) = 153.5 (C), 143.1 (C), 141.9 (CH), 134.5 (C), 131.5 (CH) 130.0 (CH), 129.6 (CH), 128.2 (CH), 127.2 (CH), 126.3 (CH), 119.3 (CH), 115.7 (CH), 111.6 (CH), 108.1 (CH), 28.6 (CH <sub>2</sub> ), 15.4 (CH <sub>3</sub> ).
<b>Elemental analysis</b>	Calcd for C <sub>14</sub> H <sub>14</sub> O: C, 84.81; H, 7.12 Found: C, 84.73; H, 7.01.
<b>GC/MS (EI)</b>	198 [M] <sup>+</sup> , 183 [M-CH <sub>3</sub> ] <sup>+</sup> , 169 [M-C <sub>2</sub> H <sub>5</sub> ] <sup>+</sup> .

### (*E*)-5-(2-(Furan-2-yl)vinyl)pyrimidine (21c)

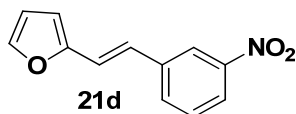


<b>Yield</b>	42%; colorless oil; $R_f$ = 0.40 (PE/EA, 7:3).
<b>Mol. Formula</b>	C <sub>14</sub> H <sub>14</sub> O
<b>IR</b> (CHCl <sub>3</sub> )	$\nu_{max}$ (cm <sup>-1</sup> ) = 3411, 3019, 1604, 1405, 1214.
<b><sup>1</sup>H NMR</b> (CDCl <sub>3</sub> , 200 MHz)	$\delta_H$ (ppm) = 9.03 (s, 1H), 8.79 (s, 2H), 7.43 (s, 1H), 7.05-6.83 (m, 2H), 6.45 (s, 2H).
<b><sup>13</sup>C NMR</b> (CDCl <sub>3</sub> , 50 MHz)	$\delta_C$ (ppm) = 157.0 (CH), 153.5 (C), 154.0 (CH), 130.8 (CH), 143.3 (C), 120.0 (CH), 119.2 (CH), 112.0 (CH), 111.0 (CH).
<b>Elemental analysis</b>	Calcd for C <sub>14</sub> H <sub>14</sub> O: C, 69.76; H, 4.68 Found: C, 69.66; H, 4.53.

### (*E*)-2-(3-Nitrostyryl)furan (21d)

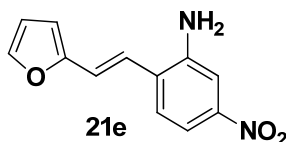


## Chapter 2



<b>Yield</b>	67%; brown solid; $R_f = 0.76$ (PE/EA, 7:3).
<b>Melting Point</b>	116.6-119.4°C
<b>Mol. Formula</b>	$C_{12}H_9NO_3$
<b>IR</b> ( $CHCl_3$ )	$\nu_{max}$ ( $cm^{-1}$ ) = 3686, 3015, 2402, 1601, 1522, 1342, 1205.
<b><math>^1H</math> NMR</b> ( $CDCl_3$ , 200 MHz)	$\delta_H$ (ppm) = 8.28-8.26 (m, 1H, CH), 8.08-8.02 (m, 1H, CH), 7.74-7.68 (m, 1H, CH), 7.51-7.43 (m, 2H, CH), 7.0 (s, 1H, CH), 6.47-6.43 (m, 2H, CH).
<b><math>^{13}C</math> NMR</b> ( $CDCl_3$ , 50 MHz)	$\delta_C$ (ppm) = 152.2 (C), 148.6 (C), 142.9 (CH), 138.8 (C), 132.0 (CH), 129.5 (CH), 129.2 (CH), 124.2 (CH), 124.1 (CH), 123.4 (CH), 121.8 (CH), 120.5 (CH), 119.1 (CH), 111.8 (CH), 110.4 (CH).
<b>Elemental analysis</b>	Calcd for $C_{12}H_9NO_3$ : C, 66.97; H, 4.22; N, 6.51 Found: C, 66.86; H, 4.30; N, 6.56.

### (*E*)-2-(2-(Furan-2-yl)vinyl)-5-nitroaniline (**21e**)

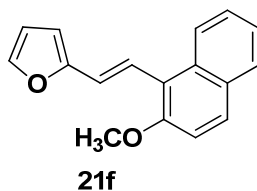


<b>Yield</b>	54%; brown solid; $R_f = 0.52$ (PE/EA, 7:3).
<b>Melting Point</b>	104.6-105.2°C
<b>Mol. Formula</b>	$C_{12}H_9NO_3$
<b>IR</b> ( $CHCl_3$ )	$\nu_{max}$ ( $cm^{-1}$ ) = 3680, 3020, 2400, 1614, 1532, 1352, 1215.
<b><math>^1H</math> NMR</b> ( $CDCl_3$ , 200 MHz)	$\delta_H$ (ppm) = 7.82-7.61 (m, 4H, CH), 7.46 (s, 1H, CH), 7.17-7.04 (m, 2H, CH), 6.66-6.61 (m, 2H,

## Chapter 2

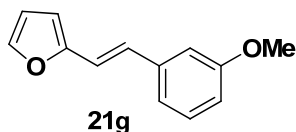
	<i>CH</i> ), 4.3 (s, 2H, <i>CH</i> ).
<b><sup>13</sup>C NMR</b> (CDCl <sub>3</sub> , 50 MHz)	$\delta_C$ (ppm) = 152.6 (C), 144.4 (C), 143.0 (CH), 129.3 (C), 128.3 (CH), 126.8 (CH), 125.8 (CH), 120.8 (CH), 120.0 (CH), 113.8 (CH), 112.0 (CH), 110.6 (CH), 110.4 (CH).
<b>Elemental analysis</b>	Calcd for C <sub>12</sub> H <sub>9</sub> NO <sub>3</sub> : C, 62.60; H, 4.38 Found: C, 62.58; H, 4.43.
<b>GC/MS (EI)</b>	230 [M] <sup>+</sup> , 213 [M-NH <sub>2</sub> ] <sup>+</sup> , 201 [M-C <sub>2</sub> H <sub>5</sub> ] <sup>+</sup> .

### (*E*)-2-(2-(2-Methoxynaphthalen-1-yl)vinyl)furan (21f)



<b>Yield</b>	70%; brown semi-solid; $R_f$ = 0.50 (PE/EA, 7:3).
<b>Mol. Formula</b>	C <sub>17</sub> H <sub>14</sub> O <sub>2</sub>
<b>IR</b> (CHCl <sub>3</sub> )	$\nu_{\max}$ (cm <sup>-1</sup> ) = 3012, 2389, 1625, 1525, 1340, 1210.
<b><sup>1</sup>H NMR</b> (CDCl <sub>3</sub> , 200 MHz)	$\delta_H$ (ppm) = 7.74-7.14 (m, 7H, <i>CH</i> ), 6.54-6.26 (m, 2H, <i>CH</i> ), 3.74 (s, 3H, OCH <sub>3</sub> ).
<b><sup>13</sup>C NMR</b> (CDCl <sub>3</sub> , 50 MHz)	$\delta_C$ (ppm) = 153.6 (C), 150.6 (C), 144.6 (C), 132.9 (CH), 131.0 (C), 129.6 (CH), 129.2 (CH), 128.8 (CH), 127.9 (CH), 127.5 (CH), 127.4 (CH), 125.9 (CH), 124.1 (CH), 115.2 (CH), 114.6 (CH), 113.4 (CH), 112.1 (CH), 56.7 (OCH <sub>3</sub> ).
<b>Elemental analysis</b>	Calcd for C <sub>17</sub> H <sub>14</sub> O <sub>2</sub> : C, 81.58; H, 5.64 Found: C, 81.64; H, 5.71.

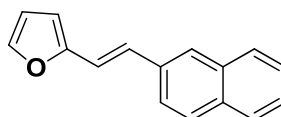
### (*E*)-2-(3-Methoxystyryl)furan (21g)



## Chapter 2

<b>Yield</b>	83%; brown semi-solid; $R_f = 0.60$ (PE/EA, 7:3).
<b>Mol. Formula</b>	$C_{13}H_{12}O_2$
<b>IR</b> ( $CHCl_3$ )	$\nu_{max}$ ( $cm^{-1}$ ) = 3012, 2392, 1612, 1521, 1323, 1205.
<b><math>^1H</math> NMR</b> ( $CDCl_3$ , 200 MHz)	$\delta_H$ (ppm) = 7.23-6.97 (m, 7H, CH), 6.83-6.77 (m, 2H, CH), 3.73 (s, 3H, $OCH_3$ ).
<b><math>^{13}C</math> NMR</b> ( $CDCl_3$ , 50 MHz)	$\delta_C$ (ppm) = 160.3 (C), 153.1 (C), 142.1 (CH), 138.4 (CH), 130.4 (C), 129.5 (CH), 127.0 (CH), 123.6 (CH), 122.7 (CH), 118.9 (CH), 117.1 (CH), 116.7 (CH), 113.2 (CH), 112.9 (CH), 111.6 (CH), 111.5 (CH), 108.6 (CH), 55.3 ( $OCH_3$ ).
<b>Elemental analysis</b>	Calcd for $C_{13}H_{12}O_2$ : C, 77.98; H, 6.04 Found: C, 78.01; H, 5.98.
<b>GC/MS (EI)</b>	200 $[M]^+$ , 185 $[M-CH_3]^+$ , 171 $[M-C_2H_5]^+$ .

### (*E*)-2-(2-(Naphthalen-2-yl)vinyl)furan (21h)



**21h**

<b>Yield</b>	60%; yellow solid; $R_f = 0.51$ (PE/EA, 7:3).
<b>Melting Point</b>	80.8-82.9°C
<b>Mol. Formula</b>	$C_{16}H_{12}O$
<b>IR</b> ( $CHCl_3$ )	$\nu_{max}$ ( $cm^{-1}$ ) = 3005, 2405, 1610, 1514, 1350, 1220.
<b><math>^1H</math> NMR</b> ( $CDCl_3$ , 200 MHz)	$\delta_H$ (ppm) = 7.77-6.81 (m, 11H, CH), 6.29-6.22 (m, 2H, CH).
<b><math>^{13}C</math> NMR</b> ( $CDCl_3$ , 50 MHz)	$\delta_C$ (ppm) = 153.3 (C), 147.0 (C), 142.2 (CH), 134.5 (CH), 133.7 (CH), 133.3 (C), 133.0 (CH), 132.3 (C), 130.6 (CH), 128.3 (CH), 127.9 (CH), 127.8 (CH), 127.6 (CH), 127.5 (CH), 127.2 (CH), 127.1 (CH), 126.5 (CH), 126.3 (CH), 125.8 (CH), 123.2 (CH), 119.4 (CH), 119.1 (CH), 116.8 (CH).

## Chapter 2

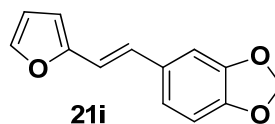
108.7 (CH).

### Elemental analysis

Calcd for  $C_{16}H_{12}O$ : C, 87.25; H, 5.49

Found: C, 87.41; H, 5.40.

### (*E*)-5-(2-(Furan-2-yl)vinyl)benzo[*d*][1,3]dioxale (21i)



### Yield

60%; yellow syrup;  $R_f = 0.55$  (PE/EA, 7:3).

### Mol. Formula

$C_{13}H_{10}O_3$

### IR (CHCl<sub>3</sub>)

$\nu_{\max}$  (cm<sup>-1</sup>) = 3030, 2465, 1625, 1520, 1325, 1212.

### <sup>1</sup>H NMR

(CDCl<sub>3</sub>, 200 MHz)

$\delta_H$  (ppm) = 7.38-7.37 (m, 1H, CH), 6.99-6.67 (m, 5H, CH) 6.41-6.39 (m, 1H, CH), 6.31-6.29 (m, 1H, CH), 5.96 (s, 2H, CH<sub>2</sub>).

### <sup>13</sup>C NMR

(CDCl<sub>3</sub>, 50 MHz)

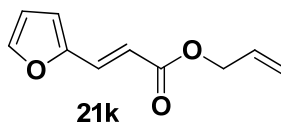
$\delta_C$  (ppm) = 153.3 (C), 148.1 (C), 147.3 (CH), 141.9 (CH), 131.6 (CH), 126.9 (CH), 121.3 (CH), 115.0 (CH), 111.6 (CH), 108.4 (CH), 108.0 (CH), 105.3 (CH), 102.4 (CH), 101.1 (CH).

### Elemental analysis

Calcd for  $C_{13}H_{10}O_3$ : C, 72.89; H, 4.71

Found: C, 72.82; H, 4.65.

### (*E*)-Allyl 3-(furan-2-yl)acrylate (21k)



### Yield

60%; yellow syrup;  $R_f = 0.50$  (PE/EA, 7:3).

### Mol. Formula

$C_{12}H_{10}O$

### IR (CHCl<sub>3</sub>)

$\nu_{\max}$  (cm<sup>-1</sup>) = 3023, 2932, 2404, 1735, 1625, 1525, 1415, 1218.

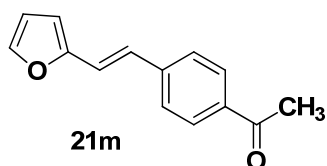
### <sup>1</sup>H NMR

(CDCl<sub>3</sub>, 200 MHz)

$\delta_H$  (ppm) = 7.45-7.34 (m, 2H, CH), 6.57-6.26 (m, 3H, CH) 6.03-5.84 (m, 1H, CH), 5.36-5.17 (m,

## Chapter 2

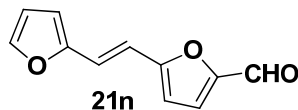
	2H, CH), 4.67-4.63 (s, 2H, CH <sub>2</sub> ).
<b><sup>13</sup>C NMR</b> (CDCl <sub>3</sub> , 50 MHz)	δ <sub>C</sub> (ppm) = 166.4 (C), 150.7 (C), 144.7 (CH), 132.2 (CH), 115.3 (CH <sub>2</sub> ), 114.7 (CH), 112.1 (CH), 64.9 (CH <sub>2</sub> ).
<b>Elemental analysis</b>	Calcd for C <sub>12</sub> H <sub>9</sub> O: C, 67.41; H, 5.66 Found: C, 67.35; H, 5.41.
<b>GC/MS (EI)</b>	178 [M] <sup>+</sup> .
<b>(E)-1-(4-(2-furan-2-yl)vinyl)phenyl)ethanone (21m)</b>	



<b>Yield</b>	53%; white yellow solid; <i>R<sub>f</sub></i> = 0.64 (PE/EA, 8:2).
<b>Melting Point</b>	98.8-100.5°C
<b>Mol. Formula</b>	C <sub>14</sub> H <sub>12</sub> O <sub>2</sub>
<b>IR (CHCl<sub>3</sub>)</b>	<i>v</i> <sub>max</sub> (cm <sup>-1</sup> ) = 3683, 3447, 3019, 2976, 2400, 2294, 1675, 1600, 1523, 1421, 1215, 1046.
<b><sup>1</sup>H NMR</b> (CDCl <sub>3</sub> , 200 MHz)	δ <sub>H</sub> (ppm) = 7.92 (d, <i>J</i> = 8.5 Hz, 2H, CH), 7.52 (d, <i>J</i> = 8.5 Hz, 2H, CH), 7.43 (m, 1H, CH), 7.02-7.01 (m, 2H, CH), 6.44-6.43 (m, 2H, CH), 2.60 (s, 3H, CH <sub>3</sub> ).
<b><sup>13</sup>C NMR</b> (CDCl <sub>3</sub> , 50 MHz)	δ <sub>C</sub> (ppm) = 197.5 (C), 152.7 (C), 142.8 (CH), 141.7 (C), 135.8 (C), 128.8 (CH), 126.2 (CH), 125.7 (CH), 118.9 (CH), 111.9 (CH), 110.1 (CH), 26.6 (CH <sub>3</sub> ).
<b>Elemental analysis</b>	Calcd for C <sub>14</sub> H <sub>12</sub> O <sub>2</sub> : C, 79.22; H, 5.70 Found: C, 79.28; H, 5.78.
<b>GC/MS (EI)</b>	212 [M] <sup>+</sup> .

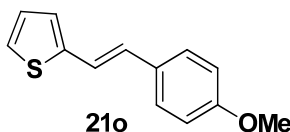
### **(E)-5-(2-furan-2-yl)vinyl)furan-2-carbaldehyde (21n)**

## Chapter 2



<b>Yield</b>	40%; yellow solid; $R_f = 0.2$ (PE/EA, 8:2).
<b>Melting Point</b>	120-122°C
<b>Mol. Formula</b>	$C_{11}H_8O_3$
<b>IR</b> ( $CHCl_3$ )	$\nu_{max}$ ( $cm^{-1}$ ) = 3680, 3442, 2855, 2401, 1675, 1605, 1425, 1215, 1046.
<b><math>^1H</math> NMR</b> ( $CDCl_3$ , 200 MHz)	$\delta_H$ (ppm) = 9.57 (s, 1H, CHO), 7.53-7.45 (m, 1H, CH), 7.31-7.24 (m, 2H, CH), 7.18-7.15 (m, 1H, CH), 6.92-6.73 (m, 1H, CH), 6.55-6.46 (m, 2H, CH).
<b><math>^{13}C</math> NMR</b> ( $CDCl_3$ , 50 MHz)	$\delta_C$ (ppm) = 177.0 (CHO), 158.5 (C), 152.0 (C), 151.6 (C), 144.0 (CH), 143.5 (CH), 120.4 (CH), 113.0 (CH), 112.2 (CH), 111.9 (CH), 110.8 (CH), 109.6 (CH), 107.4 (CH).
<b>Elemental analysis</b>	Calcd for $C_{11}H_8O_3$ : C, 70.21; H, 4.29 Found: C, 70.29; H, 4.35.
<b>GC/MS (EI)</b>	415 $[M]^+$ .

### (*E*)-2-(4-methoxystyryl)thiophene (21o)

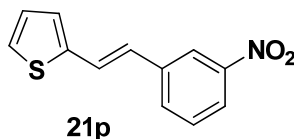


<b>Yield</b>	40%; orange solid; $R_f = 0.8$ (PE/EA, 7:3).
<b>Melting Point</b>	100-104°C
<b>Mol. Formula</b>	$C_{13}H_{12}OS$
<b>IR</b> ( $CHCl_3$ )	$\nu_{max}$ ( $cm^{-1}$ ) = 3012, 2923, 2843, 1604, 1571, 1508, 1461, 1279, 1248, 1215, 1178, 1111, 1078, 1034.
<b><math>^1H</math> NMR</b>	$\delta_H$ (ppm) = 7.54-6.83 (m, 8H, CH), 6.66-6.62 (m,

## Chapter 2

(CDCl <sub>3</sub> , 200 MHz)	1H, CH), 3.71 (s, 3H, OCH <sub>3</sub> ).
<b><sup>13</sup>C NMR</b> (CDCl <sub>3</sub> , 50 MHz)	δ <sub>C</sub> (ppm) = 159.4 (C), 143.2 (C), 138.1 (CH), 129.6 (C), 128.6 (CH), 127.5 (CH), 126.2 (CH), 125.3 (CH), 123.7 (CH), 119.7 (CH), 116.3 (CH), 114.1 (CH), 55.2 (OCH <sub>3</sub> ).
<b>Elemental analysis</b>	Calcd for C <sub>13</sub> H <sub>12</sub> OS: C, 72.19; H, 5.59 Found: C, 72.27; H, 5.51.
<b>GC/MS (EI)</b>	216 [M] <sup>+</sup> .

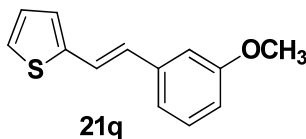
### (*E*)-2-(3-nitrostyryl)vinylthiophene (21p)



<b>Yield</b>	80%; orange solid; <i>R<sub>f</sub></i> = 0.7 (PE/EA, 7:3).
<b>Melting Point</b>	102.7-104.7°C
<b>Mol. Formula</b>	C <sub>12</sub> H <sub>9</sub> NO <sub>2</sub> S
<b>IR</b> (CHCl <sub>3</sub> )	ν <sub>max</sub> (cm <sup>-1</sup> ) = 3445, 3020, 2401, 1685, 1630, 1510, 1424, 1216, 1045.
<b><sup>1</sup>H NMR</b> (CDCl <sub>3</sub> , 200 MHz)	δ <sub>H</sub> (ppm) = 8.32-8.25 (m, 1H, CH), 8.12-8.05 (m, 1H, CH), 7.76-7.65 (m, 1H, CH), 7.54-7.46 (m, 1H, CH), 7.40-7.26 (m, 2H, CH), 7.16-7.14 (m, 1H, CH), 7.08-6.85 (m, 2H, CH).
<b><sup>13</sup>C NMR</b> (CDCl <sub>3</sub> , 50 MHz)	δ <sub>C</sub> (ppm) = 148.7 (C), 141.7 (C), 138.8 (C), 131.9 (CH), 129.6 (C), 128.6 (CH), 127.5 (CH), 125.6 (CH), 124.7 (CH), 121.9 (CH), 120.6 (CH).
<b>Elemental analysis</b>	Calcd for C <sub>12</sub> H <sub>9</sub> NO <sub>2</sub> S: C, 62.32; H, 3.92 Found: C, 62.39; H, 3.98.
<b>GC/MS (EI)</b>	231 [M] <sup>+</sup> .

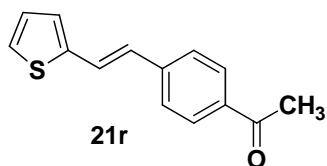
### (*E*)-2-(3-methoxystyryl)vinylthiophene (21q)

## Chapter 2



<b>Yield</b>	60%, orange solid; $R_f = 0.6$ (PE/EA, 7:3).
<b>Melting Point</b>	104.2-108.5°C
<b>Mol. Formula</b>	$C_{14}H_{12}OS$
<b>IR</b> ( $CHCl_3$ )	$\nu_{max}$ ( $cm^{-1}$ ) = 3445, 3020, 2401, 1685, 1630, 1510, 1424, 1216, 1045.
<b><math>^1H</math> NMR</b> ( $CDCl_3$ , 200 MHz)	$\delta_H$ (ppm) = 7.23-6.84 (m, 9H, CH), 3.77 (s, 3H, $OCH_3$ ).
<b><math>^{13}C</math> NMR</b> ( $CDCl_3$ , 50 MHz)	$\delta_C$ (ppm) = 142.6 (C), 142.6 (C), 138.4 (C), 130.5 (CH), 123.7 (CH), 119.7 (CH), 117.1 (CH), 113.0 (CH), 111.4 (CH), 55.37 ( $OCH_3$ ).
<b>Elemental analysis</b>	Calcd for $C_{14}H_{12}OS$ : C, 62.32; H, 3.92 Found: C, 62.39; H, 3.98.

### (*E*)-1-(4-(2-(thiophene-2-yl)vinyl)phenyl)ethanone (21r)



<b>Yield</b>	60%; orange solid; $R_f = 0.6$ (PE/EA, 7:3).
<b>Mol. Formula</b>	$C_{14}H_{12}OS$
<b>IR</b> ( $CHCl_3$ )	$\nu_{max}$ ( $cm^{-1}$ ) = 3446, 3021, 2400, 1682, 1425, 1215, 1046.
<b><math>^1H</math> NMR</b> ( $CDCl_3$ , 200 MHz)	$\delta_H$ (ppm) = 7.88 (d, $J = 8.5$ Hz, 2H, CH), 7.46 (d, $J = 8.3$ Hz, 2H, CH), 7.21-6.83 (m, 5H, CH), 2.54 (s, 3H, $CH_3$ ).
<b><math>^{13}C</math> NMR</b> ( $CDCl_3$ , 50 MHz)	$\delta_C$ (ppm) = 197.3 (C), 142.2 (C), 141.6 (C), 135.7 (C), 128.9 (CH), 128.8 (CH), 127.7 (CH), 127.2



## Chapter 2

(CH), 127.1 (CH), 126.8 (CH), 126.2 (CH), 125.3 (CH), 124.3 (CH), 26.6 (CH<sub>3</sub>).

### Elemental analysis

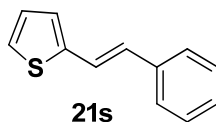
Calcd for C<sub>14</sub>H<sub>12</sub>OS: C, 73.65; H, 5.30

Found: C, 73.71; H, 5.22.

### GC/MS (EI)

228 [M]<sup>+</sup>, 213 [M-CH<sub>3</sub>]<sup>+</sup>, 184 [M-CO<sub>2</sub>]<sup>+</sup>.

### (*E*)-2-styrylthiophene (21s)



### Yield

50%; orange solid; *R<sub>f</sub>* = 0.5 (PE/EA, 7:3).

### Mol. Formula

C<sub>12</sub>H<sub>10</sub>S

### IR (CHCl<sub>3</sub>)

$\nu_{\max}$  (cm<sup>-1</sup>) = 3446, 3021, 2400, 1682, 1425, 1215, 1046.

### <sup>1</sup>H NMR

(CDCl<sub>3</sub>, 200 MHz)

$\delta_{\text{H}}$  (ppm) = 7.65-7.14 (m, 8H, CH), 7.05-6.94 (m, 2H, CH).

### <sup>13</sup>C NMR

(CDCl<sub>3</sub>, 50 MHz)

$\delta_{\text{C}}$  (ppm) = 143.0 (C), 136.9 (C), 131.5 (CH), 130.0 (CH), 128.9 (CH), 128.6 (CH), 128.3 (CH), 127.5 (CH), 127.1 (CH), 126.8 (CH), 126.2 (CH), 126.1 (CH), 125.6 (CH), 124.3 (CH), 121.7 (CH).

### Elemental analysis

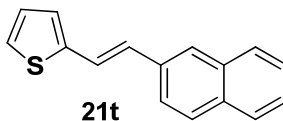
Calcd for C<sub>12</sub>H<sub>10</sub>S: C, 77.37; H, 5.41

Found: C, 77.31; H, 5.47.

### GC/MS (EI)

186 [M]<sup>+</sup>, 171 [M-CH<sub>3</sub>]<sup>+</sup>.

### (*E*)-2-(2-(naphthalen-2-yl)vinyl)thiophene (21t)



### Yield

70%; orange solid; *R<sub>f</sub>* = 0.5 (PE/EA, 7:3).

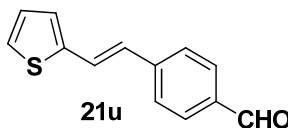
### Melting Point

143-144°C

## Chapter 2

<b>Mol. Formula</b>	C <sub>16</sub> H <sub>12</sub> S
<b>IR</b> (CHCl <sub>3</sub> )	$\nu_{\max}$ (cm <sup>-1</sup> ) = 3681, 3843, 3743, 3678, 3648, 3619, 3055, 2921, 2851, 1740, 1706, 1694, 1647, 1625, 1531, 1511, 1463, 1427, 1213.
<b><sup>1</sup>H NMR</b> (CDCl <sub>3</sub> , 200 MHz)	$\delta_{\text{H}}$ (ppm) = 7.89-7.12 (m, 10H, CH), 7.03-6.93 (m, 2H, CH).
<b><sup>13</sup>C NMR</b> (CDCl <sub>3</sub> , 50 MHz)	$\delta_{\text{C}}$ (ppm) = 142.9 (C), 134.4 (C), 133.6 (C), 132.9 (C), 128.5 (CH), 128.4 (CH), 128.3 (CH), 127.9 (CH), 127.8 (CH), 127.7 (CH), 127.6 (CH), 126.4 (CH), 126.3 (CH), 126.2 (CH), 125.9 (CH), 125.8 (CH), 124.4 (CH), 123.2 (CH), 122.1 (CH).
<b>Elemental analysis</b>	Calcd for C <sub>16</sub> H <sub>12</sub> S: C, 81.31; H, 5.12 Found: C, 81.38; H, 5.19.

### (*E*)-4-(2-(thiophene-2-yl)vinyl)benzaldehyde (**21u**)



<b>Yield</b>	80%; orange solid; $R_f$ = 0.6 (PE/EA, 7:3).
<b>Melting Point</b>	114°C
<b>Mol. Formula</b>	C <sub>13</sub> H <sub>10</sub> OS
<b>IR</b> (CHCl <sub>3</sub> )	$\nu_{\max}$ (cm <sup>-1</sup> ) = 3685, 3445, 2403, 1681, 1621, 1428, 1220, 1040.
<b><sup>1</sup>H NMR</b> (CDCl <sub>3</sub> , 200 MHz)	$\delta_{\text{H}}$ (ppm) = 9.91 (s, 1H, CHO), 7.78 (d, $J$ = 8.2 Hz, 2H, CH), 7.52 (d, $J$ = 8.3 Hz, 2H, CH), 7.20-7.19 (m, 1H, CH), 7.08-7.07 (m, 1H, CH), 6.97-6.95 (m, 1H, CH).
<b><sup>13</sup>C NMR</b> (CDCl <sub>3</sub> , 50 MHz)	$\delta_{\text{C}}$ (ppm) = 191.6 (CHO), 143.1 (C), 142.0 (C), 135.2 (C), 130.2 (CH), 127.8 (CH), 127.6 (CH), 126.7 (CH), 126.6 (CH), 125.7 (CH), 125.1 (CH).

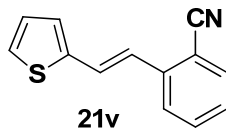
## Chapter 2

### Elemental analysis

Calcd for  $C_{13}H_{10}OS$ : C, 72.87; H, 4.70

Found: C, 72.81; H, 4.76.

### (*E*)-2-(2-(thiophen-2-yl)vinyl)benzonitrile (**21v**)



### Yield

75%; orange solid;  $R_f = 0.7$  (PE/EA, 7:3).

### Melting Point

129-131°C

### Mol. Formula

$C_{13}H_9NS$

### IR (CHCl<sub>3</sub>)

$\nu_{\max}$  (cm<sup>-1</sup>) = 3678, 2922, 2852, 2224, 1770, 1740, 1724, 1706, 1693, 1647, 1625, 1595.

### <sup>1</sup>H NMR

(CDCl<sub>3</sub>, 200 MHz)

$\delta_H$  (ppm) = 7.78-7.53 (m, 6H, CH), 7.36-7.25 (m, 2H, CH), 7.21-7.15 (m, 2H, CH).

### <sup>13</sup>C NMR

(CDCl<sub>3</sub>, 50 MHz)

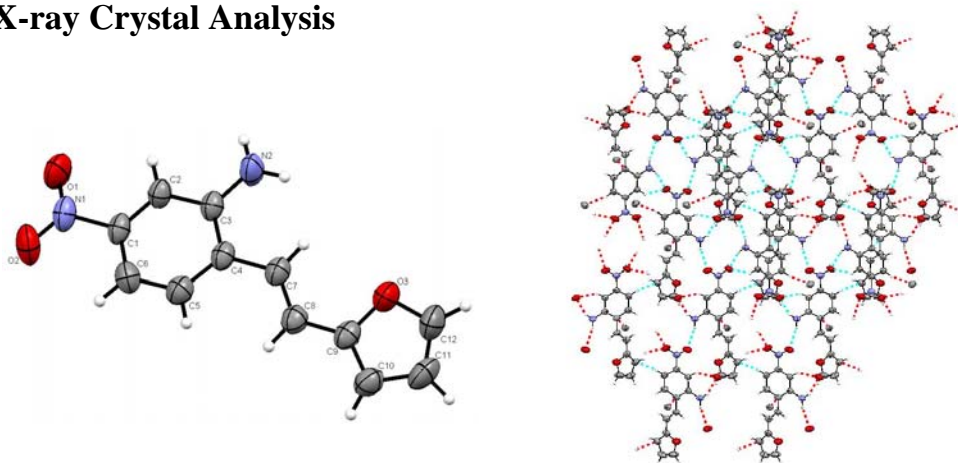
$\delta_C$  (ppm) = 143.3 (C), 139.8 (C), 139.7 (C), 136.9 (C), 134.5 (C), 133.6 (CH), 133.3 (CH), 133.1 (CH), 132.9 (CH), 132.8 (CH), 130.6 (CH), 129.5 (CH), 129.2 (CH), 129.1 (CH), 128.3 (CH), 127.8 (CH), 127.7 (CH), 125.7 (CH), 125.2 (CH), 124.5 (CH), 118.8 (CH), 117.8 (CH).

### Elemental analysis

Calcd for  $C_{13}H_9NS$ : C, 73.90; H, 4.29

Found: C, 73.97; H, 4.34.

### X-ray Crystal Analysis



## Chapter 2

---

**Table 3.** Crystal data and structure refinement for compound **21e**.

Empirical formula	C <sub>12</sub> H <sub>10</sub> N <sub>2</sub> O <sub>3</sub>	
Formula weight	230.22	
Temperature	273(2) K	
Wavelength	0.71073 Å	
Crystal system	Monoclinic	
Space group	P21/c	
Unit cell dimensions	a = 7.515(4) Å	α = 90°
	b = 9.855(5) Å	β = 100.829 (8)°.
	c = 15.415(8) Å	γ = 90°.
Volume	1121.3(10) Å <sup>3</sup>	
Z	4	
Density (Calcd)	1.364 Mg/m <sup>3</sup>	
Absorption coefficient	0.100 mm <sup>-1</sup>	
F(000)	480	
Crystal size	210 x 113 x 10 mm <sup>3</sup>	
Theta range for data collection	2.47 to 28.22°.	
Index ranges	-9<=h<=9, -6<=k<=13, -19<=l<=20	
Reflections collected	6432	
Independent reflections	2540 [R(int) = 0.0360]	
Completeness to theta = 28.22°	98.3 %	
Absorption correction	Semi-empirical from equivalents	
Refinement method	Full-matrix least-squares on F <sup>2</sup>	
Data / restraints / parameters	2540 / 0 / 154	
Goodness-of-fit on F <sup>2</sup>	1.173	
Final R indices [I>2sigma(I)]	R1 = 0.0707, wR2 = 0.1541	
R indices (all data)	R1 = 0.1111, wR2 = 0.1706	
Largest diff. peak and hole	0.261 and -0.177 e. Å <sup>-3</sup>	

## Chapter 2

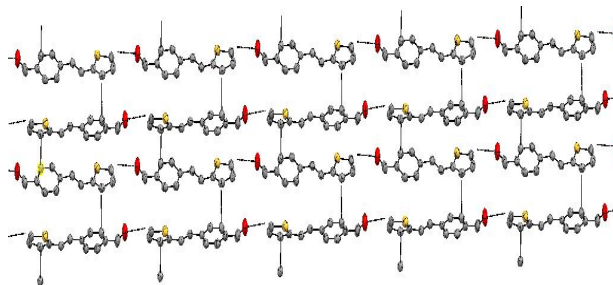
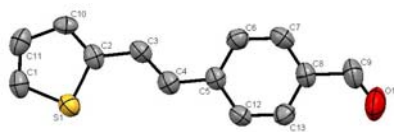


**Table 4.** Crystal data and structure refinement for compound **21u**.

Empirical formula	C <sub>13</sub> H <sub>10</sub> OS	
Formula weight	214.27	
Temperature	296(2) K	
Wavelength	0.71073 Å	
Crystal system	Monoclinic	
Space group	P21/c	
Unit cell dimensions	a = 5.904(4) Å	α = 90°
	b = 7.560(5) Å	β = 97.837(10)°
	c = 12.324(9) Å	γ = 90°
Volume	544.9(6) Å <sup>3</sup>	
Z	2	
Density (Calcd)	1.306 Mg/m <sup>3</sup>	
Absorption coefficient	0.264 mm <sup>-1</sup>	
F(000)	224	
Crystal size	317 x 173 x 17 mm <sup>3</sup>	
Theta range for data collection	1.67 to 28.03°	
Index ranges	-7<=h<=5, -9<=k<=9, -16<=l<=16	
Reflections collected	6798	
Independent reflections	2596 [R(int) = 0.0376]	
Completeness to theta = 28.03°	99.1 %	
Absorption correction	Semi-empirical from equivalents	
Refinement method	Full-matrix least-squares on F <sup>2</sup>	
Data / restraints / parameters	2596 / 1 / 137	
Goodness-of-fit on F <sup>2</sup>	1.068	
Final R indices [I>2sigma(I)]	R1 = 0.0540, wR2 = 0.1465	
R indices (all data)	R1 = 0.0695, wR2 = 0.1655	
Absolute structure parameter	0.68(12)	

## Chapter 2

---

---

Extinction coefficient	0.000(6)
Largest diff. peak and hole	0.453 and -0.270 e. Å <sup>-3</sup>

---

### 2.7 References

1. For representative reviews, see: (a) Trost, B. M. *Tetrahedron* **1977**, *33*, 2615; (b) Tsuji, J. *Top. Curr. Chem.* **1980**, *91*, 29; (c) Kumada, M. *Pure Appl. Chem.* **1980**, *52*, 669; (d) Negishi, E. I. *Acc. Chem. Res.* **1982**, *15*, 340; (e) Tsuji, J. *Organic Synthesis with Palladium Compounds*; Springer-Verlag: Berlin, 1980; (f) Baeckvall, J. E. *Pure Appl. Chem.* **1983**, *55*, 1669; (g) Heck, R. H. *Palladium Reagents for Organic Synthesis*; Academic Press: New York, 1985. Oppolzer, W. *Angew. Chem.* **1989**, *101*, 39; (h) Trost, B. M. *Acc. Chem. Res.* **1990**, *23*, 34; (i) Larock, R. C. *Adv. Met.-Org. Chem.* **1994**, *3*, 97; (j) Venkatraman, S.; Li, C.-J. *Org. Lett.* **1999**, *1*, 1133.
2. (a) Bloome, K. S.; McMahan, R. L.; Alexanian, E. J. *J. Am. Chem. Soc.* **2011**, *133*, 20146; (b) Mehnert, C. P.; Weaver, D. W.; Ying, J. Y. *J. Am. Chem. Soc.* **1998**, 12289; (c) Newman, S. G.; Lautens, M. *J. Am. Chem. Soc.* **2011**, *133*, 1778.
3. (a) Maleczka, R. E.; Gallagher, W. P. *J. Am. Chem. Soc.* **2000**, *122*, 384; (b) Gallagher, W. P.; Maleczka, R. E. *J. Org. Chem.* **2005**, *70*, 841.
4. (a) Liang, B.; Dai, M.; Chen, J. *J. Org. Chem.* **2005**, *70*, 391; (b) Schilz, M.; Plenio, H. *J. Org. Chem.* **2012**, *77*, 2798.
5. (a) Zhang, C.; Huang, J.; Trudell, M. L.; Nolan, S. P. *J. Org. Chem.* **1999**, *64*, 3804; (b) Kim, J.; Kim, J.; Shokouhimehr, M.; Lee, Y. *J. Org. Chem.* **2005**, *70*, 6714.
6. (a) Goossen, L. J. *Science* **2006**, *313*, 662; (b) Baudoin, O. *Angew. Chem. Int. Ed.* **2007**, *46*, 1373.
7. (a) Beck, E. M.; Grimster, N. P.; Hatley, R.; Gaunt, M. J. *J. Am. Chem. Soc.* **2006**, *128*, 2528; (b) Shi, Z.; Li, B.; Wan, X.; Cheng, J.; Fang, Z.; Cao, B.; Qin, C.; Wang, Y. *Angew. Chem. Int. Ed.* **2007**, *46*, 5554; (c) Lane, B. S.; Brown, M. A.; Sames, D. *J. Am. Chem. Soc.* **2005**, *127*, 8050.
8. (a) Voutchkova, A.; Coplin, A.; Leadbeater, E.; Crabtree, R. H. *Chem. Commun.* **2008**, 6312; (b) Tanaka, D.; Myers, A. G. *Org. Lett.* **2004**, *6*, 433; (c) Paetzold, J. *Angew. Chem. Int. Ed.* **2002**, *41*, 1237; (d) Goossen, L. J.; Rodríguez, N.; Linder, C. *J. Am. Chem. Soc.* **2008**, *130*, 15248; (e) Ohlmann,

## Chapter 2

---

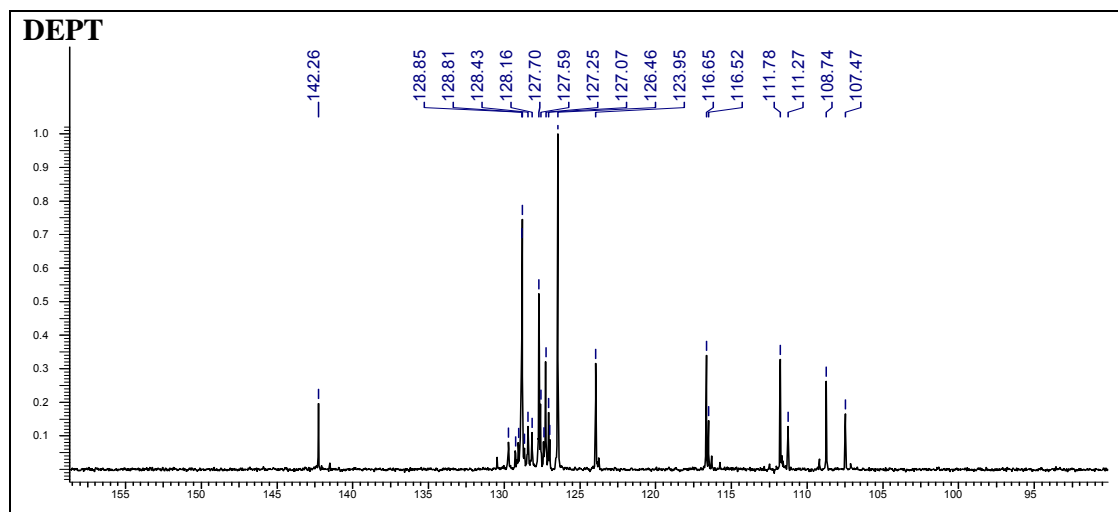
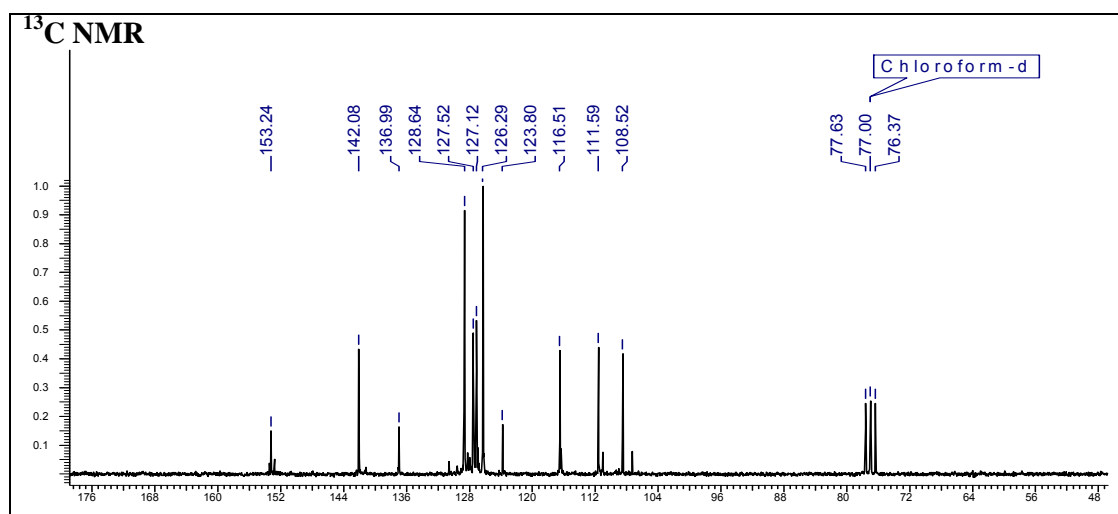
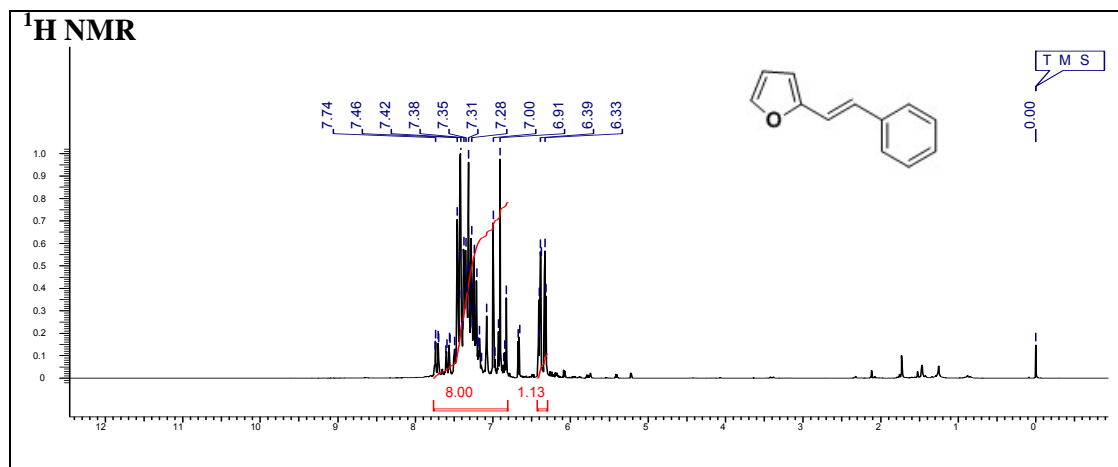
- D. M.; Tschauder, N.; Stockis, J-P.; Goossen, K.; Dierker, M.; Goossen, L. J. *J. Am. Chem. Soc.* **2012**, *134*, 13716; (f) Bhadra, S.; Dzik, W. I.; Goossen, L. J. *J. Am. Chem. Soc.* **2012**, *134*, 9938.
9. Nilsson, M. *Acta Chem. Scand.*, **1958**, *12*, 537.
10. Myers, A. G.; Tanaka, D.; Mannion, M. R. *J. Am. Chem. Soc.* **2002**, *124*, 11250.
11. (a) Goossen, L. J.; Rodri, N.; Melzer, B.; Linder, C.; Deng, G.; Levy, L. M. *J. Am. Chem. Soc.* **2007**, *129*, 4824; (b) Goossen, L. J.; Koley, D.; Hermann, H. L.; Thiel, W. *J. Am. Chem. Soc.* **2005**, *127*, 11102; (c) Goossen, L. J.; Rodríguez, N.; Melzer, B.; Linder, C.; Deng, G.; Levy, L. M. *J. Am. Chem. Soc.* **2007**, *129*, 4824.
12. Zeni, G.; Alves, D.; Braga, A. L.; Stefani, A.; Nogueira, C. W. *Tetrahedron Lett.* **2004**, *45*, 4823.
13. Antonioletti, R.; Bonadies, F.; Ciammaichella, A.; Viglianti, A. *Tetrahedron* **2008**, *64*, 4644.
14. Aouf, C.; Thiery, E.; Bras, J. L.; Muzart, J. *Org. Lett.* **2009**, *11*, 4096.
15. Forgione, P.; Brochu, M.-C.; St-Onge, M.; Thesen, K. H.; Bailey, M. D.; Bilodeau, F. *J. Am. Chem. Soc.* **2006**, *128*, 11350.



## 2.8 Appendix D: Characterization data of synthesized compounds

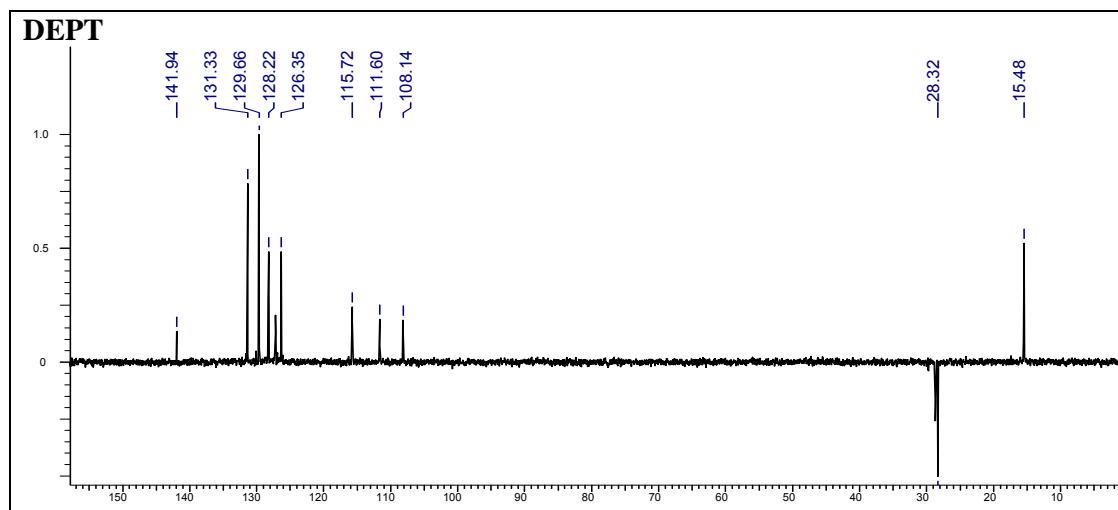
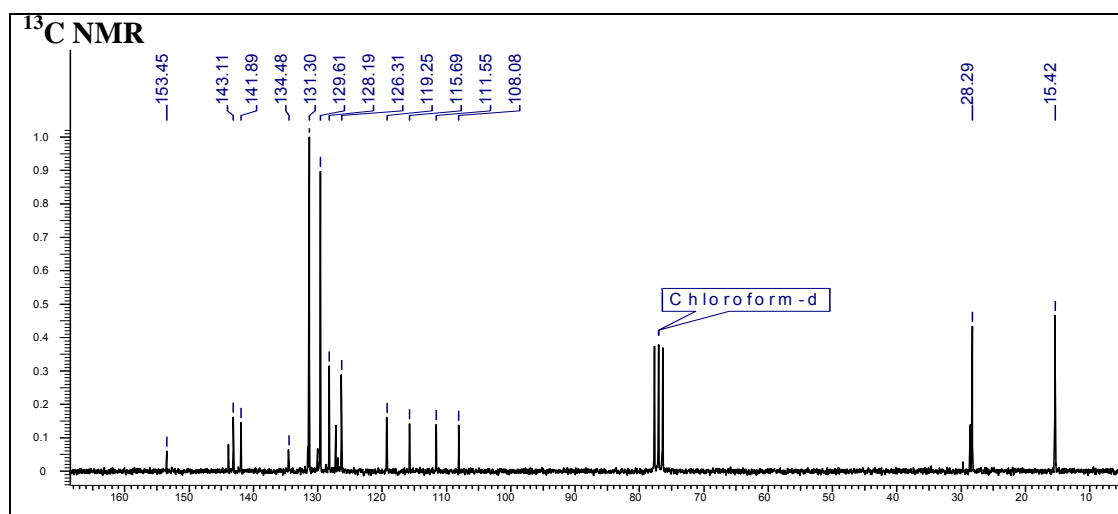
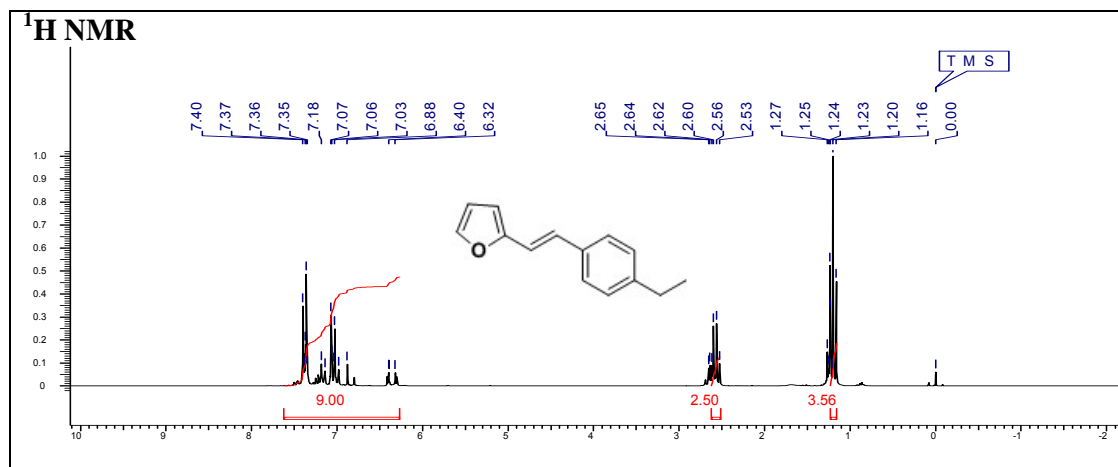
Compound	Description	Page No.
Compound <b>21a</b>	$^1\text{H}$ NMR, $^{13}\text{C}$ NMR, DEPT-NMR	161
Compound <b>21b</b>	$^1\text{H}$ NMR, $^{13}\text{C}$ NMR, DEPT-NMR	162
Compound <b>21c</b>	$^1\text{H}$ NMR, $^{13}\text{C}$ NMR, DEPT-NMR	163
Compound <b>21d</b>	$^1\text{H}$ NMR, $^{13}\text{C}$ NMR, DEPT-NMR	164
Compound <b>21e</b>	$^1\text{H}$ NMR, $^{13}\text{C}$ NMR, DEPT-NMR	165
Compound <b>21f</b>	$^1\text{H}$ NMR, $^{13}\text{C}$ NMR, DEPT-NMR	166
Compound <b>21g</b>	$^1\text{H}$ NMR, $^{13}\text{C}$ NMR, DEPT-NMR	167
Compound <b>21h</b>	$^1\text{H}$ NMR, $^{13}\text{C}$ NMR, DEPT-NMR	168
Compound <b>21i</b>	$^1\text{H}$ NMR, $^{13}\text{C}$ NMR, DEPT-NMR	169
Compound <b>21k</b>	$^1\text{H}$ NMR, $^{13}\text{C}$ NMR, DEPT-NMR	170
Compound <b>21m</b>	$^1\text{H}$ NMR, $^{13}\text{C}$ NMR, DEPT-NMR	171
Compound <b>21n</b>	$^1\text{H}$ NMR, $^{13}\text{C}$ NMR, DEPT-NMR	172
Compound <b>21o</b>	$^1\text{H}$ NMR, $^{13}\text{C}$ NMR, DEPT-NMR	173
Compound <b>21p</b>	$^1\text{H}$ NMR, $^{13}\text{C}$ NMR, DEPT-NMR	174
Compound <b>21r</b>	$^1\text{H}$ NMR, $^{13}\text{C}$ NMR, DEPT-NMR	175
Compound <b>21s</b>	$^1\text{H}$ NMR, $^{13}\text{C}$ NMR, DEPT-NMR	176
Compound <b>21t</b>	$^1\text{H}$ NMR, $^{13}\text{C}$ NMR, DEPT-NMR	177
Compound <b>21u</b>	$^1\text{H}$ NMR, $^{13}\text{C}$ NMR, DEPT-NMR	178
Compound <b>21v</b>	$^1\text{H}$ NMR, $^{13}\text{C}$ NMR, DEPT-NMR	179

# Chapter 2



**(E)-2-Styrylfuran (21a)**

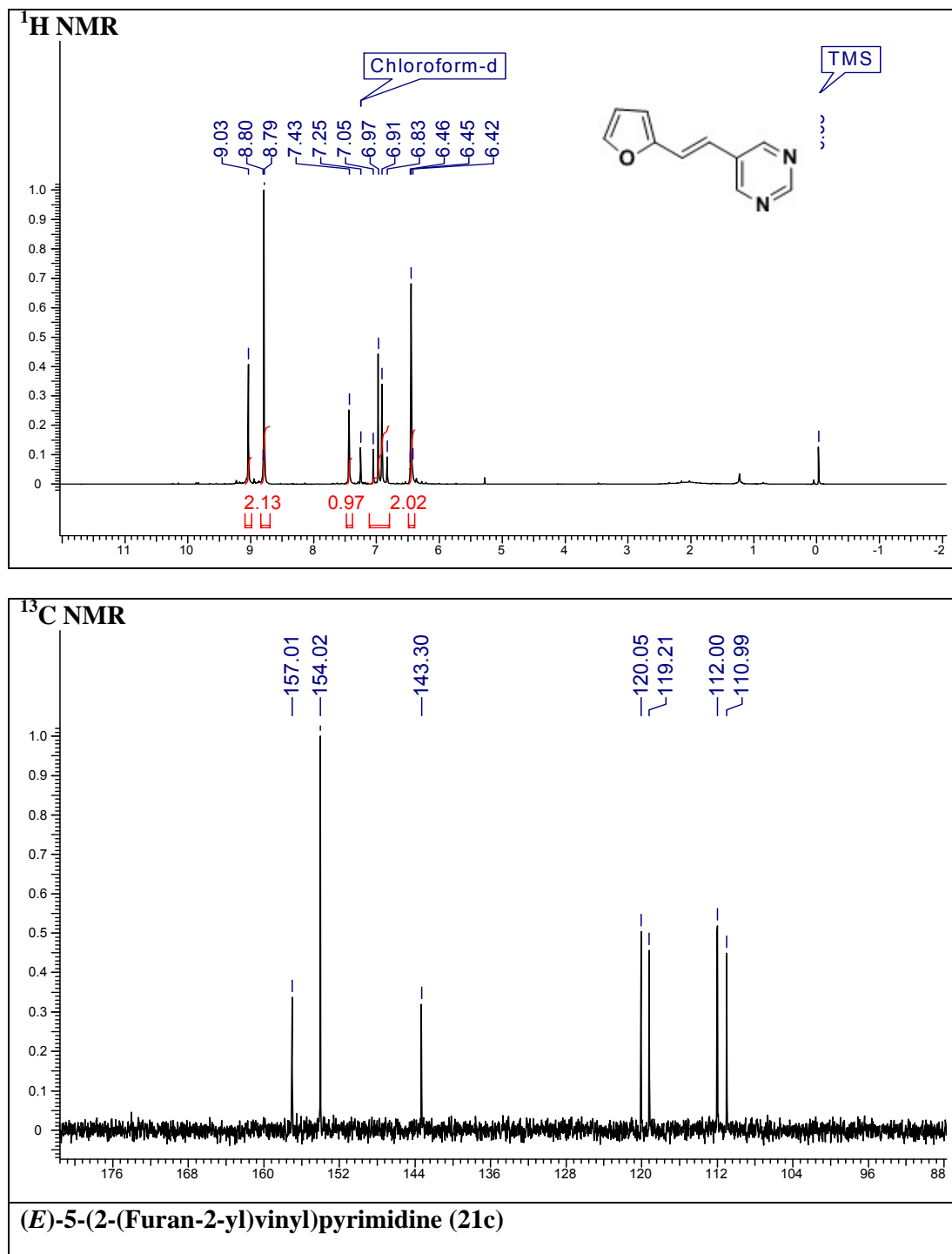
# Chapter 2



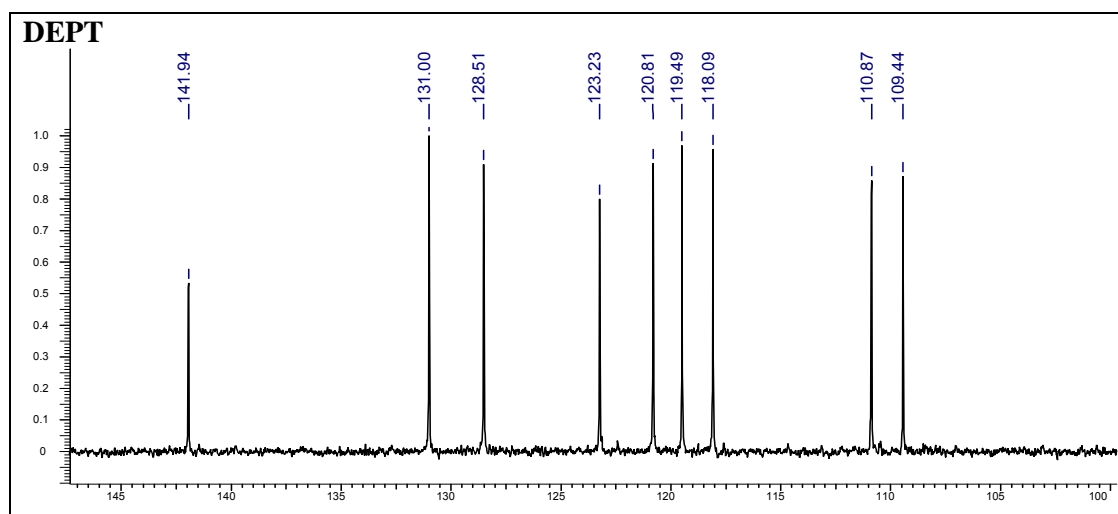
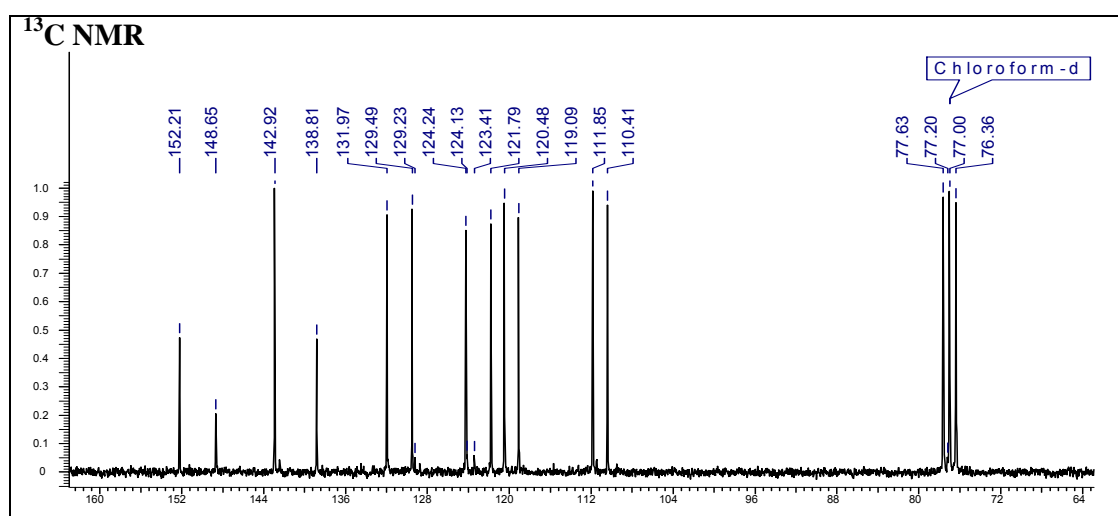
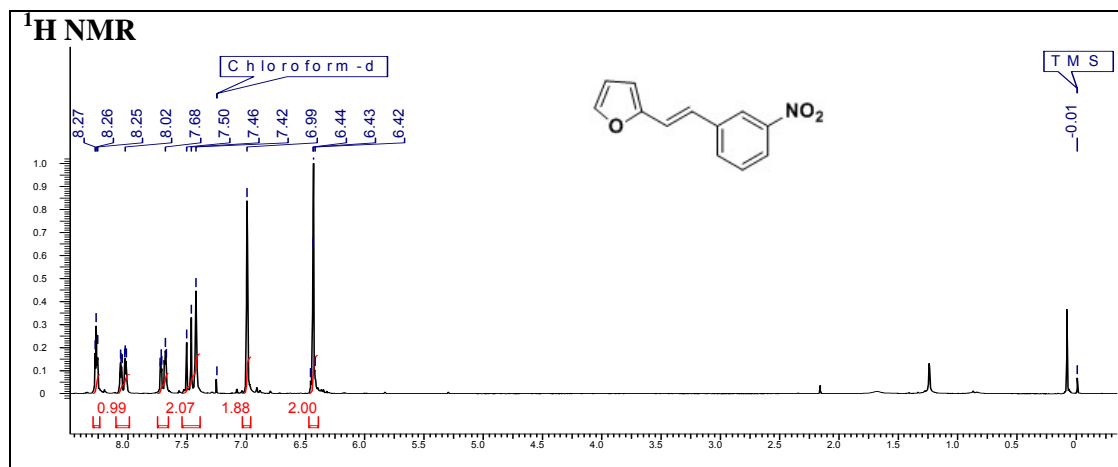
**(E)-2-(4-Ethyl)styryl furan (21b)**

T. Kaur, *PhD thesis*, University of Pune, 2013

# Chapter 2



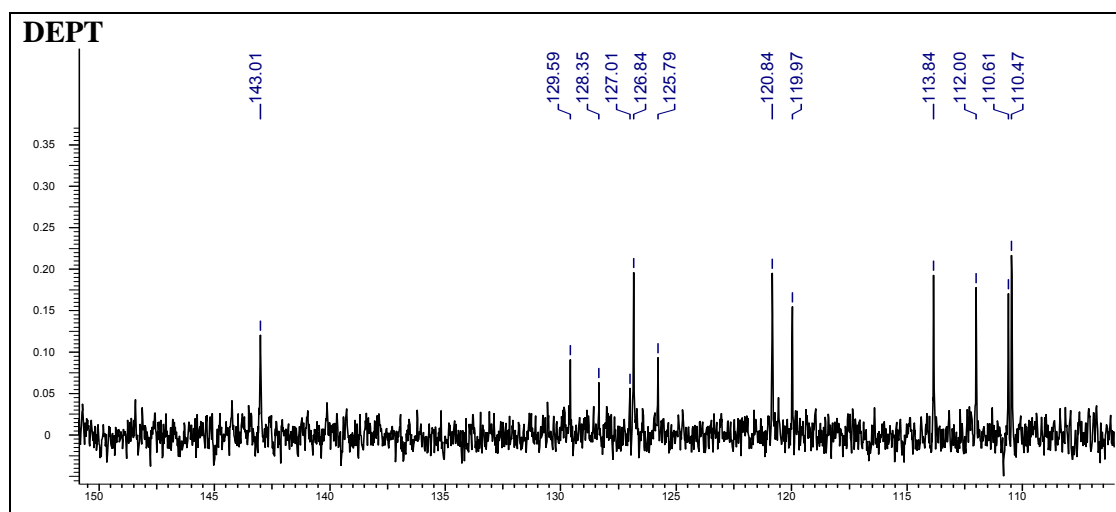
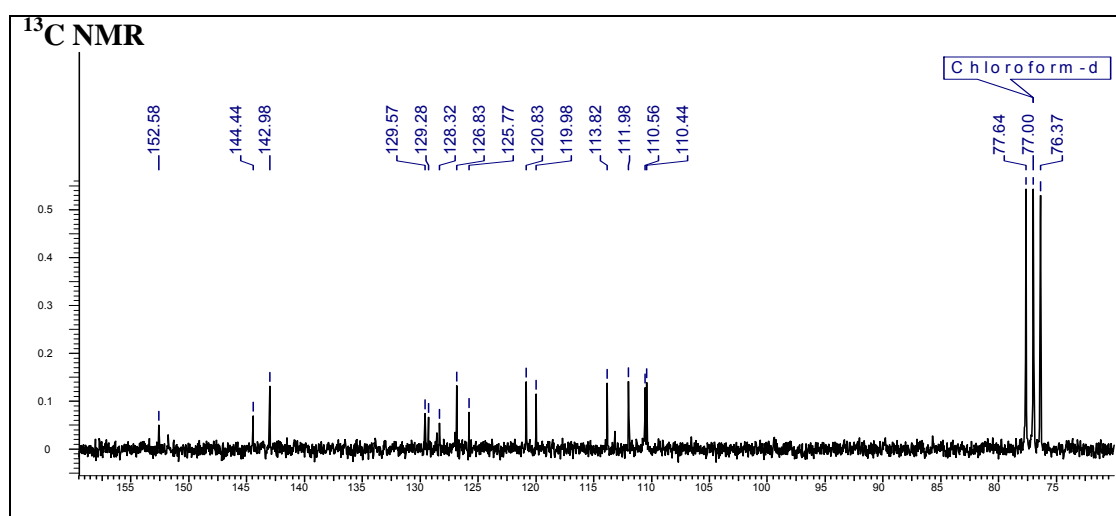
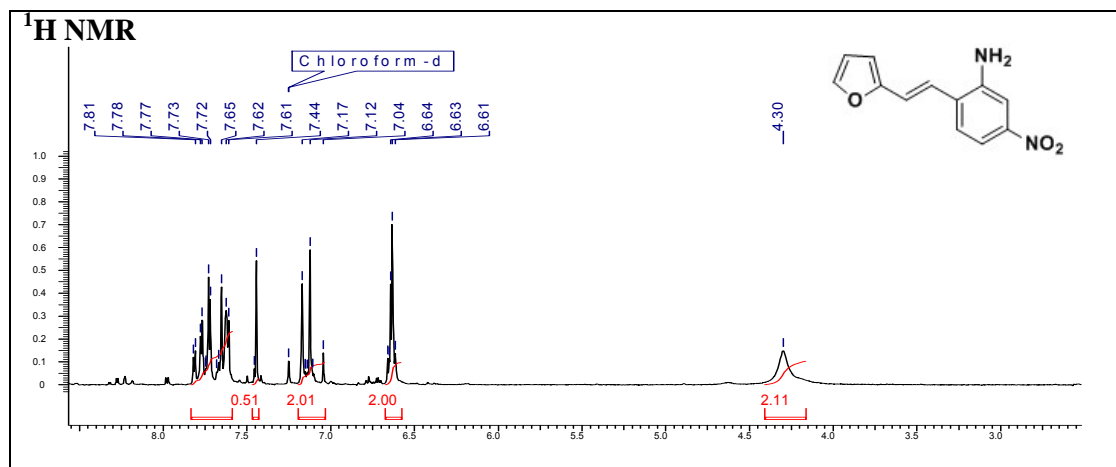
# Chapter 2



**(E)-2-(3-Nitrostyryl)furan (21d)**

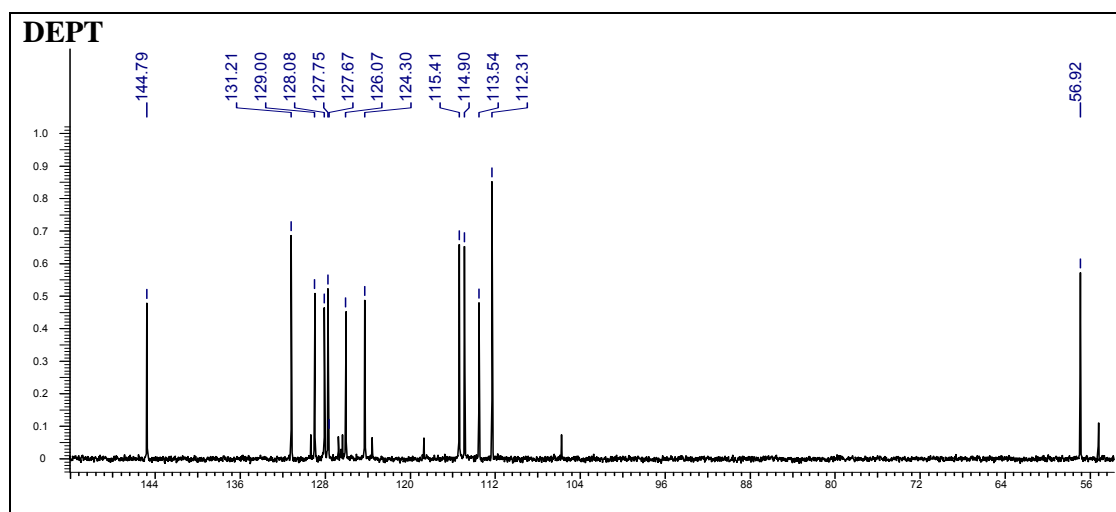
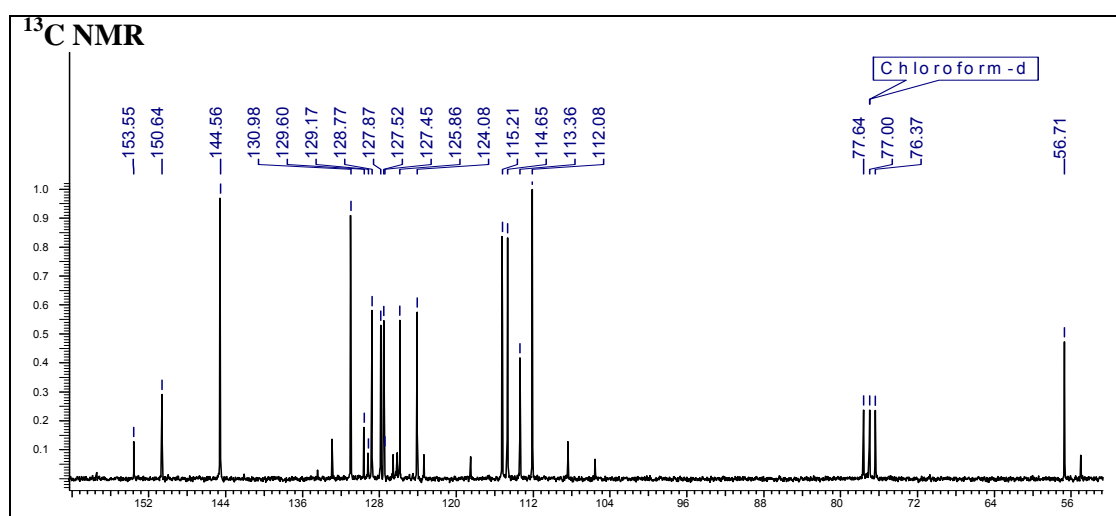
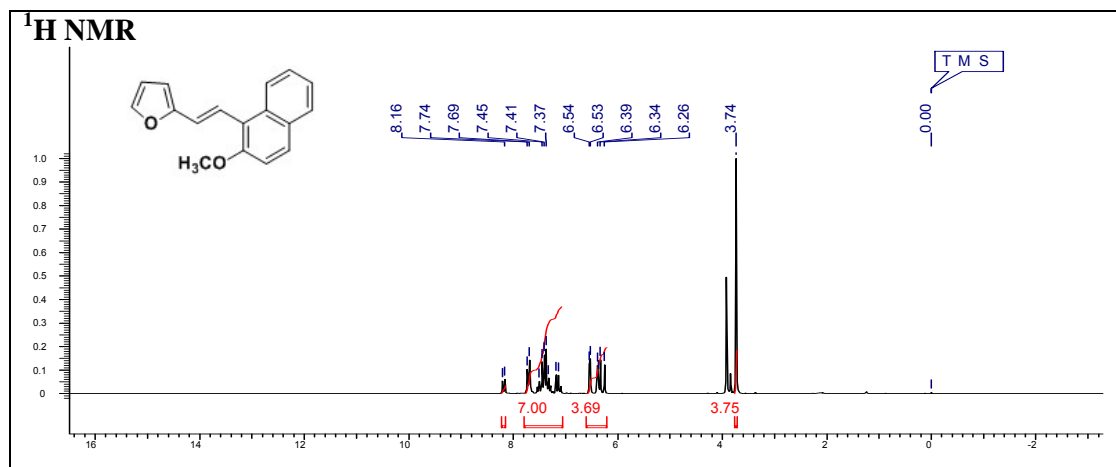
T. Kaur, *PhD thesis*, University of Pune, 2013

# Chapter 2



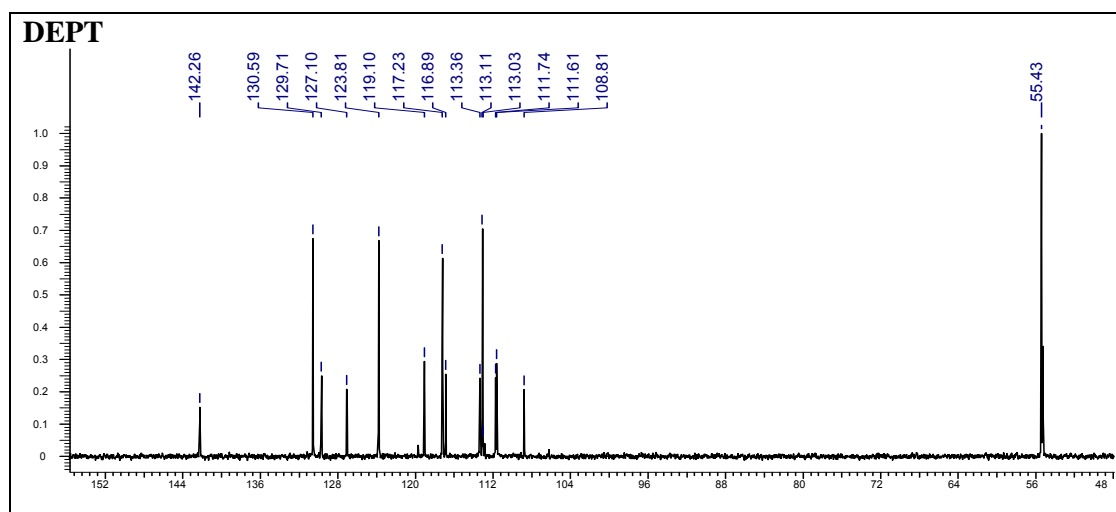
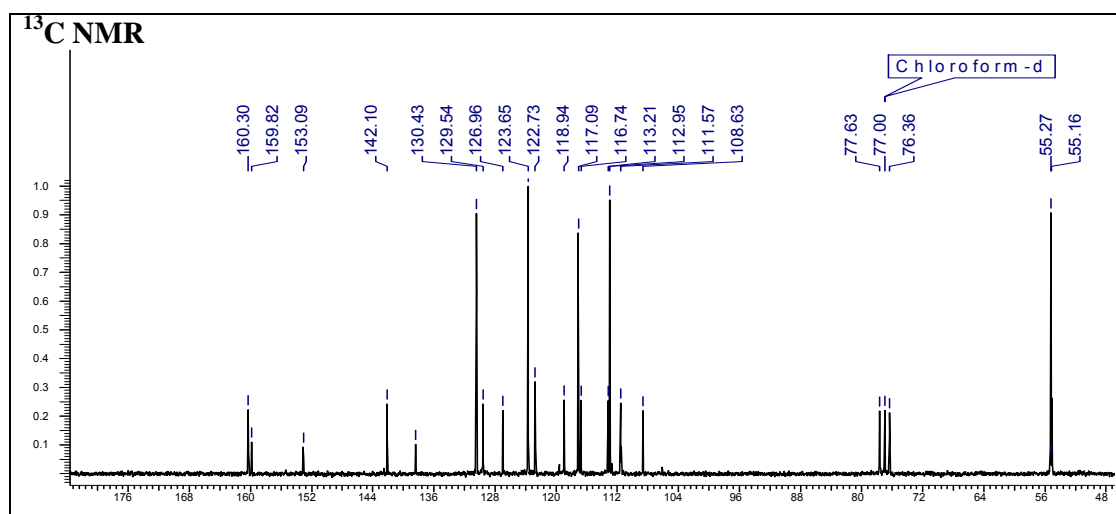
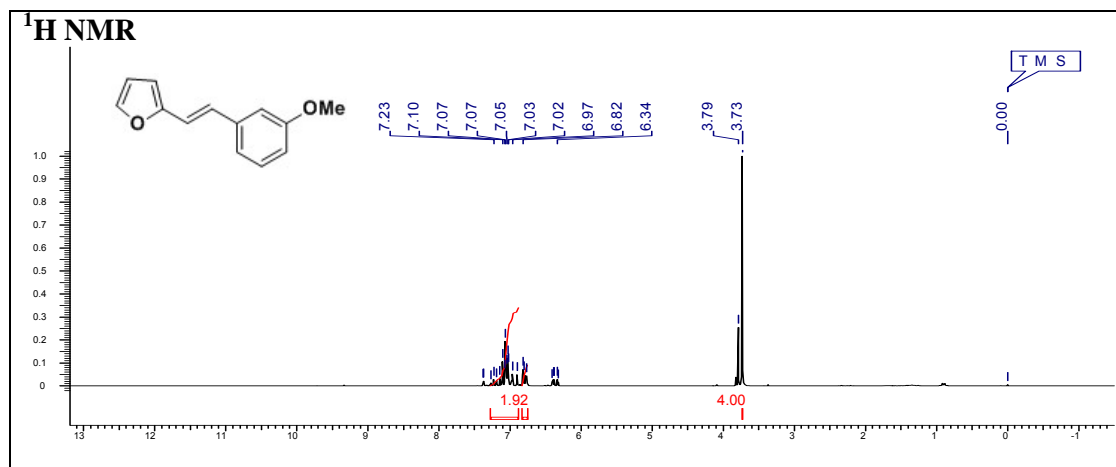
**(E)-2-(2-(Furan-2-yl)vinyl)-5-nitroaniline (21e)**

# Chapter 2



**(E)-2-(2-(2-Methoxynaphthalen-1-yl)vinyl)furan (21f)**

# Chapter 2

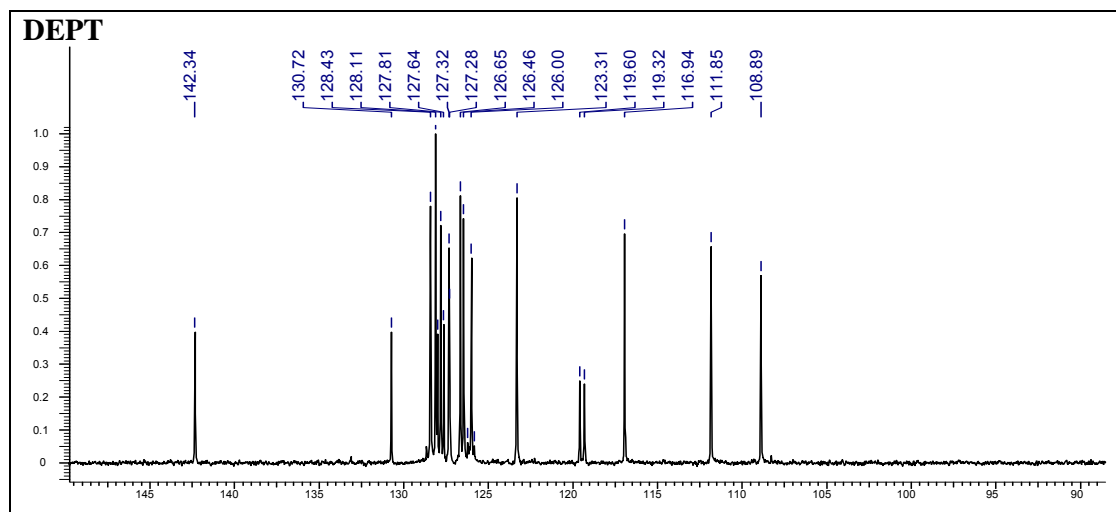
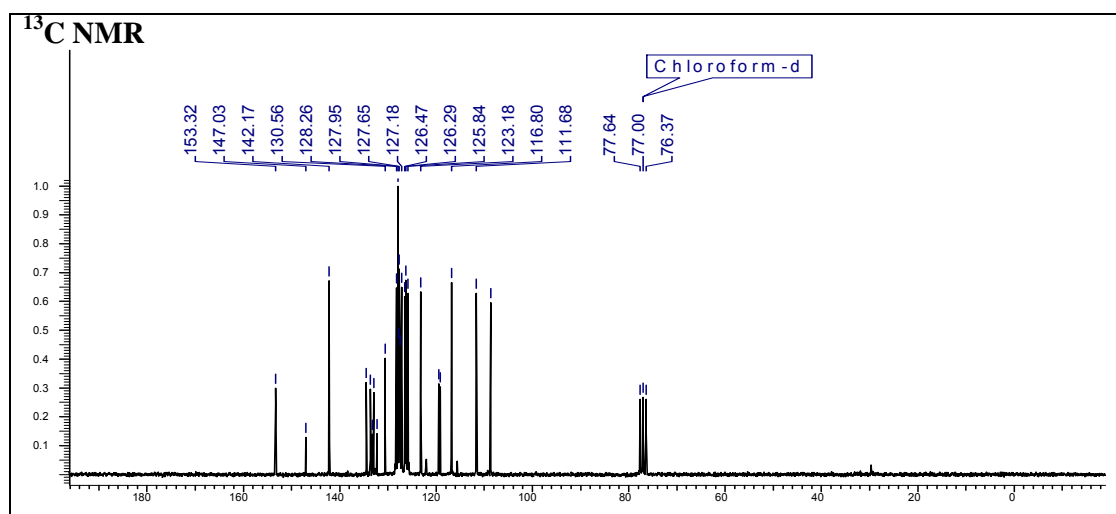
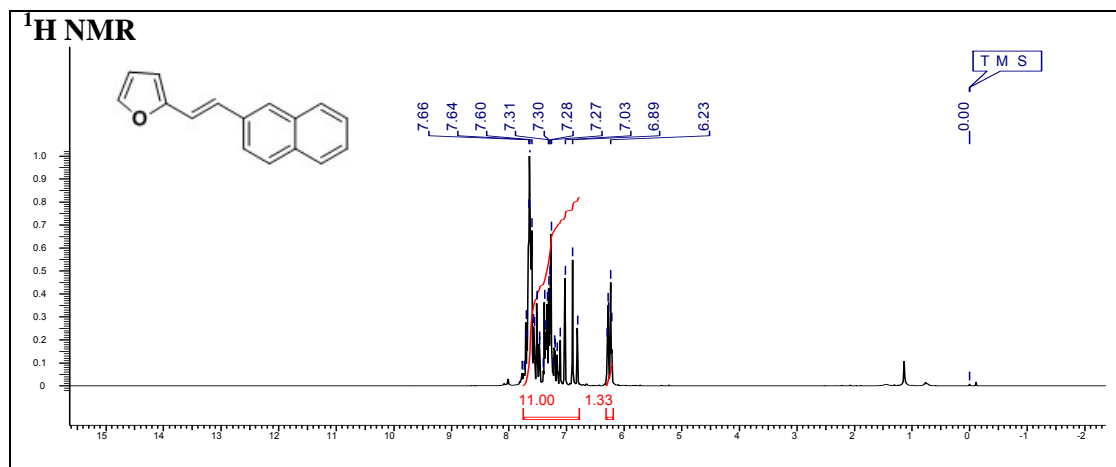


**(E)-2-(3-Methoxystyryl)furan (21g)**

T. Kaur, *PhD thesis*, University of Pune, 2013

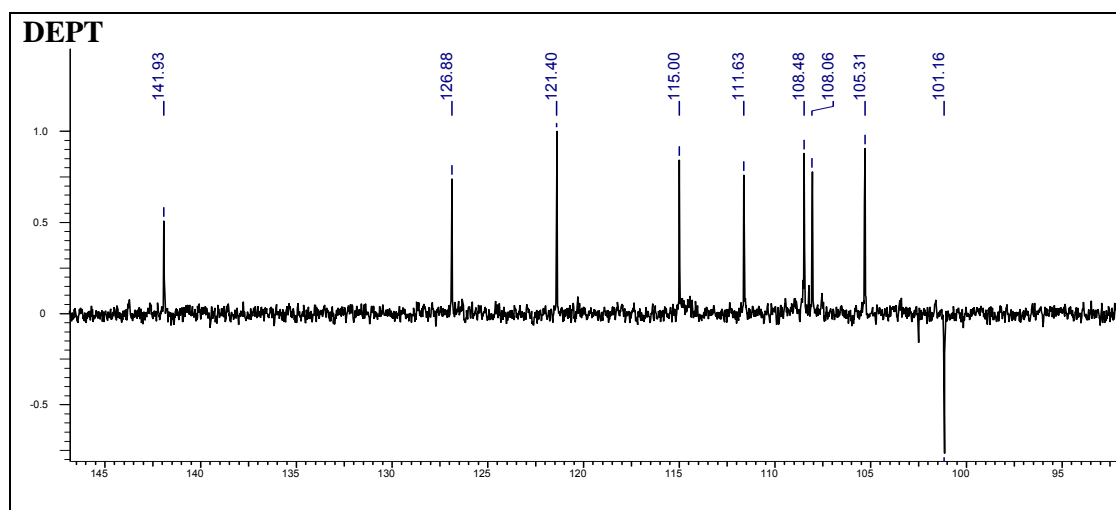
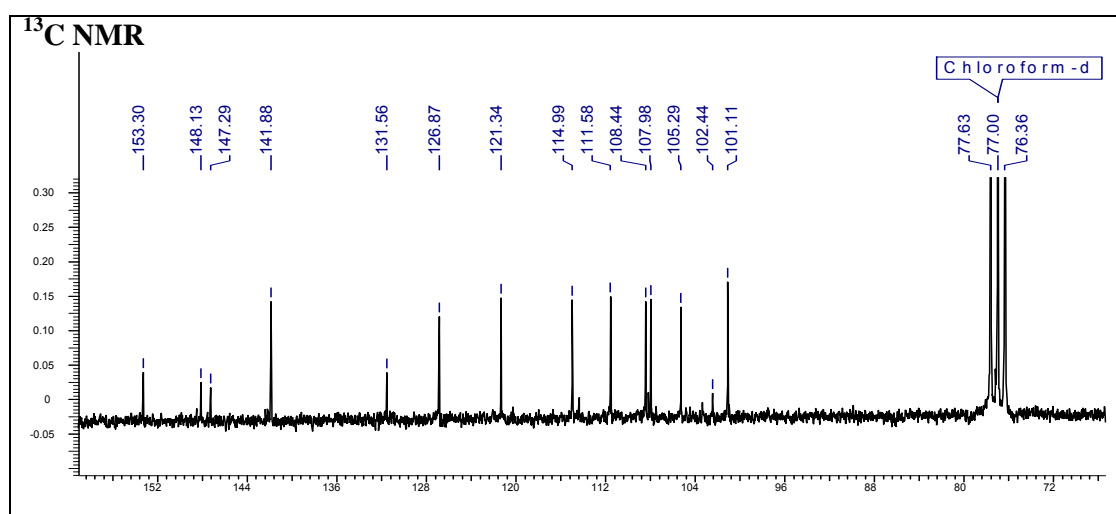
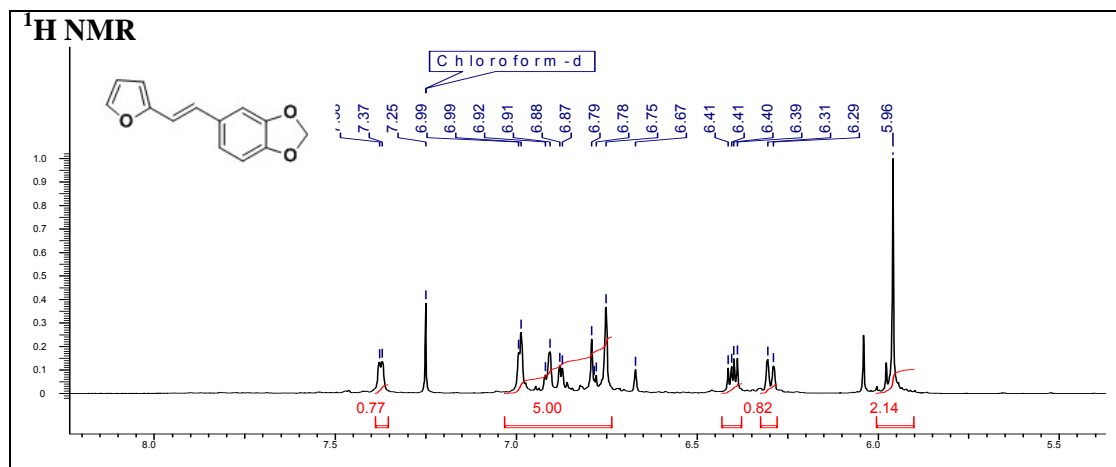


# Chapter 2



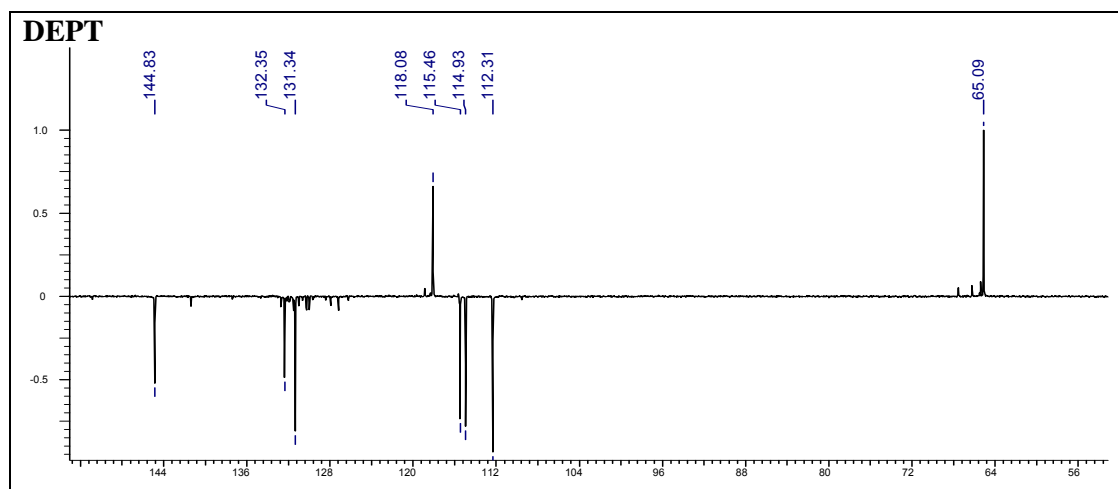
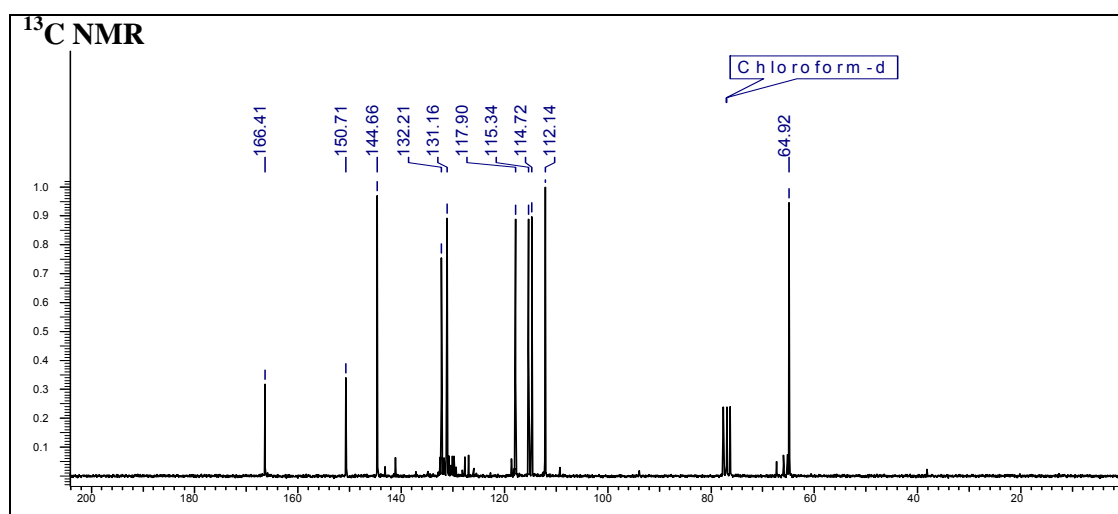
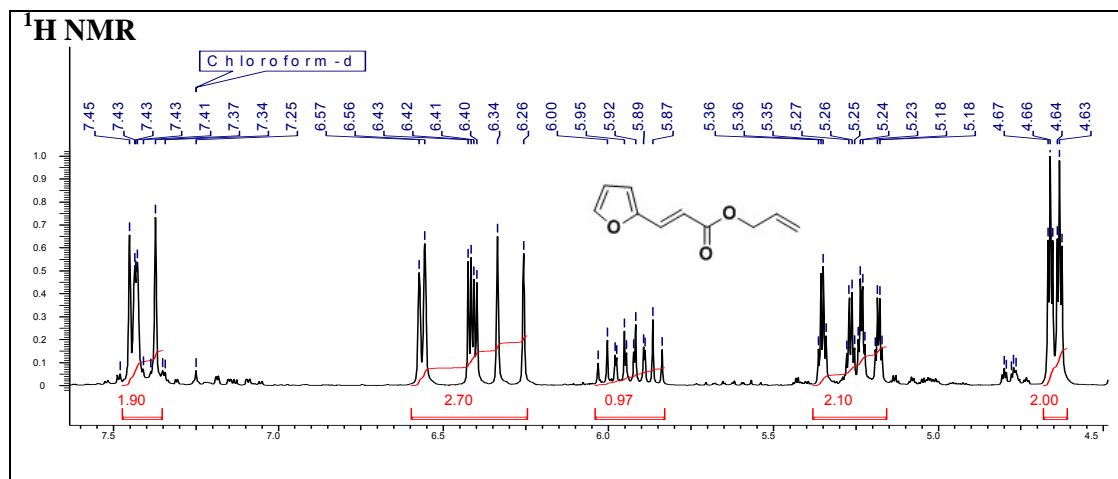
**(E)-2-(2-(Naphthalen-2-yl)vinyl)furan (21h)**

# Chapter 2



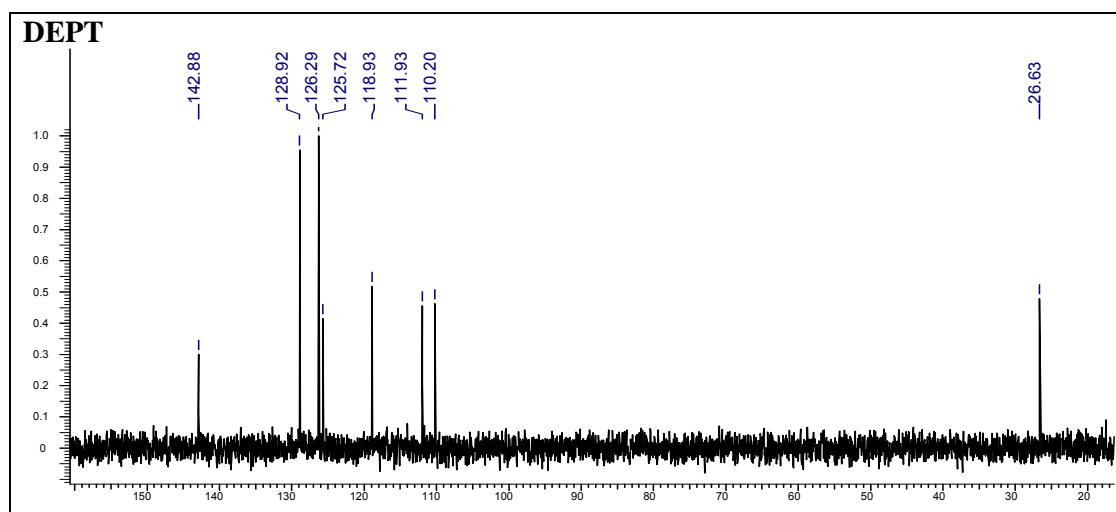
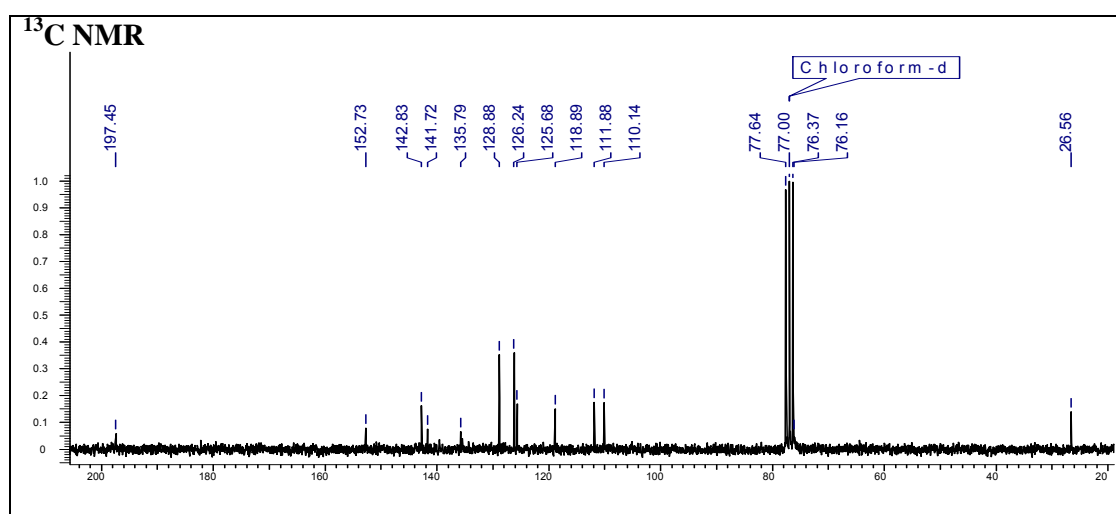
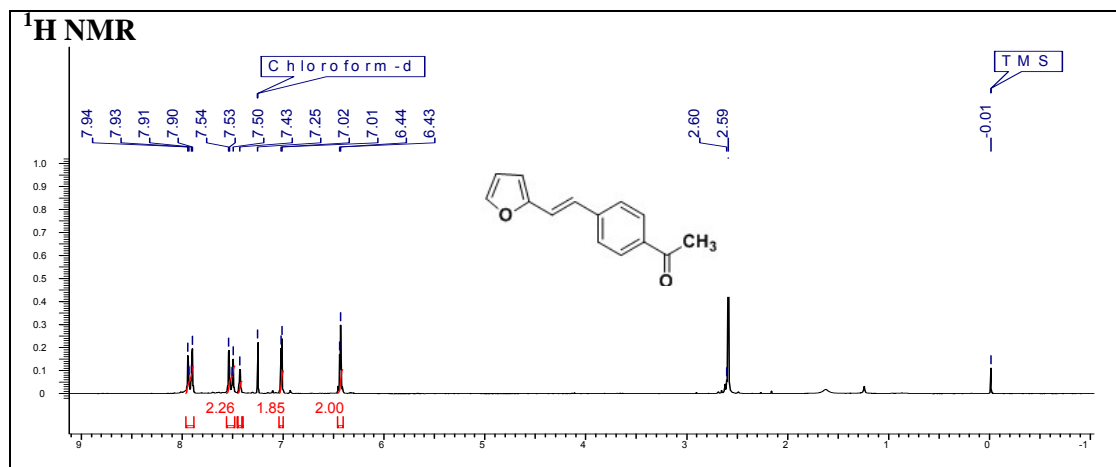
**(E)-5-(2-(Furan-2-yl)vinyl)benzo[d][1,3]dioxale (21i)**

# Chapter 2



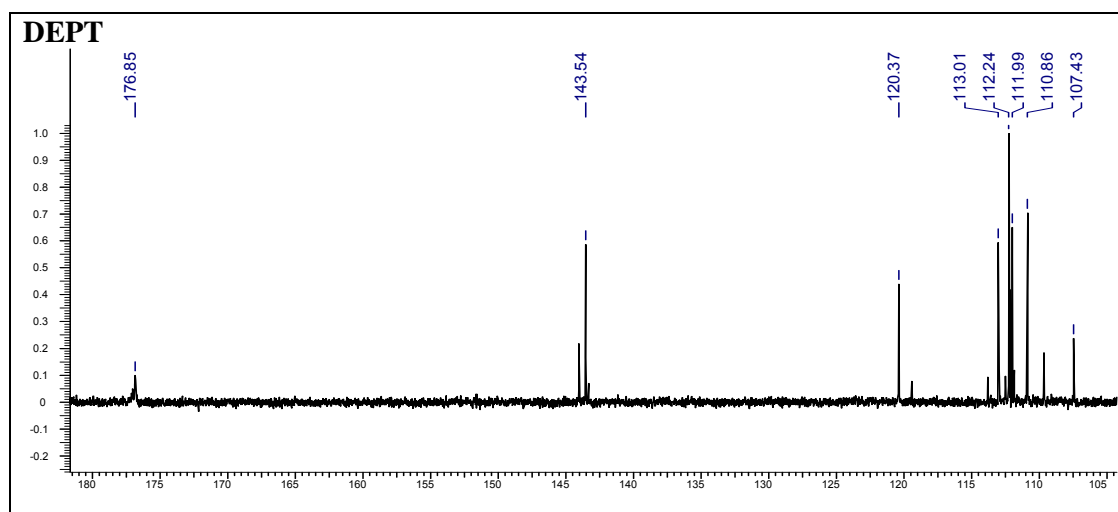
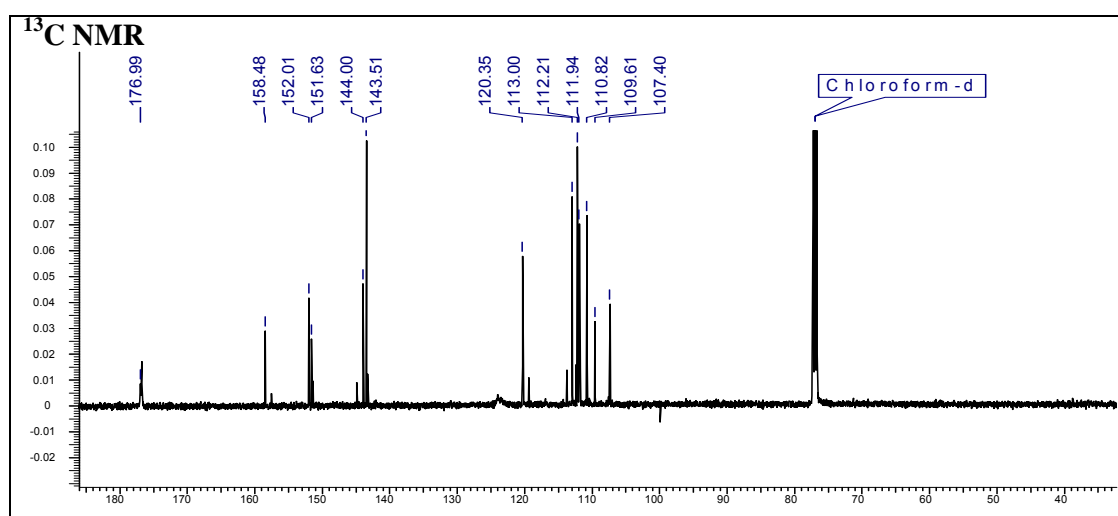
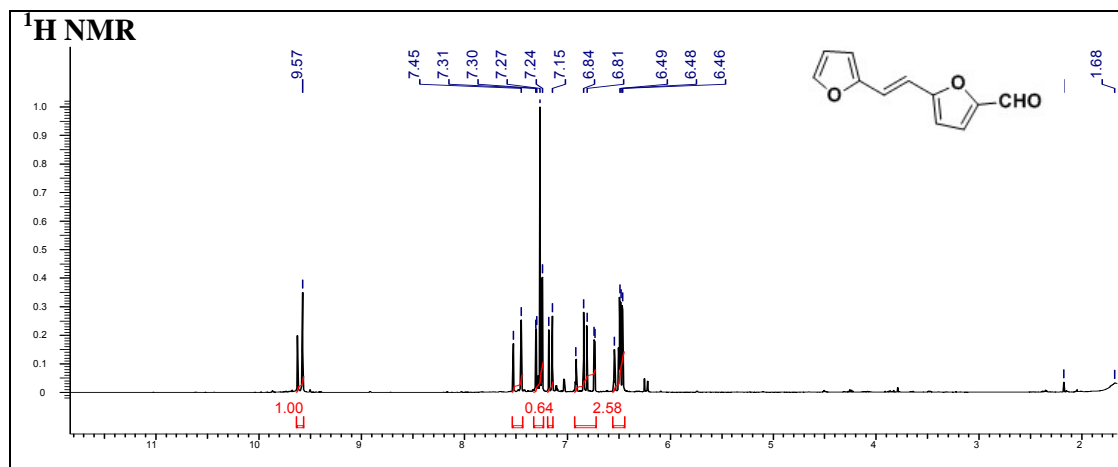
**(E)-Allyl 3-(furan-2-yl)acrylate (21k)**

# Chapter 2



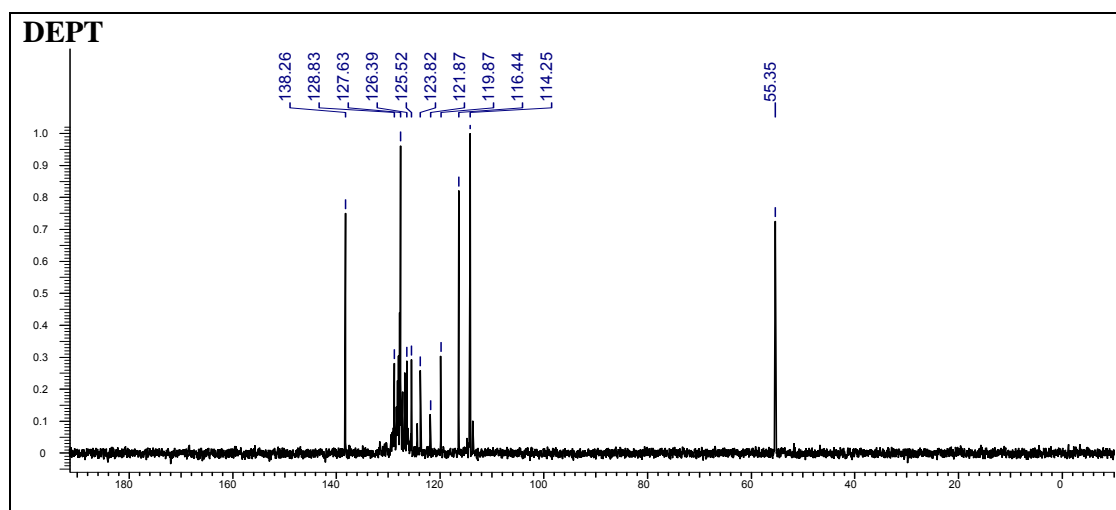
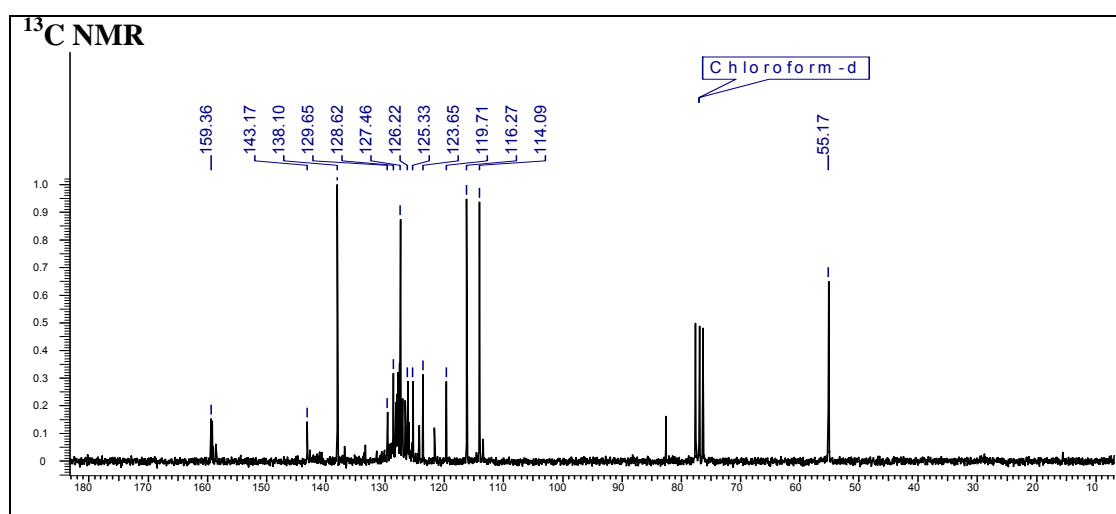
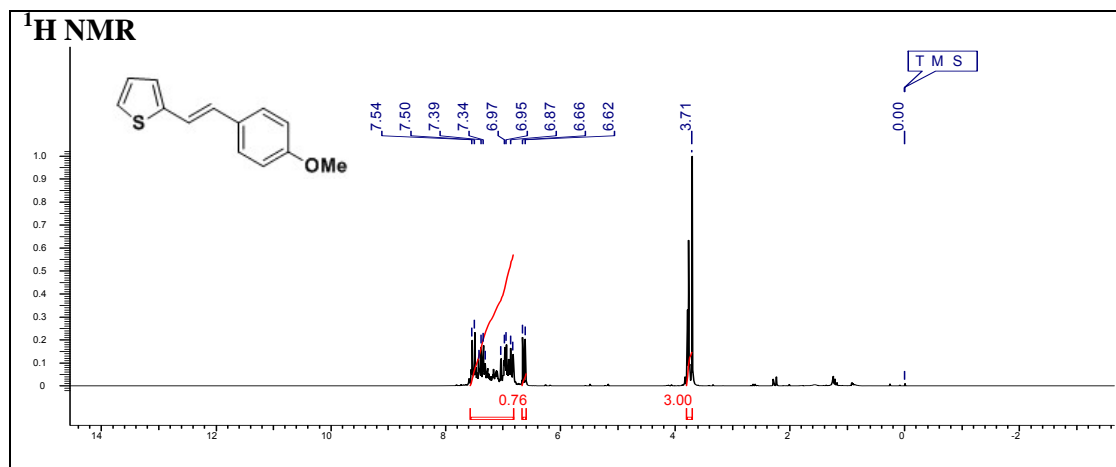
**(E)-1-(4-(2-Furan-2-yl)vinyl)phenyl)ethanone (21m)**

# Chapter 2



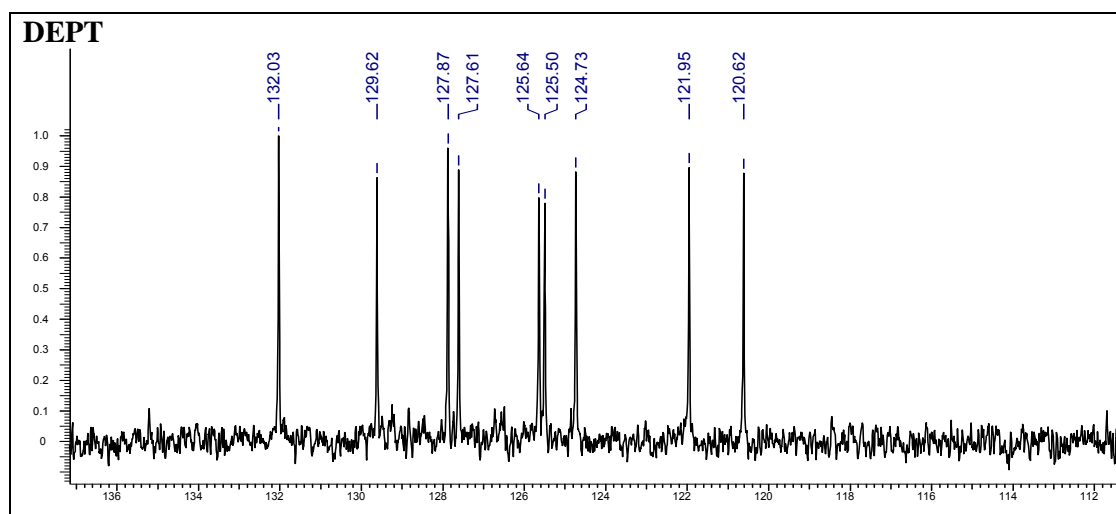
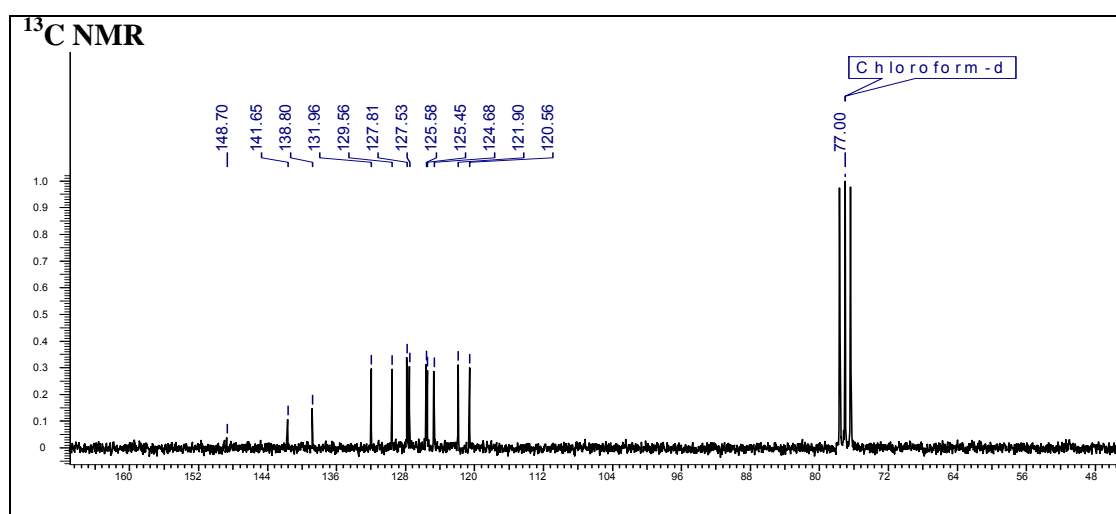
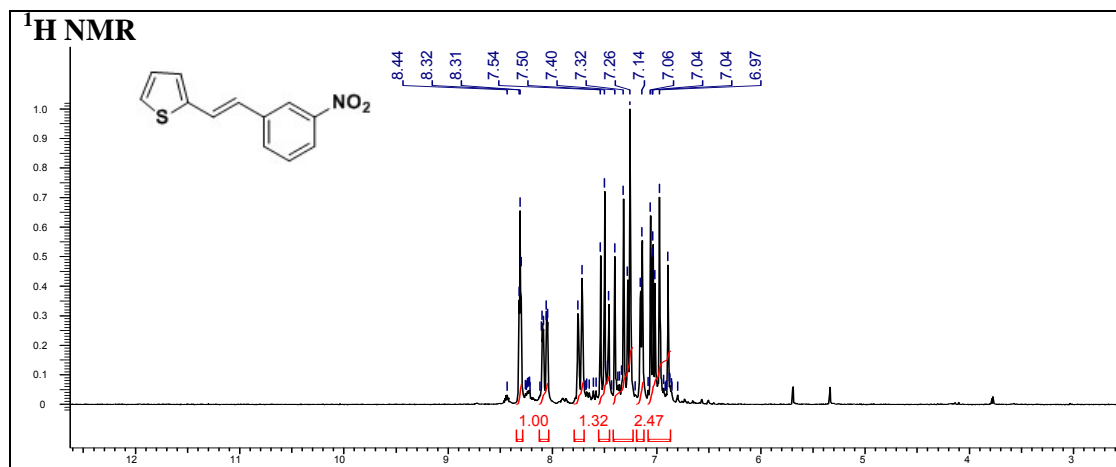
**(E)-5-(2-Furan-2-yl)vinylfuran-2-carbaldehyde (21n)**

# Chapter 2



**(E)-2-(4-Methoxystyryl)vinylthiophene (21o)**

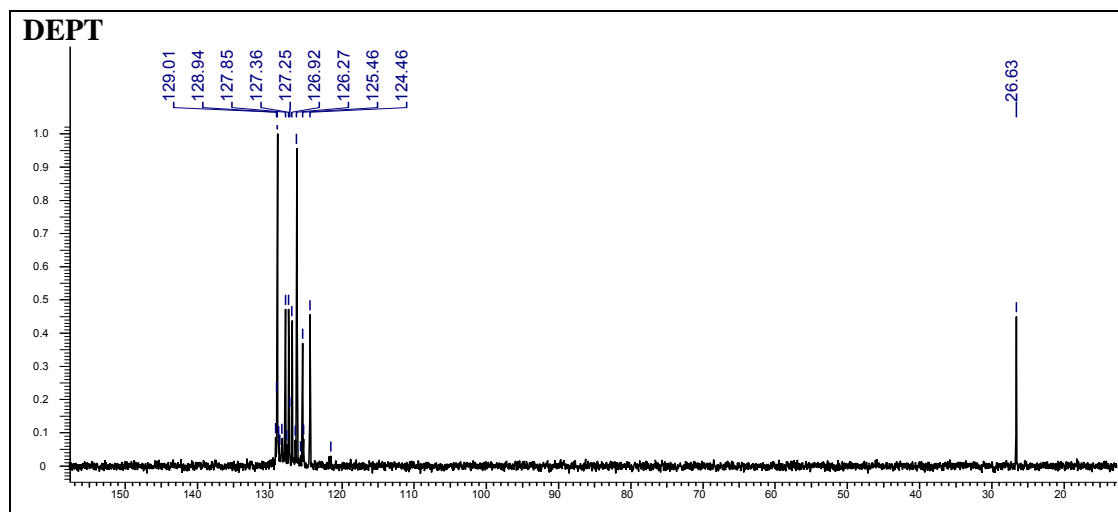
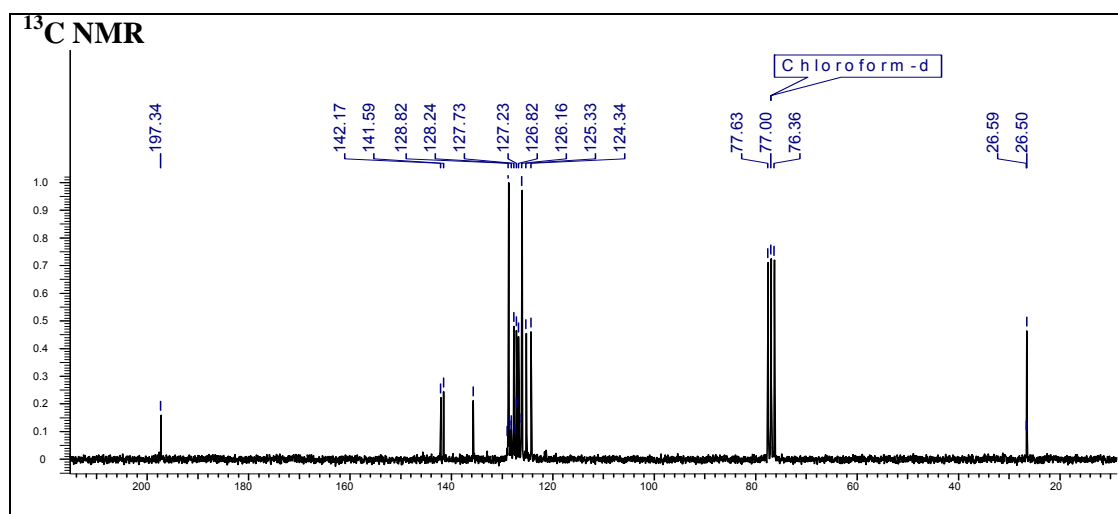
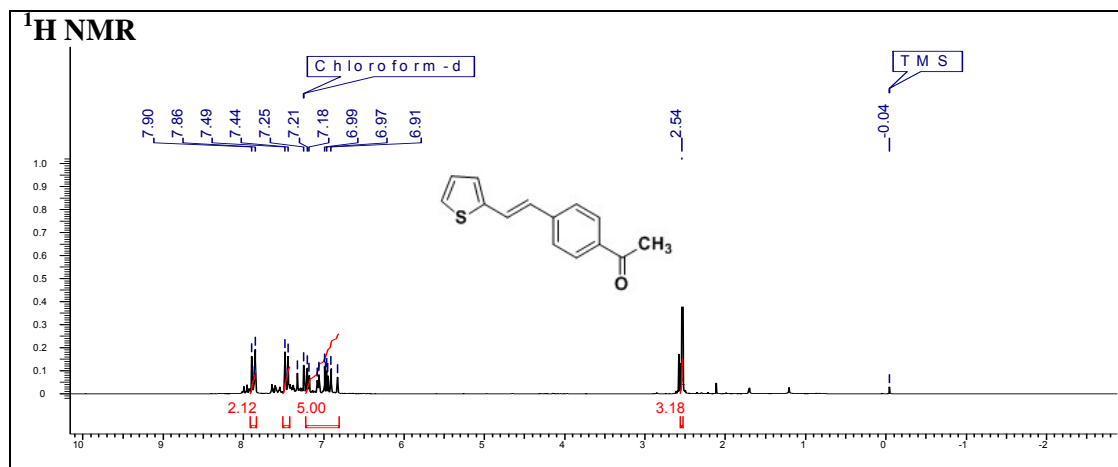
# Chapter 2



**(E)-2-(3-Nitrostyryl)vinylthiophene (21p)**

T. Kaur, *PhD thesis*, University of Pune, 2013

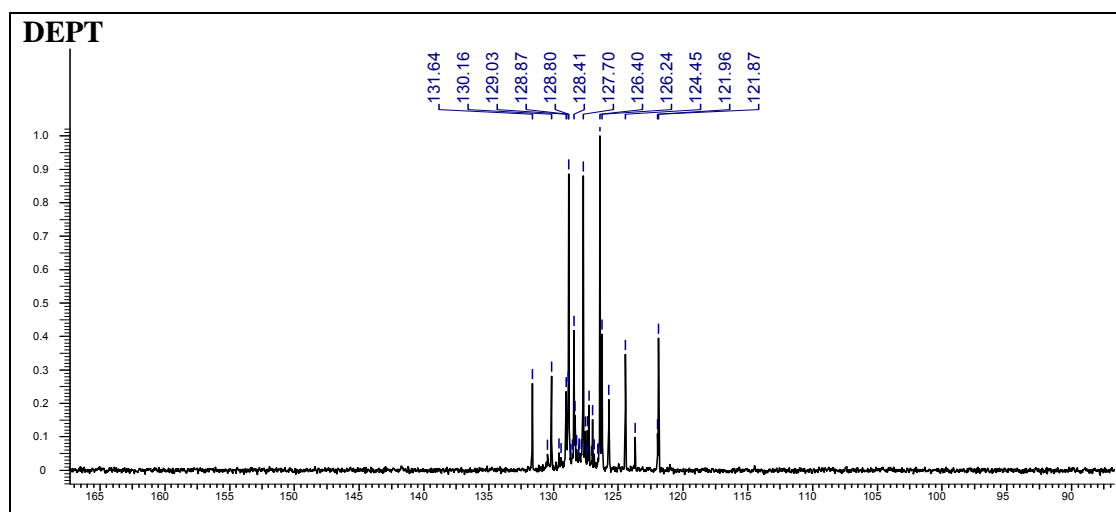
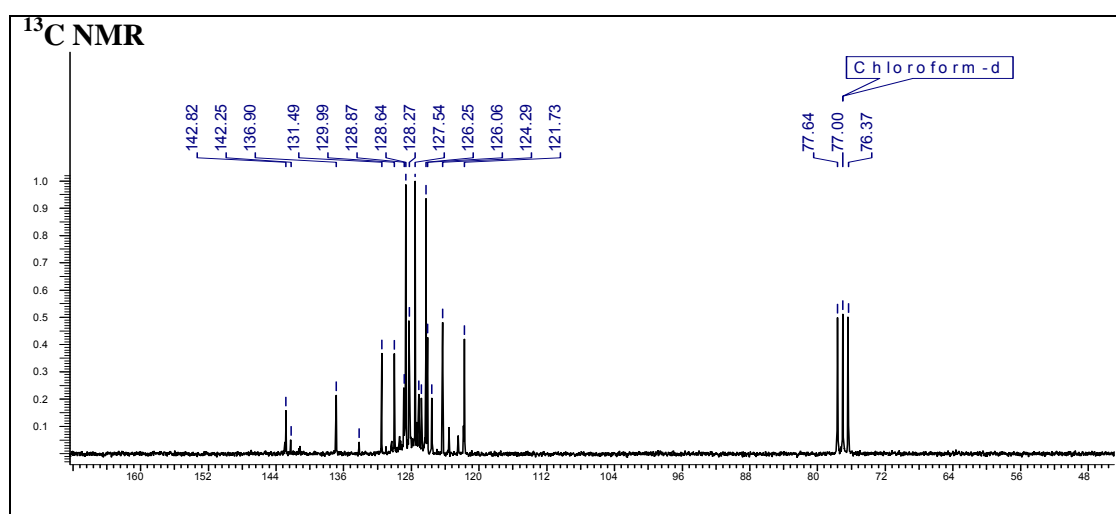
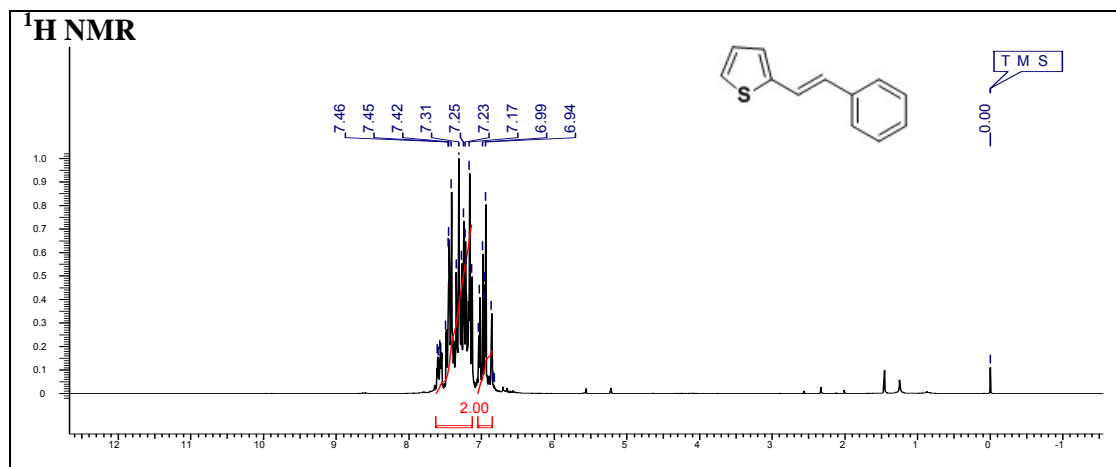
# Chapter 2



**(E)-1-(4-(2-(Thiophene-2-yl)vinyl)phenyl)ethanone (21r)**



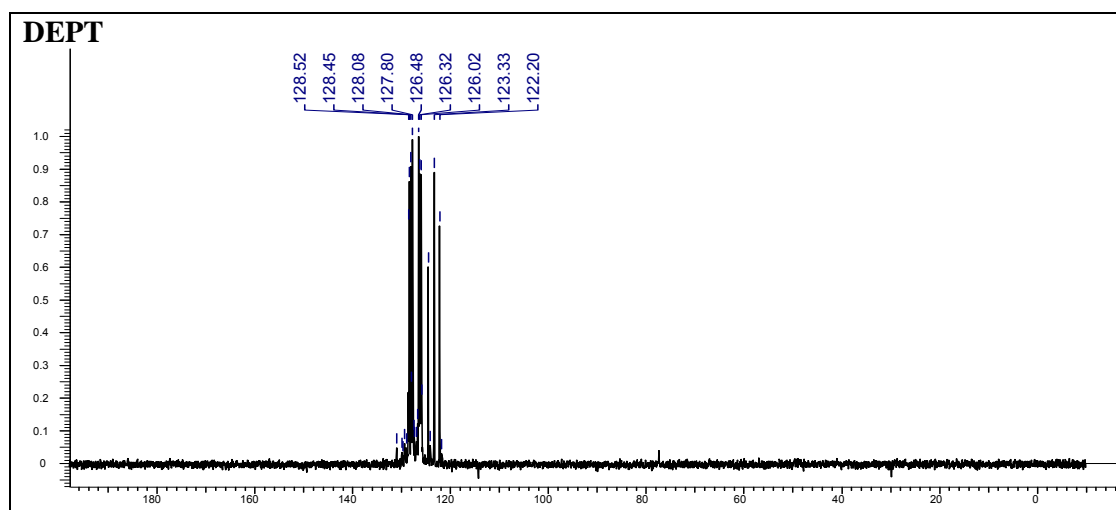
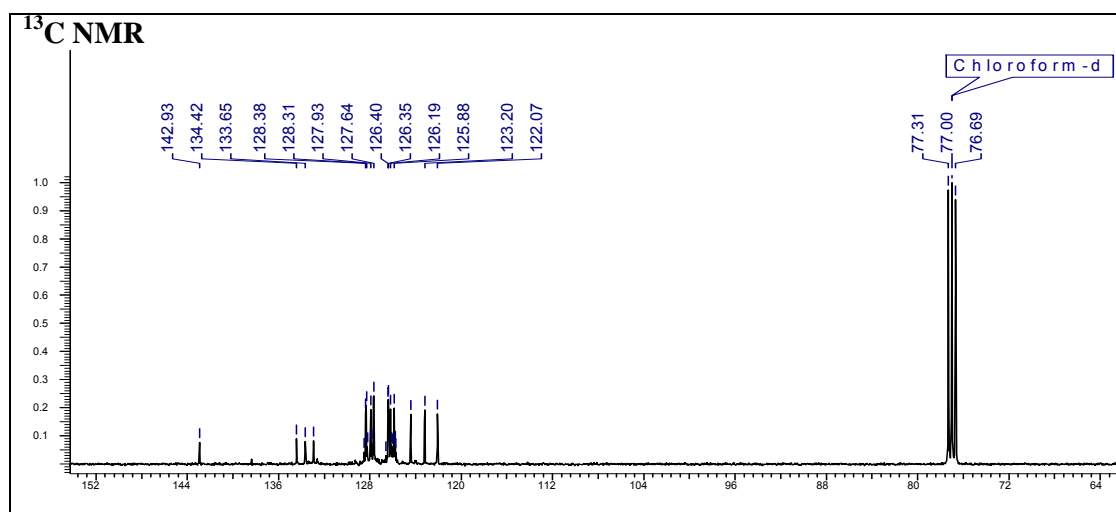
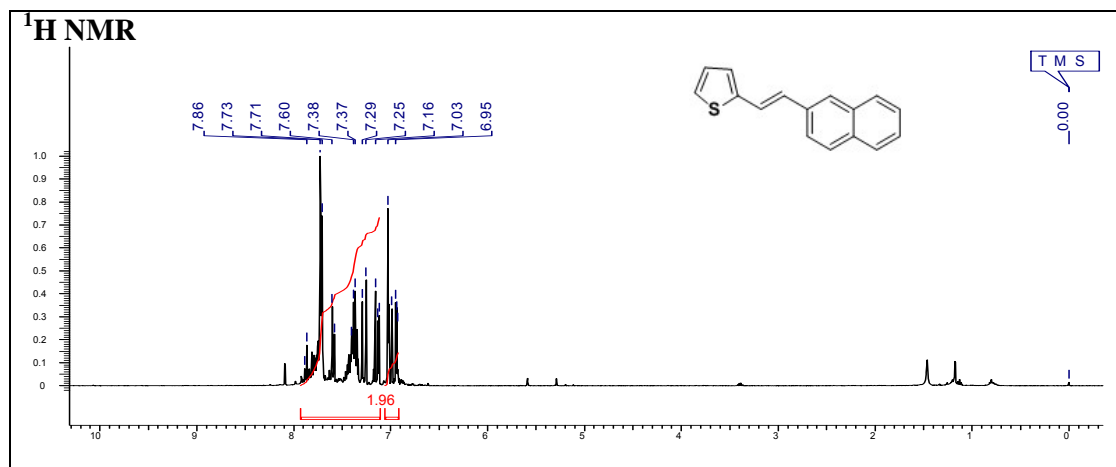
# Chapter 2



**(E)-2-Styrylthiophene (21s)**

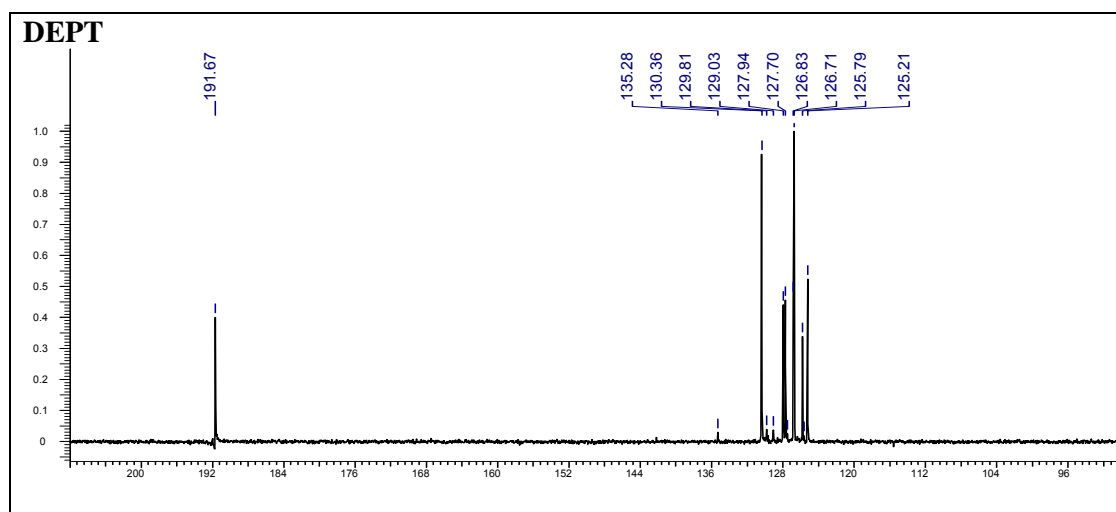
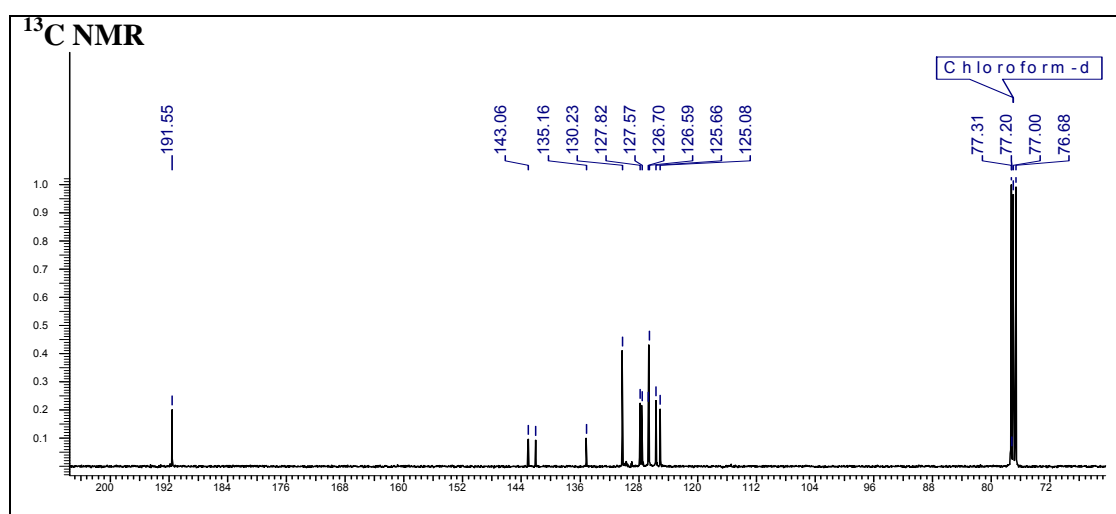
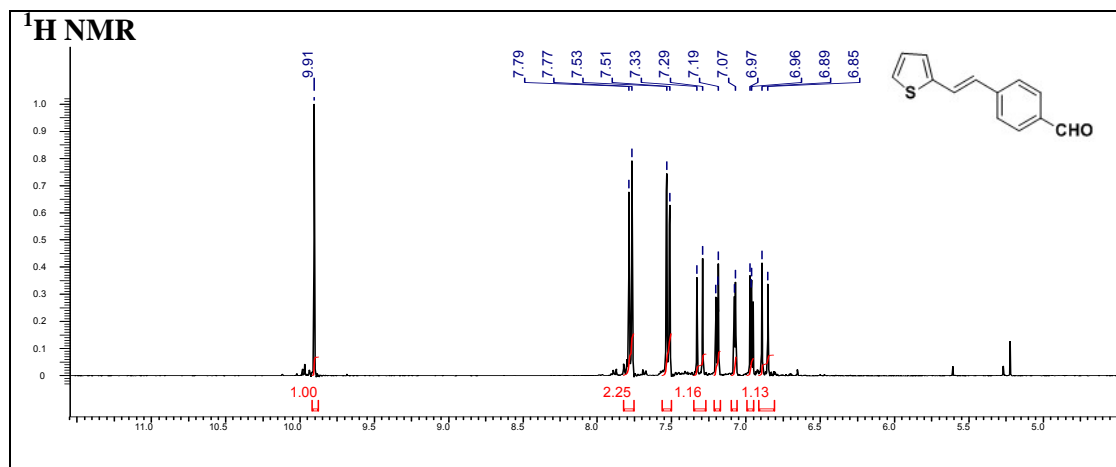
T. Kaur, *PhD thesis*, University of Pune, 2013

# Chapter 2



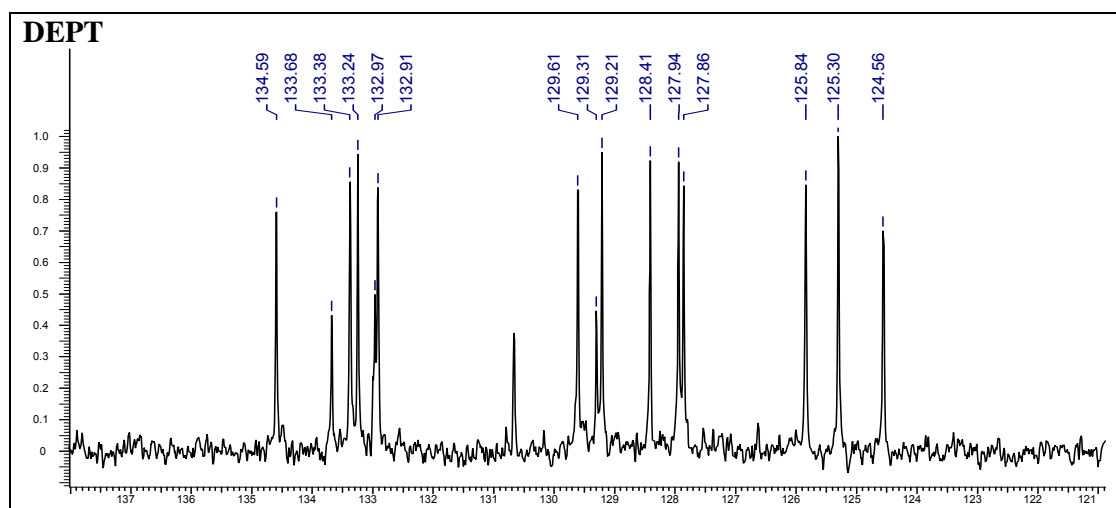
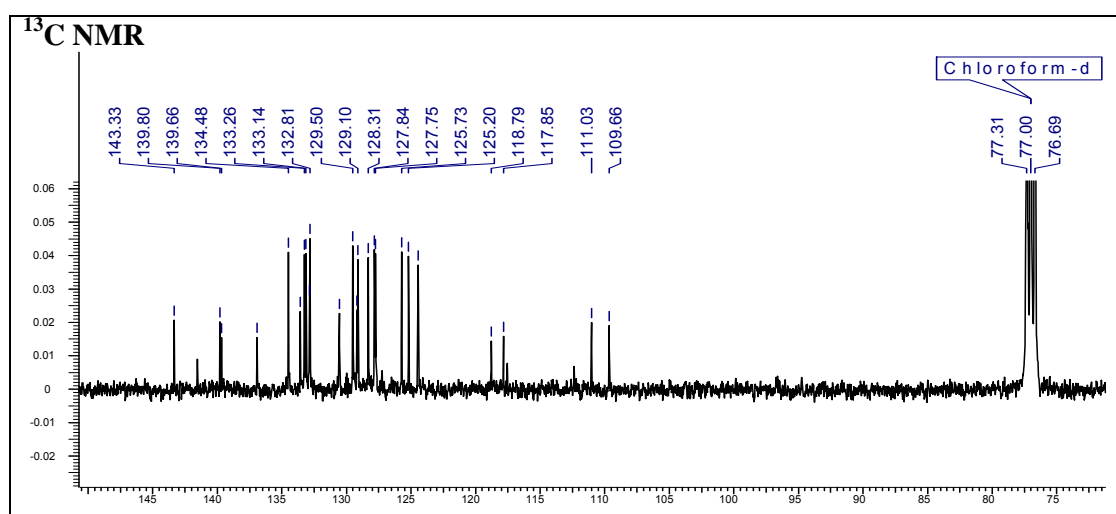
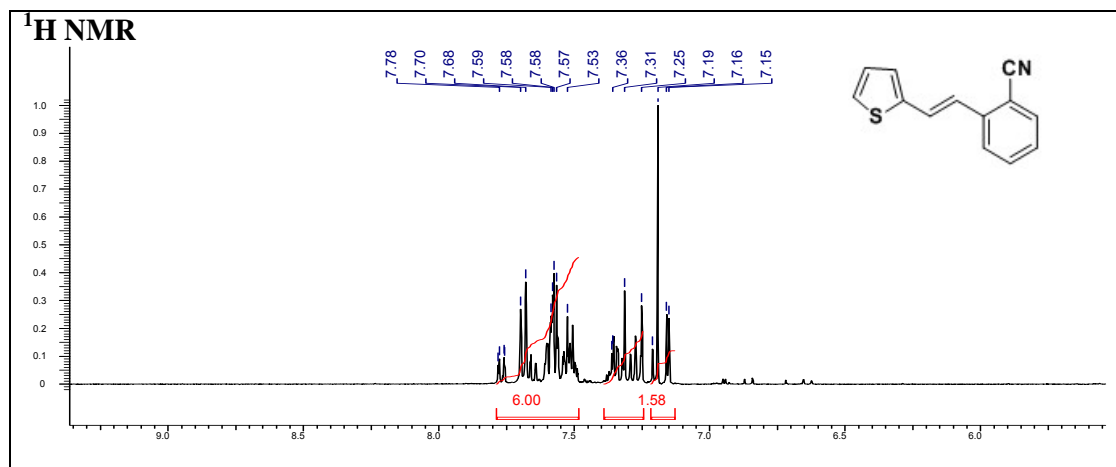
**(E)-2-(2-(Naphthalen-2-yl)vinyl)thiophene (21t)**

# Chapter 2



**(E)-4-(2-(Thiophene-2-yl)vinyl)benzaldehyde (21u)**

# Chapter 2



**(E)-2-(2-(Thiophen-2-yl)vinyl)benzonitrile (21v)**

# *Chapter 2*

## **New Synthetic Methodologies**

---

### *Section B*

#### **Synthesis of Biologically active Alpha-Aminophosphonates**

---

This section deals with the development of new routes for the synthesis of Alpha-aminophosphonates. It also discusses previous literature routes for the synthesis of this class of molecules.

## 2.1 Introduction

$\alpha$ -Aminophosphonates are an important class of compounds due to their structural similarity to the corresponding  $\alpha$ -amino acids and transition-state mimics of peptide hydrolysis.  $\alpha$ -Aminophosphonates can act as enzyme inhibitors,<sup>1</sup> peptide mimics,<sup>2</sup> antibiotics and pharmacologic agents,<sup>3</sup> herbicidal and haptens of catalytic antibodies.<sup>4</sup>

The simplest natural aminophosphonic acid, 2-aminoethanephosphonic acid (AEP) **1**, was isolated from ciliated sheep rumen protozoa in 1959 by Horiguchi and Kandatsu.<sup>5</sup> This acid is also present in dietary and bacterial material in high amounts (Figure 1). AEP acts as marker of microbial nitrogen entering duodenum of sheep. Tyrosine plays crucial role in phosphorylation and dephosphorylation which is useful in cellular signal transduction and in cell growth control and carcinogenesis. The only naturally occurring aminophosphonic acid is (-)-1-amino-2-(4-hydroxyphenyl)ethylphosphonic acid **2** found to be useful for studying the mechanism of cell growth and carcinogenesis.<sup>5</sup>

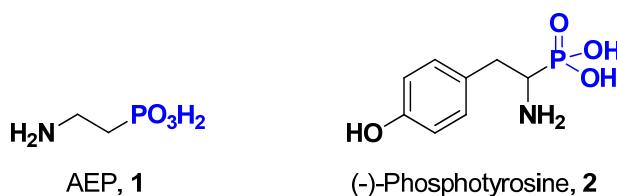


**Figure 1.** Structure of naturally occurring 2-aminoethanephosphonic acid (AEP) derivatives.

Alafosfalin **3**,<sup>6</sup> and renin inhibitor **4**<sup>7</sup> are some synthetically designed examples of this class (Figure 2). Hassell and Allen *et al.* in 1979 designed and synthesized Alafosfalin (alaphosphin) **3**.<sup>3</sup> Compound **3** was found to be highly active against *E. coli* and moderately active against *Serratia*, *Klebsiella*, *Enterobacter* and *Citrobacter* bacterial strains. When Alafosfalin **3** was exposed to different bacterial strains, it resulted in the generation of alanine and 2-aminoethylphosphonic acid (AEP), **1**. The latter compound inhibits the cell wall synthesis and hence resulting in antibacterial activity.<sup>7</sup>

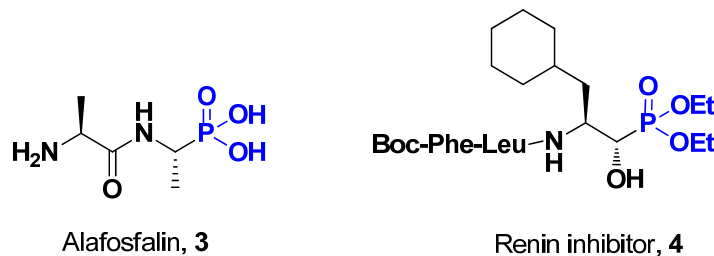


**Figure 2.** Structure of synthetic  $\alpha$ -aminophosphonic acid derivatives.

Compound **4** was designed and found to be renin inhibitor. This molecule has dipeptide of phenylalanine and leucine on one end and hydroxyl phosphonate on the other end. This compound after hydrolysis generates active hydroxyl phosphonate intermediate. This intermediate was found to act as potent renin inhibitor. So, in short aminophosphonic acid and esters possess different biological activities.<sup>7</sup>

Although the phosphonic and carboxylic acid groups differ considerably in terms of shape, size and acidity, derivatives of phosphonic acid are considered as structural analogues of natural  $\alpha$ -amino acids. They are potent transition-state mimics of peptide hydrolysis like  $\alpha$ -amino acids. They are known as “phosphorus analogues” of amino acids, in which the carboxylic acid group is replaced by a phosphonic acid group. These analogues are important in understanding the physiological processes in living organisms. These phosphonic acid derivatives have negligible mammalian toxicity. They can act as antimetabolites, which compete with their carboxylic acid counterparts for the active sites of enzymes and other cell receptors. They represent a promising class of potential drugs.<sup>5</sup>

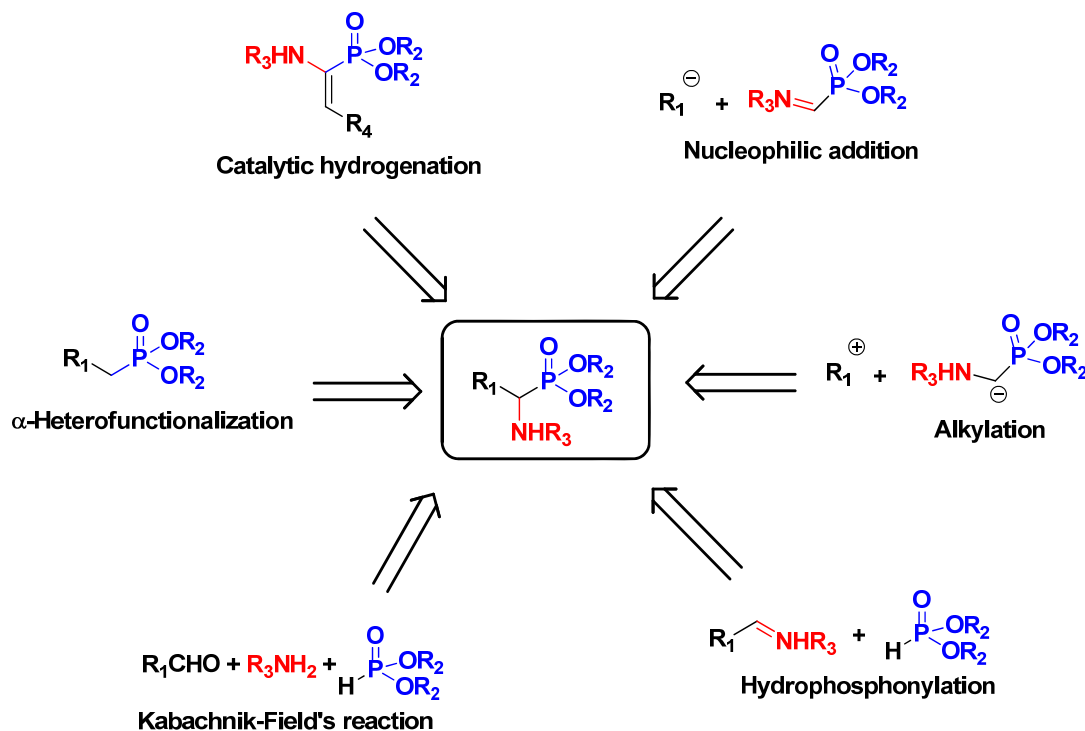
Bismuth is 83<sup>rd</sup> element in the periodic table and known as heaviest stable element. The word Bismuth has been derived from the German word *weisse masse* ‘wismuth’ (white mass).<sup>8</sup> Bismuth is isolated from the ores bismuthinite (bismuth sulphide) and bismite (bismuth oxide), and also isolated in its elemental form. Despite being heavy metal these salts are considered as non-toxic and non-carcinogenic. Many bismuth salts exhibits less toxicity than that of table salt (NaCl).<sup>8</sup> Bismuth has an electronic configuration of  $[\text{Xe}]4f^{14}5d^{10}6s^26p^3$  and due to weak

shielding exhibited by 4f electrons (Lanthanide contraction), bismuth salts (III) shows Lewis acid character. These salts are relatively less toxic and can tolerate small amounts of moisture.

Due to some of the above advantages several bismuth salts have gained tremendous applications in organic syntheses, chemical transformations etc. One of the bismuth salt, bismuth nitrate has emerged as an efficient Lewis acid.<sup>9</sup> Bismuth nitrate (III), due to presence of nitrate ligands can act as a Lewis acid. Being a mild Lewis acid, it is relatively less toxic, cheaply available and tolerant towards trace amounts of water. Hence,  $\text{Bi}(\text{NO}_3)_3 \cdot 5\text{H}_2\text{O}$  is considered as an Lewis acid.

## 2.1.1 Previous Reports

$\alpha$ -Aminophosphonates have attracted attention of organic and medicinal chemists due to their biological activities. In recent times, several synthetic approaches have been reported in the literature for the synthesis of  $\alpha$ -aminophosphonates. Several synthetic approaches have been reported as discussed in Scheme 1.

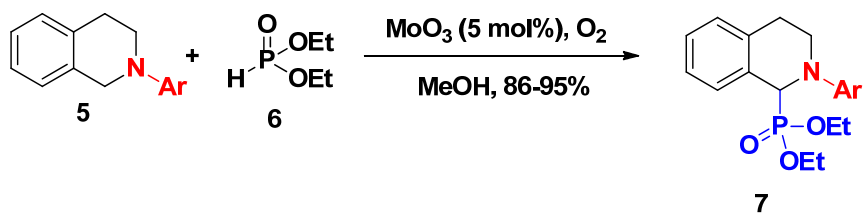




The previous reports include (i)  $\alpha$ -Heterofunctionalization,<sup>10</sup> (ii) Catalytic hydrogenation,<sup>11</sup> (iii) Nucleophilic addition,<sup>12</sup> (iv) Alkylation,<sup>13</sup> (v) Hydrophosphonation<sup>7</sup> and (vi) Kabachnik-Field's reaction<sup>14</sup> for the synthesis of  $\alpha$ -aminophosphonates.

### 2.1.1a $\alpha$ -Heterofunctionalization

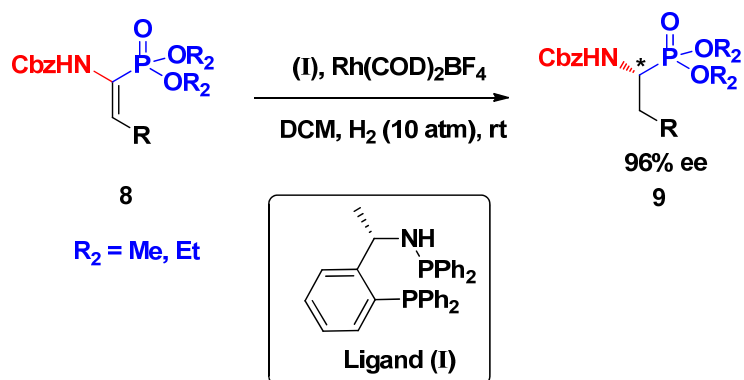
In this approach, oxidative cross-dehydrogenative-coupling (CDC) method for C-H bond functionalization of *N*-aryl tetrahydroisoquinoline derivatives **5** was carried out. This method provides excellent avenue from C-H bond oxidation to achieve C-P bond formed products. Here, molybdenum oxide acts as oxidant under aerobic conditions in order to facilitate the attack of diethylphosphite **6** to furnish  $\alpha$ -aminophosphonate **7** (Scheme 2).<sup>10</sup>



**Scheme 2.** Synthesis of iso-quinoline phosphonates using  $\alpha$ -heterofunctionalization.

### 2.1.1b Catalytic hydrogenation

In this approach, Rh-catalyzed asymmetric hydrogenation of various substituted dimethyl *R*-enamido-phosphonate derivatives **8** was carried out in the presence of phosphine (I) and aminophosphine ligands (Scheme 3).<sup>11</sup>

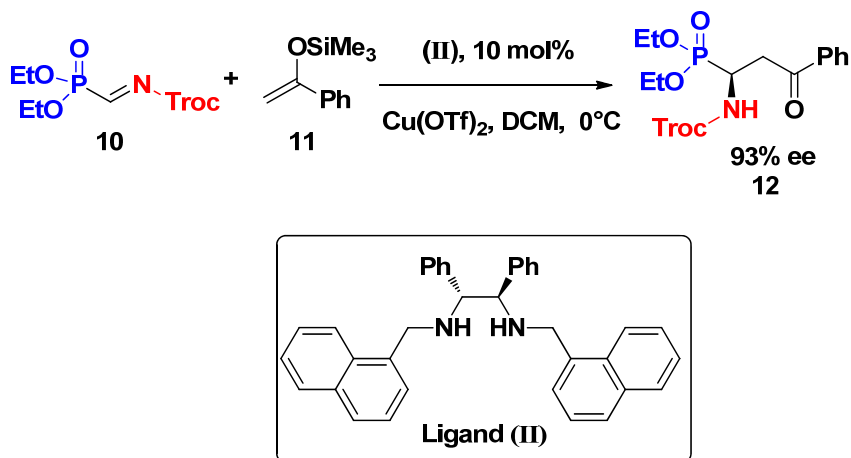


**Scheme 3.** Catalytic hydrogenation method for the synthesis of  $\alpha$ -aminophosphonates.

The enantioselective excesses (*ee*'s) largely depends on the type of chiral bidentate phosphorus ligand employed during the course of the reaction.

### 2.1.1c Nucleophilic addition

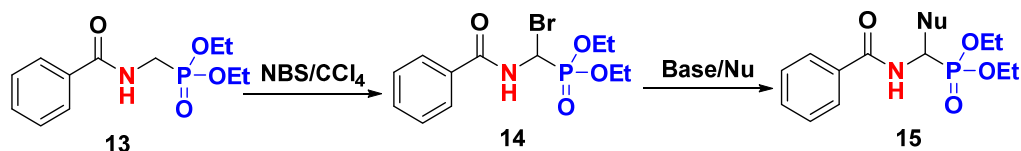
In this approach, *N*-acyl-iminophosphonates **10** were treated with silicone enolates **11** in the presence of diamine ligand (**II**) and copper triflate as catalyst to have  $\alpha$ -aminophosphonates **12** in high enantiomeric excess 93% *ee*'s (Scheme 4).<sup>12</sup>



**Scheme 4.** Enantioselective Michael addition to synthesize  $\alpha$ -aminophosphonates.

### 2.1.1d Alkylation

In this approach,<sup>13</sup>  $\alpha$ -aminophosphonate derivative **13**, was brominated using *N*-bromosuccinimide to achieve bromo derivative **14**. Bromo derivative **14** was reacted with base in the presence of various nucleophiles to furnish substituted  $\alpha$ -aminophosphonate derivatives **15** (Scheme 5).<sup>13</sup>

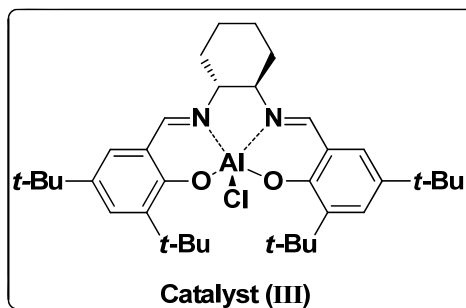
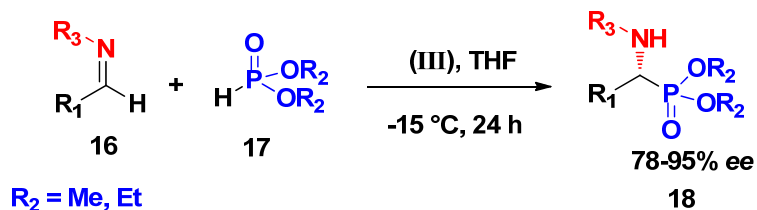


**Scheme 5.** Synthesis of  $\alpha$ -aminophosphonates using alkylation method.

### 2.1.1e Hydrophosphonylation

In this approach, imines **16** were treated with dialkyl phosphonates **17** in the presence of lewis acid based catalyst (**II**) in order to obtain  $\alpha$ -aminophosphonates **18** in good to excellent enantiomeric excess (*ee*'s).<sup>7</sup>

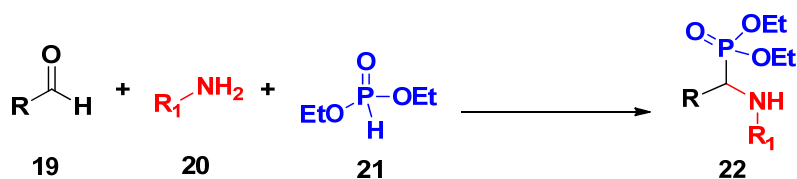
T. Kaur, *PhD thesis*, University of Pune, 2013



**Scheme 6.** Synthesis of  $\alpha$ -aminophosphonates using hydrophosphonylation.

### 2.1.1f Kabachnik-Field's reaction

Kabachnik and Field's developed a new multicomponent reaction in which aldehydes or ketones **19**, ammonia **20**, and diethyl phosphonates **21** were treated in one pot to furnish  $\alpha$ -aminophosphonates **22** (Scheme 7).<sup>14</sup>



**Scheme 7.** One pot synthesis of  $\alpha$ -aminophosphonates.

## 2.2 Present Work: Rationale and Objective

$\alpha$ -aminophosphonates are the biologically important class of compounds and their synthesis has got world-wide attention in synthetic as well as in medicinal chemistry. Several synthetic approaches have been reported in the literature for the synthesis of  $\alpha$ -aminophosphonates but the most preferred method is nucleophilic addition of phosphites to imines, which is either catalyzed by an alkali metal alkoxide or Lewis acid *e.g.* NaOEt or Lewis acids such as  $\text{BF}_3 \cdot \text{Et}_2\text{O}$ ,  $\text{SnCl}_2$ ,  $\text{SnCl}_4$ ,  $\text{ZnCl}_2$  and  $\text{MgBr}_2$ .<sup>15-16</sup> However, one-pot protocols from a carbonyl compound, an amine and a phosphite could not proceed faster because the water, generated during the course of

reaction can decompose or deactivate Lewis acid. There are some recent advancements using lanthanide triflates/MgSO<sub>4</sub>,<sup>17</sup> InCl<sub>3</sub>,<sup>18</sup> ZrCl<sub>4</sub><sup>16</sup> and TaCl<sub>5</sub>-SiO<sub>2</sub> to eliminate these drawbacks.<sup>19</sup> However, some of the major drawbacks are involvement of stoichiometric amount of catalysts, expensive reagents, longer reaction times, and in addition, many methods use harmful organic solvents such as CH<sub>2</sub>Cl<sub>2</sub>, THF or CH<sub>3</sub>CN.<sup>20-25</sup> Hence, there is still a room to develop an efficient, environment friendly and practically potent protocol for the synthesis of  $\alpha$ -aminophosphonates.

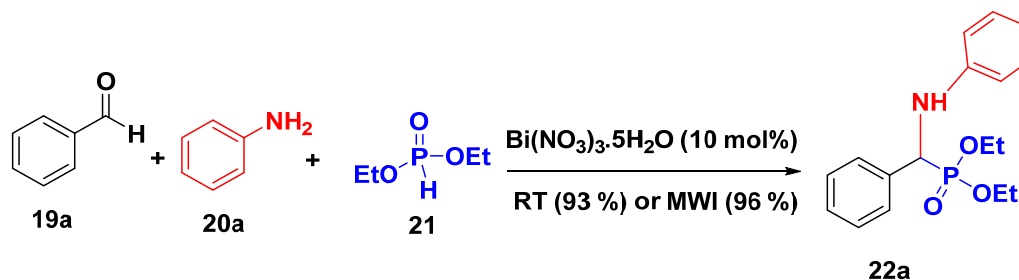
Bismuth nitrate is relatively less toxic, cheaply available and tolerant towards trace amounts of water. Hence, Bi(NO<sub>3</sub>)<sub>3</sub>.5H<sub>2</sub>O is considered as an Lewis acid. A new Bi(NO<sub>3</sub>)<sub>3</sub>.5H<sub>2</sub>O catalyzed one-pot synthesis of structurally diverse  $\alpha$ -aminophosphonates from carbonyl compounds, amines and diethylphosphite was developed. Being a mild Lewis acid, it can be used in several organic transformations like Michael conjugate addition, acylals synthesis, oxidation of secondary alcohols to aldehydes, oxidation of sulphides to sulfoxides, nitration of xylenes, Hantzsch oxidation of 1,4-dihydropyridines to pyridines, oxidation of acetals to aldehydes *etc.*<sup>9</sup>

### 2.3 Results and Discussion

In literature very few reports deal with the synthesis of  $\alpha$ -aminophosphonates using mild Lewis acid catalyst. So, it is highly desirable to develop a synthetic method employing eco-friendly catalyst for the synthesis of  $\alpha$ -aminophosphonates. Bi(NO<sub>3</sub>)<sub>3</sub>.5H<sub>2</sub>O being mild Lewis acid catalyst, was utilized in catalyzing one-pot synthesis of structurally diverse  $\alpha$ -aminophosphonates by reacting carbonyl compounds, amines and diethylphosphite in one pot. The role of bismuth atom is in coordination with the imine nitrogen and further facilitating the nucleophilic attack of diethylphosphite to render the desired product in excellent yields.

Initially, the reaction of benzaldehyde **19a** with aniline **20a** and diethylphosphite **21**, was carried out at room temperature in the presence of Bi(NO<sub>3</sub>)<sub>3</sub>.5H<sub>2</sub>O (10 mol %) (Scheme 8). The corresponding  $\alpha$ -aminophosphonate

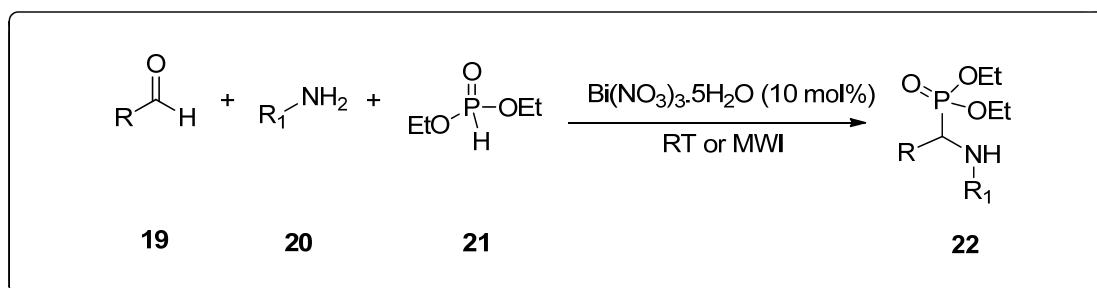
**22a** was obtained in 93% yield and in 10 h time. The same reaction was carried out under Microwave irradiation (MWI) and the product was formed in 96% yield and in 4 minutes. The use of MWI greatly enhanced the yield and was reduced the reaction time. The synthesized  $\alpha$ -aminophosphonate **22a** was identified by its spectral data. The formation of  $\alpha$ -aminophosphonate **22a** was confirmed by the presence of peak in  $^1\text{H-NMR}$  at 4.76 ppm (d,  $^1J_{\text{PH}} = 26.0$  Hz, 1H) and in  $^{13}\text{C-NMR}$  56.4 (d,  $^1J_{\text{PC}} = 150.1$  Hz, CH). IR stretching for **22a** was observed at  $\nu_{\text{max}}$  3300 (NH stretching), 1600 (C=O, stretching), 1214 (C-O, stretching) further confirms the formation of product.



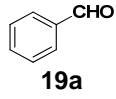
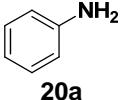
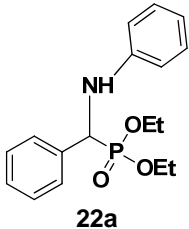
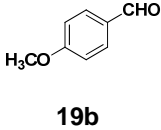
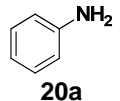
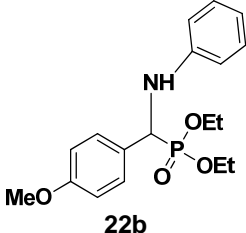
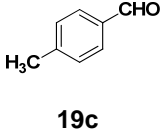
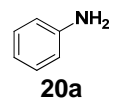
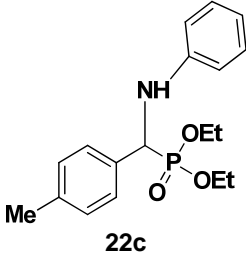
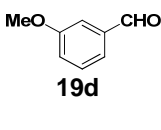
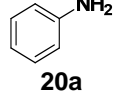
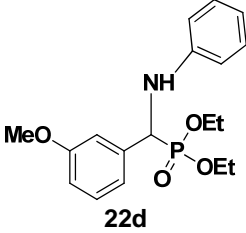
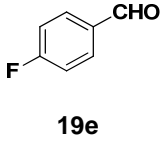
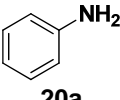
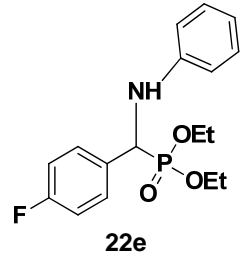
**Scheme 8.** Bismuth nitrate catalyzed synthesis of  $\alpha$ -aminophosphonates.

To establish versatility of the reaction various aldehydes (aliphatic/aromatic), amines (primary/secondary) and diethylphosphite were subjected to developed one-pot reaction conditions. The structurally diverse carbonyl compounds were subjected to this novel procedure in the presence of catalytic amount (10 mol %) of  $\text{Bi}(\text{NO}_3)_3 \cdot 5\text{H}_2\text{O}$  and converted to the corresponding  $\alpha$ -aminophosphonates in high to excellent yields (see Table 1). In all the cases, the three-component reaction proceeded smoothly and furnished  $\alpha$ -aminophosphonates.

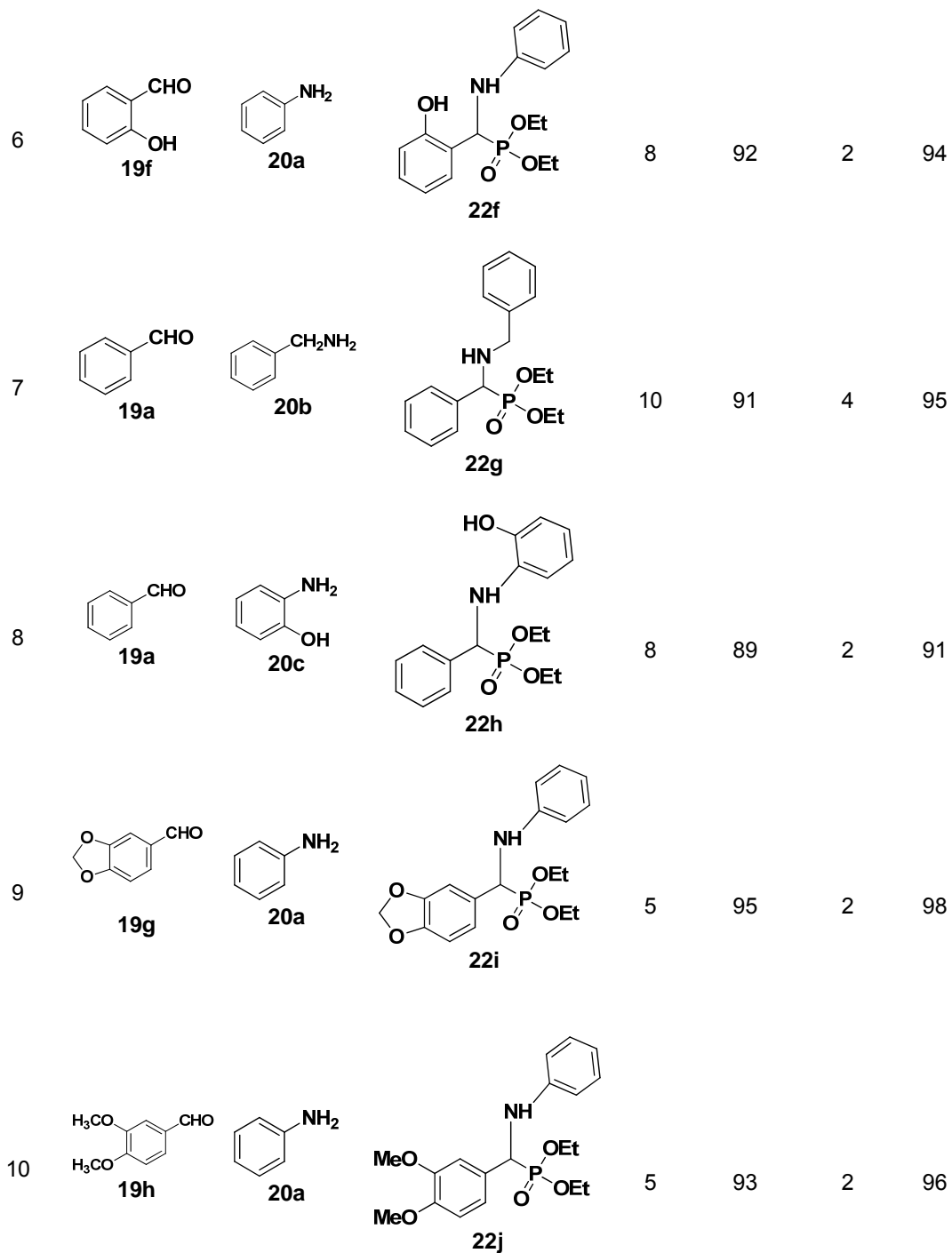
**Table 1.** One-pot synthesis of  $\alpha$ -aminophosphonates catalyzed by  $\text{Bi}(\text{NO}_3)_3 \cdot 5\text{H}_2\text{O}$ .



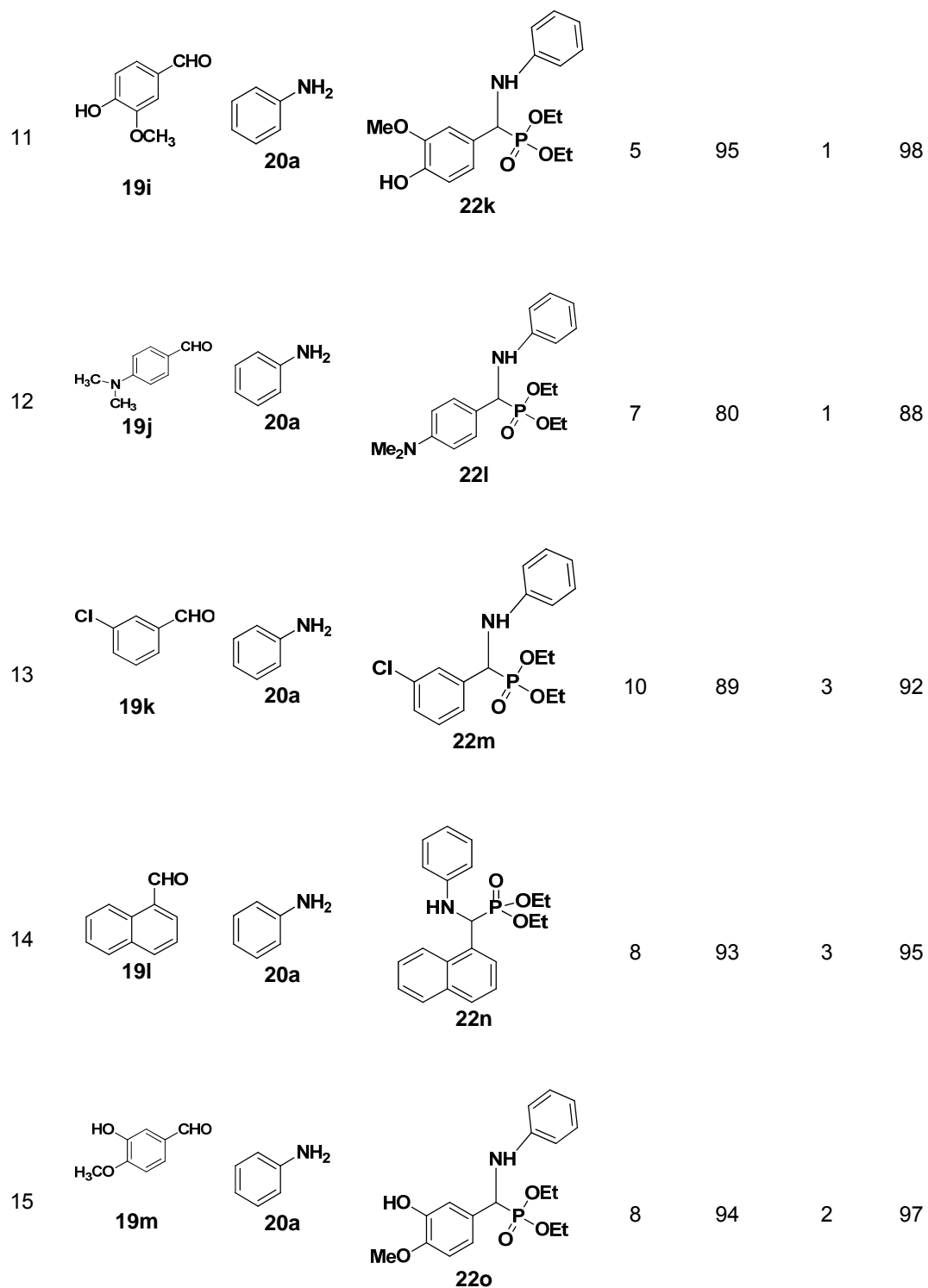
# Chapter 2

Sl. No.	RCHO	R'NH <sub>2</sub>	Product	Method A <sup>a</sup>		Method B <sup>b</sup>	
				Time (h)	Yield (%)	Time (min)	Yield (%)
1	 19a	 20a	 22a	10	93	4	96
2	 19b	 20a	 22b	10	93	2	95
3	 19c	 20a	 22c	10	94	2	96
4	 19d	 20a	 22d	8	91	3	95
5	 19e	 20a	 22e	8	90	4	92

# Chapter 2

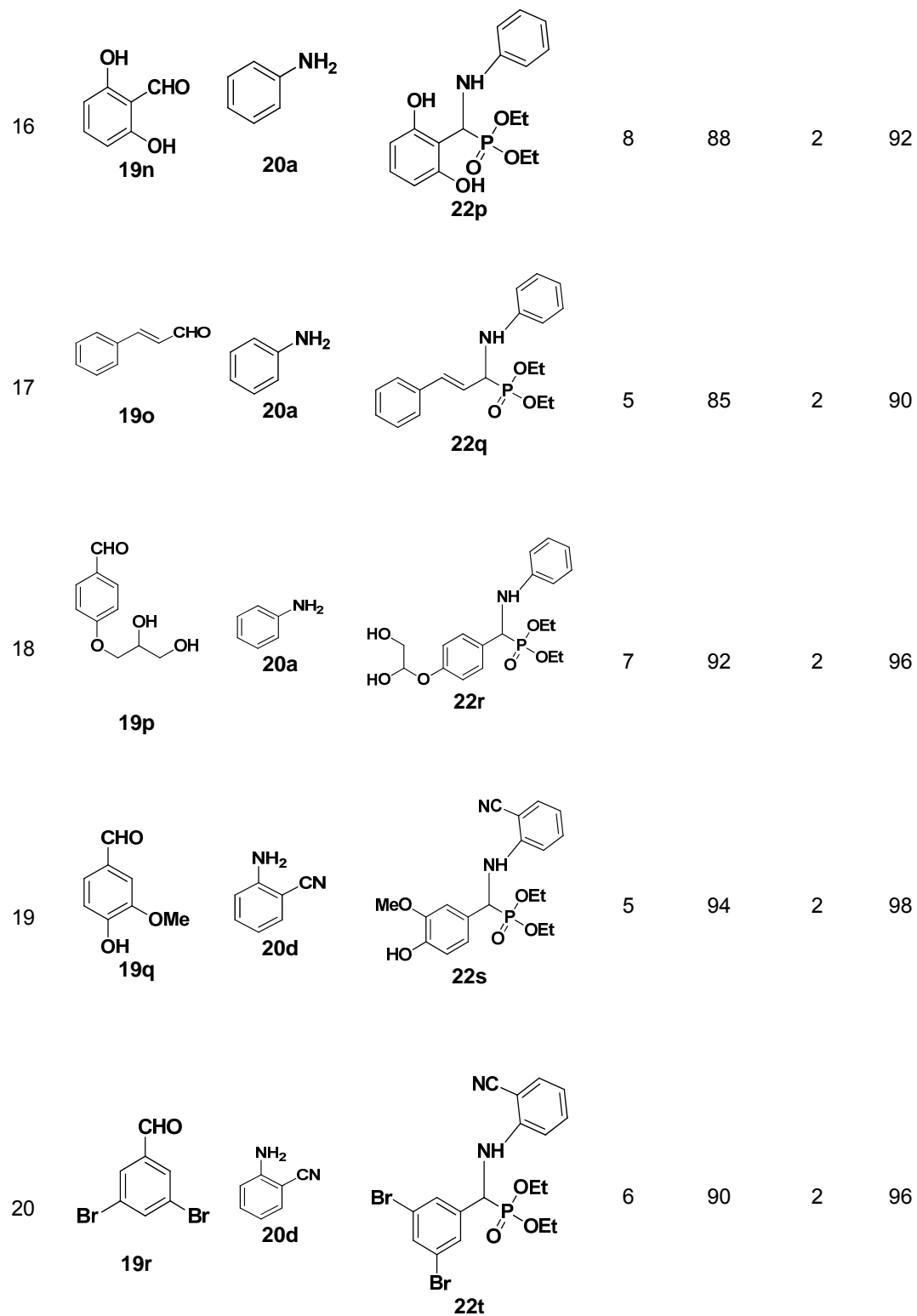


# Chapter 2

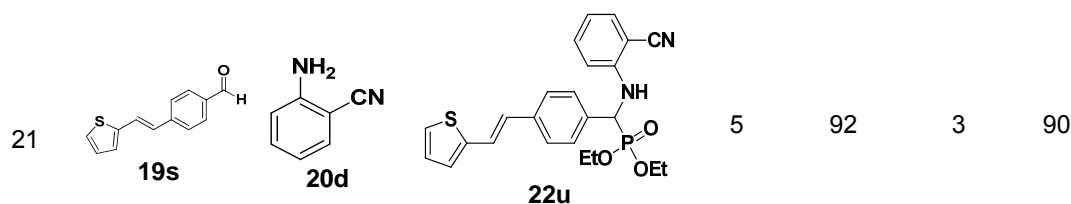




# Chapter 2



## Chapter 2



<sup>a</sup>Method A: Reaction mixtures stirred at room temperature.

<sup>b</sup>Method B: Reactions carried out under microwave irradiation (MWI).

\*Yields refer to those of pure isolated products fully characterized by its spectral data.

Higher reactivity of aromatic aldehydes than aliphatic aldehydes, leads good to excellent yields of corresponding  $\alpha$ -aminophosphonates. However, conjugated aldehydes resulted in low yields of products. The reaction was compatible with various functional groups such as methylenedioxy, methoxy ethers, hydroxyl, halides and olefinic groups. Electron-withdrawing groups at the *para*-position in the aldehyde ring resulted in higher yields while at the *meta*-position in lower yields. Electron-donating groups at the *para*-position in the aldehyde ring resulted in lower yields. Excellent yields were observed for substrates having halogen (entries 5, 13, 20) substituents. 1,4-conjugate addition was not Found in case of cinnamaldehyde (entry 17), *O*-Me group (entries 4, 10, 11, 15, 19) was remained intact and sterically hindered aldehyde (entry 16) was well tolerated. Also, different substituted amines 2-aminophenol (entry 8), 2-cyano aniline (entries 19, 20, 21) and benzylamine (entry 7) were tolerated during the course of reaction. However, longer reaction times were needed for various sterically hindered substrates and electron deficient aromatic amines. The present reaction worked well on all substrates. The formation of  $\alpha$ -aminophosphonates was confirmed by the presence of peak in  $^1\text{H}$  NMR at 4.67-5.66 ppm ( $^1J_{\text{PH}} = 23.1\text{-}26.1$  Hz) and in  $^{13}\text{C}$  NMR 51.2-55.8 ( $^1J_{\text{PC}} = 149.2\text{-}153.8$  Hz). This was further confirmed by the  $^{31}\text{P}$  NMR peak at 18.92-20.69 ppm.

$\alpha$ -Aminophosphonate **22t** was crystallized from methanol/DCM (1:9) and its single crystal X-ray analysis proved the structure (Figure 3).

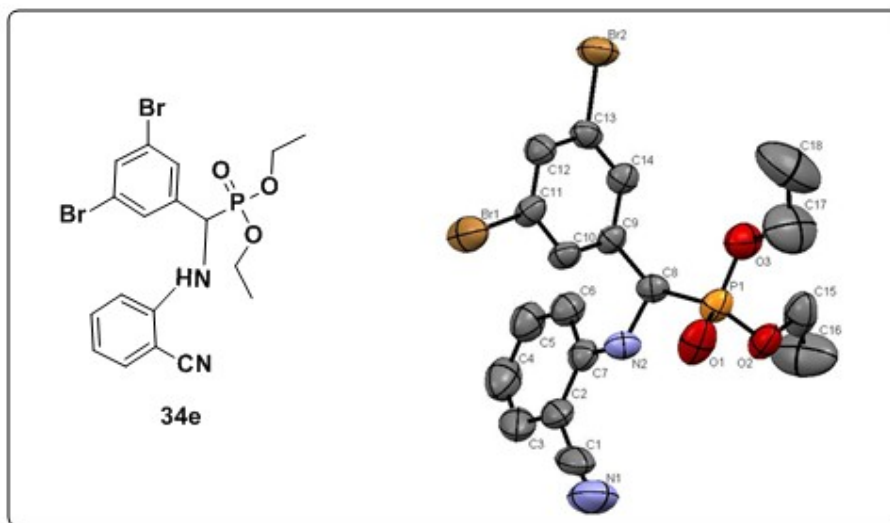
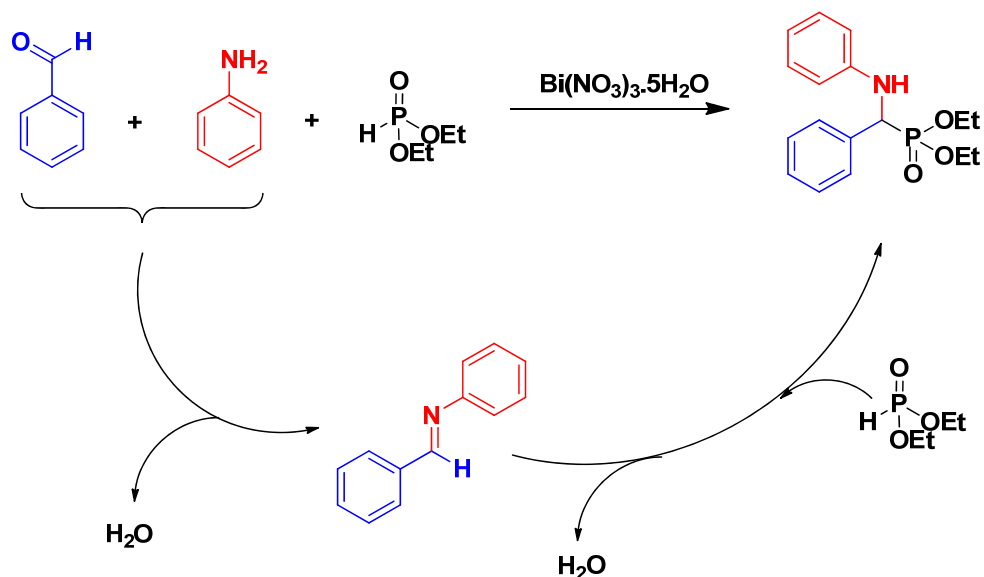


Figure 3. ORTEP diagram of  $\alpha$ -aminophosphonate derivative, **22t**.

## 2.4 Postulated mechanism

The formation of  $\alpha$ -aminophosphonates generally follows two different reaction pathways *i.e.* (i) formation of imine intermediate and nucleophilic attack of diethylphosphite or (ii) formation of hydroxyphosphonate and nucleophilic attack of phosphite yields the product. The synthesis of  $\alpha$ -aminophosphonates catalyzed by  $\text{Bi}(\text{NO}_3)_3 \cdot 5\text{H}_2\text{O}$  could be described by the first mechanistic pathway. Initially, imine formed which further reacts with diethylphosphite to furnish the desired product. Detailed mechanistic studies were done on the Kabachnik-Field's reaction and plausible mechanism is based on the observations by Cherkasov and Galkin using anilines and its substituted derivatives. A plausible mechanism for the formation of  $\alpha$ -aminophosphonates in one-pot catalyzed by  $\text{Bi}(\text{NO}_3)_3 \cdot 5\text{H}_2\text{O}$  is depicted in Scheme 9. The reaction was started with imine formation which was generated by the treatment of aldehyde and amine. Then the lone pair of phosphorus attacked on the imine intermediate generating the desired  $\alpha$ -aminophosphonates.



Scheme 9. Postulated mechanism for the synthesis of  $\alpha$ -aminophosphonates.

## 2.5 Conclusion

In summary, Bismuth (III) nitrate pentahydrate<sup>26</sup> was proved to be an efficient catalyst for three-component (3CR) one-pot reaction for the synthesis of  $\alpha$ -aminophosphonates. The advantages are such as (i) highly versatile and environmentally friendly catalyst, (ii) excellent yields (iii) solvent-free reaction condition, and (iv) the use of non-toxic reagent. This methodology provides better yields of products which will help in understanding the biological processes in detail. The present protocol is not only a potent method for the synthesis of biologically important class of compounds, but also an environmentally benign process.

## 2.6 Experimental

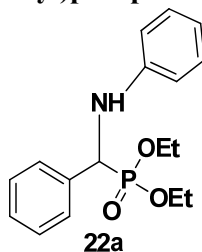
### 2.6.1 General procedures

#### Typical Experimental Procedure:

**Method A:** To a mixture of carbonyl compound (1 mmol), and amine (1 mmol), bismuth nitrate pentahydrate (10 mol %) was added and stirred at room temperature for 5 min and then slowly diethylphosphite (1 mmol) was added. The stirring of the reaction mixture was continued for the appropriate time (see Table 1) till the completion (TLC) of reaction. The reaction mixture was diluted with water and extracted with EtOAc. The EtOAc extract was washed with brine, dried (anhydrous  $\text{Na}_2\text{SO}_4$ ), evaporated to furnish crude product, which was purified by column chromatography (PE/Ea, 7:3) over silica gel to provide pure  $\alpha$ -aminophosphonates. All the products were characterized by spectral data.

**Method B:** To a mixture of carbonyl compound (1 mmol), amine (1 mmol), and diethylphosphite (1 mmol), bismuth nitrate (10 mol %) was added and the reaction mixture was irradiated with microwave (Kenstar Model No. OM-9918C; 2450 MHz, 2350 W) for the specified period of time in an open vessel. Work-up of the reaction was carried out as described in Method A.

#### Diethyl (phenyl(phenylamino)methyl)phosphonate (22a)



<b>Yield</b>	96%; colorless syrupy oil; $R_f = 0.20$ (PE/Ea, 8:2).
<b>Mol. Formula</b>	$\text{C}_{17}\text{H}_{22}\text{NO}_3\text{P}$
<b>IR</b> ( $\text{CHCl}_3$ )	$\nu_{\text{max}}$ ( $\text{cm}^{-1}$ ) = 3300, 1600, 1214.
<b><math>^1\text{H}</math> NMR</b> ( $\text{CDCl}_3$ , 200 MHz)	$\delta_{\text{H}}$ (ppm) = 7.49-7.06 (m, 7H), 6.72-.586 (m, 3H), 4.76 (d, $^1J_{\text{PH}} = 26.0$ Hz, 1H), 4.16-3.61 (m, 4H),

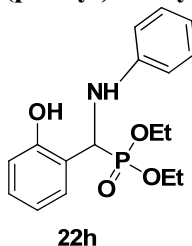
**$^{13}\text{C}$  NMR**  
( $\text{CDCl}_3$ , 50 MHz)

1.28 (t,  $J = 7.3$  Hz, 3H), 1.11 (t,  $J = 7.3$  Hz, 3H).  
 $\delta_{\text{C}}$  (ppm) = 146.8 (s, Ph), 146.6 (s, Ph), 136.3 (s, Ph), 129.6 (s, Ph), 128.2 (s, Ph), 118.8 (s, Ph), 114.2 (s, Ph), 63.7 (d,  $^2J_{\text{PC}} = 7.0$  Hz,  $-\text{OCH}_2\text{CH}_3$ ), 56.4 (d,  $^1J_{\text{PC}} = 150.0$  Hz,  $-\text{CHP}$ ), 16.8 (d,  $^3J_{\text{PC}} = 5.8$  Hz,  $-\text{OCH}_2\text{CH}_3$ ), 16.6 (d,  $^3J_{\text{PC}} = 5.8$  Hz,  $-\text{OCH}_2\text{CH}_3$ ).

**Elemental analysis**

Calcd for  $\text{C}_{17}\text{H}_{22}\text{NO}_3\text{P}$ : C, 63.94; H, 6.94; N, 4.39  
 Found: C, 63.89; H, 6.99; N, 4.45.

**Diethyl-(2-hydroxyphenylamino)(phenyl)methyl-phosphonate (22h)**



**Yield**

91%; colorless syrupy oil;  $R_f = 0.20$  (PE/EA, 6:4).

**Mol. Formula**

$\text{C}_{17}\text{H}_{22}\text{NO}_4\text{P}$

**IR** ( $\text{CHCl}_3$ )

$\nu_{\text{max}}$  ( $\text{cm}^{-1}$ ) = 3687, 3018, 2399, 1215, 757.

**$^1\text{H}$  NMR**

( $\text{CDCl}_3$ , 200 MHz)

$\delta_{\text{H}}$  (ppm) = 7.46-6.46 (m, 9H), 4.89 (d,  $^1J_{\text{PH}} = 26.0$  Hz, 1H), 4.33-3.61 (m, 4H), 1.30 (t,  $J = 7.0$  Hz, 3H), 1.10 (t,  $J = 7.0$  Hz, 3H).

**$^{13}\text{C}$  NMR**

( $\text{CDCl}_3$ , 50 MHz)

$\delta_{\text{C}}$  (ppm) = 145.2 (s, Ph), 135.6 (s, Ph), 134.7 (s, Ph), 128.4 (s, Ph), 128.4 (s, Ph), 128.1 (s, Ph), 127.8 (s, Ph), 127.7 (s, Ph), 119.7 (s, Ph), 118.1 (s, Ph), 114.3 (s, Ph), 111.8 (s, Ph), 64.2 (d,  $^2J_{\text{PC}} = 7.3$  Hz,  $-\text{OCH}_2\text{CH}_3$ ), 63.70 (d,  $^2J_{\text{PC}} = 7.0$  Hz,  $-\text{OCH}_2\text{CH}_3$ ), 55.8 (d,  $^1J_{\text{PC}} = 153.0$  Hz,  $-\text{CHP}$ ), 16.4 (d,  $^3J_{\text{PC}} = 5.5$  Hz,  $-\text{OCH}_2\text{CH}_3$ ), 16.0 (d,  $^3J_{\text{PC}} = 5.9$  Hz,  $-\text{OCH}_2\text{CH}_3$ ).

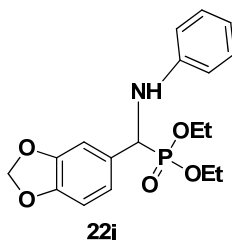
**Elemental analysis**

Calcd for  $\text{C}_{17}\text{H}_{22}\text{NO}_4\text{P}$ : C, 60.89; H, 6.61; N, 4.18

## Chapter 2

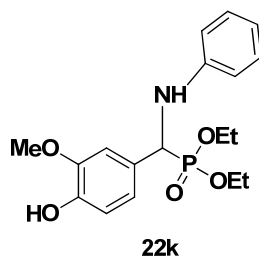
Found: C, 60.72; H, 6.58; N, 4.10.

### Diethylbenzo[d][1,3]dioxol-5-yl(phenylamino) methyl-phosphonate (22i)



<b>Yield</b>	98%; white solid; $R_f = 0.60$ (PE/EA, 7:3).
<b>Melting Point</b>	112-3°C
<b>Mol. Formula</b>	$C_{18}H_{22}NO_5P$
<b>IR</b> ( $CHCl_3$ )	$\nu_{max}$ ( $cm^{-1}$ ) = 3380, 3001, 2400, 1210.
<b><math>^1H</math> NMR</b> ( $CDCl_3$ , 200 MHz)	$\delta_H$ (ppm) = 7.16-6.57 (m, 8H), 5.94 (s, 2H), 4.72 (d, $^1J_{PH} = 23.1$ Hz, 1H), 4.17-3.70 (m, 4H), 1.30 (t, $J = 7.0$ Hz, 3H), 1.17 (t, $J = 7.0$ Hz, 3H).
<b><math>^{13}C</math> NMR</b> ( $CDCl_3$ , 50 MHz)	$\delta_C$ (ppm) = 146.9 (s, Ph), 146.8 (s, Ph), 146.4 (s, Ph), 146.1 (s, Ph), 145.4 (s, Ph), 128.9 (s, Ph), 127.1 (s, Ph), 127.0 (s, Ph), 120.8 (s, Ph), 120.7 (s, Ph), 114.4 (s, Ph), 113.7 (s, Ph), 110.2 (s, Ph), 63.3 (d, $^2J_{PC} = 7.0$ Hz, $-OCH_2CH_3$ ), 63.1 (d, $^2J_{PC} = 7.1$ Hz, $-OCH_2CH_3$ ), 55.7 (s, $-OCH_3$ ), 55.5 (d, $^1J_{PC} = 152.1$ Hz, $-CHP$ ), 16.2 (d, $^3J_{PC} = 5.8$ Hz, $-OCH_2CH_3$ ), 16.1 (d, $^3J_{PC} = 6.0$ Hz, $-OCH_2CH_3$ ).
<b>Elemental analysis</b>	Calcd for $C_{18}H_{22}NO_5P$ : C, 59.50; H, 6.10; N, 3.85 Found: C, 59.32; H, 6.05; N, 3.78.

### Diethyl-(4-hydroxy-3-methoxyphenyl) (phenylamino) methylphosphonate (22k)

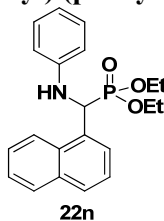


T. Kaur, *PhD thesis*, University of Pune, 2013

## Chapter 2

<b>Yield</b>	98%; white solid; $R_f = 0.30$ (PE/EA, 7:3).
<b>Mol. Formula</b>	$C_{18}H_{22}NO_5P$
<b>IR</b> ( $CHCl_3$ )	$\nu_{max} (cm^{-1}) = 3308, 3012, 2401, 1200.$
<b><math>^1H</math> NMR</b> ( $CDCl_3$ , 200 MHz)	$\delta_H$ (ppm) = 7.14-6.58 (m, 8H), 4.67 (d, $^1J_{PH} = 24.0$ Hz, 1H), 4.16-3.67 (m, 4H), 3.83 (s, 3H), 1.27 (t, $J = 7.0$ Hz, 3H), 1.13 (t, $J = 7.0$ Hz, 3H).
<b><math>^{13}C</math> NMR</b> ( $CDCl_3$ , 50 MHz)	$\delta_C$ (ppm) = 146.9 (s, Ph), 146.8 (s, Ph), 146.5 (s, Ph), 146.2 (s, Ph), 145.5 (s, Ph), 129.1 (s, Ph), 121.0 (s, Ph), 120.8 (s, Ph), 118.3 (s, Ph), 114.4 (s, Ph), 113.8 (s, Ph), 110.2 (s, Ph), 110.1 (s, Ph), 63.4 (d, $^2J_{PC} = 7.0$ Hz, $-OCH_2CH_3$ ), 63.2 (d, $^2J_{PC} = 7.3$ Hz, $-OCH_2CH_3$ ), 55.8 (s, $-OCH_3$ ), 55.7 (d, $^1J_{PC} = 152.0$ Hz, $-CHP$ ), 16.4 (d, $^3J_{PC} = 5.8$ Hz, $-OCH_2CH_3$ ), 16.2 (d, $^3J_{PC} = 5.8$ Hz, $-OCH_2CH_3$ ).
<b>Elemental analysis</b>	Calcd for $C_{18}H_{22}NO_5P$ : C, 59.17; H, 6.62; N, 3.83 Found: C, 59.05; H, 6.45; N, 3.78.

### Diethyl-(2-hydroxy-6-methoxyphenyl) (phenylamino) methylphosphonate (22n)



<b>Yield</b>	95%; white solid; $R_f = 0.20$ (PE/EA, 7:3).
<b>Melting Point</b>	110-12°C
<b>Mol. Formula</b>	$C_{21}H_{24}NO_3P$
<b>IR</b> ( $CHCl_3$ )	$\nu_{max} (cm^{-1}) = 3302, 3010, 1209.$
<b><math>^1H</math> NMR</b> ( $CDCl_3$ , 200 MHz)	$\delta_H$ (ppm) = 8.26 (d, $J = 8.3$ Hz, 1H), 7.91-7.76 (m, 3H), 7.66-7.39 (m, 3H), 7.08-7.00 (m, 2H), 6.68-6.53 (m, 3H), 5.66 (d, $^1J_{PH} = 24.1$ Hz, 1H), 4.26-4.12 (m, 2H), 3.79-3.67 (m, 1H), 3.26-3.14 (m,



**<sup>13</sup>C NMR**

(CDCl<sub>3</sub>, 50 MHz)

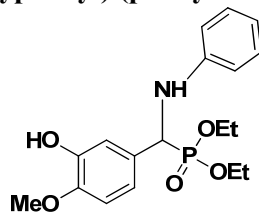
1H), 1.32 (t, *J* = 7.3 Hz, 3H), 0.72 (t, *J* = 7.0 Hz, 3H).

δ<sub>C</sub> (ppm) = 146.1 (s, Ph), 145.8 (s, Ph), 133.7 (s, Ph), 133.6 (s, Ph), 131.6 (s, Ph), 131.5 (s, Ph), 131.4 (s, Ph), 131.3 (s, Ph), 129.0 (s, Ph), 128.4 (s, Ph), 128.3 (s, Ph), 126.1 (s, Ph), 125.5 (s, Ph), 125.4 (s, Ph), 125.3 (s, Ph), 125.2 (s, Ph), 122.8 (s, Ph), 122.7 (s, Ph), 118.1 (s, Ph), 113.4 (s, Ph), 63.3 (d, <sup>2</sup>*J*<sub>PC</sub> = 7.3 Hz, -OCH<sub>2</sub>CH<sub>3</sub>), 63.1 (d, <sup>2</sup>*J*<sub>PC</sub> = 7.0 Hz, -OCH<sub>2</sub>CH<sub>3</sub>), 51.2 (d, <sup>1</sup>*J*<sub>PC</sub> = 152.6 Hz, -CHP), 16.3 (d, <sup>3</sup>*J*<sub>PC</sub> = 5.9 Hz, -OCH<sub>2</sub>CH<sub>3</sub>), 15.6 (d, <sup>3</sup>*J*<sub>PC</sub> = 5.9 Hz, -OCH<sub>2</sub>CH<sub>3</sub>).

**Elemental analysis**

Calcd for C<sub>21</sub>H<sub>24</sub>NO<sub>3</sub>P: C, 68.28; H, 6.55; N, 3.79  
Found: C, 68.20; H, 6.50; N, 3.72.

**Diethyl-(3-hydroxy-4-methoxyphenyl) (phenylamino) methylphosphonate (22o)**



**22o**

**Yield**

97%; colorless syrupy liquid; *R<sub>f</sub>* = 0.20 (PE/EA, 7:3).

**Mol. Formula**

C<sub>18</sub>H<sub>24</sub>NO<sub>5</sub>P

**IR (CHCl<sub>3</sub>)**

*v*<sub>max</sub> (cm<sup>-1</sup>) = 3300, 3005, 2402, 1218.

**<sup>1</sup>H NMR**

(CDCl<sub>3</sub>, 200 MHz)

δ<sub>H</sub> (ppm) = 7.12-6.57 (m, 8H), 4.66 (d, <sup>1</sup>*J*<sub>PH</sub> = 24.0 Hz, 1H), 4.15-3.68 (m, 4H), 3.79 (s, 3H), 1.26 (t, *J* = 7.0 Hz, 3H), 1.12 (t, *J* = 7.0 Hz, 3H).

**<sup>13</sup>C NMR**

(CDCl<sub>3</sub>, 50 MHz)

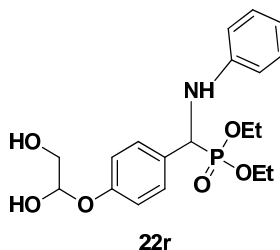
δ<sub>C</sub> (ppm) = 146.7 (s, Ph), 146.3 (s, Ph), 146.0 (s, Ph), 128.8 (s, Ph), 128.2 (s, Ph), 119.3 (s, Ph), 119.1 (s, Ph), 118.0 (s, Ph), 114.3 (s, Ph), 113.7 (s,

Ph), 110.8 (s, Ph), 63.3 (d,  $^2J_{PC} = 7.0$  Hz, -OCH<sub>2</sub>CH<sub>3</sub>), 55.6 (s, -OCH<sub>3</sub>), 55.2 (d,  $^1J_{PC} = 153.8$  Hz, -CHP), 16.1 (d,  $^3J_{PC} = 5.5$  Hz, -OCH<sub>2</sub>CH<sub>3</sub>), 15.9 (d,  $^3J_{PC} = 5.8$  Hz, -OCH<sub>2</sub>CH<sub>3</sub>).

**Elemental analysis**

Calcd for C<sub>18</sub>H<sub>24</sub>NO<sub>5</sub>P: C, 59.17; H, 6.62; N, 3.83  
 Found: C, 59.12; H, 6.48; N, 3.78.

**Diethyl-[4-(2,3-dihydroxypropoxy) phenyl] (phenyl-amino)methylphosphonate (22r)**



**Yield**

96%; colorless syrupy liquid;  $R_f = 0.40$  (PE/EA, 1:9).

**Mol. Formula**

C<sub>20</sub>H<sub>28</sub>NO<sub>6</sub>P

**IR (CHCl<sub>3</sub>)**

$\nu_{\max}$  (cm<sup>-1</sup>) = 3302, 3020, 2389, 1219.

**<sup>1</sup>H NMR**

(CDCl<sub>3</sub>, 200 MHz)

$\delta_H$  (ppm) = 7.37-6.55 (m, 9H), 4.70 (d,  $^1J_{PH} = 25.6$  Hz, 1H), 4.13-3.62 (m, 8H), 1.25 (t,  $J = 7.0$  Hz, 3H), 1.11 (t,  $J = 6.8$  Hz, 3H).

**<sup>13</sup>C NMR**

(CDCl<sub>3</sub>, 50 MHz)

$\delta_C$  (ppm) = 158.3 (s, Ph), 158.2 (s, Ph), 146.4 (s, Ph), 146.1 (s, Ph), 129.1 (s, Ph), 129.0 (s, Ph), 127.9 (s, Ph), 120.19 (s, Ph), 118.4 (s, Ph), 114.7 (s, Ph), 114.6 (s, Ph), 113.8 (s, Ph), 70.3 (s, -CHOH), 69.0 (s, -CH<sub>2</sub>OH), 63.6 (d,  $^2J_{PC} = 7.3$  Hz, -OCH<sub>2</sub>CH<sub>3</sub>), 63.4 (d,  $^2J_{PC} = 7.3$  Hz, -OCH<sub>2</sub>CH<sub>3</sub>), 55.2 (d,  $^1J_{PC} = 151.0$  Hz, -CHP), 16.3 (d,  $^3J_{PC} = 5.5$  Hz, -OCH<sub>2</sub>CH<sub>3</sub>), 16.2 (d,  $^3J_{PC} = 5.5$  Hz, -OCH<sub>2</sub>CH<sub>3</sub>).

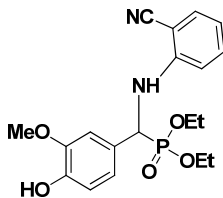
**Elemental analysis**

Calcd for C<sub>20</sub>H<sub>28</sub>NO<sub>6</sub>P: C, 58.67; H, 6.89; N, 3.42

## Chapter 2

Found: C, 58.50; H, 6.78; N, 3.36.

### Diethyl(((2-cyanophenyl)amino)(4-hydroxy-3-methoxyphenyl) methyl) phosphonate (22s)



22s

<b>Yield</b>	98%; white solid; $R_f$ = 0.30 (PE/EA, 7:3).
<b>Melting Point</b>	116°C
<b>Mol. Formula</b>	$C_{19}H_{23}N_2O_5P$
<b>IR</b> ( $CHCl_3$ )	$\nu_{max}$ ( $cm^{-1}$ ) = 3396, 2984, 2931, 2400, 2213, 1604, 1215.
<b><math>^1H</math> NMR</b> ( $CDCl_3$ , 200 MHz)	$\delta_H$ (ppm) = 7.49 (d, $J$ = 7.6 Hz, 1H), 7.36-7.33 (m, 1H), 7.07 (s, 1H), 7.01-6.93 (m, 2H), 6.79 (t, $J$ = 7.3 Hz, 3H), 6.63 (d, $J$ = 8.2 Hz, 1H), 4.81 (d, $^1J_{PH}$ = 23.5 Hz, 1H), 4.21-3.95 (m, 4H), 3.94 (s, 3H), 1.35 (t, $J$ = 7.0 Hz, 3H), 1.30 (t, $J$ = 7.0 Hz, 3H).
<b><math>^{13}C</math> NMR</b> ( $CDCl_3$ , 50 MHz)	$\delta_C$ (ppm) = 148.8 (s, Ph), 148.7 (s, Ph), 147.0 (s, Ph), 145.8 (s, Ph), 134.0 (s, Ph), 132.7 (s, Ph), 126.0 (s, Ph), 120.7 (s, Ph), 120.6 (s, Ph), 118.0 (s, Ph), 117.3 (s, Ph), 114.6 (s, Ph), 112.4 (s, Ph), 112.3 (s, Ph), 109.8 (s, Ph), 97.4 (s, Ph), 63.6 (d, $^2J_{PC}$ = 7.3 Hz, $-OCH_2CH_3$ ), 63.4 (d, $^2J_{PC}$ = 6.8 Hz, $-OCH_2CH_3$ ), 55.9 (s, $-OCH_3$ ), 55.6 (d, $^1J_{PC}$ = 152.4 Hz, $-CHP$ ), 16.3 (d, $^3J_{PC}$ = 5.5 Hz, $-OCH_2CH_3$ ), 16.2 (d, $^3J_{PC}$ = 5.7 Hz, $-OCH_2CH_3$ ).
<b><math>^{31}P</math> NMR</b> ( $CDCl_3$ , 200 MHz)	$\delta_P$ (ppm) = 20.69.
<b>Elemental analysis</b>	Calcd for $C_{19}H_{23}N_2O_5P$ : C, 58.46; H, 5.94; N,

## Chapter 2

7.18

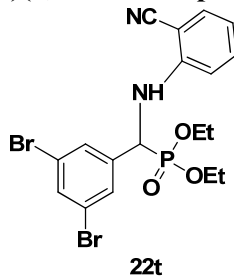
Found: C, 58.40; H, 5.87; N, 7.10.

### HRMS

Calcd for  $C_{19}H_{23}N_2O_5P$ : 413.1242 (M+Na)<sup>+</sup>

Found: 413.1240.

### Diethyl (((2-cyanophenyl)amino)(3, 5-dibromophenyl)methyl)phosphonate (22t)



### Yield

96%; white solid;  $R_f$  = 0.40 (PE/EA, 7:3).

### Melting Point

124°C

### Mol. Formula

$C_{18}H_{19}Br_2N_2O_3P$

### IR (CHCl<sub>3</sub>)

$\nu_{\max}$  (cm<sup>-1</sup>) = 3843, 3619, 1922, 2215, 1740, 1693, 1646, 1246, 1214.

### <sup>1</sup>H NMR

(CDCl<sub>3</sub>, 200 MHz)

$\delta_H$  (ppm) = 7.67-7.66 (m, 1H), 7.60 (s, 2H), 7.51 (d,  $J$  = 6.1 Hz, 1H), 7.37-7.32 (m, 1H), 6.84 (t,  $J$  = 7.3 Hz, 1H), 6.46 (d,  $J$  = 8.5 Hz, 1H), 5.52-5.49 (m, 1H), 4.76 (d,  $^1J_{PH}$  = 24.7 Hz, 1H), 4.23-4.06 (m, 4H), 1.36 (t,  $J$  = 7.0 Hz, 3H), 1.34 (t,  $J$  = 7.0 Hz, 3H).

### <sup>13</sup>C NMR

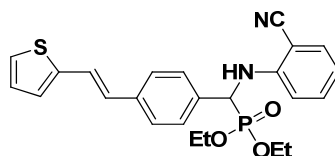
(CDCl<sub>3</sub>, 50 MHz)

$\delta_C$  (ppm) = 148.1 (s, Ph), 148.0 (s, Ph), 139.3 (s, Ph), 139.2 (s, Ph), 134.3 (s, Ph), 134.1 (s, Ph), 134.0 (s, Ph), 133.0 (s, Ph), 129.2 (s, Ph), 129.1 (s, Ph), 123.4 (s, Ph), 123.3 (s, Ph), 118.6 (s, Ph), 117.0 (s, Ph), 112.0 (s, Ph), 97.8 (s, Ph), 64.0 (d,  $^2J_{PC}$  = 7.5 Hz, -OCH<sub>2</sub>CH<sub>3</sub>), 63.7 (d,  $^2J_{PC}$  = 7.0 Hz, -OCH<sub>2</sub>CH<sub>3</sub>), 55.2 (d,  $^1J_{PC}$  = 149.2 Hz, -CHP), 16.4 (d,  $^3J_{PC}$  = 5.7 Hz, -OCH<sub>2</sub>CH<sub>3</sub>), 16.2 (d,  $^3J_{PC}$  = 5.9 Hz, -OCH<sub>2</sub>CH<sub>3</sub>).

## Chapter 2

<b><math>^{31}\text{P}</math> NMR</b> ( $\text{CDCl}_3$ , 200 MHz)	$\delta_{\text{P}}$ (ppm) = 18.92.
<b>Elemental analysis</b>	Calcd for $\text{C}_{18}\text{H}_{19}\text{Br}_2\text{N}_2\text{O}_3\text{P}$ : C, 43.05; H, 3.81; N, 5.58 Found: C, 42.98; H, 3.89; N, 5.51.
<b>HRMS (ESI)</b>	Calcd for $\text{C}_{18}\text{H}_{19}\text{Br}_2\text{N}_2\text{O}_3\text{P}$ : 522.9398 ( $\text{M}+\text{Na}$ ) <sup>+</sup> Found: 522.9395.

**(*E*)-Diethyl(((2-cyanophenyl)amino)(4-(2-(thiophen-2-yl)vinyl)phenyl) methyl) phosphate (22u)**



<b>Yield</b>	90%; colorless syrupy liquid; $R_f$ = 0.30 (PE/EA, 7:3).
<b>Mol. Formula</b>	$\text{C}_{24}\text{H}_{25}\text{N}_2\text{O}_3\text{PS}$
<b>IR</b> ( $\text{CHCl}_3$ )	$\nu_{\text{max}}$ ( $\text{cm}^{-1}$ ) = 3012, 2923, 2843, 2214, 1740, 1693, 1604, 1248, 1214, 1178, 1078.
<b><math>^1\text{H}</math> NMR</b> ( $\text{CDCl}_3$ , 200 MHz)	$\delta_{\text{H}}$ (ppm) = 7.22-7.19 (m, 5H), 7.09-6.96 (m, 3H), 6.86-6.76 (m, 2H), 6.68 (d, $J$ = 16 Hz, 1H), 6.50 (t, $J$ = 7.8 Hz, 1H), 6.30 (d, $J$ = 8.2 Hz, 1H), 5.36 (d, $J$ = 16.9 Hz, 1H), 4.65 (d, $^1J_{\text{PH}}$ = 24.3 Hz, 1H), 3.92-3.72 (m, 4H), 1.08 (t, $J$ = 7.3 Hz, 3H), 1.03 (t, $J$ = 6.9 Hz, 3H).
<b><math>^{13}\text{C}</math> NMR</b> ( $\text{CDCl}_3$ , 50 MHz)	$\delta_{\text{C}}$ (ppm) = 148.4 (s, Ph), 148.3 (s, Ph), 142.3 (s, Ph), 136.8 (s, Ph), 136.7 (s, Ph), 133.9 (s, Ph), 133.6 (s, Ph), 132.6 (s, Ph), 127.7 (s, Ph), 127.6 (s, Ph), 127.4 (s, Ph), 127.3 (s, Ph), 127.1 (s, Ph), 126.4 (s, Ph), 126.2 (s, Ph), 124.4 (s, Ph), 122.1 (s, Ph), 117.8 (s, Ph), 117.1 (s, Ph), 111.9 (s, Ph), 97.1 (s, Ph), 63.4 (d, $^2J_{\text{PC}}$ = 7.7 Hz, $-\text{OCH}_2\text{CH}_3$ ),

63.2 (d,  $^2J_{PC} = 6.7$  Hz, -OCH<sub>2</sub>CH<sub>3</sub>), 55.3 (d,  $^1J_{PC} = 150.5$  Hz, -CHP), 16.1 (d,  $^3J_{PC} = 4.8$  Hz, -OCH<sub>2</sub>CH<sub>3</sub>), 16.0 (d,  $^3J_{PC} = 4.8$  Hz, -OCH<sub>2</sub>CH<sub>3</sub>).

### Elemental analysis

Calcd for C<sub>24</sub>H<sub>25</sub>N<sub>2</sub>O<sub>3</sub>PS:C, 63.7; H, 5.57; N, 6.19  
Found: C, 62.68; H, 5.62; N, 6.26.

---

### X-ray Crystal Structure

X-ray diffraction data for all the crystallized compounds were collected at  $T = 296$  K, on SMART APEX CCD Single Crystal X-ray diffractometer using Mo-K $\alpha$  radiation ( $\lambda = 0.7107$  Å) to a maximum  $\theta$  range of  $25.00^\circ$ . Crystal to detector distance was 6.05 cm, 512 x 512 pixels / frame and other conditions used are oscillation / frame ( $-0.3^\circ$ ), maximum detector swing angle ( $-30.0^\circ$ ), beam center (260.2, 252.5) and in plane spot width (1.24). SAINT integration and SADABS correction were also applied. The structures were solved by direct methods using SHELXTL. All the data were corrected for Lorentzian, polarisation and absorption effects. SHELX-97 (ShelxTL) was used for structure solution and full matrix least squares refinement on F2. Hydrogen atoms were included in the refinement as per the riding model. The refinements were carried out using SHELXL-97.

Single crystals of the compound were found to grow best in solution mixture of ethanol and dichloromethane by slow evaporation. Colorless needle like crystal of approximate size 0.13 x 0.05 x 0.03 mm, was used for data collection. Multirun data acquisition, total scans (3), total frames (1818), exposure / frame (15.0 sec),  $\theta$  range ( $1.80$  to  $28.56^\circ$ ) and completeness to  $\theta$  of  $28.56^\circ$  (94%) were registered. The compound has molecular formula C<sub>18</sub> H<sub>19</sub> Br<sub>2</sub> N<sub>2</sub> O<sub>3</sub> and molecular weight of 502.14. Crystals belong to Monoclinic system with P21/c space group with unit cell dimensions as  $a = 16.518$  (12),  $b = 12.174$  (9),  $c = 10.948$  (8) Å. Other parameters like volume 2081(3) Å<sup>3</sup>,  $Z = 4$ ,  $D_c = 1.603$  g/cc, absorption coefficient  $\mu$  (Mo-K $\alpha$ ) =

## Chapter 2

3.991 mm<sup>-1</sup> were also recorded. 11542 reflections measured of which 2874 are unique. The final R indices [ $I > 2\sigma(I)$ ] are R1 (0.0493) and wR2 (0.1332).

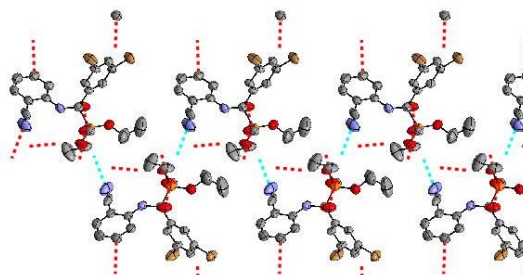
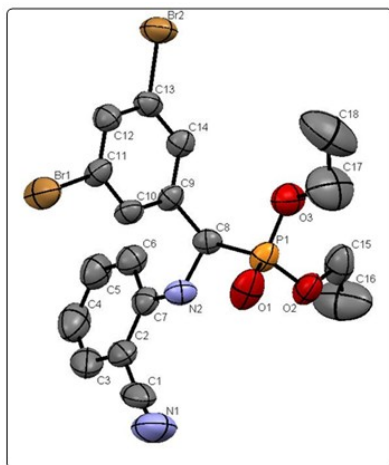


**Table 2.** Crystal data and structure refinement for compound **22t**.

Empirical formula	C <sub>18</sub> H <sub>19</sub> Br <sub>2</sub> N <sub>2</sub> O <sub>3</sub> P	
Formula weight	502.14	
Temperature	296(2) K	
Wavelength	0.71073 Å	
Crystal system	Monoclinic	
Space group	P21/c	
Unit cell dimensions	a = 16.518(12) Å	α = 90°
	b = 12.174(9) Å	β = 109.044 (16)°
	c = 10.948(8) Å	γ = 90°
Volume	2081(3) Å <sup>3</sup>	
Z	4	
Density (Calcd)	1.603 Mg/m <sup>3</sup>	
Absorption coefficient	3.991 mm <sup>-1</sup>	
F(000)	1000	
Crystal size	0.13 x 0.05 x 0.03 mm	
Theta range for data collection	1.30 to 28.56°	
Index ranges	-22 ≤ h ≤ 22, -14 ≤ k ≤ 16, -11 ≤ l ≤ 14	
Reflections collected	13963	
Independent reflections	4991 [R(int) = 0.0673]	

## Chapter 2

---

---

Completeness to theta = 28.56°	94.0%
Absorption correction	Semi-empirical from equivalents
Refinement method	Full-matrix least-squares on F <sup>2</sup>
Data / restraints / parameters	4991/0/237
Goodness-of-fit on F <sup>2</sup>	0.843
Final R indices [I>2sigma(I)]	R1 = 0.0493, wR2 = 0.1332
R indices (all data)	R1 = 0.1203, wR2 = 0.1805
Largest diff. peak and hole	0.497 and -0.850 e.Å <sup>-3</sup>

---



### 2.7 References

1. (a) Giannousis, P. P.; Bartlett, P. *J. Med. Chem.* **1987**, *30*, 1603; (b) Allen, M. C.; Fuhrer, W.; Tuck, B.; Wade, R.; Wood, J. M. *J. Med. Chem.* **1989**, *32*, 1652.
2. (a) Kafarski, P.; Leczak, B. *Phosphorus Sulfur Silicon Relat. Elem.* **1991**, *63*, 193; (b) R. Hildebrand. *The role of Phosphonates in Living system*; CRC Press: Boca Raton, **1983**.
3. (a) Atherton, F. R.; Hassal, C. H.; Lambert, R. W. *J. Med. Chem.* **1986**, *29*, 29; (b) Allen, J. G.; Atherton, F. R.; Hall, M. J.; Hassal, C. H.; Lambert, R. W.; Nisbet, L. J.; Ringrose, P. S. *Antimicrob. Agents Chemother.* **1979**, *15*, 684.
4. (a) Hirschmann, R.; Smith III, A. B.; Taylor, C. M.; Benkovic, P. A.; Taylor, S. D.; Yager, K. M.; Sprengler, P. A.; Venkovic, S. J. *Science* **1994**, *265*, 234; (b) Smith III, A. B.; Taylor, C. M.; Venkovic, S. J.; Hirschmann, R. *Tetrahedron Lett.* **1994**, *37*, 6854.
5. Kolio D. Troev, 'Chemistry and Application of H-Phosphonates' Elsevier press, The Netherlands, 1<sup>st</sup> edition, 2006, 336.
6. Maruyama, H. B.; Arisawa, M.; Sawada, T. *Antimicrob. Agents Chemother.* **1979**, *16*, 444.
7. Merino, P.; Marqués-López, E.; Herrera, R. P. *Adv. Syn. Cat.* **2008**, *350*, 1195.
8. Mohan, R. *Nature Chem.* **2010**, *2*, 336.
9. (a) Eash, K.; Pulia, M.; Wieland, L.; Mohan, R. S. *J. Org. Chem.* **2000**, *65*, 8399; (b) Srivastava, N.; Banik, B. K. *J. Org. Chem.* **2003**, *68*, 2109; (c) Aggen, D. H.; Arnold, J. N.; Hayes, P. D.; Smoter, N.; Mohan, R. S. *Tetrahedron* **2004**, *60*, 3675.
10. Alagiri, K.; Devadig, P.; Prabhu, K. R. *Tetrahedron Lett.* **2012**, *53*, 1456.
11. Kadyrov, R.; Holz, J.; Schäffner, B.; Zayas, O.; Almena, J.; Börner, A. *Tetrahedron: Asymmetry* **2008**, *19*, 1189.
12. Kobayashi, S.; Kiyohara, H.; Nakamura, Y.; Matsubara, R. *J. Am. Chem. Soc.* **2004**, *126*, 6558.
13. Boukallaba, K.; Elachqar, A.; El Hallaoui, A.; Alami, A.; El Hajji, S.; Labriti, B.; Atmani, A.; El Bali, B.; Lachkar, M.; Allouchi, H.; Martinez, J.; Rolland, V. *Phosphorus Sulfur Silicon Relat. Elem.* **2007**, *182*, 1045.

T. Kaur, *PhD thesis*, University of Pune, **2013**

## Chapter 2

---

14. Kaboudin, B.; Jafari, E. *Synlett* **2008**, 2008, 1837; (b) Kabachnik, M.; Minaeva, L.; Beletskaya, I. *Synthesis* **2009**, 2009, 2357.
15. (a) Petrov, K. A.; Chauzov, V. A.; Erokhina, T. S. *Usp. Khim.* **1974**, 43, 2045; *Chem. Abstr.* **1975**, 82, 43486. (b) Kirby, A. J.; Warren, S. G. *The Organic Chemistry of Phosphorus*; Elsevier: Amsterdam, London, New York, 1967.
16. Reddy, B. V. S.; Raj, K. S.; Reddy, K. B.; Prasad, A. R. *Synthesis* **2001**, 2277.
17. (a) Qian, C.; Huang, T. *J. Org. Chem.* **1998**, 63, 4125; (b) Lee, S.; Park, J. H.; Lee, J. K.; Kang, J. *Chem. Commun.* **2001**, 1698.
18. Ranu, B. C.; Hajra, A.; Jana, U. *Org. Lett.* **1999**, 1, 1141.
19. Chandrasekhar, S.; Prakash, S. J.; Jagadeshwar, V.; Narsihmulu, C. *Tetrahedron Lett.* **2001**, 42, 5561.
20. Manabe, K.; Kobayashi, S. *Chem. Commun.* **2000**, 669.
21. Paraskar, A. S.; Sudalai, A. *Arkivoc* **2006**, 2006, 183.
22. Kaboudin, B.; Rahmani, A. *Synthesis* **2003**, 2705.
23. Sultana, S. S.; Saritha, B.; Prakash, S. J. *Synlett* **2001**, 505.
24. Kaboudin, B. *Tetrahedron Lett.* **2003**, 44, 1051.
25. Zhan, Z.; Li, J. *Synthetic Commun.* **2005**, 35, 2501.
26. Bhattacharya, A. K.; Kaur, T. *Synlett* **2007**, 745.

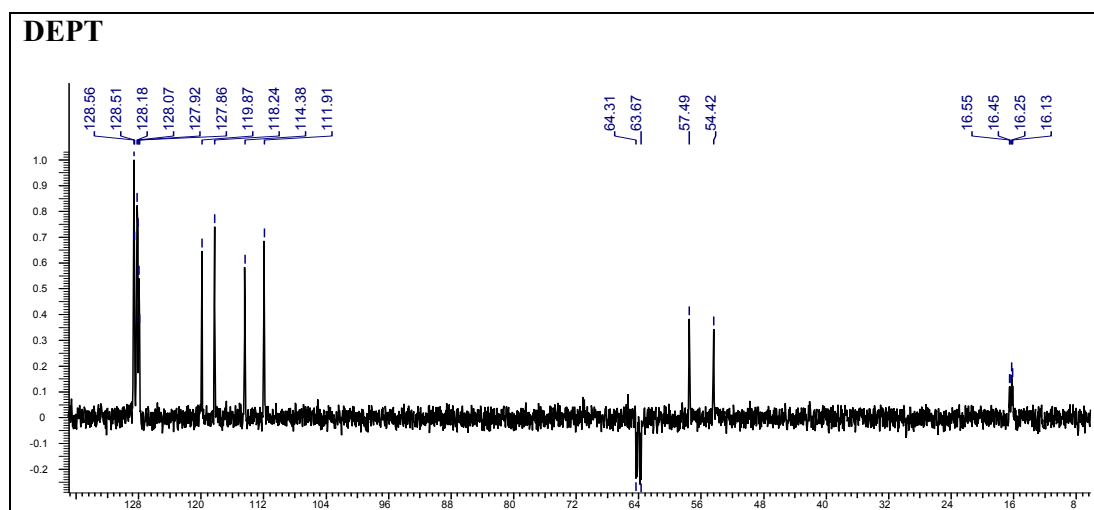
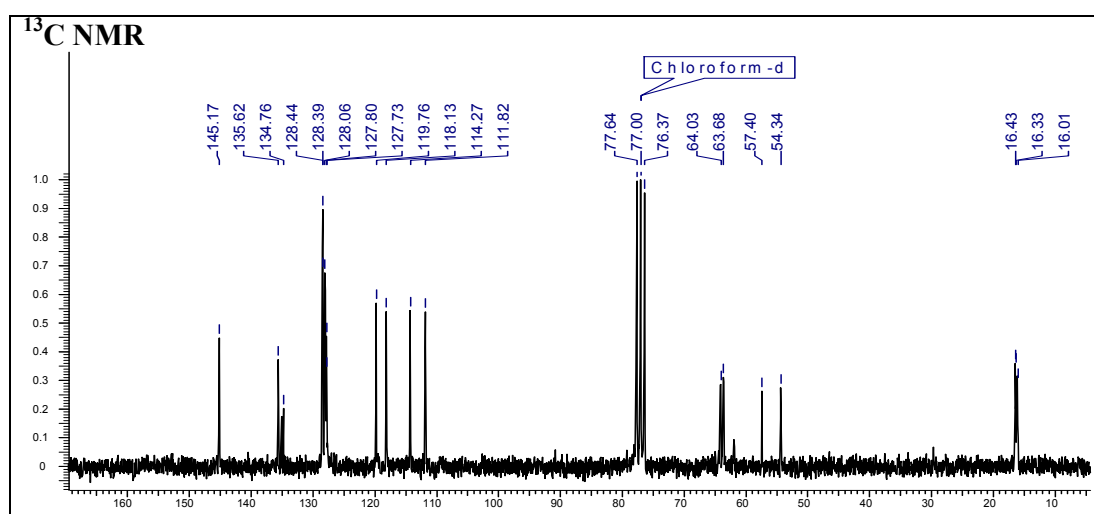
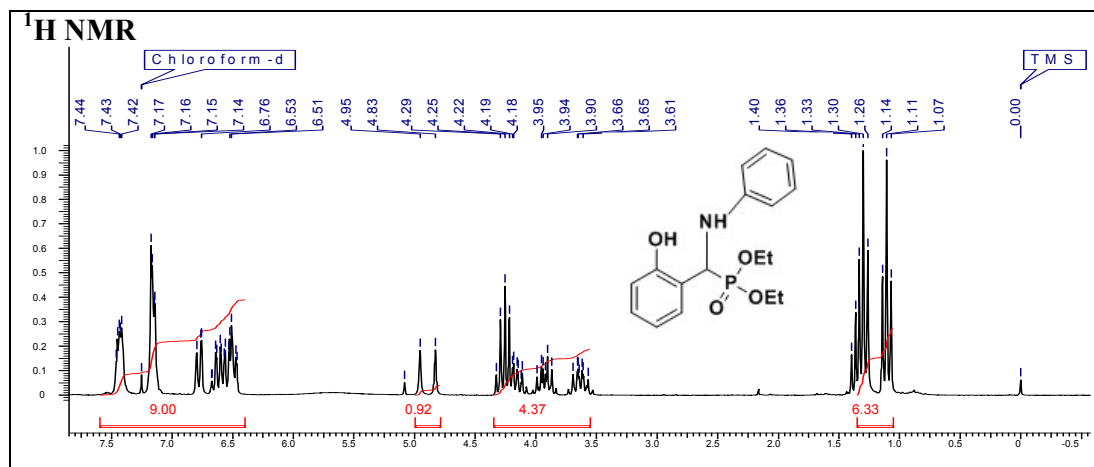
## Chapter 2

---

### 2.8 Appendix E: Characterization data of synthesized compounds

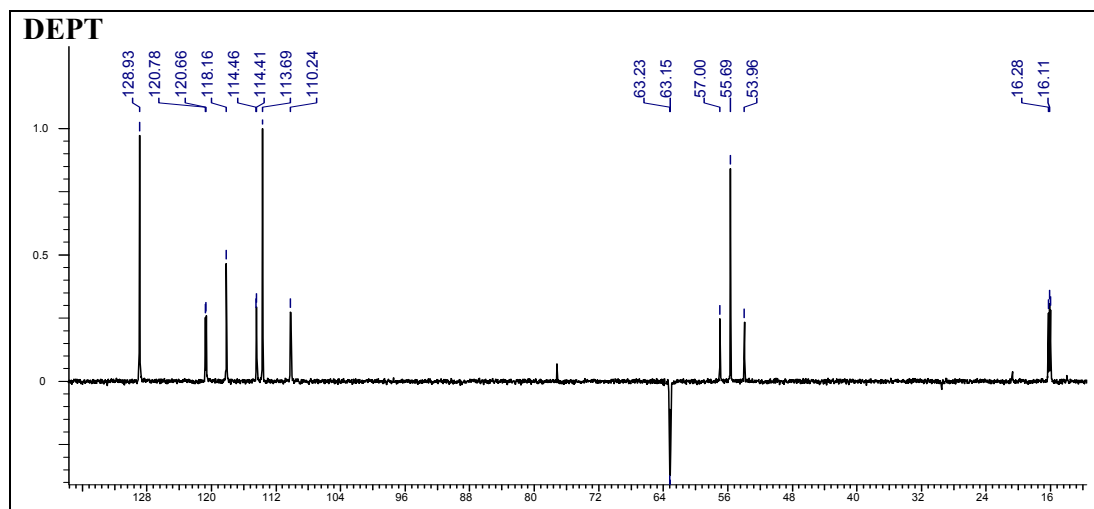
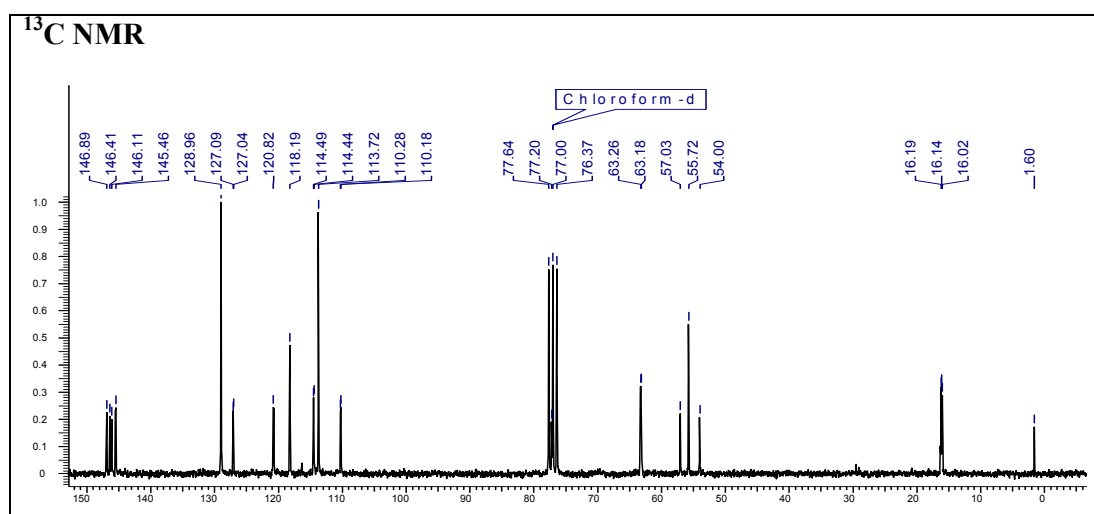
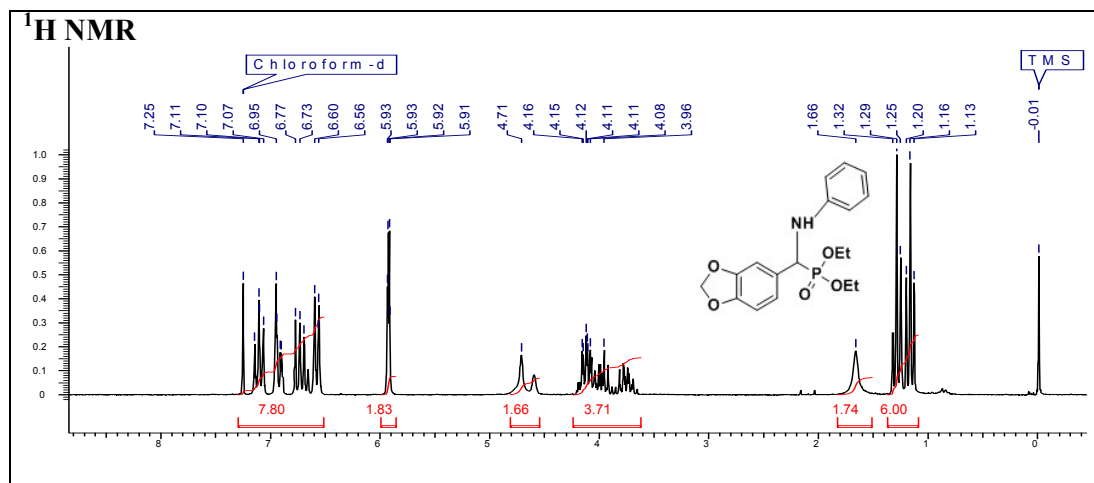
Compound	Description	Page No.
Compound <b>22h</b>	$^1\text{H}$ NMR, $^{13}\text{C}$ NMR, DEPT-NMR	211
Compound <b>22i</b>	$^1\text{H}$ NMR, $^{13}\text{C}$ NMR, DEPT-NMR	212
Compound <b>22k</b>	$^1\text{H}$ NMR, $^{13}\text{C}$ NMR, DEPT-NMR	213
Compound <b>22n</b>	$^1\text{H}$ NMR, $^{13}\text{C}$ NMR, DEPT-NMR	214
Compound <b>22s</b>	$^1\text{H}$ NMR, $^{13}\text{C}$ NMR, DEPT-NMR, FT-IR, $^{31}\text{P}$ NMR, HR-MS	215-217
Compound <b>22t</b>	$^1\text{H}$ NMR, $^{13}\text{C}$ NMR, DEPT-NMR, FT-IR, $^{31}\text{P}$ NMR, HR-MS	218-220
Compound <b>22t</b>	$^1\text{H}$ NMR, $^{13}\text{C}$ NMR, DEPT-NMR	221

# Chapter 2



**Diethyl-(2-hydroxyphenylamino)(phenyl)methyl-phosphonate (22h)**

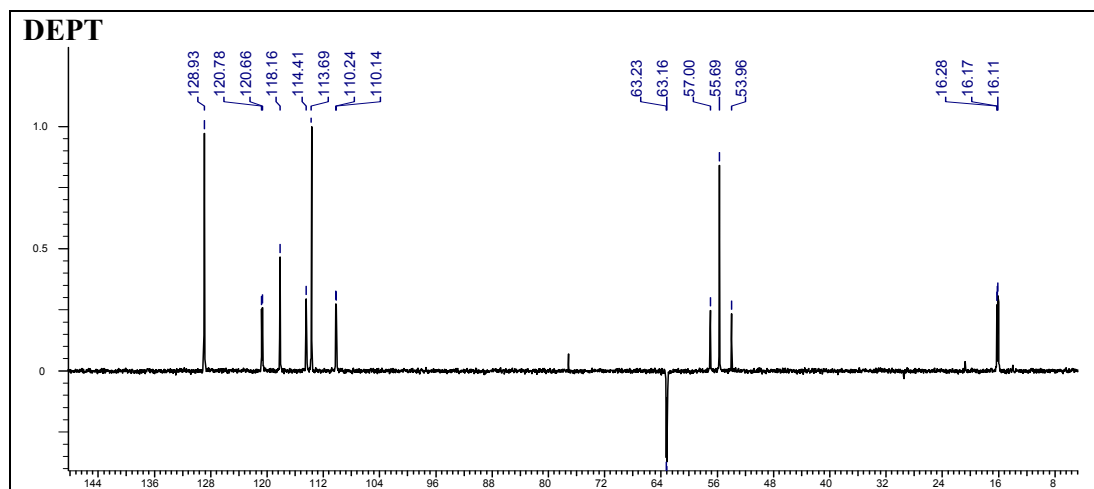
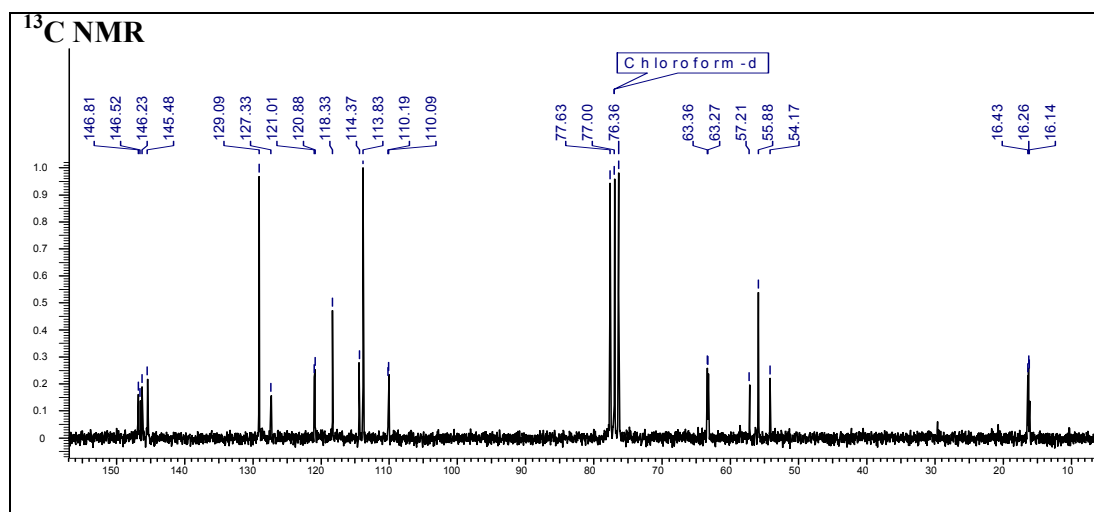
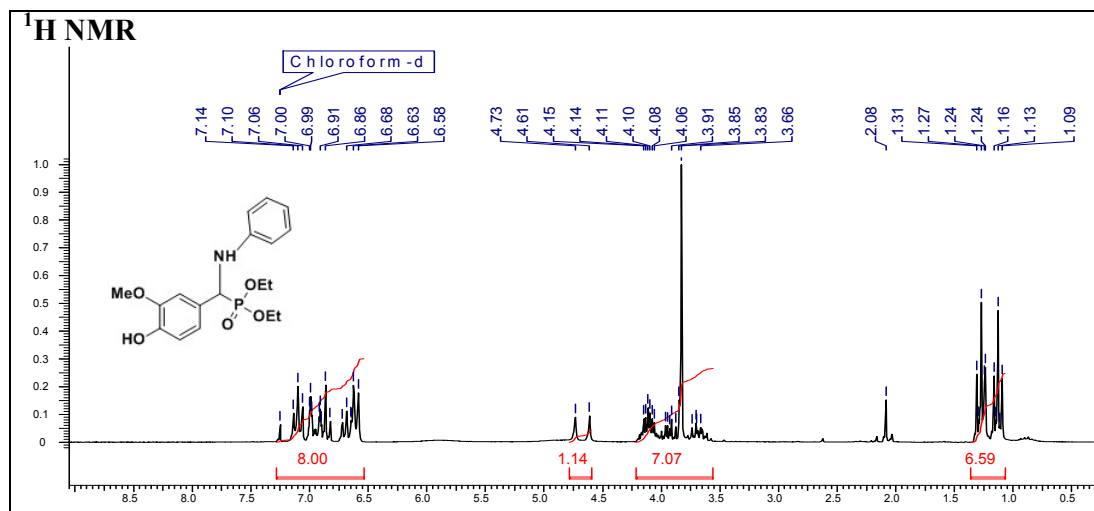
# Chapter 2



**Diethylbenzo[d][1,3]dioxol-5-yl(phenylamino)methyl-phosphonate (22i)**

T. Kaur, *PhD thesis*, University of Pune, 2013

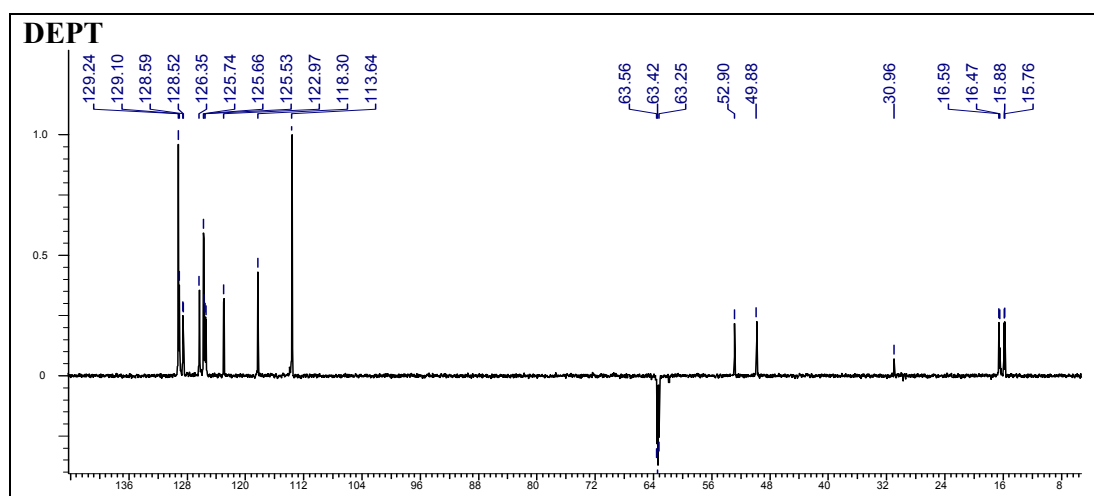
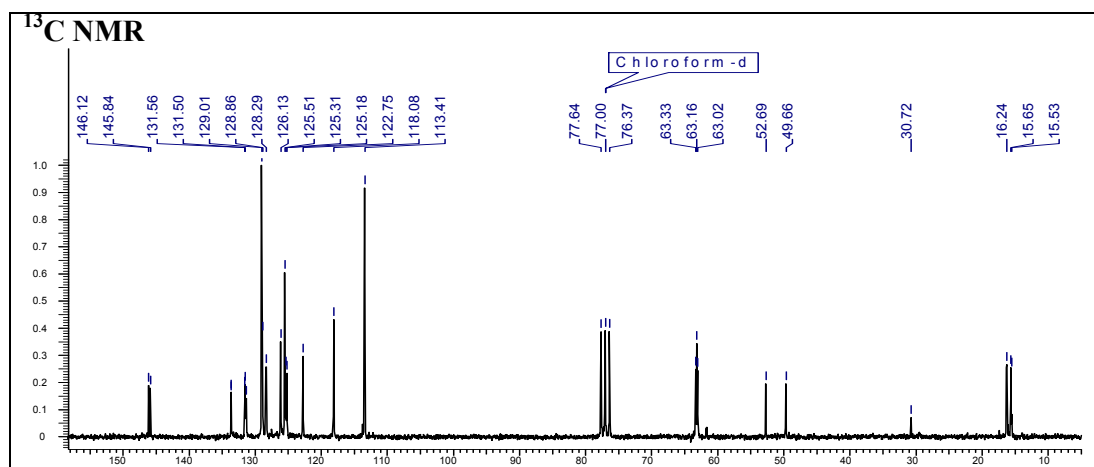
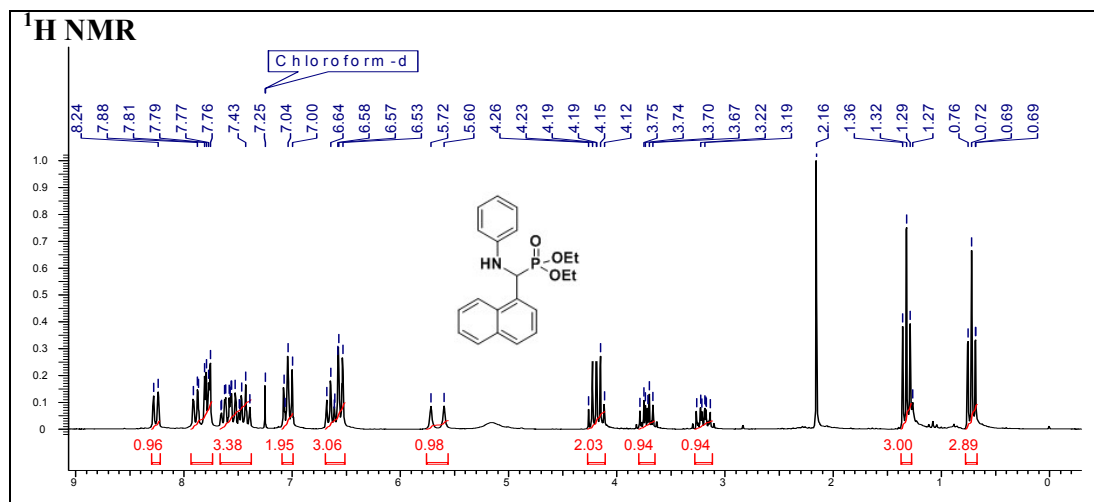
# Chapter 2



**Diethyl-(4-hydroxy-3-methoxyphenyl) (phenylamino) methylphosphonate (22k)**

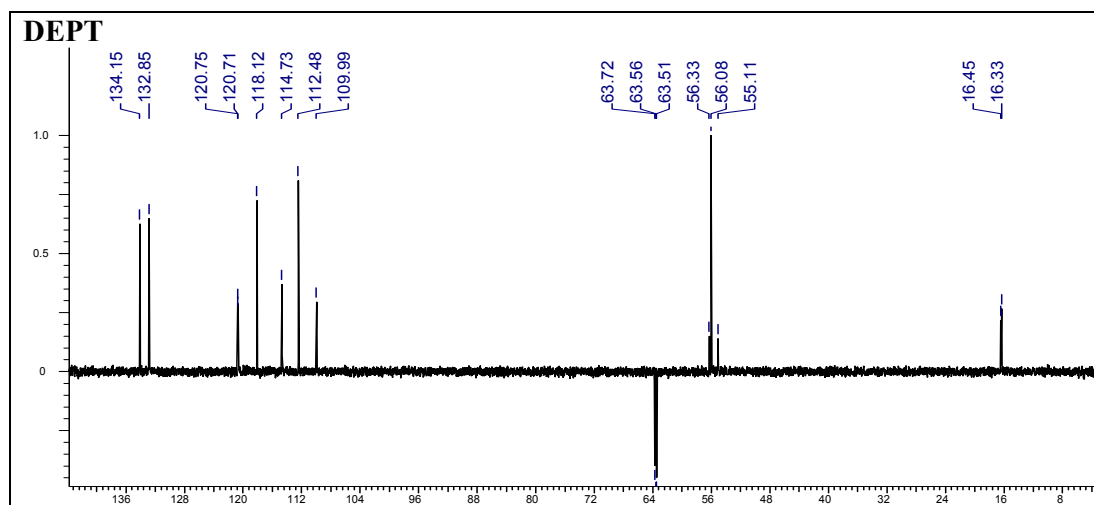
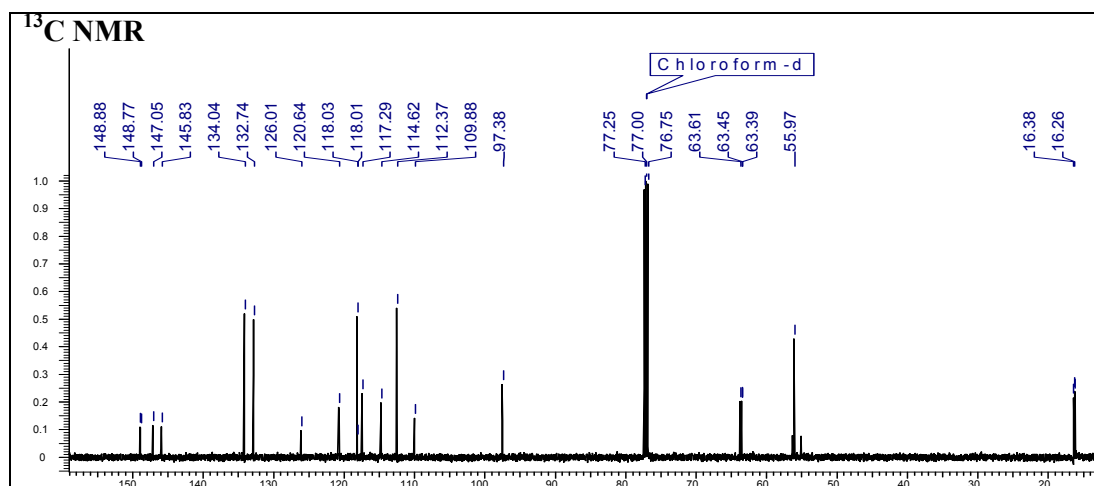
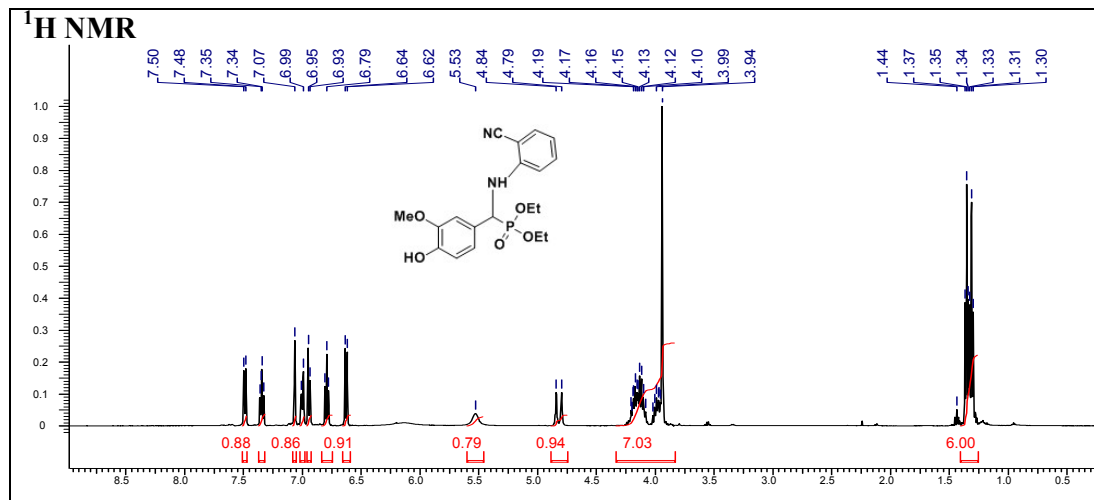
T. Kaur, *PhD thesis*, University of Pune, 2013

# Chapter 2



**Diethyl(naphthalen-1-yl(phenylamino)methyl)phosphonate (22n)**

# Chapter 2

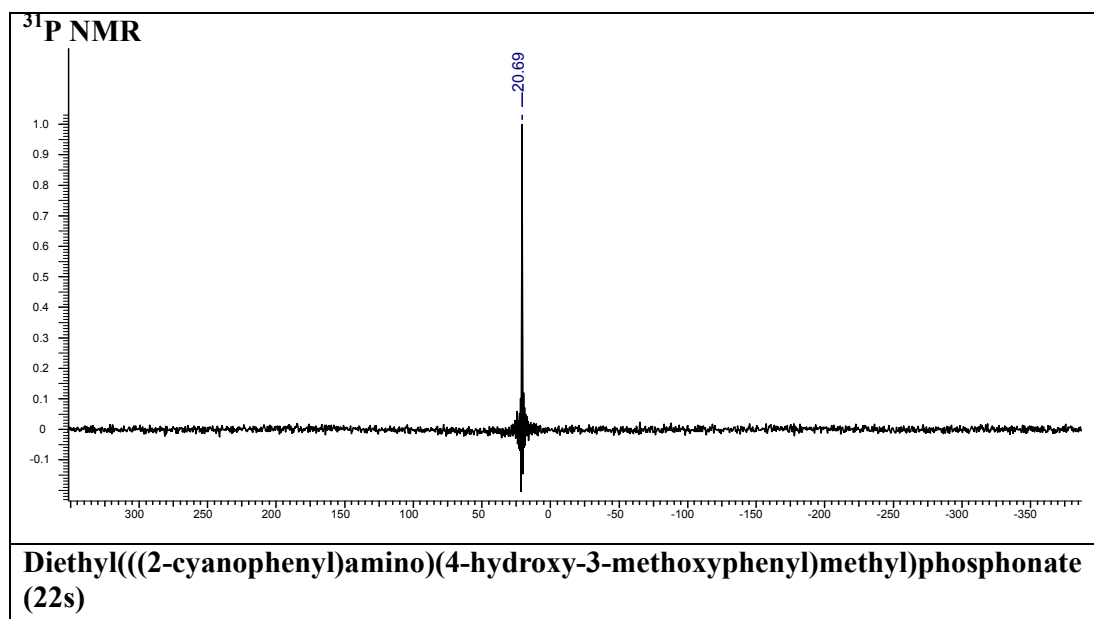
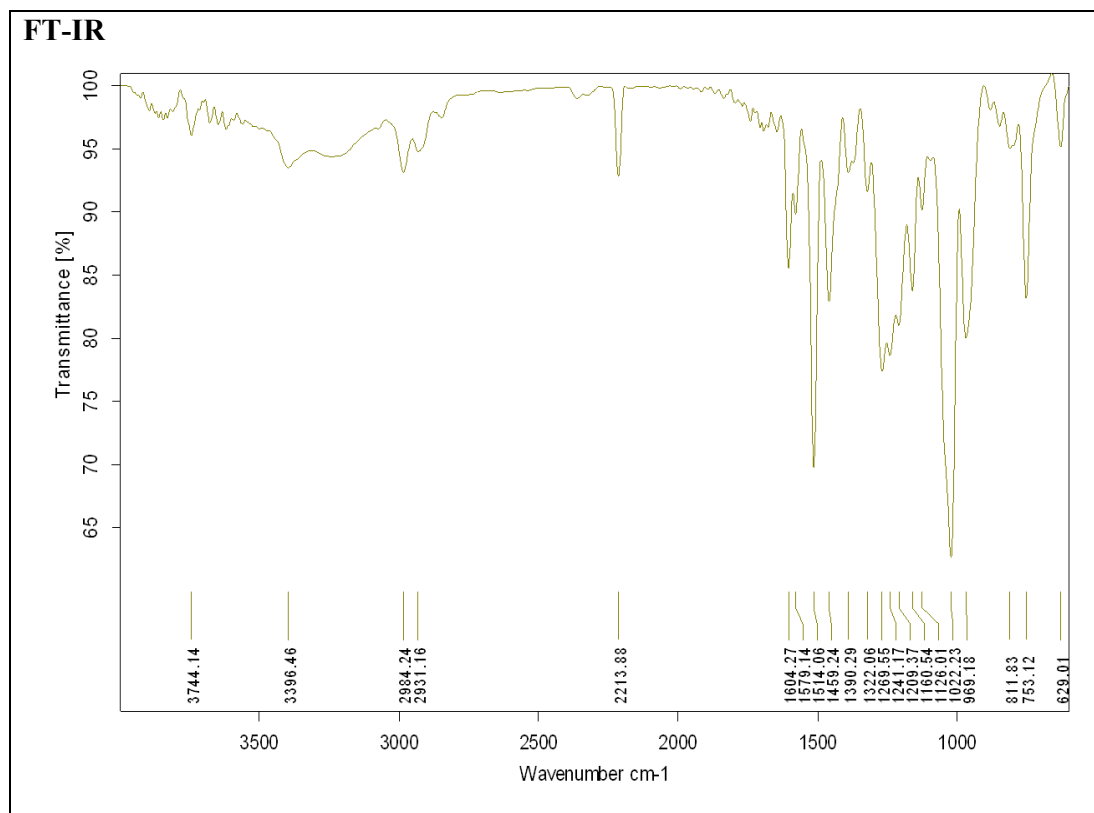


**Diethyl(((2-cyanophenyl)amino)(4-hydroxy-3-methoxyphenyl)methyl)phosphonate (22s)**

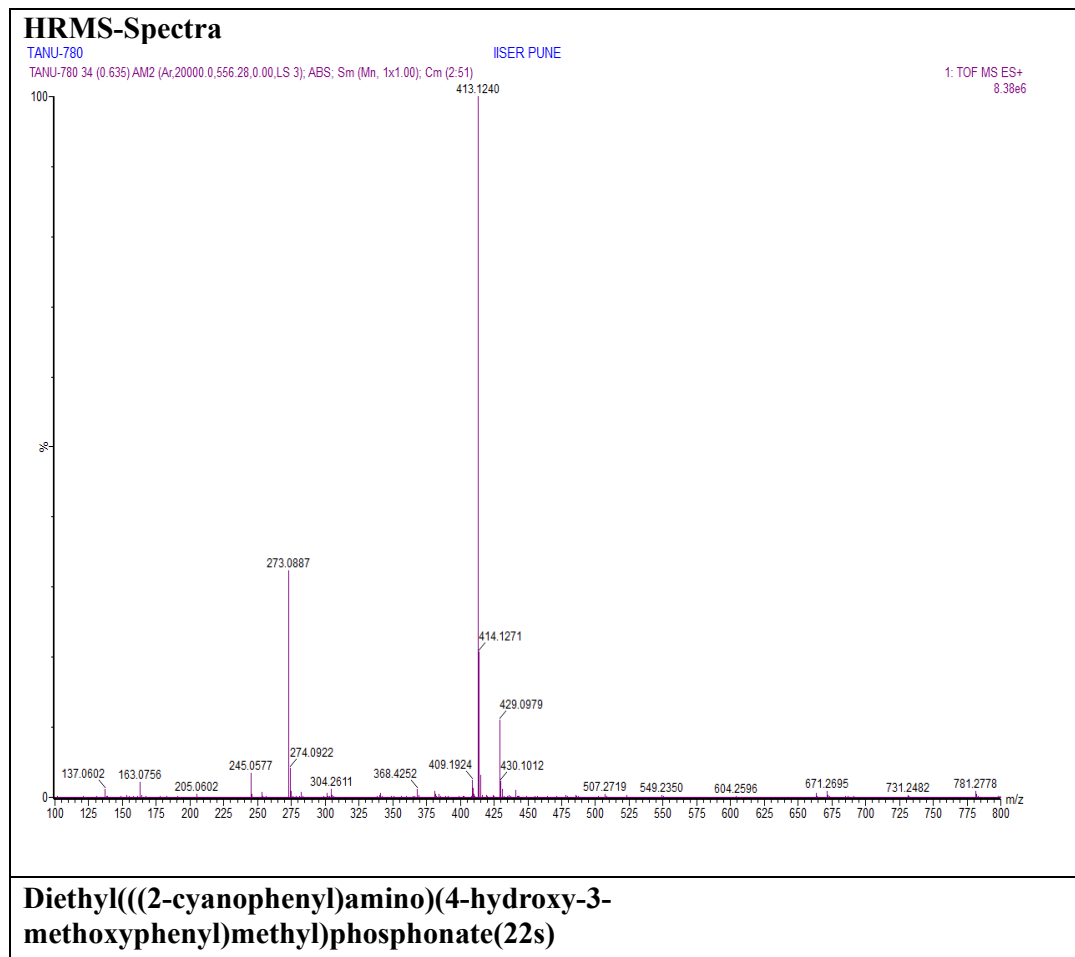
T. Kaur, *PhD thesis*, University of Pune, 2013



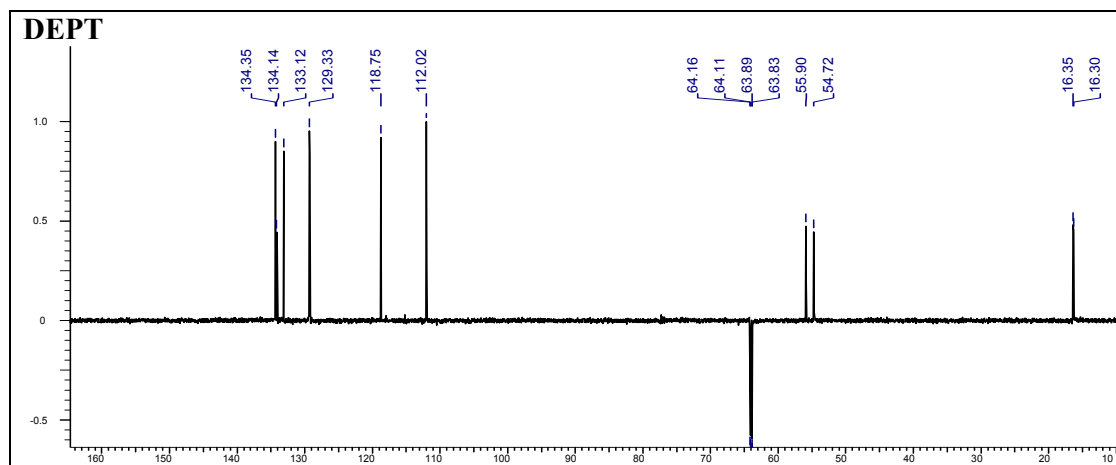
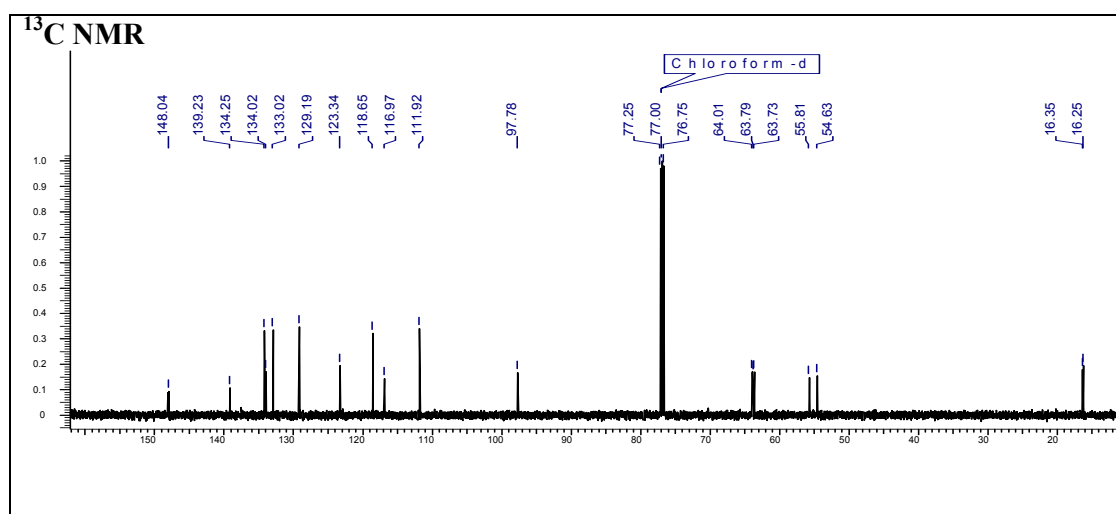
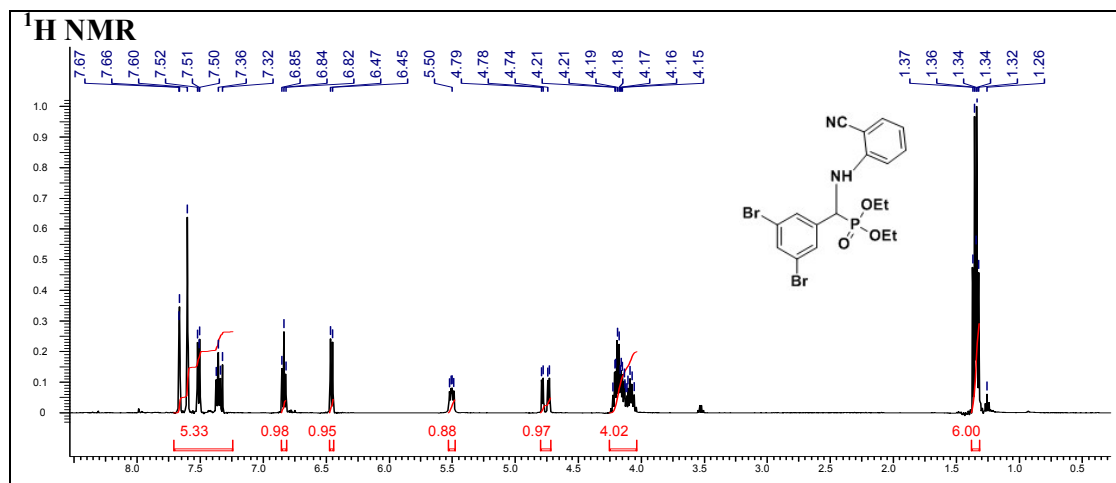
## Chapter 2



# Chapter 2



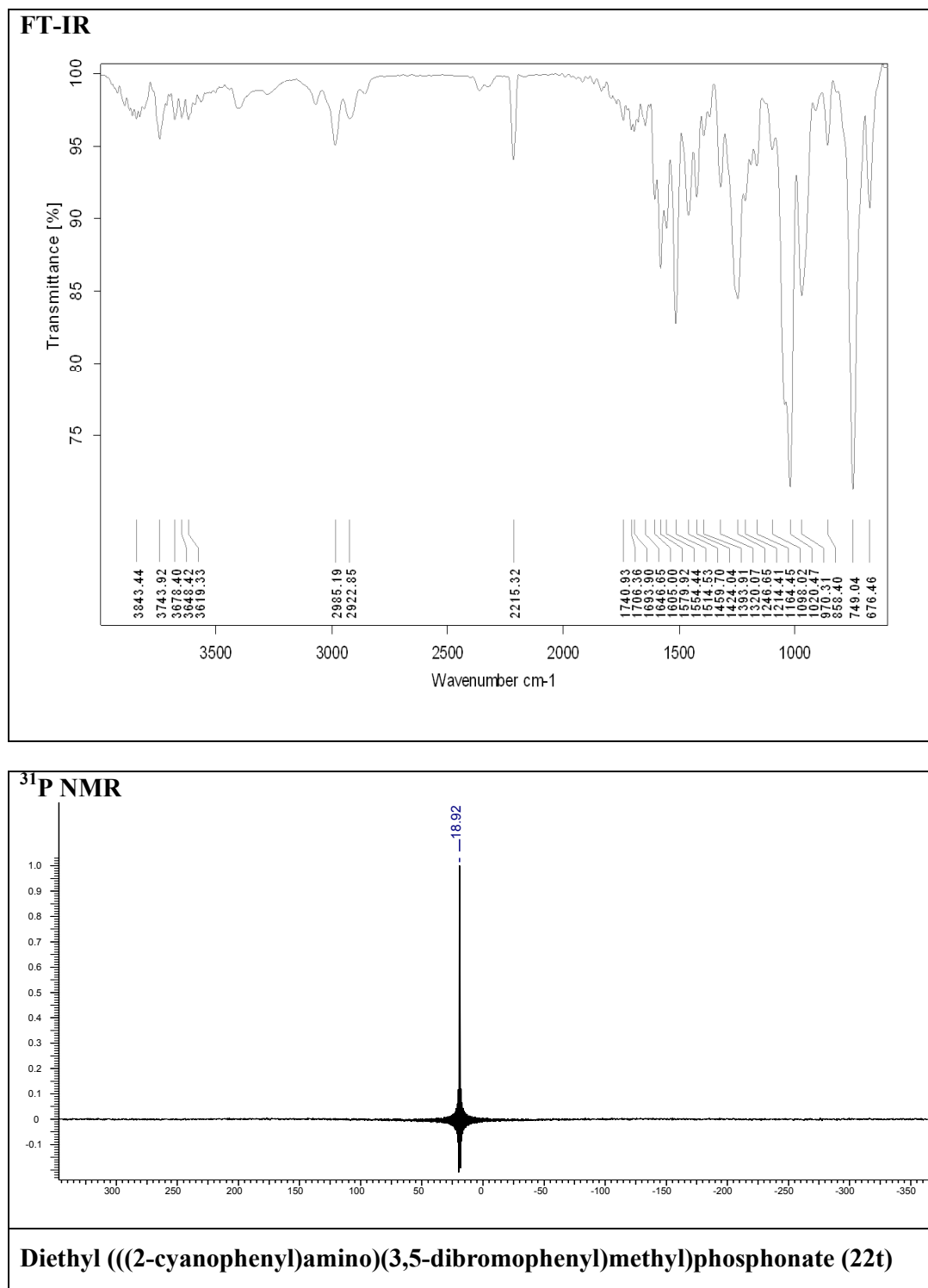
# Chapter 2



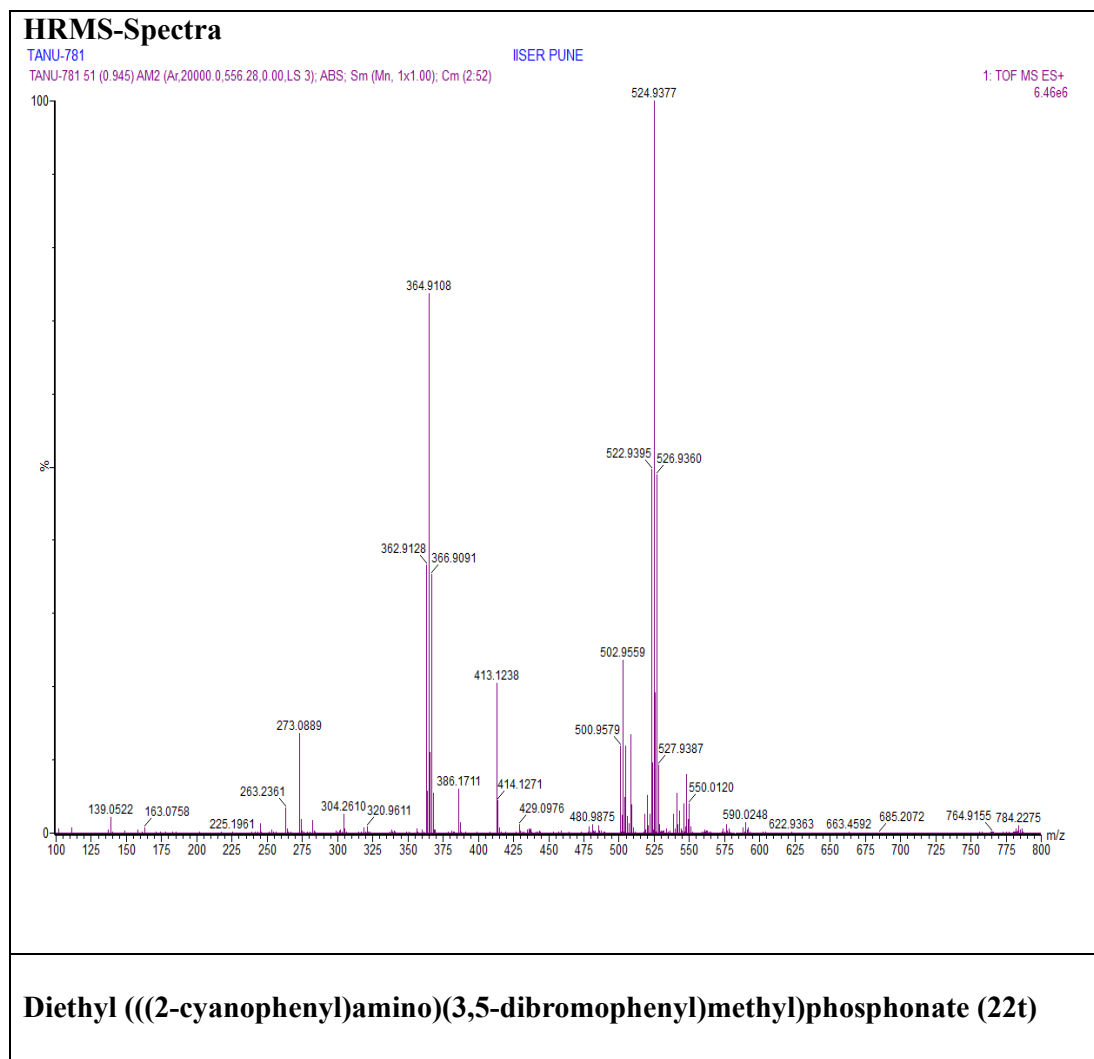
**Diethyl (((2-cyanophenyl)amino)(3,5-dibromophenyl)methyl)phosphonate (22t)**

T. Kaur, *PhD thesis*, University of Pune, 2013

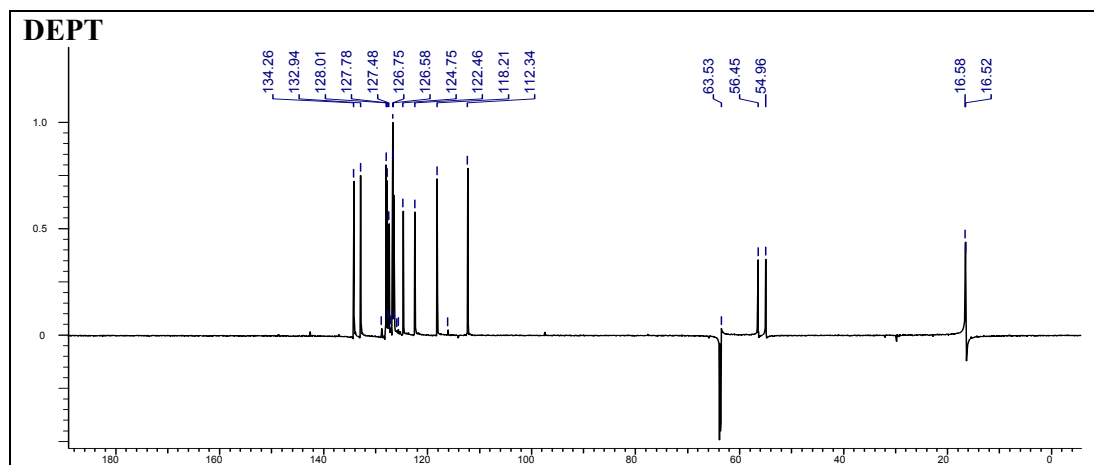
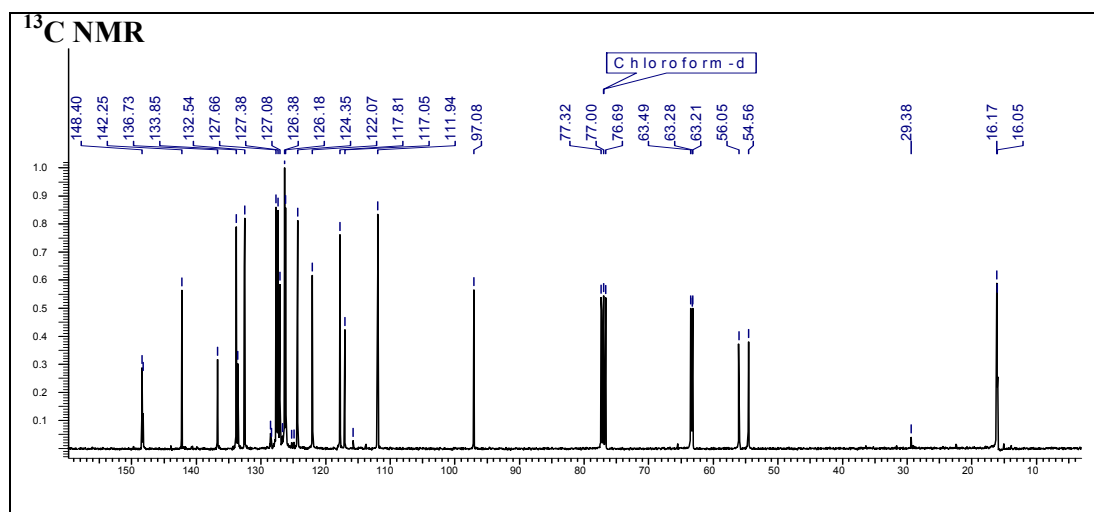
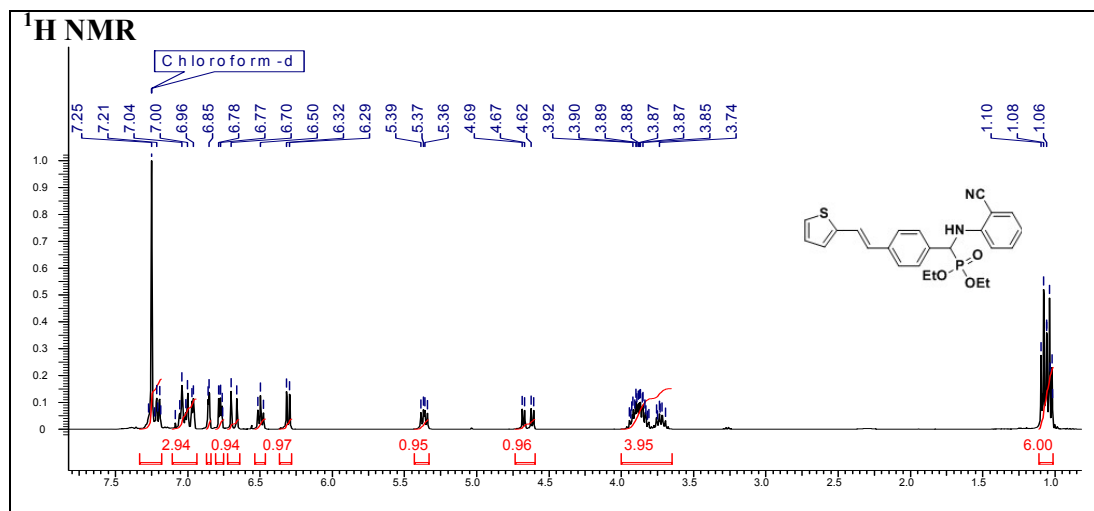
## Chapter 2



# Chapter 2



# Chapter 2



**(E)-Diethyl(((2-cyanophenyl)amino)(4-(2-(thiophen-2-yl)vinyl)phenyl)methyl)phosphate (22u)**

T. Kaur, *PhD thesis*, University of Pune, 2013

# Chapter 3

---

## **Design, Synthesis and Metal Complexation Studies of *Aminoethyl Glycyl* Polyamides**

This section deals with the synthesis of metal complexing ligands linked to polyamide *aminoethyl glycyl* backbone and their subsequent oligomerization on the Solid Phase. These polyamide oligomers were investigated for their metal binding properties.

### 3.1 Introduction

Nature uses simpler units in intricate ways and in numerous combinations to orchestrate complex processes that support and sustain life. This is exemplified in biopolymers such as proteins and polypeptides which participate in various cellular events like signalling cascades, biochemical pathways; polysaccharides that constitute structural units like cellulose, exoskeleton, cell walls; and nucleic acids which play the crucial role of storing and passing on the genetic information. In particular, comprehending the chemical origin of the properties of deoxyribonucleic acids (DNA) and emergence of complex functions from their sophisticated architectures has been an extremely tantalizing research area.<sup>1</sup> Nature, thus presents synthetic chemists with the challenge to construct or to mimic such assemblies. It was this endeavour which led to the emergence of the field of artificial DNA/DNA mimics, locked nucleic acid (LNA) and peptide nucleic acid (PNA).

Molecular recognition events in biological systems regulate various functions such as transport, catalysis, signal initiation and regulation, which are caused by the three-dimensional structural architectures adopted by the bio-polymers. The structural assembly which mediates the process of recognition by the receptors is driven by non-covalent forces such as hydrogen bonding, aromatic-stacking, solvophobic and van der Waals interactions.<sup>2</sup>

This section in the thesis presents studies on the synthesis of modified oligomers based on aminoethyl glyceryl (*aeg*) backbone of PNA. It provides an overview of background literature for undertaking the research work and gives an account of recent advancements in the synthesis of metal complexing ligands.

#### 3.1.1 Nucleic acids: chemical structure

Nucleic acids (DNA, RNA) form the basic hereditary material in all cells and are essential biopolymers of life. The double-helical structure of DNA was proposed by Watson and Crick in 1953 (Figure 1).<sup>3</sup> DNA is a polymer made up of repeating nucleotide unit that consists of a nitrogenous base, a deoxyribose sugar and a phosphate residue. Alternating sugar-phosphate units constitute the backbone of DNA



## Chapter 3

and each base adenine (A), thymine (T), guanine (G) and cytosine (C) is connected to sugar moiety *via* a  $\beta$ -glycosyl linkage.

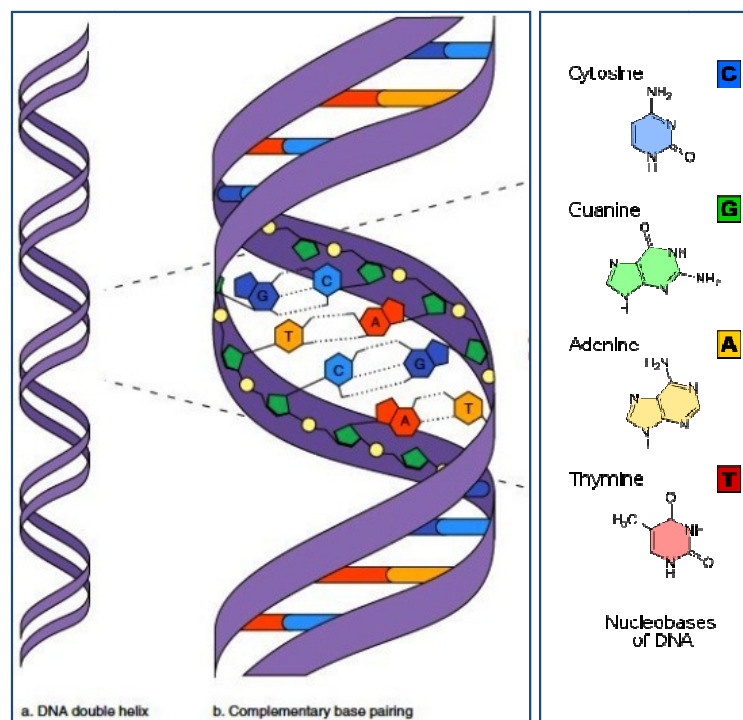


**Figure 1.** Structure of DNA duplex and nucleobases.

The nitrogenous bases adenine (A), thymine (T), guanine (G) and cytosine (C) are paired by hydrogen bonds between complementary pairs (A:T, G:C) and these hold the two strands in a duplex form. The double helical structure of DNA is nature's simplest and most elegant way of storing, retrieving and transferring the genetic information of a living organism. Ribonucleic acid (RNA) contains ribose instead of the deoxyribose sugar unit with the base composition of adenine (A), uracil (U), guanine (G) and cytosine (C).

### ***Base pairing via hydrogen bonding***

Watson and Crick recognized the the hydrogen-bonding capability of A:T and G:C base pairs, the consequent complementarity and the inherent advantage of such a scheme in the replication of this informational biopolymer through DNA model-building studies (Figure 2). The amine groups of the bases are potent H-bond donors. On the other hand, the  $sp^2$ -hybridized electron pairs on the oxygens of the base C=O groups and on the ring nitrogens are much better H-bond acceptors. The interactions

between acceptor:donor groups comprising hydrogen bonds are largely ionic in character.

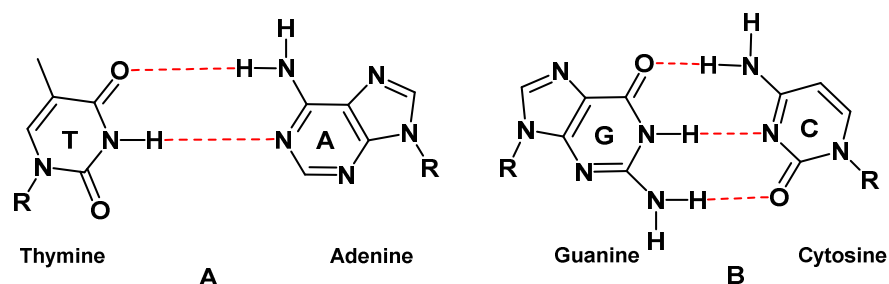


**Figure 2.** Hydrogen-bonding interactions between (A) A-T and (B) G-C base pairs.

This base pairing pattern, known as **Watson-Crick pairing**, consists of two hydrogen bonds holding A:T base pair and three hydrogen bonds holding G:C base pair.<sup>4</sup>

### 3.1.2 DNA modifications

Decades of intensive research in the development of oligonucleotides based therapeutics has yielded several synthetic oligonucleotides with various modifications to the deoxyribonucleotide unit. The objective of the several of these modifications was to achieve better stability under physiological conditions, longer *in vivo* half-life, enhanced cellular internalization and improved binding specificity, especially for the modulation of specific gene expressions *via* binding to complementary RNA and genomic DNA through antisense and antigene technology, respectively. Based on the incorporation of unnatural bases, modified sugars and altered phosphate backbone, the synthetic DNA mimics can be considered to have evolved in three generations (Figure 3).

‘First generation’ ONs, the best known example is phosphorothioate (PS)<sup>5</sup> in which one of the non-bridging oxygen atoms in the phosphodiester bond is replaced by sulphur. These were shown to have cellular toxicity and found to exert slightly reduced affinity towards complementary RNA molecules in comparison to their corresponding phosphodiester oligodeoxynucleotides.

‘Second generation’ ONs are consists of nucleotides with alkyl modifications at the 2’ position of the ribose<sup>6</sup> and have 2’-*O*-methyl and 2’-*O*-methoxy-ethyl RNA are the most important members of this generation of antisense ONs and are known to be less toxic than PS DNAs.

## Chapter 3

In order to improve properties such as target affinity, nuclease resistance and pharmacokinetics, the concept of conformational restriction has been widely utilised for enhanced binding affinity and biostability, paving way for the development of ‘third generation’ ONs encompassing variety of modified nucleotides.

These include several DNA and RNA analogs with modified phosphate linkages or riboses as well as nucleotides with completely different chemical moieties substituting the furanose ring.

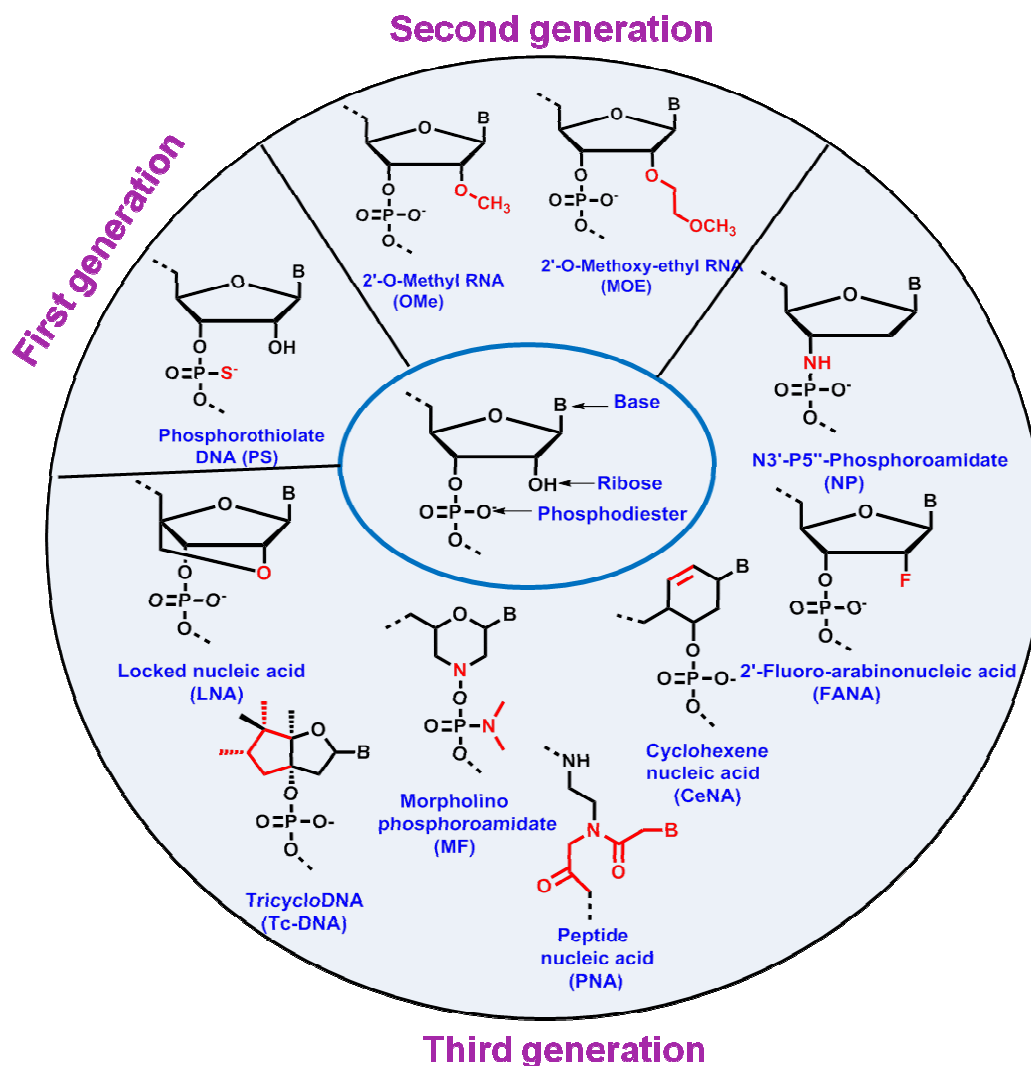


**Figure 3.** Chemical modifications in the development of oligonucleotides.

‘Third generation’ ONs includes modified phosphate derivative ***N3'-P5''*** phosphoroamidates (NPs), in which the 3'-hydroxyl group of the 2'-deoxyribose ring is replaced by a 3'-amino group.<sup>7</sup> Another first uniformly sugar-modified ONs is **2'-Deoxy-2'-fluoro-β-D-arabino nucleic acid (FANA)**, which is reported to induce RNase-H cleavage of a bound RNA molecule.<sup>8</sup> The most proven class of chemically

modified nucleotide is **Locked nucleic acid (LNA)**, which contains a methylene bridge that connects the 2'-oxygen of the ribose with the 4'-carbon.<sup>9</sup>

**Morpholino oligonucleotides (MF)** are nonionic DNA analogs in which ribose unit replaced by morpholino moiety and phosphoramidate linkages instead of phosphodiester bonds in backbone.<sup>10</sup> The replacement of the five-membered furanose ring by a six-membered ring lead to **Cyclohexene nucleic acid (CeNA)**, which are characterized by a high degree of conformational rigidity of the oligomers.<sup>11</sup> **Tricyclo-DNA (tcDNA)** exhibited enhanced binding to complementary sequences.<sup>12</sup> **Peptide nucleic acid (PNA)** are most intensively studied DNA analogs besides phosphorothioate DNA and 2'-*O*-alkyl RNA.<sup>13</sup> The present work is oriented towards the development of such repeating *N*-(1-aminoethyl)-glycyl (*aeg*) units having different metal complexing ligands.

### 3.1.3 Peptide nucleic acids (PNAs)

Peptide Nucleic Acid (PNA) is a DNA mimic resulting from the replacement of sugar-phosphate backbone by a pseudopeptide backbone and was introduced by Nielsen *et al.* in 1991.<sup>13</sup> The structure of PNA is remarkably simple. It consists of a repeating *N*-(1-aminoethyl)-glycyl (*aeg*) units linked by amide bonds (Figure 4). A methyl carbonyl linker connects natural as well as unusual nucleotide bases to the backbone at the amino nitrogens. The pseudopeptide (polyamide) backbone of PNA was originally designed to be a good structural mimic of the ribose-phosphate backbone of nucleic acids. PNA was proven to be an efficient DNA mimic with better DNA/RNA-recognition and triplex-forming properties.<sup>14</sup>

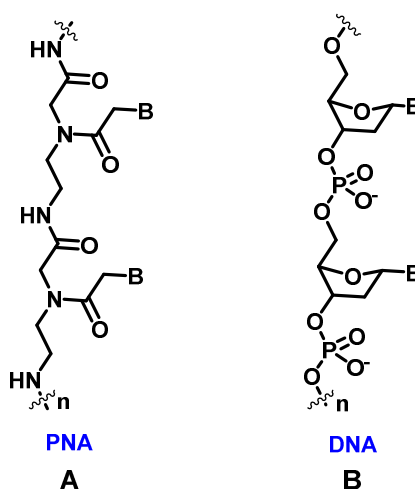


**Figure 4.** Structure of (A) PNA and (B) DNA, B = nucleobases.

## Chapter 3

PNA oligomers are better than the conventional antisense oligonucleotides, because of their high flexibility and absence of charge in the artificial backbone. They have longer life span in the cellular environment than any oligonucleotide and used to downregulate the target gene expression, being resistant to both nucleases and proteases. PNA hybridizes with complementary DNA/RNA sequences with superior thermal stability resulting from the overall decrease in electrostatic repulsion in DNA/RNA strands. Hence, they can successfully compete and eventually displace the natural complementary strand. In short, PNA has attracted wide attention in medicinal chemistry for development of gene therapeutics in antisense<sup>15</sup> and antigene<sup>16</sup> strategy and for diagnostics.

There is an increasing interest in modulating and expanding the recognition motifs of standard base pairs in PNA. Employing non-natural nucleobases in place of natural ones would help us in understanding of the recognition process in terms of various contributing factors such as hydrogen bonding, inter-nucleobase stacking *etc.* Further, new recognition motifs may have potential applications in diagnostics and nanomaterial chemistry. 2,6-Diaminopurine (Figure 5A)<sup>17</sup> offers increased affinity and selectivity for thymine/pseudoisocytosine (Figure 5B)<sup>18</sup> and is an efficient mimic of protonated cytosine for triplex formation.

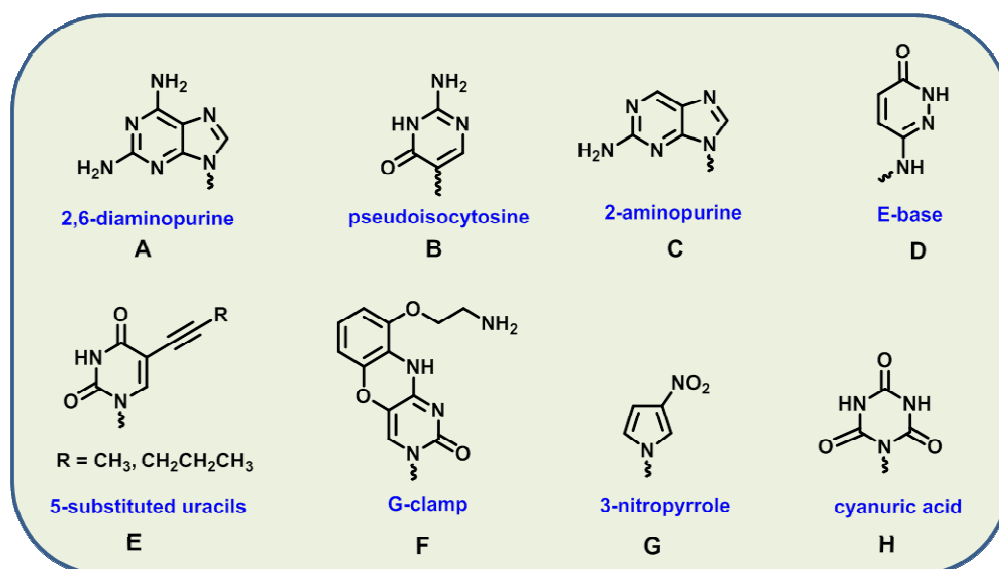


**Figure 5.** Modified nucleobases used in the synthesis of PNA oligomers.<sup>17-21</sup>

2-Aminopurine (Figure 5C) forms hydrogen bonds with U and T in reverse Watson-Crick fashion. The *E*-base (Figure 5D) was rationally designed for

recognition of A-T base pair in the major groove and forms a stable triad with T in the central position. A wide variety of 5-substituted uracils (Figure 5E) were synthesized to study their ability for triplex formation.<sup>19</sup> The G-clamp base (Figure 5F) was developed to build specific, additional bonding interactions with guanine. Unnatural heterocycles 3-nitropyrrole (Figure 5G)<sup>20</sup> and cyanuryl PNA (Figure 5H)<sup>21</sup> were also synthesized.

### 3.1.4 Metal organic complexes

Metals are nature's favourite class of guest molecules that are involved in stabilization of different three dimensional structures. These include Zn finger proteins, chlorophyll pigment, haemoglobin *etc*, which allow them to carry out vital functions like transcription process, photosynthesis and carry oxygen reversibly *etc*. Na<sup>+</sup>-K<sup>+</sup> pumps are crucial in maintaining electrolyte balance across cell membranes, metalloprotein 'haemoglobin' chooses Fe to carry out the metabolic respiration. The understanding of these recognition events has further deepened with the development of foldamers,<sup>22</sup> where the interplay of basic forces and structural assembly process is often initiated by interactions with the guest molecule.

Jean Marie Lehn<sup>23</sup> laid the foundation of supramolecular chemistry with his discovery of cryptands in the late 1980s.<sup>24</sup> These complexes are found to possess various properties for example cation transport, anionic polymerization and removal of radioisotopes. Further, he designed novel inorganic and organic hybrids for various functions. Significant contributions towards the discovery of dynamers (dynamic polymers), [2 x 2] grid complexes, 2D- and 3D-cryptands were made by this finding. Metallofoldamers developed by Lehn *et al.*<sup>25</sup> presents one of the many facets of the folding behaviour exhibited by synthetic oligomers by virtue of ion-dipole interactions, where Cs<sup>+</sup> ions drive the helical assembly of the alternating naphthyridine-pyrimidine oligomer unit (Figure 6).

## Chapter 3

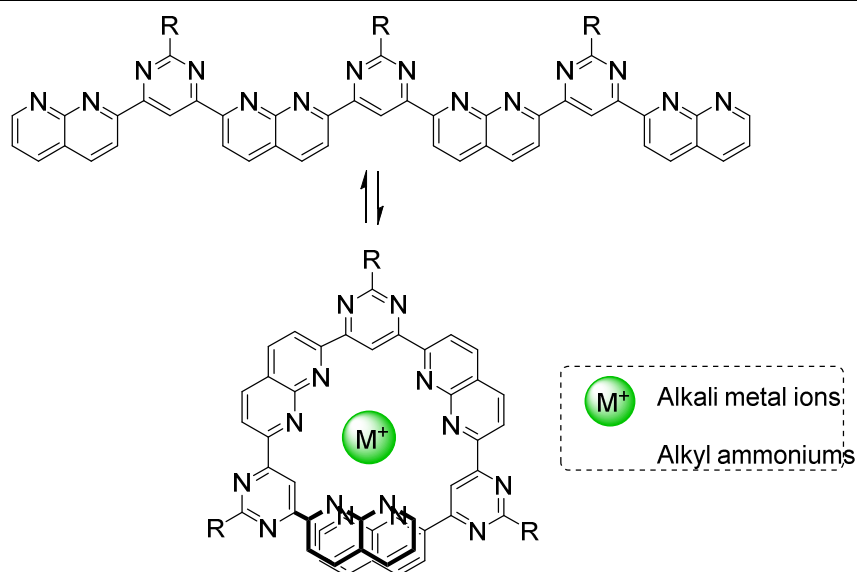


**Figure 6.** Naphthyridine–pyrimidine metallofoldamer reported by Lehn.<sup>25</sup>

The same group reported Pb<sup>2+</sup> ion binding pyridine-hydrazone oligomer that forms a helically folded complex (Figure 7).<sup>26</sup>

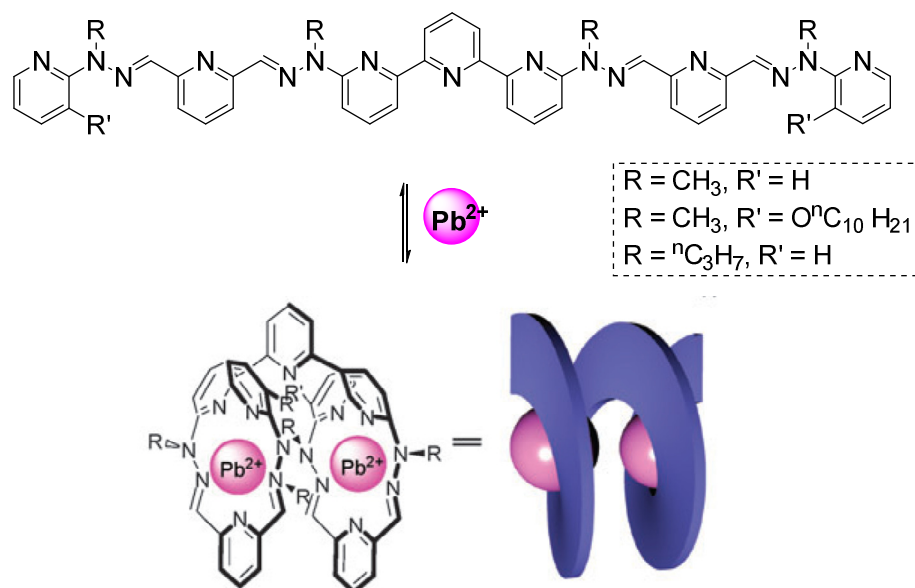


**Figure 7.** Pyridine–hydrazone metallofoldamer exhibited binding to Pb<sup>2+</sup>.<sup>26</sup>

Various other helical assemblies have been designed by different groups for *e.g.* Moore *et al.*<sup>27</sup> reported solvophobic driven folding of *m*-phenylene-ethynylene (*m*-PE) oligomers due to metal binding-induced helical conformation with participation of interacting cyano groups.

### 3.1.5 Metallo-DNAs

In addition to being the carrier of genetic information, DNA molecule has also been recognized for its superior self-assembling properties. Sequences can be designed to assemble into different types of H-bonding induced architectures such as duplexes, triplexes, quadruplexes hairpins and a variety of branched nanostructures. The DNA strands can also arrange themselves into long nanowires. Several attempts have been made to exploit and extend these properties of DNA by synthetic modifications to the backbone and nucleobases for various applications in both biological and nanomaterials chemistry. Keeping the fundamental design of the DNA double helix intact, several groups<sup>28</sup> have studied replacement of the natural base pairs of the DNA molecule with ligands that show pronounced affinity to bind to metal ions. Shionoya *et al.*<sup>29</sup> (Figure 8) replaced the natural DNA base pairs with unnatural ones that can coordinatively bind metal ions mimicking the base pairs of DNA.

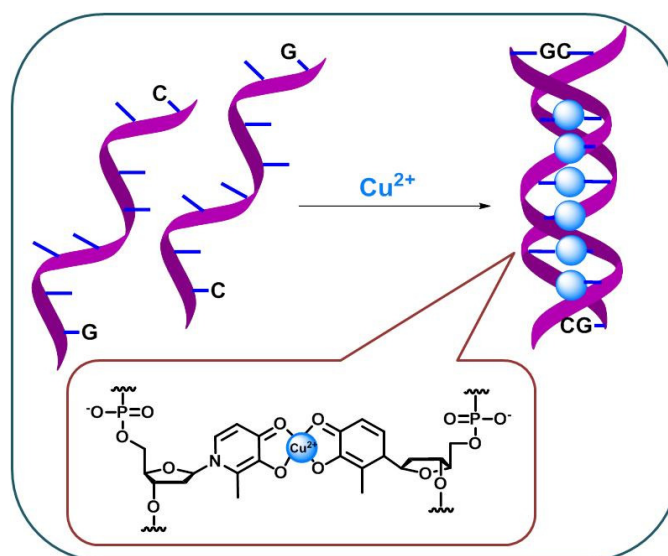


**Figure 8.**  $\text{Cu}^{2+}$ -mediated duplex formation between two artificial DNA strands in which hydroxypyridone nucleobases replace natural base pairs.<sup>29</sup>

The strategy was used to assemble copper and mercury metal ions inside the DNA molecule to generate heterometallic wires by employing different metal binding ligands as substituents for the nucleobases. Some of the synthesized inorganic bases are depicted in Figure 9, which shows variety of binding selectivities. *e.g.* *o*-amino phenol binding to  $\text{Pd}^{2+}$ , *o*-hydroxy-quinone (Hq), catechol and bipyridyl (Bpy) binding to  $\text{Cu}^{2+}$ .



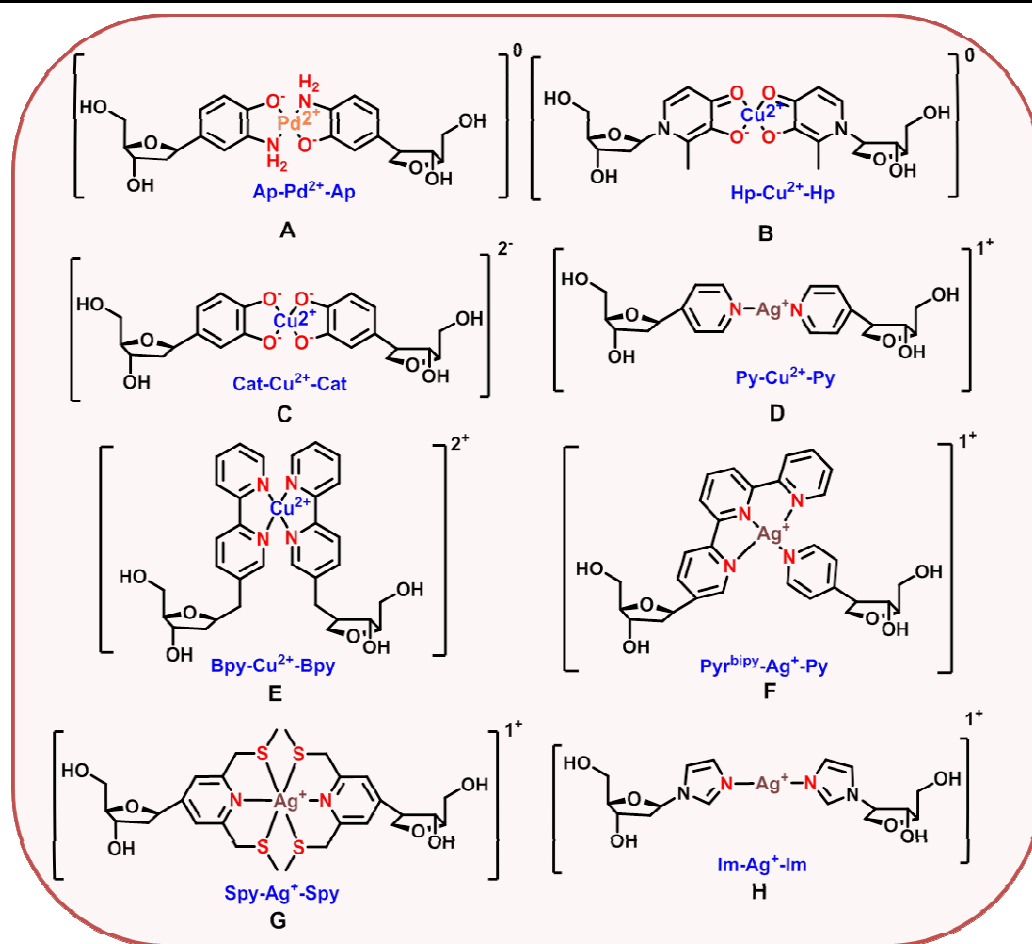


**Figure 9.** Metal binding ligands instead of A/T/G/C nucleobases used in DNA oligomers.<sup>29</sup>

The pyridyl (Py), terpyridyl (Tpy), imidazolyl (Im) and S-methylpyridyl (Spy) bind preferably to  $\text{Ag}^+$  metal ions.<sup>29</sup>

### 3.1.6 Metallo-PNAs

Over the past few years, peptide nucleic acids (PNAs) have emerged as one of the most promising new type of molecules for the recognition of nucleic acids (DNA and RNA). The successful incorporation of artificial bases in DNA molecule prompted replacement in PNA also, since latter being conceptual DNA mimic. PNA backbone also provides a great deal of synthetic versatility and this feature paves an easy access to incorporate amino acid residues, non-natural bases and metal-binding ligands into it.<sup>30</sup>

Nolte *et al.*<sup>31</sup> incorporated and studied the cellular uptake of octapeptide-cobalt complexes, which have 4 to 5 lysine residues and a guanidine group. The resulting complexes showed better results in the cellular uptake and its endosomal escape

## Chapter 3

compared to ferrocenium complexes (Figure 10). Also in order to facilitate cellular imaging experiments, fluorescent di-rhenium organometallics have been attached to the PNA oligomers, which could successfully stain both cytoplasm and nucleus of HEK-293 cells simultaneously.<sup>32</sup>

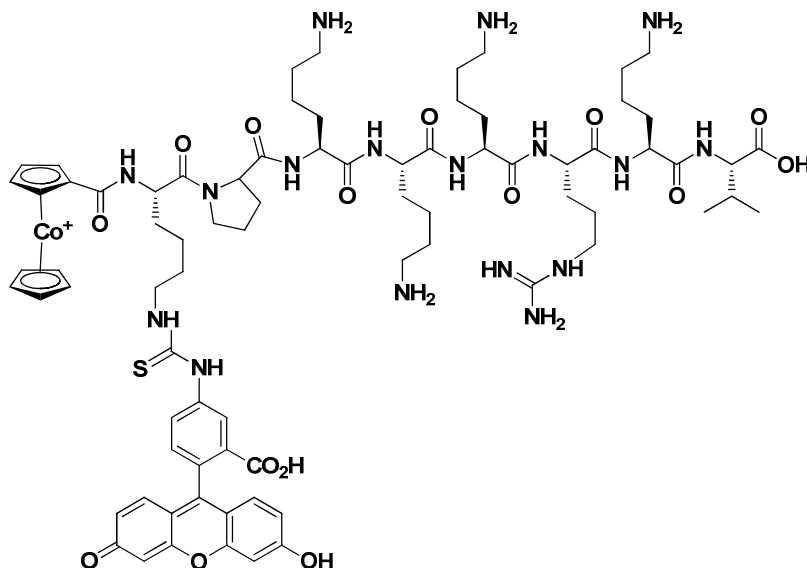


**Figure 10.** Synthesized cobaltocene peptides having lysines and guanidines.<sup>31</sup>

To construct a hybrid of metal bound PNA with *aeg* backbone properties along with the co-ordination properties of transition metals, Achim *et al.*<sup>33</sup> incorporated three consecutive 8-hydroxyquinoline (hq)<sup>33</sup> or bi-pyridine (bpy)<sup>34</sup> units into PNA oligomers. It was observed that stabilization exerted by metal ions on terminally modified duplexes surpassed the effects exerted on the central modification. These modifications showed increased or decreased stability in presence of various metal ions. It was found that greater stabilization was exerted by the  $\text{Cu}^{2+}$  or  $\text{Ni}^{2+}$  metal ions, while  $\text{Pd}^{2+}$  and  $\text{Pt}^{2+}$  did not change the melting temperatures of the duplexes generated. Due to steric effect of these large ligands, more modifications in the oligomer backbone resulted in the decreased duplex melting temperatures and have shown high mismatch tolerance.

Several groups have reported insertion of pyridyl (py), ter-pyridyl (tpy) moieties into the PNA backbone (Figure 11).<sup>35</sup> Also in order to evaluate the electrochemical behaviour of organometallic moieties within the PNA sequence, ferrocenyl click derivatives,<sup>36</sup> chromium tricarbonyl,<sup>37</sup> Fischer type carbene

## Chapter 3

complexes of tungsten<sup>38</sup> and redox active ruthenium complexes<sup>39</sup> were synthesized and have found great applications in spectroscopic analysis and bio-imaging areas.

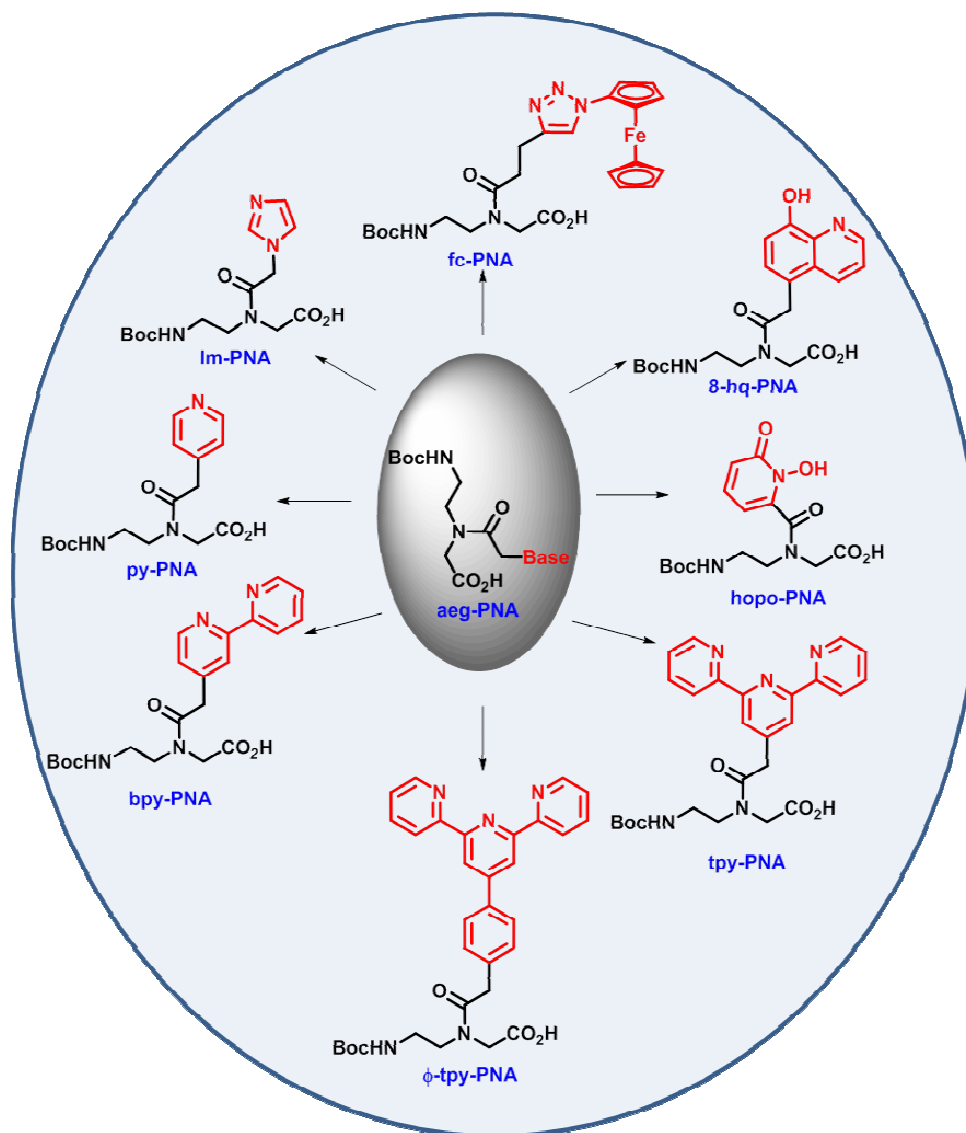


**Figure 11.** Structures of metal binding ligands attached to PNA backbone.<sup>33-36</sup>

Mokhir *et al.*<sup>40</sup> designed PNA oligomers that can bind specifically with metals which are available at higher concentrations in various organs<sup>41</sup> as well as in some cancerous cells for *e.g.*  $Zn^{2+}$ . In breast cancer tissues, zinc levels sometimes are known to increase by a factor of 72%. With this rationale in mind several bi- and tri-dentate ligands *e.g.* bis-(pyridine-2-yl-methyl)amine (dpa)-PNA conjugates were designed and found to increase in the thermal stability of PNA.DNA/RNA duplexes (Figure 12). The modified terpyridyl PNA-Zn (II) complexes also have shown increased cellular uptake.<sup>42</sup>

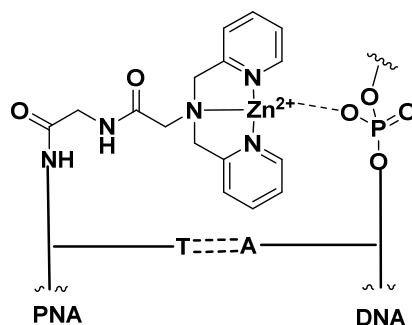


**Figure 12.** Proposed approach for metal binding of Zn-dpa probes to oligonucleotides.<sup>41</sup>

### 3.1.7 Synthetic methods and characterization of polyamide *aeg* oligomers

There are many methods to achieve synthesis of the oligomeric PNA strands. Solution phase synthesis using different coupling agents is not a preferred strategy for oligomerization of peptide mimics due to its tedious and time consuming procedure. The ease of handling and scale up procedures have made choice of solid phase peptide synthesis (SPPS) better compared to solution phase peptide synthesis (a general comparison has been discussed in Table 1).

#### 3.1.7a Solid Phase Peptide Synthesis (SPPS)

Solid Phase Peptide Synthesis (SPPS) protocols are used for the synthesis of several peptides and oligomeric PNAs.<sup>42</sup> The method allows easy access to incorporation of a large number of analogues which are useful in binding and elicit biological properties. There are several features that are beneficial in solid phase peptide synthesis like no loss of material during work-up as the peptide is never taken out of the reaction vessel. No purification of the intermediates is required during the synthesis, and operations are repetitive enabling automation.

**Table 1.** Solid Phase Peptide Synthesis (SPPS) vs Solution Phase Peptide Synthesis.

Solid Phase Peptide Synthesis	Solution phase peptide synthesis
❖ Time saving process.	❖ Tedious process.
❖ Practically possible for small as well as lengthy peptide sequences.	❖ Practically difficult, as purification of polar intermediate peptides is not feasible.
❖ Isolation and purification of intermediates is not needed.	❖ Isolation and purification of intermediates is desirable for next step synthesis.
❖ Excess of coupling reagent and monomers	❖ Excess of coupling reagent and monomers are not desirable.

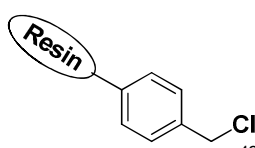
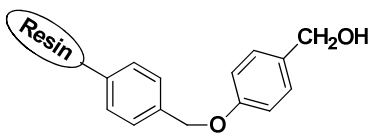
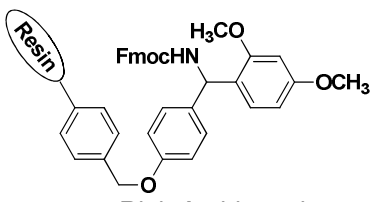

## Chapter 3

are needed.

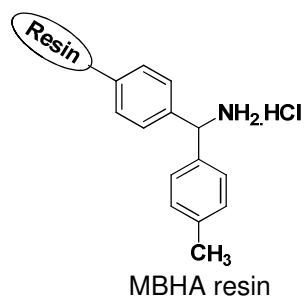
- |  |   |
|--|---|
| <ul style="list-style-type: none"> <li>❖ Racemization is not observed.</li> <li>❖ Limited scope of protecting groups of side chains.</li> <li>❖ Fast and good yielding synthesis.</li> </ul> | <ul style="list-style-type: none"> <li>❖ Racemization is observed in some cases.</li> <li>❖ Several different groups can be employed as isolation of intermediates is needed.</li> <li>❖ Slow process.</li> </ul> |
|--|---|

Peptides with different functionalities can be synthesised by proper choice of resins. A brief description used for the synthesis of peptide acids, peptide hydrazides and peptide carboxamides is described in Table 2.

**Table 2.** Resins Used for Solid Phase Peptide Synthesis

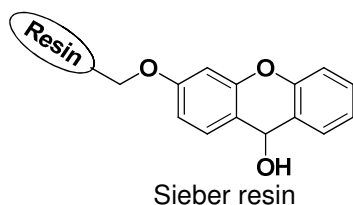
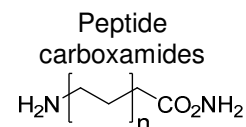
Resin Structure	Protecting Group Used	Resin Cleavage Conditions	Final Products
 Merrifield resin <sup>42</sup>	Boc	HF/ TFA HBr/ TFMSA	Peptide acids $\text{H}_2\text{N} \left[ \text{CH}_2 \text{CH}(\text{R}) \right]_n \text{CO}_2\text{H}$
 Wang resin	Fmoc	TFA	Peptide acids $\text{H}_2\text{N} \left[ \text{CH}_2 \text{CH}(\text{R}) \right]_n \text{CO}_2\text{H}$
 Rink Amide resin	Fmoc	20% TFA/DCM	Peptide carboxamides $\text{H}_2\text{N} \left[ \text{CH}_2 \text{CH}(\text{R}) \right]_n \text{CO}_2\text{NH}_2$
 SASRIN resin	Fmoc	1% TFA/DCM	Peptide acids $\text{H}_2\text{N} \left[ \text{CH}_2 \text{CH}(\text{R}) \right]_n \text{CO}_2\text{H}$

# Chapter 3



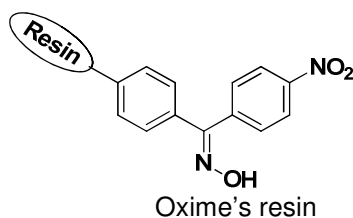
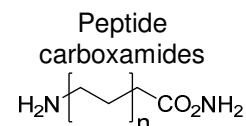
Boc

TFA/TFMSA



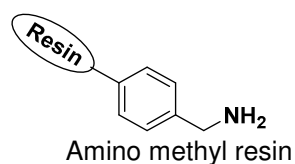
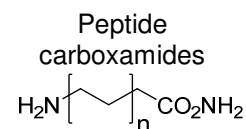
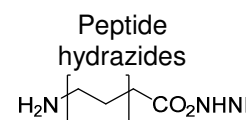
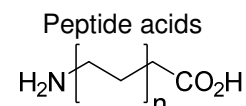
Fmoc

1%  
TFA/DCM



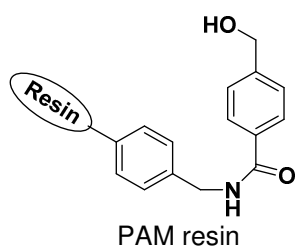
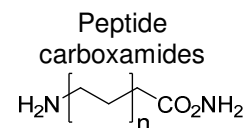
Boc

$\text{NaOH}, \text{N}_2\text{H}_4$   
 $\text{NH}_3, \text{RNH}_2$



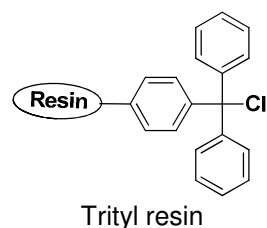
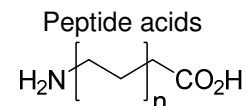
Boc/ Fmoc

20%  
TFA/DCM



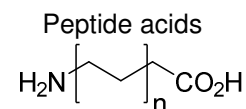
Boc

TFA/TFMSA



Fmoc

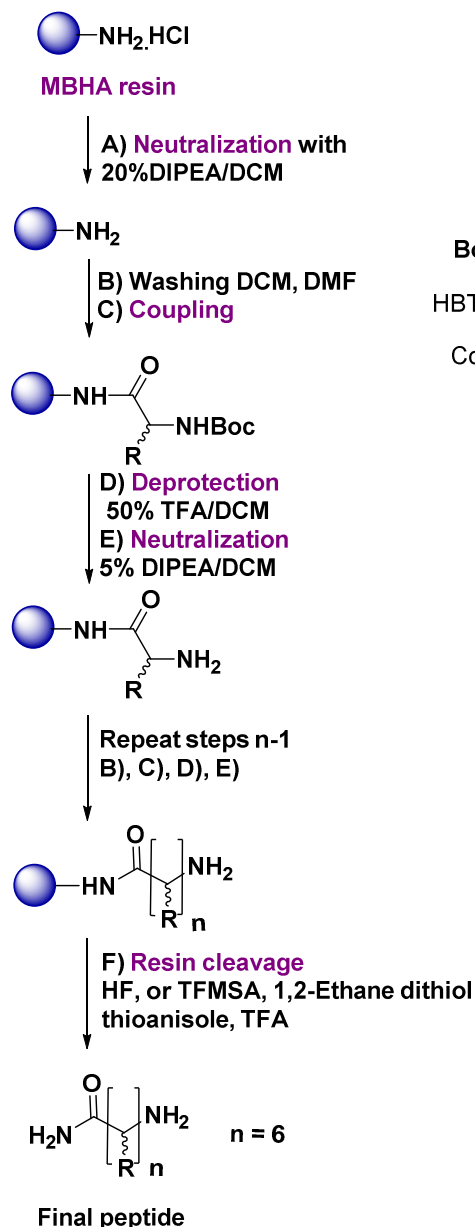
1-5%  
TFA/DCM



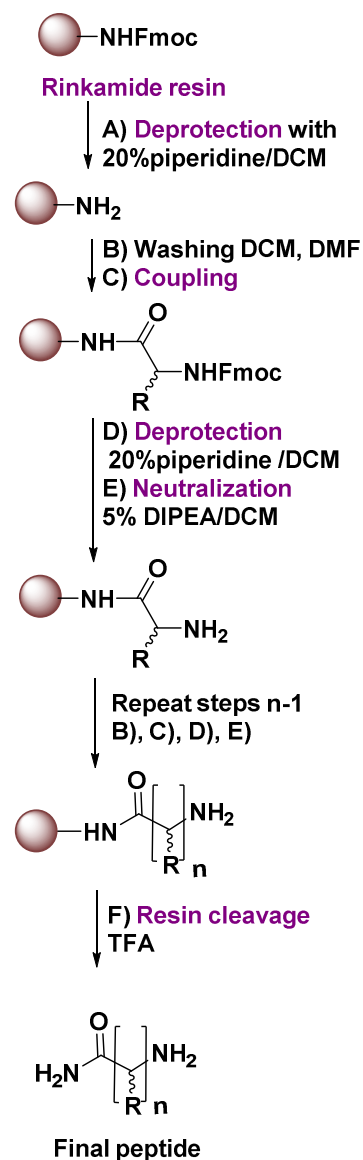
## Chapter 3

Generally in solid phase peptide synthesis, either acid labile *Boc*-group<sup>44</sup> or base labile *Fmoc*-group<sup>45</sup> (Scheme 1) is used for *N*-protection. The C-terminus amino acid can be attached directly to the resin or through a linker. Other functional groups present on the side chains are protected orthogonally with *Boc*- and *Fmoc*- protecting groups.<sup>42</sup> *Fmoc* chemistry is known for generating peptides of higher purity and in greater yield than *t*-*Boc* chemistry.

### *Boc*-chemistry



### *Fmoc*-chemistry

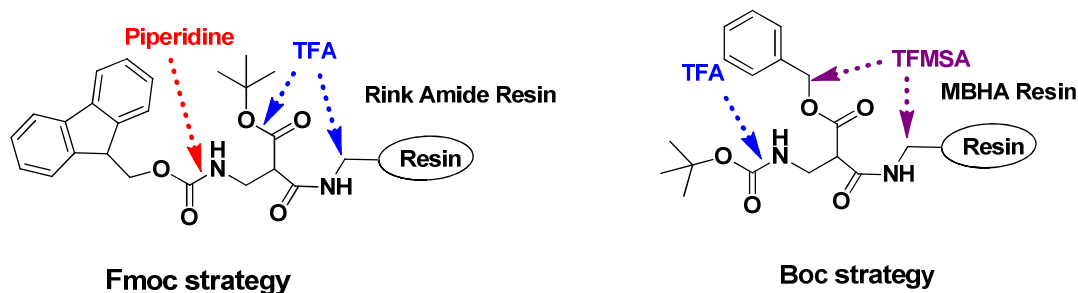


**Scheme 1.** General protocols for the synthesis of peptides *via Boc* (left) and *Fmoc*- groups (right).

The cleavage of *Boc*-group is carried out using TFA (trifluoroacetic acid) and the deprotection of *Fmoc* group is done under basic conditions using piperidine or

## Chapter 3

diethylamine. After the synthesis the peptide up to the desired length, it is cleaved from the solid support, employing different deprotection conditions for different resins. The final cleavage of resin is achieved using a strong acid such as hydrogen fluoride (HF) or trifluoromethanesulphonic acid (TFMSA) in case of *Boc* protecting method and 20% TFA in DCM for the *Fmoc* protecting method (Scheme 2).

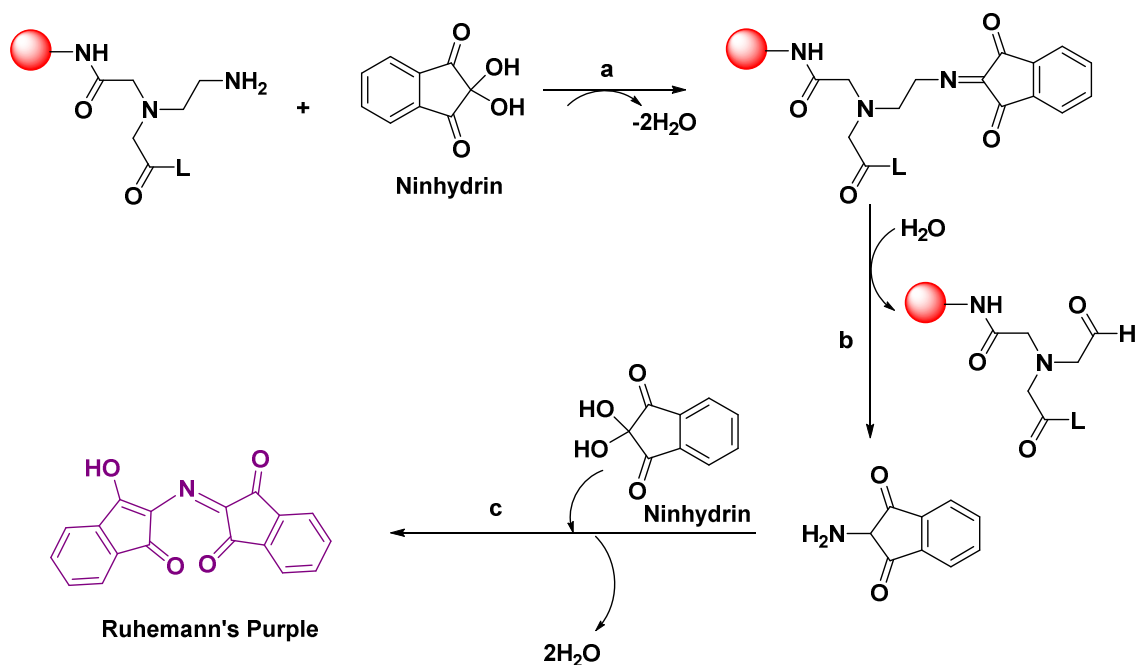


Scheme 2. General strategies for *Boc* and *Fmoc* protecting groups.

### Monitoring of coupling on resin

Successful coupling of amino acid on the resin can be estimated by detecting the amount of unreacted amino groups on the resin.

**Kaiser's test** is the most widely used qualitative test to detect the presence or absence of free amino groups (deprotection/coupling).



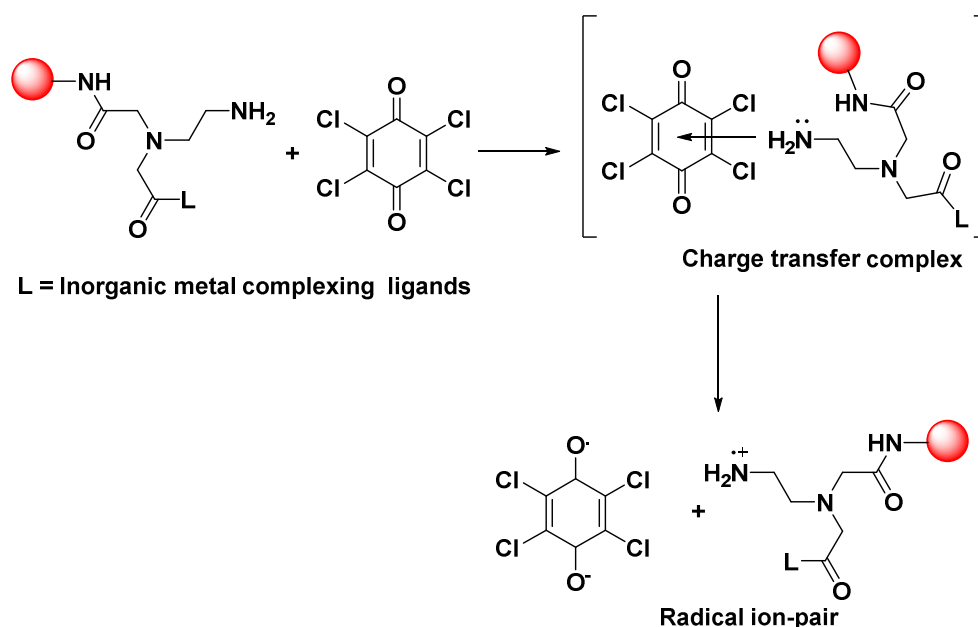
**Scheme 3.** Proposed mechanism for Ninhydrin test: (a) Amine reacts with ninhydrin to generate Schiff's base; (b) Hydrolysis generates amine and aldehyde; (c) Amine reacts with another molecule of nindrin to generate colored compound, Rheumann's purple.



## Chapter 3

It is used to monitor the completion of *t*-Boc deprotection and hence an efficient amide bond (peptide bond) formation. When free amines are present on surface of the resin, it reacts with ninhydrin to produce the purple coloured, Rheumann's purple (Scheme 3). Kaiser's test is negative upon completion of the coupling reaction and the resin beads remain colourless.<sup>47</sup>

**Chloranil test** is highly sensitive towards unreacted primary as well as secondary amines present on the resin beads. Resin is taken in a small test tube, reacted with chloranil and acetone or acetaldehyde. For detection of primary amines, acetaldehyde is added and for secondary amines, acetone is added. The resin beads are left at room temperature for 5 min and colour is checked. When free amines are present on surface of the resin after deprotection, chloranil reacts with it and produces blue colored charge-transfer complex (Scheme 4). On the other hand, upon completion of the coupling reaction, the resin beads remain colourless.



**Scheme 4.** Proposed mechanism for the formation of charge-transfer complex between chloranil and peptides.

### 3.1.7b Gel Filtration Chromatography (GFC)

Gel Filtration Chromatography (GFC) is one of the separation techniques used widely in case of biomolecules. It separates molecules on the basis of size and molecular weight. The stationary phase consists of well-defined porous beads of different sizes having a fractionation range, which controls separation of molecules

based on variable molecular weights. Molecules of smaller molecular weights get trapped inside the porous beads, and eluted in the end, while the high molecular weight biomolecules do not enter the gel pores and are excluded/eluted first.<sup>48</sup>

### 3.1.7c High Performance Liquid Chromatography (HPLC)

High Performance Liquid Chromatography (HPLC) is one of the chromatographic techniques used to separate a complex mixture of compounds. It enables purification and quantification of the individual components in the mixture. It has wide application in analytical chemistry and biochemical research involving separation of wide variety of organic biomolecules and in pharmaceutical industry.

The HPLC instrument typically includes a sample injector, pumps and a detector all under computer control. The sample injector delivers the sample mixture into the mobile phase stream, which is carried into the column and is under the control of gradient mixer. The pump controls the flow and passes the solvents through the column. The detector generates a signal proportional to the amount of sample component emerging from the column, hence allowing quantitative analysis of the sample components. Various detectors used in HPLC are UV/Vis, photodiode array (PDA), refractive index, fluorescence *etc.* HPLC can also be used in a preparative mode to collect the peak of interest for further characterization.

### 3.1.7d High Resolution-Mass Spectrometry (HR-MS)

**Mass spectrometry (MS)** is the science of displaying the *spectra* of masses of the molecules. It is useful in determination of elemental composition, the masses, and the chemical structures of molecules of various classes. It works by ionizing chemical compounds to generate charged molecules or molecule fragments and measuring their mass-to-charge ratios. A *mass spectrometer* instrument consists of four modules:

- ❖ **Inlet probe** for injecting samples.
- ❖ **Ionizer** for converting sample into positively or negatively charged ions.
- ❖ **Mass analyzer** sorts the ions by mass either by *electric field* or by *magnetic field*.
- ❖ **Detector and Amplifier** for converting charged ions into electric current.

The digitalized signal was further processed for getting the mass spectra of the compounds.

The synthesized small peptide units purified by HPLC can be characterized by HR-MS. MS is commonly used in analytical laboratories that study physical, chemical, or biological properties of a great variety of compounds.<sup>49</sup> It can be coupled to liquid chromatography and each peak eluted can be directly characterized by its mass.

### **3.1.7e Matrix Assisted Laser Desorption Ionization-Time of Flight (MALDI-TOF)**

Matrix Assisted Laser Desorption Ionization (MALDI) was first introduced for proteins by M. Karas and F. Hillenkamp (1988) that allows determination of intrinsic molecular masses of nucleic acids.

MALDI-TOF is a key technology which employs 'soft ionization' method.<sup>50</sup> The nucleic acid and protein samples are embedded in a crystalline matrix of a light absorbing molecules (*e.g.*  $\alpha$ -cyano-*p*-hydroxycinnamic acid, nicotinic acid & sinapinic acid).<sup>51</sup> This target is excited by a pulse from an ultraviolet laser beam that in high vacuum results in intact molecules of the sample becoming desorbed into the gas phase and ionized by the UV radiation to give (mostly) singly charged ions. The matrix assists in desorption and ionization of the analyte and molecular weight >500 kDa can be analyzed. The basic concept of TOF mass analyzer (Time Of Flight) is that the ions are separated based on the time taken by the ion to drift down the flight tube to the detector. Lighter ions have higher velocities than heavier ions and reach the detector first.

This technique is very much utilised for oligomers with high molecular weights.

### **3.1.7f X-ray crystal structure determination**

X-ray crystallography is the ultimate method of structure characterization of organic, inorganic and biomolecules. The atoms arranged in the crystal lattice enables X-rays to diffract them in specific angles. After getting the diffraction pattern, electron density map of the structure is derived. This diffraction pattern helps in rendering the important information regarding position of the atoms, specific arrangements as well as chemical bonds and their disorders.<sup>52</sup>

### 3.1.7g Determination of $pK_a$

The acid dissociation constant ( $pK_a$ ) is an important physicochemical parameter of a substance, and its knowledge is of fundamental requisite in a wide range of applications in various research areas.<sup>53</sup> In the pharmaceutical industry,  $pK_a$  is an important factor for drug design and development. The acid–base property of any biomolecule is the key parameter in terms of determining solubility, absorption, distribution, metabolism and elimination.

There are several methods for the determination of dissociation constants like the traditional potentiometry and UV–Vis absorption spectrometry *etc.* In the present studies potentiometry method has been used. Potentiometric titration is a high-precision technique for determining the  $pK_a$  values of substances. It is commonly used due its accuracy and the commercial availability of fast, automated instruments.

### 3.1.8 Metal binding studies of polyamide *aeg* oligomers

The metal binding studies of polyamides is generally performed using optical spectroscopy. The present section focuses on detailed study of optical spectroscopy in the characterization, stoichiometry and binding constants of the metal-ligand complexes.

#### 3.1.8a UV-Vis spectroscopy

Optical spectroscopy is one of the most widely used techniques for the study of stoichiometry and binding constants of metal-ligand complexes.<sup>54</sup> For successful measurements, significant spectral change should occur during complex formation. In any spectrophotometric method, equivalence point is detected due to the difference in the molar absorptivities (at the wavelength selected) of the various species present in the mixture. The appearance of an absorbing species will give a concentration dependent change in absorbance resulting in two straight lines that intersect at the equivalence point. The selection of the analytical wavelength requires care, since at least three components are present that may absorb light: the original substance, the DNA/RNA/oligomer, metal salts and the resulting metal complex. The usual procedure is to select a wavelength at which only one component absorbs. The resulting spectral curves will pass through a common point of intersection, called an

isosbestic point, which shows presence of more than one species in the solution. (Figure 13).

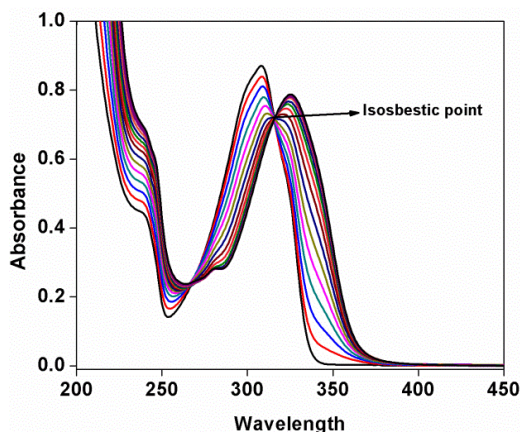


**Figure 13.** Representation of isosbestic point in UV-Vis spectroscopy.

For a successful spectrophotometric titration it is necessary that the measured species adhere roughly to Lambert-Beer's law, and the necessary precautions must be taken to maintain the relation  $A = \epsilon cl$ . To avoid the effects caused by dilution on absorbance, titrant should have 10 times more concentration than the titrated solution.

**Job's Method** was introduced by P. Job (1928) and is used to determine the stoichiometry of components.<sup>55</sup> This method is known as the method of continuous variation and is used to derive quantitative binding relationships in chemical reactions. The total molar concentrations of two binding partners (*i.e.* metal and ligand) are held constant, but the relative mole fractions are varied. The absorption values from the complexation are plotted against the mole fractions of the two components. The maxima or minima on the plot correspond to the stoichiometry of the two binding species (Figure 14).

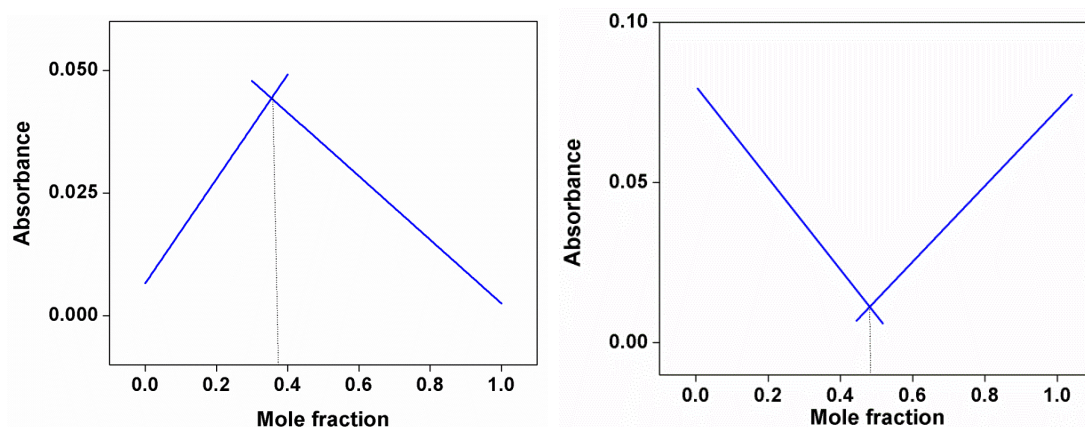


**Figure 14.** Representation of maxima and minima in Job's plot.

There are several conditions that must be considered for Job's method:

- ❖ The system must follow Lambert-Beer law within the concentration range
- ❖ The total mole fractions of two components should be held constant throughout the experiment
- ❖ Total absorption should be in the range of 0.1-1.0
- ❖ pH and ionic strength must be maintained constant

In the present work, studies on the interaction of monomers and oligomers with metal salts have been extensively investigated using UV spectroscopy.

### 3.1.8b Binding constant measurements

The extent of interactions between the two species / complexation is derived from binding constant values. Herein, few techniques employed for the calculation the binding constants have been comprehensively discussed.

#### Optical spectroscopy

The intrinsic binding constant,  $K$ , of the metal complex to monomer/polyamide oligomers can be determined from a Benesi-Hildebrand plot.<sup>56</sup> It is often applied in one-to-one complex systems, such as charge-transfer complexes and host-guest molecular complexation. Benesi-Hildebrand equation has the following form for 1:1 binding systems (Eq. 1):

$$\frac{1}{\Delta A} = \frac{1}{\Delta A_{max}} + \left[ \frac{1}{K[L]} \times \frac{1}{\Delta A_{max}} \right] \quad (\text{Eq. 1})$$

Benesi-Hildebrand equation has the following form for 1:2 binding systems (Eq. 2):

$$\frac{1}{\Delta A} = \frac{1}{\Delta A_{max}} + \left[ \frac{1}{K[L]^2} \times \frac{1}{\Delta A_{max}} \right] \quad (\text{Eq. 2})$$

Where,  $\Delta A = A - A_0$ ,  $A$  is absorbance intensity of ligands in the presence of metal salts.  $A_0$  is absorbance intensity of ligands in the absence of metal salts.  $K$  is equilibrium/ binding constant for the reaction and  $L$  is the ligand concentration. The binding constant ( $K$ ) is determined from the intercept to slope ratio of Benesi-Hildebrand plot. The experiment involves measuring the change in the

absorption/emission spectra of the reaction before and after the formation of the product.

### Magnetic Resonance Spectroscopy (MRS)

NMR is widely used for the binding studies. It throws light on the complexes in the solution. Difference in the chemical shifts of the ligand and metal complexes directly gives evidence in terms of binding as well as site of binding.

### Isothermal Titration Calorimetry (ITC)

Calorimetry is a technique in which the heat of a reaction is measured. The commonly used method for measurement of enthalpy change associated with a binding interaction is isothermal titration calorimetry (ITC).<sup>57</sup> It is utilised for almost any bimolecular binding interaction at a fixed and constant temperature. From the binding isotherms, the equilibrium-binding constant ( $K_b = K_a$ ) and binding stoichiometry ( $n$ ) can be determined.

## 3.2 Present work: Rationale and Objective

The primary idea behind replacing the natural bases linked to *aeg* backbone with ligands that have affinity towards metals, is to generate molecular assembly or molecular wires based on metal-ligand interactions (Figure 15).

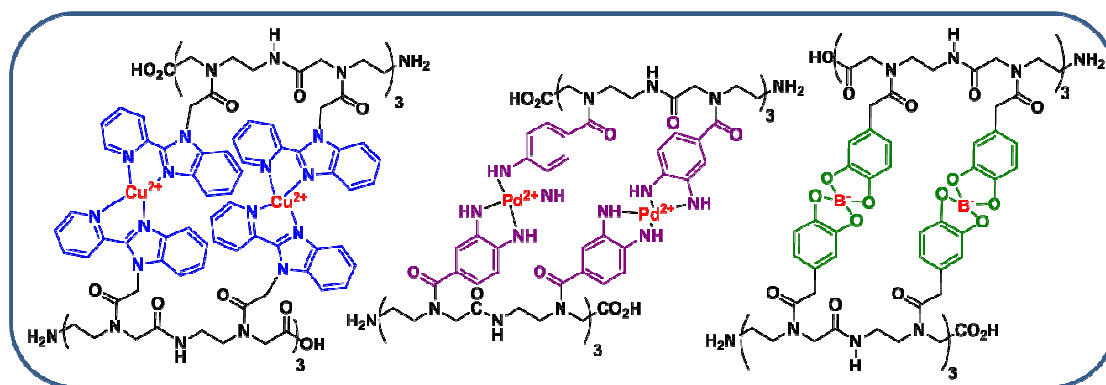


**Figure 15.** Metal complexes with designed ligands linked to *aeg* backbone.

The properties of metal complexes can be tuned by changing metal ions and ligands such as: (1) thermodynamics and kinetics of complexation and decomplexation, (2) change in coordination numbers and geometries, (3) physical and chemical properties such as redox-, magnetic-, optical- and Lewis acidity, and (4)

rational control of assembling properties of the derived oligomers. With above mentioned characteristics in mind, 2-pyridyl benzimidazole (PBI) **1**, phenylenediamine (PDA) **2**, catechol (CAT) **3** were chosen as metal chelating ligands for incorporation of metal ions in *aeg* backbone (Figure 16).

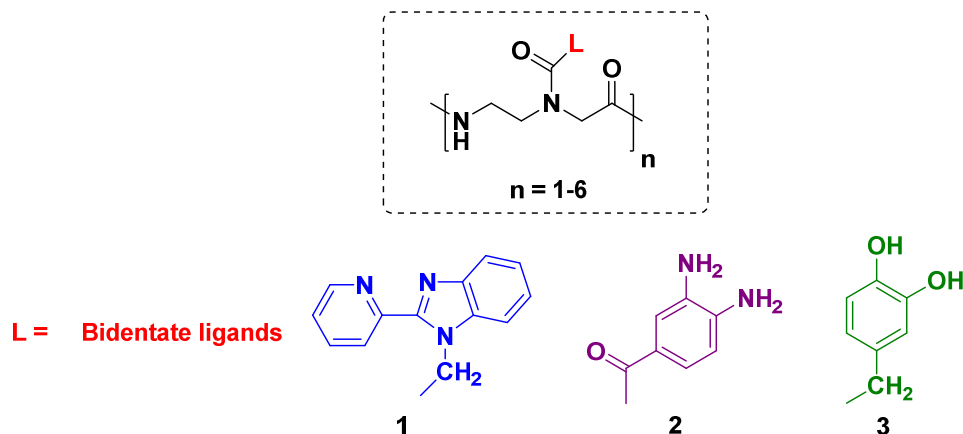


**Figure 16.** Designed novel *aeg* linked bidentate ligands.

Amongst these, 2-pyridylbenzimidazole (PBI) **1** has venerable history in coordination chemistry. The choice of the ligands was made with a view of ease of synthesis, donor/acceptor properties of imidazole and pH triggered assembly and disassembly. Phenylenediamine (PDA) **2** was chosen due to its property of strong affinity towards palladium and gold ions. Catechol (CAT) **3** linked *aeg* ligand was designed for its promising application in drug delivery as it is likely to be a good candidate to form stable complexes with boron. Thus, these peptidic catechols can potentially bind to boron and help deliver to the target tissues/cells. The designed ligands and oligomers are anticipated to form 2:1 metal complexes with different metals *e.g.* PBI with  $\text{Cu}^{2+}$ , PDA with  $\text{Pd}^{2+}$  and CAT with B<sup>-</sup> *etc.*

The designed *aeg* linked ligands are bidentate ligands *i.e.* each ligand has two binding sites. In case of PBI, two quaternary nitrogens are responsible for binding with copper, in PDA two aromatic amines are needed to bind with palladium and in CAT, boron is attached to both of the phenolic groups.

The rationally designed “metallo-oligomers” can form either parallel or antiparallel duplexes upon complexation with metal ions. They can also be useful in generating multimetallic structures analogous to DNA based heterometallic nanowires by metal-coordination based self-assembly of modified aminoethyl glycine (*aeg*)



polyamides. Incorporation of metal ions into aminoethyl glycine (*aeg*) would result in stable complexes as well as a variety of metal based functions (Figure 17).

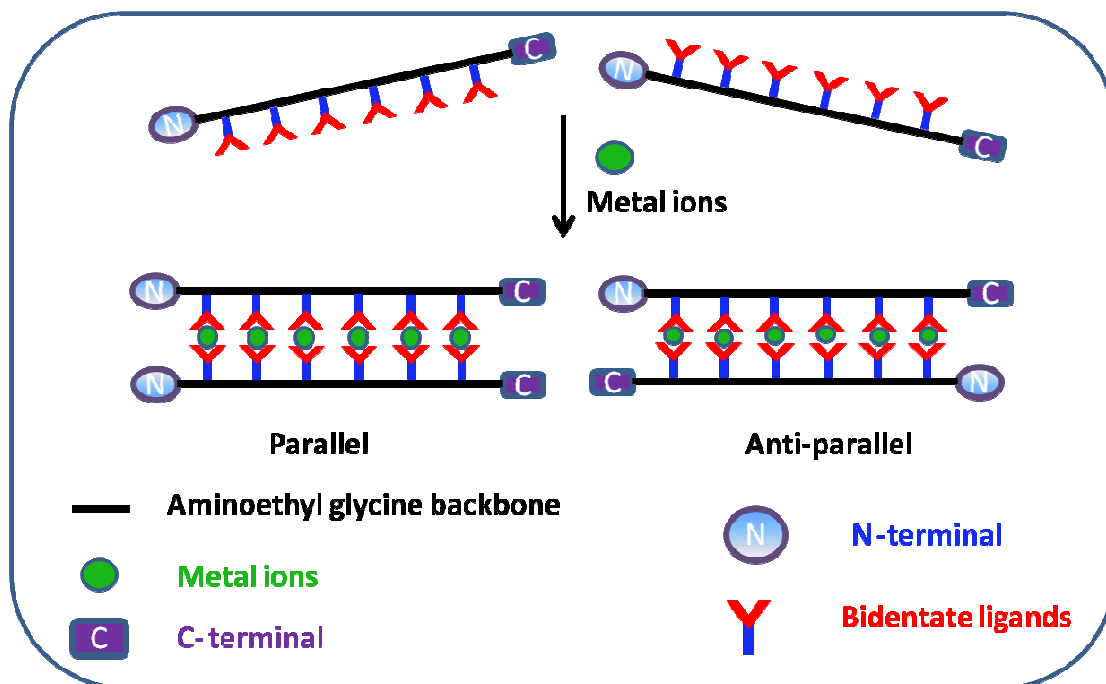


**Figure 17.** Metal mediated duplex formation in modified ligand aminoethyl glycine (*aeg*) strands.

The specific objectives of this work are:

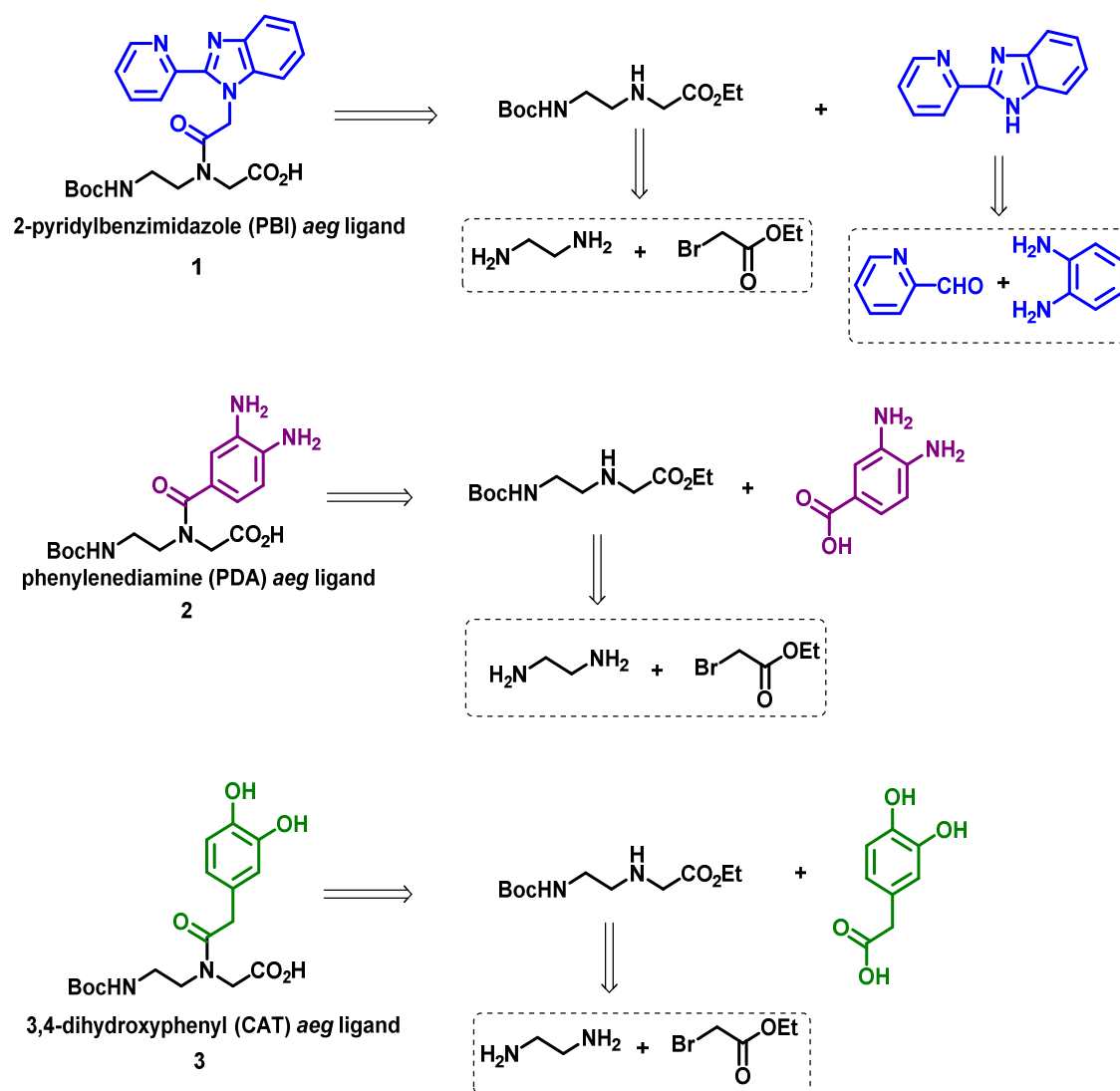
- ❖ Synthesis of metal chelating aminoethyl glycine (*aeg*) linked ligands and their oligomerization.
- ❖ Study of the metal-complexation properties of ligand linked aminoethyl glycine (*aeg*) modified monomers and oligomers.

### 3.3 Results and Discussion

The retrosynthetic pathway (Scheme 5) for each of the target molecule suggests that 1,2-diaminoethane can act as prompt precursor for their synthesis. It can later be functionalized with different reagents and reacted with different substrates to achieve the target monomers. 2-Pyridylbenzimidazole (PBI) **1** *aeg* linked ligand would be obtained from mono-*N*-alkylated-1,2-diaminoethane and 2-pyridylbenzimidazole, which in turn could be synthesized from pyridine-2-aldehyde and *o*-phenylenediamine.<sup>58</sup> *o*-Phenylenediamine (PDA) **2** *aeg* linked ligand could be synthesized from mono-*N*-alkylated-1,2-diaminoethane and 3,4-diaminobenzoic

## Chapter 3

acid. Catechol (CAT) **3** linked *aeg* ligand could be obtained from mono-*N*-alkylated-1,2-diaminoethane and 3,4-dihydroxyphenylacetic acid.

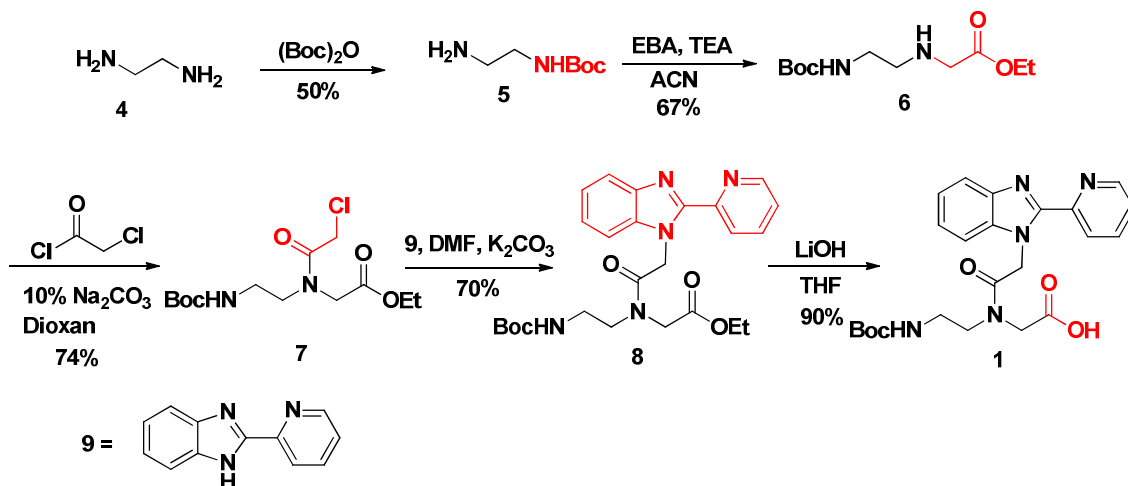


**Scheme 5.** Retrosynthetic pathways towards the synthesis of target *aeg* linked ligands.

### 3.3.1 Synthesis of *N*-Boc-aminoethyl 2-pyridylbenzimidazole (PBI) glycinate

In this account, the synthesis of *aeg* linked ligands were carried out as literature<sup>59</sup> reports starting from the readily available 1, 2-diaminoethane (Scheme 6). The monoprotected derivative of ethylenediamine was prepared by treating a large excess of 1,2-diaminoethane with (Boc)<sub>2</sub>O in dioxane: water under high dilution conditions to minimize the formation of *N*<sup>1</sup>, *N*<sup>2</sup> di-Boc derivative. The formation of product **5** was confirmed by its spectral analysis which was in accordance to the literature data. Compound **5** was *N*-monoalkylated using ethylbromoacetate in

acetonitrile to furnish compound **6** whose structure was confirmed by spectral analysis. Due to the instability of compound **6** at room temperature, it was immediately treated with chloroacetyl chloride in aqueous dioxan containing  $\text{Na}_2\text{CO}_3$  to yield *N*-acyl compound **7** in good yield.



**Scheme 6.** Synthesis of *N*-Boc-aminoethyl-2-pyridylbenzimidazole (PBI) glycinate **1**.

Compound **7** was treated with 2-pyridylbenzimidazole (PBI) to furnish compound **8**, whose structure was confirmed by the appearance of new peaks at  $\delta$  8.57, 8.49 (d, 2H, *CH*) ppm for aromatic protons in  $^1\text{H}$  NMR spectrum. Final hydrolysis of compound **8** with 1N LiOH resulted in the desired monomer **1**, obtained as a white solid in 90% yield. The formation of product **1** was confirmed by its spectral analysis. In  $^1\text{H}$  NMR spectrum, the absence of signals due to ester group protons confirmed the formation of acid **1**.

### 3.3.1a Synthesis of palladium complex with *N*-Boc-aminoethyl-2-pyridyl benzimidazole (PBI) glycinate

*N*-Boc-aminoethyl-2-pyridylbenzimidazole (PBI) glycinate **8** was crystallized from a mixture of ethanol and dichloromethane (2:8), and its structure was confirmed by single crystal X-ray analysis (Figure 18). This was treated with different metal salts to synthesize the corresponding metal complexes. *N*-Boc-aminoethyl-2-pyridylbenzimidazole (PBI) glycinate **8** was reacted with various palladium salts such as sodium tetrachloropalladate, palladium acetylacetonate, palladium nitrate and palladium-*dba* salt, in different molar ratios which resulted in either the formation of a precipitate or viscous liquid. It was found that treatment with palladium acetate in dry

DMF resulted in formation of yellow crystals. The structure of *N*-Boc-aminoethyl-2-pyridylbenzimidazole (PBI) glycinate **8**-Pd complex was determined by single crystal X-ray diffraction analysis.

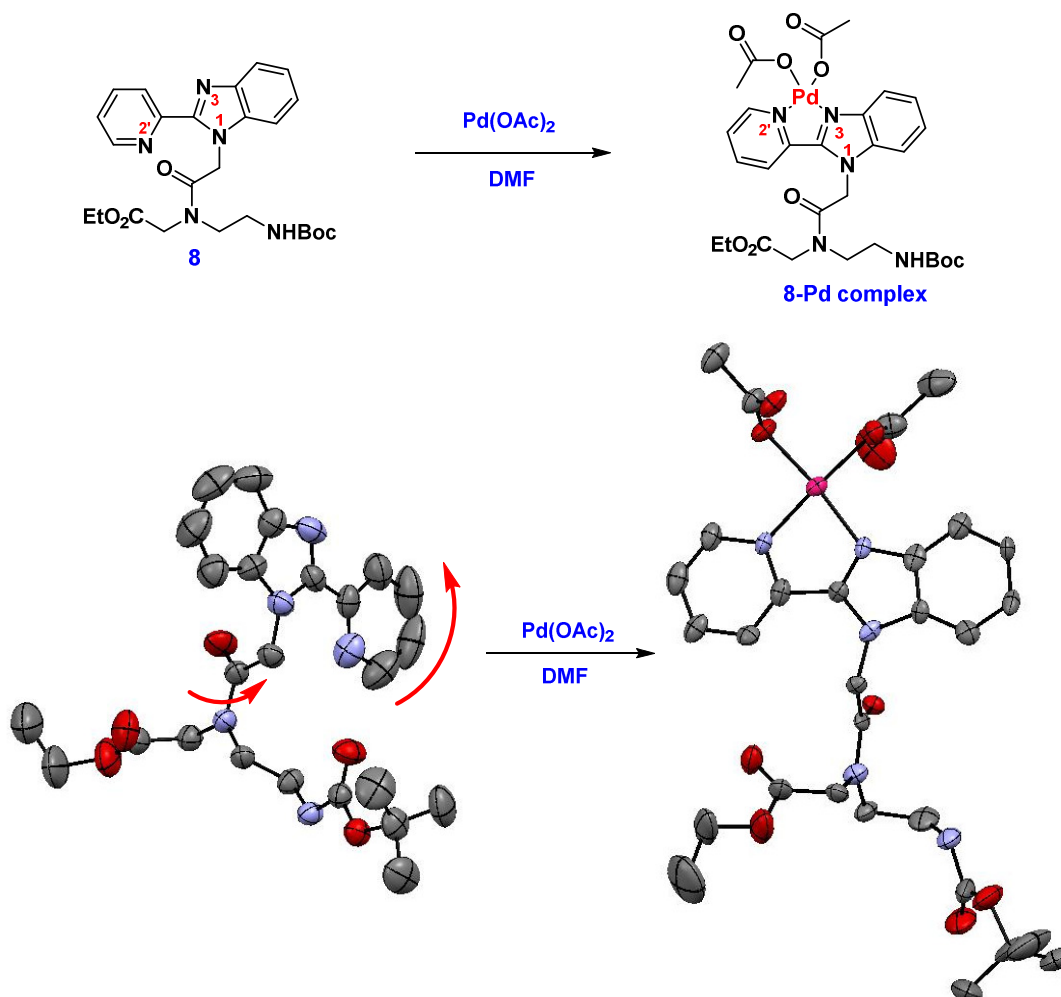


**Figure 18.** ORTEP diagram of *N*-Boc-aminoethyl-2-pyridylbenzimidazole (PBI) glycinate **8** and Pd complex.

The crystal analysis of *N*-Boc-aminoethyl-2-pyridylbenzimidazole (PBI) glycinate **8**-Pd revealed following features:

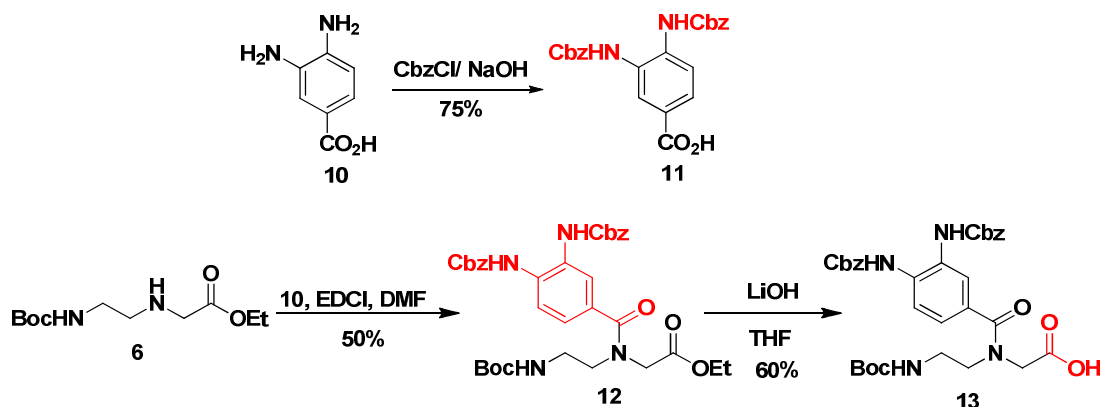
- ❖ The complexation of metal involved two nitrogens, one each from the 2-pyridyl unit (2') and the benzimidazole ring (N<sup>3</sup>).
- ❖ Only 1:1 complex of metal and the *N*-Boc-aminoethyl (PBI) glycinate **8** was observed rather than the expected 2:1 complex.
- ❖ The orientation of the pyridyl nitrogen (2') that act as metal binding site in free ligand shows rotation by 90°.

- ❖ In the *trans* conformation, the pyridyl nitrogen (2') and the nitrogen atom (N<sup>1</sup>) of benzimidazole attached to the *aeg* backbone are in the same plane, while in the *cis* conformation pyridyl nitrogen (2') and other nitrogen atom (N<sup>3</sup>) of benzimidazole are in the same plane (Figure 19).
- ❖ The original *trans* conformation of pyridyl nitrogen (2') and the *N*-benzimidazole moiety (N<sup>1</sup>) switched to *cis* conformation for effective metal complexation.
- ❖ In the ORTEP diagram of *N*-Boc-aminoethyl (PBI) glycinate **8**, it is clear that carbonyl group is oriented towards the glycinate part, while in *N*-Boc-aminoethyl (PBI) glycinate **8-Pd** projection of carbonyl group is towards the *Boc* group.

Similar reaction with other metal salts *i.e.* cobalt nitrate, copper nitrate, nickel nitrate, zinc nitrate did not result in formation of any crystals.

### 3.3.2 Synthesis of *N*-Boc-aminoethyl-*o*-phenylenediamine (PDA) glycinate

3,4-diaminobenzoic acid **10** was treated with *Cbz*Cl in NaOH to obtain the *bis-N,N'*-protected analogue **11** in 75% yield. The identity of compound **11** was confirmed by MALDI-MS, which showed a peak *m/z* at 420, indicating that both the amino groups are protected with *Cbz* group. Compound **6** was treated with the *bis-N,N'*-*Cbz*-protected benzoic acid **11**, in the presence of EDC.HCl and HOBT, to furnish compound **12** in 50% yield. The structural identity of product **12** was confirmed by its spectral analysis (Scheme 7).

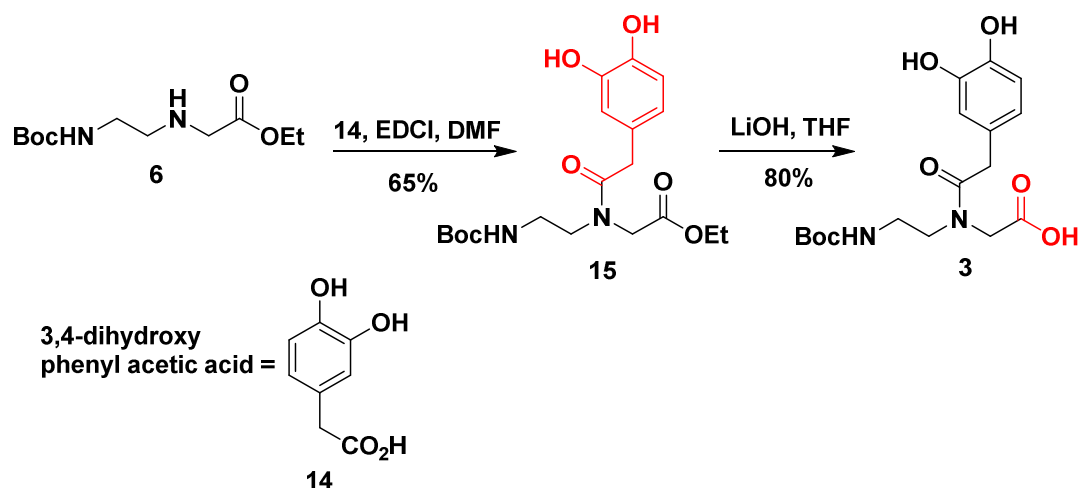


**Scheme 7.** Synthesis of *N*-Boc-aminoethyl-*o*-phenylenediamine (PDA) glycinate **13**.

In  $^1\text{H}$  NMR spectrum, peaks at  $\delta$  7.35-7.24 ppm and in  $^{13}\text{C}$  NMR spectrum, peaks at  $\delta$  135.9, 128.7, 128.5 ppm were observed confirming the attachment of aromatic ring to the *aeg* backbone. The hydrolysis of compound **12** with LiOH (1N) resulted in the desired monomer **13**, in 60% yield. The formation of product **13** was confirmed by its  $^1\text{H}$  NMR spectrum, which showed absence of ester ethyl group protons as expected for product **1**.

### 3.3.3 Synthesis of *N*-Boc-aminoethyl-3,4-dihydroxyphenyl (CAT) glycinate

Compound **6** was treated with 3,4-dihydroxyphenyl acetic acid **14**, in the presence of EDC.HCl and HOBT to furnish compound **15** in 65% yield. The characterization of product **15** was done by its  $^1\text{H}$  NMR spectrum (Scheme 8).



**Scheme 8.** Synthesis of *N*-Boc-aminoethyl-3,4-dihydroxyphenyl (CAT) glycinate **3**.

The presence of peaks at  $\delta$  6.71-6.50 (m, 3H, CH) ppm confirmed the successful coupling of aromatic ring to the *aeg* backbone. The hydrolysis of compound **12** with LiOH (1N) resulted in the desired monomer **3**, whose identity was confirmed by its  $^1\text{H}$  NMR spectrum, which showed the absence of signals due to ethyl ester group protons. Extensive efforts of crystallization culminated in the formation of crystals of compound **15** as white needles (Figure 19). The structure showed the orientation of carbonyl group towards the glycine ester moiety with respect to the phenolic hydroxyl groups.

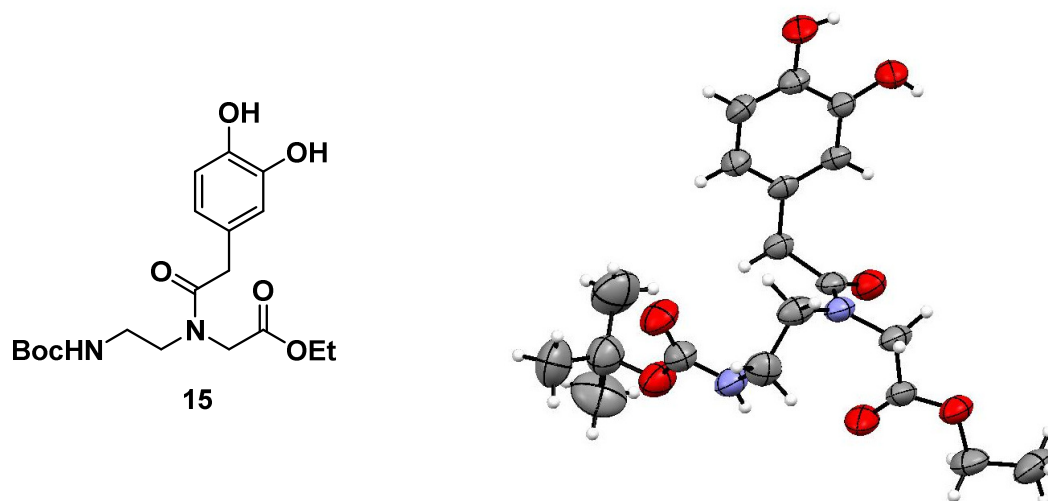
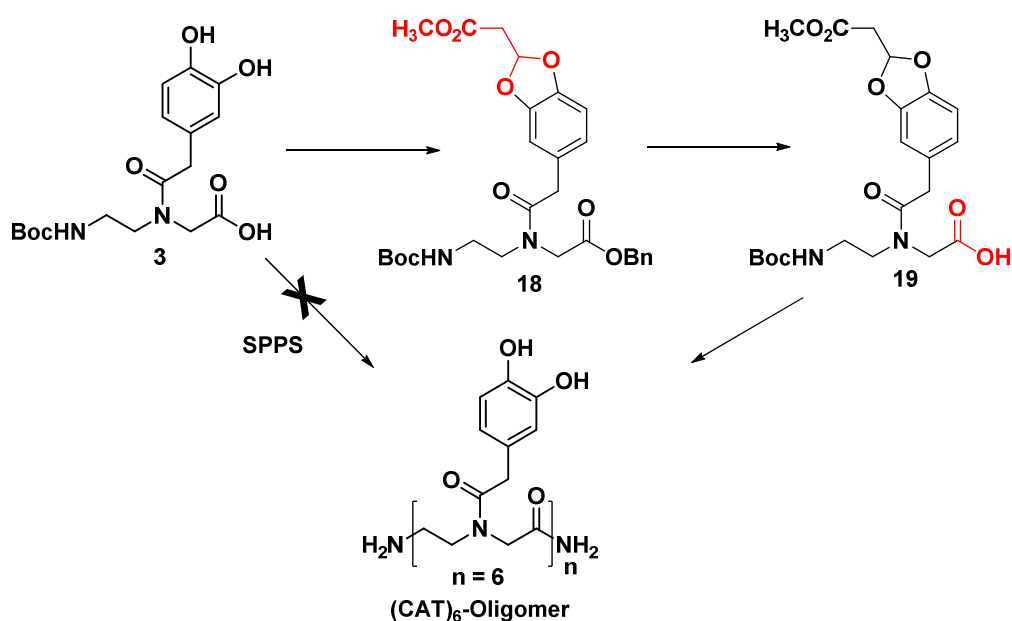


Figure 19. ORTEP diagram of compound 15.

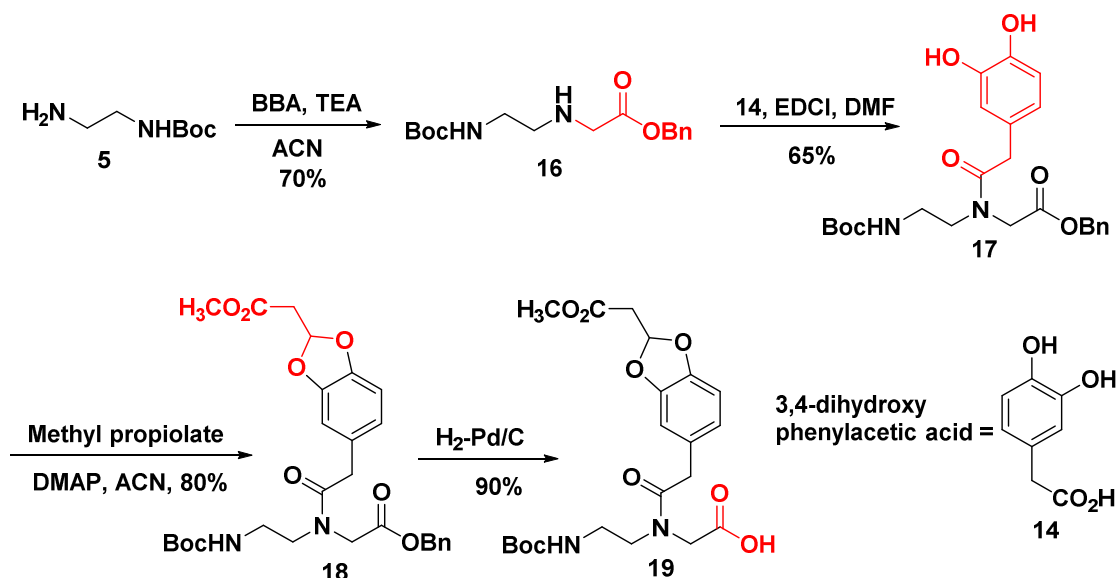
In order to synthesize the catechol derived (CAT)<sub>6</sub> polyamide oligomer, compound **3** was subjected for solid phase peptide synthesis but failed to furnish the desired oligomer, due to presence of unprotected phenolic groups. Thus, a slightly modified synthetic protocol was employed, in which mono-*Boc*-ethylenediamine was alkylated using benzyl bromoacetate instead of ethyl bromoacetate. To synthesize product **18**, catechol hydroxyls should be derivatized with base labile protecting group like 2-moc-ethylidene (acetal) (Scheme 9). The deprotection of benzyl group avoids base and hence would be suited for the present synthesis. The benzyl group of compound **18** could be removed under hydrogenolysis and would furnish title compound **19**.



Scheme 9. Revised synthetic scheme for the synthesis of (CAT)<sub>6</sub> oligomer.

## Chapter 3

Compound **5** was *N*-alkylated using benzyl bromoacetate in acetonitrile to furnish compound **16** (Scheme 10). The formation of product **16** was confirmed by its spectral analysis. In  $^1\text{H}$  NMR spectrum, peaks  $\delta$  7.28-7.25 (*benzyl*) ppm and in  $^{13}\text{C}$  NMR spectrum, peaks at  $\delta$  60.6 ( $\text{OCH}_2$ ) and 14.0 ( $\text{CH}_3$ ) ppm were observed. Due to the instability of compound **16** at room temperature, it was further treated with 3,4-dihydroxyphenyl acetic acid **14**, in presence of EDC.HCl and HOBt to furnish compound **17** in 65% yield. The hydroxyl groups of compound **17** were protected as its 2-Moc-ethylidene (*Mocdene*) acetal derivative **18**, confirmed by the presence of peaks in  $^1\text{H}$  NMR spectrum, at  $\delta$  6.43 (t,  $J = 5.5$  Hz, CH), 3.67 (s,  $\text{OCH}_3$ ) and 2.89 (d,  $J = 5.5$  Hz,  $\text{CH}_2$ ) ppm and in  $^{13}\text{C}$  NMR spectrum, at  $\delta$  109.2 (CH), 51.7 ( $\text{OCH}_3$ ), 48.5 ( $\text{CH}_2$ ) and  $\delta$  168.3 ppm. The debenzoylation of compound **18** using  $\text{H}_2/\text{Pd-C}$  resulted in the desired monomer **19**, in 90% yield, which was confirmed by  $^1\text{H}$  NMR spectrum which also showed the absence of signals due to benzyl group protons.



**Scheme 10.** Synthesis of *Mocdene* protected- *N*-Boc-aminoethyl-3,4-dihydroxyphenyl (CAT) glycinate **19**.

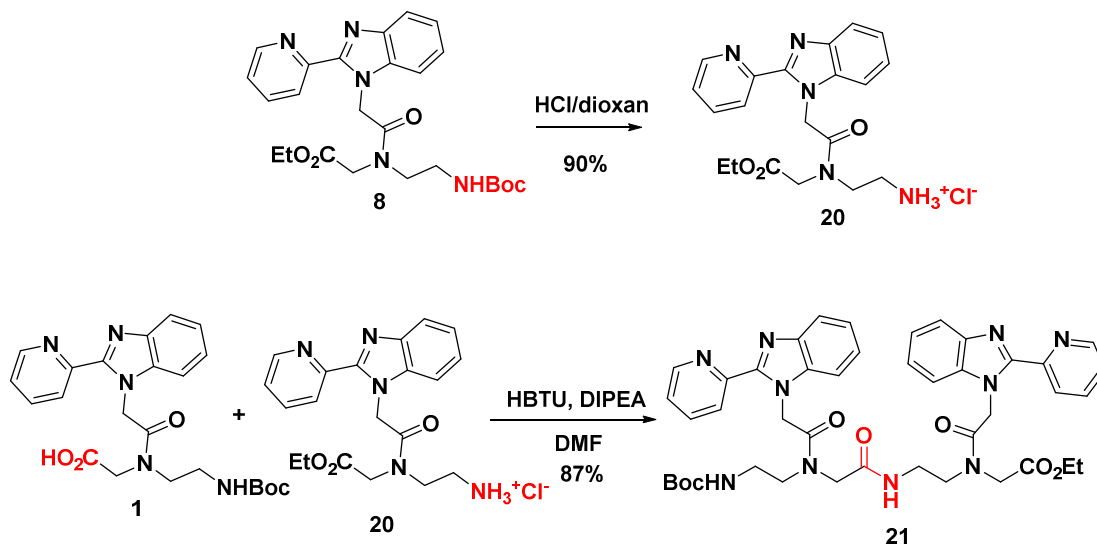
### 3.3.4 Synthesis of *N*-Boc-aminoethyl 2-pyridylbenzimidazole (PBI)<sub>2</sub> (glycinate)<sub>2</sub>

As the length of the *aeg* backbone increases, the resulting metal-linked duplex should become more rigid, giving rise to stronger electronic interactions between adjacent metal centers. Dimerization of the designed metal binding monomers can potentially introduce increasing electronic complexity which can be observed as changes in spectroscopy. With this rationale, dimer of 2-pyridylbenzimidazole was



## Chapter 3

synthesized. The synthesis of *N*-Boc-aminoethyl-2-pyridyl benzimidazole (PBI)<sub>2</sub> (glycinate)<sub>2</sub> **21** was carried out with the coupling of hydrochloride salt of primary amine **20** and acid derivative **1** in the presence of HBTU/DMF in 87% yield (Scheme 11).



**Scheme 11.** Synthesis of *N*-Boc-aminoethyl 2-pyridyl benzimidazole (PBI)<sub>2</sub> (glycinate)<sub>2</sub> **21**.

### Summary

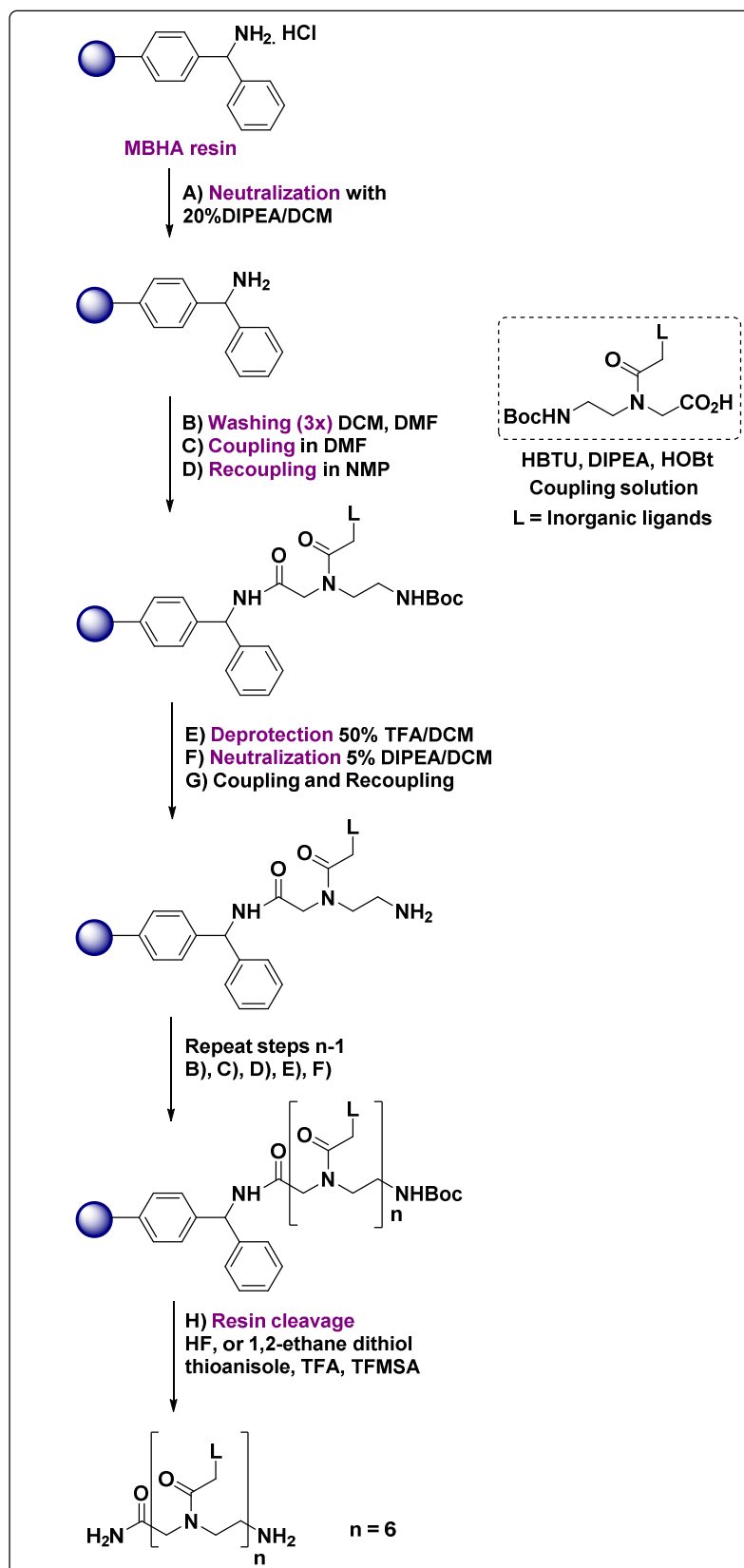
This section has presented the design, synthesis and characterization of novel *aeg*-linked ligand compounds by the successful conjugation of 2-pyridylbenzimidazole (PBI), phenylenediamine (PDA) and catechol (CAT) moiety to *aeg* backbone. All metal complexing monomers have been derived from a common precursor unit, 1,2-diaminoethane. All the intermediates and new compounds have been characterized by <sup>1</sup>H, <sup>13</sup>C NMR spectroscopy and with other appropriate analytical data. Crystal structures of *N*-Boc-aminoethyl 3,4-dihydroxyphenyl (CAT) glycinate **15**, *N*-Boc-aminoethyl (PBI) glycinate **8** and *N*-Boc-aminoethyl (PBI) glycinate **8-Pd** were obtained. The crystal analysis of product **8** and **8-Pd** suggested a conformational switching from *trans* to *cis* for effective complexation.

### 3.4 Synthesis of the polyamide oligomers

The aminoethyl glycyl (*aeg*) polyamide oligomers having metal complexing ligands (**22-28**) were synthesized by manual solid phase peptide synthesis on the readily available 4-methyl-benzhydryl amine (MBHA) resin using standard *t*-Boc protocol from the C-terminus to the N-terminus. The resin after synthesis of polyamide oligomers was cleaved to yield the C-terminal amide peptide.

#### 3.4.1 Solid phase method followed for polyamide oligomers

The hydrochloride salt of MBHA resin was neutralised with 50% DIPEA-DCM and the monomers were coupled as free acids using *in situ* activation with 3 eq. of monomer, HBTU as a coupling reagent and DIPEA, HOBt as catalyst and racemization-suppressant respectively. Subsequently the resin bound *Boc*-group was cleaved with 50% TFA/DCM before coupling the next amino acid. The deprotection and coupling reactions were monitored using Ninhydrin (Kaiser) and chloranil test. A positive color test after the coupling which indicates incomplete reaction and in such cases recoupling was carried out. To avoid deletion of sequences, a capping step with Ac<sub>2</sub>O/DIPEA in DCM was performed. The polyamide oligomers **22-28** were cleaved from the resin at final stage using TFA and TFMSA.



**Scheme 12.** Schematic representation of Solid Phase Peptide Synthesis (SPPS).

In order to complex metal ions on polyamide backbone using metal complexing monomers [2-pyridylbenzimidazole (PBI), phenylenediamine (PDA), catechol (CAT)] and obtain metal linked duplexes, target *homo*-oligomers (PBI)<sub>6</sub> **22**, (PDA)<sub>6</sub> **23**, (CAT)<sub>6</sub> **24** were designed (Figure 20). To study the effect of two different metal complexing units in the same molecule, *hetero*-oligomers of 2-pyridyl benzimidazole (PBI) and catechol (CAT) and those containing 2-pyridyl benzimidazole (PBI) and *o*-phenylenediamine (PDA) either in block units (PBI)<sub>3</sub>-(PDA)<sub>3</sub> **25**, (PBI)<sub>3</sub>-(CAT)<sub>3</sub> **27** or in alternating units (PBI-PDA)<sub>3</sub> **26**, (PBI-CAT)<sub>3</sub> **28** were designed (Figure 21).

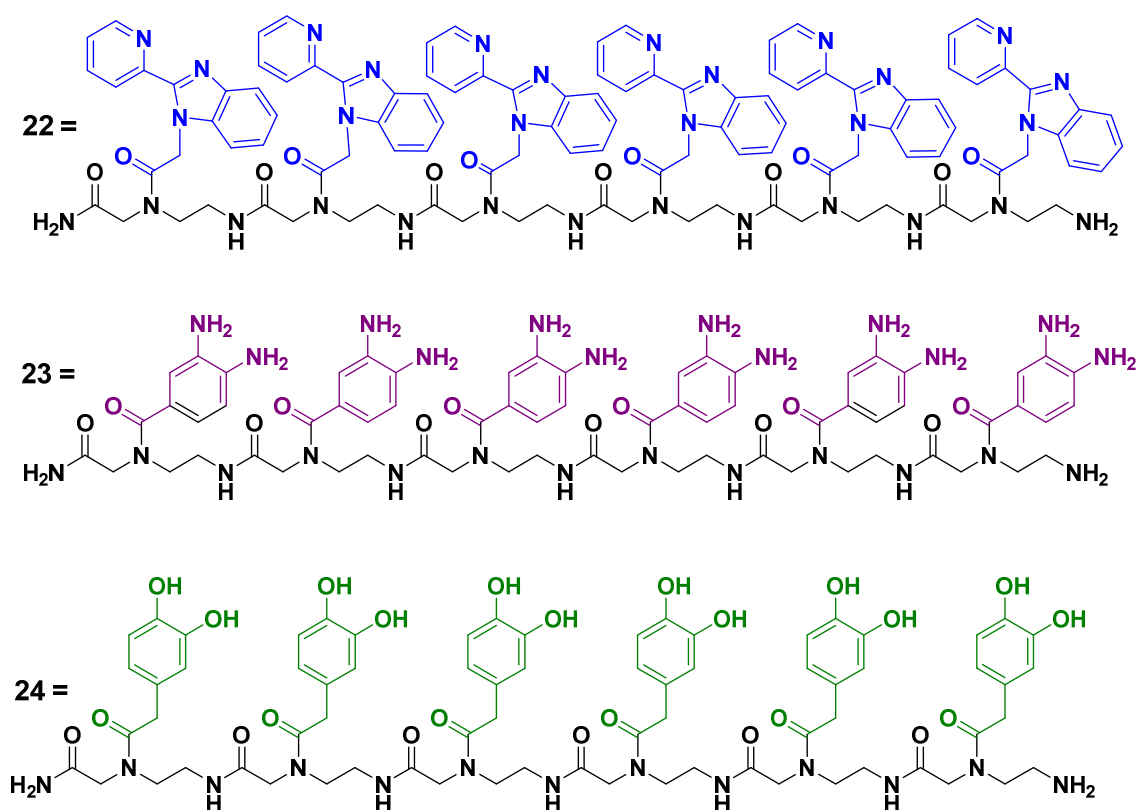


**Figure 20.** Structure of polyamide *homo*-oligomers (PBI)<sub>6</sub> **22**, (PDA)<sub>6</sub> **23**, (CAT)<sub>6</sub> **24**.

### 3.4.2 Cleavage of the oligomers from the solid support

The oligomers were cleaved from the solid support (MBHA resin), using trifluoromethanesulphonic acid (TFMSA) in the presence of trifluoroacetic acid (TFA) to yield *aeg* polyamide oligomers having amide at their C-termini. After cleavage, the polyamide oligomers obtained in solution were precipitated by addition

of cold dry diethyl ether. Various polyamide oligomers synthesized for the present study are shown in Table 3.

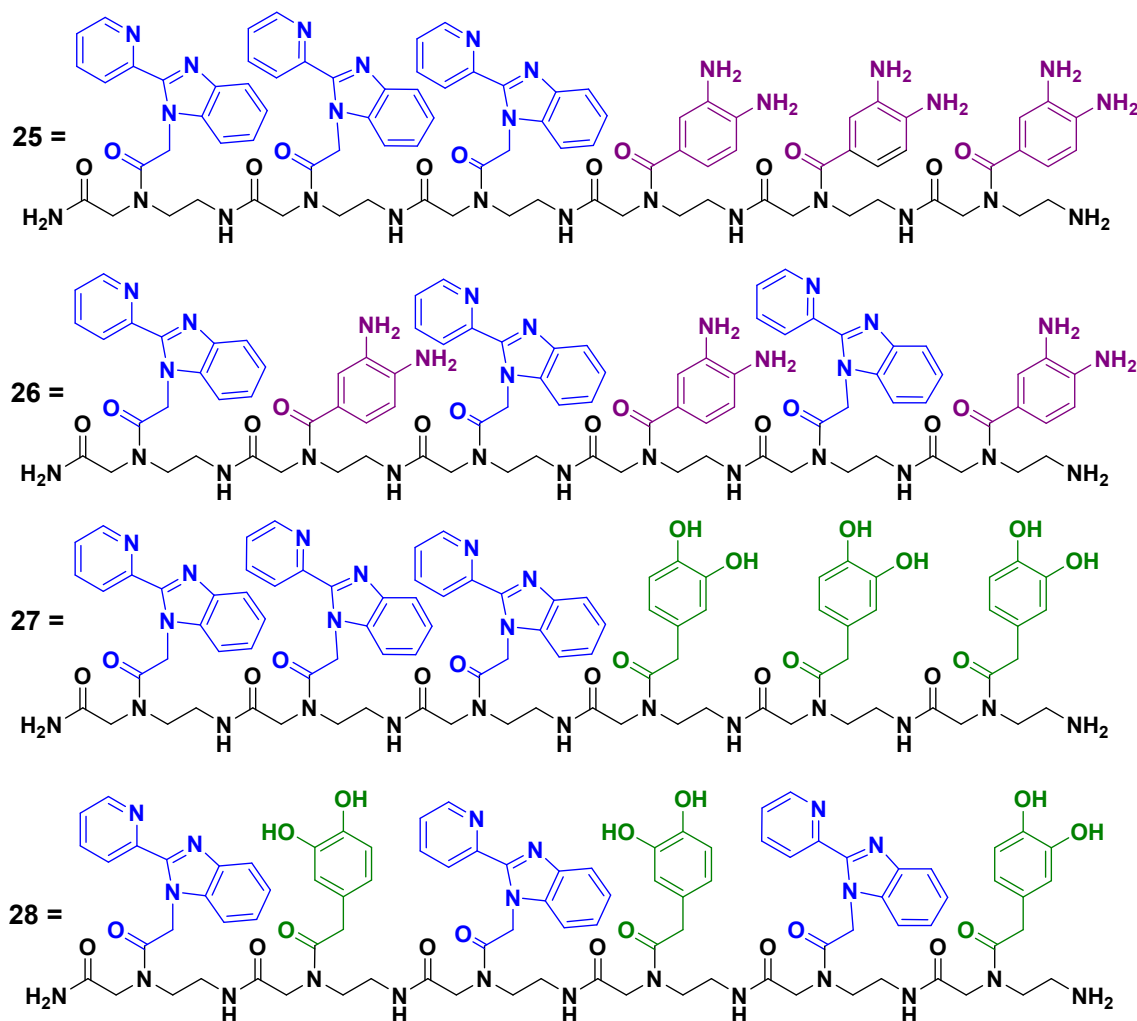


**Figure 21.** Structure of polyamide hetero-oligomers (PBI)<sub>3</sub>-(PDA)<sub>3</sub> **25**, (PBI-PDA)<sub>3</sub> **26**, (PBI)<sub>3</sub>-(CAT)<sub>3</sub> **27** and (PBI-CAT)<sub>3</sub> **28**.

### 3.5 Purification and characterization of the polyamide oligomers

Purification of polyamides has been performed using gel filtration chromatography in which all the cleaved oligomers were passed through sephadex NAP column to remove low molecular weight impurities and their purities were ascertained by HPLC. MALDI-TOF mass spectrometric measurements were done on MDS-SCIEX 4800 mass spectrometer.

### 3.5.1 High Performance Liquid Chromatography (HPLC)

The polyamide oligomers were subsequently purified by RP-HPLC on a semi-preparative C18 column (C18 column, acetonitrile:water system) in 95-99% purity and their purity were ascertained by analytical RP-HPLC. The HPLC retention time and mass data of the synthesized polyamide oligomers are given in Table 3 and their representative HPLC profiles are shown in Figure 22.

**Table 3.** HPLC retention time and MALDI-TOF mass spectral analysis of oligomers

Oligomers	HPLC (RT min)	Mol. Formula	$M_{(Calcd)}^*/M_{(Found)}$
(PBI) <sub>6</sub> <b>22</b>	14.2	C <sub>108</sub> H <sub>105</sub> N <sub>31</sub> O <sub>12</sub>	2029.19/ 2052.048 [M+Na] <sup>+</sup>
(PDA) <sub>6</sub> <b>23</b>	4.11	C <sub>66</sub> H <sub>87</sub> N <sub>25</sub> O <sub>12</sub>	1422.5573/ 1445.036 [M+Na] <sup>+</sup>
(CAT) <sub>6</sub> <b>24</b>	11.0	C <sub>72</sub> H <sub>87</sub> N <sub>13</sub> O <sub>24</sub>	1518.5339/ 1541.479 (M+Na) <sup>+</sup>
(PBI) <sub>3</sub> - (PDA) <sub>3</sub> <b>25</b>	9.24	C <sub>87</sub> H <sub>96</sub> N <sub>28</sub> O <sub>12</sub>	1725.8735/ 1725.771
(PBI-PDA) <sub>3</sub> <b>26</b>	11.9	C <sub>87</sub> H <sub>96</sub> N <sub>28</sub> O <sub>12</sub>	1725.8735/ 1748.844 [M+Na] <sup>+</sup>
(PBI) <sub>3</sub> - (CAT) <sub>3</sub> <b>27</b>	12.6	C <sub>90</sub> H <sub>96</sub> N <sub>22</sub> O <sub>18</sub>	1772.7273/ 1796.793 [M+Na] <sup>+</sup>
(PBI-CAT) <sub>3</sub> <b>28</b>	13.0	C <sub>90</sub> H <sub>96</sub> N <sub>22</sub> O <sub>18</sub>	1772.7273/ 1796.413 [M+Na] <sup>+</sup>

\*Molecular weights were calculated using chemdraw 12.0.

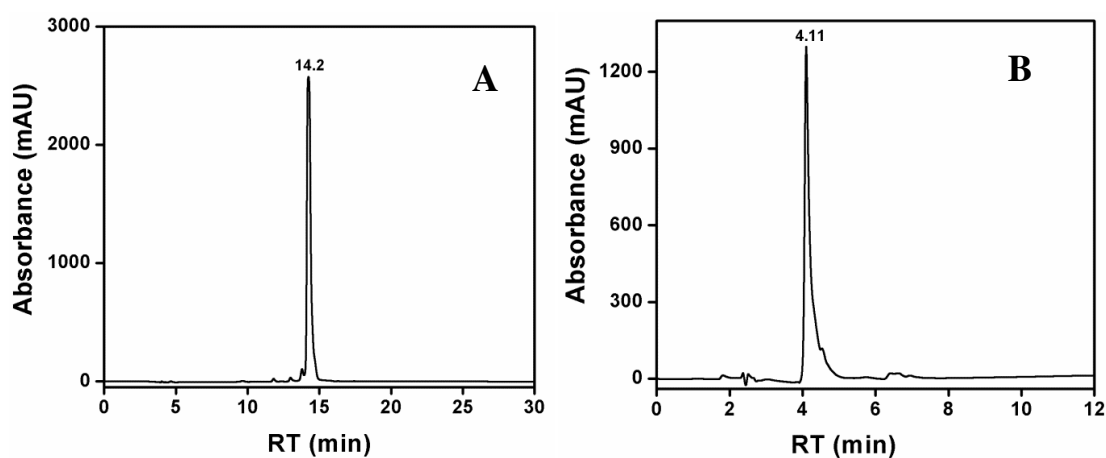


**Figure 22.** HPLC of polyamide oligomers (A) (PBI)<sub>6</sub> **22**, (B) (PDA)<sub>6</sub> **23**.

### 3.5.2 Matrix Assisted Laser Desorption Ionization-Time of Flight (MALDI-TOF) characterization

The molecular weights of polyamide oligomers were confirmed by MALDI-TOF mass spectrometric analysis. The observed molecular weight along with the calculated molecular weight and the molecular formula of all the polyamide oligomers are given in Table 3. The MALDI-TOF data for the synthesized polyamide oligomers were shown in Figure 23. All the oligomers exhibited corresponding  $[M]^+$  or  $[M + Na]^+$  peaks.

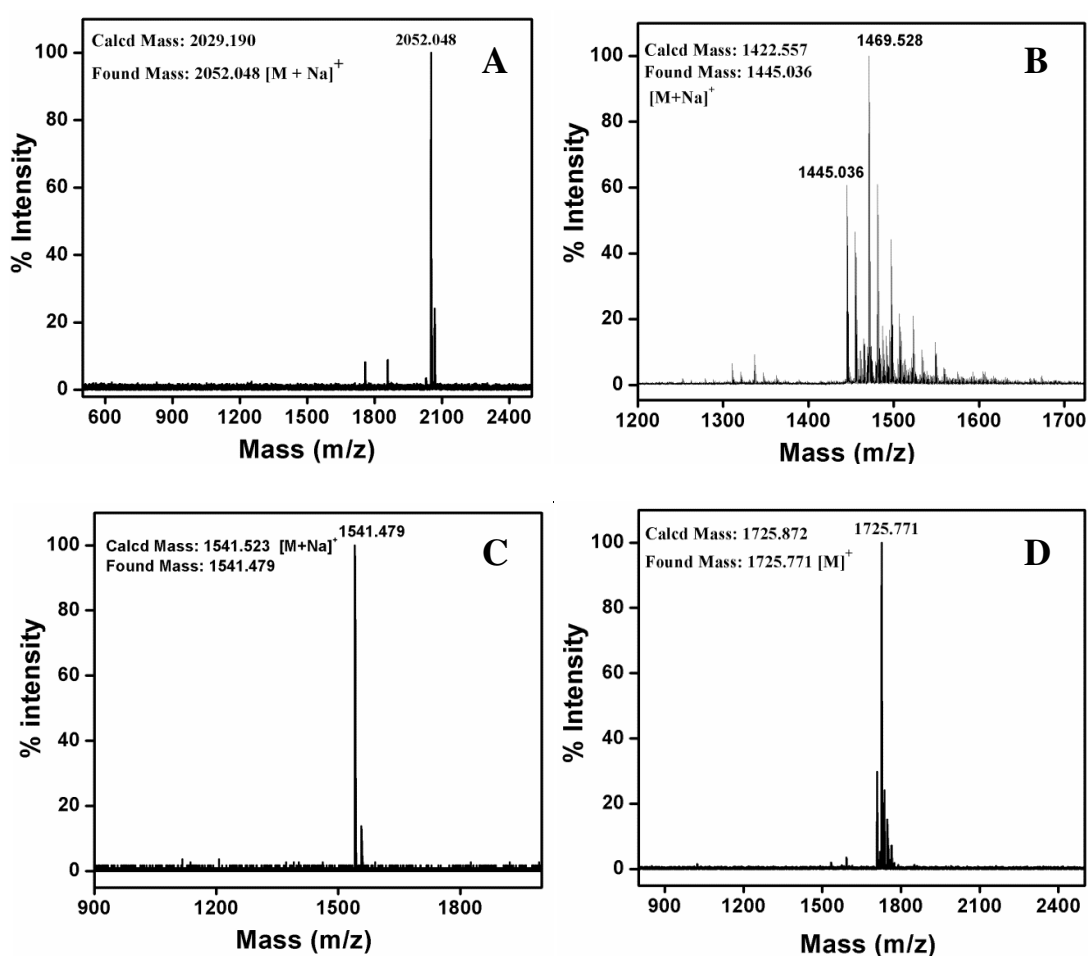


**Figure 23.** MALDI-TOF of polyamide oligomers (A) (PBI)<sub>6</sub> **22**, (B) (PDA)<sub>6</sub> **23**, (C) (CAT)<sub>6</sub> **24** and (D) (PBI)<sub>3</sub>-(PDA)<sub>3</sub> **25**.

### 3.6 Molar Extinction Coefficients of polyamide oligomers

Determination of the exact concentration of the small amounts of peptides is always difficult. Initially the empty microfuge tubes are weighed and the solution containing HPLC purified peptides oligomers (PBI)<sub>6</sub> **22**, (PDA)<sub>6</sub> **23**, (CAT)<sub>6</sub> **24**, (PBI)<sub>3</sub>-(PDA)<sub>3</sub> **25**, (PBI-PDA)<sub>3</sub> **26**, (PBI)<sub>3</sub>-(CAT)<sub>3</sub> **27** and (PBI-CAT)<sub>3</sub> **28** is transferred. The solvent is evaporated further, dried under vacuum for several hours and the peptide is stored over phosphorus pentoxide (P<sub>2</sub>O<sub>5</sub>). The weight of the peptide is determined by deducting the empty weight from the recorded weight of the microfuge tubes after drying.

The synthesized polyamide oligomers were dissolved in precise amount of water to get accurate concentration (Figures 24-26). The molar extinction coefficients were determined from UV-Vis spectrophotometric method. According to the Lambert-Beer's law, if the absorbing species has a molar concentration  $c$  and the sample thickness or path length is  $l$ , the absorbance is given by

$$A = \epsilon cl$$

where,  $\epsilon$  is defined as the molar absorption coefficient or molar extinction coefficient. In order to calculate the molar extinction coefficient, known amounts of the de-ionized water was added and the absorbance spectra of the different concentrations of oligomeric solutions were recorded on UV-Vis spectrophotometer.

The concentration is plotted against absorbance and a linear fitting gives the slope which is known as the molar extinction coefficient ( $\epsilon$ ) of the oligomers solution. The representative plots for molar extinction coefficient ( $\epsilon$ ) are mentioned in the Tables 4-10 below.

Conventionally, molar extinction coefficient ( $\epsilon$ ) for the monomer units is calculated and for the higher oligomers, the value is calculated by the multiplication of the number of repeating monomer units in the same solvent. This method also helps in evaluating presence of any secondary structures.



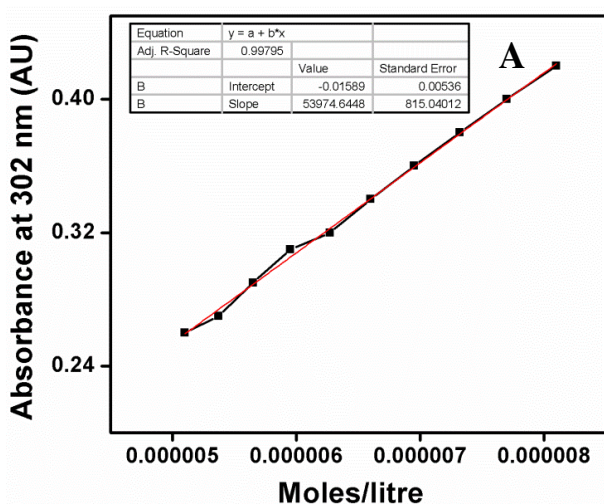


**Table 4:** Conc. vs absorbance plot at 302 nm for (PBI)<sub>6</sub> **22**

Conc. (μM)	Absorbance at 302 nm
8.0	0.42
7.6	0.40
7.3	0.38
6.9	0.36
6.6	0.34
6.3	0.32
5.9	0.31
5.6	0.29
5.4	0.27
5.1	0.26

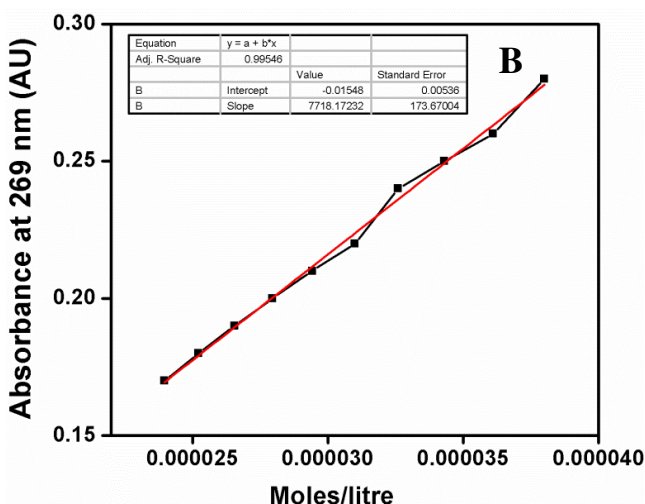


**Table 5:** Conc. vs absorbance plot at 269 nm for (PDA)<sub>6</sub> **23**

Conc. (μM)	Absorbance at 269 nm
38.0	0.28
36.1	0.26
34.3	0.25
32.6	0.24
31.0	0.22
29.4	0.21
27.9	0.20
26.5	0.19
25.2	0.18
23.9	0.17

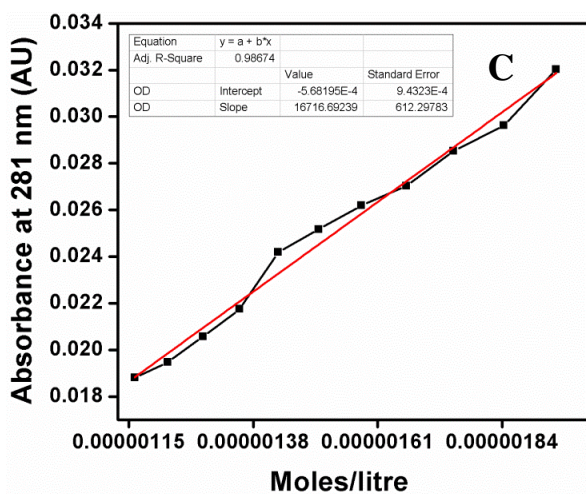


**Table 6:** Conc. vs absorbance plot at 281 nm for (CAT)<sub>6</sub> **24**

Conc. (μM)	Absorbance at 281 nm
1.94	0.032
1.84	0.029
1.75	0.028
1.66	0.027
1.58	0.026
1.42	0.025
1.35	0.024
1.28	0.021
1.22	0.019
1.16	0.018

**Figure 24.** Concentration vs absorbance plots for calculating molar extinction coefficient ( $\epsilon$ ) for polyamide oligomer (A) (PBI)<sub>6</sub> **22** (B) (PDA)<sub>6</sub> **23** (C) (CAT)<sub>6</sub> **24**.

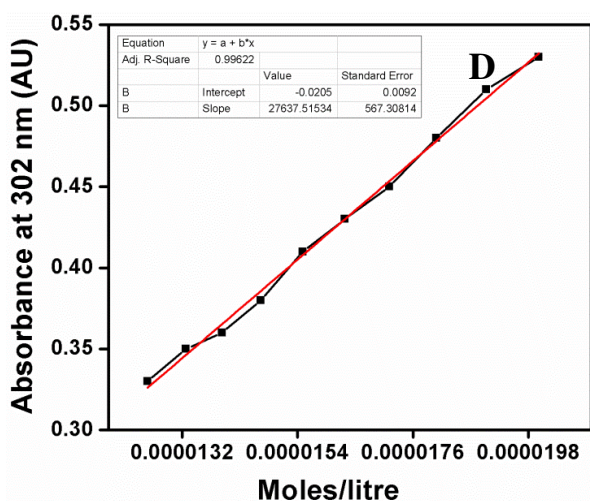


**Table 7:** Conc. vs absorbance plot at 302 nm for (PBI)<sub>3</sub>-(PDA)<sub>3</sub> **25**

Conc. (μM)	Absorbance at 302 nm
20.0	0.53
19.0	0.51
18.1	0.48
17.2	0.45
16.3	0.43
15.5	0.41
14.7	0.38
13.9	0.36
13.3	0.35
12.6	0.33

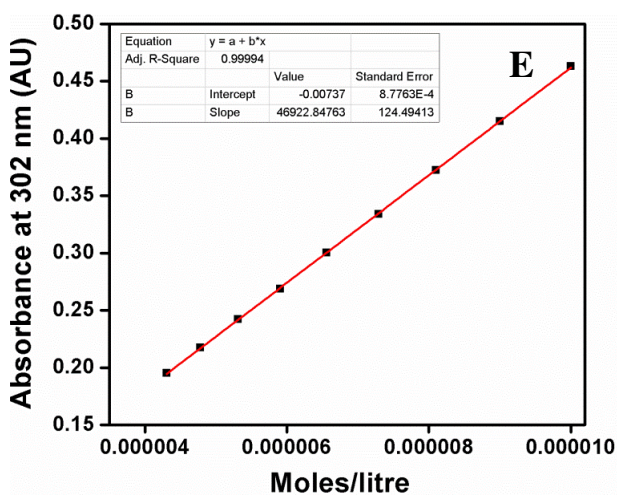


**Table 8:** Conc. vs absorbance plot at 302 nm for (PBI-PDA)<sub>3</sub> **26**

Conc. (μM)	Absorbance at 302 nm
10.0	0.46
9.0	0.41
8.1	0.37
7.29	0.33
6.56	0.30
5.90	0.27
5.31	0.24
4.78	0.22
4.30	0.19

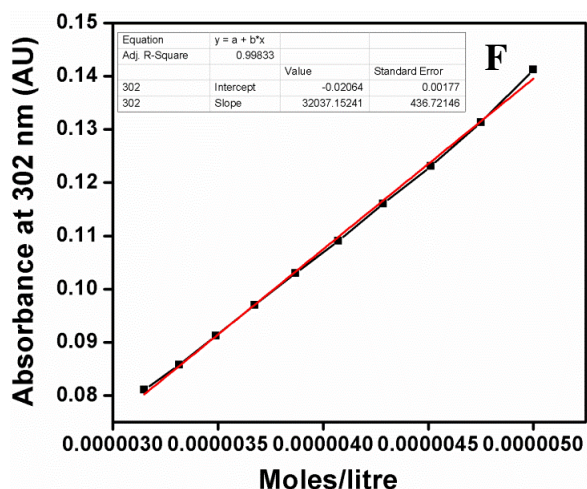


**Table 9:** Conc. vs absorbance plot at 302 nm for (PBI)<sub>3</sub>-(CAT)<sub>3</sub> **27**

Conc. (μM)	Absorbance at 302 nm
5.0	0.141
4.75	0.131
4.51	0.123
4.29	0.116
4.07	0.109
3.86	0.102
3.67	0.099
3.49	0.091
3.31	0.085
3.15	0.081

**Figure 25.** Concentration vs absorbance plots for calculating molar extinction coefficient ( $\epsilon$ ) for polyamide oligomer (D) (PBI)<sub>3</sub>-(PDA)<sub>3</sub> **25**, (E) (PBI-PDA)<sub>3</sub> **26** (F) (PBI)<sub>3</sub>-(CAT)<sub>3</sub> **27**.

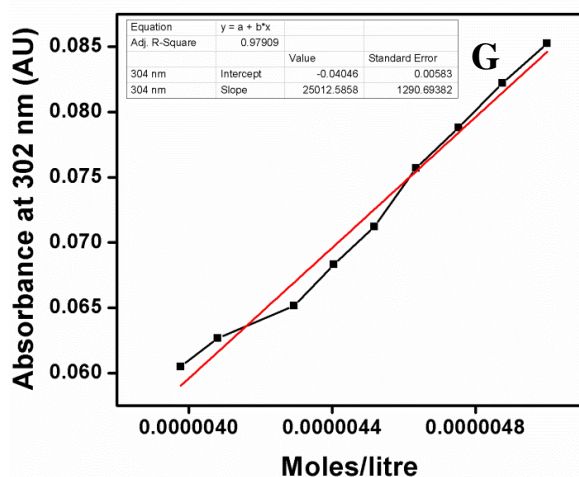


**Table 10:** Conc. vs absorbance plot at 302 nm for (PBI-CAT)<sub>3</sub> **28**

Conc. (μM)	Absorbance at 302 nm
5.0	0.085
4.87	0.082
4.75	0.078
4.63	0.076
4.52	0.071
4.41	0.068
4.29	0.065
4.08	0.063
3.98	0.061

**Figure 26.** Concentration vs absorbance for calculating molar extinction coefficient ( $\epsilon$ ) for polyamide oligomer (G) (PBI-CAT)<sub>3</sub> **28**.

The synthesized polyamide oligomers were solubilized in deionized water and their molar extinction coefficients are summarized in Table 11.

**Table 11.** Molar Extinction Coefficients ( $\epsilon$ ) for the polyamide oligomers

Oligomer	Molar Extinction Coefficient ( $\epsilon$ ) (mM <sup>-1</sup> cm <sup>-1</sup> )
(PBI) <sub>6</sub> <b>22</b>	53.9
(PDA) <sub>6</sub> <b>23</b>	7.72
(CAT) <sub>6</sub> <b>24</b>	16.7
(PBI) <sub>3</sub> - (PDA) <sub>3</sub> <b>25</b>	27.6
(PBI-PDA) <sub>3</sub> <b>26</b>	46.9
(PBI) <sub>3</sub> - (CAT) <sub>3</sub> <b>27</b>	32.0
(PBI-CAT) <sub>3</sub> <b>28</b>	25.0

In conclusion, it was seen that (PBI)<sub>6</sub> had the highest value of the molar extinction coefficient than all the other polyamide oligomers synthesized, perhaps due to its higher conjugation.

The polyamide oligomer (PBI-PDA)<sub>3</sub> **26** is found to have almost double the value of molar extinction coefficient in comparison to (PBI)<sub>3</sub>-(PDA)<sub>3</sub> **25**, this may be attributed to stable dimeric assembly formed by the former; Exactly the opposite was observed in case of oligomer (PBI-CAT)<sub>3</sub> **28**, which has lesser molar extinction coefficient as compared to (PBI)<sub>3</sub>-(CAT)<sub>3</sub> **27**. In general polyamide oligomers of 2-pyridylbenzimidazole (PBI) and phenylenediamine (PDA) possess comparatively larger molar extinction coefficient value than that of -pyridylbenzimidazole (PBI) and catechol (CAT) oligomers. The reason may be that PDA is devoid of one extra methylene carbon of the aminoethyl glycol (*aeg*) chain, providing better conjugation.

### 3.7 Determination of $pK_a$ of synthesized oligomers

Potentiometric titration is a high-precision technique for determination of  $pK_a$  values of compounds. It is commonly used due its accuracy and the commercial availability of fast, automated instruments. The dissociation constant of uncharged substances (hydrophobic organic molecules) in aqueous-organic mixtures is not only ruled by electrostatic interactions but also with specific solute-solvent interactions (solvation effects).

In order to determine aqueous  $pK_a$  values, synthesized polyamide oligomers were subjected to potentiometric titrations. The pH of oligomers (8-20  $\mu$ M, 2 mL) in deionized water was first adjusted to 2.0-2.5 using HCl (50%). This solution was titrated with 2.5  $\mu$ L aliquots of aq. NaOH (0.5 M). After each addition of NaOH solution aliquot, pH of the solution was recorded. The pH of the sample solution changes rapidly at the  $pK_a$  of the functional group. The  $pK_a$  values were derived from the first derivative of the plot of pH vs volume of NaOH (Figure 27).

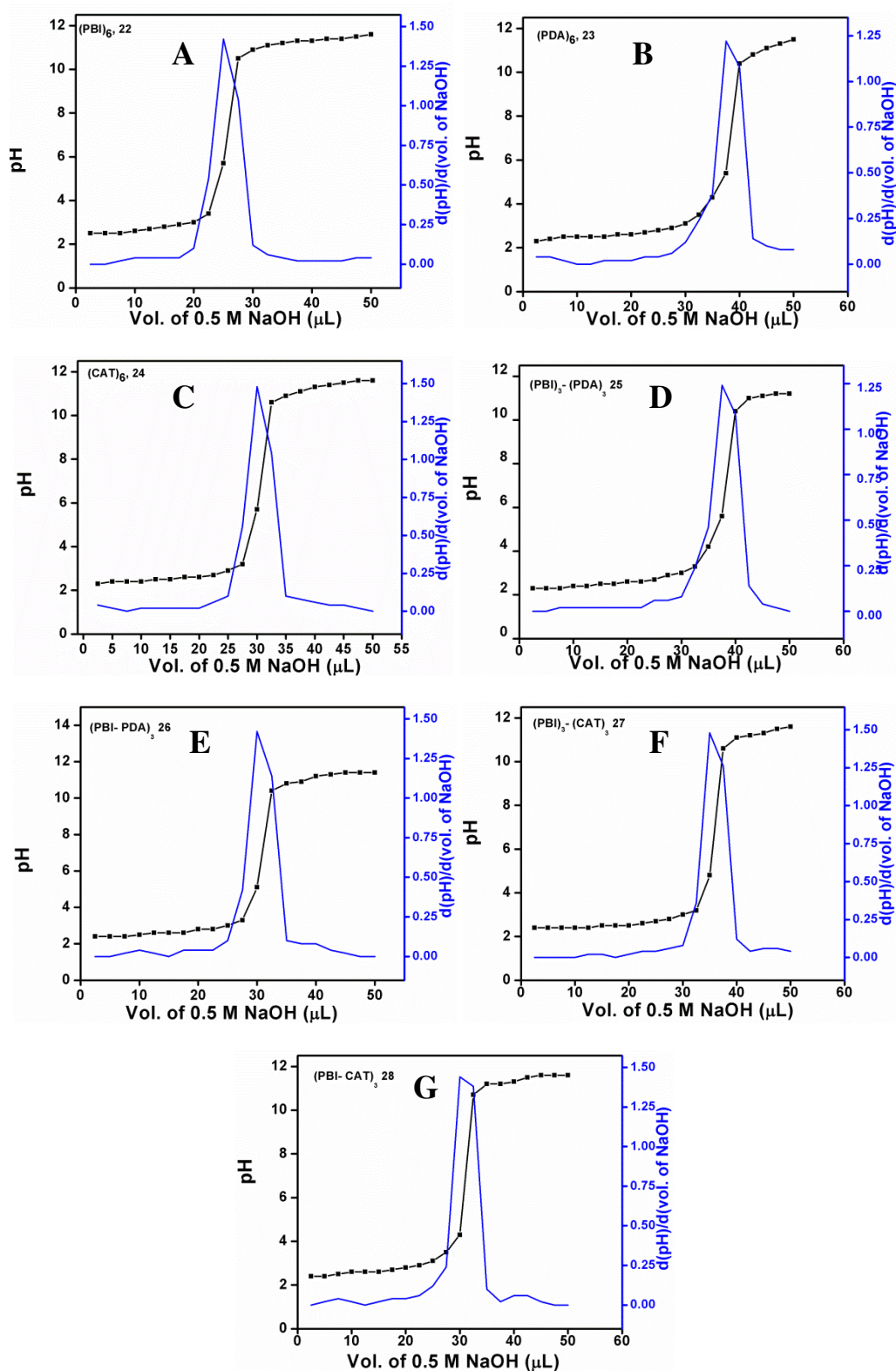


**Figure 27.** Potentiometric pH titration of polyamide oligomers with NaOH (0.5 M) (A)  $(\text{PBI})_6$  22, (B)  $(\text{PDA})_6$  23, (C)  $(\text{CAT})_6$  24, (D)  $(\text{PBI})_3-(\text{PDA})_3$  25, (E)  $(\text{PBI-PDA})_3$  26, (F)  $(\text{PBI})_3-(\text{CAT})_3$  27, (G)  $(\text{PBI-CAT})_3$  28.

The  $pK_a$  values for the synthesized polyamide ligands are shown in Table 12.

**Table 12.**  $pK_a$  for the synthesized polyamide oligomers and reported derivatives

Oligomer	$pK_a$	Literature reports <sup>53</sup>	$pK_a$
(PBI) <sub>6</sub> <b>22</b>	5.7	Pyridine	5.2
(PDA) <sub>6</sub> <b>23</b>	5.4	Benzimidazole	5.5
(CAT) <sub>6</sub> <b>24</b>	5.7	3,4-Dihydroxybenzoic acid	4.5
(PBI) <sub>3</sub> <sup>-</sup> (PDA) <sub>3</sub> <b>25</b>	5.6	<i>o</i> -Phenylenediamine	4.6
(PBI-PDA) <sub>3</sub> <b>26</b>	5.1		
(PBI) <sub>3</sub> <sup>-</sup> (CAT) <sub>3</sub> <b>27</b>	4.8		
(PBI-CAT) <sub>3</sub> <b>28</b>	4.3		

(PBI)<sub>6</sub> **22** has two nitrogens, one from the pyridine (N2') and other from the benzimidazole (N3) are quite acidic and in literature,<sup>53</sup>  $pK_a$  values for the pyridine and benzimidazole has been reported to be 5.2 and 5.5, respectively. The presence of different nitrogens in the molecule with closer  $pK_a$  values often leads to only single. However, it is to be noted that the  $pK_a$  of 2-pyridylbenzimidazole may be slightly different when it is part of a larger peptide chain. The  $pK_a$  for (PBI)<sub>6</sub> was observed to be 5.7 (Figure 28).

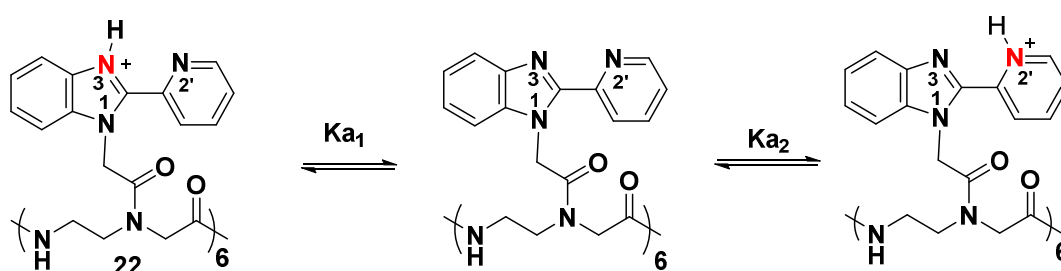


**Figure 28.** Acid base equilibria of (PBI)<sub>6</sub> polyamide oligomer **22**.

In case of (PDA)<sub>6</sub> polyamide oligomers **23**, both the 3,4-diamino groups are acidic and display a single transition. In literature,<sup>53</sup>  $pK_a$  for the *o*-phenylenediamine has been reported to be 4.6 and  $pK_a$  obtained for the (PDA)<sub>6</sub> is 5.4 (Figure 29). Thus, an increment of 0.8  $pK_a$  was observed for the oligomer.

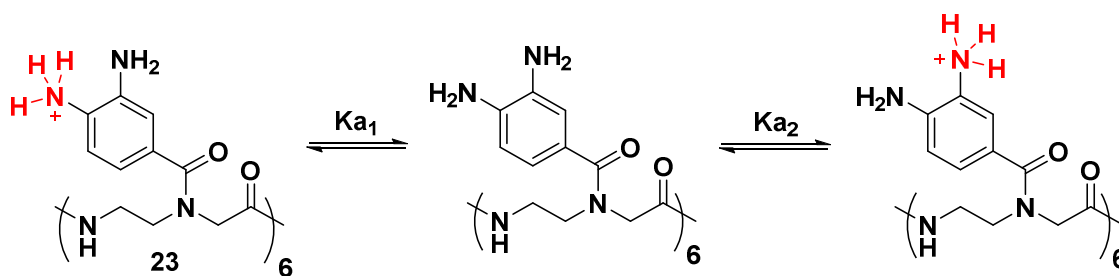


**Figure 29.** Acid base equilibria of (PDA)<sub>6</sub> polyamide oligomers **23**.

(CAT)<sub>6</sub> polyamide oligomer **24**, also possesses acidic 3,4-dihydroxy groups. The  $pK_a$  for the (CAT)<sub>6</sub> was observed to be 5.7 and literature<sup>53</sup> value of  $pK_a$  for the 3,4-dihydroxybenzoic acid has been reported to be 4.5 (Figure 30). Thus, an increment of 1.2  $pK_a$  was observed for the (CAT)<sub>6</sub> oligomer.

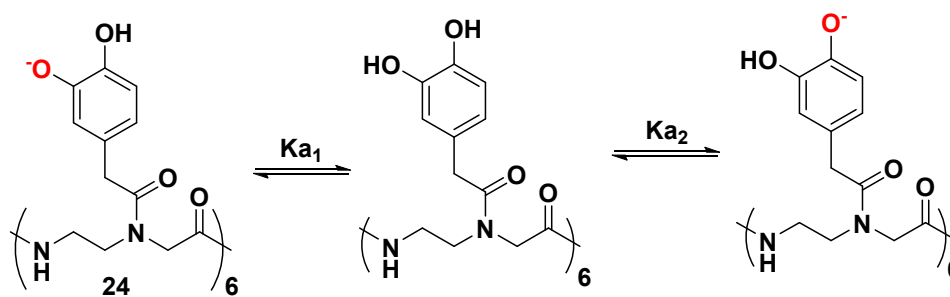


**Figure 30.** Acid base equilibria of (CAT)<sub>6</sub> polyamide oligomers **24**.

In conclusion, it is observed that both (PBI)<sub>6</sub> **22**, (CAT)<sub>6</sub> **24** possess same values of  $pK_a$  (5.7) and (PDA)<sub>6</sub> **23** possess slightly lower value of  $pK_a$  (5.4). The oligomers (PBI)<sub>6</sub> **22**, (CAT)<sub>6</sub> **24** are less acidic (larger  $pK_a$ ) as compared to (PDA)<sub>6</sub> **23**. In case of *hetero*-oligomers it is difficult to state that observed  $pK_a$  is due to which functional group. *Hetero*-oligomers of 2-pyridylbenzimidazole (PBI) and phenylenediamine (PDA) possess comparatively larger  $pK_a$  values and hence are less acidic than those of 2-pyridylbenzimidazole (PBI) and catechol (CAT).

## Summary

This section has demonstrated the synthesis of novel polyamide oligomers by incorporation of metal binding 2-pyridylbenzimidazole (PBI), phenylenediamine (PDA) and catechol (CAT) moieties utilizing the solid phase peptide synthesis (SPPS). It deals with the synthesis of polyamide oligomers having two units of different monomers either in block or alternative arrangements. All the synthesized

## Chapter 3

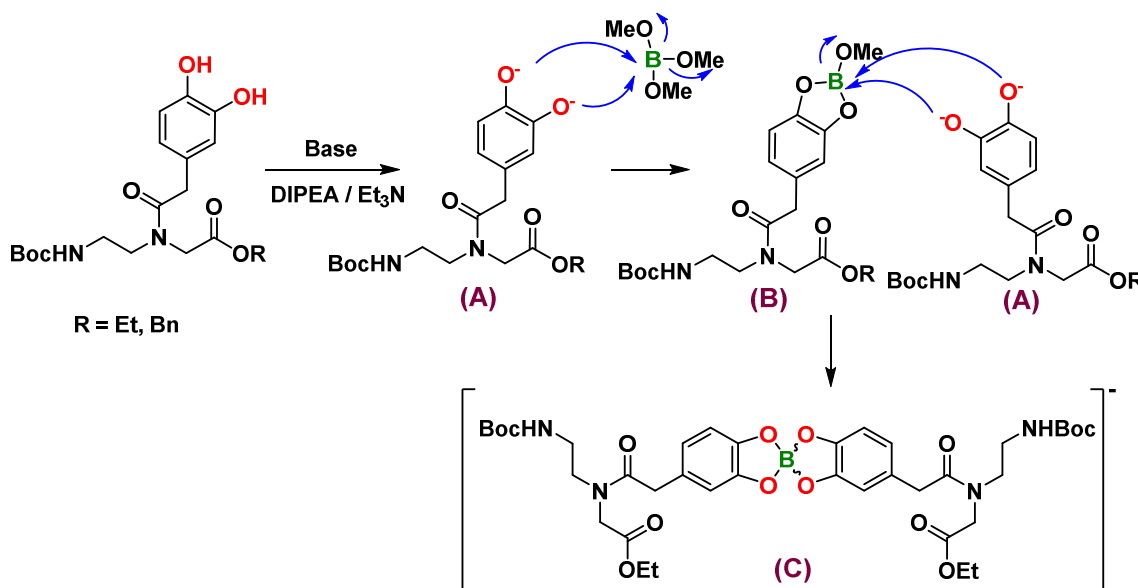
---

polyamide oligomers were purified by High Pressure Liquid Chromatography (HPLC), and subsequently their molecular weights were confirmed by the MALDI-TOF analysis. Molar extinction coefficients ( $\epsilon$ ) were calculated from the calibration curve of absorbance versus concentration.  $pK_a$  of the synthesized polyamide oligomers were calculated according to the potentiometric methods.<sup>53</sup>



### 3.8 NMR studies

In order to assess the binding characteristics of catechol with trimethylborate, NMR studies were undertaken as reported in the literature.<sup>60</sup> Phenolic hydroxyl groups are acidic in nature and capable of binding with different metal ions. Catechols bind efficiently with boron ions and the complexation-decomplexation can be tuned with pH change. The postulated mechanism for catechol (CAT) linked *aeg* ligand and boron complexation is depicted in Scheme 13.



**Scheme 13.** Postulated mechanism of catechol (CAT) linked *aeg* ligands with trimethyl borate.

The mechanism involves deprotection of the catechol groups with bases like triethylamine or diisopropyl ethylamine to furnish the phenoxide intermediate (A). The generated phenoxide intermediate (A) reacts with trimethyl borate to form intermediate (B), which subsequently reacts with another molecule of (A) to generate the desired the final complex (C).

#### 3.8.1 NMR studies on ethyl-*N*-Boc-aminoethyl-3,4-dihydroxyphenyl (CAT) glycinate **15**

Ethyl-*N*-Boc-aminoethyl-3,4-dihydroxyphenyl (CAT) glycinate **15** was first reacted with triethylamine to generate the phenoxide ions and was subsequently treated with stoichiometric amounts of trimethylborate to form the metal complexes. In  $^1\text{H}$  NMR spectra of ethyl-*N*-Boc-aminoethyl-3,4-dihydroxyphenyl (CAT) glycinate **15**, signals for the phenolic hydroxyl group appeared at  $\delta$  8.80 in  $\text{DMSO}-d_6$  and after

complexation with boron, this signal disappeared and a new signal due to triethylamine salt appeared at  $\delta$  8.31 ppm (Figure 31).

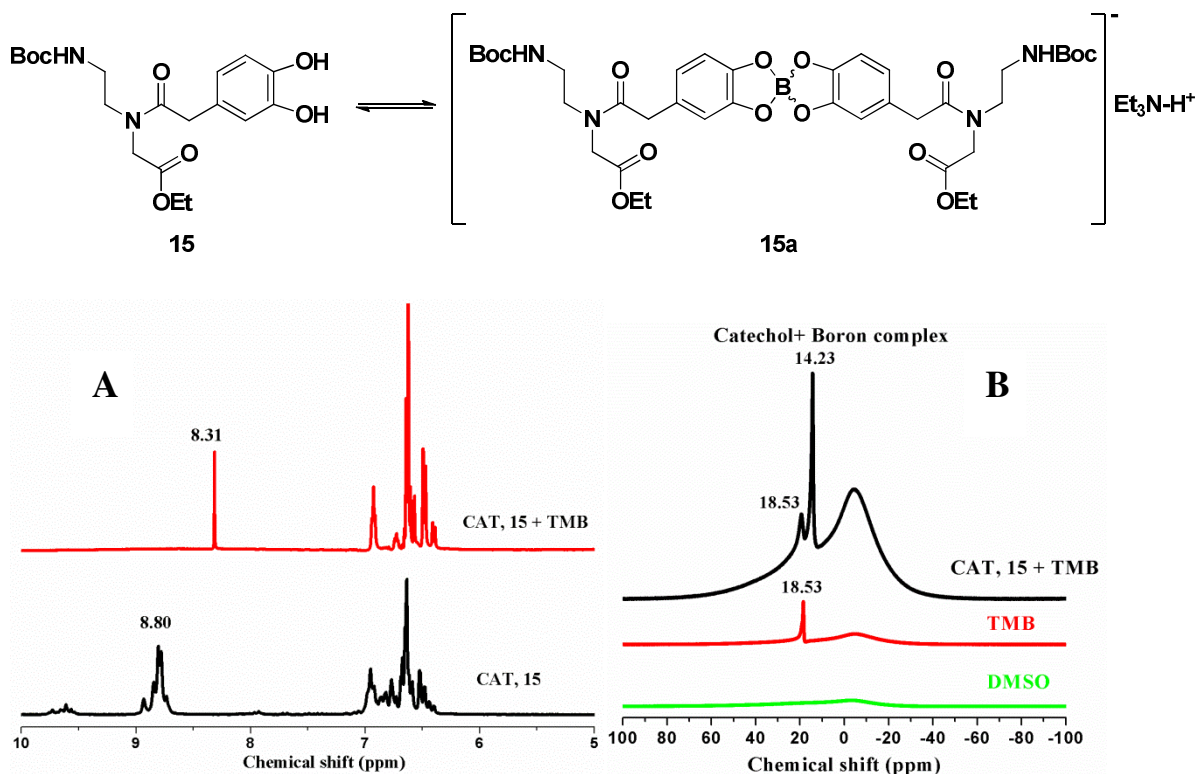


**Figure 31.** NMR studies of ethyl-*N*-Boc-aminoethyl-3,4-dihydroxyphenyl (CAT) glycinate **15** and trimethyl borate (A)  $^1\text{H}$  NMR, (B)  $^{11}\text{B}$  NMR in  $\text{DMSO-}D_6$ .

In  $^{11}\text{B}$  NMR, the signal for the trimethyl borate appeared at  $\delta$  18.53 ppm, whereas in the complex, it appeared upfield at  $\delta$  14.23 ppm. These results clearly indicate the binding of catechol groups with trimethyl borate, to form the 2:1 [Ethyl-*N*-Boc-aminoethyl-3,4-dihydroxyphenyl (CAT) glycinate **15**:boron] complex **15a**.

### 3.8.2 NMR studies on the benzyl *N*-Boc-aminoethyl-3,4-dihydroxy phenyl (CAT) glycinate, **17**

Just as with the ethyl ester derivative, benzyl-*N*-Boc-aminoethyl-3,4-dihydroxyphenyl (CAT) glycinate **17** upon treatment with trimethyl borate provided a 2:1 complex. In  $^1\text{H}$  NMR spectra, resonances for the aromatic protons that appears at  $\delta$  6.59 of the benzyl-*N*-Boc-aminoethyl-3,4-dihydroxyphenyl (CAT) glycinate **17**-boron complex in  $\text{DMSO-}d_6$  appeared upfield at  $\delta$  6.30 ppm upon complexation. Consequently, the proton signals at  $\delta$  8.73 ppm (OH) coming from the phenolic hydroxyl group completely disappeared upon its complexation with boron (Figure 32).

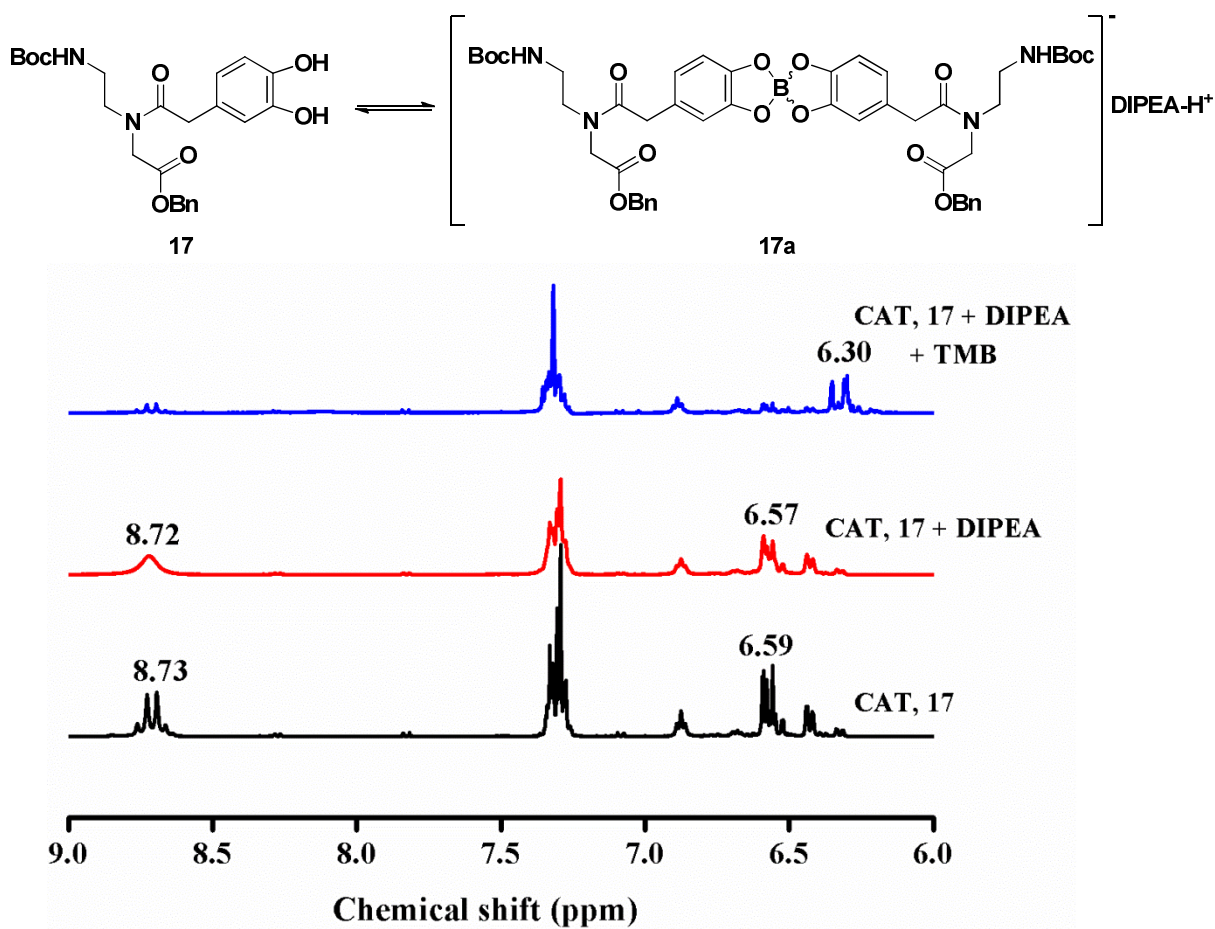


**Figure 32.**  $^1\text{H}$  NMR studies of benzyl-*N*-Boc-aminoethyl-3,4-dihydroxyphenyl (CAT) glycinate **17** and trimethyl borate in  $\text{DMSO-d}_6$ .

In conclusion, both the designed ethyl and benzyl-*N*-Boc-aminoethyl-3,4-dihydroxyphenyl (CAT) glycinate **15** and **17** reacted with trimethyl borate to form the 2:1 complex (Figure 33).

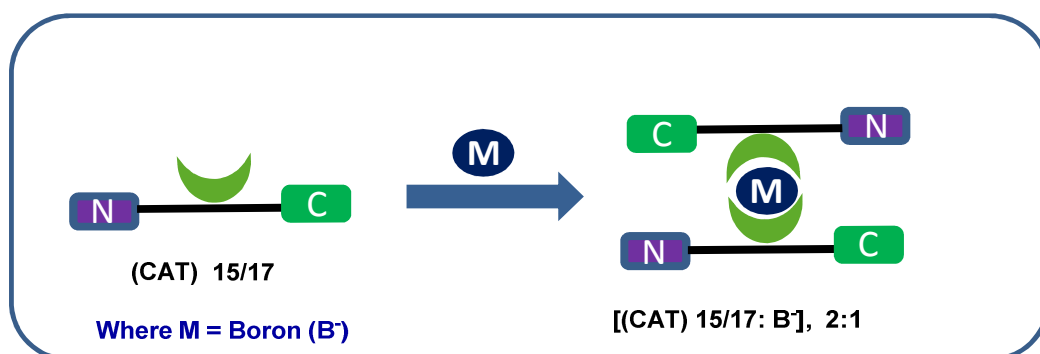


**Figure 33.** Pictorial representation of ethyl and benzyl-*N*-Boc-aminoethyl-3,4-dihydroxyphenyl (CAT) glycinate **15** and **17** with boron ion.

### 3.9 High Resolution-Mass spectrometry (HR-MS) Studies

High Resolution-Mass Spectrometry (HR-MS) was used for additional characterization of the synthesized *aeg* linked ligands (Figure 34). Both *N*-Boc-aminoethyl (PBI) glycinate **8** and *N*-Boc-aminoethyl (PBI)<sub>2</sub> (glycinate)<sub>2</sub> **21** were treated with metal salts. After stirring the stoichiometric mixture of the *aeg* ligands and metal salts overnight, the complexes were purified on an alumina column. Electrospray Ionization-Time of Flight (ESI-TOF) mass spectra was recorded to confirm metal complexation.

#### 3.9.1 HR-MS studies on ethyl-*N*-Boc-aminoethyl-2-pyridylbenzimidazole (PBI) glycinate **8**

Ethyl-*N*-Boc-aminoethyl-2-pyridylbenzimidazole (PBI) glycinate **8** was treated with copper chloride salt and its high resolution mass spectrum was recorded, which showed the presence of two types of molecular stoichiometry (Figure 35A) i.e. molecular ion peaks at  $m/z$  579.0979 (Calculated: 579.0847) and 1060.6124 (Calculated: 1060.3635). The former and latter peak corresponded to molecular stoichiometry of 1:1 [ethyl-*N*-Boc-aminoethyl-2-pyridylbenzimidazole (PBI) glycinate **8**: Cu<sup>2+</sup>] and 2:1 [ethyl-*N*-Boc-aminoethyl-2-pyridylbenzimidazole (PBI) glycinate **8**: Cu<sup>2+</sup>], respectively.

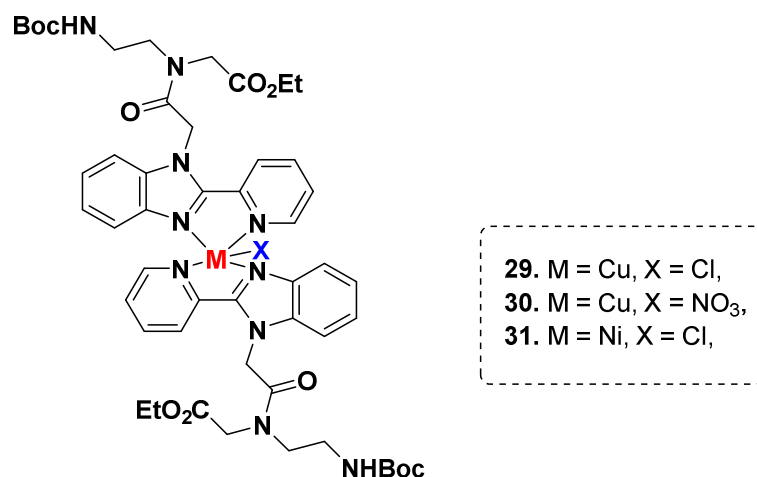


**Figure 34.** Structures of complexes of ethyl-*N*-Boc-aminoethyl-2-pyridylbenzimidazole (PBI) glycinate **8** with various metal salts.

In the same way, on treating ethyl-*N*-Boc-aminoethyl-2-pyridylbenzimidazole (PBI) glycinate **8** with copper nitrate, the high resolution mass spectrum displayed a desired molecular ion peak at  $m/z$  1087.4622 (Calculated: 1087.3825) corresponding

to molecular complex stoichiometry of 2:1 [ethyl-*N*-Boc-aminoethyl-2-pyridylbenzimidazole (PBI) glycinate **8**: Cu<sup>2+</sup>] (Figure 35B) and peak corresponding to 1:1 molecular stoichiometry was absent.

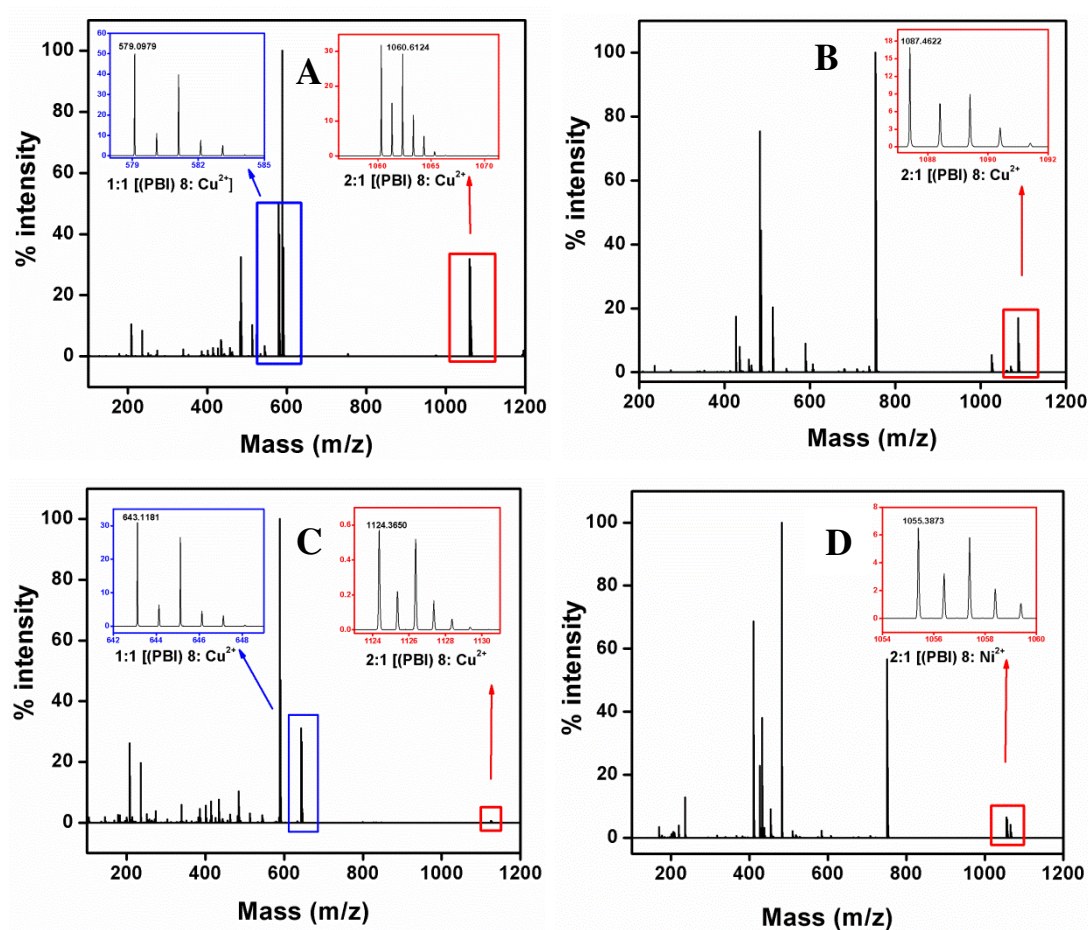


**Figure 35.** HR-MS spectra for ethyl-*N*-Boc-aminoethyl-2-pyridylbenzimidazole (PBI) glycinate **8** with (A) copper chloride, (B) copper nitrate, (C) copper perchlorate and (D) nickel chloride.

Copper perchlorate complex with ethyl-*N*-Boc-aminoethyl-2-pyridylbenzimidazole (PBI) glycinate **8** revealed high resolution molecular ion peaks at *m/z* 643.1181 (Calculated: 643.1106) and 1124.3650 (Calculated: 1124.3846), respectively for molecular stoichiometry of 1:1 [ethyl-*N*-Boc-aminoethyl-2-pyridylbenzimidazole (PBI) glycinate **8**: Cu<sup>2+</sup>] and 2:1 [ethyl-*N*-Boc-aminoethyl-2-pyridylbenzimidazole (PBI) glycinate **8**: Cu<sup>2+</sup>] (Figure 35C). And for nickel chloride at *m/z* 1055.3873 (Calculated: 1055.3692) corresponded to molecular stoichiometry of 2:1 [ethyl-*N*-Boc-aminoethyl-2-pyridylbenzimidazole (PBI) glycinate **8**: Ni<sup>2+</sup>] (Figure 35D) with no 1:1 molecular stoichiometry.

In conclusion, it was observed that (PBI) **8** binds with all the four metal salts *i.e.* copper chloride, copper nitrate, copper perchlorate and nickel chloride and forms stable duplexes in either in 1:1 or 2:1 molecular stoichiometry (Figure 36).

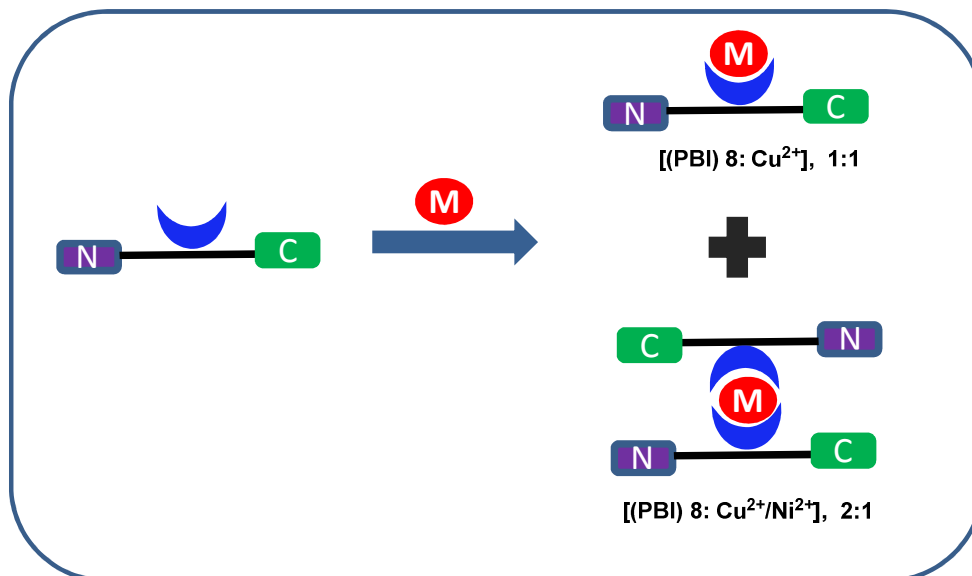


**Figure 36.** Schematic representation of *aeg* linked ethyl-*N*-Boc-aminoethyl-2-pyridylbenzimidazole (PBI) glycinate **8** with copper and nickel metal salts.

### 3.9.2 HR-MS studies on ethyl-*N*-Boc-aminoethyl-2-pyridylbenzimidazole (PBI)<sub>2</sub> (glycinate)<sub>2</sub> **21**

In a similar fashion, *N*-Boc-aminoethyl (PBI)<sub>2</sub> (glycinate)<sub>2</sub> **21** was also examined for metal complexation with all aforesaid metal salts, but only copper chloride yielded fruitful results (Figure 37).

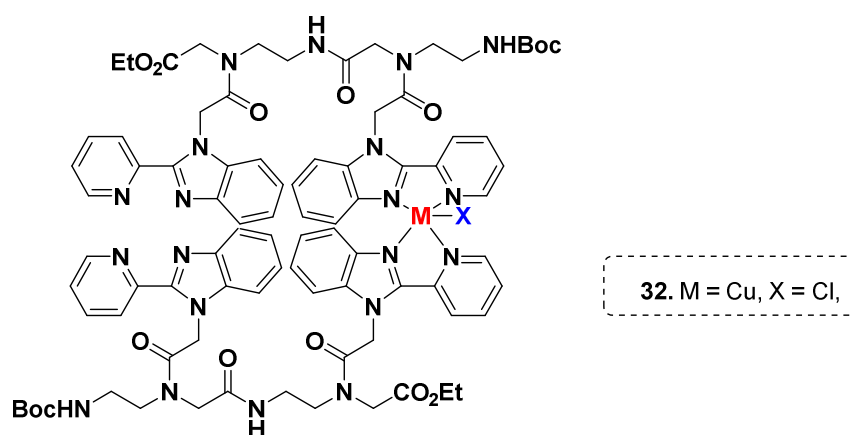


**Figure 37.** Structure of *N*-Boc-aminoethyl (PBI)<sub>2</sub> (glycinate)<sub>2</sub> **21** and copper chloride complex.

## Chapter 3

*N*-Boc-aminoethyl (PBI)<sub>2</sub> (glycinate)<sub>2</sub> **21** treated with copper chloride showed the presence of peak at  $m/z$  1730.6259 (Calculated: 1730.6399) suggesting single metal incorporation between ligands (Figure 38).

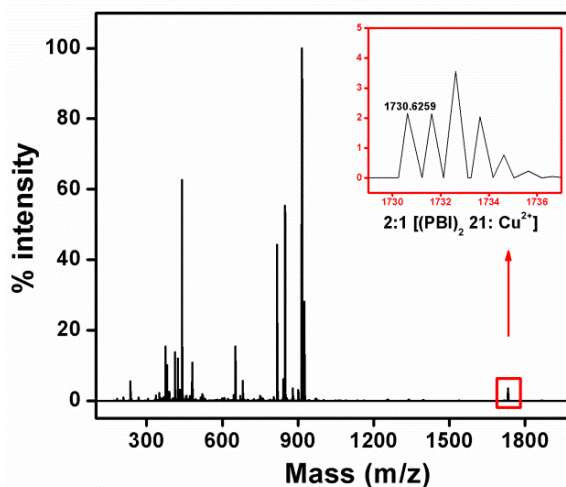


**Figure 38.** HR-MS spectra of *N*-Boc-aminoethyl (PBI)<sub>2</sub> (glycinate)<sub>2</sub> **21** with copper chloride.

In conclusion, both *N*-Boc-aminoethyl (PBI) glycinate **8** and *N*-Boc-aminoethyl (PBI)<sub>2</sub> (glycinate)<sub>2</sub> **21** both displayed metal complexation. Though (PBI)<sub>2</sub> **21** showed metal complexation with all metal salts, but HR-MS data could only be obtained with copper chloride. A pictorial depiction of the plausible complexation is presented below in Figure 39.

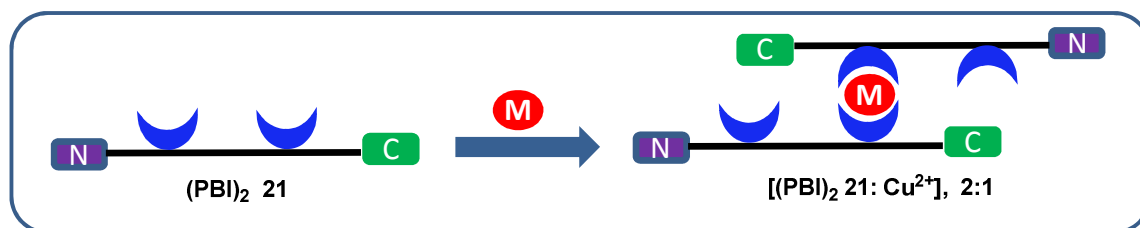


**Figure 39.** Schematic representation of *N*-Boc-aminoethyl (PBI)<sub>2</sub> (glycinate)<sub>2</sub> **21** with copper chloride.

### 3.10 UV-Vis spectroscopic studies

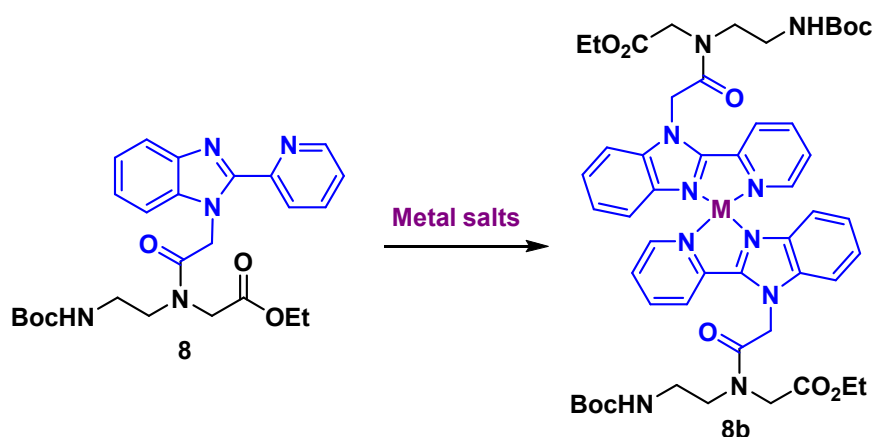
Since metal coordination is accompanied by the appearance of a peak in the UV-Vis absorption spectrum, spectrophotometric titrations were used as a probe to monitor the metal complexation of synthesized *aeg* linked ligands.

#### 3.10.1 UV-Vis spectrophotometric titrations of (PBI) and (CAT) *aeg* linked ligands

UV-Vis titrations were performed by incremental addition of metal ions into a methanolic solution of methanolic solutions *N*-Boc-aminoethyl (PBI) glycinate **8** and *N*-Boc-aminoethyl (CAT) glycinate **17** of known concentrations.

##### 3.10.1a UV-Vis spectrophotometric titrations of the *N*-Boc-aminoethyl-2-pyridylbenzimidazole (PBI) glycinate **8**

The binding studies of *N*-Boc-aminoethyl-2-pyridylbenzimidazole (PBI) glycinate **8** was carried out with different metal salts *i.e.* copper nitrate, nickel nitrate, palladium nitrate, lead nitrate, iron nitrate, zinc nitrate, cobalt nitrate, ruthenium trichloride, silver nitrate, gold chloride *etc* (Scheme 14). A change in the ultraviolet (UV) absorption upon complexation with  $\text{Cu}^{2+}/\text{Ni}^{2+}$  ions were used as quantitative structural probe to verify  $\text{Cu}^{2+}/\text{Ni}^{2+}$  mediated duplex formation. Thus, titration studies followed by UV-Vis spectroscopic studies were undertaken for *N*-Boc-aminoethyl-2-pyridylbenzimidazole (PBI) glycinate **8**.



**Scheme 14.** Metal Complexation of the *N*-Boc-aminoethyl-2-pyridylbenzimidazole (PBI) glycinate **8**.

**Cu(NO<sub>3</sub>)<sub>2</sub>:** The electronic spectra of *N*-Boc-aminoethyl-2-pyridylbenzimidazole (PBI) glycinate **8** in methanol showed maximum absorption ( $\lambda_{\text{max}}$ ) at 308 nm. Upon addition



of aliquots of  $\text{Cu}(\text{NO}_3)_2$ , intensity of the peak at 308 nm reduces and a new red shifted absorption band ( $\lambda_{\text{max}}$ ) at 324 nm (+16 nm) appears. This new absorption band along with two isosbestic points at 256 and 314 nm indicate the formation of  $\text{Cu}^{2+}$ - *N*-Boc-aminoethyl (PBI) glycinate **8** complex.

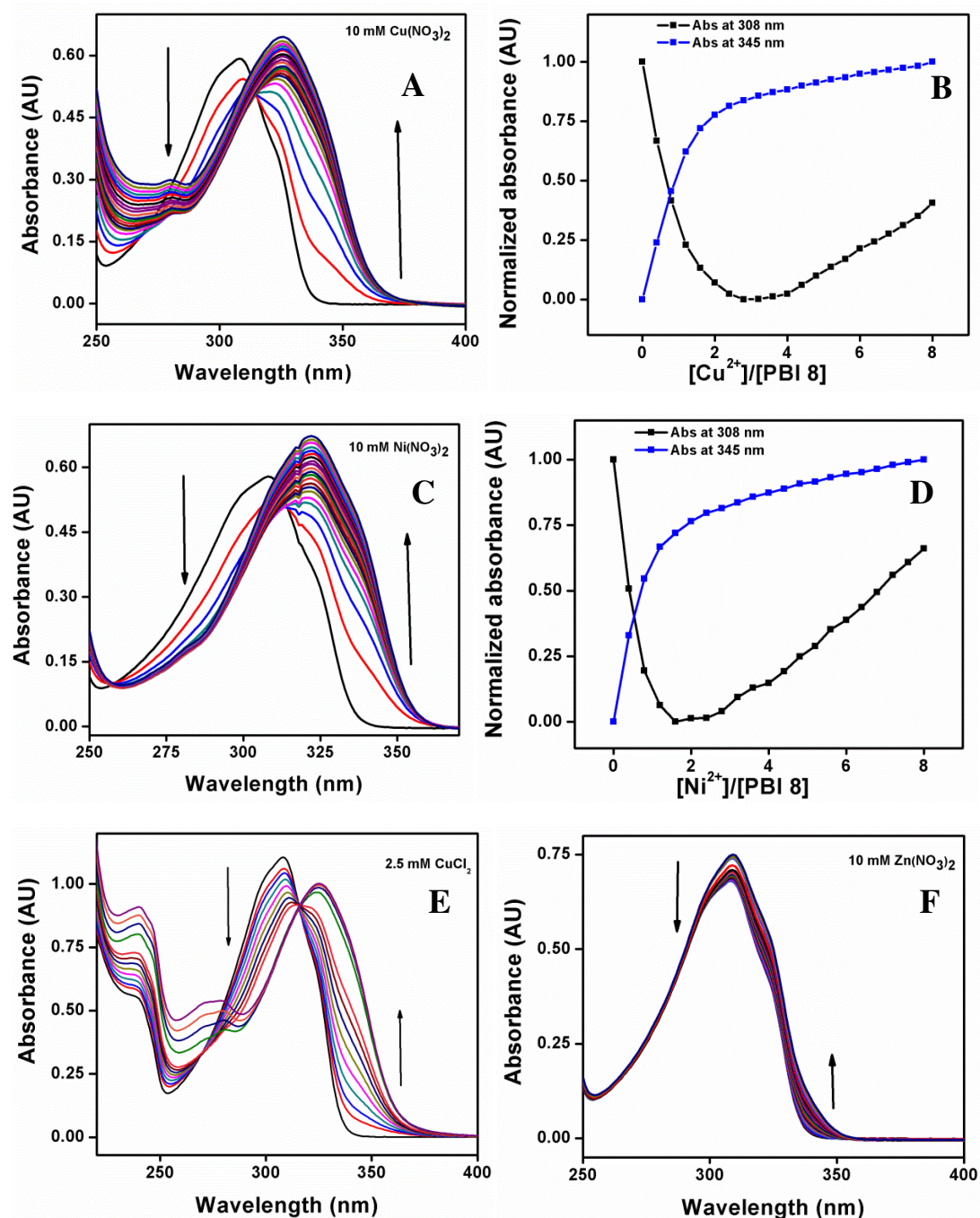


**Figure 40.** Changes in the absorption spectra of the *N*-Boc-aminoethyl-2-pyridylbenzimidazole (PBI) glycinate **8** (25  $\mu\text{M}$ ) in methanol upon the addition of metal salts (A)  $\text{Cu}(\text{NO}_3)_2$  (10 mM), (C)  $\text{Ni}(\text{NO}_3)_2$  (10 mM), (E)  $\text{CuCl}_2$  (2.5 mM) and (F)  $\text{Zn}(\text{NO}_3)_2$  (10 mM). Plot of the change in absorbance at 308 and 345 nm as a function of molar ratio of metal to (PBI) **8** (B)  $\text{Cu}(\text{NO}_3)_2$ , (D)  $\text{Ni}(\text{NO}_3)_2$ .

The titration curve, plotted as the change in absorbance against as a function of (PBI) **8** concentration, is shown in Figure 40A & B. The plot of molar absorptivity at 308 nm vs equivalents of  $\text{Cu}^{2+}$  added shows a saturation ca. 2 equivalents of  $\text{Cu}(\text{NO}_3)_2$  in methanol.

**Ni(NO<sub>3</sub>)<sub>2</sub>**: Similarly, titrations were carried out by adding the aliquots of  $\text{Ni}(\text{NO}_3)_2$  into the *N*-Boc-aminoethyl-2-pyridylbenzimidazole (PBI) glycinate **8** solution. This new absorption band at ( $\lambda_{\text{max}}$ ) at 308 nm with two isosbestic points at 265 and 314 nm indicated the formation of  $\text{Ni}^{2+}$ -*N*-Boc-aminoethyl-2-pyridylbenzimidazole (PBI) glycinate **8** complete with a saturation approx. with 2 equiv. of  $\text{Ni}(\text{NO}_3)_2$  in methanol (Figure 40C & D).

**CuCl<sub>2</sub>**: *N*-Boc-aminoethyl-2-pyridylbenzimidazole (PBI) glycinate **8** was also titrated with copper chloride and showed appreciable binding, with two isosbestic points at 256 and 315 nm (Figure 40E). Among copper salts, copper nitrate was carried out further due to its better binding results observed.

**Zn(NO<sub>3</sub>)<sub>2</sub>**: UV-Vis titration studies of *N*-Boc-aminoethyl-2-pyridylbenzimidazole (PBI) glycinate **8** with zinc nitrate salt results in the weak binding (Figure 40F).

**AuCl<sub>3</sub>**: UV-Vis titrations were carried out with  $\text{AuCl}_3$  (10 mM), but unfortunately absorption change due to the monomer was completely masked by the gold absorption itself. So, in order to attain the equivalence point, titration was carried out at a lower concentration of  $\text{AuCl}_3$  (2.5 mM) (Figure 41).

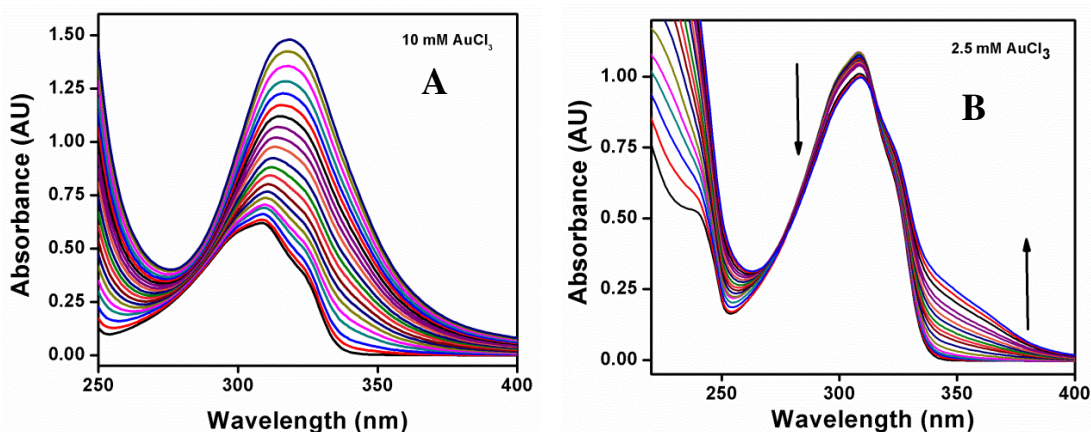


**Figure 41.** Changes in the absorption spectra of the *N*-Boc-aminoethyl-2-pyridylbenzimidazole (PBI) glycinate **8** (25  $\mu\text{M}$ ) in methanol upon the addition of metal salts (A)  $\text{AuCl}_3$  (10 mM) and (B)  $\text{AuCl}_3$  (2.5 mM).

## Chapter 3

Although an isobestic point was observed at 315 nm, the emergent absorption at 350 failed to saturate even at as high molar equivalence as 10 perhaps indicating transient binding of the metal to the ligands. However, no significant spectral change was observed.

UV-Vis titration results have been summarised in Table 13.

**Table 13.** Summary of UV-Vis titrations for *N*-Boc-aminoethyl-2-pyridylbenzimidazole (PBI) glycinate **8**

SI No.	Metal salts (2.5/10 mM)	Observation	Inflection points	Isosbestic points
1.	Copper nitrate	Binding	308 and 324	256 and 314
	Copper chloride	Binding	308 and 324	269 and 315
2.	Nickel nitrate	Binding	308 and 324	265 and 314
3.	Gold chloride	Weak binding	-	-
4.	Zinc nitrate	Weak binding		

\*No appreciable binding with palladium nitrate, lead nitrate, iron nitrate, cobalt nitrate, ruthenium trichloride, silver nitrate, gold chloride

The continuous variation Job's method provides information about binding stoichiometry between metal and *N*-Boc-aminoethyl-2-pyridylbenzimidazole (PBI) glycinate **8** (Figure 42), which was examined by keeping the overall concentration constant and plotted against the mole fraction of  $\text{Cu}^{2+}/\text{Ni}^{2+}$ .

Various stoichiometric mixtures of *N*-Boc-aminoethyl-2-pyridylbenzimidazole (PBI) glycinate **8**:metal salts in varying molar ratios (100:0, 90:10, 80:20, 70:30, 60:40, 50:50, 40:60, 30:70, 20:80, 10:90 and 0:100) were prepared keeping concentration of *N*-Boc-aminoethyl (PBI) glycinate **8** as 100  $\mu\text{M}$  in methanol. The intersection point in the Job's plot was found to be at 0.50, which indicates binding stoichiometry 1:1 for the complexes *N*-Boc-aminoethyl-2-pyridylbenzimidazole (PBI) glycinate **8** with both copper nitrate and nickel nitrates.

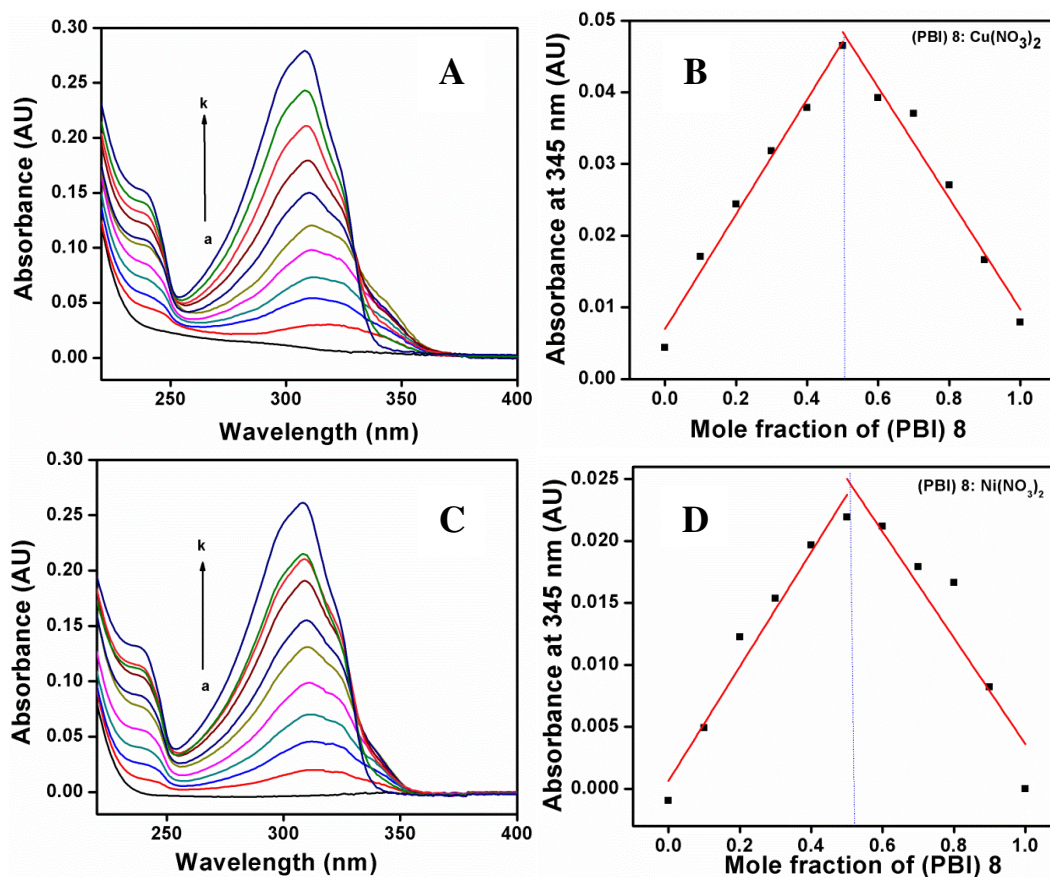


**Figure 42.** UV-Vis absorption spectra of *N*-Boc-aminoethyl-2-pyridylbenzimidazole (PBI) glycinate **8** with metal salts in molar ratios of (a) 0:100 (b) 10:90 (c) 20:80 (d) 30:70 (e) 40:60 (f) 50:50 (g) 60:40 (h) 70:30 (i) 80:20 (j) 90:10 (k) 100:0; (A) UV spectra and (B) Job's plot with  $\text{Cu}(\text{NO}_3)_2$  (C) UV spectra and (D) Job's plot with  $\text{Ni}(\text{NO}_3)_2$ .

Benesi-Hildebrand (BH) equation, is highly useful in determining binding constants for 1:1 and 1:2 [(Metal:ligand) or (Host:guest) or (DNA/RNA:peptides)] systems. For *N*-Boc-aminoethyl-2-pyridylbenzimidazole (PBI) glycinate **8**, Job's plot indicated the binding stoichiometry of 1:1 and it was subsequently fitted in the BH equation. In this equation, concentration was plotted against the change in the metal concentration. After selecting proper binding model, BH equation results in the straight line, which is observed in graphs.

The binding constant ( $K$ ) was determined from the intercept to slope ratio of the Benesi-Hildebrand plot and the values calculated were  $6.71 \times 10^3$  and  $1.82 \times 10^3$   $[\text{M}]^{-1}$  for  $\text{Cu}(\text{NO}_3)_2$  and  $\text{Ni}(\text{NO}_3)_2$ , respectively, which indicate the comparable strength of binding with both the metals (Figure 43, inset).

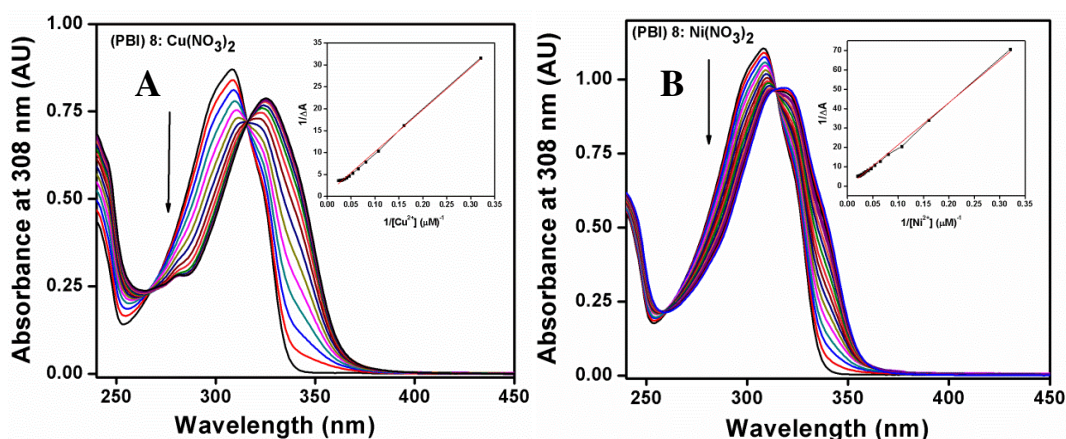


**Figure 43.** Benesi Hildebrand's plots (A) UV-Vis absorption spectra of *N*-Boc-aminoethyl-2-pyridylbenzimidazole (PBI) glycinate **8** with (A)  $\text{Cu}(\text{NO}_3)_2$  and (B)  $\text{Ni}(\text{NO}_3)_2$ . Arrows indicate decrease in absorption at 308 nm from 0 to 2.5 mM metal concentration. The Benesi Hildebrand plots are represented as insets.

In conclusion, *N*-Boc-aminoethyl-2-pyridylbenzimidazole (PBI) glycinate **8** strongly binds in 1:1 stoichiometry with methanolic solution of  $\text{Cu}(\text{NO}_3)_2$  and  $\text{Ni}(\text{NO}_3)_2$ , while no appreciable binding is observed with zinc, cobalt and gold metal salts.

These binding models are only proposed models and at present no direct evidence is available. Based on the present investigations using UV-Vis spectroscopy (1:1), single crystal X-ray diffraction studies (1:1), HRMS (2:1) and ITC analyses, it can be concluded that *N*-Boc-aminoethyl-2-pyridylbenzimidazole (PBI) glycinate **8** predominantly forms both 2:1 and 1:1 complexes with metal salts (Figure 44).

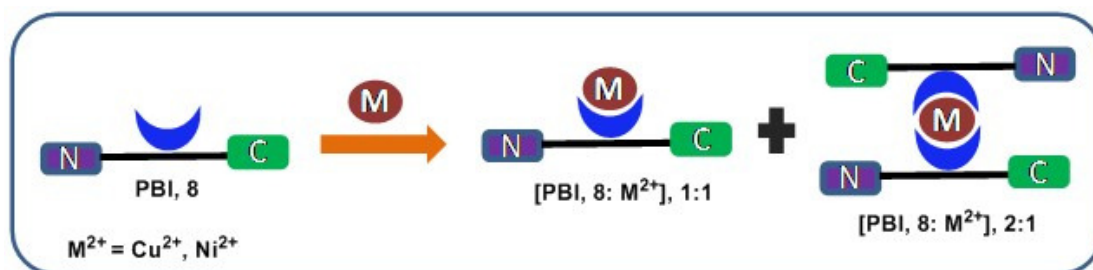
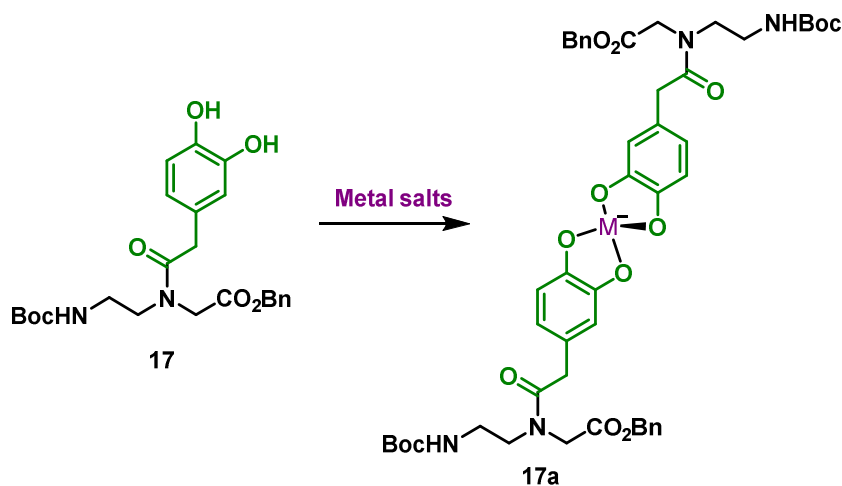


**Figure 44.** Proposed model of *N*-Boc-aminoethyl-2-pyridylbenzimidazole (PBI) glycinate **8** with copper and nickel nitrates.

### 3.10.1b UV-Vis spectrophotometric titrations of *N*-Boc-aminoethyl-catechol (CAT) glycinate **17**

Metal binding studies of the synthesized *N*-Boc-aminoethyl-catechol (CAT) glycinate **17** with various metal salts were done (Scheme 15).



**Scheme 15.** Metal complexation of *N*-Boc-aminoethyl-catechol (CAT) glycinate **17**.

The electronic spectra of *N*-Boc-aminoethyl-catechol (CAT) glycinate **17** in methanol showed maximum absorption ( $\lambda_{\text{max}}$ ) at 283 nm. UV-Vis experiments of *N*-Boc-aminoethyl-catechol (CAT) glycinate **17** were studied with different metal ions ( $\text{Cu}^{2+}$ ,  $\text{Ni}^{2+}$ ,  $\text{Zn}^{2+}$ ,  $\text{Ru}^{3+}$ ,  $\text{Pd}^{2+}$ ,  $\text{Fe}^{3+}$ ,  $\text{Ag}^+$ ,  $\text{Au}^{3+}$ ,  $\text{Tl}^{3+}$ ,  $\text{Ln}^{3+}$ ) as their nitrate/chloride salts.

**Phenylboronic acid:** *N*-Boc-aminoethyl-catechol (CAT) glycinate **17** was examined for its metal binding studies with phenylboronic acid and exhibited significant spectral change in the absorbance spectra (Figures 45).

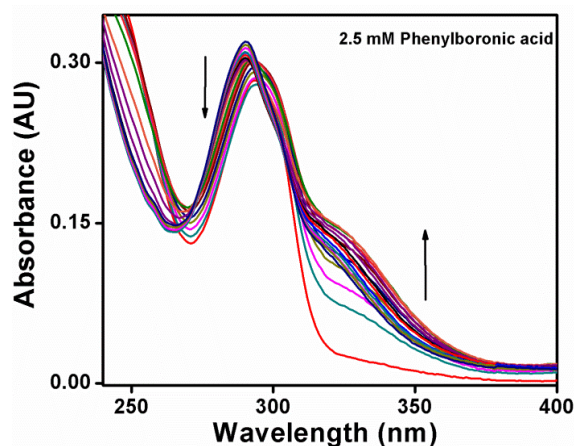


**Figure 45.** Changes in the absorption spectra of *N*-Boc-aminoethyl-catechol (CAT) glycinate **17** ( $50 \mu\text{M}$ ) in methanol upon the addition of phenylboronic acid (2.5 mM).

The methanolic solution of *N*-Boc-aminoethyl-catechol (CAT) glycinate **17** showed maximum absorption ( $\lambda_{\text{max}}$ ) at 283 nm and upon adding aliquots of phenylboronic acid (2.5 mM), the intensity of the peak at 283 nm decreases and intensity of new peak at 328 nm increases. Since, isosbestic points were not clearly indicative, important information regarding stoichiometry could not be obtained.

Metal salts *i.e.* copper nitrate, nickel nitrate, ruthenium trichloride and ferric nitrate, exhibited visible change in the absorbance spectra. Ruthenium trichloride showed absorbance change in the 550 nm that can be attributed to the formation of ruthenium nanoparticles. UV-Vis titration spectra for  $\text{Cu}^{2+}$ ,  $\text{Ni}^{2+}$ ,  $\text{Zn}^{2+}$ ,  $\text{Ru}^{3+}$  are displayed below (Figure 46).

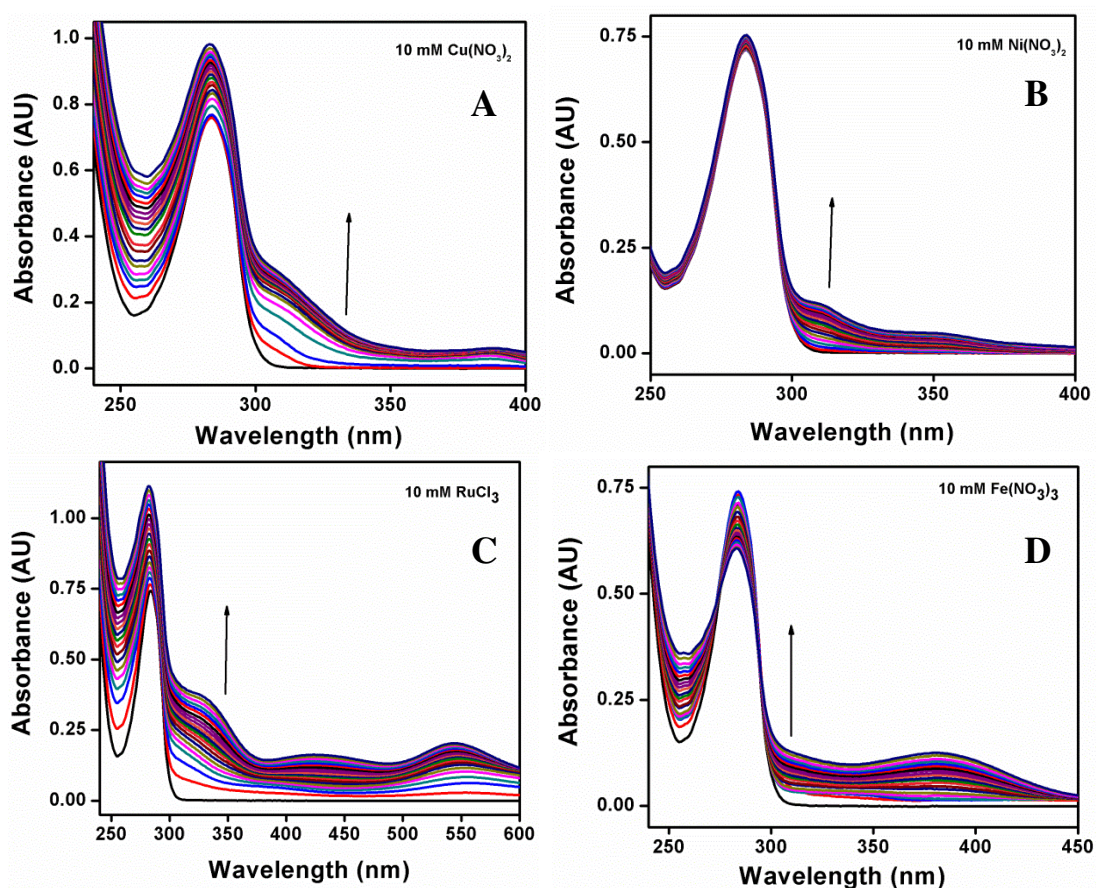


**Figure 46.** Changes in the absorption spectra of *N*-Boc-aminoethyl-catechol (CAT) glycinate **17** (50  $\mu\text{M}$ ) in methanol upon the addition of metal salts (A)  $\text{Cu}(\text{NO}_3)_2$  (10 mM), (B)  $\text{Ni}(\text{NO}_3)_2$  (10 mM), (C)  $\text{Zn}(\text{NO}_3)_2$  (10 mM) and (D)  $\text{RuCl}_3$  (10 mM).

Similar results were also observed for silver nitrate (Figure 47). However, no significant spectral change was observed by the addition of palladium nitrate, thallium nitrate and lanthanum nitrate.

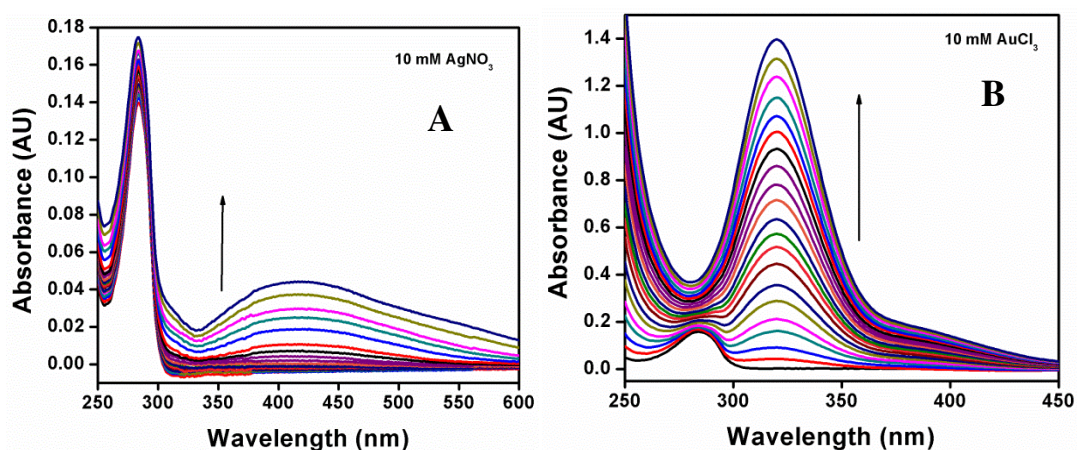


**Figure 47.** Changes in the absorption spectra of *N*-Boc-aminoethyl-catechol (CAT) glycinate **17** (50  $\mu$ M) in methanol upon the addition of metal salts (A) AgNO<sub>3</sub> (10 mM) and (B) AuCl<sub>3</sub> (10 mM).

Summary of metal binding for the *N*-Boc-aminoethyl-catechol (CAT) glycinate **17** is displayed in Table 14.

**Table 14.** Summary of UV-Vis titration results for the *N*-Boc-aminoethyl-catechol (CAT) glycinate **17**.

Metal salts (10 mM)	Observation
Phenylboronic acid	Binding
Copper nitrate	Weak binding
Nickel nitrate	Weak binding
Ruthenium trichloride	Ru-Nanoparticles
Ferric nitrate	Weak binding
Gold chloride	Weak binding
Silver nitrate	Ag-Nanoparticles

\*palladium nitrate, thallium nitrate and lanthanum nitrate did not show any significant spectral change.

In conclusion, (CAT) **17** showed binding with phenylboronic acid, whereas other metal salts did not exhibit appreciable binding.

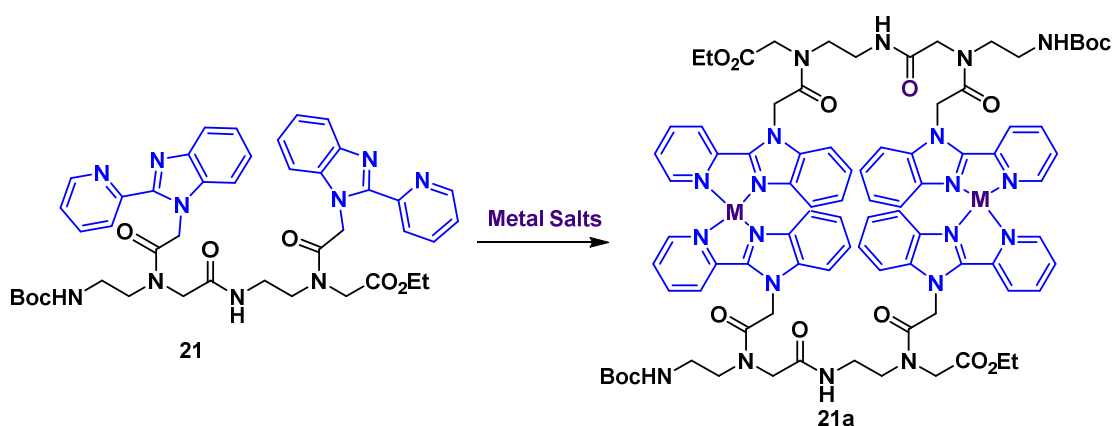


### 3.10.2 UV-Vis spectrophotometric titrations of (PBI) Dimer

UV-Vis titrations were performed by incremental addition of metal ions into a methanolic solution of methanolic solutions *N*-Boc-aminoethyl (PBI)<sub>2</sub> glycinate<sub>2</sub> **21** of known concentrations.

#### 3.10.2a UV-Vis spectrophotometric titrations of *N*-Boc-aminoethyl 2-pyridylbenzimidazole (PBI)<sub>2</sub> (glycinate)<sub>2</sub> **21**

(PBI)<sub>2</sub> structure possesses two pyridyl-benzimidazole units linked to *aeg*-backbone, providing total of two sites for metal complexation (Scheme 16).



**Scheme 16.** Schematic representation of metal complexation of the *N*-Boc-aminoethyl 2-pyridylbenzimidazole (PBI)<sub>2</sub> (glycinate)<sub>2</sub> **21**.

**Cu(NO<sub>3</sub>)<sub>2</sub>:** The electronic spectra of *N*-Boc-aminoethyl 2-pyridylbenzimidazole (PBI)<sub>2</sub> (glycinate)<sub>2</sub> **21** obtained from on UV-Vis Spectrophotometric titration carried out in methanol showed maximum absorption at  $\lambda_{\text{max}}$  308 nm and shows inflection point approximately at 2 equivalents of Cu(NO<sub>3</sub>)<sub>2</sub> in methanol. Similar to (PBI) **8**, upon addition of aliquots of Cu(NO<sub>3</sub>)<sub>2</sub>, a new red shifted absorption band at  $\lambda_{\text{max}}$  321 nm (13 nm) was observed at the expense of reduction of intensity of the peak at 308 nm. Isosbestic points at 266 and 316 nm indicated the formation of Cu<sup>2+</sup>-*N*-Boc-aminoethyl 2-pyridylbenzimidazole (PBI)<sub>2</sub> (glycinate)<sub>2</sub> **21** complex (Figure 48).

**Ni(NO<sub>3</sub>)<sub>2</sub>:** For Ni(NO<sub>3</sub>)<sub>2</sub>, same value of red shifted absorption band was noted ( $\lambda_{\text{max}}$ ) at 321 nm (+13 nm), but different isosbestic points at 261 and 317 nm, indicating the formation of complex.

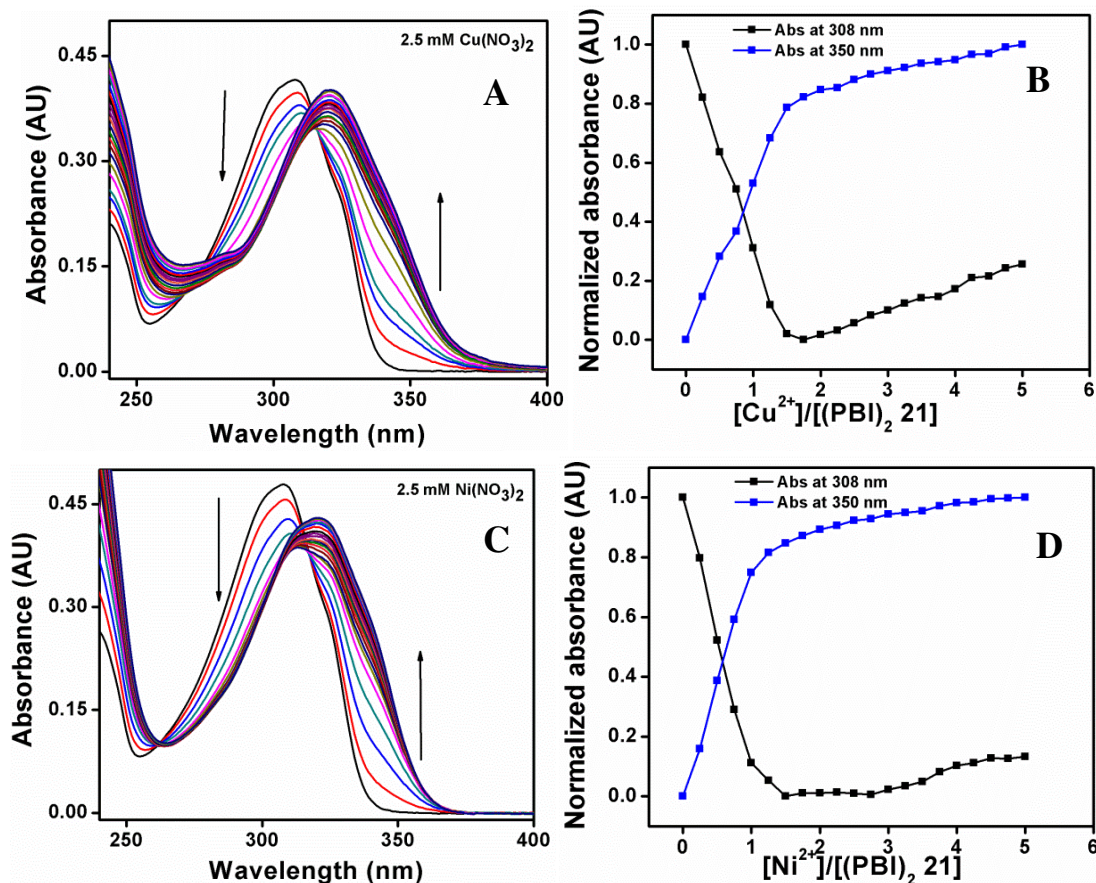


**Figure 48.** Changes in the absorption spectra of *N*-Boc-aminoethyl 2-pyridylbenzimidazole (PBI)<sub>2</sub> (glycinate)<sub>2</sub> **21** (10 μM) in water upon the addition of metal salts (A) Cu(NO<sub>3</sub>)<sub>2</sub> (2.5 mM) (C) Ni(NO<sub>3</sub>)<sub>2</sub> (2.5 mM). Plot of the change in absorbance at 308 and 350 nm as a function of molar ratio of metal to peptides (B) Cu(NO<sub>3</sub>)<sub>2</sub> and (D) Ni(NO<sub>3</sub>)<sub>2</sub>.

Summary of metal binding for the *N*-Boc-aminoethyl 2-pyridylbenzimidazole (PBI)<sub>2</sub> (glycinate)<sub>2</sub> **21** is displayed in Table 15.

**Table 15.** Summary of UV-Vis titration for the *N*-Boc-aminoethyl 2-pyridylbenzimidazole (PBI)<sub>2</sub> (glycinate)<sub>2</sub> **21**.

Metal salts (2.5 mM)	Observation	Inflection points	Isosbestic points
Nickel nitrate	Binding	308 and 321	266 and 316
Copper nitrate	Binding	308 and 321	261 and 317

Using Job's method, the concentrations of metal salts and *N*-Boc-aminoethyl 2-pyridylbenzimidazole (PBI)<sub>2</sub> (glycinate)<sub>2</sub> **21** were examined by keeping the overall concentration constant. The Job's plot (Figure 49) indicated an intersection point around 0.40, suggesting binding stoichiometry of 2:3 for *N*-Boc-aminoethyl 2-

pyridylbenzimidazole (PBI)<sub>2</sub> (glycinate)<sub>2</sub> **21**:Cu(NO<sub>3</sub>)<sub>2</sub> complex. In comparison, *N*-Boc-aminoethyl 2-pyridylbenzimidazole (PBI)<sub>2</sub> (glycinate)<sub>2</sub> **21**: Ni(NO<sub>3</sub>)<sub>2</sub> complex showed intersection point around 0.60 in Job's plot indicating a binding stoichiometry to be 3:2.

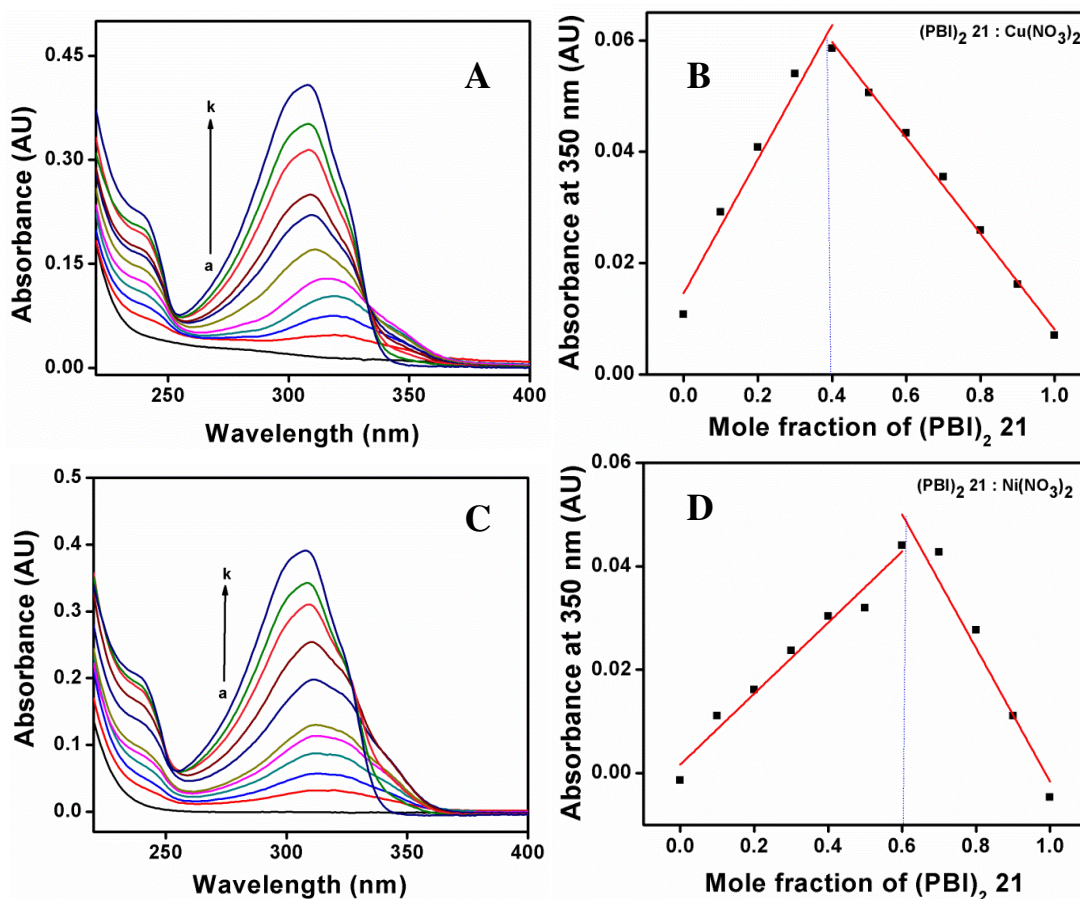


**Figure 49.** UV-Vis absorption spectra of *N*-Boc-aminoethyl 2-pyridylbenzimidazole (PBI)<sub>2</sub> (glycinate)<sub>2</sub> **21** with metal salts in molar ratios of (a) 0:100 (b) 10:90 (c) 20:80 (d) 30:70 (e) 40:60 (f) 50:50 (g) 60:40 (h) 70:30 (i) 80:20 (j) 90:10 (k) 100:0; (A) UV spectra and (B) Job's plot with Cu(NO<sub>3</sub>)<sub>2</sub>; (C) UV spectra and (D) Job's plot with Ni(NO<sub>3</sub>)<sub>2</sub>.

Benesi Hildebrand equation holds good fitting values only in case of either 1:1 or 1:2 binding models. However, Job's plot for *N*-Boc-aminoethyl 2-pyridylbenzimidazole (PBI)<sub>2</sub> (glycinate)<sub>2</sub> **21** with Cu(NO<sub>3</sub>)<sub>2</sub> and Ni(NO<sub>3</sub>)<sub>2</sub> yielded the binding stoichiometry 2:3 [*N*-Boc-aminoethyl 2-pyridylbenzimidazole (PBI)<sub>2</sub> (glycinate)<sub>2</sub> **21**: Cu(NO<sub>3</sub>)<sub>2</sub>], and 3:2 [*N*-Boc-aminoethyl 2-pyridylbenzimidazole (PBI)<sub>2</sub> (glycinate)<sub>2</sub> **21**: Ni(NO<sub>3</sub>)<sub>2</sub>], respectively. To avoid any ambiguity, BH equation (1:2 binding model) was used for calculating the binding constants and results in the straight line, which is observed in graphs below (Figure 50A & B, inset).

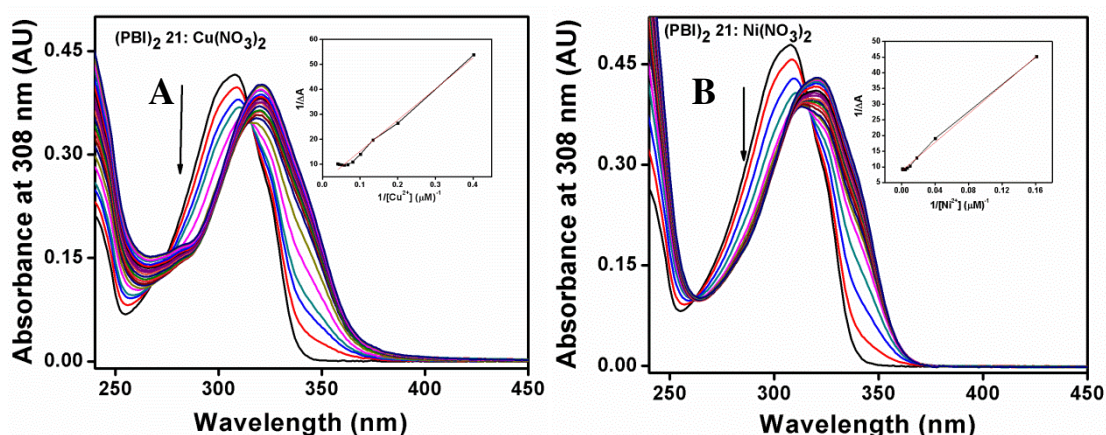


**Figure 50.** Benesi Hildebrand's plots (A) UV-Vis absorption spectra of *N*-Boc-aminoethyl 2-pyridylbenzimidazole (PBI)<sub>2</sub> (glycinate)<sub>2</sub> **21** with (A) Cu(NO<sub>3</sub>)<sub>2</sub> and (B) Ni(NO<sub>3</sub>)<sub>2</sub>. Arrows indicate decrease in absorption at 308 nm from 0 to 2.5 mM metal concentration. The Benesi Hildebrand plots are represented as insets.

The calculated values of binding constant (*K*) were found to be  $2.24 \times 10^4$  [M]<sup>-1</sup> for Cu(NO<sub>3</sub>)<sub>2</sub> and  $3.18 \times 10^4$  [M]<sup>-1</sup> for Ni(NO<sub>3</sub>)<sub>2</sub> in 1:2 binding models (Table 16), which implies better and strong binding in comparison to (PBI) **8**.

**Table 16.** Calculation of binding constants for (PBI)<sub>2</sub> (glycinate)<sub>2</sub> **21** using UV-Vis spectroscopy

Ligands	Metal salts	UV-Vis <i>K</i> (M) <sup>-1</sup>
(PBI) <sub>2</sub> <b>21</b>	Cu(NO <sub>3</sub> ) <sub>2</sub>	$2.24 \times 10^4$
	Ni(NO <sub>3</sub> ) <sub>2</sub>	$3.18 \times 10^4$

The present investigations into the metal binding ability of *N*-Boc-aminoethyl 2-pyridylbenzimidazole (PBI)<sub>2</sub> (glycinate)<sub>2</sub> **21** shows that it binds to both Cu(NO<sub>3</sub>)<sub>2</sub> and Ni(NO<sub>3</sub>)<sub>2</sub>. However unlike the monomeric units (PBI) **8**, the binding stoichiometries of the dimer *N*-Boc-aminoethyl 2-pyridylbenzimidazole (PBI)<sub>2</sub> (glycinate)<sub>2</sub> **21** is different for its complexes with the two metal ions. In view of the results obtained from the above studies, the geometry of the complexes and considering the tetracoordinate nature of Cu<sup>2+</sup>, hexacoordinate nature of Ni<sup>2+</sup> the following plausible model models as depicted in Figure 51 can be proposed.

## Chapter 3

In the model proposed here, *N*-Boc-aminoethyl 2-pyridylbenzimidazole (PBI)<sub>2</sub> (glycinate)<sub>2</sub> **21** and copper, the tetracoordinate character of Cu<sup>2+</sup> has been fulfilled by the attachment of two bidentate ligands. Thus, two *N*-Boc-aminoethyl 2-pyridylbenzimidazole (PBI)<sub>2</sub> (glycinate)<sub>2</sub> **21** strands are held together by three copper metal ions. In case of nickel, the hexacoordinate character of Ni<sup>2+</sup> could be fulfilled by the attachment of three bidentate ligands. Therefore, three *N*-Boc-aminoethyl 2-pyridylbenzimidazole (PBI)<sub>2</sub> (glycinate)<sub>2</sub> **21** units are likely to be held together in either parallel or in antiparallel manner by two nickel metal ions.

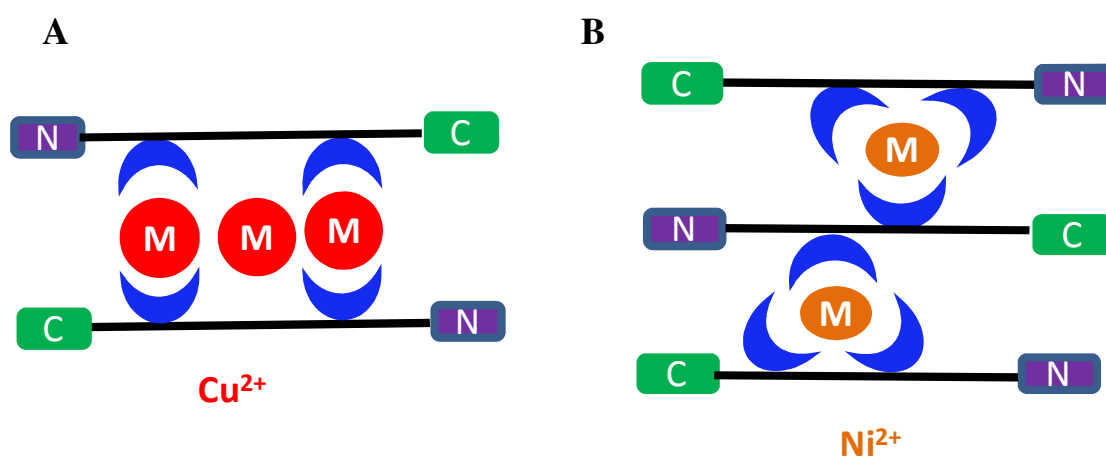


**Figure 51.** Proposed model for *N*-Boc-aminoethyl 2-pyridylbenzimidazole (PBI)<sub>2</sub> (glycinate)<sub>2</sub> **21** (A) with Cu(NO<sub>3</sub>)<sub>2</sub> and (B) Ni(NO<sub>3</sub>)<sub>2</sub>.

Figure 51 shows only two examples (for both copper and nickel metal ions) of the possible isomers that results from antiparallel vs parallel alignment of polyamide oligomers inside the formed duplexes.

### 3.10.3 UV-Vis spectrophotometric titrations of polyamide *homo*-oligomers

This section discusses the metal binding properties of synthesized polyamide *homo*-oligomers (PBI)<sub>6</sub> **22**, (PDA)<sub>6</sub> **23** and (CAT)<sub>6</sub> **24** with diverse metal salts.

#### 3.10.3a UV-Vis spectrophotometric titrations of 2-pyridyl-benzimidazole (PBI)<sub>6</sub> oligomer, **22**

(PBI)<sub>6</sub> structure provides total of six sites for metal complexation (Figure 52).

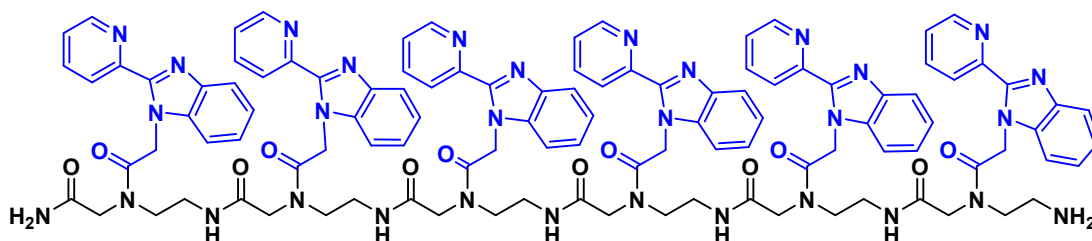


**Figure 52.** Structure of 2-pyridylbenzimidazole (PBI)<sub>6</sub> oligomer **22**.

UV-Vis spectrophotometric titrations were performed in water, where 2-pyridylbenzimidazole (PBI)<sub>6</sub> oligomer **22** displayed maximum absorption ( $\lambda_{\text{max}}$ ) at 302 nm.

**Cu(NO<sub>3</sub>)<sub>2</sub>:** On addition of Cu(NO<sub>3</sub>)<sub>2</sub>, spectrum reveals a hyperchromic shift ( $\lambda_{\text{max}}$ ) at 324 nm (+16 nm) upon binding with and two isosbestic points at 258 and 315 nm, with inflection point ~ 3 equivalents of Cu(NO<sub>3</sub>)<sub>2</sub> in water (Figure 53A & B).

**Ni(NO<sub>3</sub>)<sub>2</sub>:** Similarly, addition of Ni(NO<sub>3</sub>)<sub>2</sub> exhibited a new red shifted absorption band ( $\lambda_{\text{max}}$ ) at 324 nm (+16 nm). This new absorption band along with two isosbestic points at 256 and 312 nm indicated the formation of Ni<sup>2+</sup>-2-pyridylbenzimidazole (PBI)<sub>6</sub> oligomer **22** complex (Figure 53). The saturation point was not clearly visible (Figure 53D), indicative of a very weak binding of 2-pyridylbenzimidazole (PBI)<sub>6</sub> oligomer **22** with Ni(NO<sub>3</sub>)<sub>2</sub>.

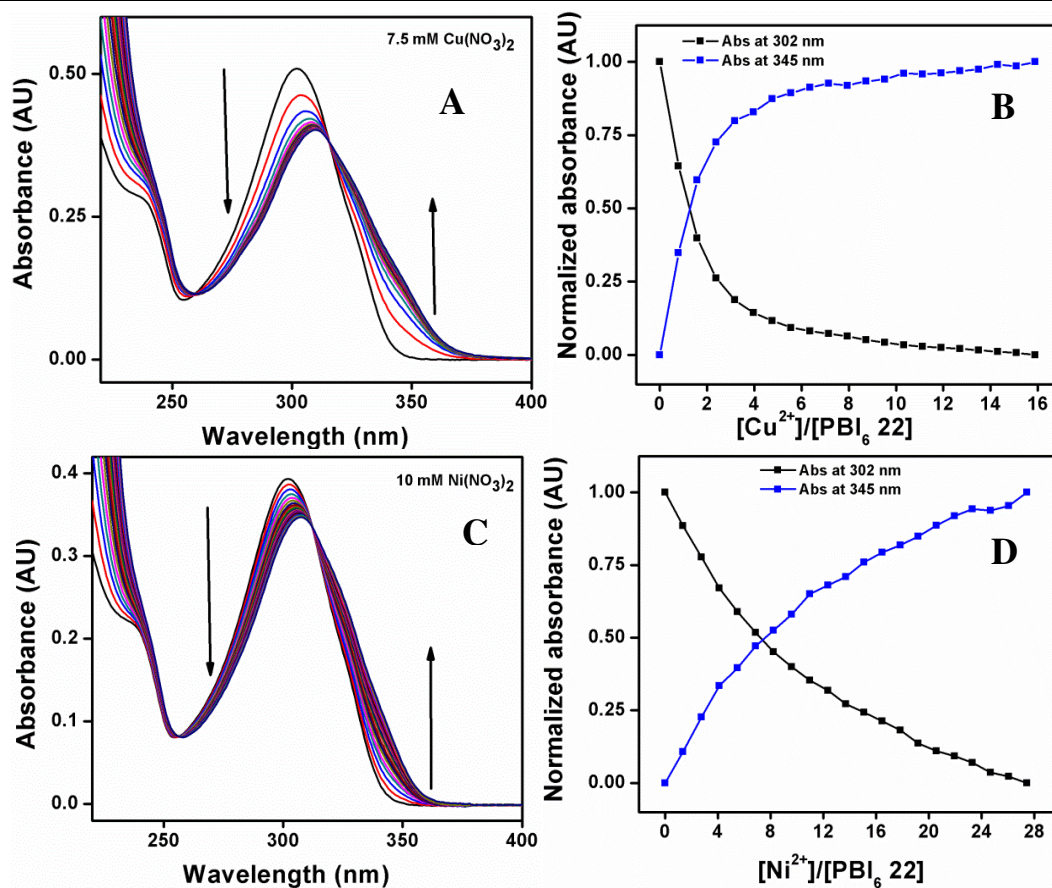


**Figure 53.** Changes in the absorption spectra of 2-pyridylbenzimidazole (PBI)<sub>6</sub> oligomer **22** (8-10 μM) in water upon the addition of metal salts (A) Cu(NO<sub>3</sub>)<sub>2</sub> (7.5 mM). (C) Ni(NO<sub>3</sub>)<sub>2</sub> (10 mM). Plot of the change in absorbance at 308 and 323 nm as a function of molar ratio of metal to peptides (B) Cu(NO<sub>3</sub>)<sub>2</sub> and (D) Ni(NO<sub>3</sub>)<sub>2</sub>.

**AuCl<sub>3</sub>:** In case of Au<sup>3+</sup>, with increasing concentration a gradual decrease in the absorbance at 302 nm was observed, but unfortunately, since the absorption changes of the ligand was completely masked by the gold absorption itself, meaningful interpretation of this result was not possible (Figure 54).

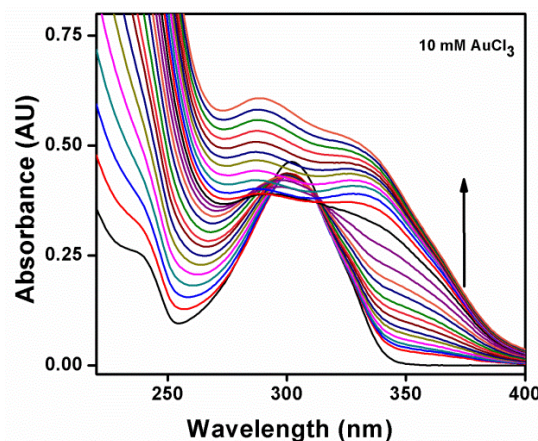


**Figure 54.** Changes in the absorption spectra of 2-pyridylbenzimidazole (PBI)<sub>6</sub> oligomer **22** (8-10 μM) in water upon the addition of AuCl<sub>3</sub> (10 mM).

UV-Vis titration experiments of 2-pyridylbenzimidazole (PBI)<sub>6</sub> oligomer **22** with several metal ions like Zn<sup>2+</sup>, Pt<sup>3+</sup>, Ag<sup>+</sup>, Tb<sup>3+</sup>, Eu<sup>3+</sup>, Cd<sup>2+</sup>, Pt<sup>2+</sup>, Pb<sup>2+</sup>, Ho<sup>3+</sup>, Mn<sup>3+</sup> *etc* were undertaken. No significant spectral changes were observed by the addition of any of these metal salts (Table 17), suggesting lack of complexation to (PBI)<sub>6</sub> **22**.

**Table 17.** Summary of UV-Vis titrations for the 2-pyridylbenzimidazole (PBI)<sub>6</sub> oligomer **22**.

Metal salts (2.5 mM)	Observation	Inflection points	Isosbestic points
Copper nitrate	Binding	302 and 324	258 and 315
Nickel nitrate	Binding	302 and 324	256 and 312
Gold chloride	Binding	302 and 350	293 and 312
Ruthenium chloride	very weak binding	-	-
Palladium nitrate	Very weak binding	-	-

\*silver nitrate, cadmium nitrate, lead nitrate, holmium nitrate, manganese acetate, iron nitrate, zinc nitrate, europium nitrate, terbium nitrate did not show metal binding.

To determine the stoichiometry of binding, Job's plot of 2-pyridylbenzimidazole (PBI)<sub>6</sub> oligomer **22** (100 μM in water) with Cu(NO<sub>3</sub>)<sub>2</sub> and Ni(NO<sub>3</sub>)<sub>2</sub> were obtained. The intersection point was obtained around 0.60, which indicated a binding stoichiometry 3:2 for the complexes (Figure 55). However, Job's plot for 2-pyridylbenzimidazole (PBI)<sub>6</sub> oligomer **22** with Cu(NO<sub>3</sub>)<sub>2</sub> and Ni(NO<sub>3</sub>)<sub>2</sub> yielded the different binding stoichiometry 2:3 [2-pyridylbenzimidazole (PBI)<sub>6</sub> oligomer **22**: Cu(NO<sub>3</sub>)<sub>2</sub>], and 1:2 [2-pyridylbenzimidazole (PBI)<sub>6</sub> oligomer **22**: Ni(NO<sub>3</sub>)<sub>2</sub>], respectively.



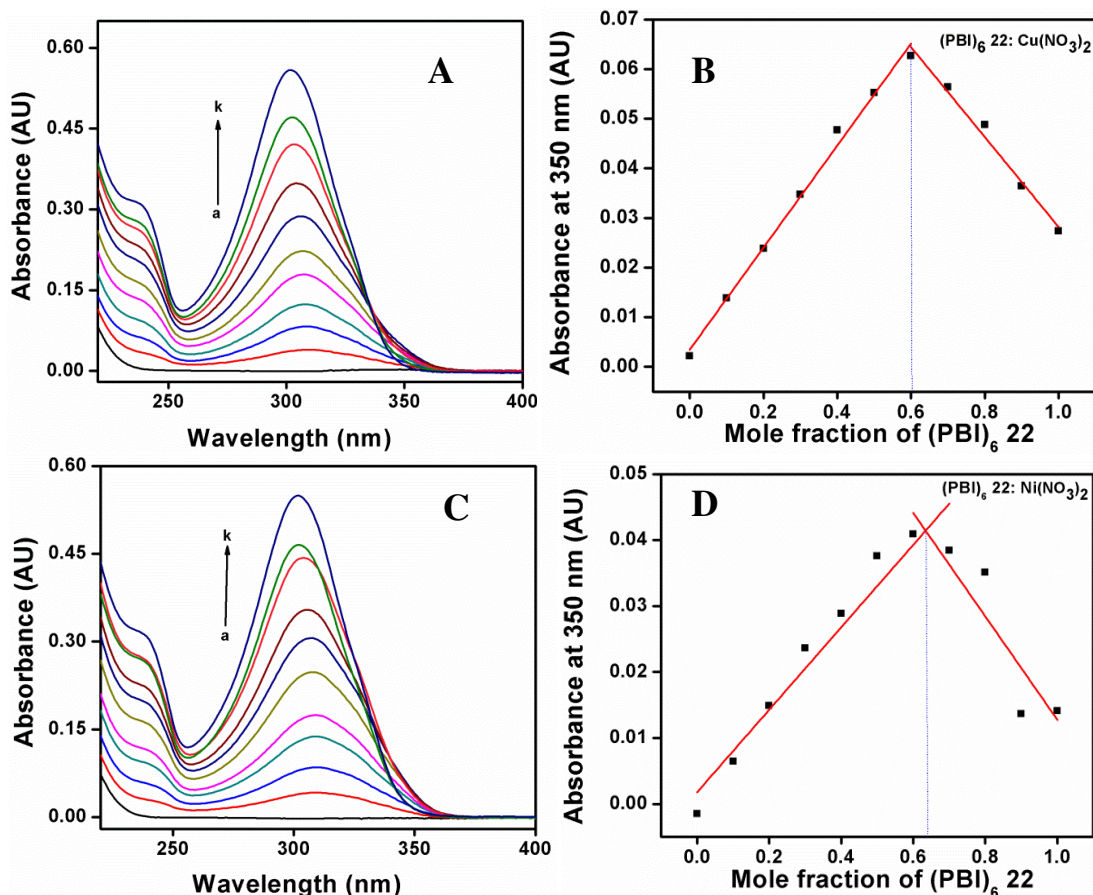


**Figure 55.** UV-Vis absorption spectra of 2-pyridylbenzimidazole ( $(\text{PBI})_6$  oligomer **22**) with metal salts in molar ratios of (a) 0:100 (b) 10:90 (c) 20:80 (d) 30:70 (e) 40:60 (f) 50:50 (g) 60:40 (h) 70:30 (i) 80:20 (j) 90:10 (k) 100:0; (A) UV spectra and (B) Job's plot with  $\text{Cu}(\text{NO}_3)_2$ ; (C) UV spectra and (D) Job's plot with  $\text{Ni}(\text{NO}_3)_2$ .

Benesi Hildebrand equation was used for calculating the binding constants and resulted in the straight line, which is shown in graphs (Figure 56A & B, inset).

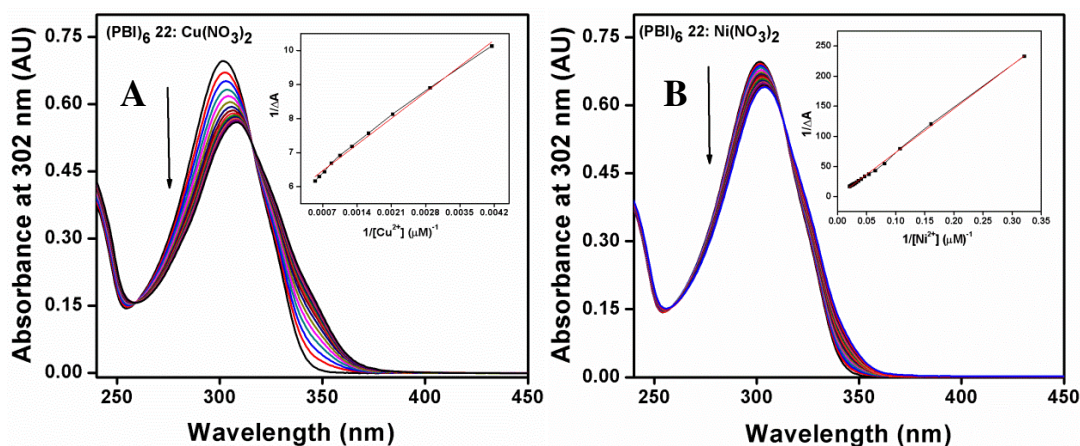


**Figure 56.** Benesi Hildebrand's plots for 2-pyridylbenzimidazole ( $(\text{PBI})_6$  oligomer **22**) (A) UV-Vis absorption spectra of with (A)  $\text{Cu}(\text{NO}_3)_2$  and (B)  $\text{Ni}(\text{NO}_3)_2$ . Arrows indicate decrease in absorption at 302 nm from 0 to 2.5 mM metal concentration. The Benesi Hildebrand plots are represented as insets.

The calculated binding constant (K) values are  $5.19 \times 10^3 \text{ [M]}^{-1}$  and  $2.61 \times 10^3 \text{ [M]}^{-1}$  for  $\text{Cu}(\text{NO}_3)_2$  and  $\text{Ni}(\text{NO}_3)_2$ , respectively. These values are comparable with those of the monomer (PBI) **8**.

In conclusion, 2-pyridylbenzimidazole (PBI)<sub>6</sub> oligomer **22**, showed binding with copper, nickel and gold metal ions.

### 3.10.3b UV-Vis spectrophotometric titrations of *o*-phenylenediamine polyamide oligomer (PDA)<sub>6</sub> **23**

As per the reports,<sup>61</sup> *o*-phenylenediamines are found to binds better with palladium, gold, mercury, cadmium *etc.* With this rationale in mind *o*-phenylenediamine oligomer (PDA)<sub>6</sub> **23** (Figure 57) consisting of *o*-phenylenediamines attached to *aeg*-backbone were titrated with dissimilar metal salts.

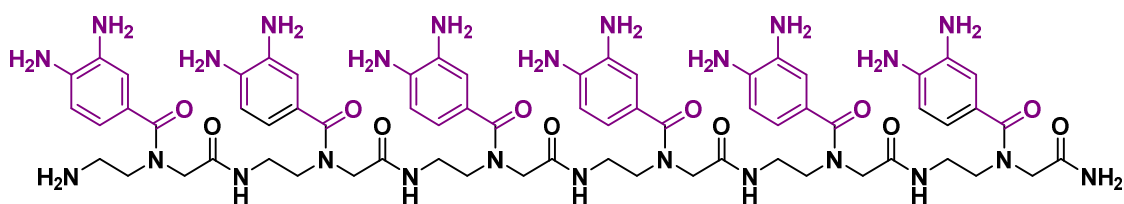


**Figure 57.** Structure of *o*-phenylenediamine oligomer (PDA)<sub>6</sub> **23**.

*o*-Phenylenediamine oligomer (PDA)<sub>6</sub> **23** was studied for its complexation behaviour towards diverse metal ions *i.e* copper nitrate, nickel nitrate and gold chloride (Figure 57).

**Cu(NO<sub>3</sub>)<sub>2</sub> and Ni(NO<sub>3</sub>)<sub>2</sub>:** The absorption spectra of aqueous solution of *o*-phenylenediamine oligomer (PDA)<sub>6</sub> **23** displays two absorption peaks ( $\lambda_{\text{max}}$ ) at 269 nm and 271 nm. UV-Vis titration experiments of *o*-phenylenediamine oligomer (PDA)<sub>6</sub> **23** with  $\text{Cu}(\text{NO}_3)_2$  and  $\text{Ni}(\text{NO}_3)_2$  were carried out at lower concentration (2.5 mM) which resulted insignificant spectral change (Figure 58A & B). Concentration of the metal salts were increased to 7.5 mM in order to shift the equilibrium towards metal complexation. The titrations also performed with  $\text{Cu}(\text{NO}_3)_2$  and  $\text{Ni}(\text{NO}_3)_2$  at higher concentration (7.5 mM), but displayed no significant spectral change (Figure 58C & D).

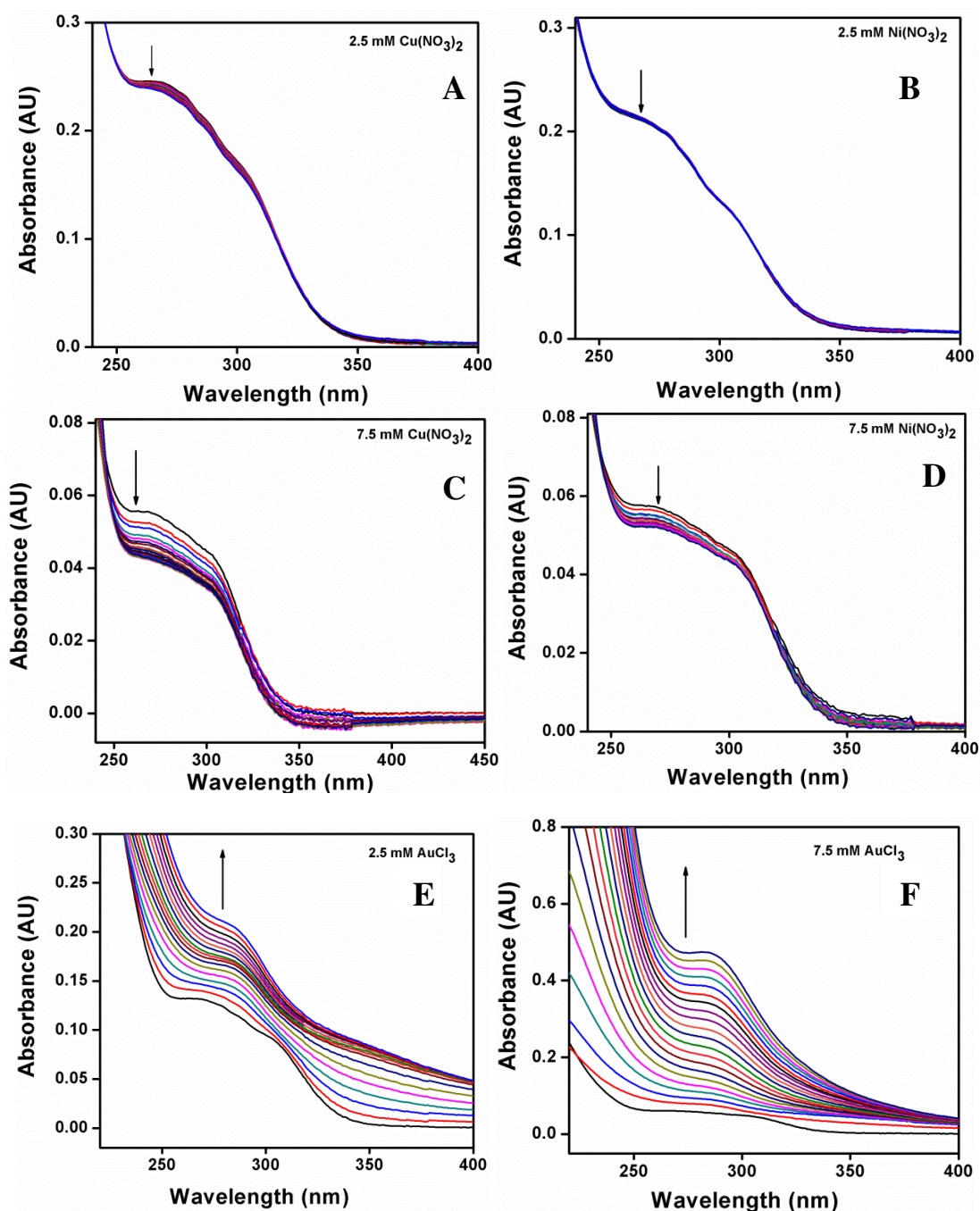


**Figure 58.** Changes in the absorption spectra of *o*-phenylenediamine oligomer (PDA)<sub>6</sub> **23** (8–10  $\mu$ M) in water upon the addition of metal salts (A) Cu(NO<sub>3</sub>)<sub>2</sub> (2.5 mM), (B) Ni(NO<sub>3</sub>)<sub>2</sub> (2.5 mM), (C) Cu(NO<sub>3</sub>)<sub>2</sub> (7.5 mM), (D) Ni(NO<sub>3</sub>)<sub>2</sub> (7.5 mM), (E) AuCl<sub>3</sub> (2.5 mM) and (F) AuCl<sub>3</sub> (7.5 mM).

**AuCl<sub>3</sub>:** Similar results were seen in the titration of *o*-phenylenediamine oligomer (PDA)<sub>6</sub> **23** with gold chloride at both lower (2.5 mM) as well as higher concentrations (7.5 mM) (Figure 59E & F). Complexation of other metal ions like Zn<sup>2+</sup>, Cd<sup>2+</sup>, Pd<sup>2+</sup>, Hg<sup>2+</sup> as their nitrate/perchlorate salts were also explored. However, no significant spectral change was observed by the addition of these metal salts (Figure 59).

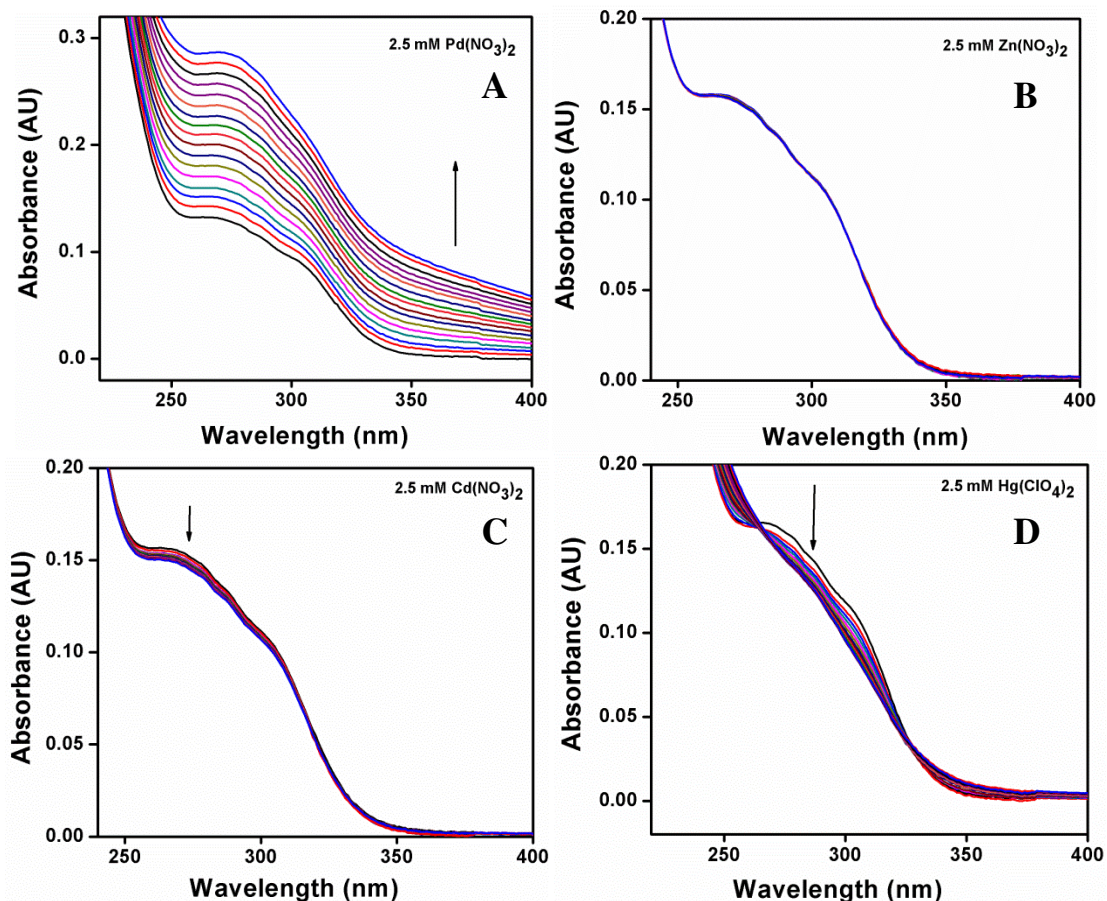


**Figure 59.** Changes in the absorption spectra of *o*-phenylenediamine oligomer (PDA)<sub>6</sub> 23 (8-10 μM) in water upon the addition of metal salts. (A) Pd(NO<sub>3</sub>)<sub>2</sub> (2.5 mM), (B) Zn(NO<sub>3</sub>)<sub>2</sub> (2.5 mM), (C) Cd(NO<sub>3</sub>)<sub>2</sub> (2.5 mM) and (D) Hg(ClO<sub>4</sub>)<sub>2</sub> (2.5 mM).

UV-Vis experiments of *o*-phenylenediamine oligomer (PDA)<sub>6</sub> 23 were done with Cu(NO<sub>3</sub>)<sub>2</sub> and Ni(NO<sub>3</sub>)<sub>2</sub> under basic conditions also (Figure 60), but no significant spectral changes were observed.

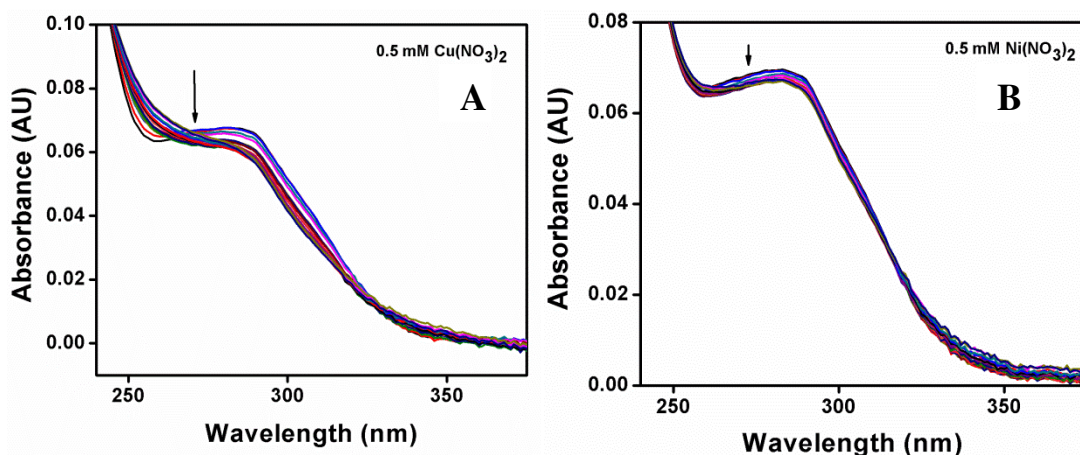


**Figure 60.** Changes in the absorption spectra of *o*-phenylenediamine oligomer (PDA)<sub>6</sub> 23 (8-10 μM) in water upon the addition of metal salts followed by NaOH (0.5 M) (A) Cu(NO<sub>3</sub>)<sub>2</sub> (0.5 mM) and (B) Ni(NO<sub>3</sub>)<sub>2</sub> (0.5 mM).

In summary, *o*-phenylenediamine oligomer (PDA)<sub>6</sub> **23** exhibited poor or negligible complexation towards various metal ions such as like Zn<sup>2+</sup>, Cd<sup>2+</sup>, Pd<sup>2+</sup>, Hg<sup>2+</sup>, Cu<sup>2+</sup>, Au<sup>3+</sup> and Ni<sup>2+</sup>.

### 3.10.3c UV-Vis spectrophotometric titrations of catechol (CAT)<sub>6</sub> Oligomer **24**

Catechol (CAT)<sub>6</sub> oligomer **24** (Figure 61) consisting of catechol units attached to *aeg*-backbone were titrated with various metal salts.

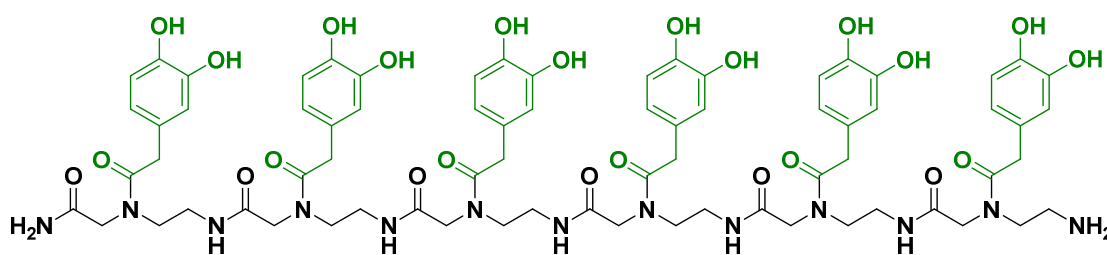


**Figure 61.** Structure of catechol (CAT)<sub>6</sub> oligomer **24**.

The electronic spectra of aqueous solution of catechol (CAT)<sub>6</sub> oligomer **24** displays absorption ( $\lambda_{\text{max}}$ ) at 281 nm. UV-Vis titration experiments of catechol (CAT)<sub>6</sub> oligomer **24** with Cu(NO<sub>3</sub>)<sub>2</sub> and Ni(NO<sub>3</sub>)<sub>2</sub> (Figure 62).

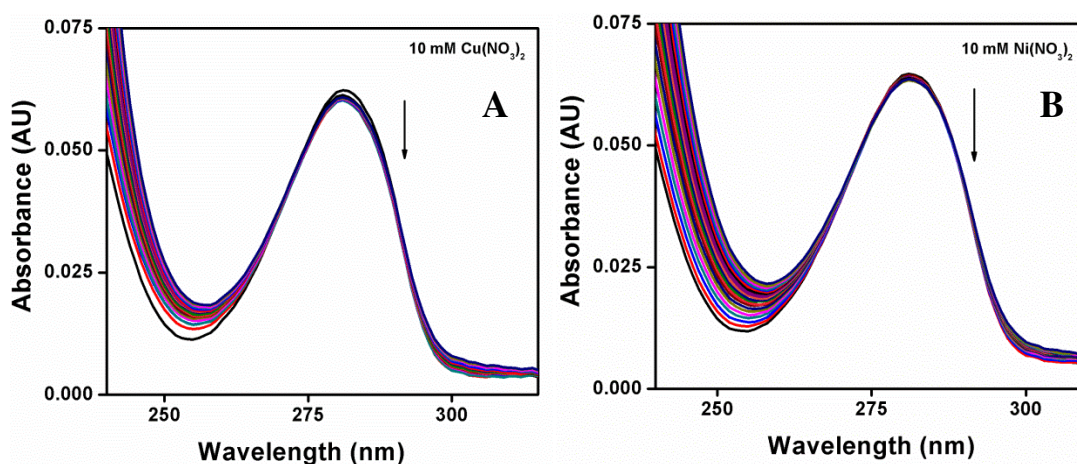


**Figure 62.** Changes in the absorption spectra of catechol (CAT)<sub>6</sub> oligomer **24** (8-10  $\mu$ M) in water upon the addition of metal salts (A) Cu(NO<sub>3</sub>)<sub>2</sub> (10 mM) and (B) Ni(NO<sub>3</sub>)<sub>2</sub> (10 mM).

Similarly, UV-Vis spectrophotometric titrations were also carried out at higher concentration (10 mM) but resulted in no significant spectral change (Figure 63).

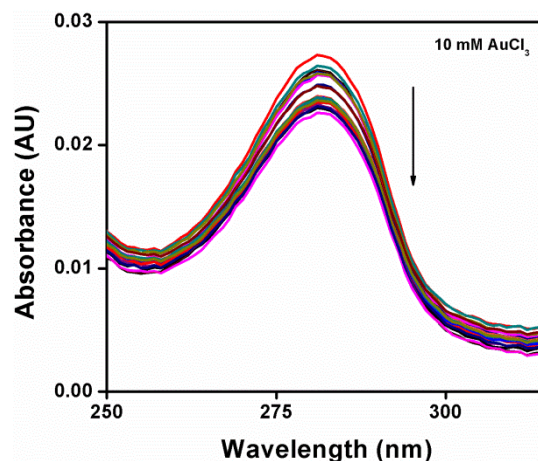


**Figure 63.** Changes in the absorption spectra of catechol (CAT)<sub>6</sub> oligomer **24** (8-10  $\mu$ M) in water upon the addition of AuCl<sub>3</sub> (10 mM).

In summary, catechol (CAT)<sub>6</sub> oligomer **24** exhibited poor complexation towards metal ions such as like Cu<sup>2+</sup>, Au<sup>3+</sup> and Ni<sup>2+</sup>.

### 3.10.4 UV-Vis spectrophotometric titrations of polyamide *hetero*-oligomers

*Hetero*-oligomers having different metal complexing ligands *e.g.* PBI/PDA or PBI/CAT expands the repertoire of metallo-polyamides. Hence, polyamide *hetero*-oligomers (PBI)<sub>3</sub>-(PDA)<sub>3</sub> **25**, (PBI-PDA)<sub>3</sub> **26**, (PBI)<sub>3</sub>-(CAT)<sub>3</sub> **27** and (PBI-CAT)<sub>3</sub> **28** were synthesized and titrated with different metal salts to investigate their metal binding properties.

#### 3.10.4a UV-Vis spectrophotometric titrations of (PBI)<sub>3</sub>-(PDA)<sub>3</sub> oligomer **25**

UV-Vis titration experiments of (PBI)<sub>3</sub>-(PDA)<sub>3</sub> oligomer **25** (Figure 64) were studied with different metal ions (Zn<sup>2+</sup>, Ru<sup>3+</sup>, Pd<sup>2+</sup>, Pt<sup>3+</sup>, Co<sup>2+</sup>, Cd<sup>2+</sup>, Pb<sup>2+</sup>, Pd<sup>2+</sup>) as their nitrate/chloride salts. UV-Vis spectrum of aqueous solution of (PBI)<sub>3</sub>-(PDA)<sub>3</sub> oligomer **25** shows absorbance ( $\lambda_{\text{max}}$ ) at 302 nm.

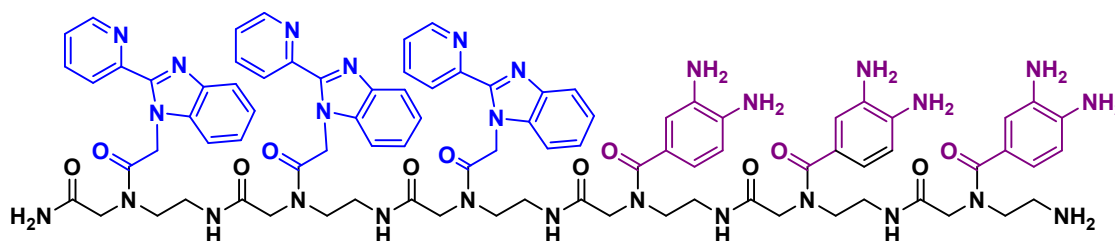


**Figure 64.** Structure of (PBI)<sub>3</sub>-(PDA)<sub>3</sub> oligomer **25**.

**Cu(NO<sub>3</sub>)<sub>2</sub> and Ni(NO<sub>3</sub>)<sub>2</sub>:** Upon addition of Cu(NO<sub>3</sub>)<sub>2</sub> and Ni(NO<sub>3</sub>)<sub>2</sub>, the new absorption band appears ( $\lambda_{\max}$ ) at 325 nm (+13 nm) and 324 nm (+12 nm) respectively, both exhibiting isosbestic points at 256 and 312 nm that indicated the formation of Cu<sup>2+</sup>-[(PBI)<sub>3</sub>-(PDA)<sub>3</sub> oligomer **25**] and Ni<sup>2+</sup>- [(PBI)<sub>3</sub>-(PDA)<sub>3</sub> oligomer **25**] complexes (Figure 65).

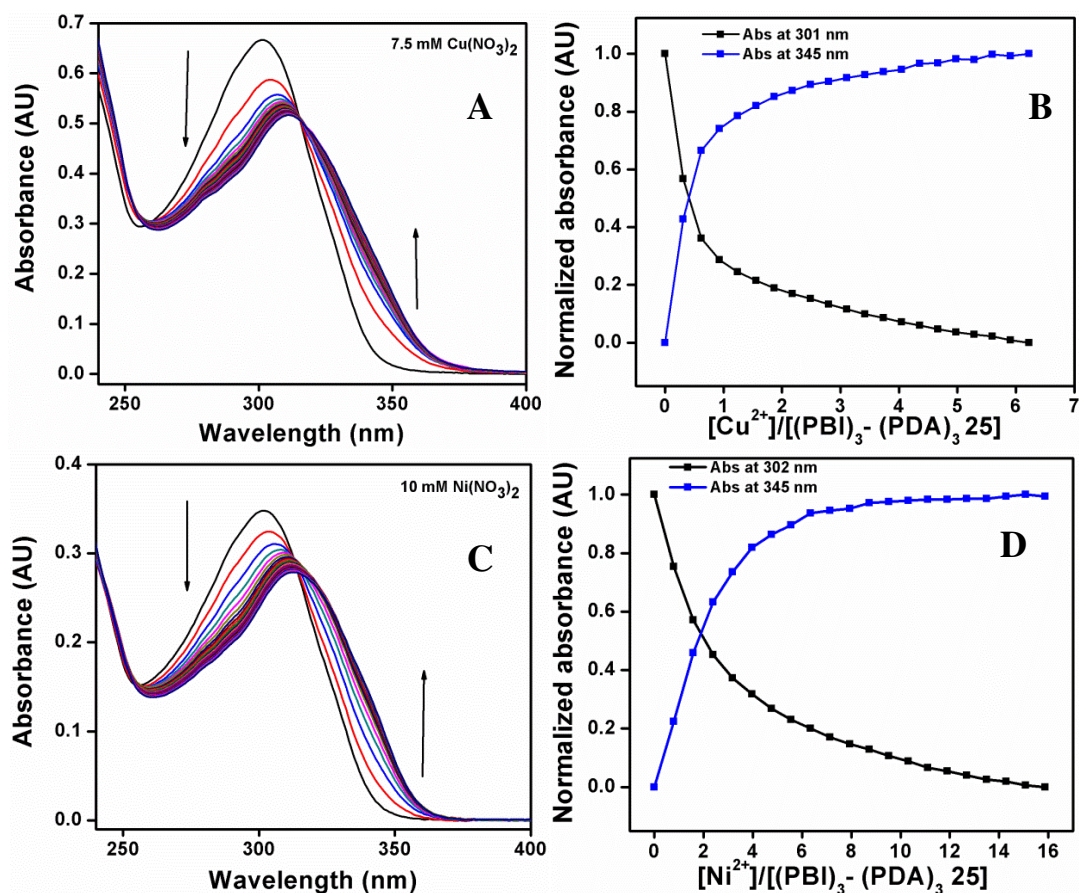


**Figure 65.** Changes in the absorption spectra of (PBI)<sub>3</sub>-(PDA)<sub>3</sub> oligomer **25** (8-10 μM) in water upon the addition of metal salts (A) Cu(NO<sub>3</sub>)<sub>2</sub> (7.5 mM) and (C) Ni(NO<sub>3</sub>)<sub>2</sub> (10 mM). Plot of the change in absorbance at 302 and 345 nm as a function of molar ratio of metal to peptides (B) Cu(NO<sub>3</sub>)<sub>2</sub> and (D) Ni(NO<sub>3</sub>)<sub>2</sub>.

It is worthy to note that synthesized *aeg* linked oligomers exhibits differential binding patterns with various metal salts. The synthesized *o*-phenylenediamine (PDA)<sub>6</sub> oligomer **23** did not show any strong binding for nickel nitrate salt, whereas *hetero*-oligomer (PBI)<sub>3</sub>-(PDA)<sub>3</sub> **25** exhibited strong binding.

**AuCl<sub>3</sub>:** Surprisingly, with an increase in the Au<sup>3+</sup> concentration the absorbance ( $\lambda_{\max}$ ) at 302 nm gradually decreased, but the absorbance was completely masked by the absorbance of gold itself. So, in order to obtain the clear isosbestic point, it was titrated with lesser amount (2.0 μL of 10 mM solution) and it revealed two isosbestic

2013 PhD thesis: T. Kaur, University of Pune

points at 286 and 332 nm suggesting the formation of  $\text{Au}^{3+}$ -[(PBI)<sub>3</sub>-(PDA)<sub>3</sub>] oligomer **25** complex (Figure 66).

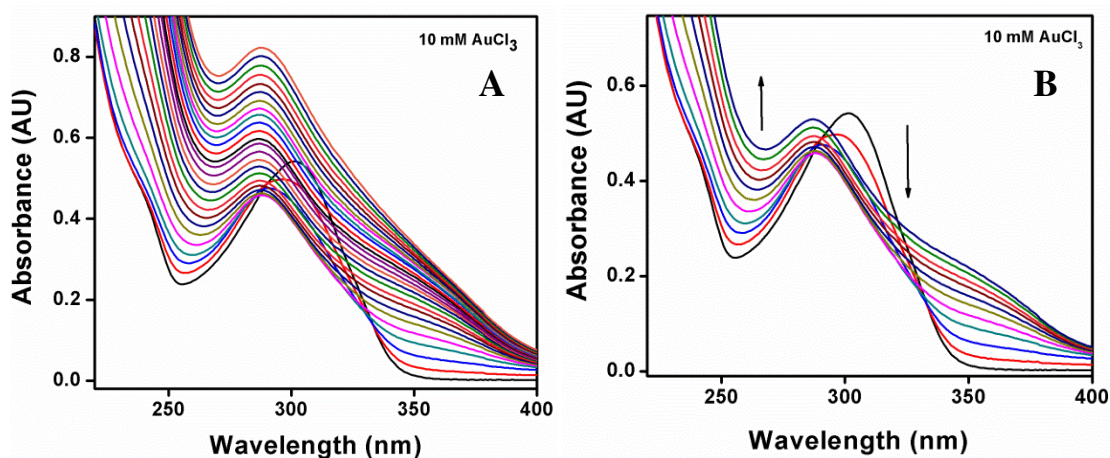


**Figure 66.** Changes in the absorption spectra of (PBI)<sub>3</sub>-(PDA)<sub>3</sub> oligomer **25** (8-10  $\mu\text{M}$ ) in water upon the addition of metal salts (A)  $\text{AuCl}_3$  (10 mM) (B)  $\text{AuCl}_3$  (10 mM).

In comparison to (PBI)<sub>6</sub> **22** (Figure 67A & B), (PBI)<sub>3</sub>-(PDA)<sub>3</sub> oligomer **25** (Figure 65C & D) binds better with similar concentration of nickel nitrate (10 mM). So, it is possible that the octahedral geometry of nickel salts could be stabilized nicely by either two PBI units and one PDA unit or *vice versa*.

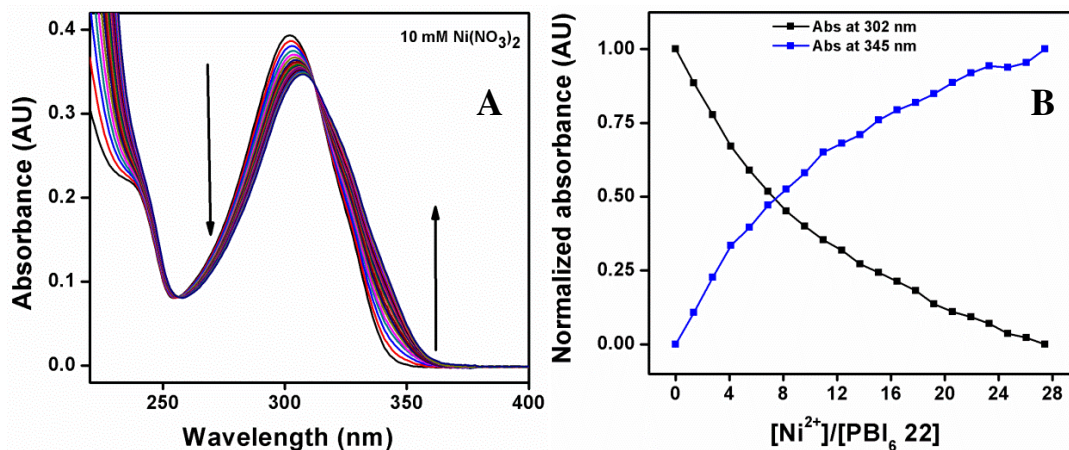


**Figure 67.** Changes in the absorption spectra of (PBI)<sub>6</sub> oligomer **22** (8-10  $\mu\text{M}$ ) in water upon the addition of metal salts (A)  $\text{Ni}(\text{NO}_3)_2$  (7.5). Plot of the change in absorbance at 302 and 345 nm as a function of molar ratio of metal to peptides (B)  $\text{Ni}(\text{NO}_3)_2$ .

UV-Vis spectral change of (PBI)<sub>3</sub>-(PDA)<sub>3</sub> oligomer **25** were studied in the presence of metal ions like zinc nitrate, ruthenium trichloride, palladium nitrate,



## Chapter 3

cobalt nitrate, lead nitrate, potassium tetrachloroplatinate and did not exhibit significant spectral change (Table 18).

**Table 18.** Summary of UV-Vis titrations for the  $(\text{PBI})_3\text{-(PDA)}_3$  oligomer **25**.

Metal salts (2.5/ 7.5/ 10 mM)	Observation	Inflection points	Isosbestic points
Copper nitrate	Binding	302 and 325	258 and 315
Nickel nitrate	Binding	302 and 324	256 and 312
Gold chloride	Weak binding	302	286 and 332

\*zinc nitrate, ruthenium trichloride, palladium nitrate, cobalt nitrate, lead nitrate, potassium tetrachloroplatinate

Determination of binding stoichiometry by Job's plot (100  $\mu\text{M}$  in water) gave intersection point  $\sim 0.60$  shows 3:2 binding stoichiometry for  $[(\text{PBI})_3\text{-(PDA)}_3 \text{ 25: Cu(NO}_3)_2]$ , implying that the duplex is assembled from two oligomeric strands linked by three copper metal ions (Figure 68).

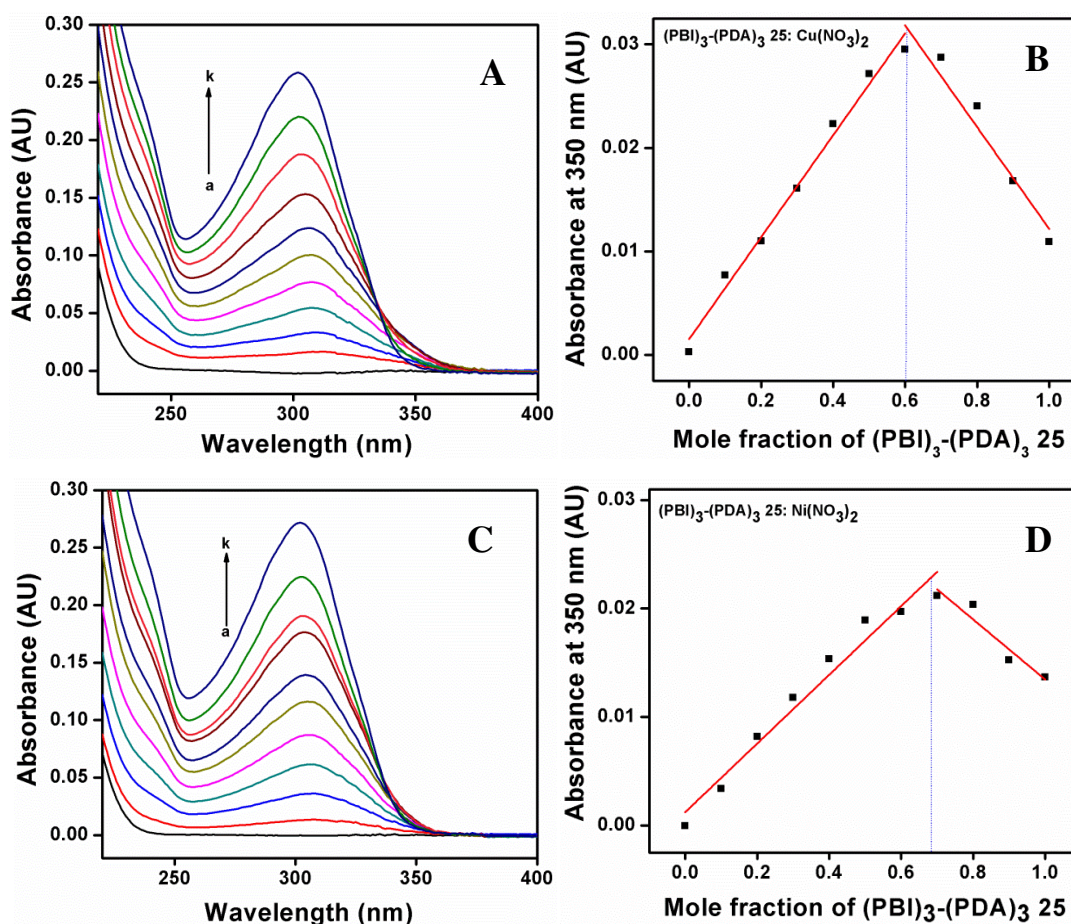


**Figure 68.** UV-Vis absorption spectra of  $(\text{PBI})_3\text{-(PDA)}_3$  **25** with metal salts in molar ratios of (a) 0:100 (b) 10:90 (c) 20:80 (d) 30:70 (e) 40:60 (f) 50:50 (g) 60:40 (h) 70:30 (i) 80:20 (j) 90:10 (k) 100:0; (A) UV spectra and (B) Job's plot with  $\text{Cu(NO}_3)_2$  (C) UV spectra and (D) Job's plot with  $\text{Ni(NO}_3)_2$ .

Job's plot of  $\text{Ni}(\text{NO}_3)_2$  and  $(\text{PBI})_3\text{-(PDA)}_3$  oligomer **25** exhibits intersection point at 0.67, shown a 1:2 binding stoichiometry for  $[(\text{PBI})_3\text{-(PDA)}_3 \text{ oligomer } \mathbf{25} : \text{Ni}(\text{NO}_3)_2]$ , suggests that two oligomeric strands are bound with four nickel metal ions.

UV-Vis spectroscopic studies confirmed that  $(\text{PBI})_3\text{-(PDA)}_3$  oligomer **25** binds better to the  $\text{Cu}(\text{NO}_3)_2$  and  $\text{Ni}(\text{NO}_3)_2$  than other metal salts. The calculated binding constants were found to be  $7.42 \times 10^4$  and  $3.34 \times 10^3 \text{ [M]}^{-1}$  for  $\text{Cu}(\text{NO}_3)_2$  and  $\text{Ni}(\text{NO}_3)_2$ , respectively (Figure 69).

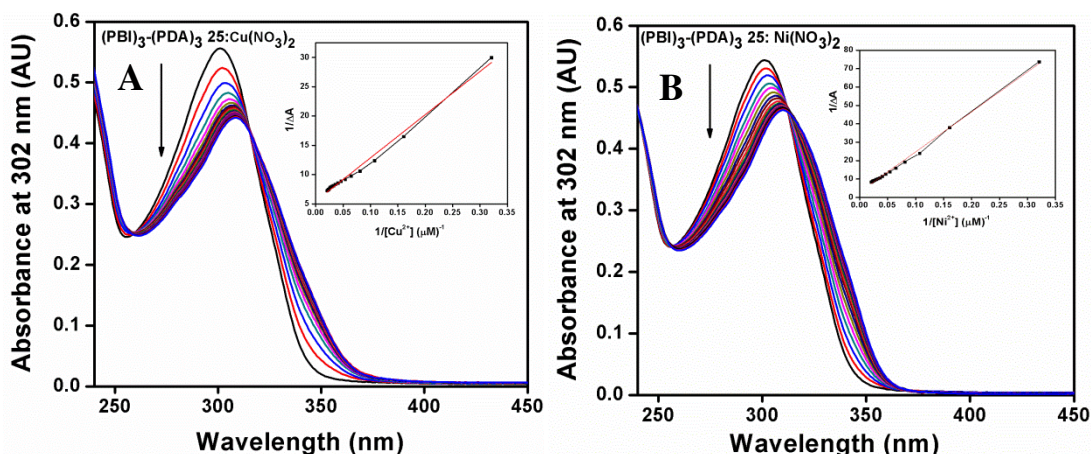


**Figure 69.** Benesi Hildebrand's plots (A) UV-Vis absorption spectra of  $(\text{PBI})_3\text{-(PDA)}_3$  oligomer **25** with (A)  $\text{Cu}(\text{NO}_3)_2$  and (B)  $\text{Ni}(\text{NO}_3)_2$ . Arrows indicate decrease in absorbance at 302 nm from 0 to 2.5 mM metal concentration. The Benesi Hildebrand plots are represented as insets.

In conclusion,  $(\text{PBI})_3\text{-(PDA)}_3$  oligomer **25**, showed binding with copper, nickel and gold metal ions.

### 3.10.4b UV-Vis spectrophotometric titrations of $(\text{PBI-PDA})_3$ oligomer **26**

Inspired by the metal binding results from the *hetero*-oligomer  $(\text{PBI-PDA})_3$  **25**, alternately linked  $(\text{PBI-PDA})_3$  oligomer **26** was also checked for its complexation studies. The UV-Vis absorbance spectra of  $(\text{PBI-PDA})_3$  oligomer **26** shows absorbance ( $\lambda_{\text{max}}$ ) at 303 nm in water (Figure 70).

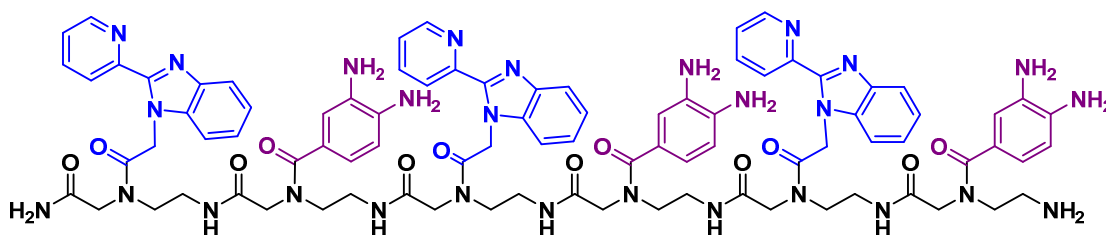


**Figure 70.** Structure of  $(\text{PBI-PDA})_3$  oligomer **26**.

**Cu(NO<sub>3</sub>)<sub>2</sub> and Ni(NO<sub>3</sub>)<sub>2</sub>:** Addition of Cu(NO<sub>3</sub>)<sub>2</sub> solution led to red shifts revealing absorbance ( $\lambda_{\text{max}}$ ) at 324 nm (+11 nm) and isosbestic points at 254 and 315 nm indicating the formation of Cu<sup>2+</sup>-(PBI-PDA)<sub>3</sub> oligomer **26** complex. So was the observation for Ni(NO<sub>3</sub>)<sub>2</sub>, but with isosbestic points at 255 and 315 nm. Similar results regarding its better binding with Ni(NO<sub>3</sub>)<sub>2</sub> can also be observed for (PBI-PDA)<sub>3</sub> oligomer **26** (Figure 71).

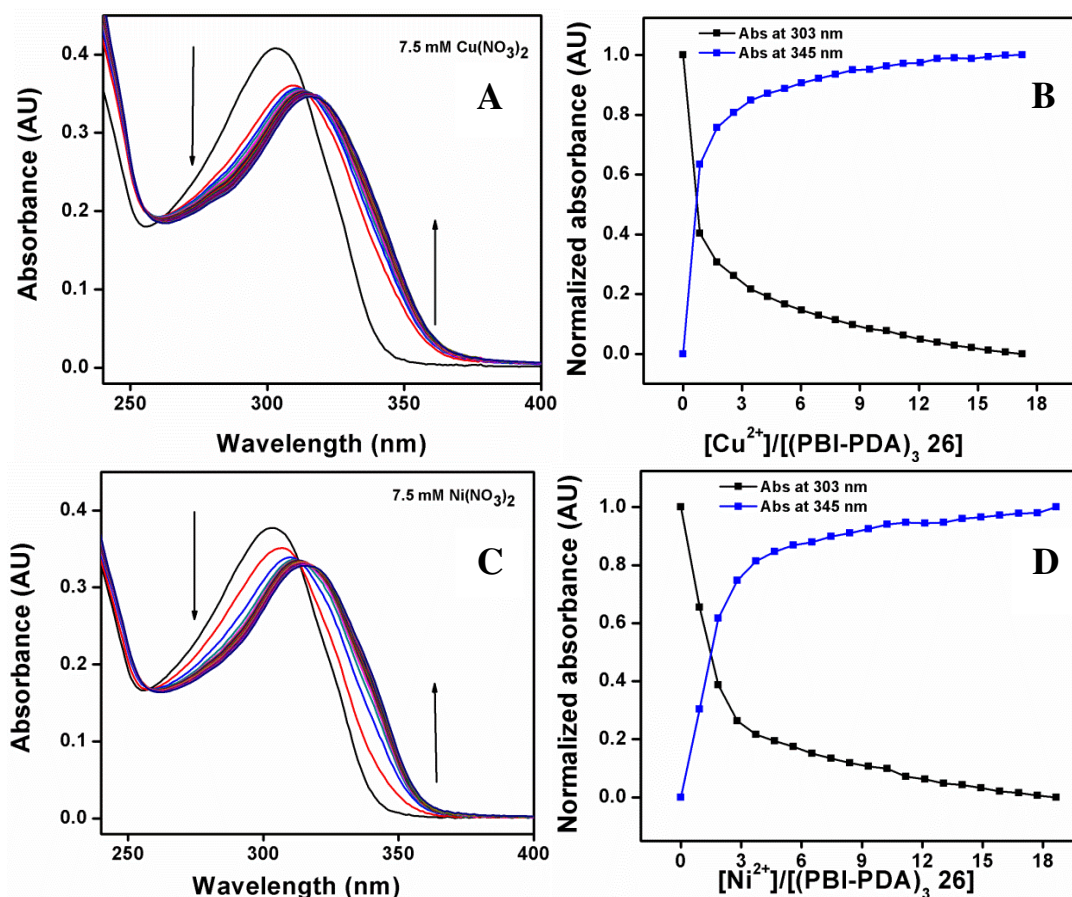


**Figure 71.** Changes in absorption spectra of (PBI-PDA)<sub>3</sub> oligomer **26** (8-10  $\mu\text{M}$ ) in water upon the addition of metal salts (A) Cu(NO<sub>3</sub>)<sub>2</sub> (7.5 mM) and (C) Ni(NO<sub>3</sub>)<sub>2</sub> (7.5 mM). Plot of the change in absorbance at 302 and 345 nm as a function of molar ratio of metal to peptides (B) Cu(NO<sub>3</sub>)<sub>2</sub> and (D) Ni(NO<sub>3</sub>)<sub>2</sub>.

**AuCl<sub>3</sub>:** Spectroscopic behaviour of (PBI-PDA)<sub>3</sub> oligomer **26** upon complexation with Au<sup>3+</sup>, showed a fall in absorbance at 302 nm was noted and presence of two isosbestic points at 288 and 333 nm indicated formation of Au<sup>3+</sup>-(PBI-PDA)<sub>3</sub> oligomer **26** complex (Figure 72).

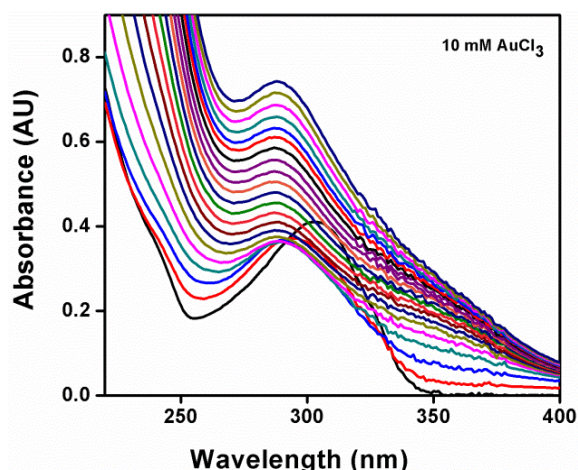


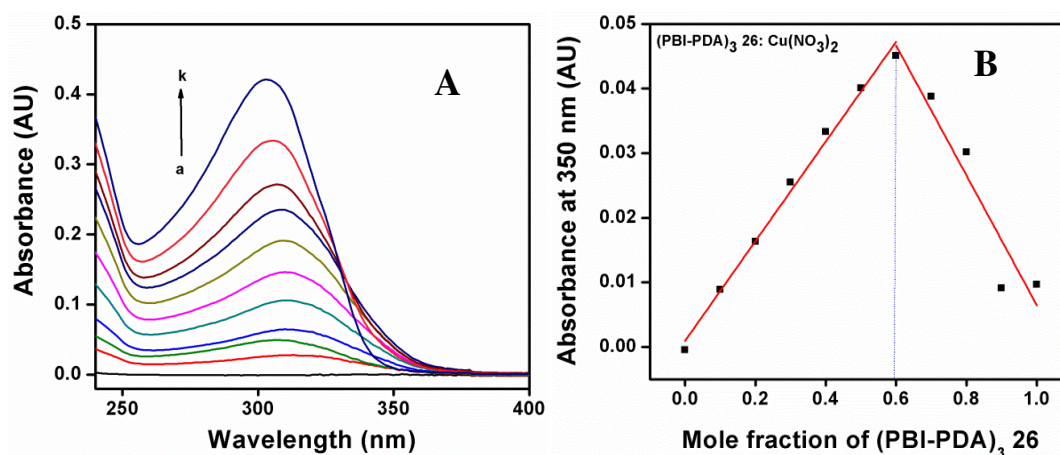
**Figure 72.** Changes in absorption spectra of (PBI-PDA)<sub>3</sub> oligomer **26** (8-10 μM) in water upon the addition of AuCl<sub>3</sub> (10 mM).

UV-Vis titration results for the (PBI-PDA)<sub>3</sub> oligomer have been summarized in Table 19.

**Table 19.** Summary of UV-Vis titrations for the (PBI-PDA)<sub>3</sub> oligomer **26**.

Metal salts (7.5/10 mM)	Observation	Inflection points	Isosbestic points
Copper nitrate	Binding	303 and 324	254 and 315
Nickel nitrate	Binding	303 and 324	255 and 315
Gold chloride	Weak binding	303	288 and 333

In the Job's continuous variation method (100 μM in water), intersection point was attained ~0.60 showing 3:2 stoichiometry for (PBI-PDA)<sub>3</sub> oligomer **26**: Cu(NO<sub>3</sub>)<sub>2</sub> complex. The two oligomeric strands are linked by three copper metal ions. In comparison Ni(NO<sub>3</sub>)<sub>2</sub> exhibits intersection point ~0.67, which shows the 1:2 stoichiometry wherein two oligomeric strands are linked by four nickel metal ions (Figure 73).



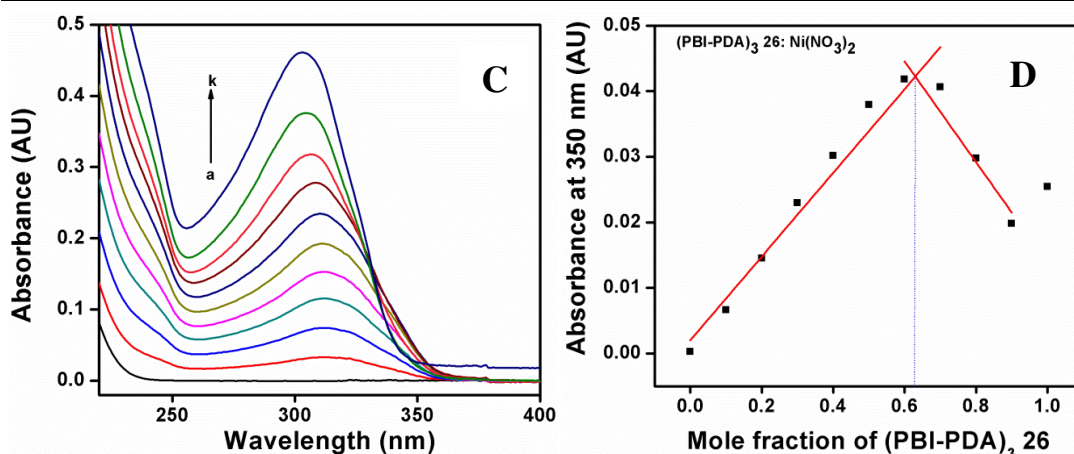


**Figure 73.** UV-Vis absorption spectra of  $(\text{PBI-PDA})_3$  oligomer **26** with metal salts in molar ratios of (a) 0:100 (b) 10:90 (c) 20:80 (d) 30:70 (e) 40:60 (f) 50:50 (g) 60:40 (h) 70:30 (i) 80:20 (j) 90:10 (k) 100:0; (A) UV spectra and (B) Job's plot with  $\text{Cu}(\text{NO}_3)_2$ ; (C) UV spectra and (D) Job's plot with  $\text{Ni}(\text{NO}_3)_2$ .

The binding constant ( $K$ ) calculated from Benesi-Hildebrand's equation were found  $1.58 \times 10^3$  and  $2.1 \times 10^3 \text{ [M]}^{-1}$  for  $\text{Cu}(\text{NO}_3)_2$  and  $\text{Ni}(\text{NO}_3)_2$ , respectively (Figure 74).

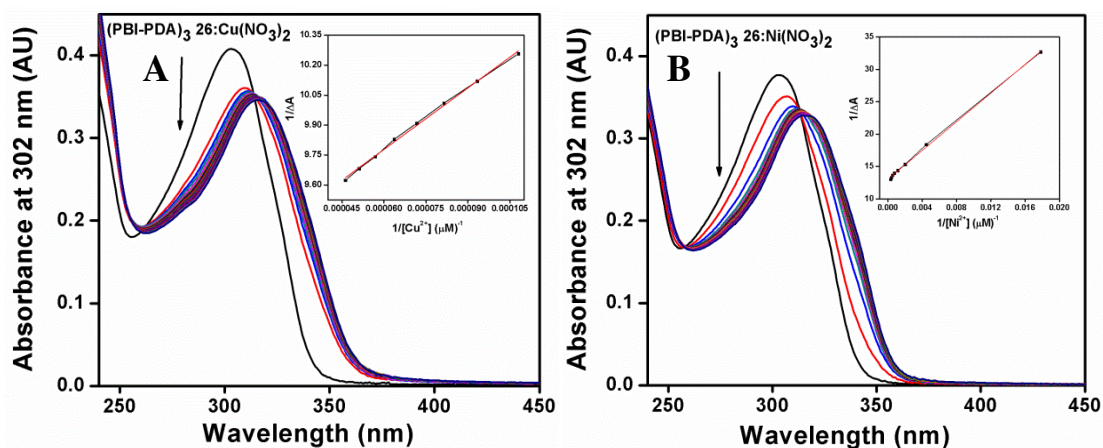


**Figure 74.** Benesi Hildebrand's plots (A) UV-Vis absorption spectra of  $(\text{PBI-PDA})_3$  oligomer **26** with (A)  $\text{Cu}(\text{NO}_3)_2$  and (B)  $\text{Ni}(\text{NO}_3)_2$ . Arrows indicate decrease in absorbance at 302 nm from 0 to 2.5 mM metal concentration. The Benesi Hildebrand plots are represented as insets.

In conclusion,  $(\text{PBI-PDA})_3$  oligomer **26**, showed binding with copper, nickel and gold metal ions.

### 3.10.4c UV-Vis spectrophotometric titrations of $(\text{PBI})_3\text{-(CAT)}_3$ Oligomer **27**

Polyamide hetero-oligomers with sequence  $(\text{PBI})_3\text{-(CAT)}_3$  oligomer **27** (hexamer unit) showed absorbance ( $\lambda_{\text{max}}$ ) at 303 nm in water (Figure 75).

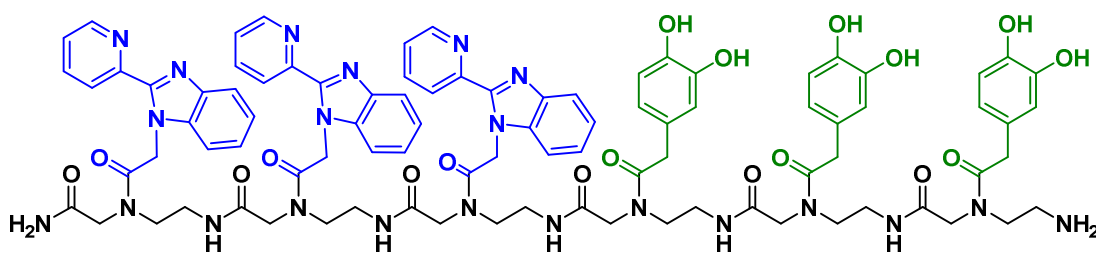


**Figure 75.** Structure of  $(\text{PBI})_3\text{-(CAT)}_3$  oligomer **27**.

**Cu(NO<sub>3</sub>)<sub>2</sub>:** The electronic spectra of  $(\text{PBI})_3\text{-(CAT)}_3$  oligomer **27** upon addition of  $\text{Cu(NO}_3)_2$  revealed binding pattern similar to that of  $\text{Cu}^{2+}\text{-(PBI-PDA)}_3$  **26** complex. Titrations with  $\text{Ni(NO}_3)_2$  exhibited a similar red shift, but a slightly more shifted isosbestic points at 260 and 313 nm indicating the formation of  $\text{Ni}^{2+}\text{-(PBI)}_3\text{-(CAT)}_3$  oligomer **27** complex (Figure 76). These changes in the absorption spectra indicated complex formation between  $(\text{PBI})_3\text{-(CAT)}_3$  oligomer **27** and metal ions ( $\text{Cu}^{2+}/\text{Ni}^{2+}$ ).

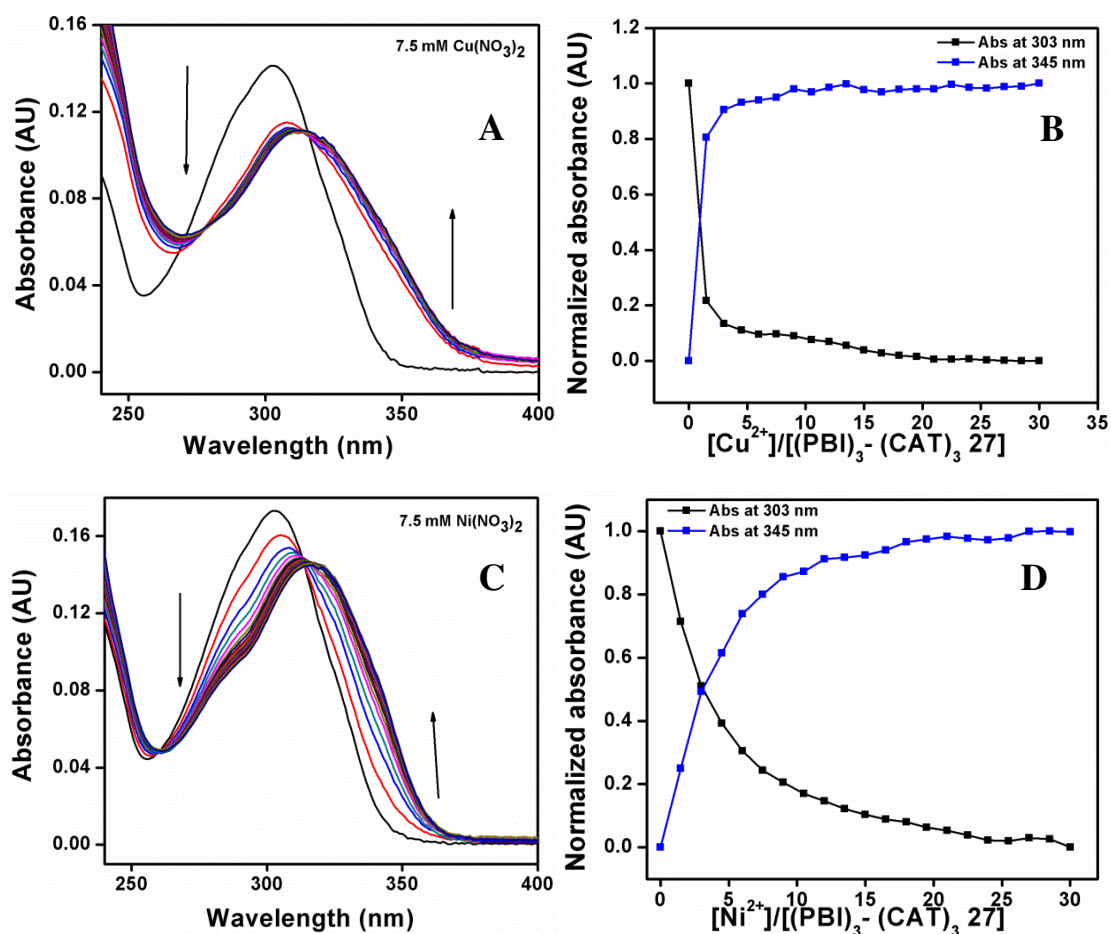


**Figure 76.** Changes in the absorption spectra of  $(\text{PBI})_3\text{-(CAT)}_3$  oligomer **27** (8-10  $\mu\text{M}$ ) in water upon the addition of metal salts (A)  $\text{Cu(NO}_3)_2$  (7.5 mM) and (C)  $\text{Ni(NO}_3)_2$  (7.5 mM)

## Chapter 3

Plot of the change in absorbance at 303 and 345 nm as a function of molar ratio of metal to peptides (B)  $\text{Cu}(\text{NO}_3)_2$  and (D)  $\text{Ni}(\text{NO}_3)_2$ .

The continuous variation method to determine molecular stoichiometry, showed intersection point  $\sim 0.60$  proving 3:2 stoichiometry for  $(\text{PBI})_3\text{-(CAT)}_3$  oligomer **27**: $\text{Cu}(\text{NO}_3)_2$ . The two oligomeric strands are possibly linked by three copper metal ions.  $(\text{PBI})_3\text{-(CAT)}_3$  oligomer **27**: $\text{Ni}(\text{NO}_3)_2$  indicated intersection point at 0.67, which indicates a binding stoichiometry of 1:2 (Figure 77).

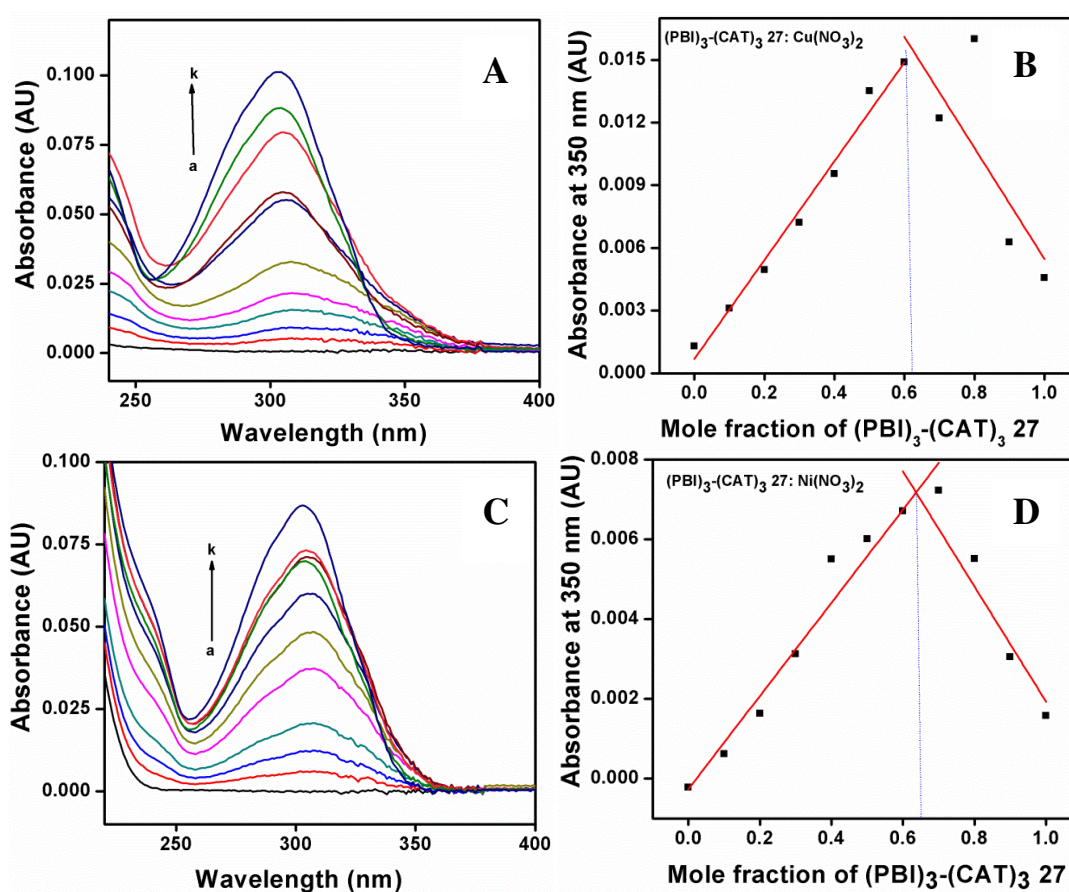


**Figure 77.** UV-Vis absorption spectra of  $(\text{PBI})_3\text{-(CAT)}_3$  oligomer **27** with metal salts in molar ratios of (a) 0:100 (b) 10:90 (c) 20:80 (d) 30:70 (e) 40:60 (f) 50:50 (g) 60:40 (h) 70:30 (i) 80:20 (j) 90:10 (k) 100:0; (A) UV spectra and (B) Job's plot with  $\text{Cu}(\text{NO}_3)_2$ ; (C) UV spectra and (D) Job's plot with  $\text{Ni}(\text{NO}_3)_2$ .

The binding constant ( $K$ ), which denotes the strength of binding, were found to be  $1.45 \times 10^4$  and  $5.16 \times 10^3 \text{ [M]}^{-1}$  in 1:2 binding model for  $\text{Cu}(\text{NO}_3)_2$  and  $\text{Ni}(\text{NO}_3)_2$ , respectively (Figure 78).

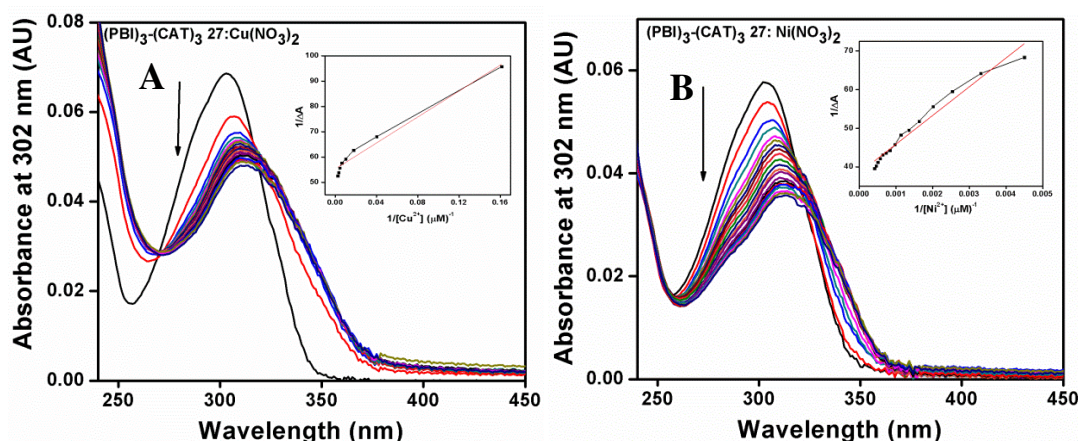


**Figure 78.** Benesi Hildebrand's plot (A) UV-Vis absorption spectra of  $(\text{PBI})_3\text{-(CAT)}_3$  oligomer **27** with (A)  $\text{Cu}(\text{NO}_3)_2$  and (B)  $\text{Ni}(\text{NO}_3)_2$ . Arrows indicate decrease in absorption at 302 nm from 0 to 2.5 mM metal concentration. The Benesi Hildebrand plots are represented as insets.

UV-Vis titration results have been summarized in Table 20.

**Table 20.** Summary of UV-Vis titration for the  $(\text{PBI})_3\text{-(CAT)}_3$  oligomer **27**.

Metal salts (7.5 mM)	Observation	Inflection points	Isosbestic points
Copper nitrate	Binding	303 and 324	255 and 314
Nickel nitrate	Binding	303 and 324	260 and 313

In conclusion,  $(\text{PBI})_3\text{-(CAT)}_3$  oligomer **27** binds strongly with copper and nickel metal salts.

#### 3.10.4d UV-Vis spectrophotometric titrations of $(\text{PBI-CAT})_3$ Oligomer **28**

The electronic spectrum of alternately linked  $(\text{PBI})_3\text{-(CAT)}_3$  oligomer **28** in aqueous medium featured absorption ( $\lambda_{\text{max}}$ ) at 305 nm, which on addition of  $\text{Cu}(\text{NO}_3)_2$  shifted to ( $\lambda_{\text{max}}$ ) at 324 nm (+11 nm) with isosbestic points at 265 and 317 nm, this indicates the formation of  $\text{Cu}^{2+}\text{-(PBI-CAT)}_3\text{-28}$  complex (Figure 79).

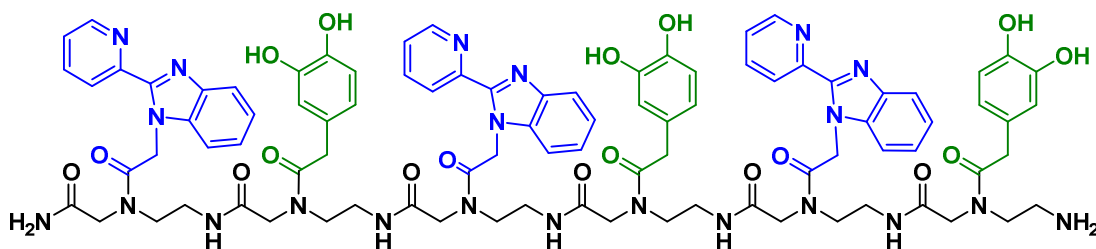


**Figure 79.** Structure of  $(\text{PBI})_3\text{-(CAT)}_3$  oligomer **28**.



A similar red shift was observed with with isosbestic points at 255 and 317 nm for the formation of  $\text{Ni}^{2+}$ -  $(\text{PBI})_3$ - $(\text{CAT})_3$  oligomer **28** complex (Figure 80).

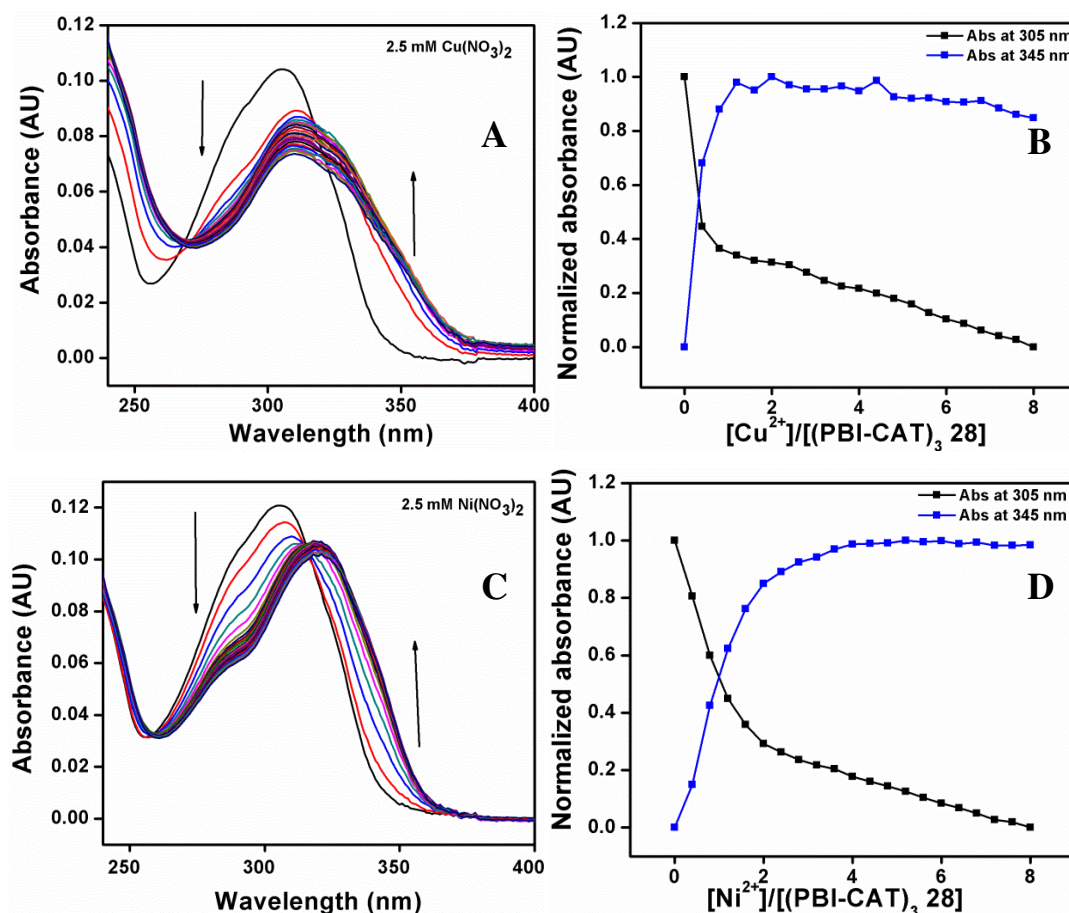


**Figure 80.** Changes in the absorption spectra of  $(\text{PBI})_3$ - $(\text{CAT})_3$  oligomer **28** (8-10  $\mu\text{M}$ ) in water upon the addition of metal salts (A)  $\text{Cu}(\text{NO}_3)_2$  (2.5 mM) and (C)  $\text{Ni}(\text{NO}_3)_2$  (2.5 mM). Plot of the change in absorbance at 305 and 350 nm as a function of molar ratio of metal to peptides (B)  $\text{Cu}(\text{NO}_3)_2$  and (D)  $\text{Ni}(\text{NO}_3)_2$ .

UV-Vis titration results have been summarized in Table 21.

**Table 21.** Summary of UV-Vis titration for the  $(\text{PBI})_3$ - $(\text{CAT})_3$  oligomer **28**.

Metal salts (2.5 mM)	Observation	Inflection points	Isosbestic points
Copper nitrate	Binding	305 and 324	265 and 317
Nickel nitrate	Binding	305 and 324	255 and 317

The Job's plot (100  $\mu\text{M}$  in water) indicated the intersection point at 0.60, proving binding stoichiometries to be 3:2 for  $(\text{PBI})_3$ - $(\text{CAT})_3$  oligomer **28**: $\text{Cu}(\text{NO}_3)_2$ . whereas, the intersection point at 0.67 for  $(\text{PBI})_3$ - $(\text{CAT})_3$  oligomer **28**: $\text{Ni}(\text{NO}_3)_2$  was indicative of 1:2 stoichiometry (Figure 81).

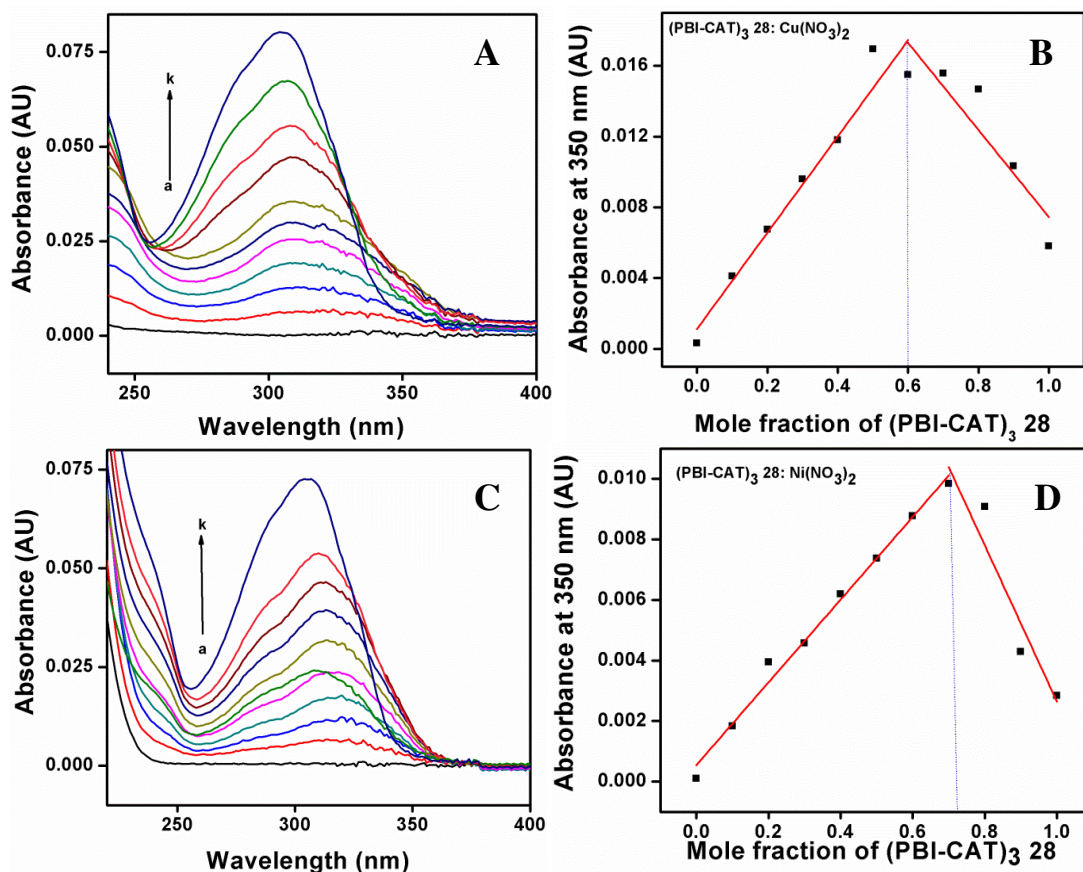


**Figure 81.** UV-Vis absorption spectra of (PBI)<sub>3</sub>-(CAT)<sub>3</sub> oligomer **28** with metal salts in molar ratios of (a) 0:100 (b) 10:90 (c) 20:80 (d) 30:70 (e) 40:60 (f) 50:50 (g) 60:40 (h) 70:30 (i) 80:20 (j) 90:10 (k) 100:0; (A) UV spectra and (B) Job's plot with Cu(NO<sub>3</sub>)<sub>2</sub>; (C) UV spectra and (D) Job's plot with Ni(NO<sub>3</sub>)<sub>2</sub>.

The binding constant (K) values obtained from Benesi-Hildebrand plot was  $7.87 \times 10^3$  and  $4.54 \times 10^4$  [M]<sup>-1</sup> for Cu(NO<sub>3</sub>)<sub>2</sub> and Ni(NO<sub>3</sub>)<sub>2</sub>, respectively (Figure 82).

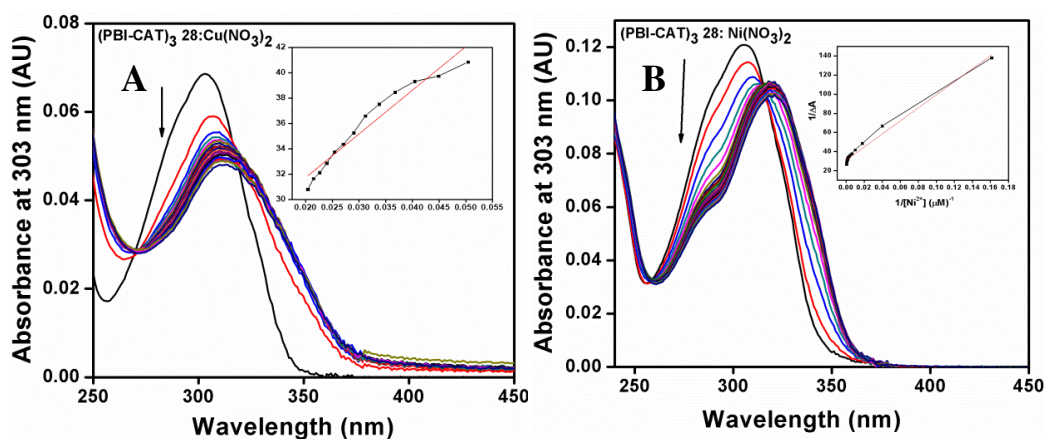


**Figure 82.** Benesi Hildebrand's plot (A) UV-Vis absorption spectra of (PBI)<sub>3</sub>-(CAT)<sub>3</sub> oligomer **28** with (A) Cu(NO<sub>3</sub>)<sub>2</sub> and (B) Ni(NO<sub>3</sub>)<sub>2</sub>. Arrows indicate decrease in absorption at 305 nm from 0 to 2.5 mM metal concentration. The Benesi Hildebrand plots are represented as insets.

In short, (PBI)<sub>6</sub> **22**-oligomer and mixed oligomers were found to bind strongly with copper and nickel metal salts. These oligomers exhibited intersection point ~0.6 which confirmed 3:2 binding stoichiometry with Cu(NO<sub>3</sub>)<sub>2</sub>. With this in mind, binding model was proposed in which two oligomer strands are held together with the three copper metal ions (Figure 83).

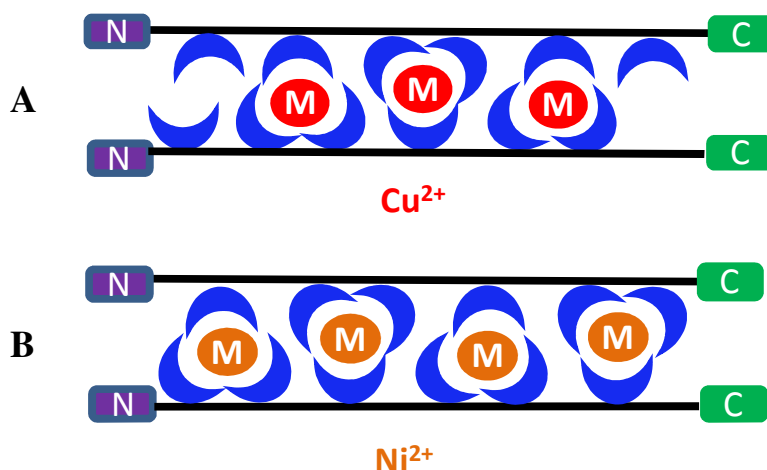


**Figure 83.** Schematic diagram of polyamide oligomers binding with (A) Cu(NO<sub>3</sub>)<sub>2</sub> and (B) Ni(NO<sub>3</sub>)<sub>2</sub>.

The polyamide *hetero*-oligomers showed 2:1 binding stoichiometry with Ni(NO<sub>3</sub>)<sub>2</sub>, which is indicative of the two oligomer units to be held together with four nickel metal ions.

### 3.11 Isothermal Titration Calorimetry (ITC)

Having established that *aeg* linked ligands bind better to Cu(NO<sub>3</sub>)<sub>2</sub> & Ni(NO<sub>3</sub>)<sub>2</sub> than other metal salts, ITC was used to investigate the equilibrium thermodynamics of *aeg* linked ligand-metal complex formation.

In the experiments, the heat changes are directly measured upon the addition of small volumes of metal salts Cu(NO<sub>3</sub>)<sub>2</sub> & Ni(NO<sub>3</sub>)<sub>2</sub> to the reaction cell containing the polyamide *homo*-oligomer (PBI)<sub>6</sub> **22** in aqueous solution. Integration of each peak after the addition of titrant yielded the calorimetric binding enthalpy ( $\Delta H$ ) as a function of the concentration of polyamide *homo*-oligomer (PBI)<sub>6</sub> **22**. In control experiments, the enthalpy of the dilution of polyamide *homo*-oligomer (PBI)<sub>6</sub> **22** was

determined and subtracted from the total change in enthalpy of the formation of the (PBI)<sub>6</sub> oligomer **22**: metal complex (Figure 84).

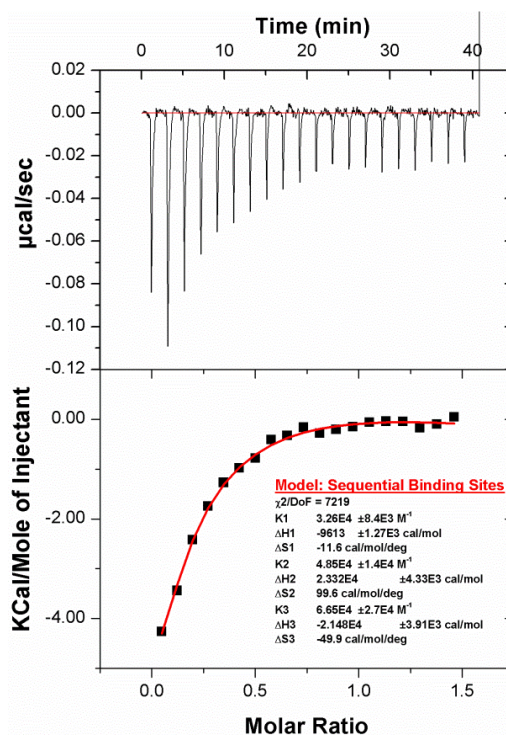


**Figure 84.** ITC figures in water for (PBI)<sub>6</sub> oligomer **22** with Cu(NO<sub>3</sub>)<sub>2</sub>.

A non-linear, least squares minimization software program (Origin 7.0 from Microcal Inc.) was used to fit the data and generate the titration curve using *one site* binding model for (PBI)<sub>6</sub> oligomer **22**: metal complex. The free-energy ( $\Delta G$ ) change during complex formation was obtained using standard thermodynamic relationships from above data. The calculated values of binding constants are  $6.65 \times 10^4$  for Cu(NO<sub>3</sub>)<sub>2</sub> and  $9.59 \times 10^4$  [M]<sup>-1</sup> for Ni(NO<sub>3</sub>)<sub>2</sub>.

Similar ITC analysis was carried out for (PBI) **8** in methanolic solution and the values of binding constants are found to be  $4.57 \times 10^5$  for Cu(NO<sub>3</sub>)<sub>2</sub> and  $2.55 \times 10^5$  [M]<sup>-1</sup> for Ni(NO<sub>3</sub>)<sub>2</sub>, respectively.

In ITC the calculated values of binding constants for polyamide *hetero*-oligomer (PBI)<sub>3</sub>- (PDA)<sub>3</sub> **25** were found to be  $1.0 \times 10^5$  and  $1.17 \times 10^4$  [M]<sup>-1</sup> for Cu(NO<sub>3</sub>)<sub>2</sub> and Ni(NO<sub>3</sub>)<sub>2</sub>, respectively (Figure 83).

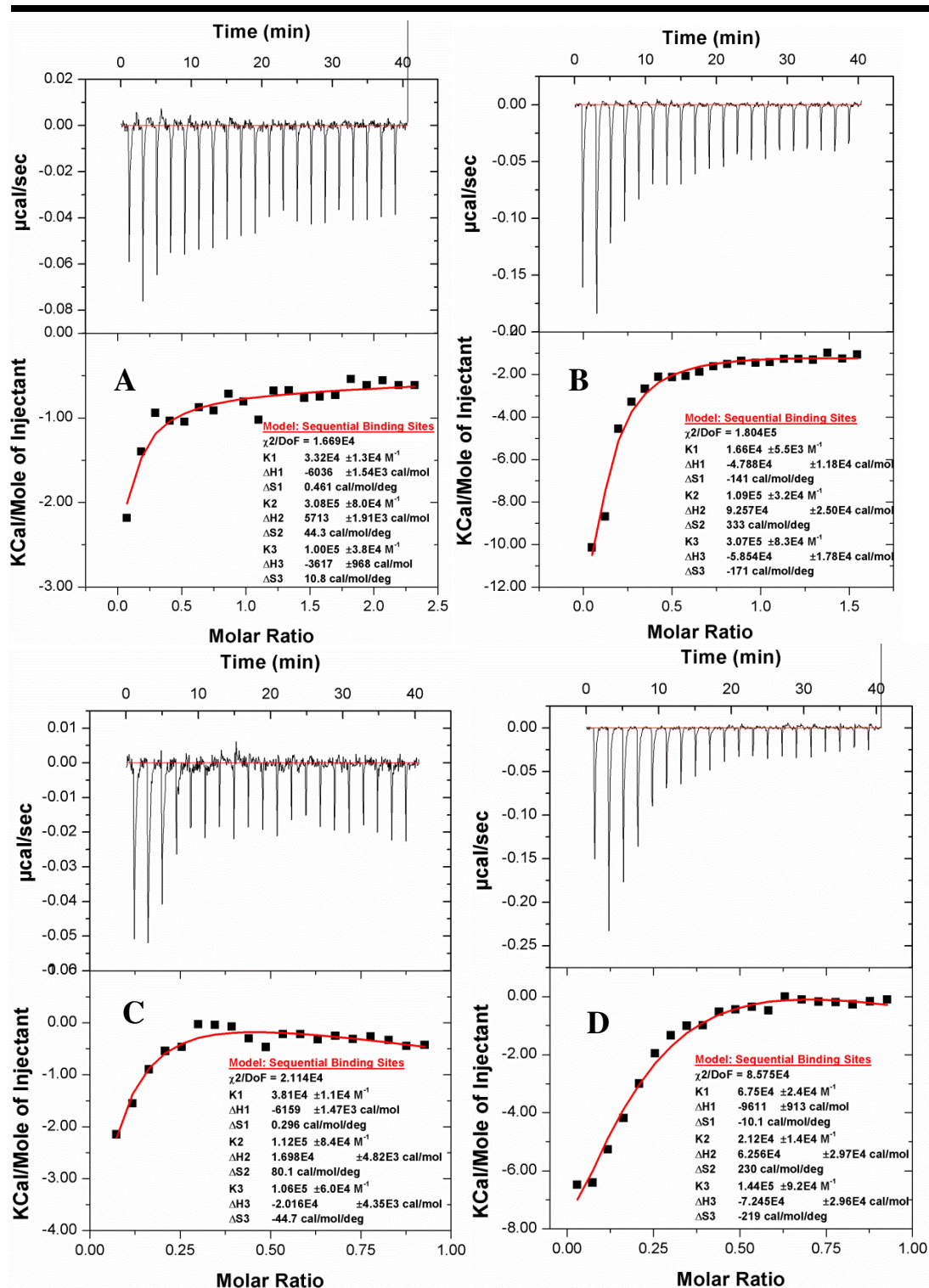


**Figure 85.** ITC figures in water for (A) (PBI)<sub>3</sub>-(PDA)<sub>3</sub> oligomer **25** with Ni(NO<sub>3</sub>)<sub>2</sub>, (B) (PBI-PDA)<sub>3</sub> oligomer **26** with Cu(NO<sub>3</sub>)<sub>2</sub>, (C) (PBI)<sub>3</sub>-(CAT)<sub>3</sub> oligomer **27** with Cu(NO<sub>3</sub>)<sub>2</sub>. (D) (PBI-CAT)<sub>3</sub> **28** in water with Cu(NO<sub>3</sub>)<sub>2</sub>.

ITC data for polyamide *hetero*-oligomer (PBI-PDA)<sub>3</sub> **26** indicated the values of binding constants to be  $3.07 \times 10^5$  and  $1.06 \times 10^4$  [M]<sup>-1</sup> Cu(NO<sub>3</sub>)<sub>2</sub> and Ni(NO<sub>3</sub>)<sub>2</sub>, respectively. The polyamide oligomer (PBI)<sub>3</sub>-(CAT)<sub>3</sub> **27** determined binding constants were  $1.06 \times 10^5$  and  $8.83 \times 10^4$  [M]<sup>-1</sup> for Cu(NO<sub>3</sub>)<sub>2</sub> and Ni(NO<sub>3</sub>)<sub>2</sub>,

## Chapter 3

respectively. The alternative oligomers (PBI-CAT)<sub>3</sub> **28** gave a values of binding constants of  $1.44 \times 10^5$  and  $2.21 \times 10^4$  [M]<sup>-1</sup> for Cu(NO<sub>3</sub>)<sub>2</sub> and Ni(NO<sub>3</sub>)<sub>2</sub>, respectively. The various thermodynamic parameters thus obtained at 273 K are listed in Table 22. Under the conditions of complexation, the value of  $\Delta G$  is negative favouring association. The complexation process is exothermic and entropy-driven. The ITC data confirm in a quantitative manner that there are 3 binding sites on the synthesized *aeg* ligands and millimolar concentrations of the metal salts (copper nitrate and nickel nitrate).

**Table 22.** ITC thermodynamic parameters describing interaction of oligomers with metal salts.

Ligands	Metal salts (0.3 mM)	Conc. (mM)	$\Delta H$ (kCal/mol)	$T\Delta S$ (kCal/mol)	$\Delta G$ (kCal/mol)	$K$ (M <sup>-1</sup> )	<b>N</b>
(PBI) <b>8</b>	Cu(NO <sub>3</sub> ) <sub>2</sub>	0.02	$-4.86 \times 10^2$	$-4.76 \times 10^2$	-9.2	$4.57 \times 10^5$	1.6
	Ni(NO <sub>3</sub> ) <sub>2</sub>	0.02	$7.56 \times 10^3$	$7.57 \times 10^3$	-10.0	$2.55 \times 10^5$	4.8
(PBI) <sub>6</sub> <b>22</b>	Cu(NO <sub>3</sub> ) <sub>2</sub>	0.02	-21.4	-14.6	-6.99	$6.65 \times 10^4$	3
	Ni(NO <sub>3</sub> ) <sub>2</sub>	0.02	-24.8	-18.03	-6.77	$9.59 \times 10^4$	3
(PBI) <sub>3</sub> -(PDA) <sub>3</sub> <b>25</b>	Cu(NO <sub>3</sub> ) <sub>2</sub>	0.02	-3.62	3.22	-6.84	$1.0 \times 10^5$	3
	Ni(NO <sub>3</sub> ) <sub>2</sub>	0.02	-3.11	2.44	-5.55	$1.17 \times 10^4$	3
(PBI-PDA) <sub>3</sub> <b>26</b>	Cu(NO <sub>3</sub> ) <sub>2</sub>	0.02	-58.5	-50.96	-7.54	$3.07 \times 10^5$	3
	Ni(NO <sub>3</sub> ) <sub>2</sub>	0.02	-170.4	-164.79	-5.61	$1.06 \times 10^4$	3
(PBI) <sub>3</sub> -(CAT) <sub>3</sub> <b>27</b>	Cu(NO <sub>3</sub> ) <sub>2</sub>	0.05	-20.1	-13.32	-6.78	$1.06 \times 10^5$	3
	Ni(NO <sub>3</sub> ) <sub>2</sub>	0.05	-3.42	3.34	-6.76	$8.83 \times 10^4$	3
(PBI-CAT) <sub>3</sub> <b>28</b>	Cu(NO <sub>3</sub> ) <sub>2</sub>	0.05	-72.4	-65.24	-7.14	$1.44 \times 10^5$	3
	Ni(NO <sub>3</sub> ) <sub>2</sub>	0.05	-43.8	-36.65	-7.14	$2.21 \times 10^5$	3

\* From these experimentally determined parameters, the free energy of binding ( $\Delta G$ ) and the entropy change ( $\Delta S$ ) are obtained using the standard thermodynamic relationship  $\Delta G = -RT \ln K = \Delta H - T\Delta S$ .

The synthesized *aeg* linked ligands bind to metal salts with binding constants in the range of  $10^4$ - $10^5$  strength. The synthesized *aeg* linked ligands in polyamides exhibit better efficiencies with copper nitrate as compared to nickel nitrate. The comparison of binding constants for polyamide oligomers calculated from both UV-Vis spectroscopy and ITC analysis are shown in Table 23. It suggests that binding constants obtained from the two different methods shown variation. Several authors<sup>62</sup>

have also reported similar trends and the proper reason is not known. ITC values about 10 times higher than that of UV-Vis.

**Table 23.** Comparison of binding constants based on UV-Vis and ITC

Ligands	Metal salts	Binding constants	Binding constants
		(UV-Vis) K (M) <sup>-1</sup>	(ITC) K (M) <sup>-1</sup>
(PBI) <b>8</b>	Cu(NO <sub>3</sub> ) <sub>2</sub>	6.71 × 10 <sup>3</sup>	4.57 × 10 <sup>5</sup>
	Ni(NO <sub>3</sub> ) <sub>2</sub>	1.82 × 10 <sup>3</sup>	2.55 × 10 <sup>5</sup>
(PBI) <sub>6</sub> <b>22</b>	Cu(NO <sub>3</sub> ) <sub>2</sub>	5.19 × 10 <sup>3</sup>	6.65 × 10 <sup>4</sup>
	Ni(NO <sub>3</sub> ) <sub>2</sub>	2.61 × 10 <sup>3</sup>	9.59 × 10 <sup>4</sup>
(PBI) <sub>3</sub> - (PDA) <sub>3</sub> <b>25</b>	Cu(NO <sub>3</sub> ) <sub>2</sub>	1.34 × 10 <sup>4</sup>	1.0 × 10 <sup>5</sup>
	Ni(NO <sub>3</sub> ) <sub>2</sub>	3.34 × 10 <sup>3</sup>	1.17 × 10 <sup>4</sup>
(PBI-PDA) <sub>3</sub> <b>26</b>	Cu(NO <sub>3</sub> ) <sub>2</sub>	1.58 × 10 <sup>3</sup>	3.07 × 10 <sup>5</sup>
	Ni(NO <sub>3</sub> ) <sub>2</sub>	2.1 × 10 <sup>3</sup>	1.06 × 10 <sup>4</sup>
(PBI) <sub>3</sub> - (CAT) <sub>3</sub> <b>27</b>	Cu(NO <sub>3</sub> ) <sub>2</sub>	1.45 × 10 <sup>4</sup>	1.06 × 10 <sup>5</sup>
	Ni(NO <sub>3</sub> ) <sub>2</sub>	5.16 × 10 <sup>3</sup>	8.83 × 10 <sup>4</sup>
(PBI-CAT) <sub>3</sub> <b>28</b>	Cu(NO <sub>3</sub> ) <sub>2</sub>	7.87 × 10 <sup>3</sup>	1.44 × 10 <sup>5</sup>
	Ni(NO <sub>3</sub> ) <sub>2</sub>	4.54 × 10 <sup>4</sup>	2.21 × 10 <sup>5</sup>

In summary, all the polyamide oligomers **22-28** bind with Cu(NO<sub>3</sub>)<sub>2</sub> better than with Ni(NO<sub>3</sub>)<sub>2</sub>.

### 3.12 Co-ordination chemistry of metal complexes

The incorporation of metals in the artificial nucleobases in the backbone resulted in the generation of metal complexes of specific geometry. The artificial nucleosides have either monodentate (one), bidentate (two) or tridentate (three) donor atoms for generating transition metal complexes. Shionoya *et al.*<sup>63</sup> found that bidentate ligand 2-hydroxypyridone forms square planar complexes with Cu<sup>2+</sup> (Hp, Figure 86A), tridentate ligand 2,6-bis(methylthiomethyl)pyridine forms octahedral complexes with Ag<sup>+</sup> (Spy, Figure 86B), monodentate ligand pyridyl forms linear complexes with Ag<sup>+</sup> (Py, Figure 86C), bidentate ligand catechol exhibits distorted tetrahedral complexes with B<sup>3+</sup> (Cat, Figure 86D) *etc* inside the formed duplexes.

William *et al.*<sup>35a</sup> also synthesized *homo*-substituted polyamide chain with chelating ligands *e.g.* monodentate pyridine or bidentate bipyridine, resulted in the generation of multimetallic structures upon co-ordination with transition metal ions.

## Chapter 3

The synthesized phenyl terpyridyl ligand ( $\phi$ -tpy, Figure 86E) and studied its complexation with  $\text{Co}^{3+}/\text{Fe}^{3+}$  in octahedral geometry.

In a similar way Achim *et al.*<sup>64</sup> synthesized the bipyridyl ligand and studied complexes of different geometries with different metal ions. It formed tetrahedral complexes with  $\text{Cu}^{2+}$  whereas both tetrahedral and octahedral complexes with  $\text{Ni}^{2+}$ .

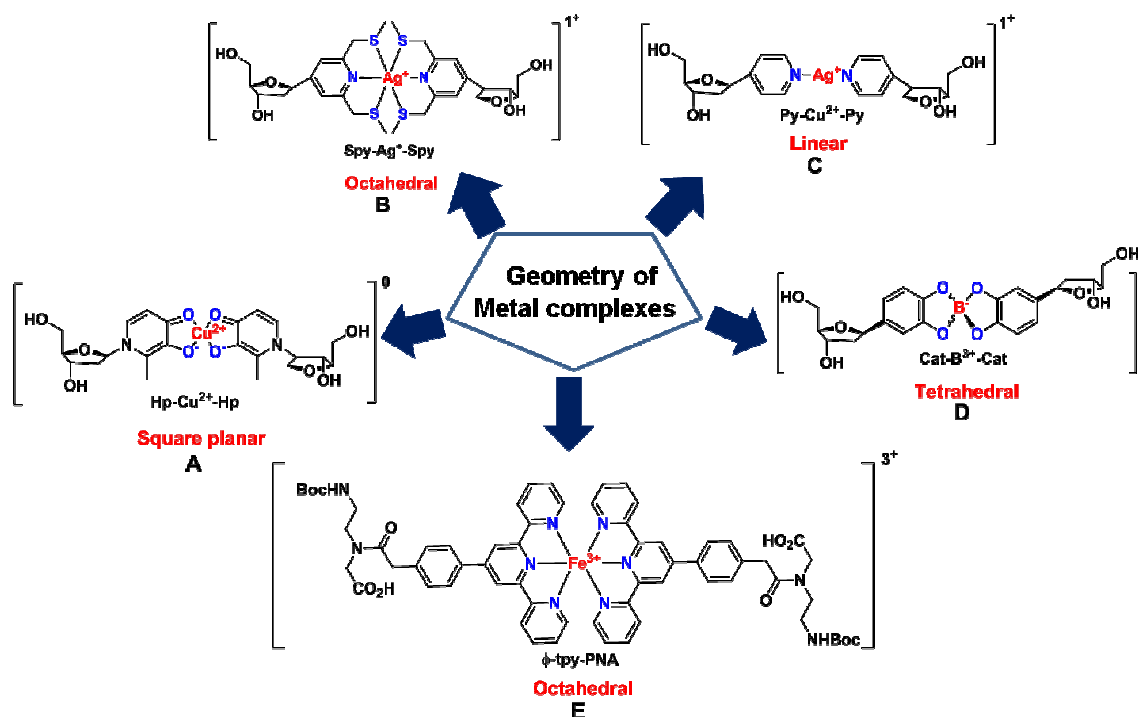


**Figure 86.** Co-ordination geometries of the reported ligands.<sup>63, 35a</sup>

In view of these facts, the synthesized bidentate ligands was seen to exhibits 2:1 [ligand: metal] complexes with different metals in specific geometries *e.g.* PBI, **1** forms square planar complexes with  $\text{Cu}^{2+}$ , PDA, **2** forms square planar complexes with  $\text{Pd}^{2+}$  and CAT, **3** forms distorted tetrahedral complexes with  $\text{B}^-$  *etc.* (Figure 87).



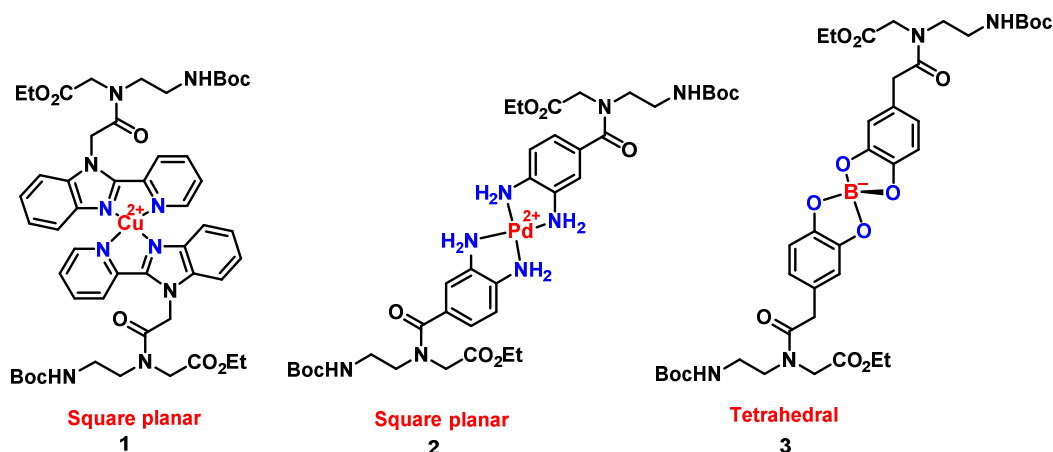


**Figure 87.** Co-ordination geometries of the synthesized *aeg* linked ligands.

Achim et al.<sup>64</sup> have studied the different behaviour exhibited by the adjacent bipyridyl ligands substituted in the PNA oligomers. They found that adjacent bipyridyl contributed towards more strong duplexes due to the supramolecular chelate effect. This effect comes into light where several bipyridyl moieties are in close proximity. With nickel salts they observed the formation of two different geometries of metal complexes; one with square planar geometry  $[\text{Ni}(\text{Bpy})_2]$  and other with octahedral geometry  $[\text{Ni}(\text{Bpy})_3]$ . By means of electron paramagnetic resonance (EPR), they confirmed the formation of different metal complexes with copper salts also; square planar geometry of  $[\text{Cu}(\text{Bpy})_2]$  and octahedral geometry of  $[\text{Cu}(\text{Bpy})_3]$  complexes.

Similar observations were found in our designed bidentate 2-pyridyl benzimidazole ligand (PBI), which is also analogous to bipyridyl ligand. 2-Pyridyl benzimidazole ligand (PBI) may form either square-planar or octahedral complexes with transition metal ions such as  $\text{Cu}^{2+}$ ,  $\text{Ni}^{2+}$  etc. In case of *N*-Boc-aminoethyl (PBI) glycinate **8**, it can only form complexes in square planar geometry and in stoichiometry of either 1:1  $[\text{PBI}:\text{Pd}^{2+}]$  or 2:1  $[\text{PBI}:\text{Cu}^{2+}/\text{Ni}^{2+}]$ . On the other hand in case of *N*-Boc-aminoethyl (PBI)<sub>2</sub> (glycinate)<sub>2</sub> **21**, it can form complexes in square planar geometry with  $\text{Cu}^{2+}$  as well as octahedral geometry  $\text{Ni}^{2+}$  metal ions.

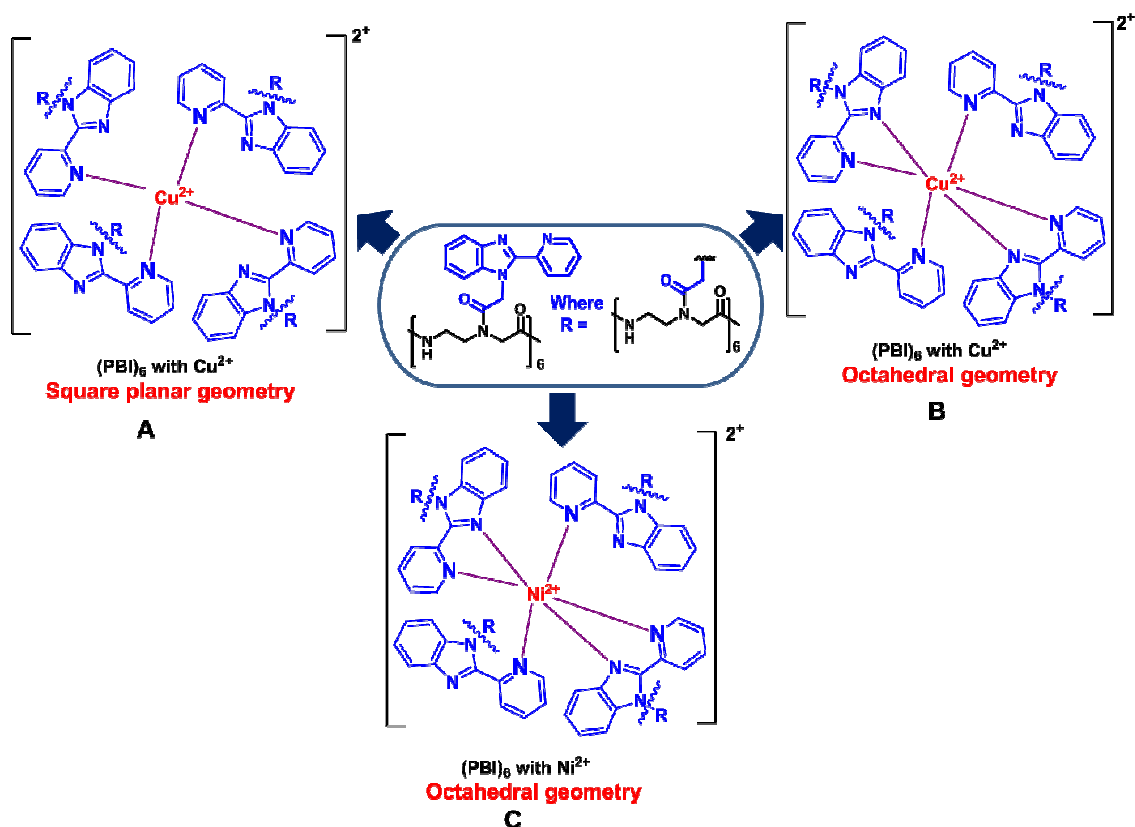


**Figure 88.** Plausible co-ordination geometries of the *aeg* linked ligands in the formed metal mediated duplexes.

On the other hand in case of *N*-Boc-aminoethyl (PBI)<sub>2</sub> (glycinate)<sub>2</sub> **21**, it can form complexes in square planar geometry with Cu<sup>2+</sup> as well as octahedral geometry Ni<sup>2+</sup> metal ions. Due to supramolecular chelate effect exerted by polyamide *homo*-oligomer (PBI)<sub>6</sub> oligomer **22**, it is possible that complexes would form either with square planar geometry (Figure 88A) or octahedral geometry (Figure 88B) with Cu<sup>2+</sup> metal ions. on the other hand with nickel metal ions, complexes of octahedral geometry is more stable (Figure 88C).

Similar results are expected from polyamide *hetero*-oligomers which has three 2-pyridylbenzimidazole ligand (PBI) units and more likely to show supramolecular chelate effect. Based on all these facts various binding models have been proposed.

### 3.13 Binding models

To summarise, copper and nickel metal salts reveal possible binding pattern as depicted pictorially below (Figure 89).

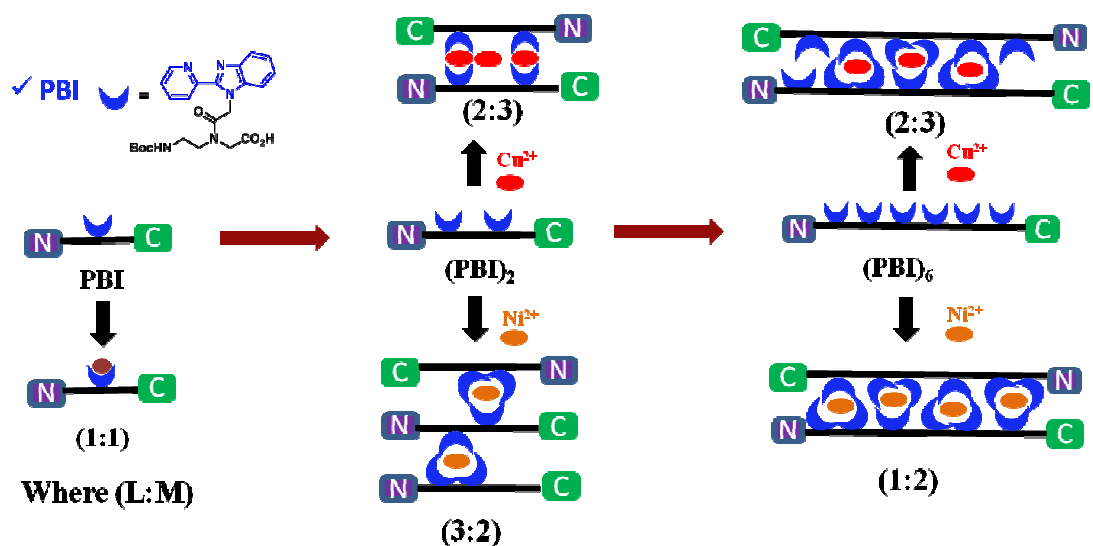


**Figure 89.** Pictorial representation of possible binding mode for 2-pyridylbenzimidazole (PBI) monomer **8**, dimer **21** and oligomers **22**.

In contrast, PDA did not result in appreciable binding with any metal salts investigated (Figure 90).

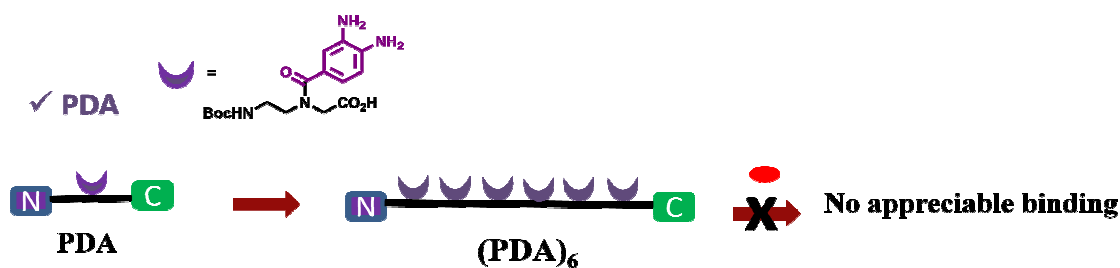


**Figure 90.** Pictorial representation of possible binding mode for (PDA) oligomers **23**.

Catechol monomer, however showed binding with boron ions at slightly basic pH, but no binding with different metal salts (Figure 91).

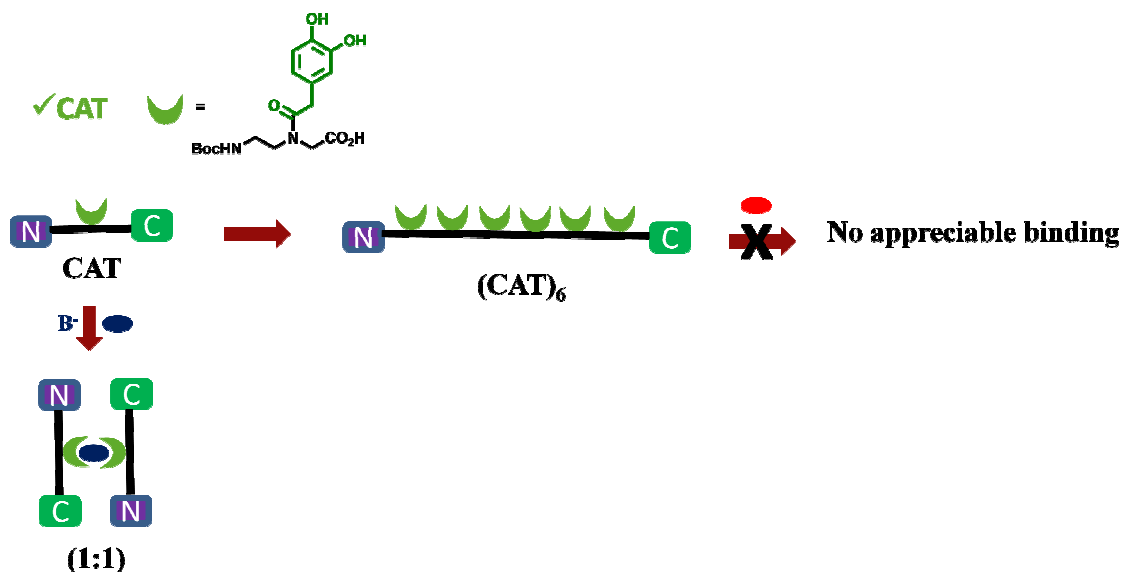


**Figure 91.** Pictorial representation of possible binding mode for (CAT) monomer 17 and oligomers 24.

It was observed that phenylenediamine oligomer was not binding to any of the metal salts, but *hetero*-oligomers of these two units exhibited better binding (Figure 92).

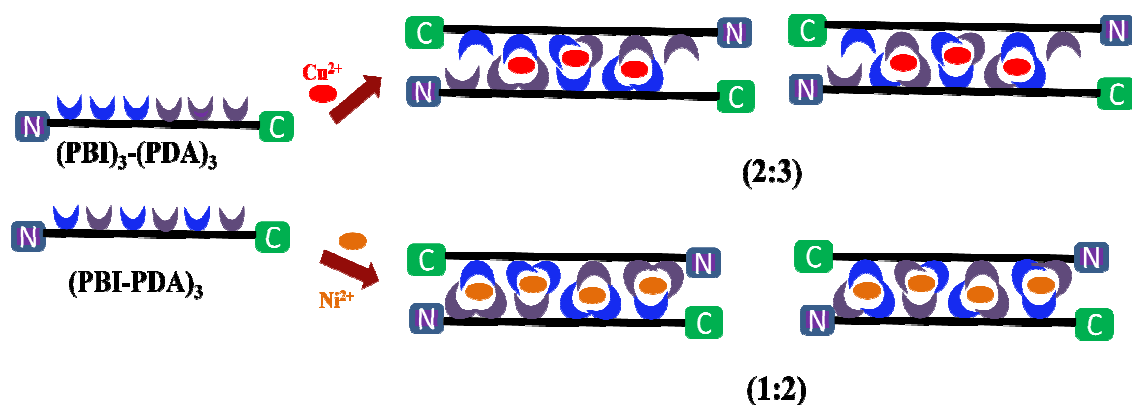


**Figure 92.** Pictorial representation of possible binding mode for 2-pyridylbenzimidazole (PBI) and *o*-phenylenediamine (PDA) *hetero*-oligomers.

So was the case of catechol oligomers, with no binding to any of the metal salts, but *hetero*-oligomers of these two units exhibited better binding (Figure 93).

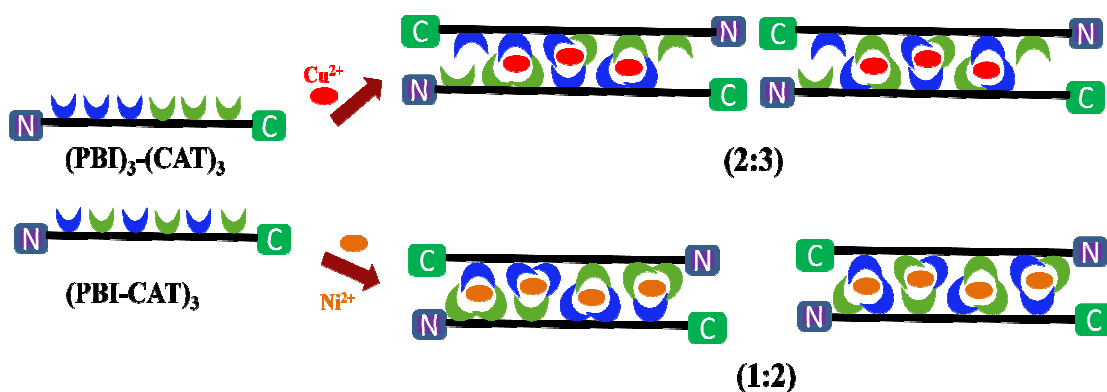


**Figure 93.** Pictorial representation of possible binding mode for 2-pyridylbenzimidazole (PBI) and catechol (CAT) *hetero*-oligomers.

### 3.14 Conclusions

In conclusion, successful synthesis of 2-pyridylbenzimidazole (PBI) *o*-phenylenediamine (PDA), catechol (CAT) monomers and its oligomer on the SPPS were achieved. This thesis presented the facile construction of supramolecular structures having multiple complexes tethered to 2-pyridylbenzimidazole (PBI), *o*-phenylenediamine (PDA), catechol (CAT) oligopeptide scaffolds. The studies here provide the necessary foundation to enable characterization of the multimetallic structures and application to design molecular motifs of increased complexity and function. Based on the denticities of the ligands attached to *aeg* backbone, it could be highly useful in designing metal sensors.

In case of  $(\text{PBI})_6$  oligomer and polyamide *hetero*-oligomers, the metal ions cross-link the strands to self assemble structures into double stranded oligopeptide duplexes with sequence dependent spectroscopic properties. It was observed that *o*-phenylenediamine (PDA) and catechol (CAT) oligomers did not exhibit metal complexation. It may be possible that presence of ring nitrogen or any *hetero* atom effects the binding properties of the designed ligands. In the literature, best rational designs are pyridyl, bipyridyl, terpyridyl, phenyl terpyridyl, hydroxyquinoline, 2-hydroxypyridone, which shows the presence of either one or two *hetero* atoms. Due to this possibility *o*-phenylenediamine (PDA) and catechol (CAT) oligomers are incapable of binding strongly.

## Chapter 3

---

It is also observed that catechol (CAT) monomer exhibited binding with boron ions under slightly basic pH. Whereas synthesized *hetero* oligomer of two different units like PBI/PDA or PBA/CAT shown strong binding affinities towards nickel nitrate. Binding constants obtained from ITC and UV-Vis is shown to have comparable binding strength of these synthesized *aeg* ligands.

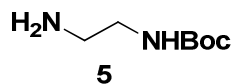
### 3.15 Experimental Section

**3.15.1 General remarks:** All reagents and chemicals were of laboratory or analytical grade obtained from commercial sources and were used without further purification unless mentioned. Thin layer chromatography (TLC) was done on precoated silica gel 60 F<sub>254</sub> plates (Merck). TLCs were visualized under UV light, iodine and/or ninhydrin spray followed by heating up to 110°C with heat gun. Silica gel 60-120 and 100-200 mesh (Merck) was used for routine column chromatography with ethyl acetate/petroleum ether or dichloromethane/methanol mixture as elution solvent depending upon the compound polarity and chemical nature. All solvents were distilled under an inert atmosphere with appropriate desiccant.

<sup>1</sup>H NMR spectra were routinely recorded at 200 MHz on a Bruker AC-200 instrument controlled by an Aspect 2000 computer. <sup>13</sup>C NMR and <sup>13</sup>C-DEPT spectra (at 50 MHz) were recorded on the same instrument. The spectra were analyzed using ACD specviewer software from ACD labs. For some compounds, NMR spectra were also recorded on 400 MHz JEOL spectrometer; and data processed Cambridge Soft's MestReNova software. All chemical shifts are referenced with respect to TMS as internal standard and are expressed in δ-scale (ppm). Mass spectra were obtained by ESI-MS technique on AP-QSTAR spectrometer. MALDI analysis were done on MDS-SCIEX 4800 MALDI TOF/TOF instrument (Applied Biosystems). High Resolution Mass Spectrometry (HRMS) was recorded on waters SYNAPT G2 MS system. Melting points of the samples were determined in open capillary tubes using Büchi Melting Point M-560 apparatus and are uncorrected. IR spectra were recorded on an Infrared Fourier Transform Spectrophotometer using chloroform. Peptide purification was carried out on High Pressure Liquid Chromatography (HPLC). HPLC system is of Dionex ICS-3000 series attached with PDA detector and SP (single pump) made. Analytical HPLC was performed using a LiChrospher 100 RP-18e 5 μM (250 mm x 10 mm) column from Merck. Preparative HPLC was carried out on a LiChrospher RP-18e 5 μM (250 mm x 10 mm). UV-vis spectrophotometric titrations were done on Perkin Elmer 950 spectrophotometer. All spectra presented for UV are drawn by Origin 8 software.

## 3.15.2 Procedures and Spectral Data

*tert*-butyl (2-aminoethyl)carbamate (**5**)<sup>32</sup>



To an ice-cold solution of 1,2-diaminoethane (20 g, 0.33 mmol) in dichloromethane (500 mL), Boc<sub>2</sub>O in dichloromethane (500 mL) was slowly added over a period of 3-4 h. The reaction mixture was stirred at rt for 24 h. After completion of the reaction, solvent was evaporated and the precipitated *N,N'*-di-Boc derivative was removed by filtration. The corresponding *N'*-mono-Boc derivative was obtained by repeated extraction of the filtrate in dichloromethane. The organic layer was separated, dried over anhydrous Na<sub>2</sub>SO<sub>4</sub>, filtered, and concentrated to give the crude product *N'*-(Boc)-1,2-diaminoethane, **5** (3.45 g).

**Yield** 50%; colorless viscous oil;  $R_f = 0.18$  (EtOAc: MeOH; 1:1).

**Mol. Formula** C<sub>7</sub>H<sub>16</sub>N<sub>2</sub>O<sub>2</sub>

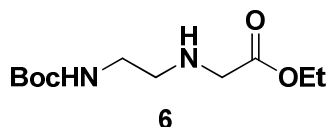
**IR** (CHCl<sub>3</sub>)  $\nu_{\max}$  (cm<sup>-1</sup>) = 3449, 3379, 3018, 2978, 2932, 2870, 2400, 1701, 1508, 1392, 1367, 1216, 1169.

**<sup>1</sup>H NMR** (CDCl<sub>3</sub>, 200 MHz)  $\delta_H$  (ppm) = 5.36 (br, 1H, NH), 3.00 (q,  $J = 5.4$  Hz, 2H, NHCH<sub>2</sub>), 2.63 (dt,  $J = 5.9$  Hz, 2H, NHCH<sub>2</sub>), 1.28 (s, 9H, (CH<sub>3</sub>)<sub>3</sub>C).

**<sup>13</sup>C NMR** (CDCl<sub>3</sub>, 50 MHz)  $\delta_C$  (ppm) = 158.1 (C), 78.8 (CH<sub>3</sub>)<sub>3</sub>C, 43.1(NHCH<sub>2</sub>), 41.6 (NHCH<sub>2</sub>), 28.2 (CH<sub>3</sub>)<sub>3</sub>C.

**Elemental analysis** Calcd for C<sub>7</sub>H<sub>16</sub>N<sub>2</sub>O<sub>2</sub>: C, 52.48; H, 10.07.  
Found: C, 52.55; H, 10.16.

Ethyl *N*-(2-Boc-aminoethyl)-glycinate (**6**)<sup>32</sup>



To an ice-cold solution of *N'*-(Boc)-1,2-diaminoethane **5** (4.0 g, 25 mmol) in acetonitrile (80 mL), triethylamine (8.6 mL, 61.8 mmol) was slowly added. After stirring at room temperature for 20 min, the solution of ethylbromoacetate (2.8 mL, 25

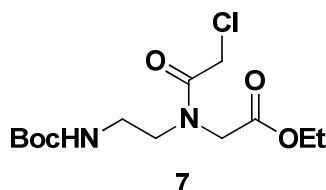


## Chapter 3

mmol) in acetonitrile (100 mL) was added. The reaction was stirred at room temperature for 12 h. After completion of the reaction, it was extracted with EtOAc (3 x 50 mL). The organic layer was washed with brine (10 mL), dried over anhydrous  $\text{Na}_2\text{SO}_4$ , and the solvent was evaporated under vacuum. The crude residue was purified by silica gel column chromatography (50% pet-ether/EtOAc) to furnish product **6** (4.3 g).

<b>Yield</b>	67%; colorless oil; $R_f = 0.5$ (EtOAc: Pet-ether; 1:1).
<b>Mol. Formula</b>	$\text{C}_{11}\text{H}_{22}\text{N}_2\text{O}_4$
<b>IR</b> ( $\text{CHCl}_3$ )	$\nu_{\text{max}}$ ( $\text{cm}^{-1}$ ) = 3338, 2977, 2935, 1694, 1515, 1455, 1391, 1366, 1247, 1160, 1027.
<b><math>^1\text{H}</math> NMR</b> ( $\text{CDCl}_3$ , 200 MHz)	$\delta_{\text{H}}$ (ppm) = 5.23 (br, 1H, NH), 4.09 (q, $J = 7.2$ Hz, 2H, $\text{CH}_2$ ), 3.12 (t, $J = 5.7$ Hz, 2H, $\text{NHCH}_2$ ), 2.65 (t, $J = 5.6$ Hz, 2H, $\text{NHCH}_2$ ), 1.34 (s, 9H, $(\text{CH}_3)_3\text{C}$ ), 1.18 (t, $J = 7.2$ Hz, 2H, $\text{CH}_3$ ) ppm.
<b><math>^{13}\text{C}</math> NMR</b> ( $\text{CDCl}_3$ , 50 MHz)	$\delta_{\text{C}}$ (ppm) = 172.3 (C), 155.9 (C), 78.9 ( $(\text{CH}_3)_3\text{C}$ ), 60.6 ( $\text{OCH}_2$ ), 50.2 ( $\text{CH}_2$ ), 48.6 ( $\text{NHCH}_2$ ), 39.9 ( $\text{NHCH}_2$ ), 28.2 ( $(\text{CH}_3)_3\text{C}$ ), 14.0 ( $\text{CH}_2\text{CH}_3$ ) ppm.
<b>Elemental analysis</b>	Calcd for $\text{C}_{11}\text{H}_{22}\text{N}_2\text{O}_4$ : C, 53.64; H, 9.00. Found: C, 53.73; H, 9.09.
<b>MALDI -TOF</b>	Calcd for $\text{C}_{11}\text{H}_{22}\text{N}_2\text{O}_4$ : 285.172 (M+K) <sup>+</sup> Found: 285.401.

### Ethyl-2-(*N*-(2-((*tert*-butoxycarbonyl)amino)ethyl)-2-chloroacetyl)-glycinate (**7**)<sup>31</sup>



To a solution of ethyl-*N*-(2-Boc-aminoethyl)-glycinate **6** (2.6 g, 11.0 mmol) in dioxan (60 mL), 10% aqueous  $\text{Na}_2\text{CO}_3$  (75 mL) and chloroacetyl chloride (1.3 mL, 11.5 mmol) was slowly added with stirring. After stirring for 1 h at room temperature, dioxan was evaporated under reduced pressure. The aqueous layer was extracted with EtOAc (3 x 50 mL). The combined organic layers were washed with brine (10 mL), dried over anhydrous  $\text{Na}_2\text{SO}_4$ , filtered and the solvent was evaporated under reduced

## Chapter 3

pressure. The crude residue was purified by silica gel column chromatography (30% pet-ether/ EtOAc) to afford product **7** (2.7 g).

**Yield** 80%; colorless oil;  $R_f = 0.4$  (EtOAc: pet ether; 3:7).

**Mol. Formula**  $C_{13}H_{23}ClN_2O_5$

**IR** ( $CHCl_3$ )  $\nu_{max}$  ( $cm^{-1}$ ) = 3366, 2980, 1741, 1700, 1657, 1509, 1454, 1398, 1368, 1247, 1208, 1164, 1025.

**$^1H$  NMR** ( $CDCl_3$ , 200 MHz)  $\delta_H$  (ppm) = 5.54 (br, 1H, NH), 4.05 (s, 2H,  $CH_2$ ), 4.06 (q,  $J = 7.3$  Hz, 2H,  $CH_2$ ), 3.92 (s, 2H,  $CH_2$ ), 3.40 (t,  $J = 5.8$  Hz, 2H,  $NHCH_2$ ), 3.14 (q,  $J = 5.6$  Hz, 2H,  $NHCH_2$ ), 1.30 (s, 9H,  $(CH_3)_3C$ ), 1.15 (t,  $J = 7.2$  Hz, 2H,  $CH_3$ ).

**$^{13}C$  NMR** ( $CDCl_3$ , 50 MHz)  $\delta_C$  (ppm) = 169.2 (C), 167.2 (C), 155.8 (C), 79.3 ( $(CH_3)_3C$ ), 61.2 ( $CH_2$ ), 49.1 ( $NHCH_2$ ), 48.5 ( $CH_2$ ), 40.5 ( $CH_2$ ), 38.2 ( $NHCH_2$ ), 27.9 ( $(CH_3)_3C$ ), 13.7 ( $CH_3$ ).

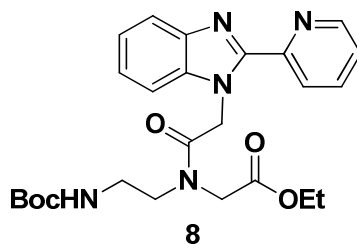
**Elemental analysis** Calcd for  $C_{13}H_{23}ClN_2O_5$ : C, 48.37; H, 7.18.

Found: C, 48.42; H, 7.26.

**MALDI -TOF** Calcd for  $C_{13}H_{23}ClN_2O_5$ : 361.883 (M+K)<sup>+</sup>

Found: 361.718.

**Ethyl-2-(N-(2-((tert-butoxycarbonyl)amino)ethyl)-2-(2-(pyridin-2-yl)-1H-benzo[d]imidazol-1-yl) acetamido)acetate (**8**)**



To a suspension of NaH (330 mg, 14 mmol) in dry DMF (7 mL) at 0 °C under  $N_2$  atmosphere, 2-pyridylbenzimidazole **9** (1.36 g, 7.0 mmol) in dry DMF (2 mL) was added. The reaction mixture was stirred for 15 min and compound (2.48 g, 7.7 mmol) in DMF (2 mL) added into it. The resulting reaction mixture was heated at 100 °C for 24 h and cooled to room temperature. After completion reaction mixture was cooled

## Chapter 3

and extracted with EtOAc (3 x 50 mL). The organic layer was washed with brine (10 mL), dried over anhydrous Na<sub>2</sub>SO<sub>4</sub> and concentrated under reduced pressure. The crude residue was purified by silica gel column chromatography (20% pet-ether/EtOAc) to afford product **8** (2.34 g).

**Yield** 70%; white solid;  $R_f = 0.57$  (EtOAc: pet ether; 1:1).

**Melting Point** 142.9-145.8°C

**Mol. Formula** C<sub>25</sub>H<sub>31</sub>N<sub>5</sub>O<sub>5</sub>

**IR** (CHCl<sub>3</sub>)  $\nu_{\max}$  (cm<sup>-1</sup>) = 3743, 3678, 3647, 3619, 3339, 2978, 2362, 1741, 1704, 1666, 1589, 1511, 1449, 1394, 1368, 1338, 1250, 1210, 1171, 1096, 1028.

**<sup>1</sup>H NMR** (CDCl<sub>3</sub>, 200 MHz)  $\delta_H$  (ppm) = 8.57 (m, 1H, CH), 8.49 (d,  $J = 8.2$  Hz, 2H, CH), 7.83-7.76 (m, 2H, CH), 7.37-7.27 (m, 5H, CH), 5.79 (s, 2H, CH<sub>2</sub>), 5.63 (s, 1H, NH), 4.10 (q,  $J = 7.3$  Hz, 2H, CH<sub>2</sub>), 3.98 (s, 2H, CH<sub>2</sub>), 3.63-3.61 (m, 2H, NHCH<sub>2</sub>), 3.38-3.34 (m, 2H, NHCH<sub>2</sub>), 1.40 (s, 9H, (CH<sub>3</sub>)<sub>3</sub>C), 1.17 (t,  $J = 7.3$  Hz, 2H, CH<sub>3</sub>).

**<sup>13</sup>C NMR** (CDCl<sub>3</sub>, 50 MHz)  $\delta_C$  (ppm) = 169.9 (C), 167.9 (C), 156.0 (C), 148.4 (C), 137.0 (C), 136.9 (C), 124.3 (C), 123.7 (C), 122.9 (C), 119.3 (C), 109.8 (C), 80.0 (CH<sub>3</sub>)<sub>3</sub>C, 61.5 (CH<sub>2</sub>), 48.9 (NHCH<sub>2</sub>), 48.8 (CH<sub>2</sub>), 46.8 (CH<sub>2</sub>), 38.6 (NHCH<sub>2</sub>), 28.3 (CH<sub>3</sub>)<sub>3</sub>C, 13.9 (CH<sub>3</sub>).

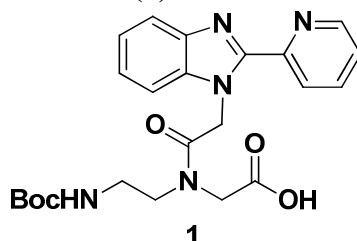
**Elemental analysis** Calcd for C<sub>25</sub>H<sub>31</sub>N<sub>5</sub>O<sub>5</sub>: C, 62.36; H, 6.49.

Found: C, 62.42; H, 6.54.

**HRMS (ESI)** Calcd for C<sub>25</sub>H<sub>31</sub>N<sub>5</sub>O<sub>5</sub>: 482.2403 (M+H)<sup>+</sup>

Found: 482.2404.

**2-(N-(2-((tert-butoxycarbonyl)amino)ethyl)-2-(2-(pyridin-2-yl)-1H-benzo[d]imidazol-1-yl) acetamido)acetic acid (1)**

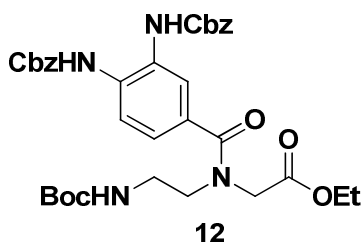


## Chapter 3

To a solution of ester **8** (0.2 g, 0.5 mmol) in MeOH at 0 °C, 10% aqueous LiOH (3 mL) was added. The resulting reaction mixture was stirred for 6 h at room temperature, and after that MeOH was removed under reduced pressure. The aqueous layer was washed with diethylether (2 x 10 mL), acidified with 1N KHSO<sub>4</sub> (8 mL) and extracted with EtOAc (3 x 20 mL). The combined organic layer was washed with brine (10 mL), filtered and dried over anhydrous Na<sub>2</sub>SO<sub>4</sub> and concentrated under reduced pressure to afford product **1** (0.17 g).

<b>Yield</b>	90%; white solid; $R_f = 0.16$ (EtOAc).
<b>Melting Point</b>	149.6-154.0°C
<b>Mol. Formula</b>	C <sub>23</sub> H <sub>27</sub> N <sub>5</sub> O <sub>5</sub>
<b>IR</b> (CHCl <sub>3</sub> )	$\nu_{\max}$ (cm <sup>-1</sup> ) = 3837, 3742, 3677, 3647, 3616, 3565, 3020, 2360, 1834, 1703, 1650, 1515, 1458, 1424, 1395, 1366, 1215, 1173.
<b><sup>1</sup>H NMR</b> (Methanol-D <sub>4</sub> , 200 MHz)	$\delta_H$ (ppm) = 8.76-8.70 (m, 1H, CH), 8.34-8.28 (m, 1H, CH), 7.99-7.91 (m, 1H, CH), 7.78-7.75 (m, 1H, CH), 7.60-7.35 (m, 5H, CH), 5.89 (s, 2H, CH <sub>2</sub> ), 5.73 (s, 1H, NH), 4.13 (s, 2H, CH <sub>2</sub> ), 3.74-3.63 (m, 2H, NHCH <sub>2</sub> ), 3.54-3.42 (m, 2H, NHCH <sub>2</sub> ), 1.47 (s, 9H, (CH <sub>3</sub> ) <sub>3</sub> C).
<b><sup>13</sup>C NMR</b> (Methanol-D <sub>4</sub> , 50 MHz)	$\delta_C$ (ppm) = 172.7 (C), 170.3 (C), 158.6 (C), 151.7 (C), 150.4 (C), 142.7 (C), 138.5 (C), 138.4 (C), 125.6 (C), 125.2 (C), 125.1 (C), 124.5 (C), 120.1 (C), 111.8 (C), 80.8 (CH <sub>3</sub> ) <sub>3</sub> C, 50.8 (CH <sub>2</sub> ), 50.4 (NHCH <sub>2</sub> ), 39.6 (CH <sub>2</sub> ), 39.3 (NHCH <sub>2</sub> ), 28.9 (CH <sub>3</sub> ) <sub>3</sub> C.
<b>Elemental analysis</b>	Calcd for C <sub>23</sub> H <sub>27</sub> N <sub>5</sub> O <sub>5</sub> : C, 60.92; H, 6.00. Found: C, 60.99; H, 6.08.
<b>HRMS (ESI)</b>	Calcd for C <sub>23</sub> H <sub>27</sub> N <sub>5</sub> O <sub>5</sub> : 454.2089 (M+H) <sup>+</sup> Found: 454.2091.
<b>Ethyl-2-(3,4-bis(((benzyloxy)carbonyl)amino)-N-(2-((tert-butoxycarbonyl)amino)ethyl) benzamido) acetate (12)</b>	

## Chapter 3

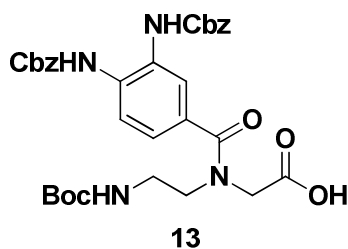


To a 0 °C cooled solution of compound **11** (4.2 g, 10.0 mmol) and compound **6** (2.46 g, 10.0 mmol) in anhydrous DMF (10 mL), DCC (3.09 g, 15.0 mmol) was slowly added into it. The reaction was stirred at room temperature for 24 h. After completion reaction mixture formed dicyclohexylurea was filtered and filtrate was extracted with EtOAc (3 x 50 mL). The combined organic layer was washed with brine (10 mL), dried over anhydrous Na<sub>2</sub>SO<sub>4</sub> and evaporated under vacuum. The crude residue was purified by silica gel column chromatography (30% pet-ether/EtOAc) to afford product **12** (3.24 g).

<b>Yield</b>	50%; orange semi-solid; $R_f = 0.33$ (EtOAc: pet ether; 1:1).
<b>Melting Point</b>	92.8-94.9°C
<b>Mol. Formula</b>	C <sub>34</sub> H <sub>40</sub> N <sub>4</sub> O <sub>9</sub>
<b>IR</b> (CHCl <sub>3</sub> )	$\nu_{\max}$ (cm <sup>-1</sup> ) = 3842, 3743, 3619, 3328, 2979, 2362, 1705, 1620, 1515, 1458, 1369, 1308, 1202, 1040.
<b><sup>1</sup>H NMR</b> (CDCl <sub>3</sub> , 200 MHz)	$\delta_H$ (ppm) = 7.35-7.24 (m, 13H, CH), 5.17 (s, 4H, CH <sub>2</sub> ), 4.21-4.14 (s, 4H, CH <sub>2</sub> ), 3.37-3.26 (m, 4H, NHCH <sub>2</sub> ), 1.36 (s, 9H, (CH <sub>3</sub> ) <sub>3</sub> C) 1.26 (t, $J = 7.3$ Hz, 2H, CH <sub>3</sub> ).
<b><sup>13</sup>C NMR</b> (CDCl <sub>3</sub> , 50 MHz)	$\delta_C$ (ppm) = 171.8 (C), 169.5 (C), 156.2 (C), 154.2 (C), 135.9 (C), 128.7 (C), 128.5 (C), 79.7 (CH <sub>3</sub> ) <sub>3</sub> C, 67.5 (CH <sub>2</sub> ), 61.5 (CH <sub>2</sub> ), 50.5 (NHCH <sub>2</sub> ), 47.8 (CH <sub>2</sub> ), 38.5 (NHCH <sub>2</sub> ), 28.5 (CH <sub>3</sub> ) <sub>3</sub> C, 14.2 (CH <sub>2</sub> ).
<b>Elemental analysis</b>	Calcd for C <sub>34</sub> H <sub>40</sub> N <sub>4</sub> O <sub>9</sub> : C, 65.71; H, 4.79. Found: C, 65.82; H, 4.86.
<b>HRMS (ESI)</b>	Calcd for C <sub>32</sub> H <sub>36</sub> N <sub>4</sub> O <sub>9</sub> : 671.2692 (M+Na) <sup>+</sup> Found: 671.2689.

### 2-(3,4-bis(((benzyloxy)carbonyl)amino)-N-(2-((tert-butoxycarbonyl)amino)ethyl)benzamido)acetic acid (**13**)

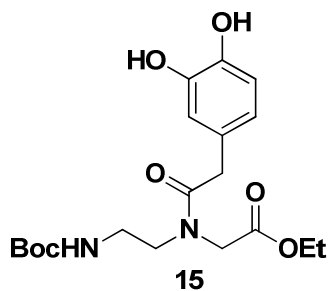
2013 PhD thesis: T. Kaur, University of Pune



To a 0 °C cooled solution of ethyl ester **12** (0.2 g, 0.30 mmol) in MeOH, aqueous 10% LiOH (2 mL) was added. The resulting reaction mixture was stirred for 4 h at room temperature, and after that MeOH was removed under reduced pressure. The aqueous layer was washed with diethylether (2 x 10 mL), acidified with 1N KHSO<sub>4</sub> (8 mL) and extracted with EtOAc (3 x 20 mL). The combined organic layer was washed with brine (10 mL), filtered and dried over anhydrous Na<sub>2</sub>SO<sub>4</sub> and concentrated under reduced pressure to afford product **13** (0.12 g).

<b>Yield</b>	60%; orange solid; $R_f = 0.3$ (EtOAc).
<b>Mol. Formula</b>	C <sub>32</sub> H <sub>36</sub> N <sub>4</sub> O <sub>9</sub>
<b>IR</b> (CHCl <sub>3</sub> )	$\nu_{\max}$ (cm <sup>-1</sup> ) = 3743, 3618, 3351, 2975, 2361, 1688, 1641, 1598, 1519, 1462, 1396, 1368, 1311, 1239, 1170, 1057.
<b>Elemental analysis</b>	Calcd for C <sub>32</sub> H <sub>36</sub> N <sub>4</sub> O <sub>9</sub> : C, 61.93; H, 5.85. Found: C, 62.02; H, 5.92.
<b>HRMS (ESI)</b>	Calcd for C <sub>32</sub> H <sub>36</sub> N <sub>4</sub> O <sub>9</sub> : 643.2379 (M+Na) <sup>+</sup> Found: 643.2371.

**Ethyl-2-(N-(2-((tert-butoxycarbonyl)amino)ethyl)-2-(3,4-dihydroxyphenyl)acetamido)acetate (15)**



To a 0 °C cooled solution of 3,4-dihydroxyphenylacetic acid **14** (0.84 g, 5.0 mmol) in anhydrous DMF (10 mL), EDC.HCl (1.24 g, 6.5 mmol) and HOBt (0.88 g, 6.5 mmol) was added. The solution of amine (1.23 g, 5.0 mmol) in anhydrous DMF (5 mL) was added into the reaction mixture. The reaction was stirred at room temperature for 24 h. The reaction mixture was diluted with water (10 mL) and extracted with EtOAc (3

## Chapter 3

x 50 mL). The organic layer was washed with brine (10 mL), dried over anhydrous  $\text{Na}_2\text{SO}_4$  and the solvent was evaporated under reduced pressure. The crude residue was purified by silica gel column chromatography (30% pet-ether/ EtOAc) to afford product **15** (2.34 g).

**Yield** 50%; white solid;  $R_f = 0.41$  (EtOAc: pet ether; 1:1).

**Melting Point** 127.8-133.7°C

**Mol. Formula**  $\text{C}_{19}\text{H}_{28}\text{N}_2\text{O}_7$

**IR** ( $\text{CHCl}_3$ )  $\nu_{\text{max}}$  ( $\text{cm}^{-1}$ ) = 3749, 3610, 3393, 3020, 2400, 1734, 1699, 1602, 1555, 1541, 1523, 1473, 1421, 1215, 1045, 929.

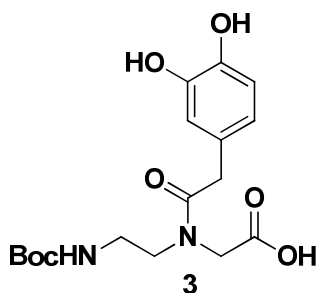
**$^1\text{H}$  NMR** ( $\delta_{\text{H}}$  (ppm) = 6.71-6.50 (m, 3H, CH), 4.18 (q,  $J = 7.3$  Hz, 2H,  $\text{CH}_2$ ), 4.07 (s, 2H,  $\text{CH}_2$ ), 3.65 (m, 2H,  $\text{NHCH}_2$ ), 3.52-3.46 (m, 2H,  $\text{NHCH}_2$ ), 3.18 (t,  $J = 5.8$  Hz, 2H,  $\text{CH}_2$ ), 1.45 (s, 9H,  $(\text{CH}_3)_3\text{C}$ ), 1.25 (t,  $J = 7.3$  Hz, 2H,  $\text{CH}_3$ ).

**$^{13}\text{C}$  NMR** ( $\delta_{\text{C}}$  (ppm) = 175.2 (C), 171.4 (C), 158.5 (C), 146.7 (C), 145.5 (C), 127.4 (C), 121.4 (C), 117.2 (C), 116.5 (C), 80.6 ( $(\text{CH}_3)_3\text{C}$ ), 62.5 ( $\text{CH}_2$ ), 41.4 ( $\text{NHCH}_2$ ), 40.4 ( $\text{CH}_2$ ), 39.6 ( $\text{NHCH}_2$ ), 28.9 ( $(\text{CH}_3)_3\text{C}$ ), 14.5 ( $\text{CH}_3$ ).

**Elemental analysis** Calcd for  $\text{C}_{19}\text{H}_{28}\text{N}_2\text{O}_7$ : C, 57.56; H, 7.12.

Found: C, 57.63; H, 7.19.

**2-(N-(2-((tert-butoxycarbonyl)amino)ethyl)-2-(3,4-dihydroxyphenyl)acetamido) acetic acid (3)**



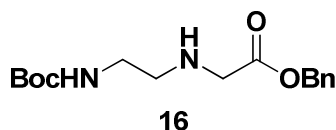
To a 0 °C cooled solution of ethyl ester **15** (0.2 g, 0.50 mmol) in MeOH, aqueous 10% LiOH (2 mL) was added. The resulting reaction mixture was stirred for 4 h at

## Chapter 3

room temperature, and after that MeOH was removed under reduced pressure. The aqueous layer was washed with diethylether (2 x 10 mL), acidified with 1N KHSO<sub>4</sub> (8 mL) and extracted with EtOAc (3 x 20 mL). The combined organic layer was washed with brine (10 mL), filtered and dried over anhydrous Na<sub>2</sub>SO<sub>4</sub> and concentrated under reduced pressure to afford product **3** (0.093 g).

<b>Yield</b>	50%; white solid; $R_f = 0.16$ (EtOAc).
<b>Melting Point</b>	103.3-108.4°C
<b>Mol. Formula</b>	C <sub>17</sub> H <sub>24</sub> N <sub>2</sub> O <sub>7</sub>
<b>IR</b> (CHCl <sub>3</sub> )	$\nu_{\max}$ (cm <sup>-1</sup> ) = 3422, 2925, 2855, 1605, 1495, 1460, 1377, 1157, 1082, 1030, 759, 728.
<b><sup>1</sup>H NMR</b> (Methanol-D <sub>4</sub> , 200 MHz)	$\delta_H$ (ppm) = 6.52-6.50 (m, 3H, CH), 3.87 (s, 2H, CH <sub>2</sub> ), 3.46 (s, 2H, CH <sub>2</sub> ), 3.02-2.99 (m, 2H, NHCH <sub>2</sub> ), 2.95-2.92 (m, 2H, NHCH <sub>2</sub> ), 1.25 (s, 9H, (CH <sub>3</sub> ) <sub>3</sub> C).
<b><sup>13</sup>C NMR</b> (Methanol-D <sub>4</sub> , 50 MHz)	$\delta_C$ (ppm) = 175.1 (C), 173.5 (C), 158.5 (C), 146.6 (C), 145.4 (C), 133.1 (CH), 130.1 (CH), 127.2 (CH), 121.5 (CH), 117.2 (CH), 116.5 (CH), 80.6 (CH <sub>3</sub> ) <sub>3</sub> C, 54.9 (CH <sub>2</sub> ), 50.1 (NHCH <sub>2</sub> ), 40.3 (CH <sub>2</sub> ), 39.6 (NHCH <sub>2</sub> ), 28.8 (CH <sub>3</sub> ) <sub>3</sub> C.
<b>Elemental analysis</b>	Calcd for C <sub>17</sub> H <sub>24</sub> N <sub>2</sub> O <sub>7</sub> : C, 55.43; H, 6.57. Found: C, 55.52; H, 6.62.

### Benzyl-*N*-(2-Boc-aminoethyl)-glycinate (**16**)



To an ice-cold solution of *N*<sup>l</sup>-(Boc)-1,2-diaminoethane **5** (9.47 g, 59 mmol) in acetonitrile (80 mL), triethylamine (8.6 mL, 61.8 mmol) was slowly added. After stirring at room temperature for 20 min, the solution of benzylbromoacetate (9.29 mL, 59 mmol) in acetonitrile (100 mL) was added. The reaction was stirred at room temperature for 12 h. After completion of the reaction, it was extracted with EtOAc (3 x 50 mL). The organic layer was washed with brine (10 mL), dried over anhydrous Na<sub>2</sub>SO<sub>4</sub>, and the solvent was evaporated under vacuum. The crude residue was

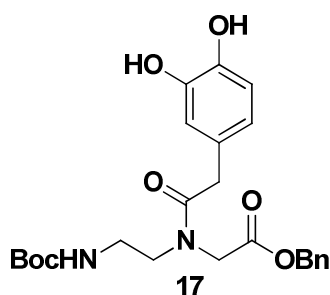


## Chapter 3

purified by silica gel column chromatography (50% pet-ether/ EtOAc) provided product **16** (12.7 g).

<b>Yield</b>	70%; colorless oil; $R_f = 0.66$ (EtOAc: pet-ether; 1:1).
<b>Mol. Formula</b>	$C_{16}H_{24}N_2O_4$
<b>IR</b> ( $CHCl_3$ )	$\nu_{max}$ ( $cm^{-1}$ ) = 3335, 2974, 2934, 1738, 1697, 1509, 1455, 1391, 1365, 1248, 1164.
<b><math>^1H</math> NMR</b> ( $CDCl_3$ , 200 MHz)	$\delta_H$ (ppm) = 7.28-7.25 (m, 5H, CH), 5.28 (br, 1H, NH), 5.09 (s, 2H, $CH_2$ ), 3.38 (s, 2H, $CH_2$ ), 3.14-3.11 (m, 2H, $NHCH_2$ ), 2.66 (t, $J = 5.9$ Hz, 2H, $NHCH_2$ ), 1.37 (s, 9H, $(CH_3)_3C$ ).
<b><math>^{13}C</math> NMR</b> ( $CDCl_3$ , 50 MHz)	$\delta_C$ (ppm) = 172.1 (C), 155.9 (C), 135.3 (CH), 128.4 (CH), 128.1 (CH), 78.8 $(CH_3)_3C$ , 66.3 ( $CH_2$ ), 50.2 ( $CH_2$ ), 48.5 ( $NHCH_2$ ), 39.9 ( $NHCH_2$ ), 28.2 ( $CH_3$ ) $_3C$ .
<b>Elemental analysis</b>	Calcd for $C_{16}H_{24}N_2O_4$ : C, 62.32; H, 7.84. Found: C, 62.39; H, 7.91.
<b>HRMS (ESI)</b>	Calcd for $C_{16}H_{24}N_2O_4$ : 309.1815 (M+H) $^+$ Found: 309.1816.

### Benzyl-2-(N-(2-((tert-butoxycarbonyl)amino)ethyl)-2-(3,4-dihydroxyphenyl)acetamido) acetate (**17**)



To a 0 °C cooled solution of 3,4-dihydroxyphenylacetic acid **14** (0.51 g, 3.0 mmol) in anhydrous DMF (10 mL), DCC (0.93 g, 4.5 mmol) was added. The solution of compound **16** (0.93 g, 3.0 mmol) in anhydrous DMF (5 mL) was added into the reaction mixture. The reaction was stirred at room temperature for 24 h. The reaction mixture was diluted with water (10 mL) and extracted with EtOAc (3 x 50 mL). The organic layer was washed with brine (10 mL), dried over anhydrous  $Na_2SO_4$  and the

## Chapter 3

solvent was evaporated under reduced pressure. The crude residue was purified by silica gel chromatography (30% pet-ether/ EtOAc) to afford product **17** (0.93 g).

**Yield** 70%; white solid;  $R_f = 0.38$  (EtOAc: pet-ether; 1:1).

**Melting Point** 102-104°C

**Mol. Formula**  $C_{24}H_{30}N_2O_7$

**IR** ( $CHCl_3$ )  $\nu_{max}$  ( $cm^{-1}$ ) = 3743, 3647, 3618, 3335, 2977, 2938, 2362, 1741, 1691, 1631, 1518, 1450, 1363, 1280, 1251, 1170, 1114, 1041.

**$^1H$  NMR** ( $\delta_H$  (ppm) = 7.19-7.16 (m, 5H, CH), 6.54-6.45 (m, 3H, CH), 5.31 (br, 1H, NH), 4.99 (s, 2H,  $CH_2$ ), 4.92 (s, 1H,  $CH_2$ ), 3.95 (s, 2H,  $CH_2$ ), 3.47 (s, 2H,  $CH_2$ ), 3.14-3.13 (m, 2H,  $NHCH_2$ ), 3.00 (t,  $J = 6.1$  Hz, 2H,  $NHCH_2$ ), 1.26 (s, 9H,  $(CH_3)_3C$ ).

**$^{13}C$  NMR** ( $\delta_C$  (ppm) = 175.2 (C), 171.2 (C), 158.5 (C), 146.6 (C), 145.5 (C), 137.3 (CH), 129.7 (CH), 129.5 (CH), 127.4 (C), 121.4 (C), 117.2 (C), 116.5 (C), 80.6  $(CH_3)_3C$ , 68.1 ( $CH_2$ ), 50.2 ( $NHCH_2$ ), 41.3 ( $CH_2$ ), 40.4 ( $CH_2$ ), 39.6 ( $NHCH_2$ ), 28.9  $(CH_3)_3C$ .

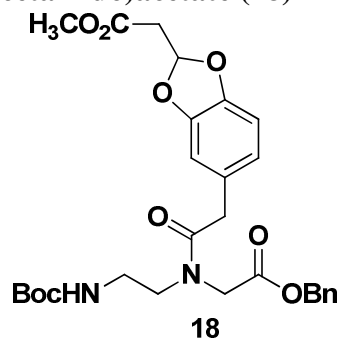
**Elemental analysis** Calcd for  $C_{24}H_{30}N_2O_7$ : C, 62.87; H, 6.59.

Found: C, 62.92; H, 6.64.

**HRMS (ESI)** Calcd for  $C_{24}H_{30}N_2O_7$ : 481.1950 ( $M+Na$ )<sup>+</sup>

Found: 481.1947.

**Benzyl-2-(N-(2-((tert-butoxycarbonyl)amino)ethyl)-2-(2-(2-methoxy-2-oxoethyl)benzo-[d][1,3]dioxol-5-yl)acetamido)acetate (18)**



To a solution of compound **17** (0.2 g, 0.43 mmol) in acetonitrile (5 mL), DMAP (79.9 mg, 0.655 mmol) was added under  $N_2$  atmosphere. The reaction mixture was stirred

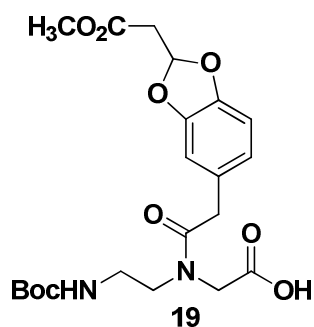
## Chapter 3

for 10 min at room temperature, followed by the slow addition of methyl propiolate (40  $\mu$ L, 0.47 mmol) into it. After stirring for 30 min, solvent was evaporated and the crude residue was purified by silica gel column chromatography (30% pet-ether/EtOAc) to afford product **18** (0.19 g).

<b>Yield</b>	80%; yellow syrup; $R_f = 0.71$ (EtOAc: pet ether; 1:1).
<b>Mol. Formula</b>	$C_{28}H_{34}N_2O_9$
<b>IR</b> ( $CHCl_3$ )	$\nu_{max}$ ( $cm^{-1}$ ) = 3893, 3860, 3843, 3743, 3677, 3647, 3618, 3395, 2944, 2830, 2361, 1740, 1695, 1640, 1497, 1446, 1395, 1361, 1245, 1169, 1101, 1026.
<b><math>^1H</math> NMR</b> ( $CDCl_3$ , 200 MHz)	$\delta_H$ (ppm) = 7.31-7.27 (m, 5H, CH), 6.70-6.61 (m, 3H, CH), 6.43 (t, $J = 5.5$ Hz, 1H, CH), 5.51 (br, 1H, NH), 5.10 (s, 2H, $CH_2$ ), 4.00 (s, 1H, $CH_2$ ), 3.67 (s, 3H, $OCH_3$ ), 3.61 (s, 2H, $CH_2$ ), 3.42 (t, $J = 5.9$ Hz, 2H, $NHCH_2$ ), 3.17-3.12 (m, 2H, $NHCH_2$ ), 2.89 (d, $J = 5.5$ Hz, 2H, $CH_2$ ), 1.39 (s, 9H, $(CH_3)_3C$ ).
<b><math>^{13}C</math> NMR</b> ( $CDCl_3$ , 50 MHz)	$\delta_C$ (ppm) = 171.7 (C), 169.6 (C), 168.3 (C), 155.7 (C), 146.9 (C), 145.6 (C), 134.9 (C), 128.3 (CH), 128.1 (CH), 127.9 (CH), 121.8 (CH), 109.2 (CH), 108.0 (CH), 107.6 (CH), 79.2 $(CH_3)_3C$ , 66.7 ( $CH_2$ ), 51.7 ( $OCH_3$ ), 48.9 ( $NHCH_2$ ), 48.5 ( $CH_2$ ), 39.6 ( $NHCH_2$ ), 39.1 ( $CH_2$ ), 38.4 ( $CH_2$ ), 28.0 $(CH_3)_3C$ .
<b>Elemental analysis</b>	Calcd for $C_{28}H_{34}N_2O_9$ : C, 61.98; H, 6.32. Found: C, 62.01; H, 6.45.
<b>HRMS (ESI)</b>	Calcd for $C_{28}H_{34}N_2O_9$ : 565.2161 (M+Na) <sup>+</sup> Found: 565.2167.

**2-(*N*-(2-((*tert*-butoxycarbonyl)amino)ethyl)-2-(2-(2-methoxy-2-oxoethyl)-benzo[d][1,3]dioxol-5-yl)acetamido)acetic acid (19)**

## Chapter 3



To a solution compound **18** (2.2 g, 4.05 mmol) in dry MeOH (10 mL), 10% Pd/C (0.2 g) was added and stirred under H<sub>2</sub> atmosphere. After stirring for 12 h at room temperature, the reaction mixture was filtered through celite. The solvent was evaporated and the crude product was purified by silica gel chromatography (100% EtOAc) to furnish the pure product **19** (1.65 g).

**Yield** 90%; white solid;  $R_f = 0.6$  (EtOAc: pet-ether; 1:1).

**Melting Point** 110-123°C

**Mol. Formula** C<sub>21</sub>H<sub>28</sub>N<sub>2</sub>O<sub>9</sub>

**IR** (CHCl<sub>3</sub>)  $\nu_{\max}$  (cm<sup>-1</sup>) = 3743, 3618, 3394, 2977, 2362, 1736, 1705, 1640, 1497, 1444, 1400, 1361, 1244, 1168, 1101, 1039.

**<sup>1</sup>H NMR** (CDCl<sub>3</sub>, 200 MHz)  $\delta_H$  (ppm) = 6.71-6.65 (m, 3H, CH), 6.47 (t,  $J = 5.0$  Hz, 1H, CH), 5.46 (br, 1H, NH), 4.00 (s, 1H, CH<sub>2</sub>), 3.73 (s, 3H, OCH<sub>3</sub>), 3.65 (s, 2H, CH<sub>2</sub>), 3.50-3.46 (m, 2H, NHCH<sub>2</sub>), 3.24-3.20 (m, 2H, NHCH<sub>2</sub>), 2.94 (d,  $J = 5.0$  Hz, 2H, CH<sub>2</sub>), 1.42 (s, 9H, (CH<sub>3</sub>)<sub>3</sub>C).

**<sup>13</sup>C NMR** (CDCl<sub>3</sub>, 50 MHz)  $\delta_C$  (ppm) = 173.0 (C), 172.3 (C), 168.7 (C), 156.2 (C), 147.3 (C), 146.0 (C), 128.1 (CH), 122.2 (CH), 109.5 (CH), 108.4 (CH), 107.9 (CH), 79.9 (CH<sub>3</sub>)<sub>3</sub>C, 52.1 (OCH<sub>3</sub>), 49.6 (NHCH<sub>2</sub>), 49.0 (CH<sub>2</sub>), 40.2 (CH<sub>2</sub>), 39.9 (NHCH<sub>2</sub>), 39.4 (CH<sub>2</sub>), 38.7 (CH<sub>2</sub>), 28.3 (CH<sub>3</sub>)<sub>3</sub>C.

**Elemental analysis** Calcd for C<sub>21</sub>H<sub>28</sub>N<sub>2</sub>O<sub>9</sub>: C, 55.75; H, 6.24.

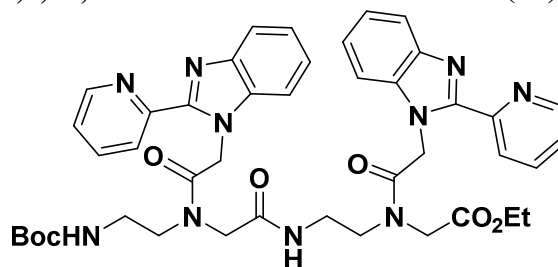
Found: C, 55.83; H, 6.32.

**HRMS (ESI)** Calcd for C<sub>21</sub>H<sub>28</sub>N<sub>2</sub>O<sub>9</sub>: 475.1692 (M+Na)<sup>+</sup>

## Chapter 3

Found: 475.1689.

**Ethyl-2,2-dimethyl-4,10-dioxo-8,14-bis(2-(2-(pyridin-2-yl)-1H-benzo[d]imidazol-1-yl) acetyl) -3-oxa-5,8,11,14-tetraazahexadecan-16-oate (21)**



To 0 °C cooled solution of compound **8** (4.8 g, 10 mmol) in dioxan (5 mL), HCl in dioxan (4M, 10 mL) was added and stirred under N<sub>2</sub> atmosphere. After stirring for 2 h at room temperature, the solvent was evaporated under reduced pressure. The formed hydrochloride salt **20** was washed with toluene (2 x 5 mL). It was dried.

To a 0 °C cooled solution of 2-pyridylbenzimidazole (PBI) *aeg* acid **1** (0.875 g, 1.93 mmol) and hydrochloride salt **20** (1.0 g, 1.93 mmol) in anhydrous DMF (10 mL), HBTU (0.88 g, 2.32 mmol) was added. DIPEA (0.671 μL, 3.864 mmol) was added into it. The reaction was stirred at room temperature for 24 h. The reaction mixture was diluted with water (10 mL) and extracted with EtOAc (3 x 50 mL). The organic layer was washed with brine (10 mL), dried over anhydrous Na<sub>2</sub>SO<sub>4</sub> and the solvent was evaporated under reduced pressure. The crude residue was purified by silica gel chromatography (5% DCM/ Methanol) to afford product **21** (1.29 g).

<b>Yield</b>	87%; white solid; $R_f = 0.6$ (Methanol: DCM; 1:9).
<b>Melting Point</b>	143-146°C
<b>Mol. Formula</b>	C <sub>43</sub> H <sub>48</sub> N <sub>10</sub> O <sub>7</sub>
<b>IR</b> (CHCl <sub>3</sub> )	$\nu_{\max}$ (cm <sup>-1</sup> ) = 3746, 3679, 3642, 3623, 3342, 2971, 2359, 1735, 1645, 1572, 1501, 1442, 1373, 1365, 1323, 1242, 1201, 1161, 1067, 1018.
<b><sup>1</sup>H NMR</b> (CDCl <sub>3</sub> , 200 MHz)	$\delta_H$ (ppm) = 8.60-8.40 (m, 5H, CH), 8.28-8.26 (m, 1H, CH), 7.76-7.70 (m, 5H, CH), 6.14 (s, 1H), 5.70-5.67 (m, 2H, CH), 5.38 (s, 1H, NH), 5.23 (s, 1H, NH), 4.18 (q, $J = 7.3$ Hz, 2H, CH <sub>2</sub> ), 3.86 (s, 2H, CH <sub>2</sub> ), 3.74 (s, 2H, CH <sub>2</sub> ), 3.35 (s, 2H, CH <sub>2</sub> ).

	3.23-3.18 (m, 2H, NHCH <sub>2</sub> ), 3.09 (m, 2H, NHCH <sub>2</sub> ), 1.39 (s, 9H, (CH <sub>3</sub> ) <sub>3</sub> C), 1.25 (t, <i>J</i> = 7.3 Hz, 2H, CH <sub>2</sub> ).
<sup>13</sup> C NMR (CDCl <sub>3</sub> , 50 MHz)	δ <sub>C</sub> (ppm) = 169.7 (C), 169.4 (C), 169.3 (C), 167.7 (C), 156.0 (C), 150.3 (CH), 150.4 (CH), 150.3 (CH), 150.1 (CH), 149.5 (C), 149.3 (C), 149.4 (C), 148.4 (C), 142.2 (C), 137.4 (CH), 137.1 (CH), 136.8 (CH), 124.4 (CH), 124.0 (CH), 123.7 (CH), 119.9 (CH), 108.6 (CH), 110.1 (CH), 79.7 (CH <sub>3</sub> ) <sub>3</sub> C, 61.7 (CH <sub>2</sub> ), 49.2 (NHCH <sub>2</sub> ), 48.5 (CH <sub>2</sub> ), 48.0 (CH <sub>2</sub> ), 46.7 (CH <sub>2</sub> ), 46.1 (NHCH <sub>2</sub> ), 28.4 (CH <sub>3</sub> ) <sub>3</sub> C, 14.1 (CH <sub>3</sub> ).
<b>Elemental analysis</b>	Calcd for C <sub>43</sub> H <sub>48</sub> N <sub>10</sub> O <sub>7</sub> : C, 63.22; H, 5.92. Found: C, 63.28; H, 5.98.
<b>HRMS (ESI)</b>	Calcd for C <sub>43</sub> H <sub>48</sub> N <sub>10</sub> O <sub>7</sub> : 817.3786 (M+H) <sup>+</sup> Found: 817.3798.

---

### 3.15.3 Solid Phase Peptide Synthesis (SPPS)

#### 3.15.3a Functionalization of the MBHA [(4-methyl benzhydryl) amine] resin

The resin (4-methylbenzhydrylamine) MBHA.HCl, from Novabiochem, [catalog number 855000, 100-200 mesh] (100 mg) was taken in sintered vessel (25 mL) and rinsed with 5 mL of dry DCM and filtered. The process was repeated 3 to 4 times and the resulting resin was kept for 2 h in DCM (10 mL) for swelling. The solvent was removed and rinsed 3 times with dry DMF and kept 2 h in dry DMF (10 mL) for swelling before the first coupling. The resin neutralisation was done with 20% DIPEA/DCM.

The resin was swollen overnight in DCM before couplings cycle. The resin was neutralized with 20% DIPEA/DCM and after that subsequent steps were repeated.

- Wash with DCM (3 x 5 mL), MeOH (3 x 5 mL) and DMF with (3 x 5 mL).
- Coupling reaction with monomer, DIPEA, HOBt and HBTU (3 eq.) in DMF (1 mL).
- Test for completion of coupling reaction (chloranil test), colorless beads.

- Wash with DMF (3 x 5 mL), and DCM with (3 x 5 mL).
- Deprotection of *t*-Boc group with 50% TFA/DCM (3 x 5 mL).
- Wash with DCM (3 x 5 mL), DMF (3 x 5 mL) and DCM with (3 x 5 mL).
- Test for complete deprotection (chloranil test), blue beads.
- Neutralization with 5% DIPEA/DCM (3 x 5 mL).
- Wash with DCM (3 x 5 mL) and DMF with (3 x 5 mL).
- Repeat of the coupling reaction in NMP for better yield.
- This cycle was repeated for every monomer.

### 3.15.3b Coupling tests (Kaiser's/Chloranil test)

These cycles were repeated for every amino acid. The coupling and deprotection reactions were monitored by a combination of Kaiser's (ninhydrin) test and chloranil test. In case of negative test after coupling the re-coupling was performed with same amino acid followed by capping of the unreacted amino groups using Ac<sub>2</sub>O, pyridine & DCM (1:1:1), in case coupling does not go to completion even after re-coupling.

### 3.15.3c Kaiser's test

Kaiser's was used to monitor the *t*-Boc/Fmoc deprotection and coupling reactions of glycine (or basically primary amines) in the solid phase peptide synthesis using three solutions.

**Solution A:** Ninhydrin (5.0 g) dissolved in ethanol (100 ml)

**Solution B:** Phenol (80.0 mg) dissolved in ethanol (20 ml)

**Solution C:** KCN (2 ml, 0.001 M aqueous solution) added to 98 ml pyridine

- Few beads of resin to be tested were taken in a test tube and washed 3 times with ethanol.
- 3-4 drops of each of the three solutions described above were added to it
- The test tube was heated to 120 °C for 4-6 min

The successful deprotection was indicated by blue resin beads while colourless beads indicate the completion of coupling step.

### 3.15.3c Chloranil test

A few beads of resin were taken in a glass test tube (5 mL capacity) and were washed with methanol followed by toluene. To this three drops of saturated chloranil solution in toluene and 200  $\mu$ L of acetone were added. The mixture was shaken for 2- 3 minutes. Blue or green color is observed on the resin beads if free amines are present.

### **3.15.4 Synthesis of polyamide oligomers incorporating 2-pyridyl-benzimidazole (PBI) *aeg* monomer, *o*-phenylenediamine (PDA) *aeg* monomer and 3,4-dihydroxyphenyl (CAT) *aeg* monomer**

The modified polyamide monomers were built into polyamide oligomers using the standard procedure on MBHA resin (initial loading value = 0.67 meq/g) using HBTU/HOBt/DIPEA in DMF/NMP as coupling reagents. The polyamide oligomers were cleaved from the resin using a TFA/TFMSA mixture and then precipitated with diethyl ether and air-dried. The oligomers were purified by reversephase HPLC (C18 column) and were characterized by MALDI-TOF mass spectrometry. The overall yields of the raw products were 55-88%.

### **3.15.5 Cleavage of the PNA oligomers from the resin**

The dry peptide-resin (10 mg) was taken in a sample vial and thioanisole (20  $\mu$ L) and 1,2-ethanedithiol (8  $\mu$ L) were added. It is kept at 0 °C for 10 min in an ice-bath, which further was treated with trifluoroacetic acid (TFA, 120  $\mu$ L) and again kept it in an ice-bath for 10 min and then trifluoromethane sulphonic acid (TFMSA, 16  $\mu$ L) was added into it. The resulting mixture was kept for 2 h by gentle shaking. The mixture was filtered through a sintered funnel and the resin was washed with TFA (3 x 1 mL). The filtrate was collected in round-bottom flask and evaporated under reduced pressure. Diethyl ether was chilled and added into it for precipitation. The off-white precipitate obtained was centrifuged. The re-precipitation procedure was done to obtain crude peptide. The crude peptide was dissolved in water and further purified on HPLC.

### **3.15.6 Purification and Characterization**

#### **3.15.6a Gel Filtration Chromatography (GFC)**

The crude peptides obtained after ether precipitation were dissolved in deionized water (~0.5 ml) and loaded onto a gel filtration G10 Sephadex column with a void volume of 1 mL. The presence of the peptide was detected by measuring the



absorbance at 254/302 nm. The fractions containing the peptides were pooled together and freeze-dried. The purity of the cleaved crude peptide was determined by analytical RP-HPLC on a C18 column.

### 3.15.6b High Performance Liquid Chromatography (HPLC)

All the cleaved polyamide oligomers were initially subjected to gel filtration over sephadex NAP column to remove low molecular weight impurities. The purity of the obtained polyamide oligomers were checked on analytical RP-HPLC (C18 column, acetonitrile:water system) and was found to be more than 80-85 % purity. These were subsequently purified by RP-HPLC on a semi-preparative C18 column to give polyamide oligomers in 95-99% purity as ascertained by analytical RP-HPLC. The representative HPLC profiles for oligomers are shown in Figure 20. An isocratic elution method with 10% CH<sub>3</sub>CN in 0.1% TFA/ H<sub>2</sub>O was used with flow rate 1.5 mL/min (linear gradient from A to B in 20 min) and the eluent was monitored at 254 nm.

The purity of the polyamide oligomers was further assessed by RP-C18 analytical HPLC column (25×0.2 cm, 5 μm) with gradient elution: A to 100% B in 20 min; A= 0.1% TFA in CH<sub>3</sub>CN:H<sub>2</sub>O (5:95); B= 0.1% TFA in CH<sub>3</sub>CN:H<sub>2</sub>O (1:1) with flow rate 1 mL/ min. The purities of the hence purified oligomers were found to be > 90%.

### 3.15.7 MALDI-TOF Characterization

MALDI-TOF mass spectra were obtained on either Voyager-Elite instrument (PerSeptive Biosystems Inc., Farmingham, MA) equipped with delayed extraction or on Voyager-De-STR (Applied Biosystems) instrument. Sinapinic acid and α-cyano-4-hydroxycinnamic acid (CHCA) both were used as matrix for peptides of which CHCA was found to give satisfactory results. A saturated matrix solution was prepared with typical dilution solvent (50:50:0.1 Water:MeCN:TFA) and spotted on the metal plate along with the oligomers. The metal plate was loaded to the instrument and the analyte ions are then accelerated by an applied high voltage (15-25 kV) in reflector mode, separated in a field-free flight tube and detected as an electrical signal at the end of the flight tube. HPLC purified peptides were characterized through this

method and were observed to give good signal to noise ratio, mostly producing higher molecular ion signals.

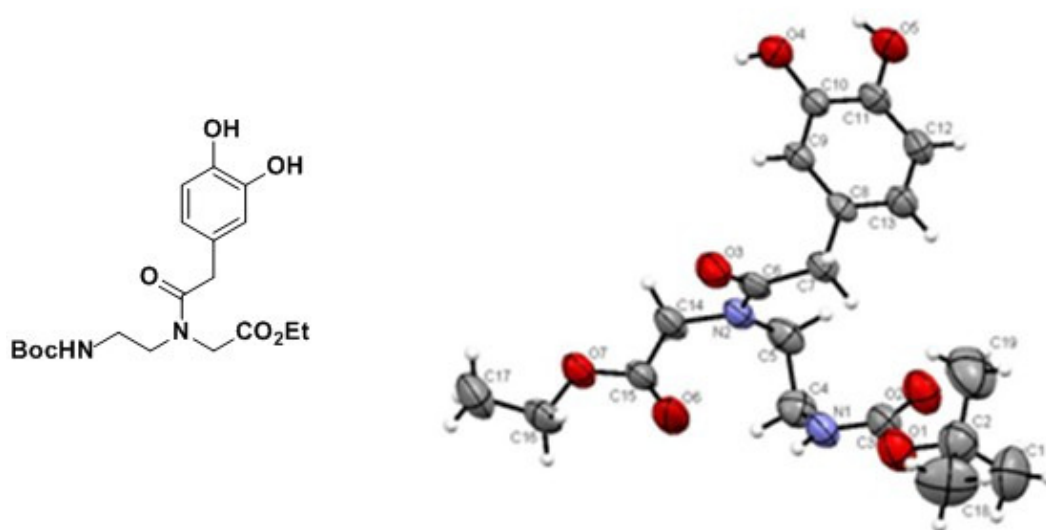
### 3.15.8 Determination of $pK_a$

The pH of polyamide oligomers **22-28** (50 mM, 1 mL) in deionized water was adjusted to 2.0 using conc. HCl. This solution was titrated with 2.5  $\mu$ L aliquots of 0.5M aq. NaOH. After each addition of NaOH solution, pH was recorded after the reading reached a stable value (1 min). The  $pK_a$  values were derived from the first derivative of the plot of pH vs volume of NaOH.

### 3.15.9 X-ray crystal structure determination

X-ray diffraction data for all the crystallized compounds were collected at  $T = 296$  K, on SMART APEX CCD Single Crystal X-ray diffractometer using Mo- $K\alpha$  radiation ( $\lambda = 0.7107$  Å) to a maximum  $\theta$  range of  $25.00^\circ$ . Crystal to detector distance was 6.05 cm, 512 x 512 pixels / frame and other conditions used are oscillation / frame ( $-0.3^\circ$ ), maximum detector swing angle ( $-30.0^\circ$ ), beam center (260.2, 252.5) and in plane spot width (1.24). SAINT integration and SADABS correction were also applied. The structures were solved by direct methods using SHELXTL. All the data were corrected for Lorentzian, polarisation and absorption effects. SHELX-97 (ShelxTL) was used for structure solution and full matrix least squares refinement on F2. Hydrogen atoms were included in the refinement as per the riding model. The refinements were carried out using SHELXL-97.

## 3,4-dihydroxyphenyl (CAT) aeg monomer 15

**Table 24.** Crystal data and structure refinement for compound 15.

Empirical formula	C <sub>19</sub> H <sub>24</sub> N <sub>2</sub> O <sub>7</sub>	
Formula weight	392.40	
Temperature	296(2) K	
Wavelength	0.71073 Å	
Crystal system	Triclinic	
Space group	P-1	
Unit cell dimensions	a = 7.621(6) Å	α = 89.819(15)°.
	b = 9.069(8) Å	β = 79.348(15)°.
	c = 17.016(14) Å	γ = 80.997(15)°.
Volume	1141.2(16) Å <sup>3</sup>	
Z	2	
Density (Calcd)	1.142 mg/m <sup>3</sup>	
Absorption coefficient	0.088 mm <sup>-1</sup>	
F(000)	416	
Crystal size	0.335 x 0.232 x 0.105 mm <sup>3</sup>	
Theta range for data collection	1.22 to 28.28°.	
Index ranges	-10 ≤ h ≤ 9, -12 ≤ k ≤ 12, -22 ≤ l ≤ 22	
Reflections collected	19181	

## Chapter 3

Independent reflections	5547 [R(int) = 0.1127]
Completeness to theta = 28.28°	98.1 %
Absorption correction	Semi-empirical from equivalents
Refinement method	Full-matrix least-squares on F <sup>2</sup>
Data / restraints / parameters	5547 / 0 / 259
Goodness-of-fit on F <sup>2</sup>	1.247
Final R indices [I>2sigma(I)]	R1 = 0.1444, wR2 = 0.3789
R indices (all data)	R1 = 0.2439, wR2 = 0.4408
Largest diff. peak and hole	1.379 and -0.494 e.Å <sup>-3</sup>

### 2-Pyridylbenzimidazole (PBI) *aeg* monomer **8**

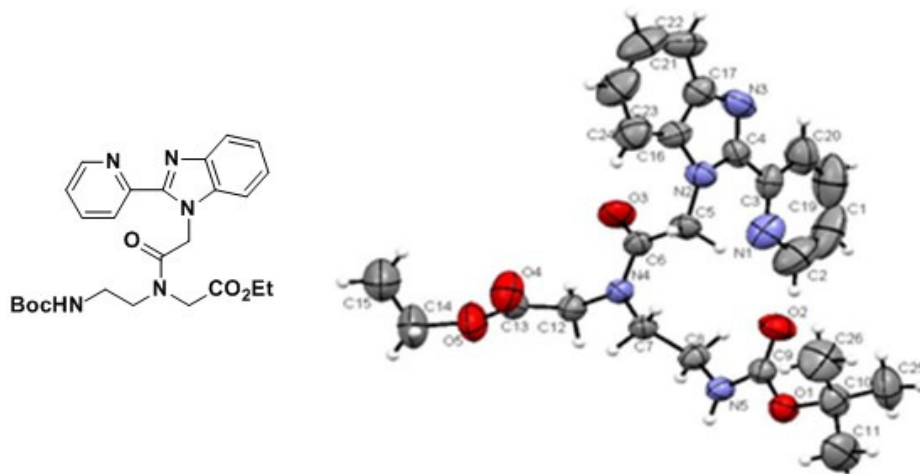


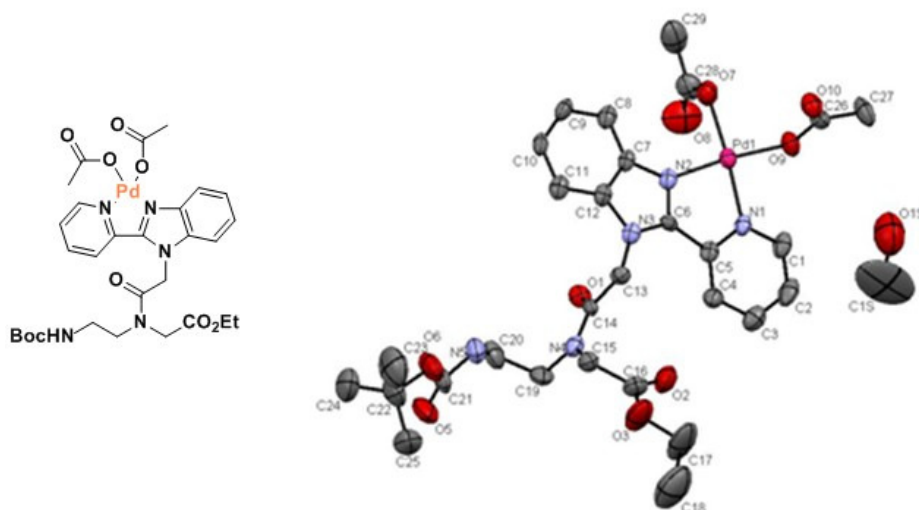
**Table 25.** Crystal data and structure refinement for compound **8**.

Empirical formula	C <sub>50</sub> H <sub>62</sub> N <sub>10</sub> O <sub>6</sub>	
Formula weight	899.10	
Temperature	296(2) K	
Wavelength	0.71073 Å	
Crystal system	Monoclinic-C	
Space group	C2/c	
Unit cell dimensions	a = 14.953(5) Å	α = 90°.
	b = 15.681(5) Å	β = 97.472(6)°.
	c = 22.700(8) Å	γ = 90°.
Volume	5277(3) Å <sup>3</sup>	

## Chapter 3

Z	4
Density (Calcd)	1.132 mg/m <sup>3</sup>
Absorption coefficient	0.076 mm <sup>-1</sup>
F(000)	1920
Crystal size	0.435 x 0.332 x 0.135 mm <sup>3</sup>
Theta range for data collection	1.81 to 28.42°.
Index ranges	-19<=h<=19, -20<=k<=20, -30<=l<=30
Reflections collected	25008
Independent reflections	6616 [R(int) = 0.0337]
Completeness to theta = 28.28°	99.6 %
Absorption correction	Semi-empirical from equivalents
Refinement method	Full-matrix least-squares on F <sup>2</sup>
Data / restraints / parameters	6616 / 0 / 321
Goodness-of-fit on F <sup>2</sup>	1.035
Final R indices [I>2sigma(I)]	R1 = 0.0568, wR2 = 0.1406
R indices (all data)	R1 = 0.1238, wR2 = 0.1706
Extinction coefficient	0.0008(2)
Largest diff. peak and hole	0.409 and -0.140 e.Å <sup>-3</sup>

### 2-Pyridylbenzimidazole (PBI) *aeg* monomer and Pd (8-Pd complex)



## Chapter 3

**Table 26.** Crystal data and structure refinement for compound **8-Pd**.

Empirical formula	C <sub>54</sub> H <sub>68</sub> N <sub>5</sub> O <sub>9</sub> Pd	
Formula weight	844.26	
Temperature	296(2) K	
Wavelength	0.71073 Å	
Crystal system	Triclinic	
Space group	P21/c	
Unit cell dimensions	a = 19.154(8) Å	α = 90°.
	b = 13.977(5) Å	β = 99.445°.
	c = 12.208(5) Å	γ = 90°.
Volume	3224(2) Å <sup>3</sup>	
Z	4	
Density (Calcd)	1.739 mg/m <sup>3</sup>	
Absorption coefficient	1.171 mm <sup>-1</sup>	
F(000)	1632	
Crystal size	0.207x 0.77x 0.26 mm <sup>3</sup>	
Theta range for data collection	1.81 to 28.32°.	
Index ranges	-24<=h<=25, -18<=k<=18, -16<=l<=15	
Reflections collected	52475	
Independent reflections	8004 [R(int) = 0.0996]	
Completeness to theta = 28.28°	99.5%	
Absorption correction	Semi-empirical from equivalents	
Refinement method	Full-matrix least-squares on F <sup>2</sup>	
Data / restraints / parameters	8004 / 0 / 404	
Goodness-of-fit on F <sup>2</sup>	4.369	
Final R indices [I>2σ(I)]	R1 = 0.1326, wR2 = 0.2904	
R indices (all data)	R1 = 0.1799, wR2 = 0.2943	
Extinction coefficient	0.0054(7)	
Largest diff. peak and hole	8.795 and -1.064 e.Å <sup>-3</sup>	

## 3.15.10 UV-Vis spectrophotometric titrations

UV-Vis titrations were carried out on Perkin Elmer 950 instrument. Titrations were performed using either methanolic solutions of known concentrations of monomer or water solutions of polyamide oligomers and Cu(NO<sub>3</sub>)<sub>2</sub>/ Ni(NO<sub>3</sub>)<sub>2</sub>. The UV spectra were recorded between 250-500 nm as a function of metal concentration. The cuvette was filled with monomer/polyamide oligomers (5-20 μM) in methanol/water, respectively. The metal salts (2.5-10 mM, 40 μl) were added into it with the help of pipette. The ΔAbs were corrected by doing the blank correction using the double beam spectrophotometer using only the metal salts. Data obtained were plotted in the Origin 8 software.

**Table 27.** Calculation of binding constants using Benesi-Hildebrand equation.

Ligands	Metal Salts	Models	Binding constants [M] <sup>-1</sup>
(PBI) <b>8</b>	Cu(NO <sub>3</sub> ) <sub>2</sub>	1:1	6.71 x 10 <sup>3</sup>
	Ni(NO <sub>3</sub> ) <sub>2</sub>	1:1	1.82 x 10 <sup>3</sup>
(PBI) <sub>2</sub> <b>21</b>	Cu(NO <sub>3</sub> ) <sub>2</sub>	1:1	2.24 x 10 <sup>4</sup>
		1:2	3.82 x 10 <sup>4</sup>
	Ni(NO <sub>3</sub> ) <sub>2</sub>	1:1	3.18 x 10 <sup>4</sup>
		1:2	3.84 x 10 <sup>4</sup>
(PBI) <sub>6</sub> <b>22</b>	Cu(NO <sub>3</sub> ) <sub>2</sub>	1:1	2.9 x 10 <sup>3</sup>
		1:2	5.19 x 10 <sup>3</sup>
	Ni(NO <sub>3</sub> ) <sub>2</sub>	1:1	4.64 x 10 <sup>2</sup>
		1:2	2.61 x 10 <sup>3</sup>
(PBI) <sub>3</sub> - (PDA) <sub>3</sub> <b>25</b>	Cu(NO <sub>3</sub> ) <sub>2</sub>	1:1	7.42 x 10 <sup>4</sup>
		1:2	1.34 x 10 <sup>4</sup>
	Ni(NO <sub>3</sub> ) <sub>2</sub>	1:1	1.36 x 10 <sup>4</sup>
		1:2	3.34 x 10 <sup>3</sup>
(PBI-PDA) <sub>3</sub> <b>26</b>	Cu(NO <sub>3</sub> ) <sub>2</sub>	1:1	6.38 x 10 <sup>4</sup>
		1:2	1.58 x 10 <sup>3</sup>
	Ni(NO <sub>3</sub> ) <sub>2</sub>	1:1	7.39 x 10 <sup>4</sup>
		1:2	2.1 x 10 <sup>3</sup>

## Chapter 3

---

(PBI) <sub>3</sub> - (CAT) <sub>3</sub> <b>27</b>	Cu(NO <sub>3</sub> ) <sub>2</sub>	1:1	1.65 x 10 <sup>5</sup>
		1:2	1.45 x 10 <sup>4</sup>
	Ni(NO <sub>3</sub> ) <sub>2</sub>	1:1	6.02 x 10 <sup>4</sup>
		1:2	5.16 x 10 <sup>3</sup>
(PBI-CAT) <sub>3</sub> <b>28</b>	Cu(NO <sub>3</sub> ) <sub>2</sub>	1:1	7.21 x 10 <sup>4</sup>
		1:2	7.87 x 10 <sup>3</sup>
	Ni(NO <sub>3</sub> ) <sub>2</sub>	1:1	7.25 x 10 <sup>4</sup>
		1:2	4.54 x 10 <sup>4</sup>

---

### 3.15.11 Isothermal Titration Calorimetry (ITC)

Isothermal titration calorimetric studies were done on MicroCal iTC200 instrument. Experiments were carried out at 20 °C. The sample cell was filled with monomer/polyamide oligomers (20 μM) in methanol/water, respectively. The metal salts (0.30 mM, 40 μl) were loaded into the syringe. The injection volumes were 1 μl each, injection time, a 120 s delay between each injection and stirring speed 1000 rpm. The integrated peaks of the heat  $q$  have been plotted as a function of molar ratio. With MicroCal origin, binding isotherms have been fitted to a one-site binding or sequential site binding model, giving values of the enthalpy of binding ( $\Delta H_{ITC}$ ), entropy ( $\Delta S_{ITC}$ ) and the binding constant ( $K_{ITC}$ ). The blank corrections were carried out by doing the titrations of the metal salts with the blank water.



### 3.16 References

1. Blackburn, G. M.; Gait, M. J. In *Nucleic acids in Chemistry and Biology*. University Press: Oxford **1990**.
2. Juwarker, H; Suk, J. -M.; Jeong, K. -S. *Chem. Soc. Rev.*, **2009**, 38, 3316.
3. (a) Watson, J. D.; Crick, F. H. C. *Nature* **1953**, 171, 737; (b) Crick, F. H. C. *J. Mol. Biol.* **1966**, 19, 548; (c) Soll, D.; Cherayil, J. D.; Bock, R. M. *J. Mol. Biol.* **1967**, 29, 97.
4. (a) Crooke, S. T. *Therapeutic Applications of Oligonucleotide*. Springer-Verlag: Heidelberg **1995**; (b) Seeman, N. C.; Rosenberg, J. M.; Rich, A. *Proc. Natl. Acad. Sci. USA.* **1976**, 73, 604.
5. (a) Eckstein, F. *Antisense Nucleic Acids Drug Dev.* **2000**, 10, 117; (b) De Clercq, E.; Eckstein, F.; Merigan, T. C. *Science* **1969**, 165, 1137.
6. (a) Kurreck, J.; Wyszko, E.; Gillen, C.; Erdmann, V. A. *Nucleic Acids Res.* **2002**, 30, 1911; (b) Crooke, S. T.; Lemonidis, K. M.; Neilson, L.; Griffey, R.; Lesnik, E. A.; Monia, B. P. *Biochem. J.* **1995**, 312, 599.
7. Gryaznov, S.; Chen, J. K. *J. Am. Chem. Soc.* **1994**, 116, 3143.
8. Damha, M. J.; Wilds, C. J.; Noronha, A.; Bruckner, I.; Borkow, G.; Arion, D.; Parniak, M. A. *J. Am. Chem. Soc.* **1998**, 120, 12976.
9. (a) Braasch, D. A.; Corey, D. R. *Chem. Biol.* **2001**, 8, 1; (b) Orum, H.; Wengel, J. *Curr. Opinion Mol. Ther.* **2001**, 3, 239.
10. Nasevicius, A.; Ekker, S. C. *Nat. Genet.* **2000**, 26, 216.
11. Wang, J.; Verbeure, B.; Luyten, I.; Lescrinier, E.; Froeyen, M.; Hendrix, C.; Rosemeyer, H.; Seela, F.; van Aerschot, A.; Herdewijn, P. *J. Am. Chem. Soc.* **2000**, 122, 8595.
12. (a) Steffens, R.; Leumann, C. J. *J. Am. Chem. Soc.* **1997**, 119, 11548; (b) Renneberg, D.; Leumann, C. J. *J. Am. Chem. Soc.* **2002**, 124, 5993.
13. (a) Nielsen, P. E.; Egholm, M.; Berg, R. H.; Buchardt, O. *Science*, **1991**, 254, 1497; (b) Egholm, M.; Nielsen, P. E.; Buchardt, O.; Berg, R. H. *J. Am. Chem. Soc.* **1992**, 114, 9677; (c) Egholm, M.; Buchardt, O.; Nielsen, P. E.; Berg, R. H. *J. Am. Chem. Soc.* **1992**, 114, 1895; (d) Egholm, M.; Behrens, C.; Christensen, L.; Berg, R. H.; Nielsen, P. E.; Buchardt, O. *J. Chem. Soc. Chem. Commun.* **1993**, 800.

## Chapter 3

---

14. (a) Ganesh, K. N.; Nielsen, P. E. *Curr. Org. Chem.* **2000**, *4*, 931; (b) Kumar, V. A.; Ganesh, K. N. *Acc. Chem. Res.* **2005**, *38*, 404; (c) Kumar, V. A. *Eur. J. Org. Chem.* **2002**, 2021; (d) Kumar, V. A.; Ganesh, K. N. *Curr. Med. Chem.* **2007**, *7*, 715.
15. (a) Hanvey, J. C.; Peffer, N. J.; Bisi, J. E.; Thomson, S. A.; Cadilla, R.; Josey, J. A.; Ricca, D. J.; Hassman, C. F.; Bonham, M. A.; Au, K. G.; Carter, S. G.; Bruckenstein, D. A.; Boyd, A. L.; Noble, S. A.; Babiss, L. E. *Science*, **1992**, *258*, 1481; (b) Knudsen, H.; Nielsen, P. E. *Nucleic Acids Res.* **1996**, *24*, 494 .
16. Nielsen, P. E.; Egholm, M.; Buchardt, O. *Gene*, **1994**, *149*, 139.
17. (a) Gangamani, B. P.; Kumar V. A. *Chem. Commun.* **1997**, 1913; (b) Gangamani, B. P.; Kumar, V. A.; Ganesh, K. N. *Biochem. Biophys. Res. Commun.* **1997**, *240*, 778.
18. Eldrup, A. B.; Dahl, O.; Nielsen, P. E. *J. Am. Chem. Soc.* **1997**, *119*, 11116.
19. (a) Wojciechowski. F.; Hudson. R. H. E. *Cur. Top. Med. Chem.* **2007**, *7*, 667; (b) Bajor, Z.; Sagi, G.; Tegye, Z.; Kraicsovits, F. *Nucleosides & Nucleotides*, **2003**, *22*, 1963; (d) Hudson, R. H. E.; Li, G.; Tse, J. *Tetrahedron Lett.* **2002**, *43*, 1381.
20. Challa, H.; Styers, M. L.; Woski, S. A. *Org. Lett.* **1999**, *1*, 1639.
21. Vysabhattar, R.; Ganesh, K. N. *Tetrahedron Lett.* **2008**, *49*, 1314.
22. (a) Hill, D. J.; Mio, M. J.; Prince, R. B.; Hughes, T. S.; Moore, J. S. *Chem. Rev.*, **2001**, *101*, 3893. (b) Hecht, S.; Huc, I. *Foldamers: Structure, Properties and Applications*, Wiley-VCH, Weinheim, **2007**.
23. Atwood, J. L.; Davies, J. E. D.; MacNicol, D. D.; Vogtle, F.; Lehn, J.-M. *Comprehensive Supramolecular Chemistry*, Ed. Pergamon, New York, 1st edn, **1996**.
24. Nic, M.; Jirat, J.; Kosata, B., Eds. (2006–). "[Cryptand](#)". *IUPAC Compendium of Chemical Terminology* (online Ed.). [doi:10.1351/goldbook.C01426](https://doi.org/10.1351/goldbook.C01426). ISBN 0-9678550-9-8.
25. (a) Petitjean, A.; Cuccia, L. A.; Lehn, J. M.; Nierengarten H.; Schmutz, M. *Angew. Chem. Int. Ed.* **2002**, *41*, 1195; (b) Berl, V.; Huc, I.; Khoury, R. G.; Krische, M. J.; Lehn, J.-M. *Nature*, **2000**, *407*, 720.
26. Stadler, A. -M.; Kyritsakas, N.; Lehn, J.-M. *Chem. Commun.*, **2004**, 2024.
27. Prince, R. B.; Okada, T.; Moore, J. S. *Angew. Chem. Int. Ed.*, **1999**, *38*, 233.

## Chapter 3

---

28. (a) Lee, J. S.; Latimer, L. J. P.; Reid, R. S. *Biochem. Cell. Biol.* **1993**, *71*, 162; (b) Katz, S. *Biochim. Biophys. Acta* **1963**, *68*, 240; (c) Kuklennyik, Z.; Marzilli, L. G. *Inorg. Chem.* **1996**, *35*, 5654.
29. (a) Molecules, H. A.; Hiraoka, S.; Harano, K.; Nakamura, T.; Shiro, M.; Shionoya, M. *Angew. Chem. Int. Ed.* **2009**, *48*, 7006; (b) Clever, G. H.; Tashiro, S.; Shionoya, M. *Angew. Chem. Int. Ed.* **2009**, *48*, 7010; (c) Hiraoka, S.; Hirata, K.; Shionoya, M. *Angew. Chem. Int. Ed.* **2004**, *43*, 3814. (d) Shionoya, M.; Tanaka, K. *Bull. Chem. Soc. Jpn.* **2000**, *73*, 1945; (e) Hatano, A.; Tanaka, K.; Shiro, M.; Shionoya, M. *Chem. Lett.* **2000**, *70*, 822; (f) Tanaka, K.; Shionoya, M. *Chem. Lett.* **2006**, *35*, 694; (g) Tanaka, K.; Shionoya, M. *Coord. Chem. Rev.* **2007**, *251*, 2732; (g) Tanaka, K.; Tasaka, M.; Cao, H.; Shionoya, M. *Eur. J. Pharma. Sci.* **2001**, *13*, 77; (h) Tanaka, K.; Tengeiji, A.; Kato, T.; Toyama, N.; Shiro, M.; Shionoya, M. *J. Am. Chem. Soc.* **2002**, *124*, 12494; (i) Tanaka, K.; Yamada, Y.; Shionoya, M. *J. Am. Chem. Soc.* **2002**, *124*, 8802; (j) Hiraoka, S.; Shiro, M.; Shionoya, M. *J. Am. Chem. Soc.* **2004**, *126*, 1214; (k) Takezawa, Y.; Tanaka, K.; Yori, M.; Tashiro, S.; Shiro, M.; Shionoya, M. *J. Org. Chem.* **2008**, *73*, 6092; (l) Tanaka, K.; Clever, G. H.; Takezawa, Y.; Yamada, Y.; Kaul, C.; Shionoya, M.; Carell, T. *Nat. Nano.* **2006**, *1*, 190.
30. (a) Haaima, G.; Hansen, H. F.; Christensen, L.; Dahl, O.; Nielsen, P. E. *Nucleic Acids Res.* **1997**, *25*, 4639; (b) Egholm, M.; Christensen, L.; Deuholm, K. L.; Buchardt, O.; Coull, J.; Nielsen, P. E. *Nucleic Acids Res.* **1995**, *23*, 217.
31. Noor, F.; Wustholz, A.; Kinscherf, R.; Metzler-Nolte, N. *Angew. Chem. Int. Ed.* **2005**, *44*, 2429.
32. Ferri, E.; Donghi, D.; Panigati, M.; Prencipe, G.; Alfonso, L. D.; Zanoni, I.; Baldoli, C.; Maiorana, S.; Alfonso, G. D.; Licandro, E. *Chem. Commun.*, **2010**, *46*, 6255.
33. Watson, R. M.; Skorik, Y. A.; Patra, G. K.; Achim, C. *J. Am. Chem. Soc.* **2005**, *127*, 14628.
34. Popescu, D.; Parolin, T. J.; Achim, C. *J. Am. Chem. Soc.* **2003**, *125*, 6354.
35. (a) Ohr, K.; Mclaughlin, R. L.; Williams, M. E. *Inorg. Chem.* **2007**, *46*, 965; (b) Myers, C. P.; Gilmartin, B. P.; Williams, M. E. *Inorg. Chem.* **2008**, *47*, 6738; (c) Coppock, M. B.; Kapelewski, M. T.; Youm, H. W.; Levine, L. A.; Miller, J. R.; Myers, C. P.; Williams, M. E. *Inorg. Chem.* **2010**, *49*, 5126; (d) Coppock, M. B.; Kapelewski, M. T.; Youm, H. W.; Levine, L. A.; Miller, J. R.; Myers, C. P.;

## Chapter 3

---

- Williams, M. E. *Inorg. Chem.* **2010**, *49*, 5126; (e) Coppock, M. B.; Miller, J. R.; Williams, M. E. *Inorg. Chem.* **2011**, *50*, 949; (f) Myers, C. P.; Miller, J. R.; Williams, M. E. *J. Am. Chem. Soc.* **2009**, *131*, 15291; (g) De Leon, A. R.; Olatunde, A. O., Morrow, J. R.; Achim, C. *Inorg. Chem.* **2012**, *51*, 12597.
36. Gasser, G.; Hüskén, N.; Köster, S. D.; Metzler-Nolte, N. *Chem. Commun.*, **2008**, *45*, 3675.
37. (a) Baldoli, C.; Maiorana, S.; Licandro, E.; Zinzalla G.; Perdicchia, D. *Org. Lett.*, **2002**, *4*, 4341; (b) Baldoli, C.; Giannini, C.; Licandro, E.; Maiorana S.; Zinzalla, G. *Synlett*, **2004**, 1044; (c) Noor, F.; Wüstholtz, A.; Kinscherf. R.; M. - N., N. *Angew. Chem., Int. Ed.*, **2005**, *44*, 2429; (d) Gasser, G.; Neukamm, M. A.; Ewers, A.; Brosch, O.; Weyhermüller, T.; Metzler-Nolte, N. *Inorg. Chem.*, **2009**, *48*, 3157.
38. Baldoli, C.; Cerea, P.; Giannini, C.; Licandro, E.; Rigamonti, C.; Maiorana, S. *Synlett.*, **2005**, *13*, 1984.
39. Nickita, N.; Gasser, G.; Bond, A. M.; Spiccia, L. *Eur. J. Inorg. Chem.*, **2009**, 2179.
40. Frederickson, C. J. *Int. Rev. Neurobiol.*, **1989**, *31*, 145; (b) Zalewski, P.D.; Millard, S. H.; Forbes, I. J.; Kapaniris, O.; Slavotinek, A.; Betts, W. H.; Ward, A. D.; Lincoln, S. F.; Mahadevan, I. *J. Histochem. Cytochem.*, **1994**, *42*, 877; (c) Zalewski, P. D.; Jian, X.; Soon, L. L.; Breed, W. G.; Seamark, R. F.; Lincoln, S. F.; Ward, A. D.; Sun, F. Z. *Reprod. Fertil. Dev.*, **1996**, *8*, 1097; (d) Margalioth, E. J.; Schenker, J. G.; Chevion, M. *Cancer Biology & Therapy*, **1983**, *52*, 868.
41. Mokhir, A.; Kra, R.; Wolf, H. *J. Am. Chem. Soc.* **2004**, *126*, 6208.
42. Füssl, A.; Schleifenbaum, A.; Göritz, M.; Riddell, A.; Schultz, C.; Kraemer, R. *J. Am. Chem. Soc.*, **2006**, *128*, 5986.
43. Erickson, B. W.; Merrifield, R. B. *Solid phase Peptide Synthesis Vol. II*, 3<sup>rd</sup> ed.; Neurath, H. and Hill, R. L. eds.; Academic Press, New York, **1976**, pp 255.
44. Merrifield, R. B. *J. Am. Chem. Soc.* **1963**, *85*, 2149.
45. Anderson, G. W.; McGreoger, A. C. *J. Am. Chem. Soc.* **1957**, *79*, 6180.
46. (a) Thomson, S. A.; Josey, J. A.; Cadilla, R.; Gaul, M. D.; Hassman, C. F.; Luzzio, M. J. *Tetrahedron*, **1995**, *51*, 6179; (b) Goodnow, R. A.; Jr. Richou, A-R.; Tam, S. *Tetrahedron Lett.* **1997**, *38*, 3195.

## Chapter 3

---

47. (a) Kaiser, E.; Colescott, R. L.; Bossinger, C. D.; Cook, P. I. *Anal. Biochem.* **1970**, *34*, 595; (b) Kaiser, E.; Bossinger, C. D.; Cplescott, R. L.; Olsen, D. B. *Anal. Chim. Acta.* **1980**, *118*, 149.
48. Gel Filtration; Principles and Methods, Amersham Biosciences
49. Edmond de Hoffman; Vincent Stroobant (2001). *Mass Spectrometry: Principles and Applications* (2nd ed.). John Wiley and Sons. ISBN 0-471-48566-7.
50. Beavis R. C.; Chait B. T. *Rapid Commun. Mass Spectrom.* **1989**, *3*, 436.
51. Beavis, R. C. *Org. Mass Spectrom.* **1992**, *27*, 156.
52. Sheldrick, G. M. *Acta Crystallogr.* **2008**, *A64*, 112.
53. (a) Perrin, D.D., *Dissociation Constants of Organic Bases in Aqueous Solution*, Butterworths, London, 1965; Supplement, 1972; (b) Serjeant, E.P., and Dempsey, B., *Ionization Constants of Organic Acids in Aqueous Solution*, Pergamon, Oxford, 1979; (c) Perrin, D.D., Dempsey, B., and Serjeant, E.P., *pKa Prediction for Organic Acids and Bases*, Chapman and Hall, London, 1981; (d) Albert, A., and Serjeant, E. P., *The Determination of Ionization Constants, Third Edition*, Chapman and Hall, London, 1984.
54. (a) Bloomfield, V. A.; Crothers, D.; Tinoco, I. *Physical Chemistry of the Nucleic Acids*. Harper and Row: New York, **1974**. (b) Freeman, W. H. *The behavior of biological macromolecules* (Cantor and Schimmel, San Francisco, **1980**, pp. 624.
55. (a) Job, P. *Ann. Chim.* **1928**, *9*, 113; (b) Cantor, C. R.; Schimmel, P. R.; *Biophys. Chem. Part III*, **1980**, 624.
56. (a) Benesi, H. A.; Hildebrand, J. H. *J. Am. Chem. Soc.* **1949**, *71*, 2703; (b) Nigam, S.; Durocher, G. *J. Phys. Chem.* **1996**, *100*, 7135.
57. (a) Haq, I.; Jenkins, T. C.; Chowdhry, B. Z.; Ren, J.; Chaires, J. B. *Meth. Enzymol.* **2000**, *323*, 373; (b) Cooper, A. *Curr. Opin. Chem. Biol.* **1999**, *3*, 557.
58. Du, L.-H.; Wa, Y.-G. *Synthesis* **2007**, *5*, 0675.
59. (a) Egholm, M.; Buchart, O.; Nielsen, P.E. *J. Am. Chem. Soc.* **1992**, *114*, 1895; (b) Egholm, M.; Nielsen, P. E.; Buchardt, O. Berg, R. H. *J. Am. Chem. Soc.* **1992**, *114*, 9677; (c) Dueholm, K. L.; Egholm, M.; Behrens, C.; Christensen, L.; Hansen, H. F.; Vulpius, T.; Petersen, K. H.; Berg, R. H.; Nielsen, P. E.; Buchardt, O. *J. Org. Chem.* **1994**, *59*, 5767.
60. Cao, H.; Tanaka, K.; Shionoya, M. *Chem. Pharm. Bull.* **2000**, *48*, 1745.
61. (a) Tanaka, K.; Cao, H.; Shionoya, M. *Nucleic Acids Symp. Ser.* **1998**, *39*, 171; (b) Tanaka, K.; Shionoya, M. *J. Org. Chem.* **1999**, *64*, 5002.

## Chapter 3

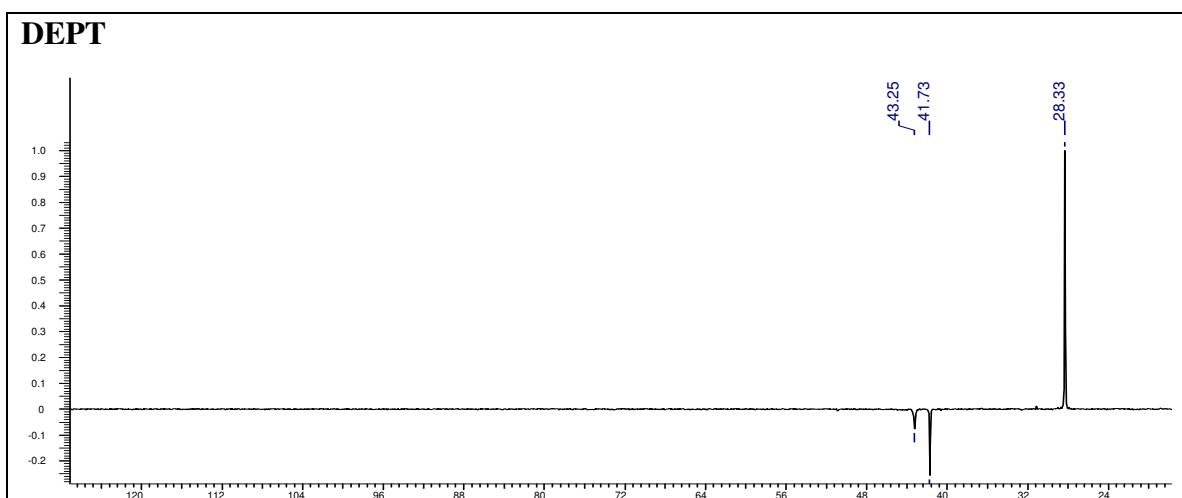
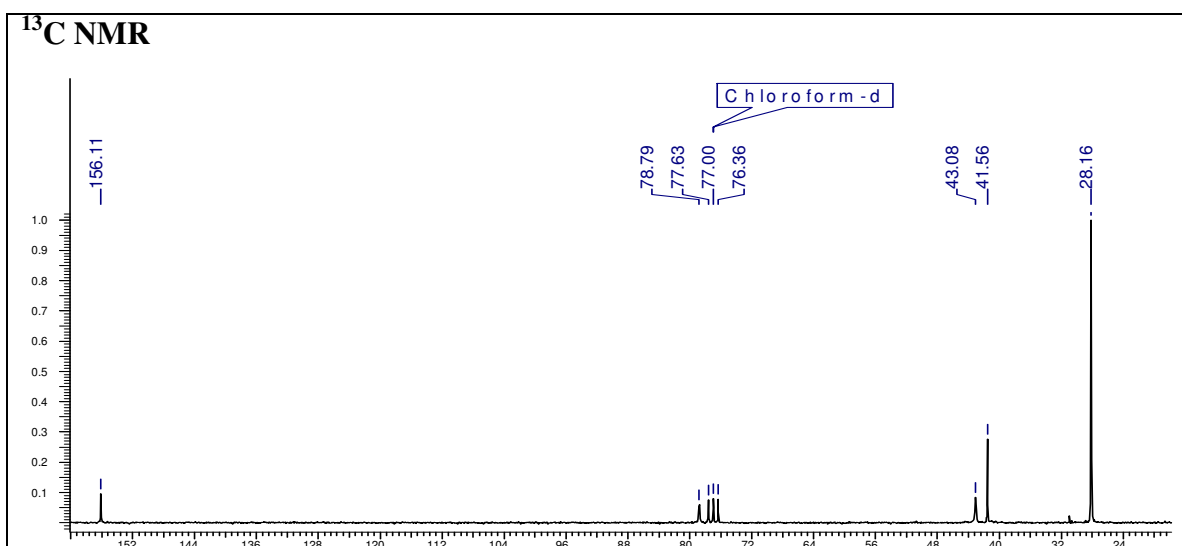
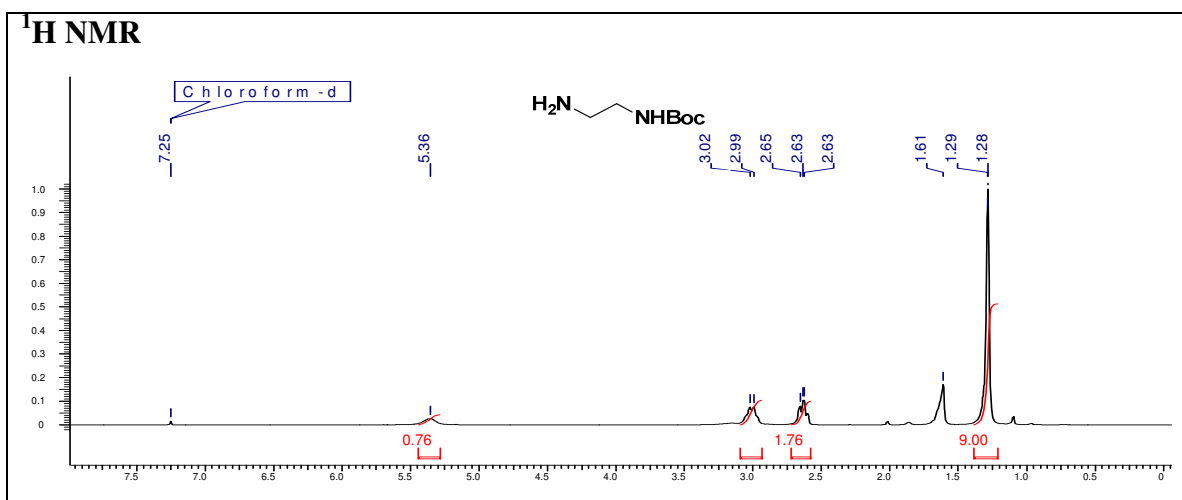
---

62. Yoo, J.; Kim, M. -S.; Hong, S. -J.; Sessler, J. L.; Lee, C. -H. *J. Org. Chem.* **2009**, *74*, 1065.
63. Tanaka, K.; Tasaka, M.; Cao, H.; Shionoya, M. *Supramol. Chem.* **2002**, *14*, 255.
64. Franzini, R. M.; Watson, R. M.; Patra, G. K.; Breece, R. M.; Tierney, D. L.; Hendrich, M. P.; Achim, C. *Inorg. Chem.*, **2006**, *45*, 9798.

## 3.16 Appendix F: Characterization data of synthesized compounds

Compound	Description	Page No.
Compound 5	<sup>1</sup> H NMR, <sup>13</sup> C NMR, DEPT-NMR	359
Compound 6	<sup>1</sup> H NMR, <sup>13</sup> C NMR, DEPT-NMR, FT-IR, MALDI-MS	360-361
Compound 7	<sup>1</sup> H NMR, <sup>13</sup> C NMR, DEPT-NMR, FT-IR, MALDI-MS	362-363
Compound 8	<sup>1</sup> H NMR, <sup>13</sup> C NMR, DEPT-NMR, FT-IR, HR-MS	364-365
Compound 1	<sup>1</sup> H NMR, <sup>13</sup> C NMR, DEPT-NMR, FT-IR, HR-MS	366-367
Compound 12	<sup>1</sup> H NMR, <sup>13</sup> C NMR, DEPT-NMR, FT-IR, HR-MS	368-369
Compound 13	HR-MS	370
Compound 15	<sup>1</sup> H NMR, <sup>13</sup> C NMR, DEPT-NMR	371
Compound 3	<sup>1</sup> H NMR, <sup>13</sup> C NMR, DEPT-NMR	372
Compound 16	<sup>1</sup> H NMR, <sup>13</sup> C NMR, DEPT-NMR, FT-IR, HR-MS	373-374
Compound 17	<sup>1</sup> H NMR, <sup>13</sup> C NMR, DEPT-NMR, FT-IR, HR-MS	375-376
Compound 18	<sup>1</sup> H NMR, <sup>13</sup> C NMR, DEPT-NMR, FT-IR, HR-MS	377-378
Compound 19	<sup>1</sup> H NMR, <sup>13</sup> C NMR, DEPT-NMR, FT-IR, HR-MS	379-380
Compound 21	<sup>1</sup> H NMR, <sup>13</sup> C NMR, DEPT-NMR, FT-IR, HR-MS	381-382
Polyamide oligomers	HPLC and MALDI-TOF spectra	383-384
Compound 8	UV-Vis spectra	385
Compound 17	UV-Vis spectra	386
Polyamide oligomers 22	UV-Vis spectra	387-390
Polyamide oligomers 25	UV-Vis spectra	390-391
Polyamide oligomers	ITC Figures	392-393

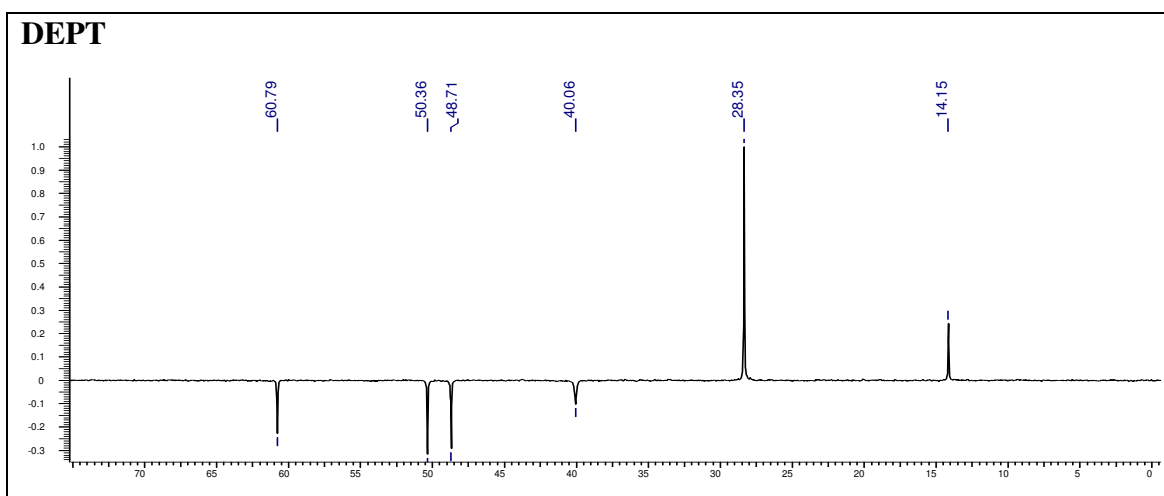
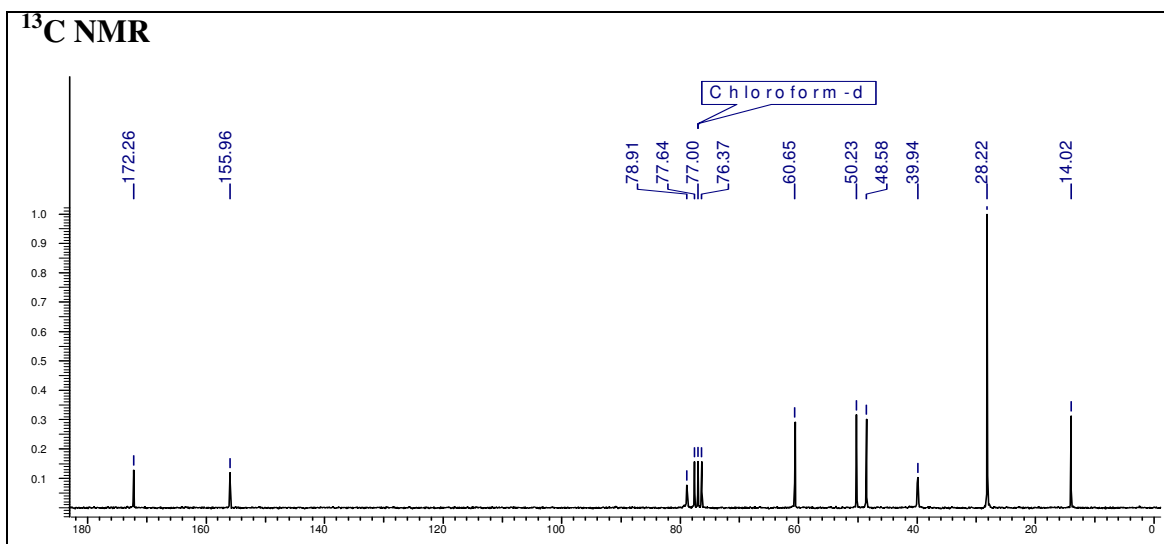
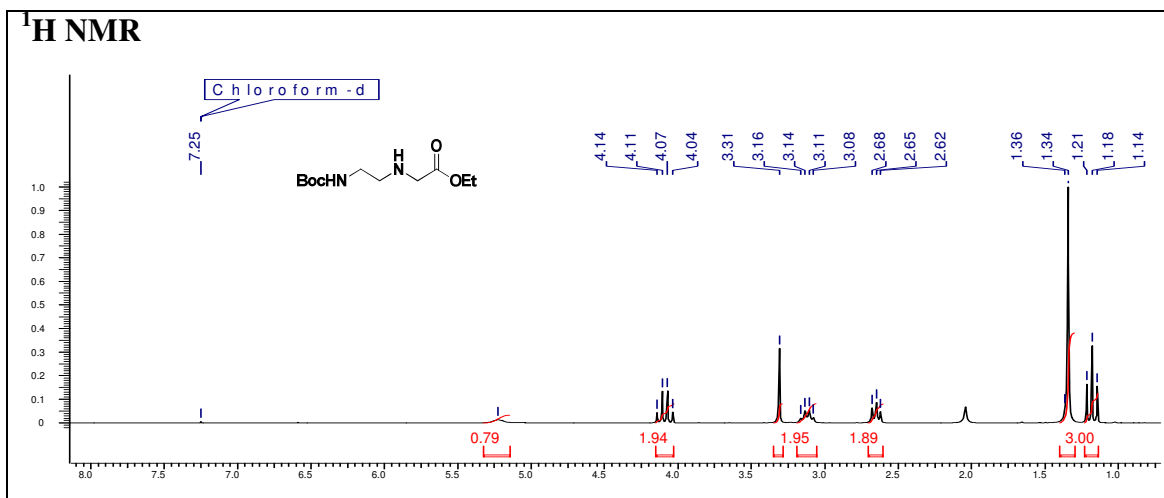
# Chapter 3



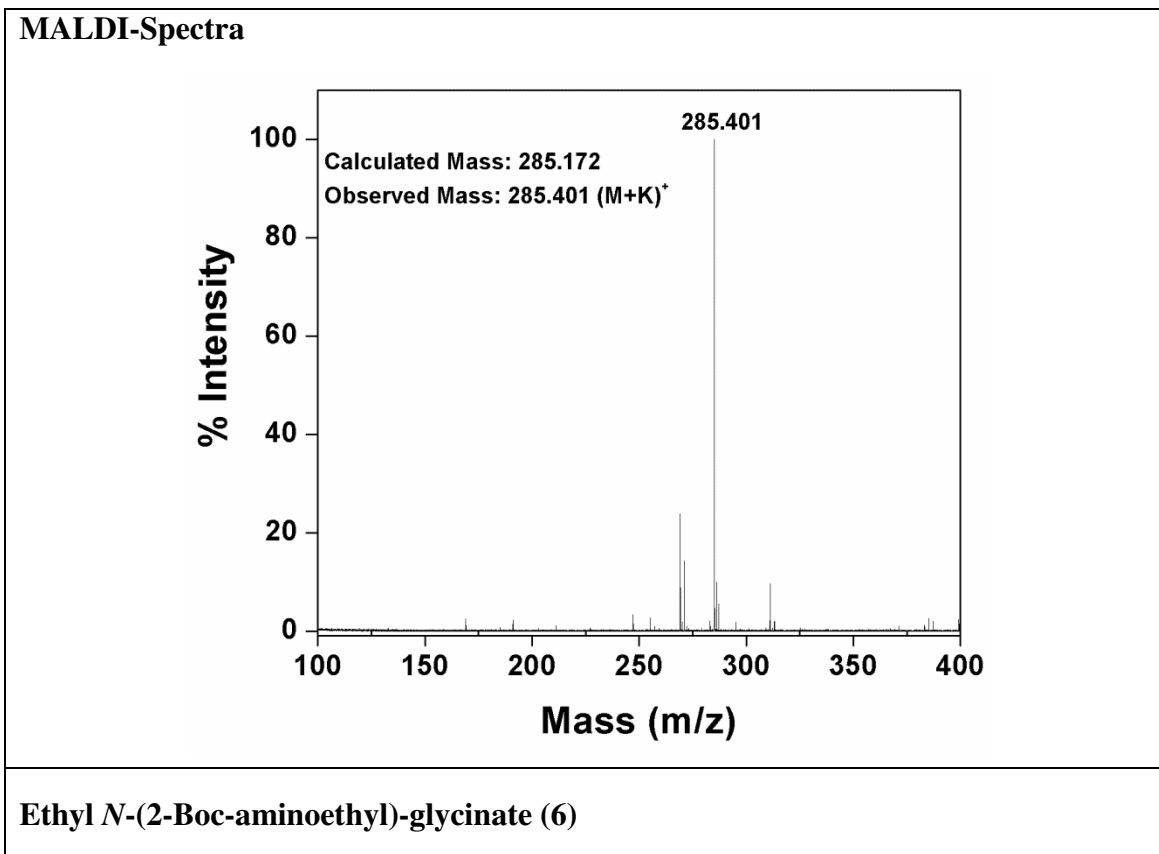
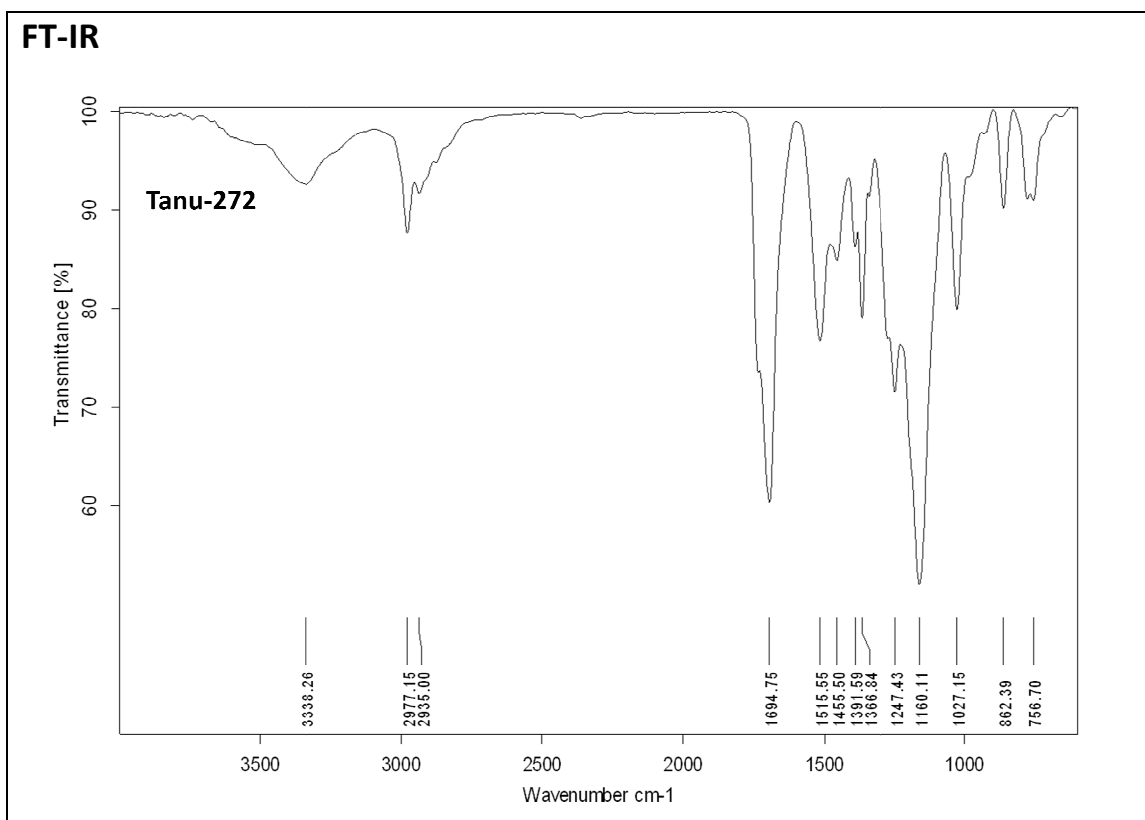
***tert*-butyl (2-aminoethyl)carbamate (5)**



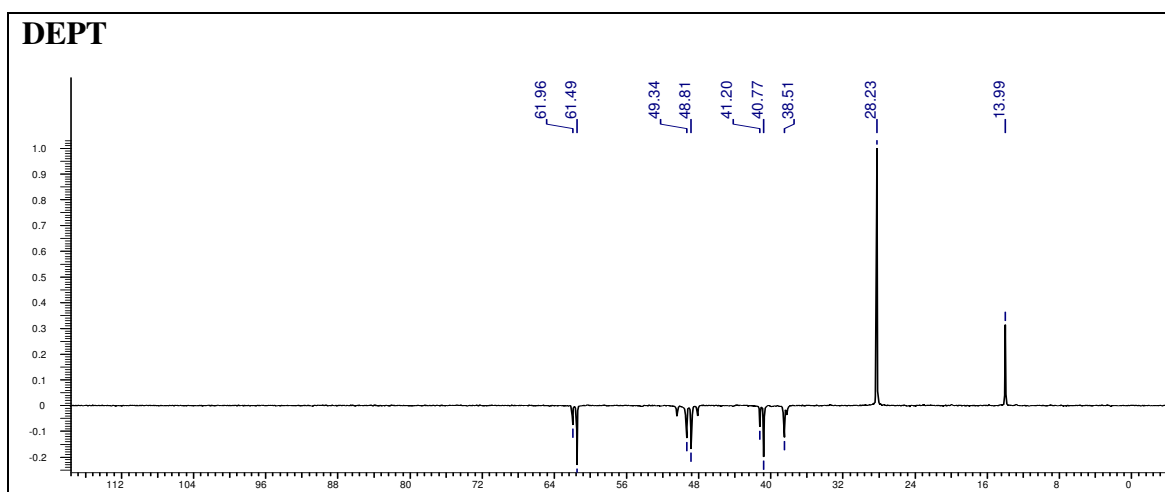
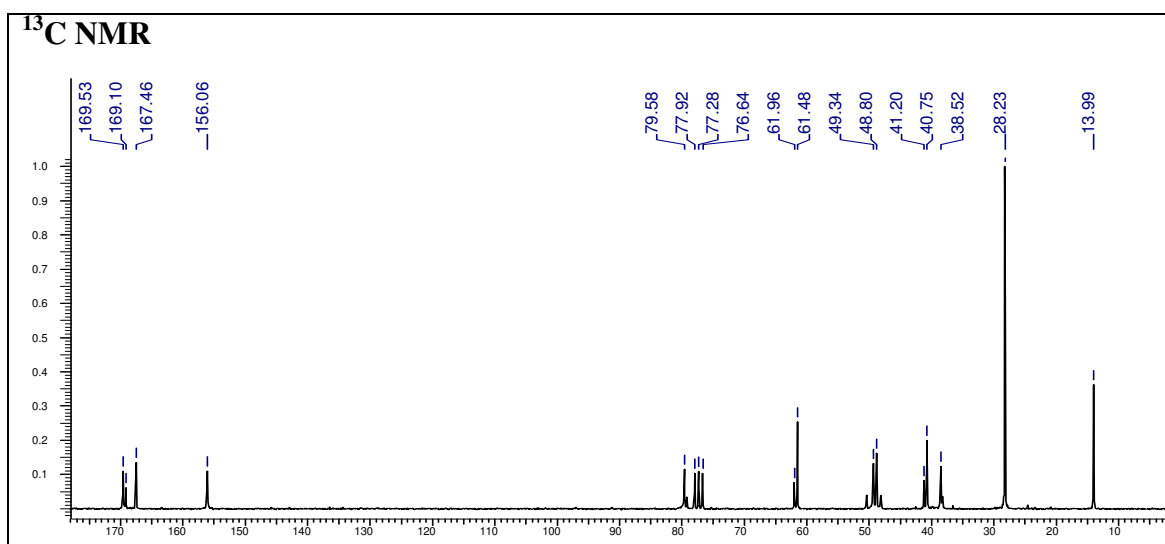
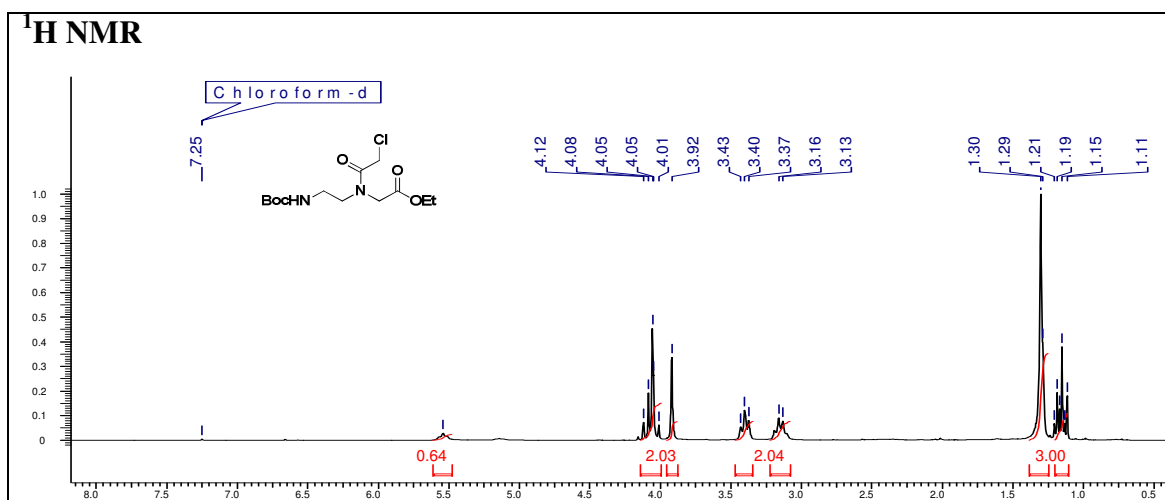
# Chapter 3



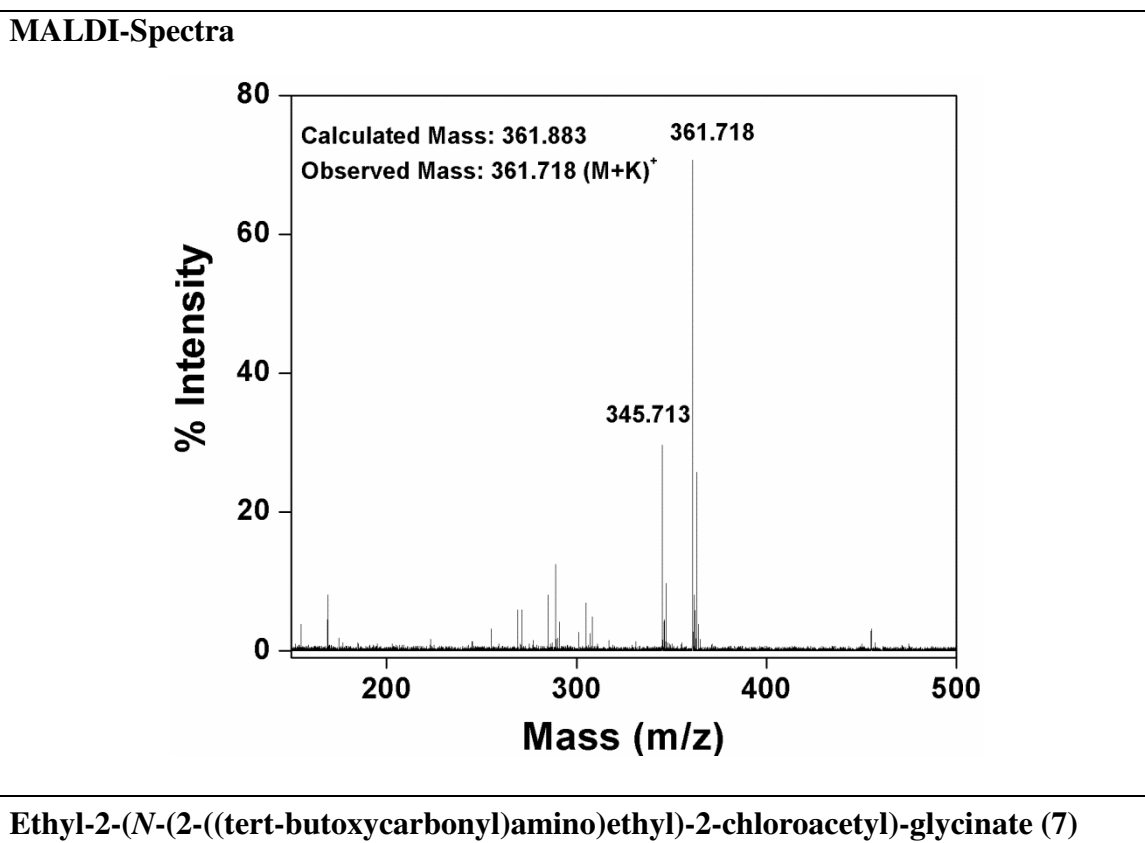
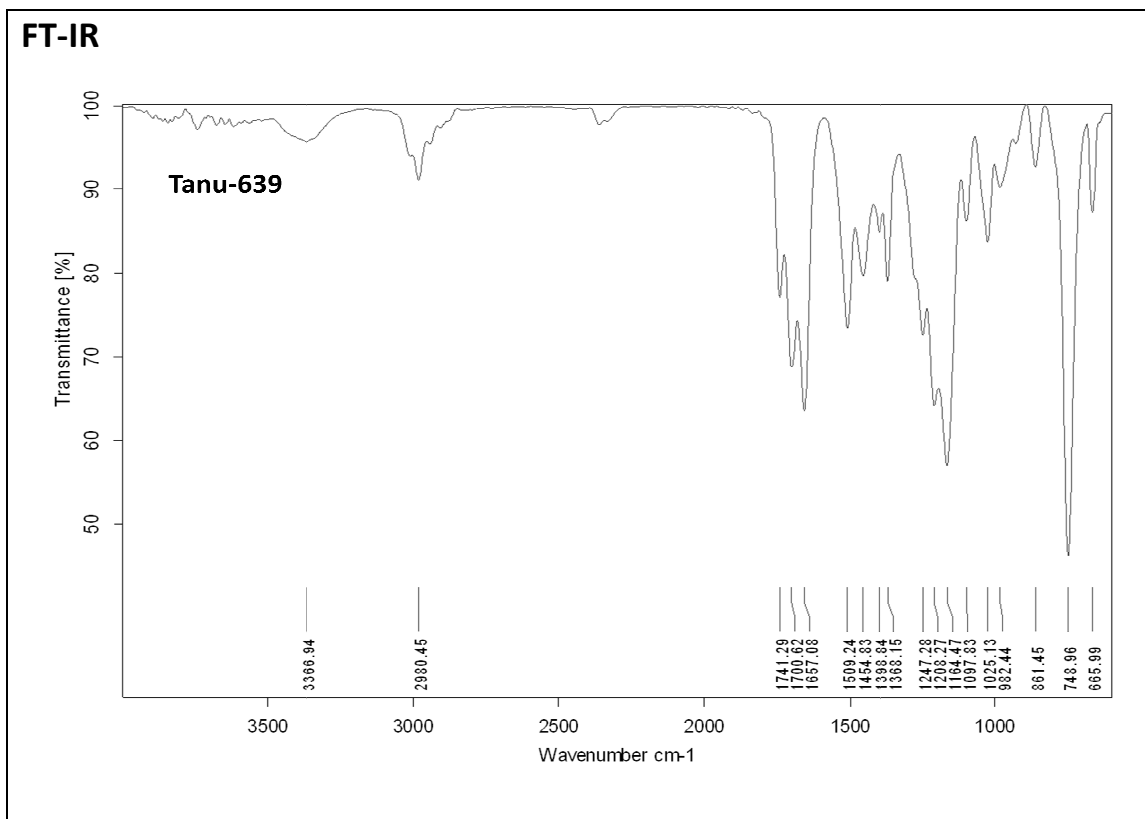
**Ethyl N-(2-Boc-aminoethyl)-glycinate (6)**



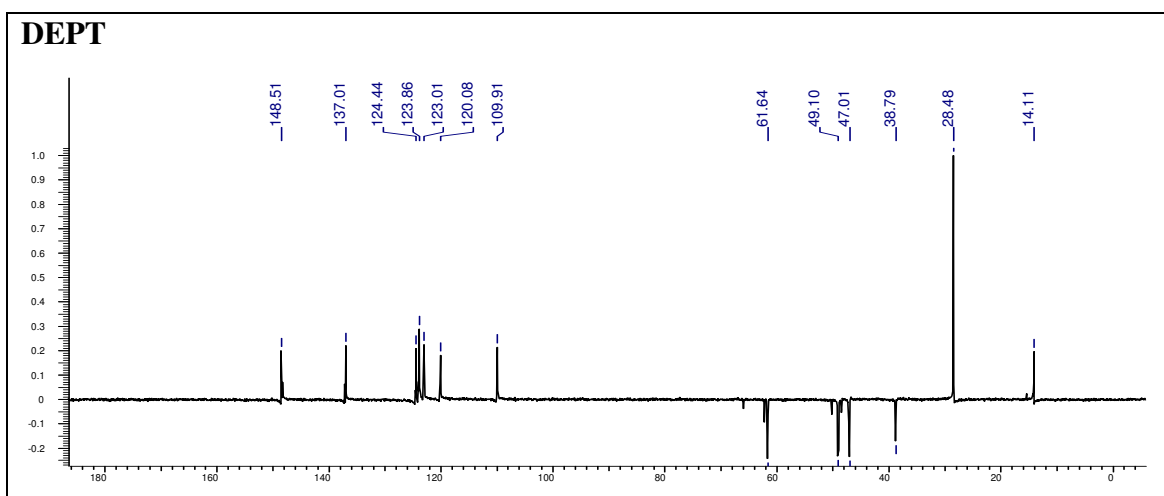
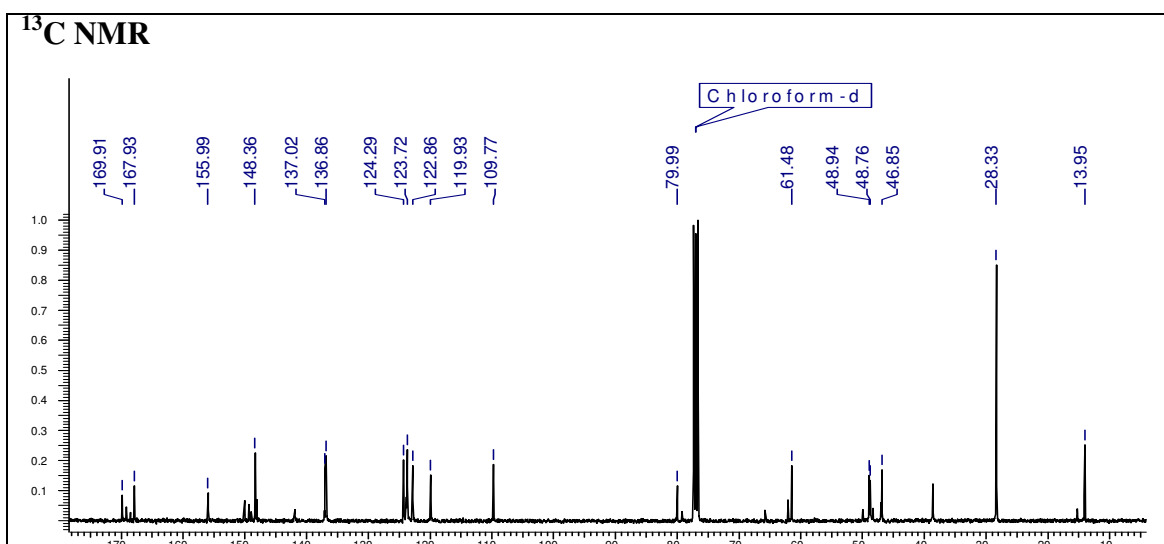
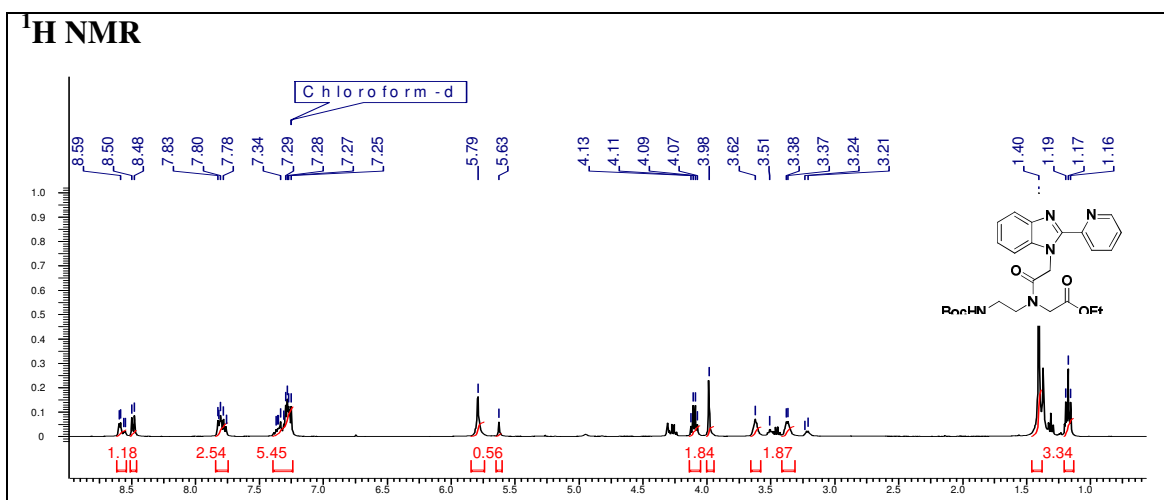
# Chapter 3



**Ethyl 2-(N-(2-((tert-butoxycarbonyl)amino)ethyl)-2-chloroacetyl)-glycinate (7)**

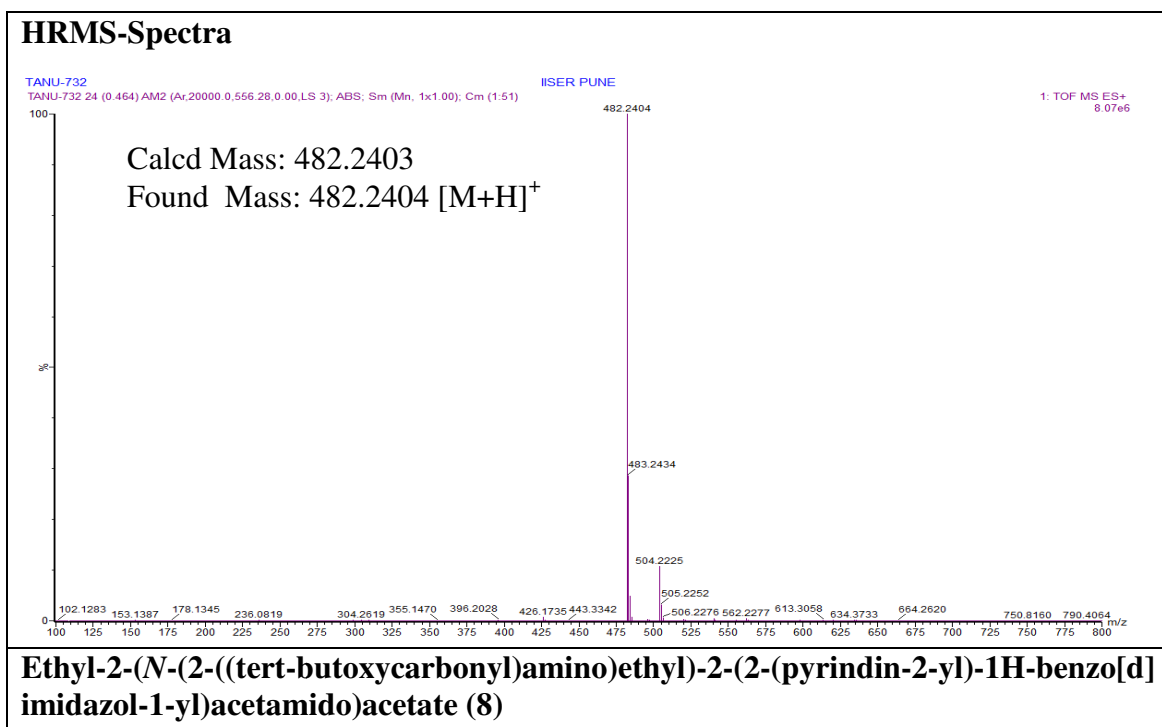
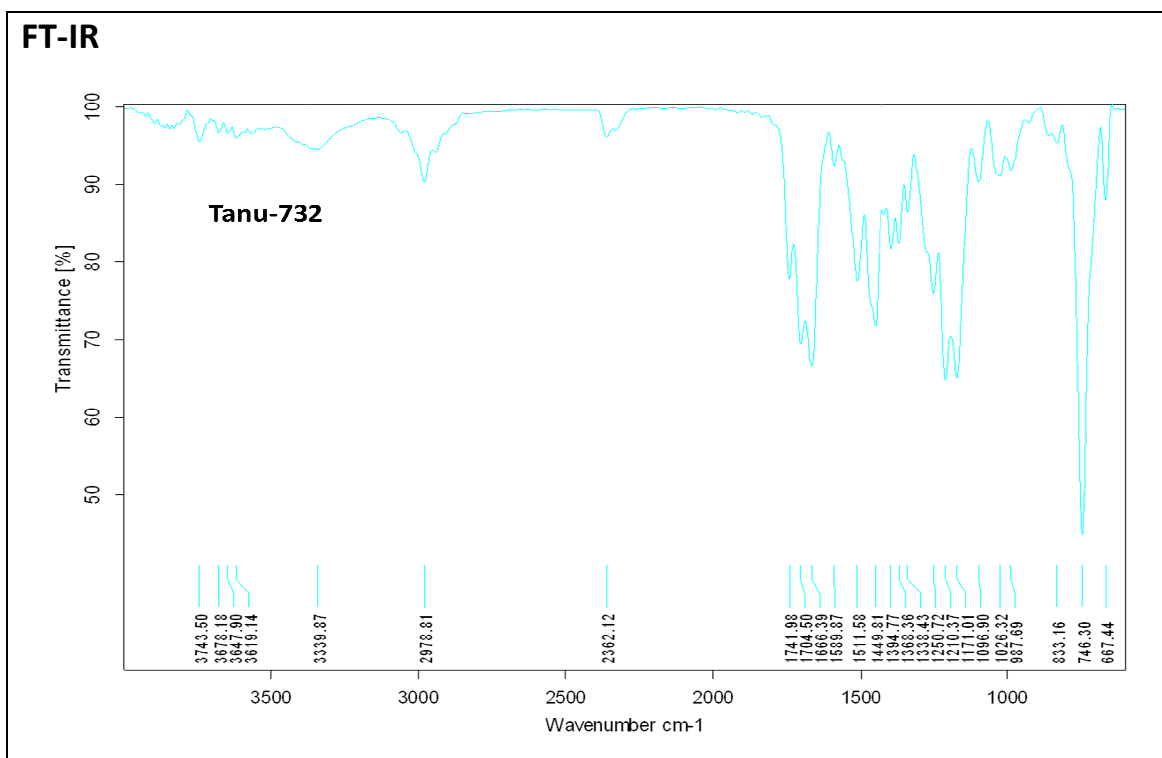


# Chapter 3

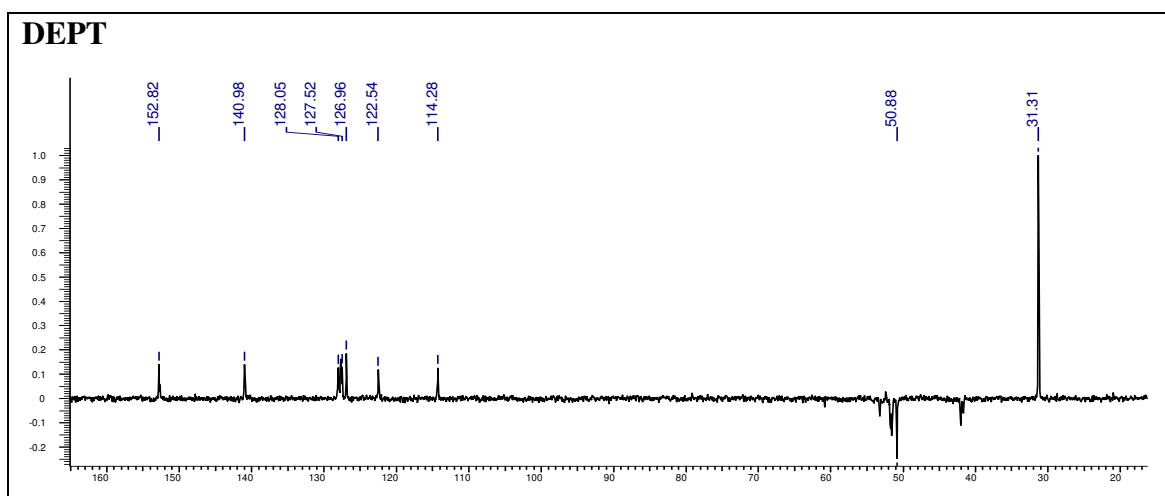
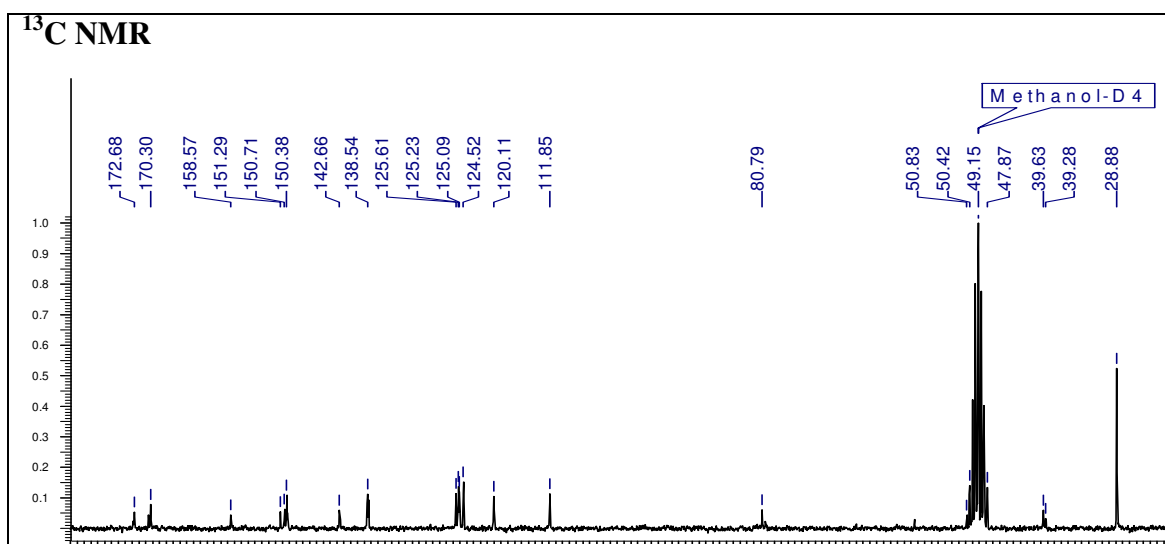
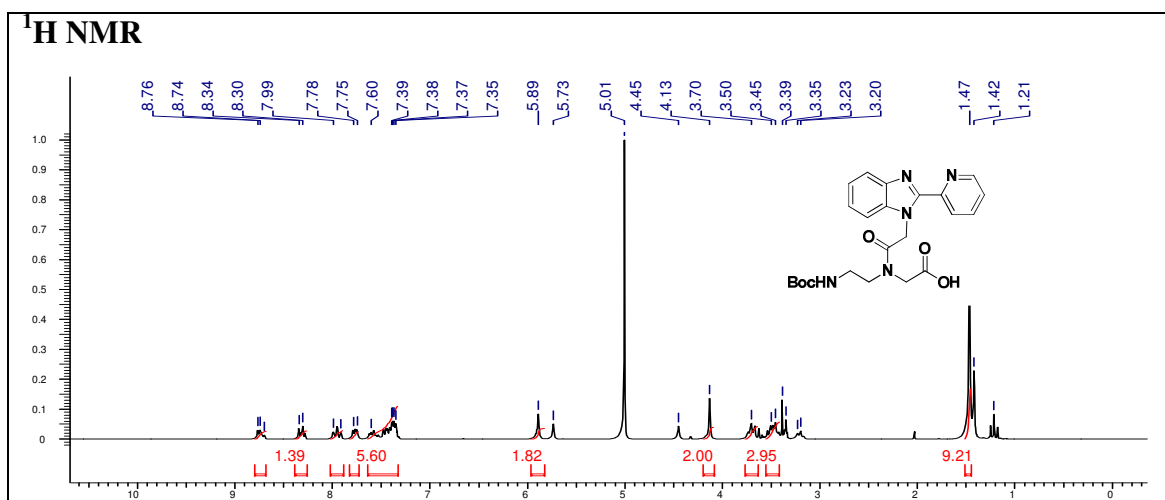


**Ethyl 2-(N-(2-((tert-butoxycarbonyl)amino)ethyl)-2-(2-(pyridin-2-yl)-1H-benzo[d]imidazol-1-yl)acetamido)acetate (8)**

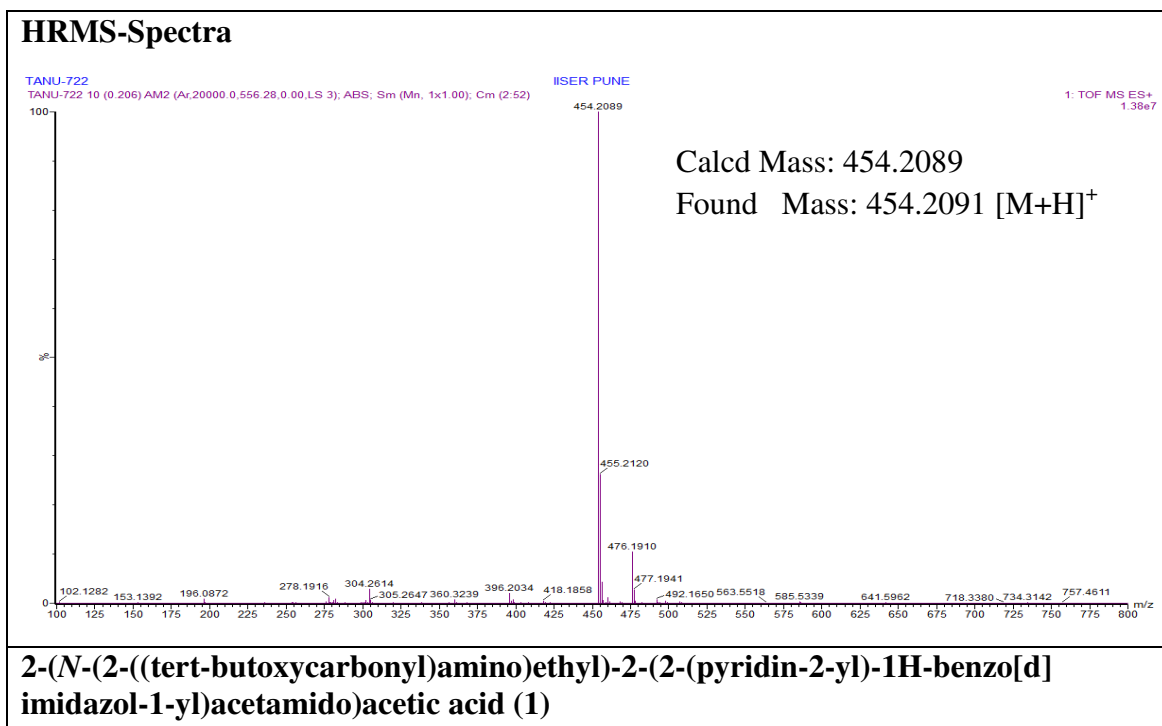
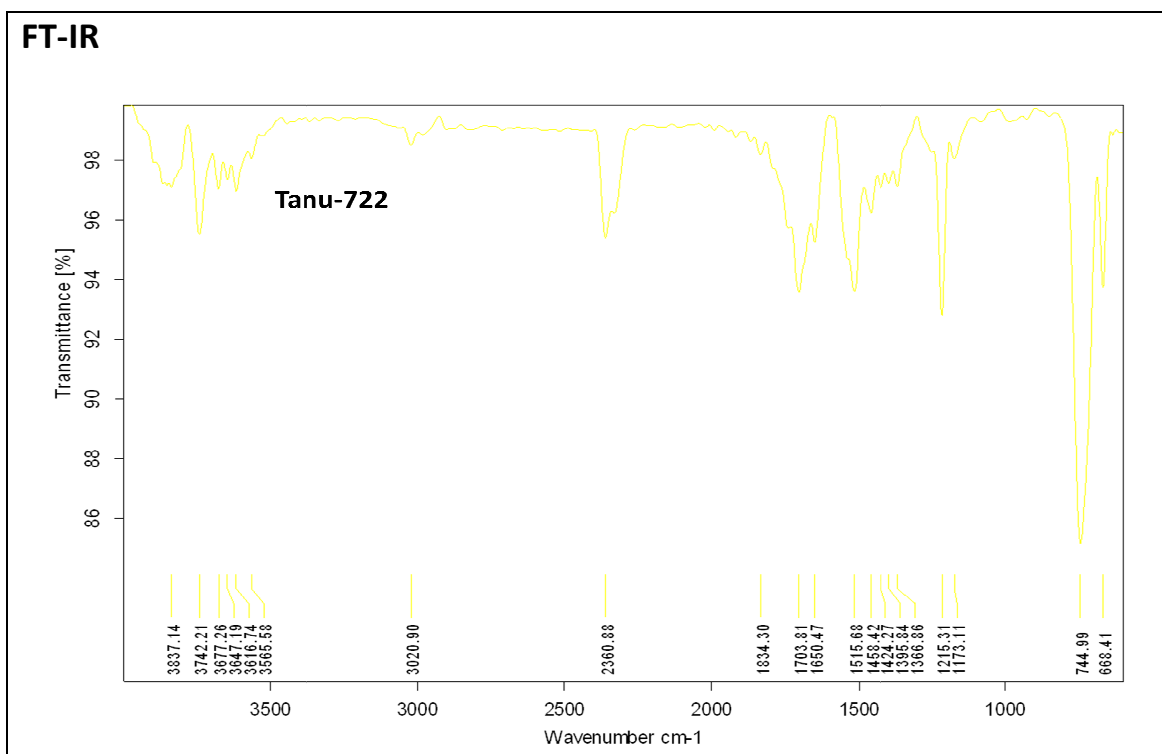
# Chapter 3



# Chapter 3

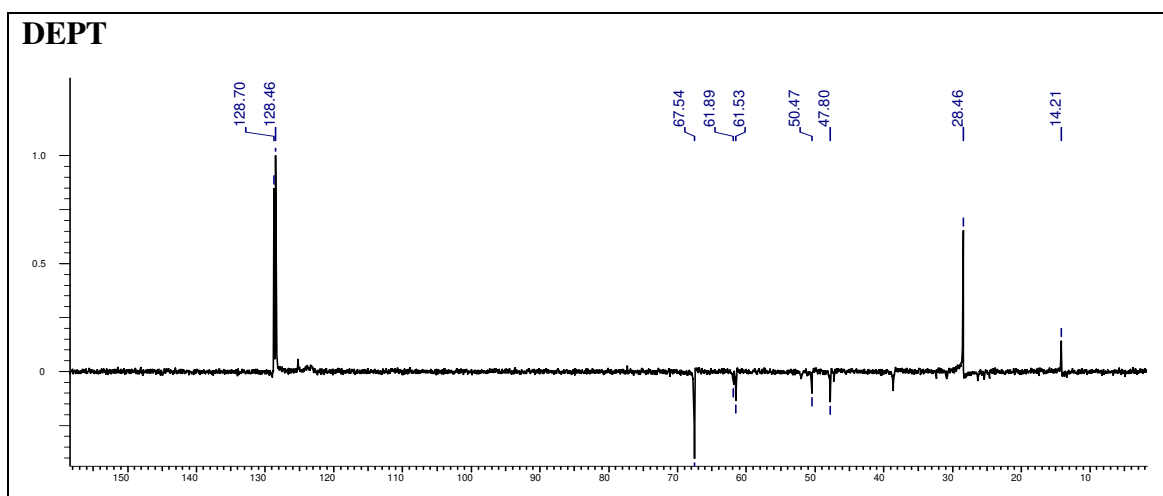
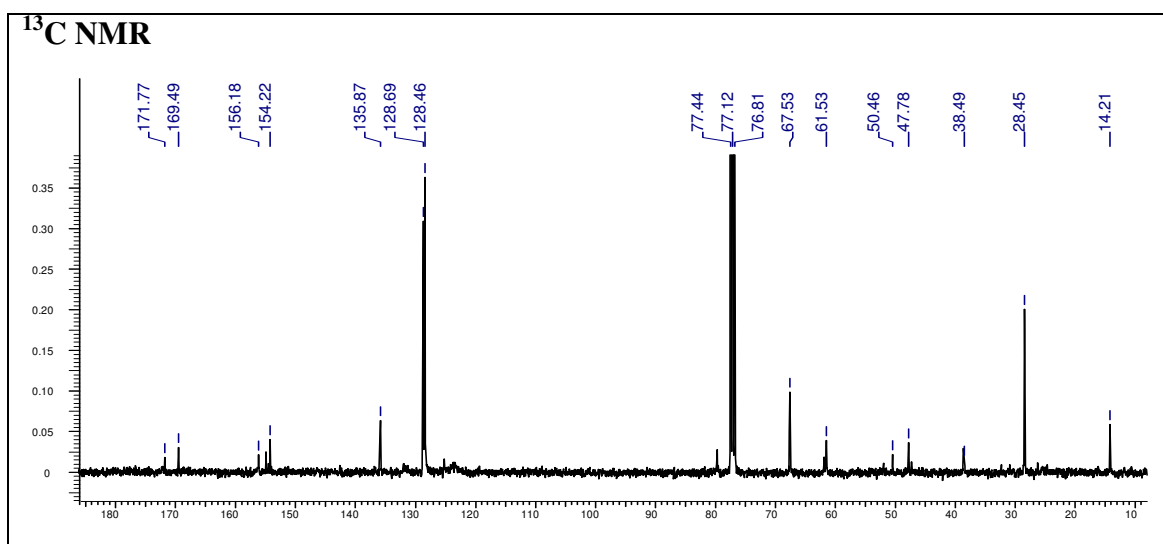
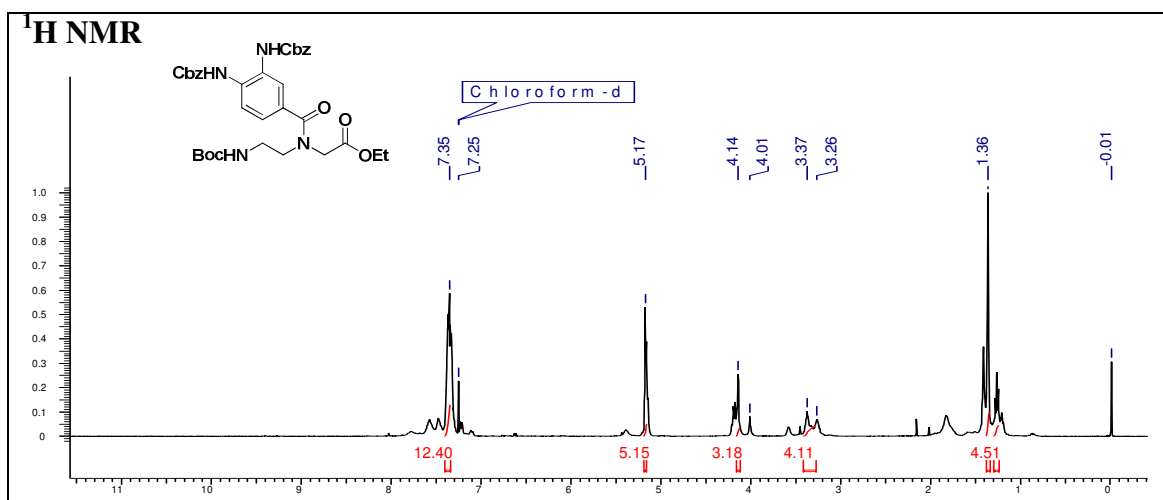


**2-(N-(2-((tert-butoxycarbonyl)amino)ethyl)-2-(2-(pyridin-2-yl)-1H-benzo[d]imidazol-1-yl)acetamido)acetic acid (1)**

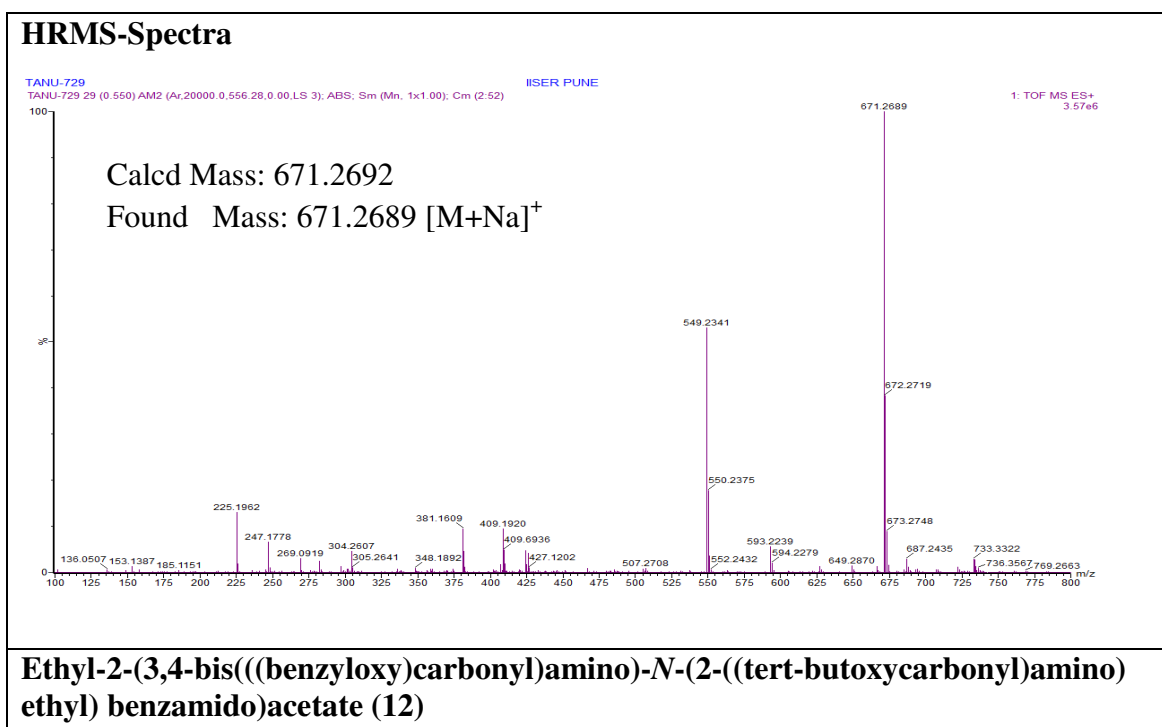
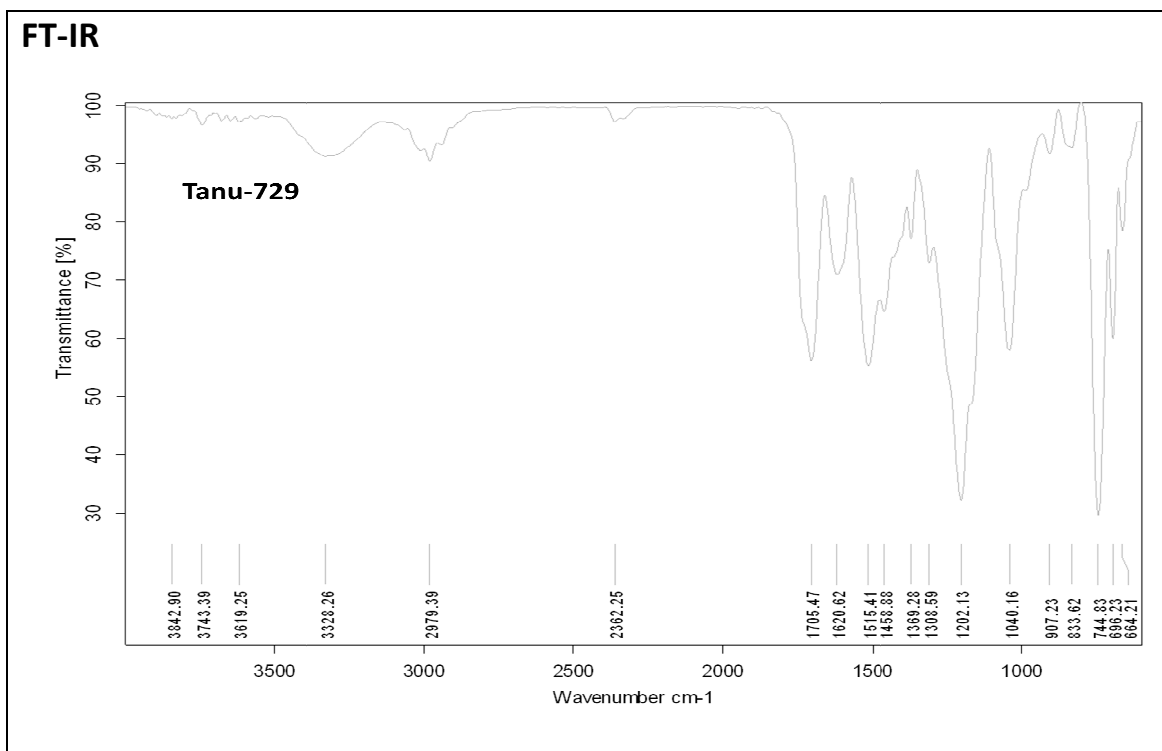




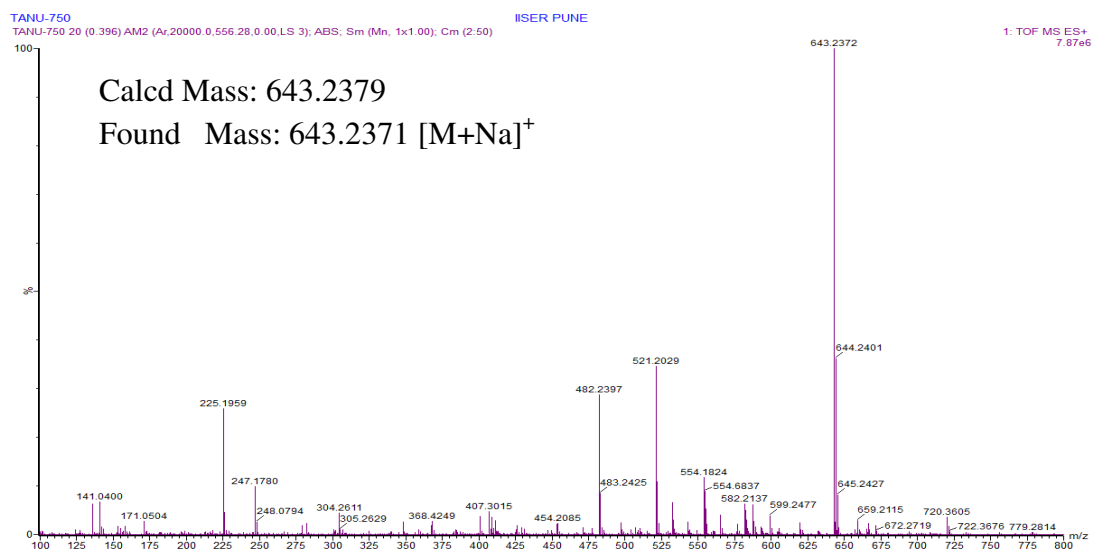
# Chapter 3



**Ethyl-2-(3,4-bis(((benzyloxy)carbonyl)amino)-N-(2-((tert-butoxycarbonyl)amino)ethyl)benzamido)acetate (12)**

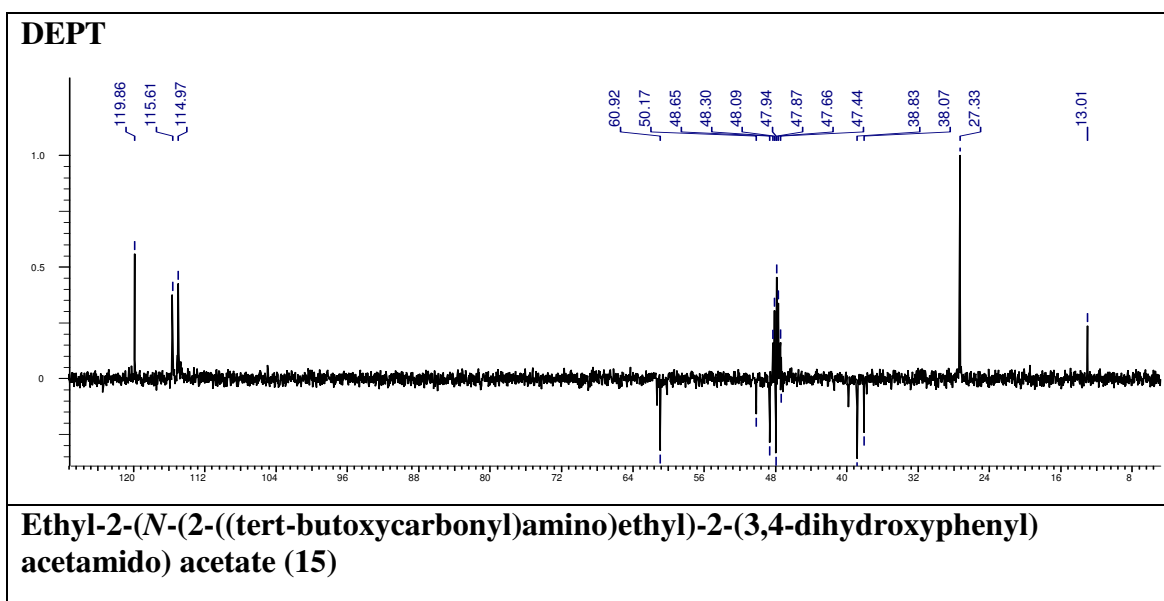
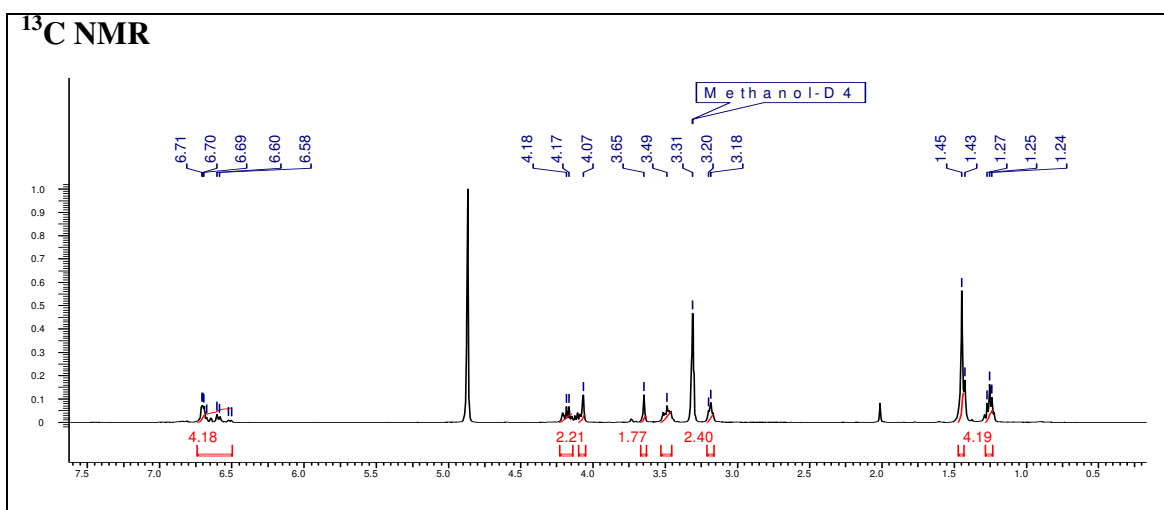
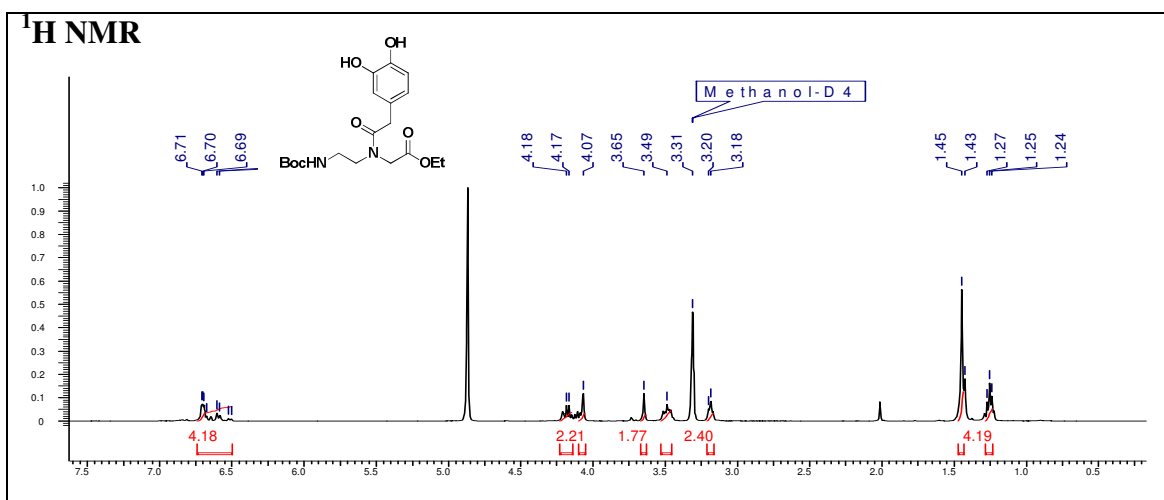


## HRMS-Spectra

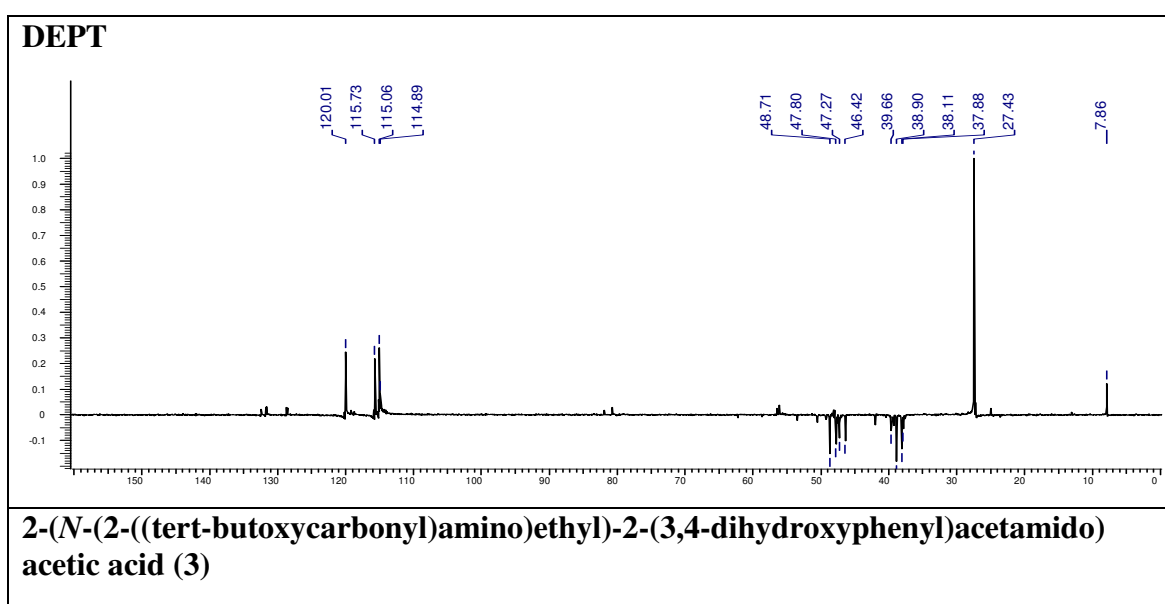
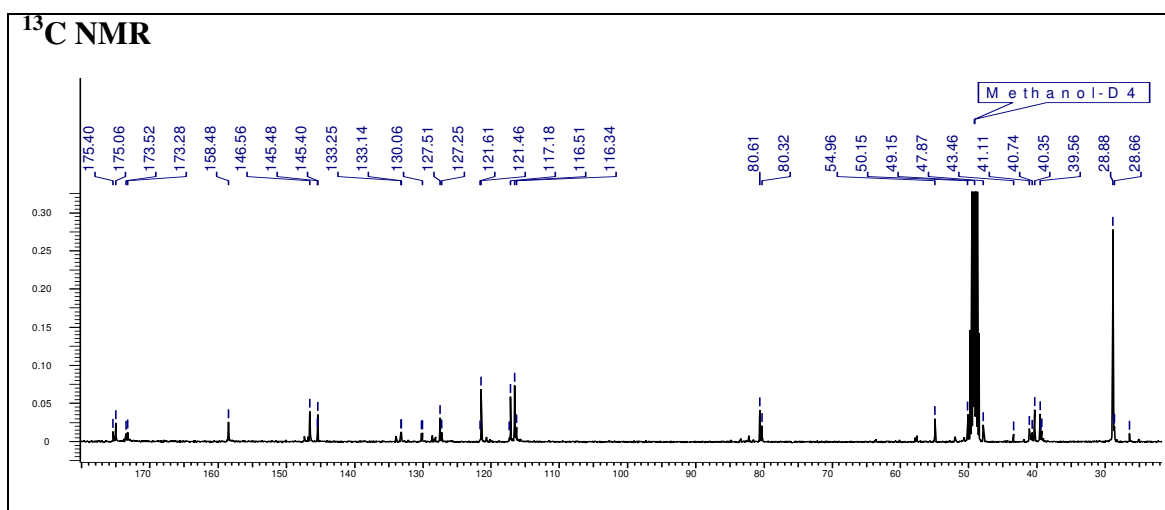
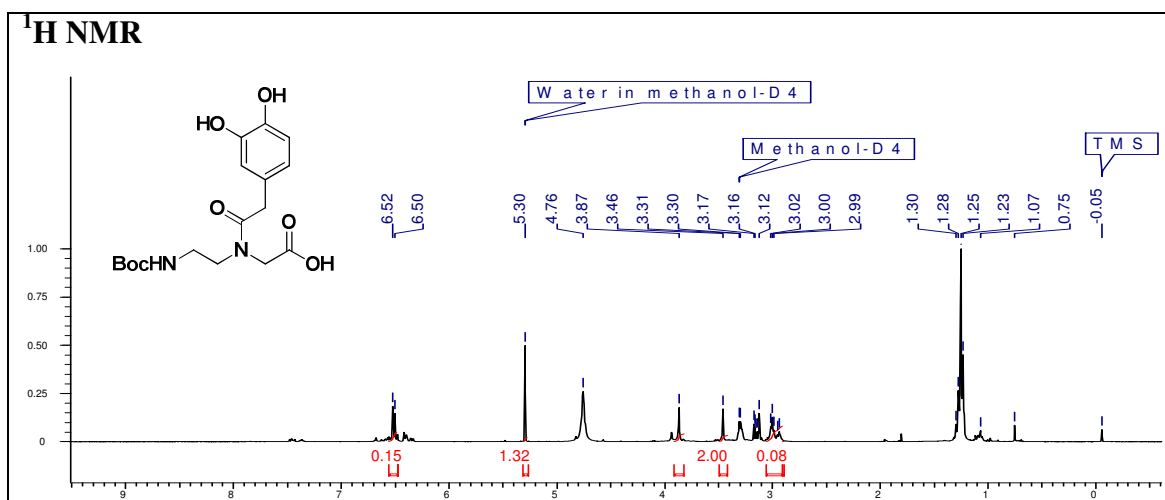


**2-(3,4-bis(((benzyloxy)carbonyl)amino)-N-(2-((tert-butoxycarbonyl)amino)ethyl)benzamido) acetic acid (13)**

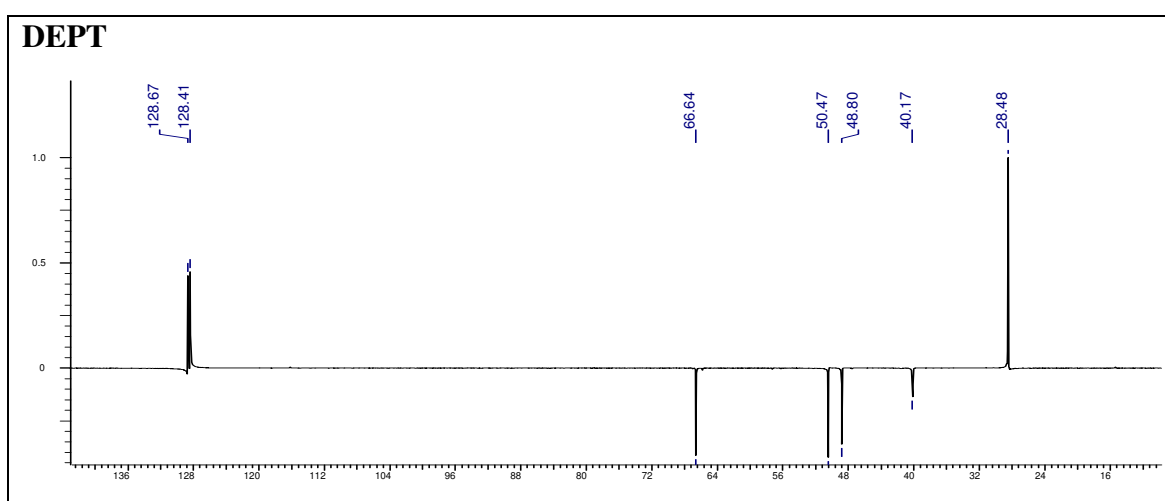
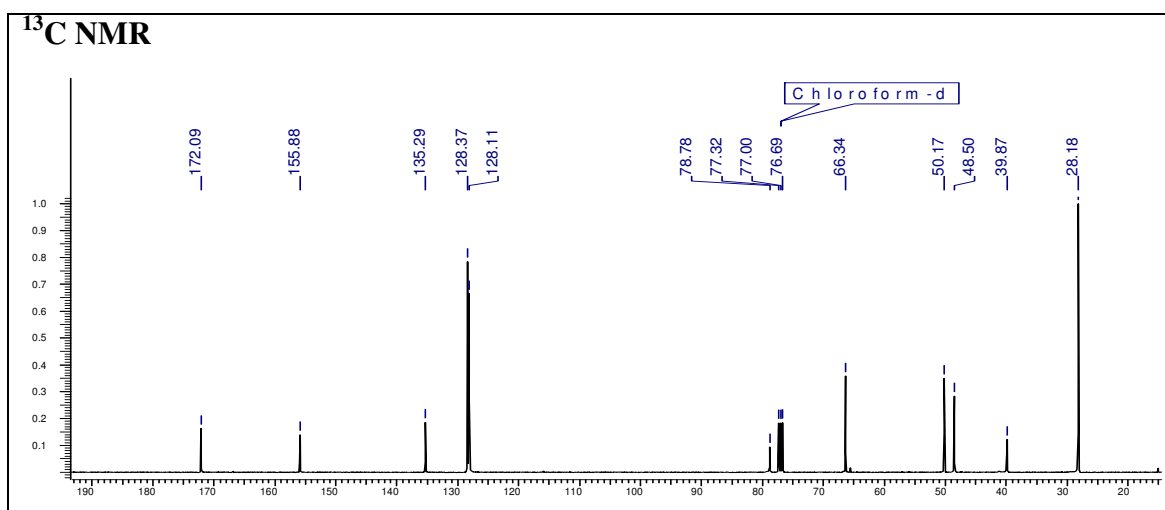
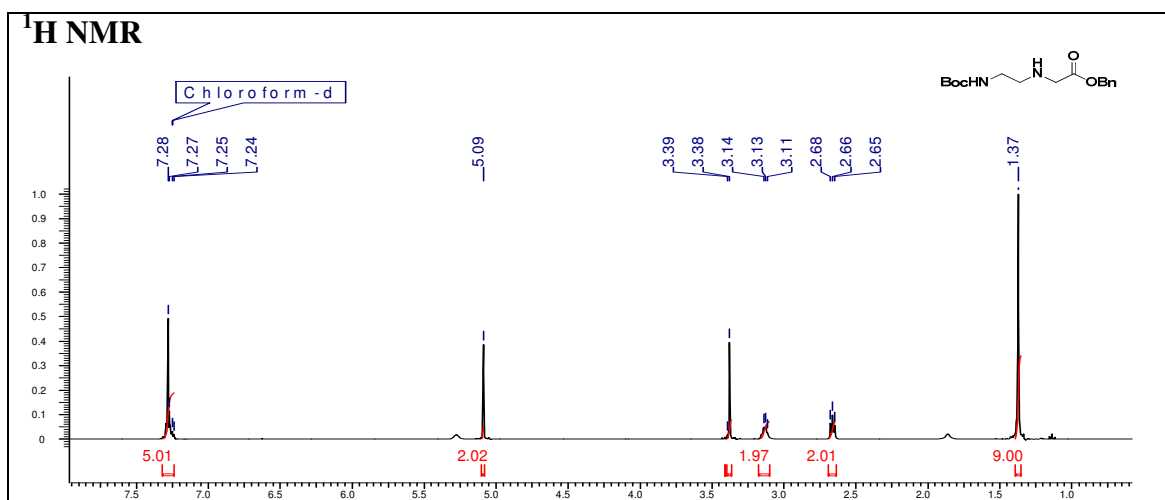
# Chapter 3



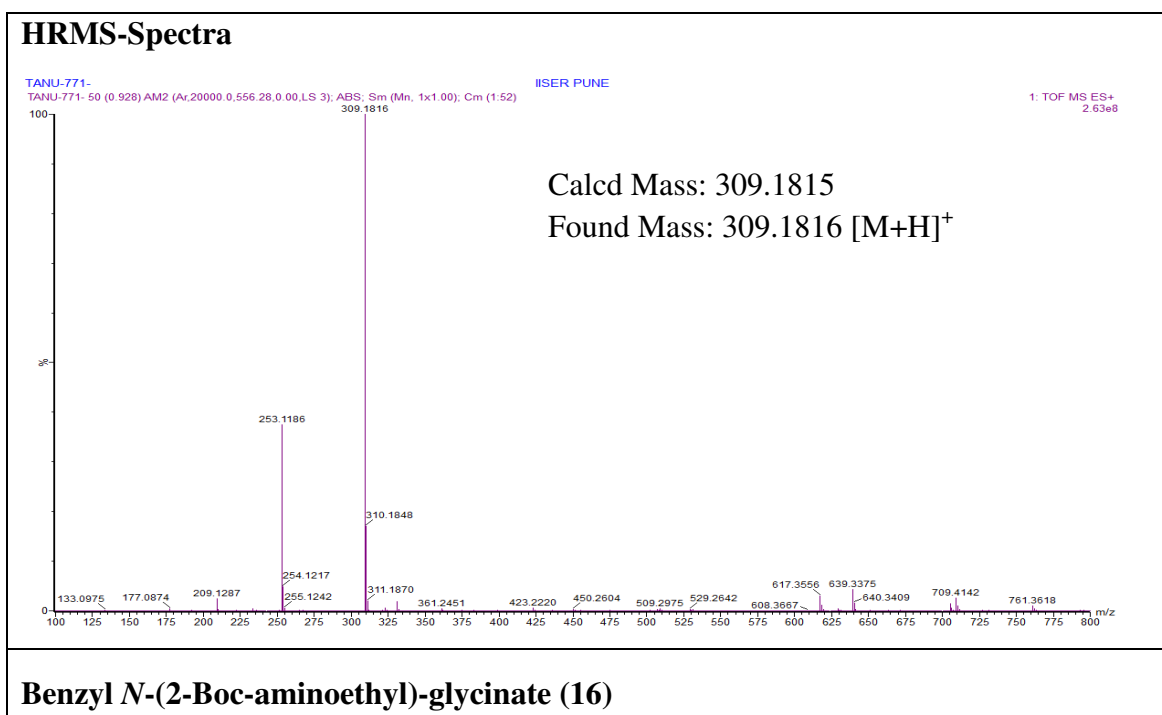
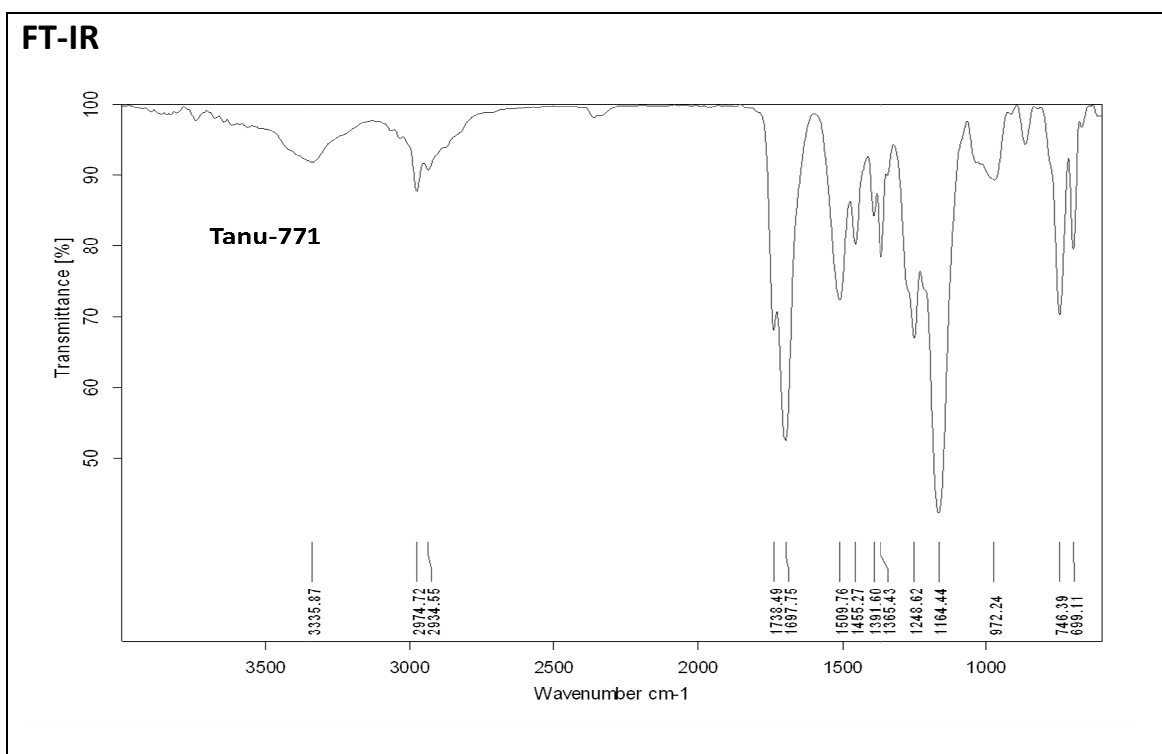
# Chapter 3



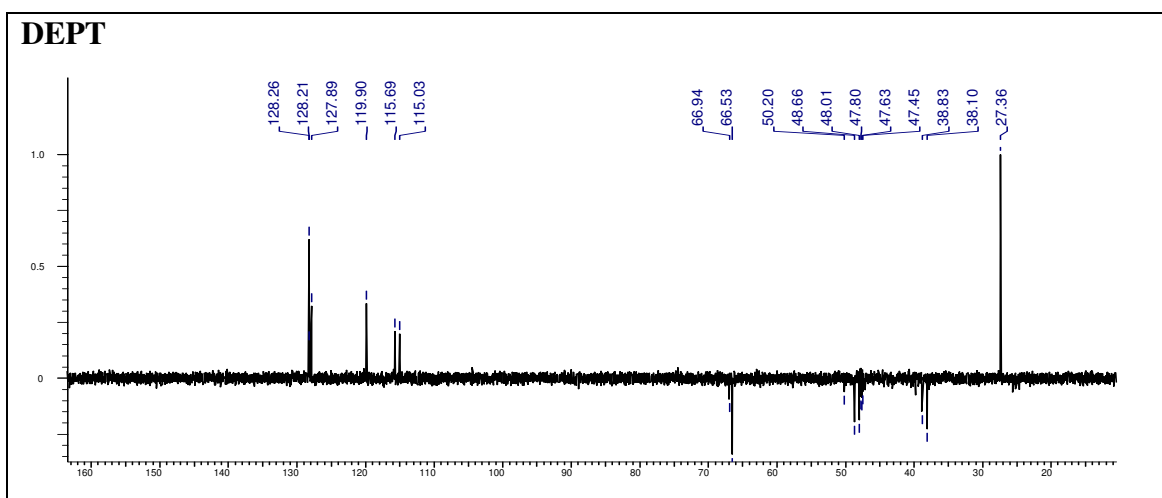
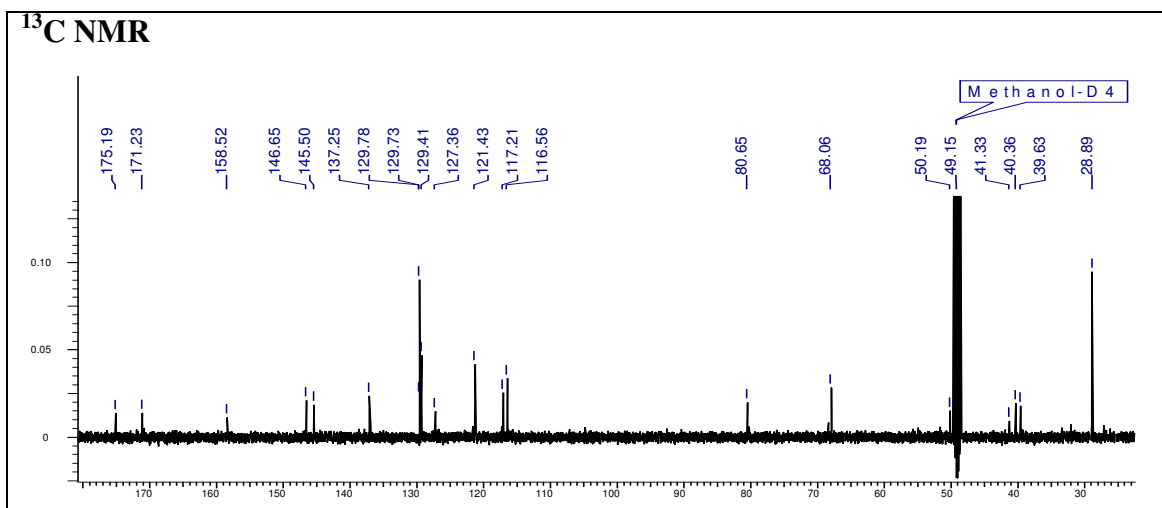
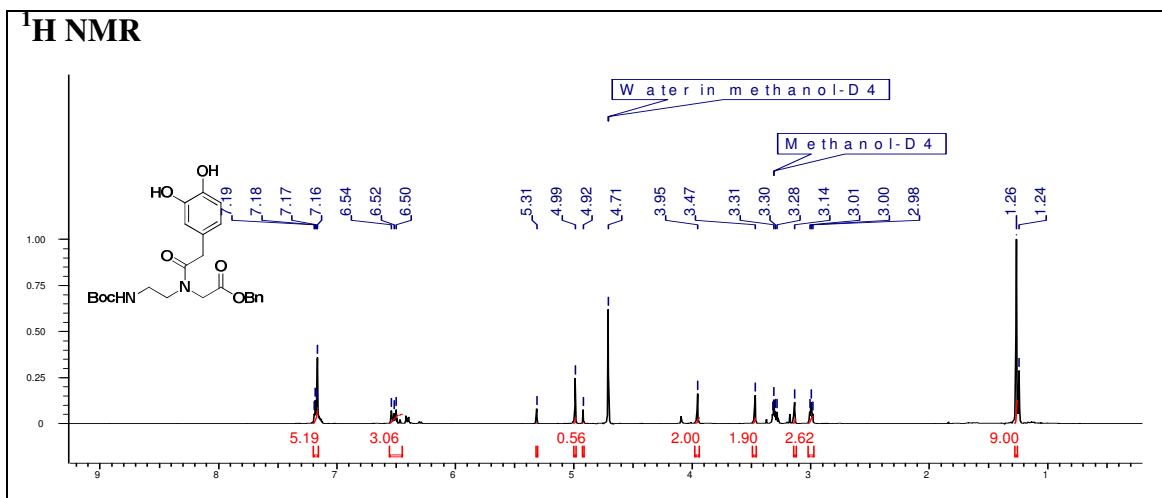
# Chapter 3



**Benzyl *N*-(2-Boc-aminoethyl)-glycinate (16)**



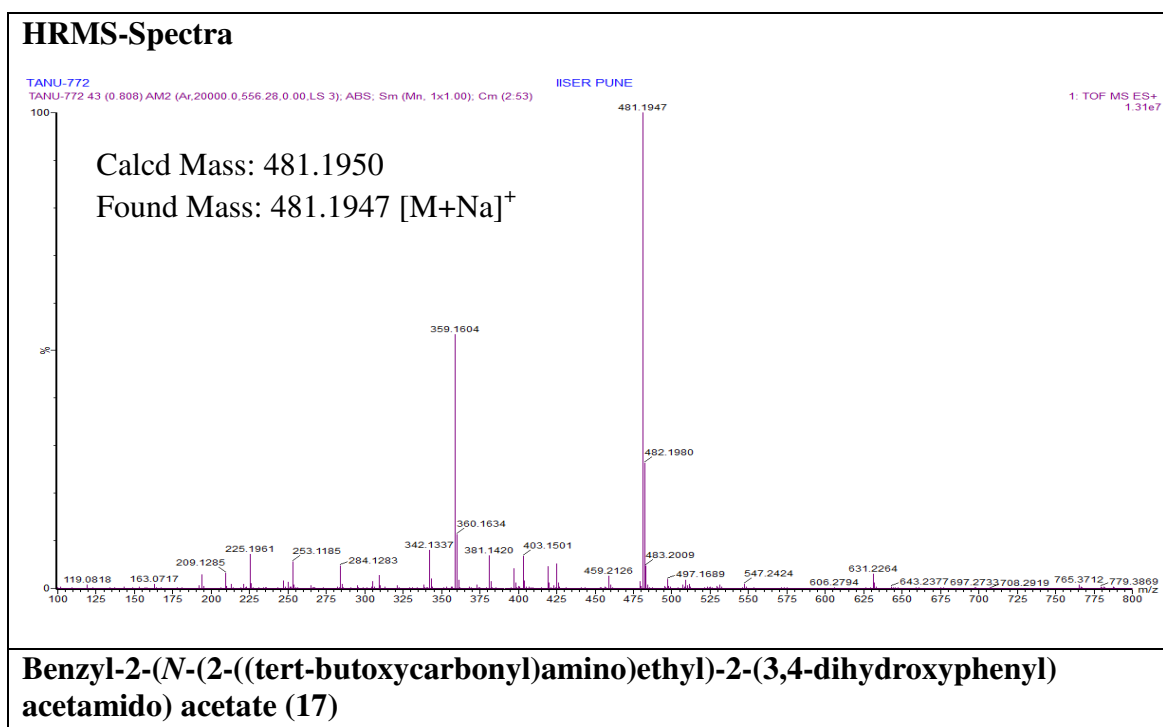
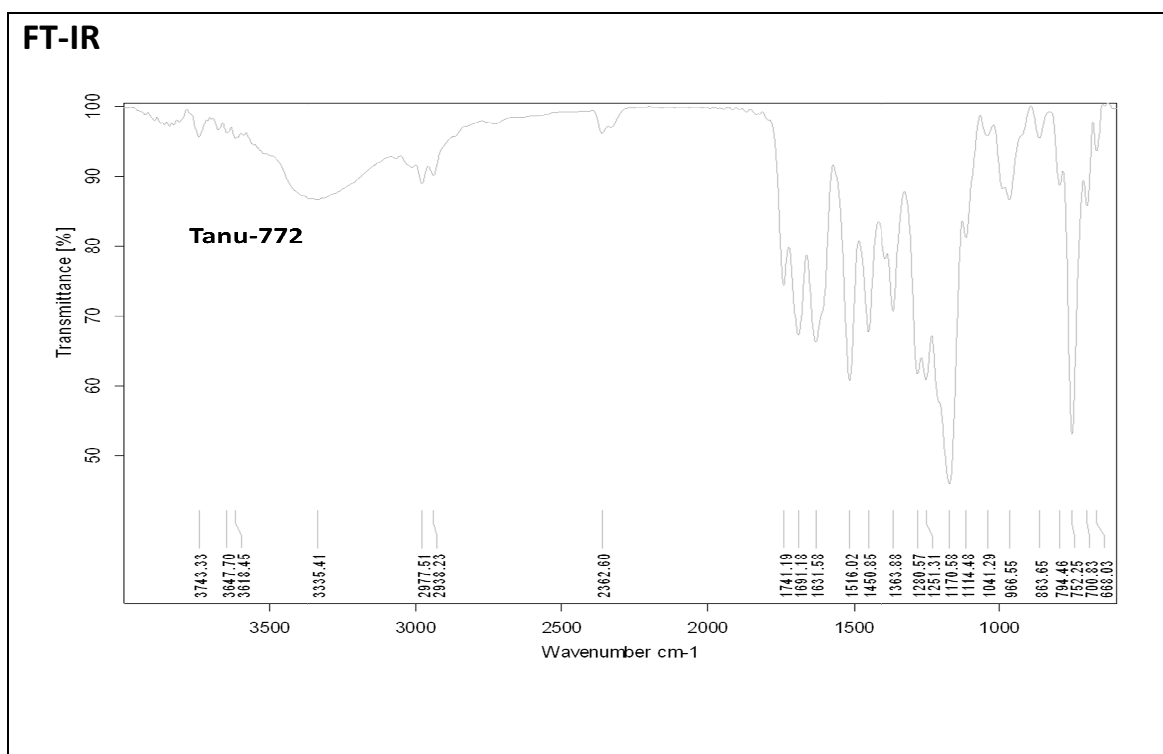
# Chapter 3



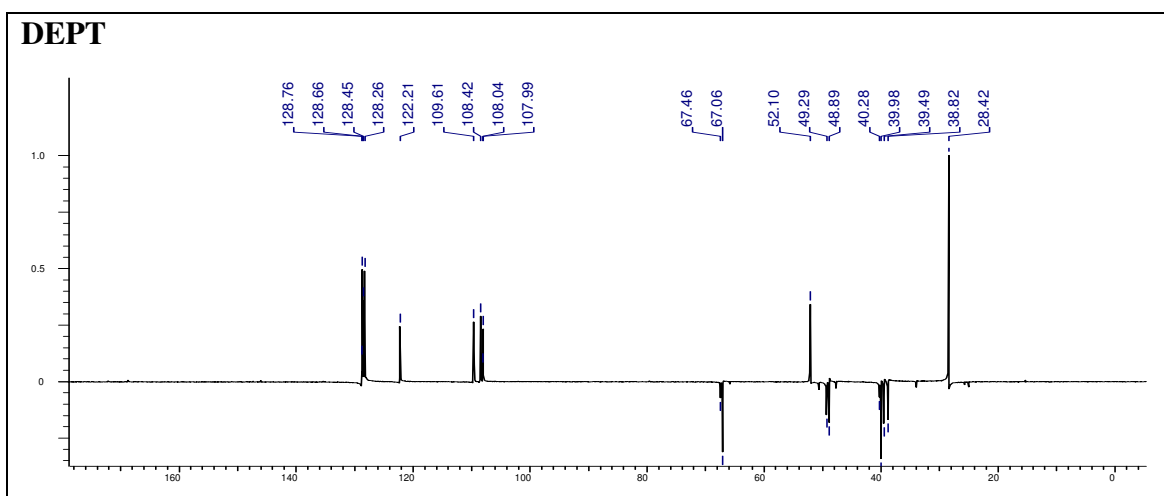
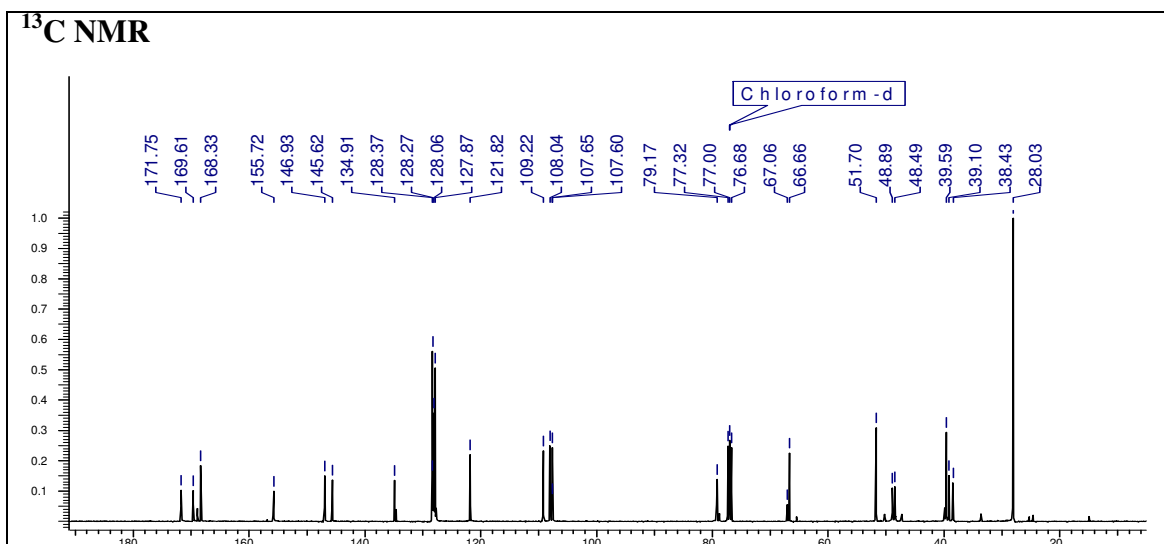
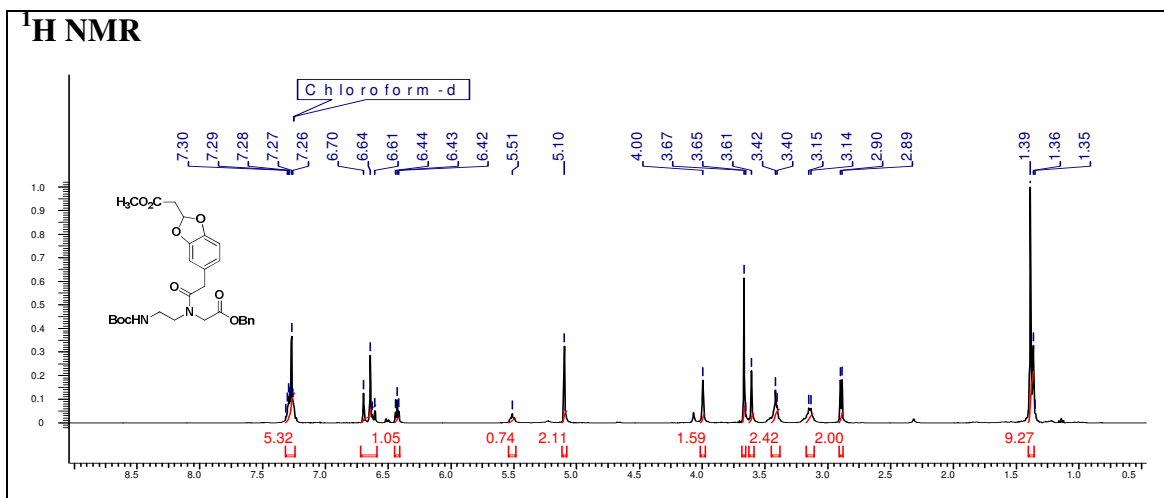
**Benzyl-2-(N-(2-((tert-butoxycarbonyl)amino)ethyl)-2-(3,4-dihydroxyphenyl)acetamido) acetate (17)**



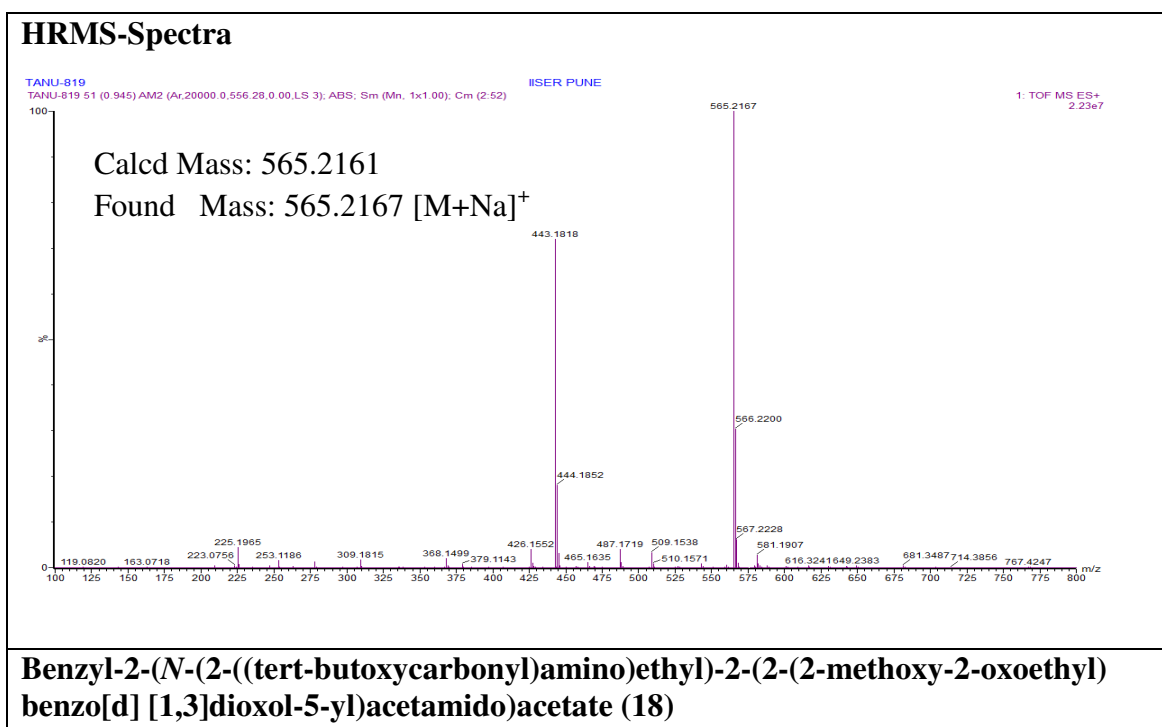
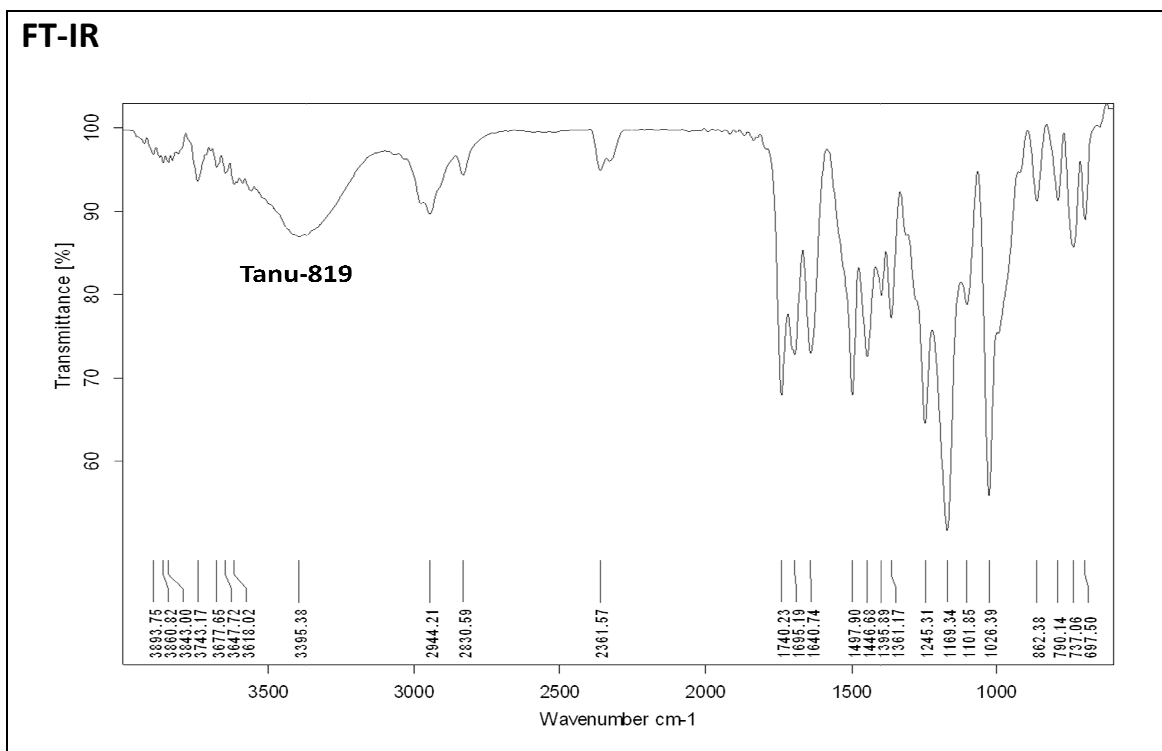
# Chapter 3



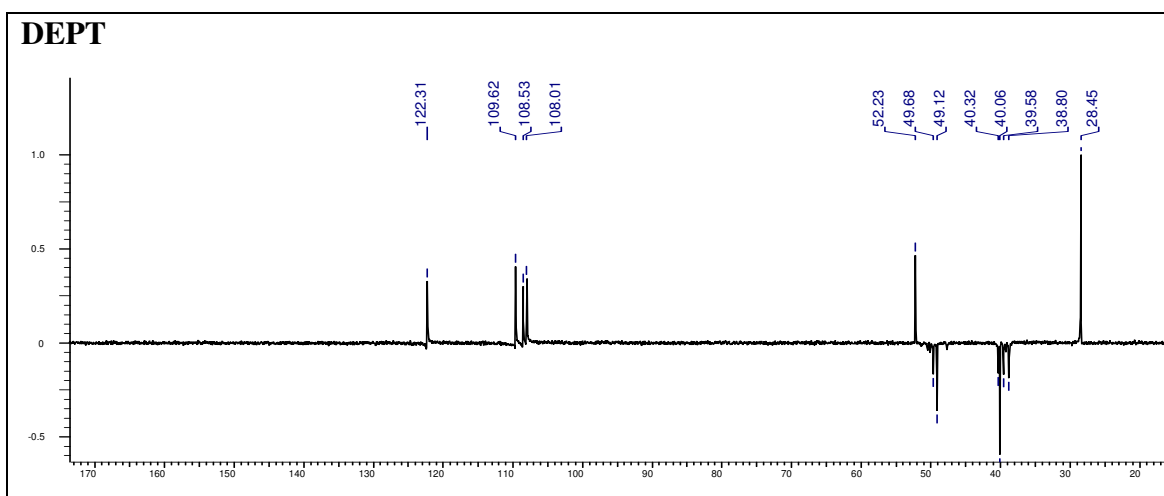
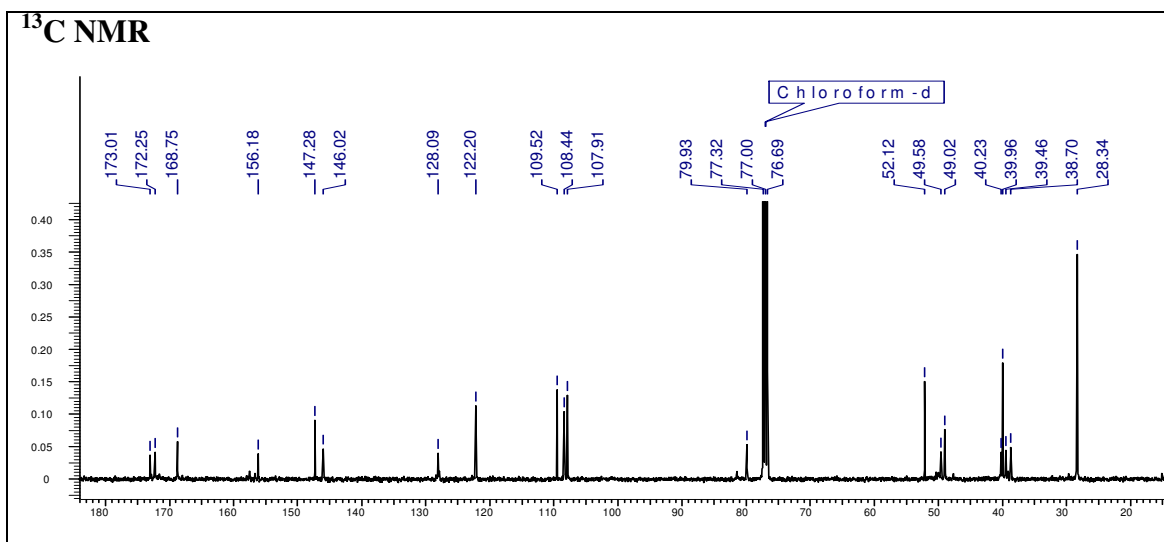
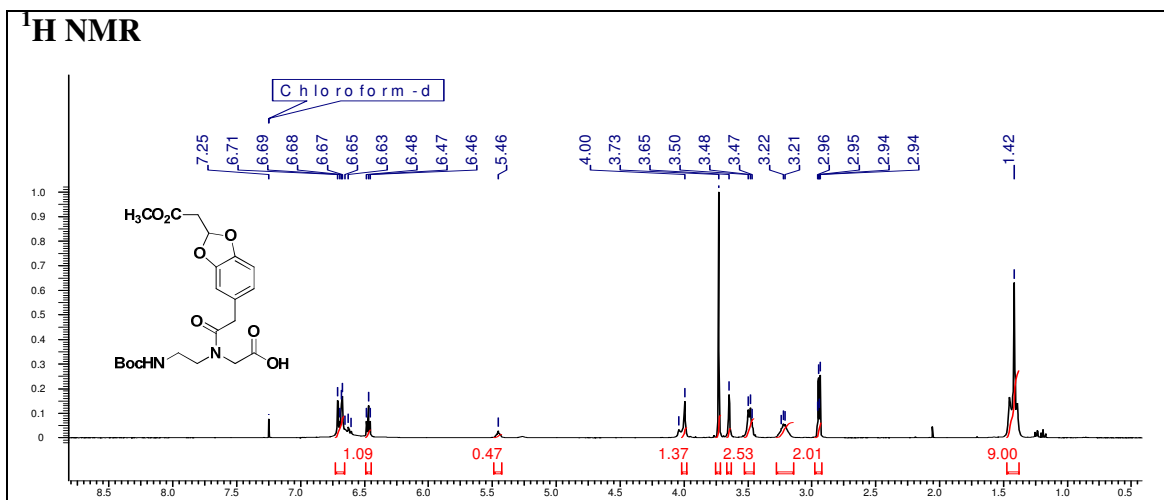
# Chapter 3



**Benzyl 2-(*N*-(2-((*tert*-butoxycarbonyl)amino)ethyl)-2-(2-(2-methoxy-2-oxoethyl)benzo [d] [1,3] dioxol-5-yl)acetamido)acetate (18)**

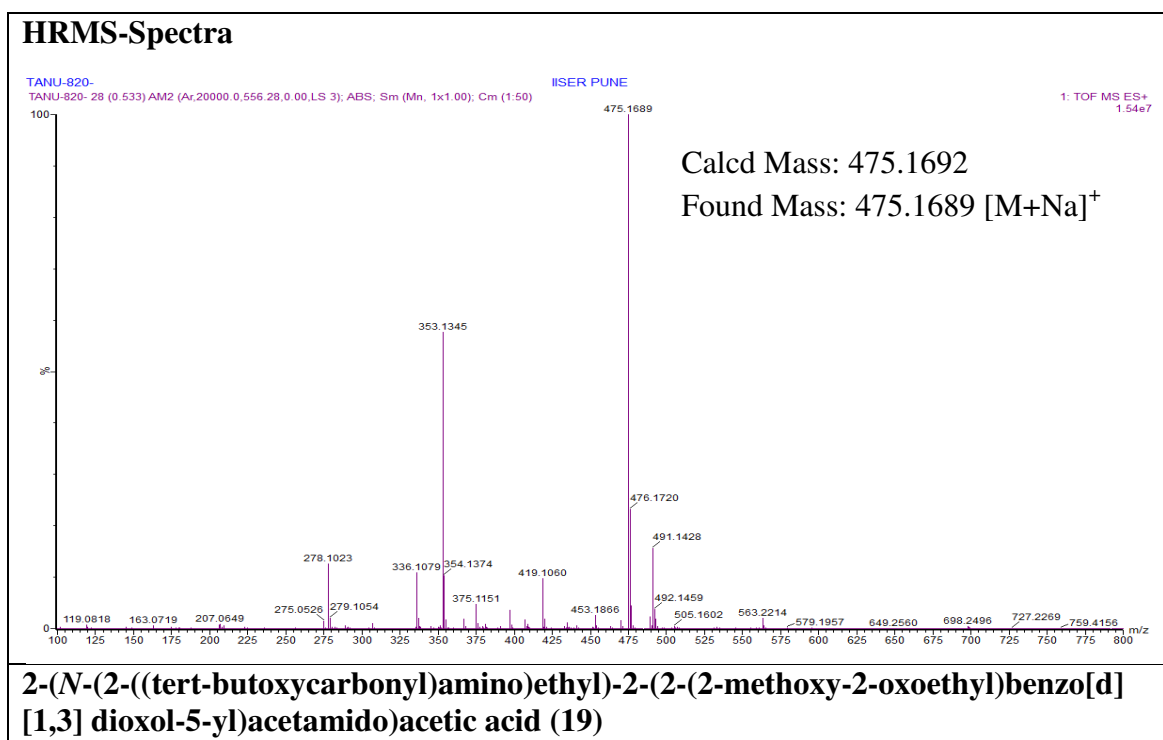
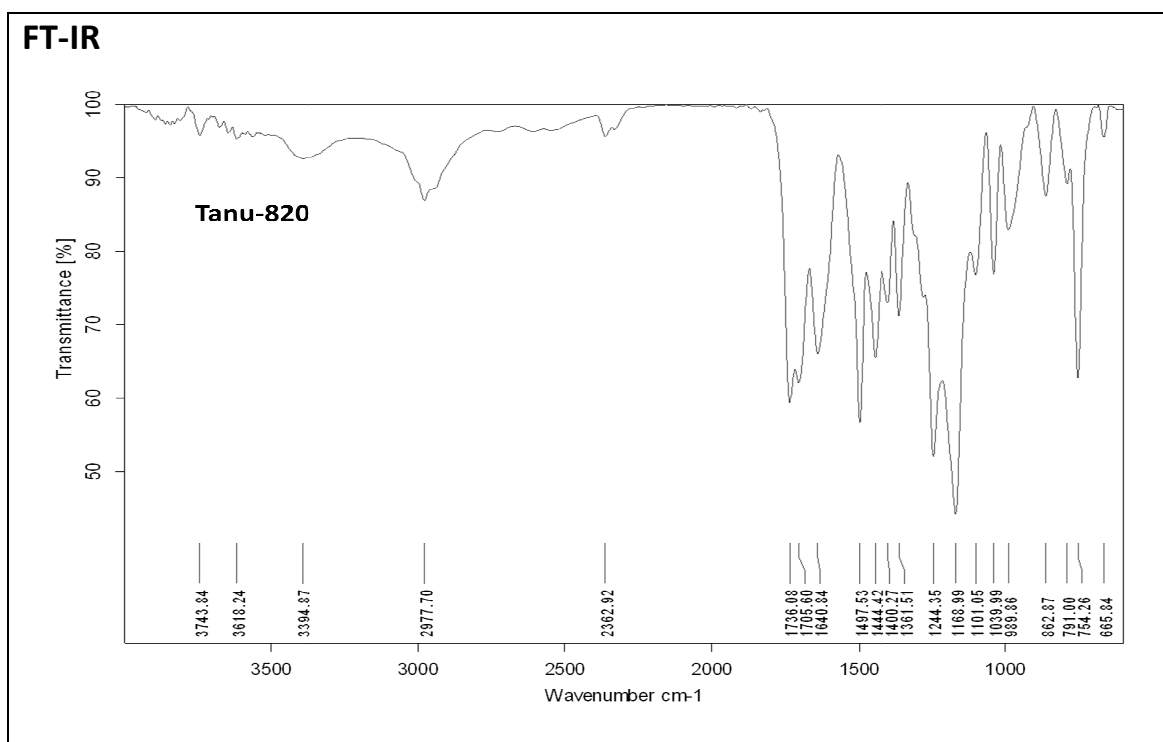


# Chapter 3

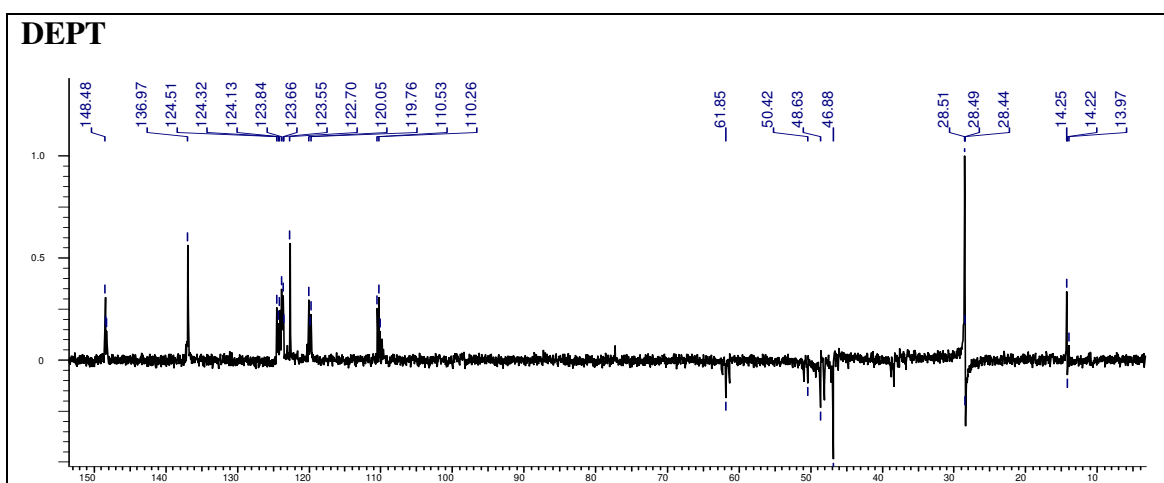
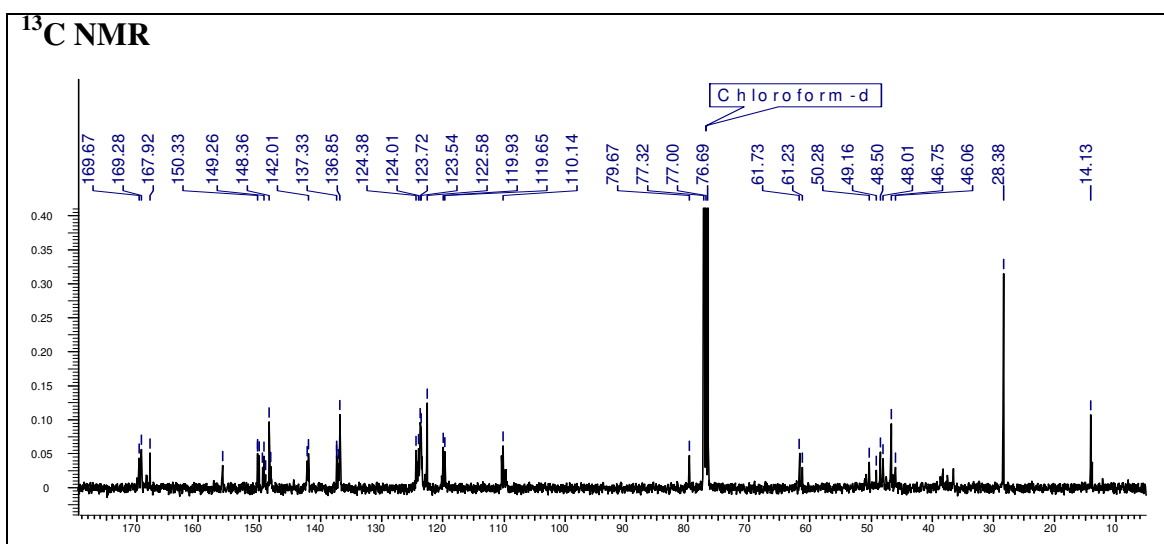
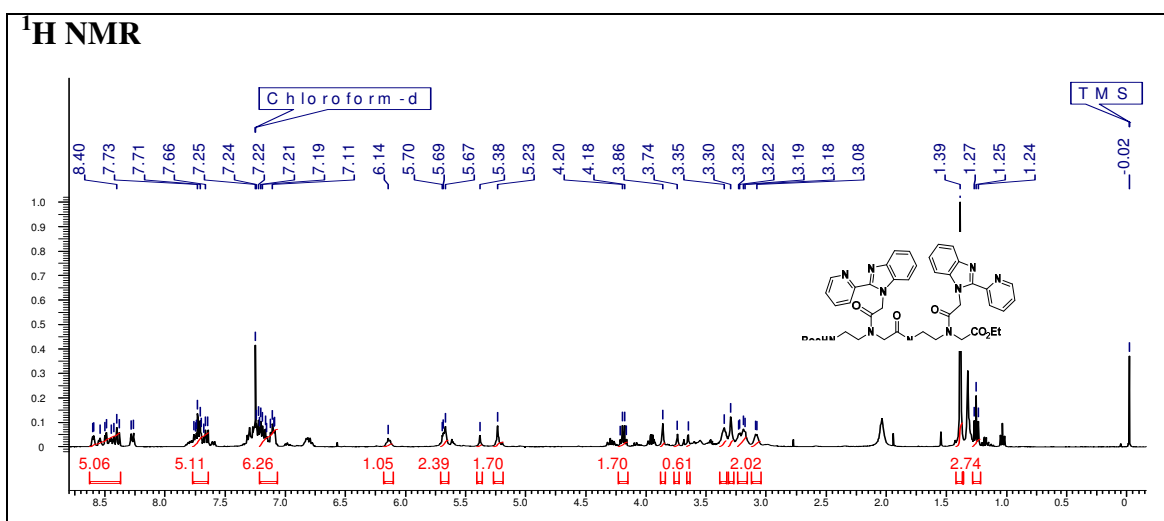


**2-(N-(2-((tert-butoxycarbonyl)amino)ethyl)-2-(2-methoxy-2-oxoethyl)benzo[d][1,3]dioxol-5-yl)acetamido)acetic acid (19)**

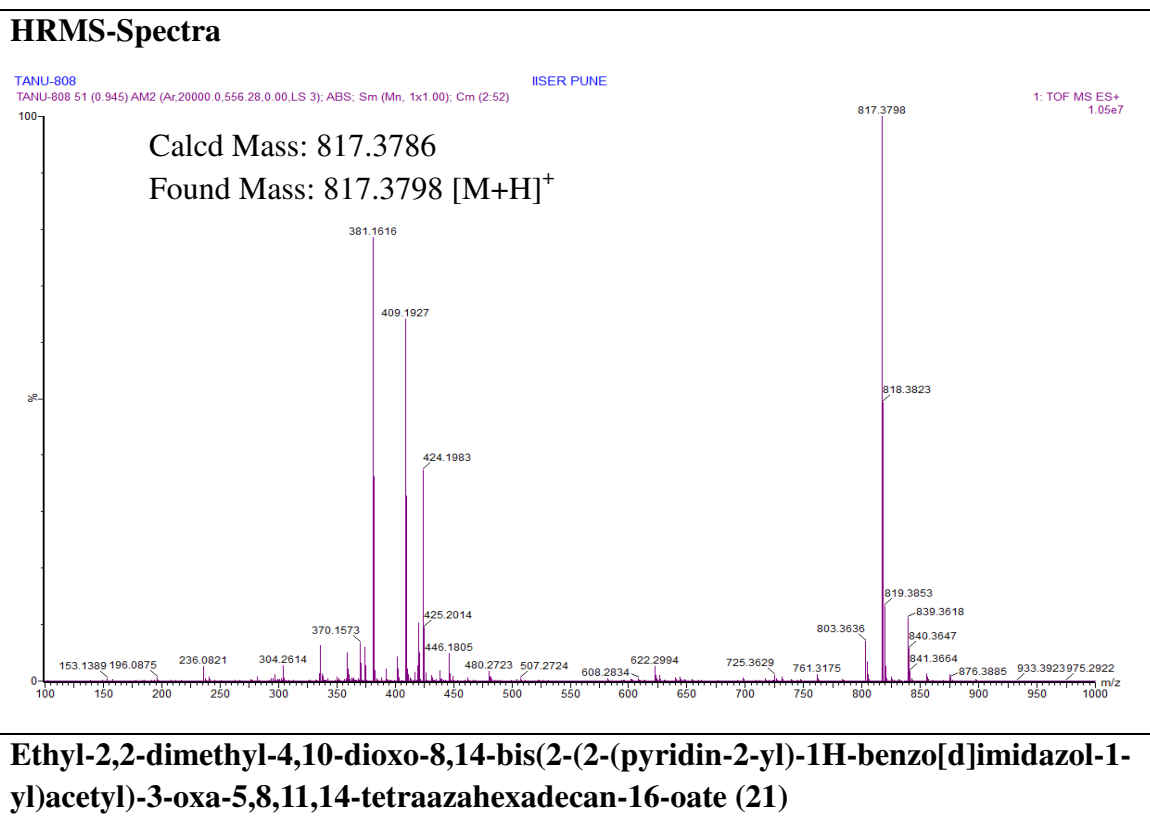
# Chapter 3

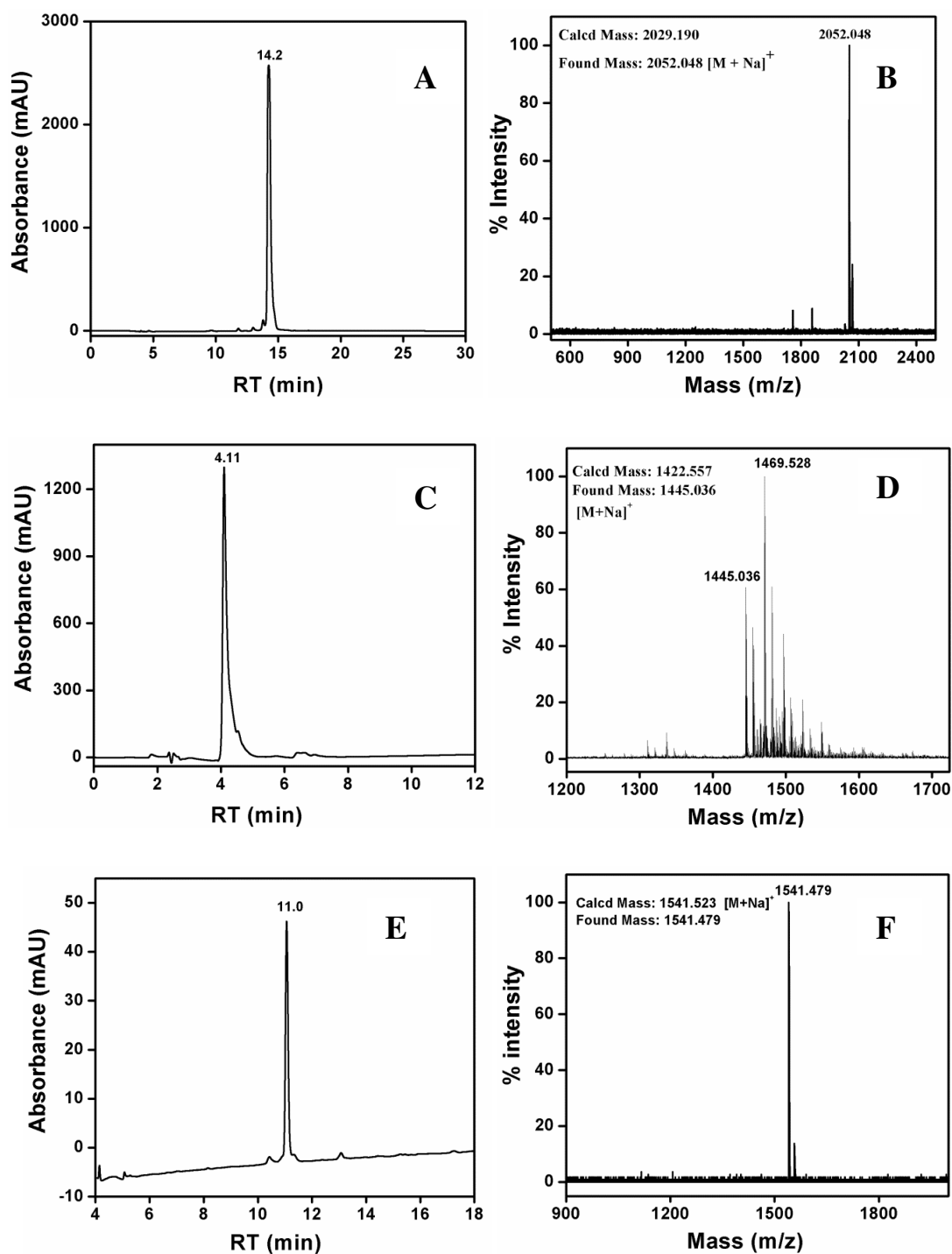


# Chapter 3



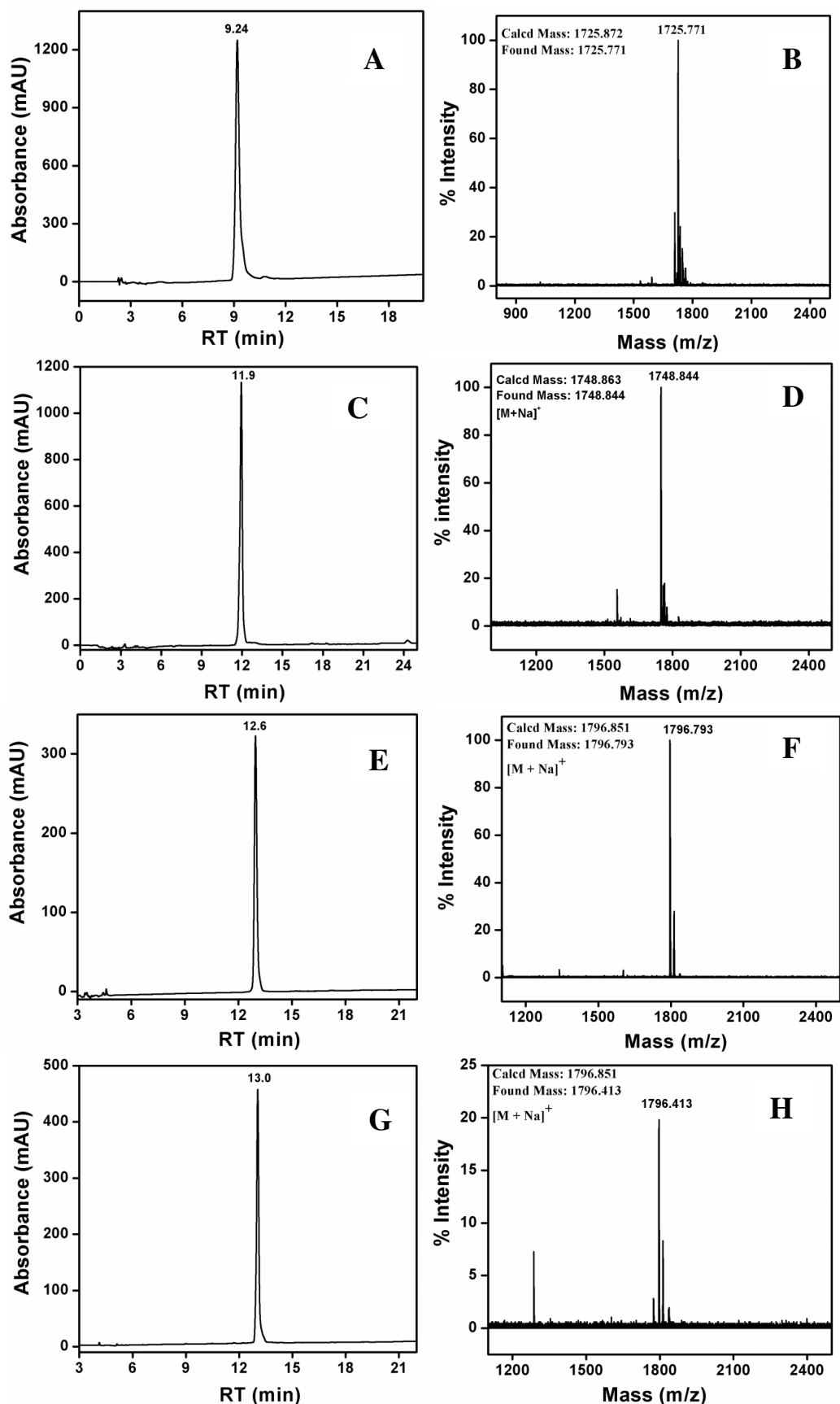
**Ethyl-2,2-dimethyl-4,10-dioxo-8,14-bis(2-(2-(pyridin-2-yl)-1H-benzo[d]imidazol-1-yl) acetyl)-3-oxa-5,8,11,14-tetraazahexadecan-16-oate (21)**





**Figure 94.** (A) HPLC of oligomers (PBI)<sub>6</sub> **22**. (B) MALDI-TOF of (PBI)<sub>6</sub> **22**. (C) HPLC of oligomer (PDA)<sub>6</sub> **23**. (D) MALDI-TOF of oligomer (PDA)<sub>6</sub> **23**. (E) HPLC of oligomer (CAT)<sub>6</sub> **24**. (F) MALDI-TOF of (CAT)<sub>6</sub> **24**.

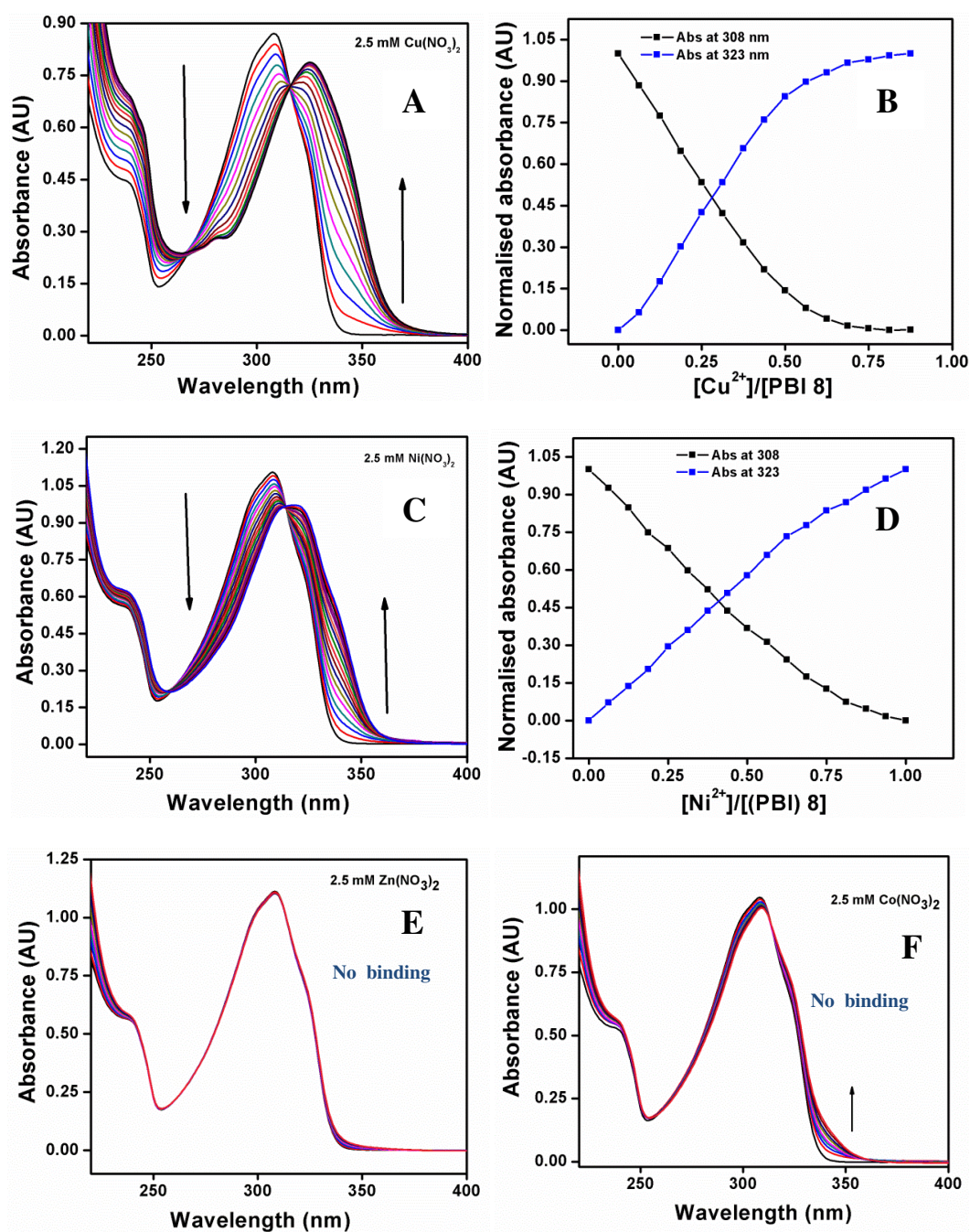




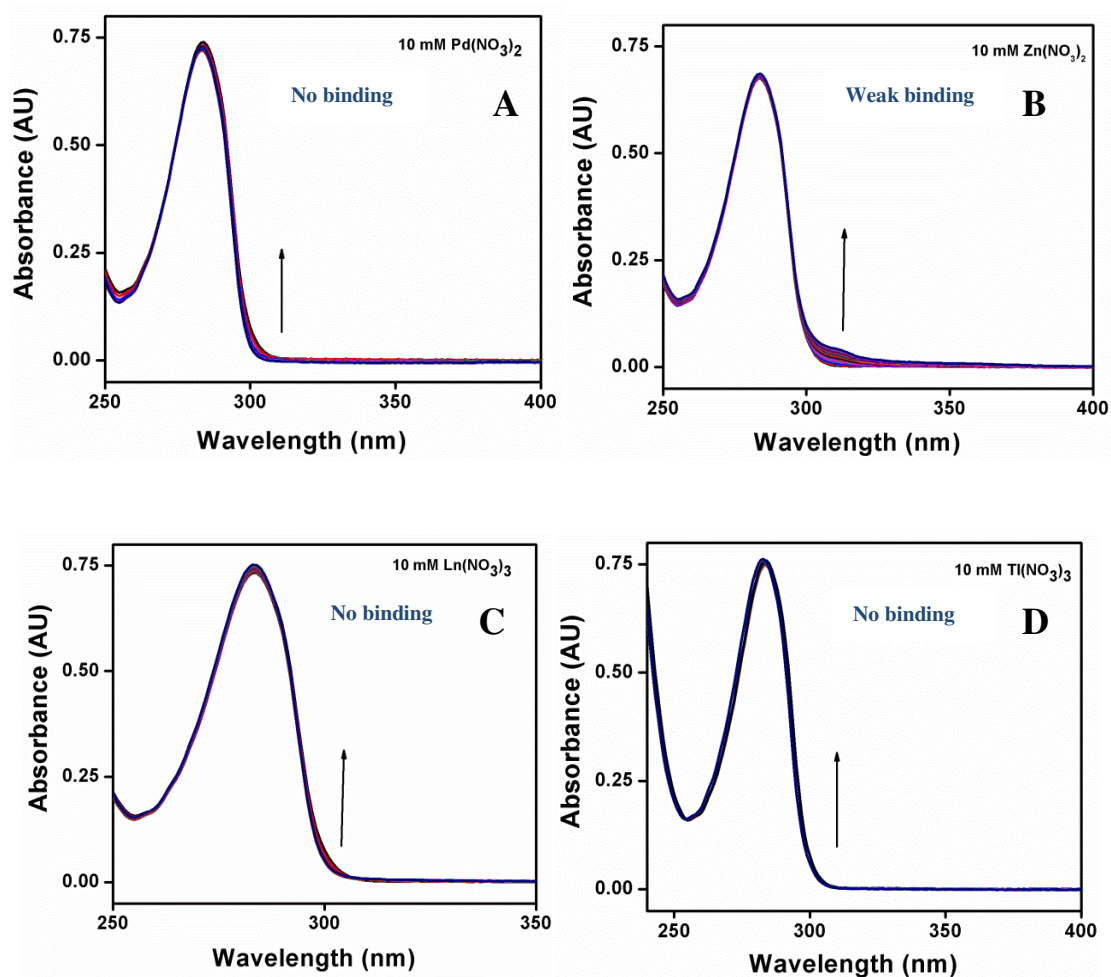
**Figure 95.** (A) HPLC of oligomer (PBI)<sub>3</sub>-(PDA)<sub>3</sub> **25**. (B) MALDI-TOF of oligomer (PBI)<sub>3</sub>-(PDA)<sub>3</sub> **25**. (C) HPLC of oligomer (PBI-PDA)<sub>3</sub> **26**. (D) MALDI-TOF of (PBI-PDA)<sub>3</sub> **26**. (E) HPLC of oligomer PBI<sub>3</sub>-(CAT)<sub>3</sub> **27**. (F) MALDI-TOF of oligomer PBI<sub>3</sub>-(CAT)<sub>3</sub> **27**. (G) HPLC of oligomer (PBI-CAT)<sub>3</sub> **28** (G) MALDI-TOF of oligomer (PBI-CAT)<sub>3</sub> **28**.

2013 PhD thesis: T. Kaur, University of Pune

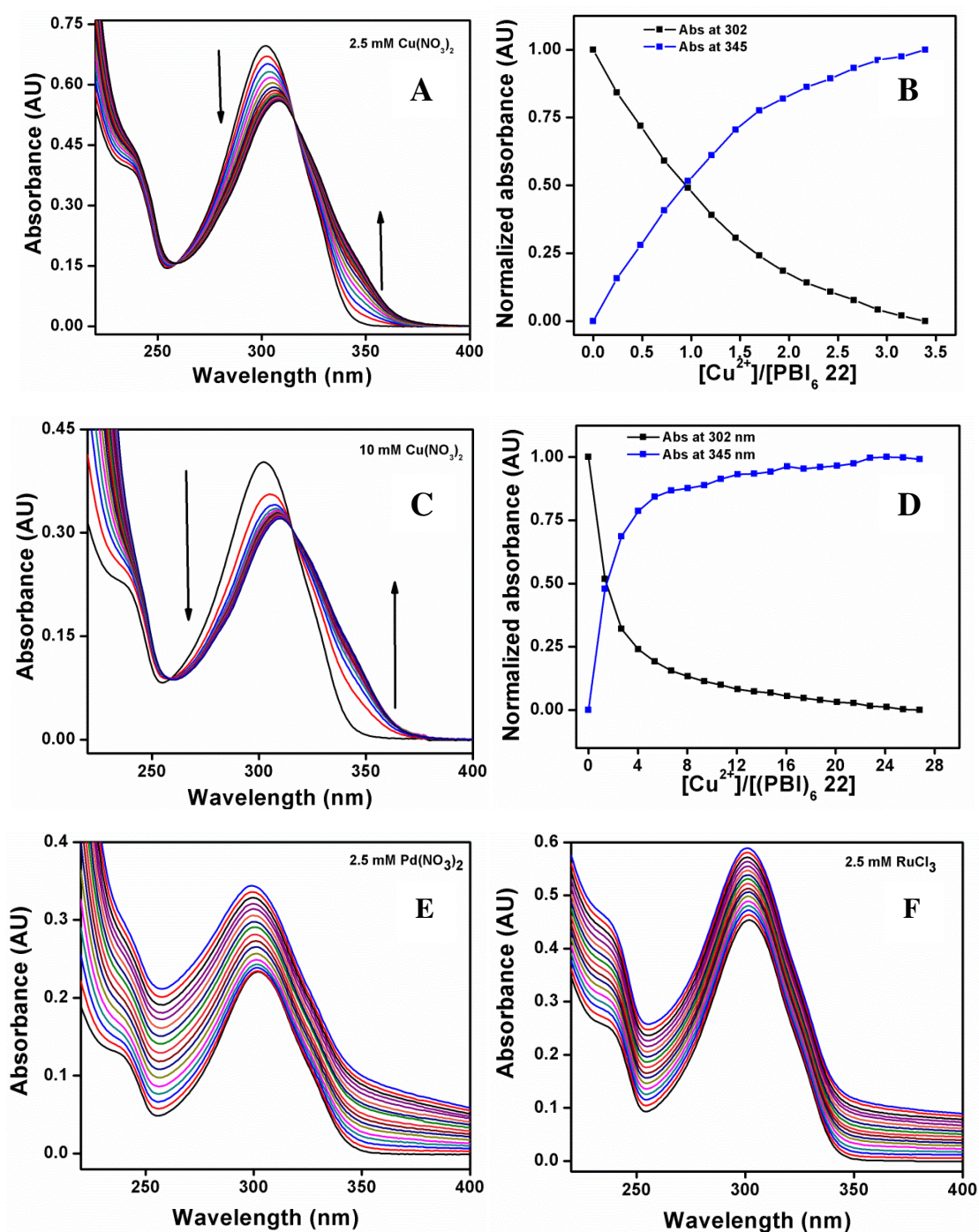
## UV-Vis spectrophotometric titrations of 2-pyridylbenzimidazole (PBI) aeg 8



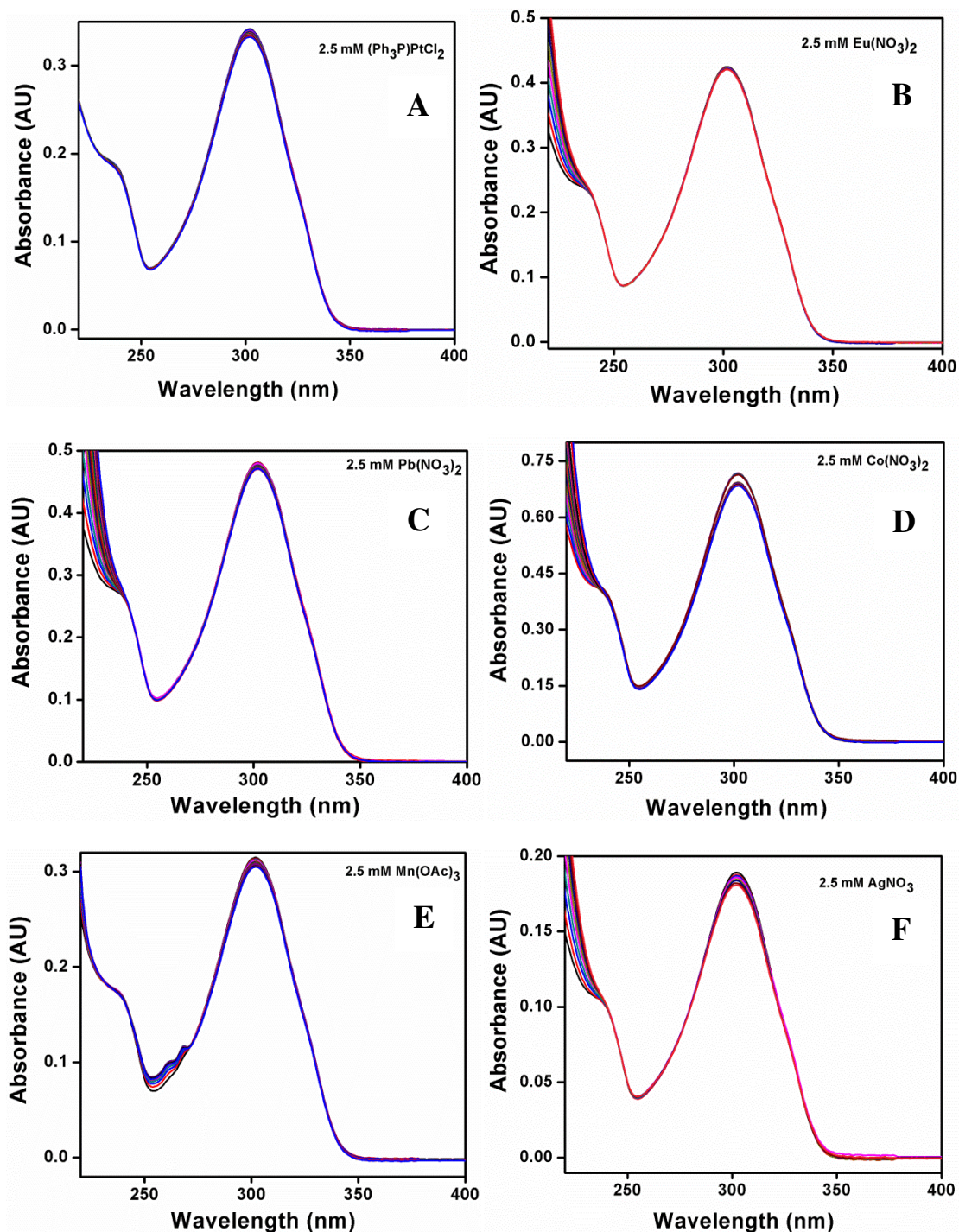
**Figure 96.** Changes in the absorption spectra of the 2-pyridylbenzimidazole (PBI) aeg 8 (25  $\mu\text{M}$ ) in methanol upon the addition of metal salts (A)  $\text{Cu}(\text{NO}_3)_2$  (2.5 mM). (C)  $\text{Ni}(\text{NO}_3)_2$  (2.5 mM). Plot of the change in absorbance at 308 and 345 nm as a function of molar ratio of metal to (PBI) 8 (B)  $\text{Cu}(\text{NO}_3)_2$  (D)  $\text{Ni}(\text{NO}_3)_2$ . (E)  $\text{Zn}(\text{NO}_3)_2$  (2.5 mM). (F)  $\text{Co}(\text{NO}_3)_2$  (10 mM).

UV-Vis spectrophotometric titrations of benzyl-*N*-Boc-aminoethyl-3,4-dihydroxyphenyl (CAT) glycinate **17**

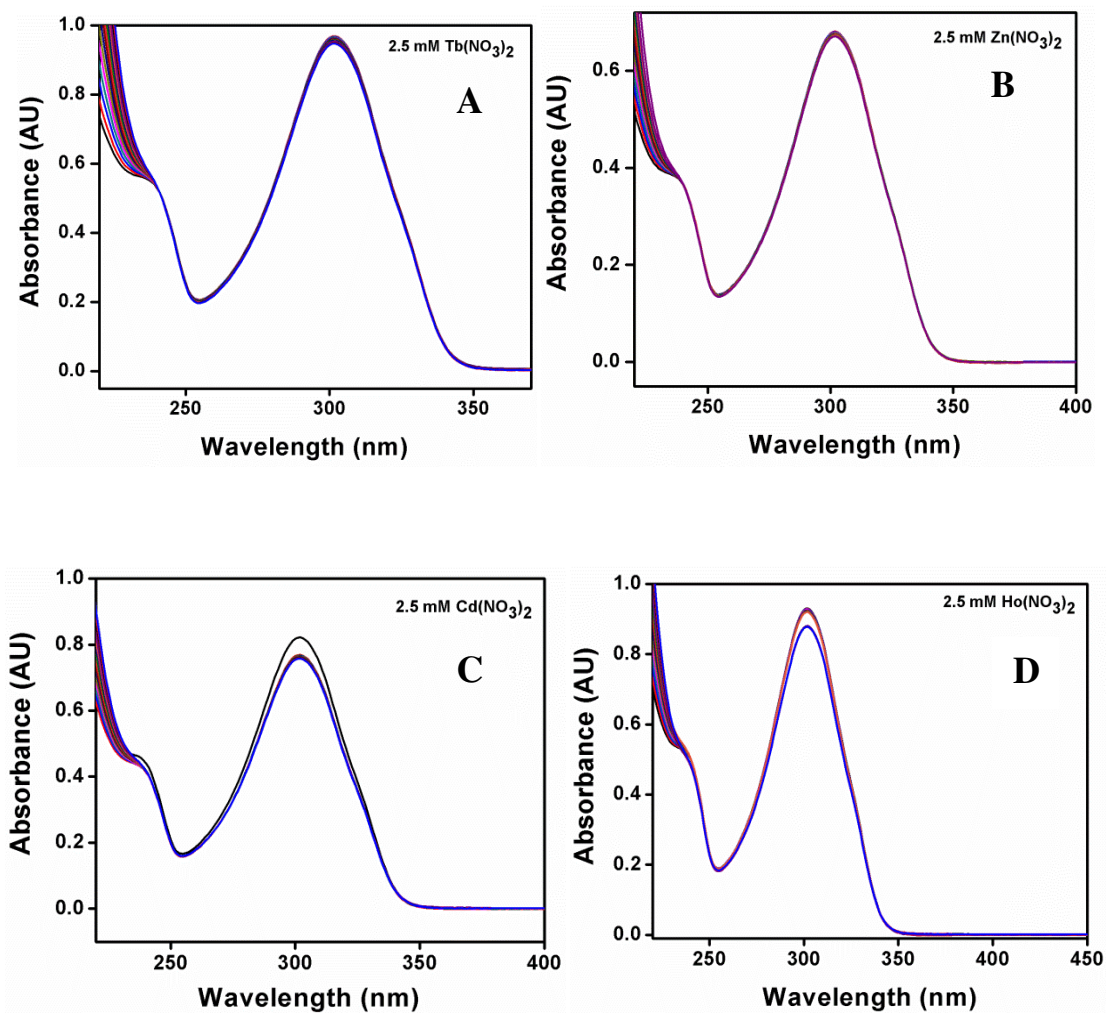
**Figure 97.** Changes in the absorption spectra of benzyl-*N*-Boc-aminoethyl-3,4-dihydroxyphenyl (CAT) glycinate **17** (8-10  $\mu$ M) in methanol upon the addition of metal salts (A)  $\text{Pd}(\text{NO}_3)_2$  (10 mM). (B)  $\text{Fe}(\text{NO}_3)_3$  (10 mM). (C)  $\text{Ln}(\text{NO}_3)_3$  (10 mM). (D)  $\text{Tl}(\text{NO}_3)_3$  (10 mM).

UV-Vis spectrophotometric titrations of 2-pyridylbenzimidazole (PBI)<sub>6</sub> oligomer 22

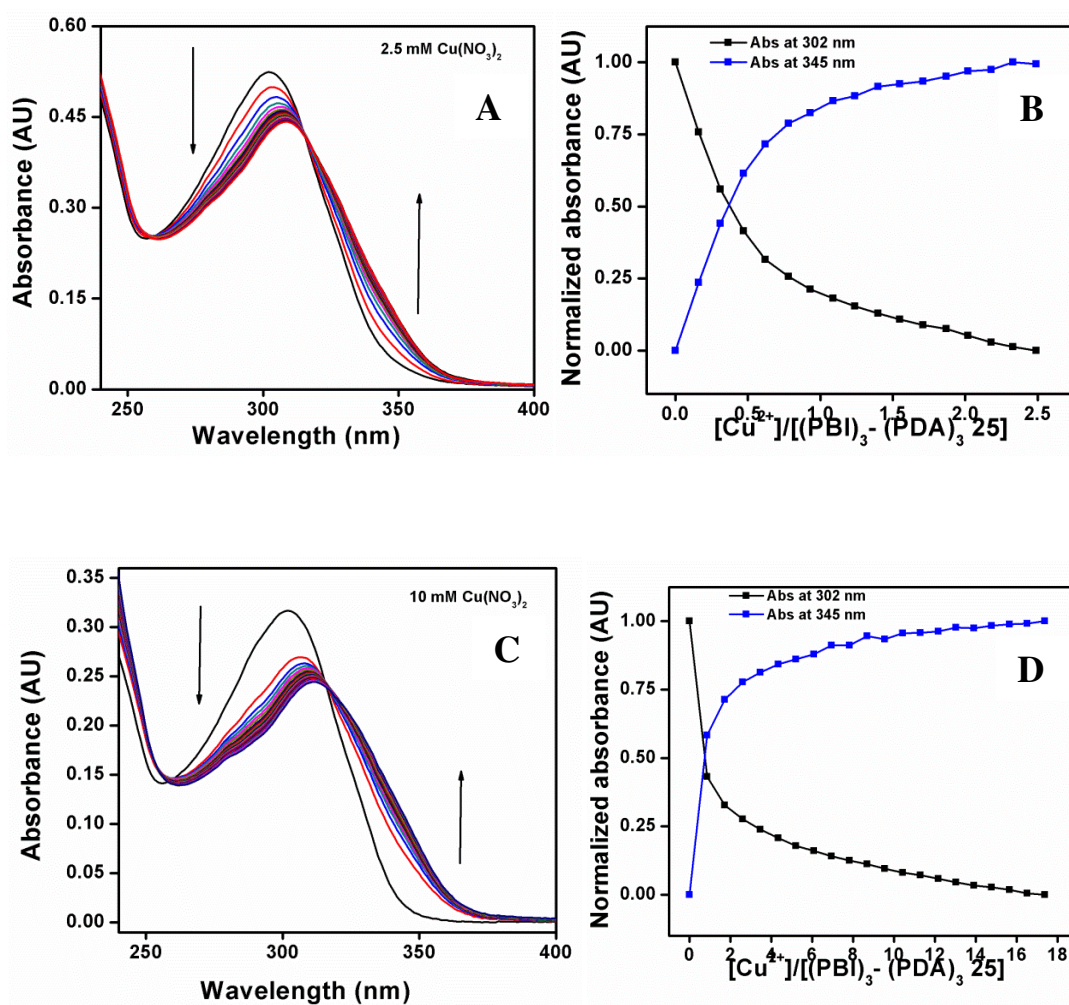
**Figure 98.** Changes in the absorption spectra of 2-pyridylbenzimidazole (PBI)<sub>6</sub> oligomer 22 (8-10  $\mu$ M) in water upon the addition of metal salts (A) Cu(NO<sub>3</sub>)<sub>2</sub> (2.5 mM). (C) Cu(NO<sub>3</sub>)<sub>2</sub> (10 mM). Plot of the change in absorbance at 302 and 345 nm as a function of molar ratio of metal to peptides (B) Cu(NO<sub>3</sub>)<sub>2</sub> and (D) Cu(NO<sub>3</sub>)<sub>2</sub>. (E) Pd(NO<sub>3</sub>)<sub>2</sub> (2.5 mM). (F) RuCl<sub>3</sub> (2.5 mM).

UV-Vis spectrophotometric titrations of 2-pyridylbenzimidazole (PBI)<sub>6</sub> oligomer **22**

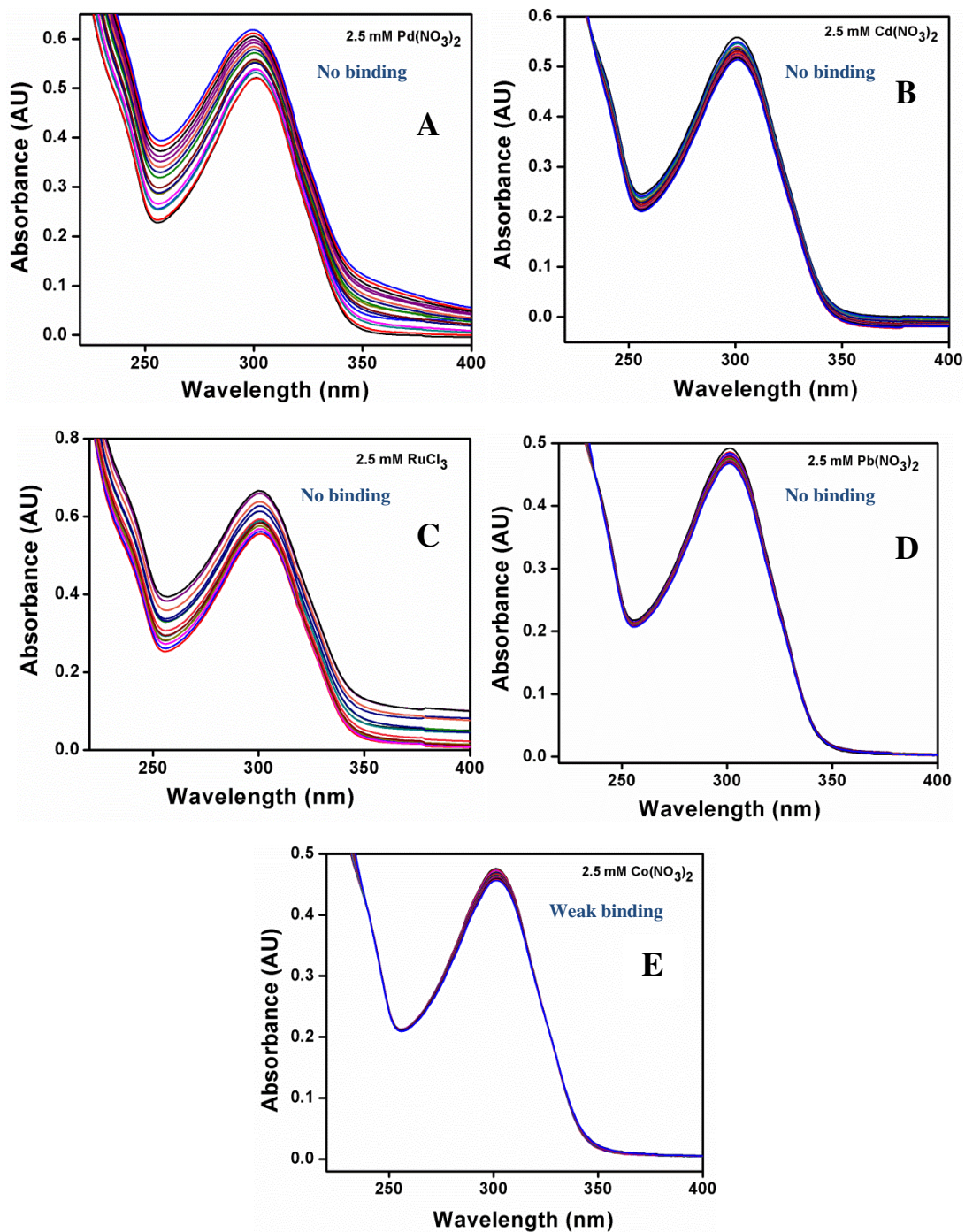
**Figure 99.** Changes in the absorption spectra of 2-pyridylbenzimidazole (PBI)<sub>6</sub> oligomer **22** (8-10  $\mu\text{M}$ ) in water upon the addition of metal salts (A)  $(\text{PPh}_3)_2\text{PtCl}_2$  (2.5 mM). (B)  $\text{Eu}(\text{NO}_3)_2$  (2.5 mM). (C)  $\text{Pb}(\text{NO}_3)_2$  (2.5 mM). (D)  $\text{Co}(\text{NO}_3)_2$  (2.5 mM). (E)  $\text{Mn}(\text{OAc})_3$  (2.5 mM). (F)  $\text{AgNO}_3$  (2.5 mM).

UV-Vis spectrophotometric titrations of 2-pyridylbenzimidazole (PBI)<sub>6</sub> oligomer **22**

**Figure 100.** Changes in the absorption spectra of 2-pyridylbenzimidazole (PBI)<sub>6</sub> oligomer **22** (8-10  $\mu\text{M}$ ) in water upon the addition of metal salts (A)  $\text{Tb}(\text{NO}_3)_2$  (2.5 mM). (B)  $\text{Zn}(\text{NO}_3)_2$  (2.5 mM). (C)  $\text{Cd}(\text{NO}_3)_2$  (2.5 mM). (D)  $\text{Ho}(\text{NO}_3)_2$  (2.5 mM).

UV-Vis spectrophotometric titrations of *hetero*-(PBI)<sub>3</sub> - (PDA)<sub>3</sub> oligomer **25**

**Figure 101.** Changes in the absorption spectra of (PBI)<sub>3</sub> - (PDA)<sub>3</sub> oligomer **25** (8-10  $\mu$ M) in water upon the addition of metal salts (A) Cu(NO<sub>3</sub>)<sub>2</sub> (2.5 mM). (C) Cu(NO<sub>3</sub>)<sub>2</sub> (10 mM). Plot of the change in absorbance at 302 and 345 nm as a function of molar ratio of metal to peptides (B) and (D) Cu(NO<sub>3</sub>)<sub>2</sub>.

UV-Vis spectrophotometric titrations of *hetero*-(PBI)<sub>3</sub> - (PDA)<sub>3</sub> oligomer **25**

**Figure 102.** Changes in the absorption spectra of (PBI)<sub>3</sub> - ((PDA)<sub>3</sub> oligomer **25** (8-10 μM) in water upon the addition of metal salts (A) Pd(NO<sub>3</sub>)<sub>2</sub> (2.5 mM). (B) Cd(NO<sub>3</sub>)<sub>2</sub> (2.5 mM). (C) RuCl<sub>3</sub> (2.5 mM). (D) Pb(NO<sub>3</sub>)<sub>2</sub> (2.5 mM). and (E) Co(NO<sub>3</sub>)<sub>2</sub> (2.5 mM).



### Isothermal Titration Calorimetry (ITC) analysis of synthesized *aeg* linked ligands with nickel nitrate

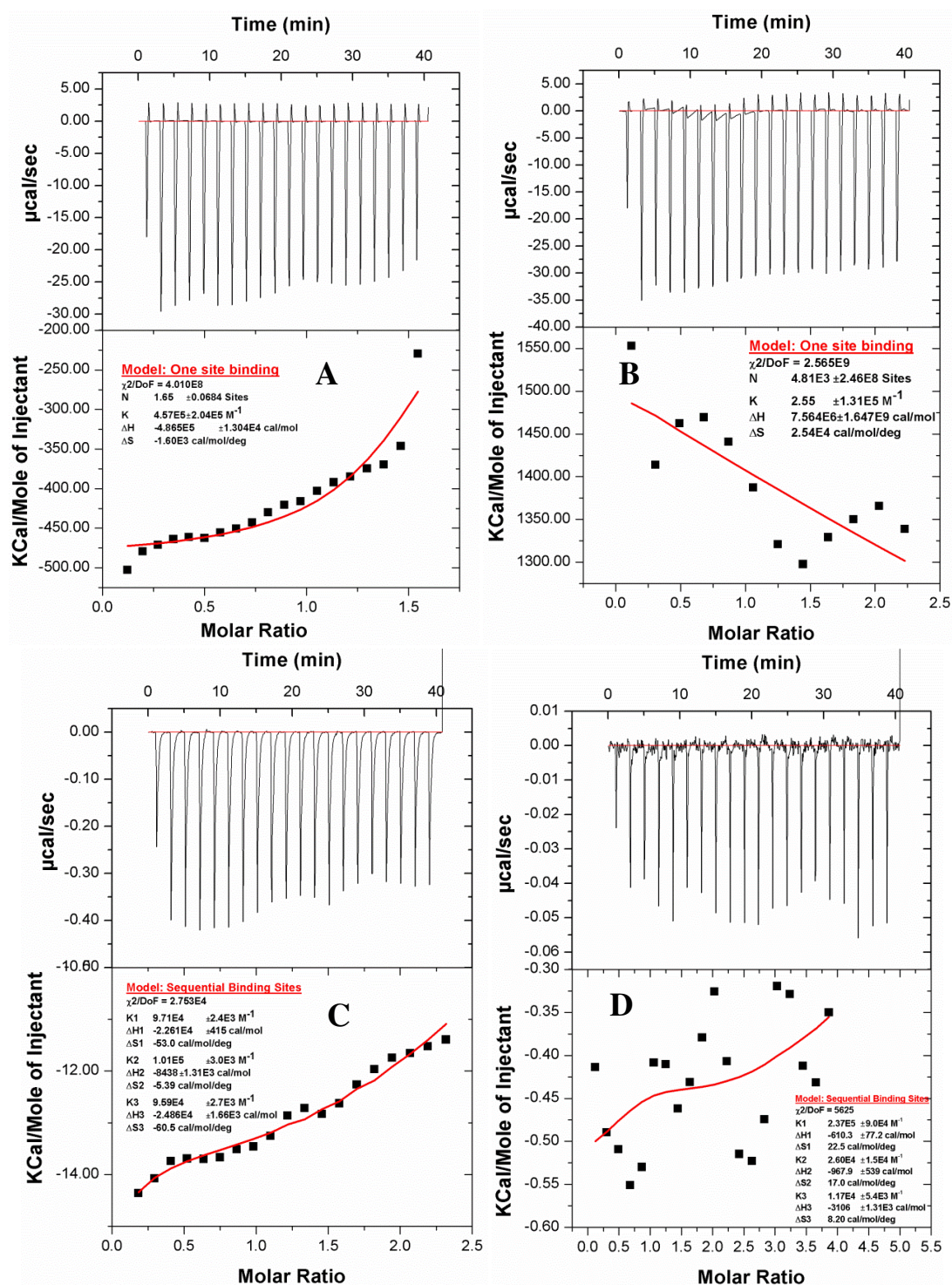


**Figure 103.** ITC figures in water (A) (PBI) **8** with Cu(NO<sub>3</sub>)<sub>2</sub> (B) (PBI) **8** with Ni(NO<sub>3</sub>)<sub>2</sub> (C) 2-pyridylbenzimidazole (PBI)<sub>6</sub> oligomer **22** with Ni(NO<sub>3</sub>)<sub>2</sub>, (D) (PBI)<sub>3</sub>- (PDA)<sub>3</sub> oligomer **25** with Ni(NO<sub>3</sub>)<sub>2</sub>.

### Isothermal Titration Calorimetry (ITC) analysis of synthesized *aeg* linked ligands with nickel nitrate

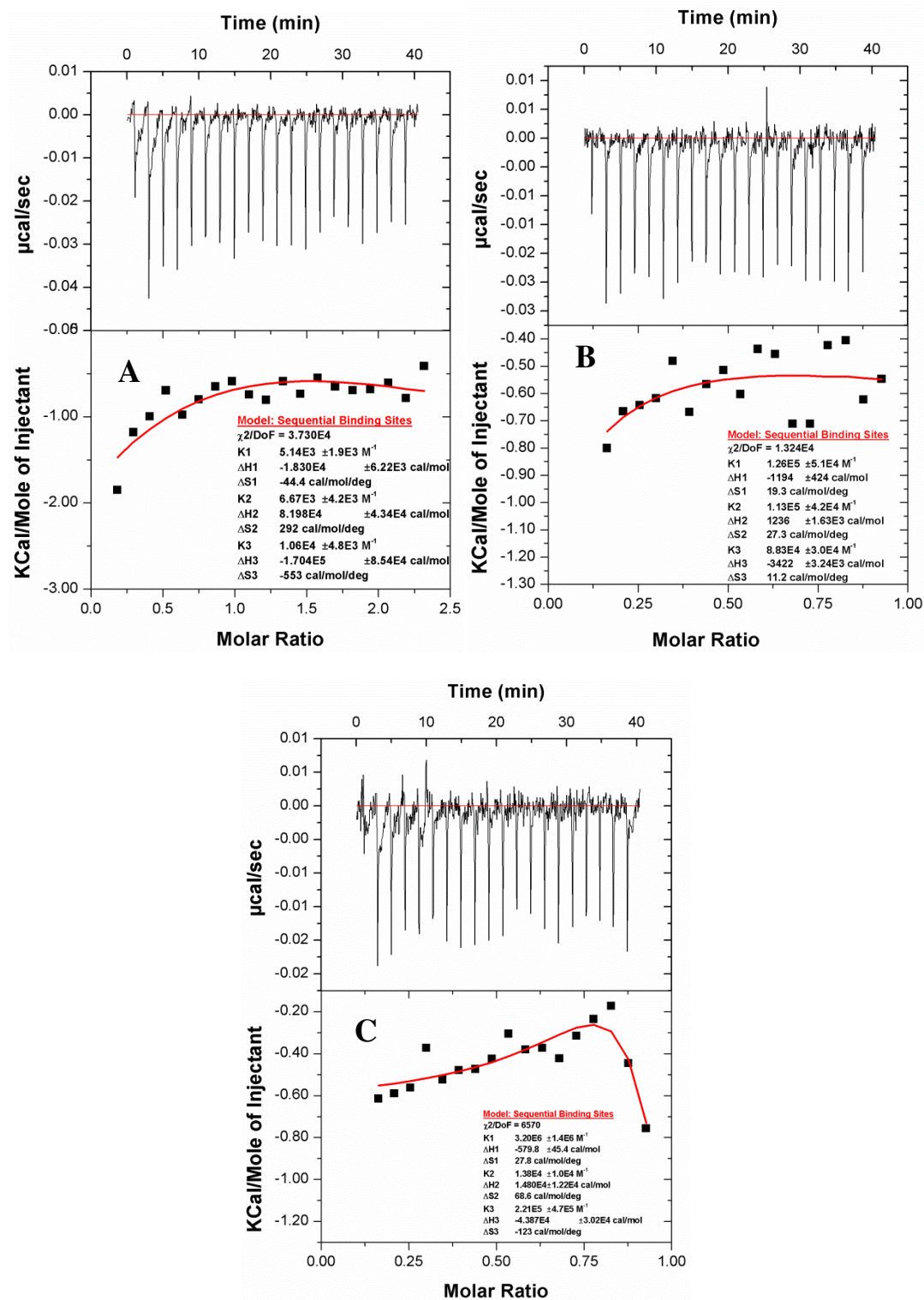


**Figure 104.** ITC figures in water (A) (PBI-PDA)<sub>3</sub> **26** in water Ni(NO<sub>3</sub>)<sub>2</sub> (B) (PBI)<sub>3</sub>-(CAT)<sub>3</sub> **27** with Ni(NO<sub>3</sub>)<sub>2</sub>. (C) (PBI-CAT)<sub>3</sub> **28** with Ni(NO<sub>3</sub>)<sub>2</sub>.

# *Erratum*

---

# An Efficient One-Pot Synthesis of $\alpha$ -Amino Phosphonates Catalyzed by Bismuth Nitrate Pentahydrate

Asish K. Bhattacharya,\* Tanpreet Kaur

Combi Chem-Bio Resource Centre and Division of Organic Chemistry (Synthesis), National Chemical Laboratory, Dr. Homi Bhabha Road, Pune 411 008, Maharashtra, India

Fax +91(20)25902624; E-mail: ak.bhattacharya@ncl.res.in

Received 30 December 2006

Respectfully dedicated to my PhD supervisor and mentor, Dr. Ram P. Sharma, FASc on the occasion of his 68<sup>th</sup> birthday

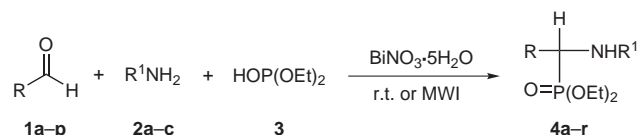
**Abstract:** A simple, efficient, and environmentally benign method has been developed for the synthesis of  $\alpha$ -amino phosphonates through a one-pot reaction of aldehydes with amines and diethyl phosphite in the presence of bismuth nitrate pentahydrate as a catalyst. Some of the major advantages of this protocol are: good yields, the involvement of a less-expensive and non-toxic catalyst, mild and solvent-free reaction conditions and also tolerance towards other functional groups present in the substrates. Eighteen examples are described, highlighting the substrate scope of the reaction.

**Key words:**  $\alpha$ -amino phosphonates, aldehydes, amines, alkyl phosphite, bismuth nitrate pentahydrate, synthetic methods

The synthesis of  $\alpha$ -amino phosphonates has attracted the attention of organic chemists and medicinal chemists worldwide as they are considered to be structural analogues of the corresponding  $\alpha$ -amino acids and transition-state mimics of peptide hydrolysis. The utilities of  $\alpha$ -amino phosphonates as enzyme inhibitors,<sup>1</sup> peptide mimics,<sup>2</sup> antibiotics and pharmacological agents,<sup>3</sup> herbicidal<sup>4</sup> and haptens of catalytic antibodies<sup>5</sup> have been reported. Several synthetic approaches have been reported but the nucleophilic addition reaction of phosphites with imines is one of the most preferred methods, which is usually catalyzed by an alkali-metal alkoxide, e.g. NaOEt or Lewis acids<sup>6</sup> such as  $\text{BF}_3\cdot\text{OEt}_2$ ,  $\text{SnCl}_2$ ,  $\text{SnCl}_4$ ,  $\text{ZnCl}_2$  and  $\text{MgBr}_2$ .<sup>7,8</sup> However, these reactions can not proceed in one pot from a carbonyl compound, an amine and a phosphite because the water that is generated during the course of reaction can decompose or deactivate Lewis acids.<sup>9</sup> This drawback has been overcome by some recent methods using lanthanide triflates/ $\text{MgSO}_4$ ,<sup>10</sup>  $\text{InCl}_3$ ,<sup>11</sup>  $\text{ZrCl}_4$ <sup>12</sup> and  $\text{TaCl}_5\text{-SiO}_2$ .<sup>13</sup> However, many of these methods involve stoichiometric amount of catalysts, expensive reagents,<sup>10</sup> longer reaction times,<sup>13</sup> low yields of products in case of aliphatic aldehydes and amines and in addition, use of harmful organic solvents<sup>10-12</sup> such as  $\text{CH}_2\text{Cl}_2$ , THF or MeCN are undesirable from the viewpoint of today's environmental consciousness. Hence, there is a need to develop an efficient, practically potential and environmentally benign method for the synthesis of  $\alpha$ -amino phosphonates.

Recently, bismuth nitrate has emerged as an efficient Lewis acid<sup>14-16</sup> due to its relatively low toxicity, readily availability at a low cost and tolerance to trace amounts of water. Hence, we considered  $\text{BiNO}_3\cdot 5\text{H}_2\text{O}$  to be an ideal Lewis acid to address some of the limitations posed by known methods. Herein, we disclose  $\text{BiNO}_3\cdot 5\text{H}_2\text{O}$ -catalyzed one-pot synthesis of structurally diverse  $\alpha$ -amino phosphonates from aldehydes, amines and diethyl phosphite.

The reaction of aldehydes with amines results in situ generation of imine intermediate which subsequently reacts with diethylphosphite and affords the  $\alpha$ -amino phosphonates in one pot. The reaction of benzaldehyde with aniline and diethylphosphite was carried out in the presence of  $\text{BiNO}_3\cdot 5\text{H}_2\text{O}$  (10 mol%) under neat conditions or microwave (Scheme 1). The bismuth atom coordinates with the imine nitrogen to facilitate the nucleophilic attack of diethylphosphite to increase the yield of the product.



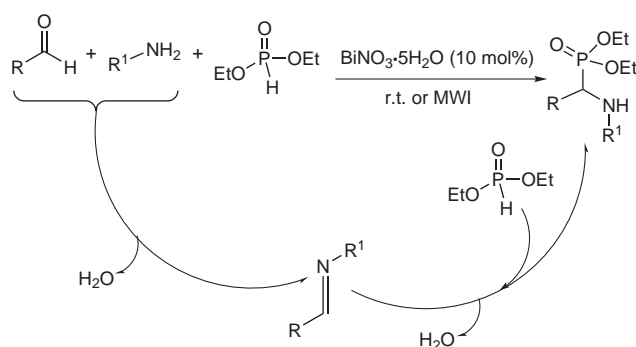
**Scheme 1**

A wide variety of structurally diverse aldehydes were subjected to this novel procedure in the presence of a catalytic amount (10 mol%) of  $\text{BiNO}_3\cdot 5\text{H}_2\text{O}$  and converted into the corresponding  $\alpha$ -amino phosphonates in high to excellent yields (see Table 1).

In all cases, the three-component reaction proceeded smoothly to furnish the corresponding  $\alpha$ -amino phosphonates. Excellent yields of the products were obtained in case of aromatic aldehydes due to their higher reactivity. However, in case of conjugated aldehydes, products were obtained in low yields. Tolerance towards various functional groups in the substrates was evident from the substrates bearing methylenedioxy, methoxy, ethers, halides, olefinic and hydroxy groups. The presence of electron-withdrawing groups at the *para* position in the aldehyde ring resulted in higher yields while at the *meta* position in lower yields. Also, the presence of electron-donating groups in the amine ring resulted in higher yields. A plausible mechanism of formation of  $\alpha$ -amino phosphonates

in one pot catalyzed by  $\text{BiNO}_3 \cdot 5\text{H}_2\text{O}$  is depicted in Scheme 2.

In conclusion,  $\text{BiNO}_3 \cdot 5\text{H}_2\text{O}$  was found to be an efficient catalyst in one-pot reaction of aldehydes, amines, and diethyl phosphite to afford  $\alpha$ -amino phosphonates. The main advantages of this method are: mild, clean and solvent-free reaction conditions, good to excellent yields, and environmentally benign reagent. In addition, our methodology might be useful for substrates containing a wide variety of other functional groups. Furthermore, this method is also expected to have much better application in organic synthesis because of the very low cost and non-toxic nature of the reagent. This reaction system not only provides a novel method for the synthesis of biologically important  $\alpha$ -amino phosphonates but is also an environmentally friendly chemical process.



**Scheme 2** Plausible mechanism of formation of  $\alpha$ -amino phosphonates catalyzed by  $\text{BiNO}_3 \cdot 5\text{H}_2\text{O}$

**Table 1** One-Pot Synthesis of  $\alpha$ -Amino Phosphonates Catalyzed by  $\text{BiNO}_3 \cdot 5\text{H}_2\text{O}$ <sup>17</sup>

Entry	RCHO	R <sup>1</sup> NH <sub>2</sub>	Product	Method A <sup>a</sup>		Method B <sup>b</sup>	
				Time (h)	Yield (%) <sup>c</sup>	Time (min)	Yield (%) <sup>c</sup>
1		1a	2a <b>4a</b>	10	93	4	96
2		1b	2a <b>4b</b>	10	93	2	95
3		1c	2a <b>4c</b>	10	94	2	96
4		1d	2a <b>4d</b>	8	91	3	95
5		1e	2a <b>4e</b>	8	90	4	92
6		1f	2a <b>4f</b>	8	92	2	94
7		1a	2b <b>4g</b>	10	91	4	95
8		1a	2c <b>4h</b>	8	89	2	91
9		1g	2a <b>4i</b>	5	95	2	98
10		1h	2a <b>4j</b>	5	93	2	96
11		1i	2a <b>4k</b>	5	95	1	98

**Table 1** One-Pot Synthesis of  $\alpha$ -Amino Phosphonates Catalyzed by  $\text{BiNO}_3 \cdot 5\text{H}_2\text{O}$ <sup>17</sup> (continued)

Entry	RCHO	R <sup>1</sup> NH <sub>2</sub>	Product	Method A <sup>a</sup>		Method B <sup>b</sup>			
				Time (h)	Yield (%) <sup>c</sup>	Time (min)	Yield (%) <sup>c</sup>		
12		1j		2a	<b>4l</b>	7	80	1	88
13		1k		2a	<b>4m</b>	10	89	3	92
14		1l		2a	<b>4n</b>	8	93	3	95
15		1m		2a	<b>4o</b>	8	94	2	97
16		1n		2a	<b>4p</b>	8	88	2	92
17		1o		2a	<b>4q</b>	5	85	2	90
18		1p		2a	<b>4r</b>	7	92	2	96

<sup>a</sup> Method A: reaction mixtures stirred at r.t.

<sup>b</sup> Method B: reactions carried out under microwave.

<sup>c</sup> Yields refer to those of pure isolated products fully characterized by spectral data.

## Acknowledgment

A.K.B. is grateful to the Director, NCL, Pune for financial support (MLP008626), to Dr. Mukund K. Gurjar, Head, Division of Organic Chemistry and Prof. Krishna N. Ganesh, J. C. Bose Fellow and Director, IISER, Pune for constant encouragement and support. T.K. is grateful to the Council of Scientific and Industrial Research (CSIR), New Delhi for a research fellowship.

## References and Notes

- (1) (a) Giannousis, P. P.; Bartlett, P. A. *J. Med. Chem.* **1987**, *30*, 1603. (b) Allen, M. C.; Fuhrer, W.; Tuck, B.; Wade, R.; Wood, J. M. *J. Med. Chem.* **1989**, *32*, 1652.
- (2) Kafarski, P.; Leczak, B. *Phosphorus, Sulfur Silicon Relat. Elem.* **1991**, *63*, 193.
- (3) (a) Atherton, F. R.; Hassall, C. H.; Lambert, R. W. *J. Med. Chem.* **1986**, *29*, 29. (b) Allen, J. G.; Atherton, F. R.; Hall, M. J.; Hassall, C. H.; Holmes, S. W.; Lambert, R. W.; Nisbet, L. J.; Ringrose, P. S. *Nature (London)* **1978**, *272*, 56. (c) Allen, J. G.; Atherton, F. R.; Hall, M. J.; Hassall, C. H.; Lambert, R. W.; Nisbet, L. J.; Ringrose, P. S. *Antimicrob. Agents Chemother.* **1979**, *15*, 684. (d) Atherton, F. R.; Hall, M. J.; Hassall, C. H.; Lambert, R. W.; Ringrose, P. S. *Antimicrob. Agents Chemother.* **1979**, *15*, 677. (e) Atherton, F. R.; Hall, M. J.; Hassall, C. H.; Lambert, R. W.; Lloyd, W. J.; Ringrose, P. S. *Antimicrob. Agents Chemother.* **1979**, *15*, 696.
- (4) Hassall, C. H.; Hahn, E. F. *Antibiotics*, Vol VI; Springer: Berlin, **1983**, 1–11.
- (5) (a) Hirschmann, R.; Smith, A. B. III; Taylor, C. M.; Benkovic, P. A.; Taylor, S. D.; Yager, K. M.; Sprengeler, P. A.; Benkovic, S. J. *Science* **1994**, *265*, 23. (b) Smith, A. B. III; Taylor, C. M.; Benkovic, S. J.; Hirschmann, R. *Tetrahedron Lett.* **1994**, *35*, 6856.
- (6) (a) Petrov, K. A.; Chauzov, V. A.; Erokhina, T. S. *Usp. Khim.* **1974**, *43*, 2045; *Chem. Abstr.* **1975**, *82*, 43486. (b) Kirby, A. J.; Warren, S. G. *The Organic Chemistry of Phosphorus*; Elsevier: Amsterdam, **1967**.
- (7) Laschat, S.; Kunz, H. *Synthesis* **1992**, 90.
- (8) Zon, J. *Pol. J. Chem.* **1981**, *55*, 643.
- (9) Genet, J. P.; Uziel, J.; Port, M.; Touzin, A. M.; Roland, S.; Thorimbert, S.; Tanier, S. *Tetrahedron Lett.* **1992**, *33*, 77.
- (10) (a) Qian, C.; Huang, T. *J. Org. Chem.* **1998**, *63*, 4125. (b) Lee, S.; Park, J. H.; Kang, J.; Lee, J. K. *Chem. Commun.* **2001**, 1698.
- (11) Ranu, B. C.; Hajra, A.; Jana, U. *Org. Lett.* **1999**, *1*, 1141.
- (12) Yadav, J. S.; Reddy, B. V. S.; Raj, K. S.; Reddy, K. B.; Prasad, A. R. *Synthesis* **2001**, 2277.

- (13) Chandrasekhar, S.; Prakash, S. J.; Jagadeshwar, V.; Narsihmulu, C. *Tetrahedron Lett.* **2001**, *42*, 5561.
- (14) Komatsu, N.; Taniguchi, A.; Uda, M.; Suzuki, H. *Chem. Commun.* **1996**, 1847.
- (15) Eash, K. J.; Pulia, M. S.; Wieland, L. C.; Mohan, R. S. *J. Org. Chem.* **2000**, *65*, 8399.
- (16) Srivastava, N.; Banik, B. K. *J. Org. Chem.* **2003**, *68*, 2109.
- (17) **Method A:** To a mixture of aldehyde (1 mmol) and amine (1 mmol), BiNO<sub>3</sub>·5H<sub>2</sub>O (10 mol%) was added and stirred at r.t. for 5 min, then diethylphosphite (1 mmol) was added dropwise. The stirring of the reaction mixture was continued for the appropriate time (see Table 1) till the completion (TLC) of reaction. The reaction mixture was diluted with H<sub>2</sub>O and extracted with EtOAc (3 × 20 mL). The combined EtOAc extract was washed with brine, dried (anhyd Na<sub>2</sub>SO<sub>4</sub>), and evaporated to furnish crude product, which was purified by column chromatography (hexane–EtOAc, 7:3) over silica gel to provide pure α-amino phosphonates. All the products were characterized by spectral data.
- Method B:** To a mixture of aldehyde (1 mmol), amine (1 mmol), and diethylphosphite (1 mmol), BiNO<sub>3</sub>·5H<sub>2</sub>O (10 mol%) was added and the reaction mixture was irradiated with microwave (Kenstar Model No. OM-9918C; 2450 MHz, 2350 W) for the specified period of time in an open vessel. Work-up of the reaction was carried out as described above.

**Diethyl [(2-Hydroxyphenyl)amino](phenylmethyl)phosphonate (4h)**

Yield 0.304 g, 91%, colorless syrupy liquid. <sup>1</sup>H NMR (200 MHz, CDCl<sub>3</sub>, TMS): δ = 7.46–6.46 (m, 9 H), 4.89 (d, <sup>1</sup>J<sub>PH</sub> = 26.0 Hz, 1 H), 3.61–4.33 (m, 4 H), 1.13 (t, *J* = 7.2 Hz, 3 H), 1.10 (t, *J* = 7.3 Hz, 3 H). <sup>13</sup>C NMR (50 MHz, CDCl<sub>3</sub>, TMS): δ = 145.29 (s, Ph), 135.73 (s, Ph), 134.88 (s, Ph), 128.56 (s, Ph), 128.51 (s, Ph), 128.18 (s, Ph), 128.07 (s, Ph), 127.85 (s, Ph), 119.88 (s, Ph), 118.25 (s, Ph), 114.38 (s, Ph), 111.94 (s, Ph), 64.31 (d, <sup>2</sup>J<sub>PC</sub> = 7.3 Hz, -OCH<sub>2</sub>CH<sub>3</sub>), 63.70 (d, <sup>2</sup>J<sub>PC</sub> = 7.0 Hz, -OCH<sub>2</sub>CH<sub>3</sub>), 55.99 (d, <sup>1</sup>J<sub>PC</sub> = 153.0 Hz, -CHP), 16.49 (d, <sup>3</sup>J<sub>PC</sub> = 5.5 Hz, -OCH<sub>2</sub>CH<sub>3</sub>), 16.19 (d, <sup>3</sup>J<sub>PC</sub> = 5.9 Hz, -OCH<sub>2</sub>CH<sub>3</sub>). Anal. Calcd for C<sub>17</sub>H<sub>22</sub>NO<sub>4</sub>P (335.33): C, 60.89; H, 6.61; N, 4.18. Found: C, 60.72; H, 6.58; N, 4.10.

**Diethyl [1,3-Benzodioxol-5-yl(phenylamino)methyl]phosphonate (4i)**

Yield 0.355 g, 98%, white solid; mp 112–13 °C. <sup>1</sup>H NMR (200 MHz, CDCl<sub>3</sub>, TMS): δ = 7.16–6.57 (m, 8 H), 5.94 (s, 2 H), 4.72 (d, <sup>1</sup>J<sub>PH</sub> = 23.1 Hz, 1 H), 4.17 (m, 4 H), 1.30 (t, *J* = 6.1 Hz, 3 H), 1.17 (t, *J* = 6.5 Hz, 3 H). <sup>13</sup>C NMR (50 MHz, CDCl<sub>3</sub>, TMS): δ = 145.29 (s, Ph), 144.80 (s, Ph), 144.51 (s, Ph), 143.92 (s, Ph), 143.85 (s, Ph), 127.35 (s, Ph), 125.49 (s, Ph), 125.44 (s, Ph), 119.21 (s, Ph), 116.59 (s, Ph), 112.12 (s, Ph), 108.67 (s, Ph), 108.58 (s, Ph), 61.64 (d, <sup>2</sup>J<sub>PC</sub> = 7.0 Hz, -OCH<sub>2</sub>CH<sub>3</sub>), 61.58 (d, <sup>2</sup>J<sub>PC</sub> = 7.1 Hz, -OCH<sub>2</sub>CH<sub>3</sub>), 54.12 (s, -OCH<sub>3</sub>), 53.91 (d, <sup>1</sup>J<sub>PC</sub> = 152.1 Hz, -CHP), 14.65 (d, <sup>3</sup>J<sub>PC</sub> = 5.8 Hz, -OCH<sub>2</sub>CH<sub>3</sub>), 14.47 (d, <sup>3</sup>J<sub>PC</sub> = 6.0 Hz, -OCH<sub>2</sub>CH<sub>3</sub>). Anal. Calcd for C<sub>18</sub>H<sub>22</sub>NO<sub>5</sub>P (363.34): C, 59.50; H, 6.10; N, 3.85. Found: C, 59.32; H, 6.05; N, 3.78.

**Diethyl [(4-Hydroxy-3-methoxyphenyl)(phenylamino)methyl]phosphonate (4k)**

Yield 0.357 g, 98%, colorless syrupy liquid. <sup>1</sup>H NMR (200 MHz, CDCl<sub>3</sub>, TMS): δ = 7.14–6.60 (m, 8 H), 4.77 (d, <sup>1</sup>J<sub>PH</sub> = 24.4 Hz, 1 H), 4.16–3.67 (m, 4 H), 3.86 (s, 3 H), 3.84 (s, 3 H), 1.28 (t, *J* = 7.43 Hz, 3 H), 1.10 (t, *J* = 7.2 Hz, 3 H). <sup>13</sup>C NMR (50 MHz, CDCl<sub>3</sub>, TMS): δ = 145.34 (s, Ph), 145.29 (s, Ph), 144.80 (s, Ph), 143.85 (s, Ph), 127.35 (s, Ph), 125.44 (s, Ph), 119.21 (s, Ph), 116.59 (s, Ph), 112.84 (s, Ph), 112.12 (s, Ph), 108.67 (s, Ph), 108.58 (s, Ph), 63.44 (d, <sup>2</sup>J<sub>PC</sub> = 7.0 Hz, -OCH<sub>2</sub>CH<sub>3</sub>), 63.39 (d, <sup>2</sup>J<sub>PC</sub> = 7.3 Hz, -OCH<sub>2</sub>CH<sub>3</sub>), 54.12 (s, -OCH<sub>3</sub>), 53.91 (d, <sup>1</sup>J<sub>PC</sub> = 152.0 Hz, -CHP), 16.48 (d, <sup>3</sup>J<sub>PC</sub> = 6.4 Hz, -OCH<sub>2</sub>CH<sub>3</sub>), 16.30 (d, <sup>3</sup>J<sub>PC</sub> = 6.0 Hz, -OCH<sub>2</sub>CH<sub>3</sub>). Anal. Calcd for C<sub>18</sub>H<sub>24</sub>NO<sub>5</sub>P (365.36): C, 59.17; H, 6.62; N, 3.83. Found: C, 59.05; H, 6.45; N, 3.78.

**Diethyl [(2-hydroxy-6-methoxyphenyl)(phenylamino)methyl]phosphonate (4n)**

Yield 0.346 g, 95%, white solid; mp 116–18 °C. <sup>1</sup>H NMR (200 MHz, CDCl<sub>3</sub>, TMS): δ = 7.13–6.64 (m, 8 H), 5.25 (d, <sup>1</sup>J<sub>PH</sub> = 24.2 Hz, 1 H), 4.21–3.86 (m, 4 H), 4.13 (s, 3 H), 1.29 (t, *J* = 7.0 Hz, 3 H), 1.10 (t, *J* = 7.0 Hz, 3 H). <sup>13</sup>C NMR (50 MHz, CDCl<sub>3</sub>, TMS): δ = 147.03 (s, Ph), 146.51 (s, Ph), 146.22 (s, Ph), 144.15 (s, Ph), 129.22 (s, Ph), 122.12 (s, Ph), 120.56 (s, Ph), 120.19 (s, Ph), 118.52 (s, Ph), 113.88 (s, Ph), 110.36 (s, Ph), 63.50 (d, <sup>2</sup>J<sub>PC</sub> = 7.2 Hz, -OCH<sub>2</sub>CH<sub>3</sub>), 56.07 (s, -OCH<sub>3</sub>), 49.58 (d, <sup>1</sup>J<sub>PC</sub> = 155.6 Hz, -CHP), 16.50 (d, <sup>3</sup>J<sub>PC</sub> = 6.1 Hz, -OCH<sub>2</sub>CH<sub>3</sub>), 16.23 (d, <sup>3</sup>J<sub>PC</sub> = 5.9 Hz, -OCH<sub>2</sub>CH<sub>3</sub>). Anal. Calcd for C<sub>18</sub>H<sub>24</sub>NO<sub>5</sub>P (365.36): C, 59.17; H, 6.62; N, 3.83. Found: C, 59.02; H, 6.42; N, 3.75.

**Diethyl [(3-Hydroxy-4-methoxyphenyl)(phenylamino)methyl]phosphonate (4o)**

Yield 0.354 g, 97%, colorless syrupy liquid. <sup>1</sup>H NMR (200 MHz, CDCl<sub>3</sub>, TMS): δ = 7.12–6.57 (m, 8 H), 4.73 (d, <sup>1</sup>J<sub>PH</sub> = 24.0 Hz, 1 H), 4.15–3.68 (m, 4 H), 3.80 (s, 3 H), 1.26 (t, *J* = 7.1 Hz, 3 H), 1.12 (t, *J* = 7.0 Hz, 3 H). <sup>13</sup>C NMR (50 MHz, CDCl<sub>3</sub>, TMS): δ = 147.02 (s, Ph), 147.00 (s, Ph), 146.37 (s, Ph), 129.19 (s, Ph), 128.59 (s, Ph), 119.60 (s, Ph), 118.37 (s, Ph), 118.18 (s, Ph), 114.67 (s, Ph), 114.01 (s, Ph), 63.55 (d, <sup>2</sup>J<sub>PC</sub> = 7.0 Hz, -OCH<sub>2</sub>CH<sub>3</sub>), 55.93 (s, -OCH<sub>3</sub>), 55.51 (d, <sup>1</sup>J<sub>PC</sub> = 153.8 Hz, -CHP), 16.47 (d, <sup>3</sup>J<sub>PC</sub> = 5.5 Hz, -OCH<sub>2</sub>CH<sub>3</sub>), 16.30 (d, <sup>3</sup>J<sub>PC</sub> = 5.8 Hz, -OCH<sub>2</sub>CH<sub>3</sub>). Anal. Calcd for C<sub>18</sub>H<sub>24</sub>NO<sub>5</sub>P (365.35): C, 59.17; H, 6.62; N, 3.83. Found: C, 59.12; H, 6.48; N, 3.78.

**Diethyl [[4-(2,3-dihydroxypropoxy)phenyl](phenylamino)methyl]phosphonate (4r)**

Yield 0.392 g, 96%, colorless syrupy liquid. <sup>1</sup>H NMR (200 MHz, CDCl<sub>3</sub>, TMS): δ = 7.39–6.57 (m, 9 H), 4.77 (d, <sup>1</sup>J<sub>PH</sub> = 25.6 Hz, 1 H), 4.14–3.65 (m, 4 H), 1.27 (t, *J* = 7.1 Hz, 3 H), 1.13 (t, *J* = 7.3 Hz, 3 H). <sup>13</sup>C NMR (50 MHz, CDCl<sub>3</sub>, TMS): δ = 158.33 (s, Ph), 158.28 (s, Ph), 146.43 (s, Ph), 146.14 (s, Ph), 129.18 (s, Ph), 129.01 (s, Ph), 128.06 (s, Ph), 120.19 (s, Ph), 118.46 (s, Ph), 114.73 (s, Ph), 114.68 (s, Ph), 113.98 (s, Ph), 70.43 (s, -CHOH), 69.08 (s, -CH<sub>2</sub>OH), 63.49 (d, <sup>2</sup>J<sub>PC</sub> = 7.3 Hz, -OCH<sub>2</sub>CH<sub>3</sub>), 63.43 (d, <sup>2</sup>J<sub>PC</sub> = 7.3 Hz, -OCH<sub>2</sub>CH<sub>3</sub>), 55.26 (d, <sup>1</sup>J<sub>PC</sub> = 151.0 Hz, -CHP), 16.42 (d, <sup>3</sup>J<sub>PC</sub> = 5.5 Hz, -OCH<sub>2</sub>CH<sub>3</sub>), 16.25 (d, <sup>3</sup>J<sub>PC</sub> = 5.5 Hz, -OCH<sub>2</sub>CH<sub>3</sub>). Anal. Calcd for C<sub>20</sub>H<sub>28</sub>NO<sub>6</sub>P (409.41): C, 58.67; H, 6.89; N, 3.42. Found: C, 58.50; H, 6.78; N, 3.36.

# Synthesis of the Antibacterial Benzoquinone Primin and its Water-Soluble Analogue, Primin Acid

Asish K. Bhattacharya,\* Tanpreet Kaur, Krishna N. Ganesh

Division of Organic Chemistry and Combi Chem-Bio Resource Centre, National Chemical Laboratory,

Dr. Homi Bhabha Road, Pune-411 008, India

Fax +91(20)25902629; E-mail: ak.bhattacharya@ncl.res.in

Received 1 December 2009; revised 14 December 2009

Dedicated to Dr. Ram P. Sharma, FASc, on the occasion of his 71<sup>st</sup> birthday

**Abstract:** The biologically active natural product, primin and its water-soluble acid analogue, primin acid are prepared in 34% and 25% overall yields, respectively, from a common intermediate using a Grignard reaction and a Johnson–Claisen rearrangement as the key steps.

**Key words:** 1,4-benzoquinones, primin, primin acid, Johnson–Claisen rearrangement, antibacterial

During a search for potential anticancer agents from the Suriname rainforest, Kingston et al.<sup>1</sup> isolated primin (2-methoxy-6-pentyl-1,4-benzoquinone) (**1**) and several other benzoquinones from the plant *Miconia lepidota* DC (Melastomataceae). Primin (**1**) (Figure 1) has been reported to occur in various plants including *Primula obconica* (primrose)<sup>2</sup> and *Miconia sp.*,<sup>3</sup> and has also been isolated from the broth extract of the endophytic fungus, *Botryosphaeria mamane* PSU-M76.<sup>4</sup> Compound **1** demonstrates antibacterial activity against *Staphylococcus aureus* ATCC 25923 and methicillin-resistant *S. aureus* SK1 with identical minimum inhibitory concentration (MIC) values of 8 µg/mL, as well as antiprotozoal, antimycobacterial and anticancer activity.<sup>1,5</sup> Primin also exhibits allergenic properties, is a strong sensitizer and can induce contact dermatitis.<sup>6</sup>

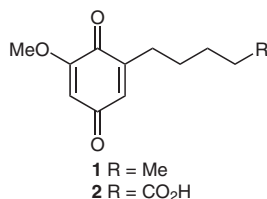
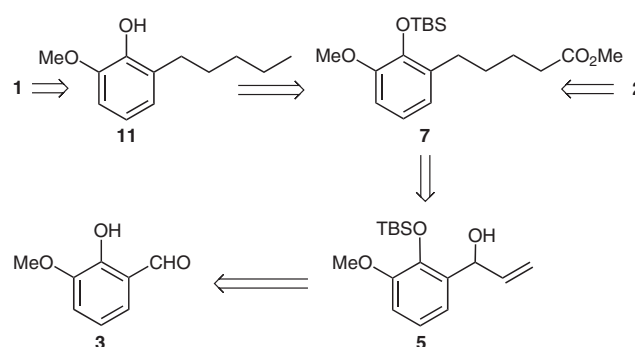


**Figure 1** Structures of primin (**1**) and primin acid (**2**)

The literature reports five synthetic approaches to primin,<sup>1,7</sup> and only one for its water-soluble analogue, primin acid (**2**).<sup>7b</sup> In continuation of our research on the synthesis of antibacterial agents and other bioactive molecules,<sup>8</sup> we were interested in the synthesis of **1** and its water-soluble analogue **2** due to their diverse biological activity.<sup>1,5</sup> Herein, we report a new and efficient synthesis

of primin (**1**) and primin acid (**2**) employing a Grignard reaction and a Johnson–Claisen rearrangement<sup>9</sup> as the key steps.

The retrosyntheses of compounds **1** and **2** are shown in Scheme 1. Compound **7** was envisaged as a common intermediate for the synthesis of **1** and **2**. Intermediate **7** could be prepared via a Johnson–Claisen rearrangement of allylic alcohol **5** followed by reduction.



**Scheme 1** Retrosyntheses of primin (**1**) and primin acid (**2**)

The synthesis of common intermediate **7** commenced from commercially available *ortho*-vanillin (**3**) (Scheme 2). Thus, protection<sup>10</sup> of the phenolic hydroxy group was accomplished using *tert*-butyldimethylsilyl chloride in *N,N*-dimethylformamide to give compound **4** in 95% yield. Reaction of aldehyde **4** with vinylmagnesium bromide, under Grignard conditions,<sup>11</sup> furnished allylic alcohol **5** in 92% yield. Next, compound **5** was subjected to Johnson–Claisen rearrangement<sup>9</sup> using trimethyl orthoacetate, xylene and a catalytic amount of propanoic acid to furnish ester **6** in 90% yield. Hydrogenation of the alkene in ester **6** resulted in formation of common intermediate **7**. Reduction of the methyl ester group in **7** with lithium aluminum hydride in tetrahydrofuran furnished alcohol **8** in 91% yield.

The primary hydroxy group of **8** was protected to give tosylate **9** which underwent reductive cleavage with lithium aluminum hydride in tetrahydrofuran to afford compound **10**. The *tert*-butyldimethylsilyl group was removed<sup>12</sup> using lithium hydroxide in *N,N*-dimethylformamide to furnish alcohol **11**. Finally, oxidation of **11** with salcomine [*N,N'*-bis(salicylidene)ethylenediaminocobalt(II)]<sup>7</sup> afforded the title compound, primin (**1**) in 81% yield.

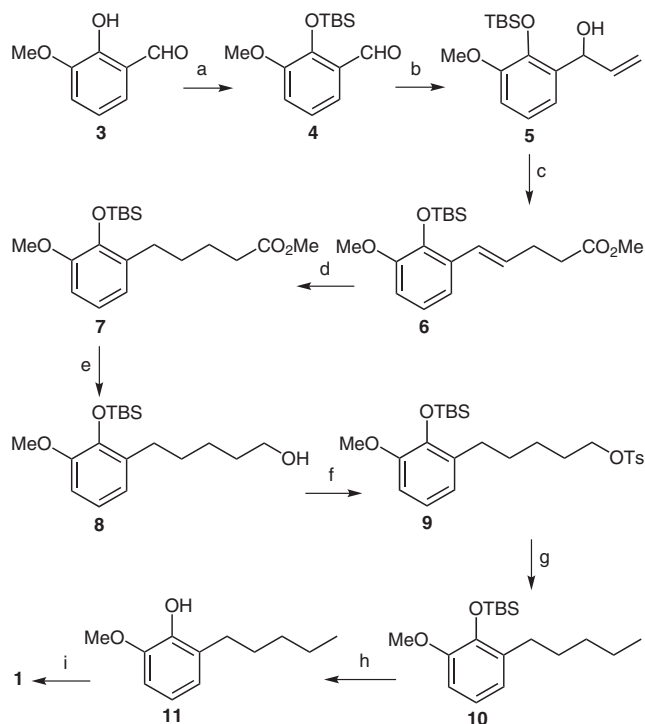
**SYNTHESIS** 2010, No. 7, pp 1141–1144

Advanced online publication: 05.02.2010

DOI: 10.1055/s-0029-1218666; Art ID: Z26109SS

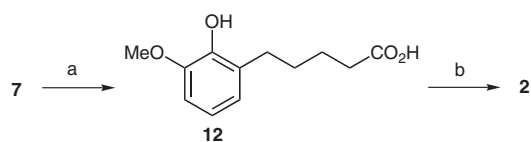
© Georg Thieme Verlag Stuttgart · New York





**Scheme 2** Reagents and conditions: (a) TBSCl, DMF, 95%; (b) vinylmagnesium bromide, THF, 92%; (c) MeC(OMe)<sub>3</sub>, xylene, propanoic acid, 90%; (d) H<sub>2</sub>, Pd/C (10%), MeOH, 94%; (e) LAH, THF, 91%; (f) TsCl, py, 93%; (g) LAH, THF, 95%; (h) LiOH, DMF, 80%; (i) *N,N'*-bis(salicylidene)ethylenediaminocobalt(II), DMF, 81%.

Cleavage of the *tert*-butyldimethylsilyl group and hydrolysis of the methyl ester of the key intermediate **7** resulted in the formation of acid **12**. Subsequent oxidation using the same conditions<sup>7</sup> as those employed for the synthesis of **1** afforded the water-soluble analogue, primin acid (**2**) in 71% yield (Scheme 3).



**Scheme 3** Reagents and conditions: (a) KOH, MeOH–H<sub>2</sub>O (3:1), 55%; (b) *N,N'*-bis(salicylidene)ethylenediaminocobalt(II), DMF, 71%.

In conclusion, the antibacterial benzoquinones, primin (**1**) and its water-soluble analogue, primin acid (**2**), have been prepared in 34% and 25% overall yields, respectively, starting from *ortho*-vanillin using a Grignard reaction and a Johnson–Claisen rearrangement as the key steps. The results described herein constitute a short, efficient and high yielding synthetic route to compounds **1** and **2** which should enable further investigation of their biological activity.

Melting points were determined in open capillaries using a Büchi B-5400 melting point apparatus and are uncorrected. Reagents and

starting materials were obtained from commercial suppliers and were used without further purification. THF was distilled over sodium/benzophenone. DMF was distilled over 3 Å molecular sieves. All reactions were conducted using flame-dried glassware under inert atmospheres. Thin layer chromatography (TLC) was performed using pre-coated silica gel F<sub>254</sub> aluminium sheets, obtained from Merck, Germany. Chromatography refers to purification by column chromatography using silica gel (100–200 mesh size; Spectrochem, India). IR spectra were recorded on a Perkin–Elmer Spectra One FT-IR spectrophotometer. <sup>1</sup>H and <sup>13</sup>C NMR spectra were recorded at 200 MHz and 50 MHz, respectively, on a Bruker AC200 spectrometer in CDCl<sub>3</sub> using TMS as the internal standard. Chemical shifts (δ) are reported in ppm. Coupling constants (*J*) are given in Hz. ESI-MS were obtained using an API-Q-Star Applied Biosystems spectrometer. The characterization data of compounds **11**,<sup>7a</sup> **1**,<sup>1</sup> **12**<sup>7b</sup> and **2**<sup>7b</sup> were in full agreement with reported data.

**CAUTION:** Primin (**1**) is a strong sensitizer and should be handled with care; contact with skin should be avoided.

#### 2-(*tert*-Butyldimethylsilyloxy)-3-methoxybenzaldehyde (**4**)

Imidazole (3.3 g, 49.0 mmol) and TBSCl (7.4 g, 49.0 mmol) were added to a soln of *ortho*-vanillin (5.0 g, 32.0 mmol) in anhyd DMF (10 mL). The reaction was complete in 7 h (TLC) and the precipitate formed during the reaction was extracted with EtOAc (3 × 50 mL). The combined organic layer was washed with brine (10 mL), dried over anhyd Na<sub>2</sub>SO<sub>4</sub> and evaporated to give a crude residue which was purified by chromatography (hexane–EtOAc, 8:2) to afford product **4**.

Colorless oil; yield: 8.3 g (95%); *R*<sub>f</sub> = 0.66 (hexane–EtOAc, 7:3).

IR (CHCl<sub>3</sub>): 3034, 2957, 1584, 1481, 1216, 1071 cm<sup>-1</sup>.

<sup>1</sup>H NMR (CDCl<sub>3</sub>): δ = 10.30 (s, 1 H), 7.16 (dd, *J* = 8.0, 8.0 Hz, 1 H), 6.86–6.70 (m, 2 H), 3.61 (s, 3 H), 0.79 (s, 9 H), 0.00 (s, 6 H).

<sup>13</sup>C NMR (CDCl<sub>3</sub>): δ = 190.3, 150.8, 149.2, 127.9, 121.2, 119.1, 116.9, 55.1, 25.9, 19.0, –4.1.

ESI-MS: *m/z* = 267 [M + H]<sup>+</sup>, 289 [M + Na]<sup>+</sup>, 305 [M + K]<sup>+</sup>.

Anal. Calcd for C<sub>14</sub>H<sub>22</sub>O<sub>3</sub>Si: C, 63.12; H, 8.32. Found: C, 63.20; H, 8.40.

#### 1-[2-(*tert*-Butyldimethylsilyloxy)-3-methoxyphenyl]prop-2-en-1-ol (**5**)

Compound **4** (3.9 g, 15.0 mmol) was dissolved in anhyd THF (10 mL) and cooled using an ice-bath. Vinylmagnesium bromide (15 mL, 15.0 mmol, 1.0 M in THF) was added over a period of 10 min and stirring was continued at 0 °C for 5 h. After completion of the reaction (TLC), aq NH<sub>4</sub>Cl soln (2 mL) was added, the reaction mixture was diluted with H<sub>2</sub>O (50 mL) and the product was extracted with EtOAc (3 × 50 mL). The organic layer was washed with brine (10 mL), dried over anhyd Na<sub>2</sub>SO<sub>4</sub>, and evaporated to furnish a crude residue which was purified by chromatography (hexane–EtOAc, 7:3) to give allylic alcohol **5**.

Colorless oil; yield: 4.05 g (92%); *R*<sub>f</sub> = 0.52 (hexane–EtOAc, 7:3).

IR (CHCl<sub>3</sub>): 3455, 3018, 2931, 1735, 1459, 1217, 1071 cm<sup>-1</sup>.

<sup>1</sup>H NMR (CDCl<sub>3</sub>): δ = 6.98–6.95 (m, 2 H), 6.83–6.81 (m, 1 H), 6.22–6.06 (m, 1 H), 5.71 (t, *J* = 4.3 Hz, 1 H), 5.44–5.21 (m, 2 H), 3.84 (s, 3 H), 1.05 (s, 9 H), 0.25 (s, 6 H).

<sup>13</sup>C NMR (CDCl<sub>3</sub>): δ = 149.7, 142.2, 139.4, 133.7, 121.3, 119.0, 114.4, 110.7, 69.0, 54.8, 26.2, 19.0, –3.7.

ESI-MS: *m/z* = 295 [M + H]<sup>+</sup>, 317 [M + Na]<sup>+</sup>, 333 [M + K]<sup>+</sup>.

Anal. Calcd for C<sub>16</sub>H<sub>26</sub>O<sub>3</sub>Si: C, 65.26; H, 8.90. Found: C, 65.36; H, 8.98.

**Methyl (4E)-5-[2-(*tert*-Butyldimethylsilyloxy)-3-methoxyphenyl]pent-4-enoate (6)**

Compound **5** (4.0 g, 13.6 mmol) in xylene (5 mL) was treated with trimethyl orthoacetate (9.79 g, 10.2 mL, 8.1 mmol) and propanoic acid (40  $\mu$ L), and the resulting mixture was heated at 140 °C for 6 h. After completion of the reaction, the xylene was evaporated under reduced pressure. The crude residue was purified by chromatography (hexane–EtOAc, 8:2) to give pure product **6**.

Colorless oil; yield: 4.28 g (90%);  $R_f$  = 0.60 (hexane–EtOAc, 7:3).

IR (CHCl<sub>3</sub>): 3021, 2955, 1738, 1480, 1252, 1086 cm<sup>-1</sup>.

<sup>1</sup>H NMR (CDCl<sub>3</sub>):  $\delta$  = 7.32–6.75 (m, 4 H), 6.26–6.13 (m, 1 H), 3.82 (s, 3 H), 3.75 (s, 3 H), 2.75–2.34 (m, 4 H), 1.15 (s, 9 H), 0.28 (s, 6 H).

<sup>13</sup>C NMR (CDCl<sub>3</sub>):  $\delta$  = 173.3, 150.6, 142.1, 129.5, 128.3, 126.4, 121.0, 118.0, 110.1, 54.8, 51.5, 33.8, 28.7, 26.1, 18.9, –4.0.

ESI-MS:  $m/z$  = 351 [M + H]<sup>+</sup>, 373 [M + Na]<sup>+</sup>, 389 [M + K]<sup>+</sup>.

Anal. Calcd for C<sub>19</sub>H<sub>30</sub>O<sub>4</sub>Si: C, 65.10; H, 8.63. Found: C, 65.20; H, 8.72.

**Methyl 5-[2-(*tert*-Butyldimethylsilyloxy)-3-methoxyphenyl]pentanoate (7)**

To compound **6** (4.5 g, 12.8 mmol) in anhyd MeOH (10 mL) was added 10% Pd/C (0.1 g) and the heterogeneous soln was stirred vigorously for 12 h under a H<sub>2</sub> atm. After completion of the reaction (TLC), the mixture was filtered over Celite. The filtrate was evaporated and the crude product was purified by chromatography (hexane–EtOAc, 8:2) to furnish pure ester **7**.

Colorless oil; yield: 4.24 g (94%);  $R_f$  = 0.51 (hexane–EtOAc, 7:3).

IR (CHCl<sub>3</sub>): 3033, 2937, 1735, 1475, 1234, 1088 cm<sup>-1</sup>.

<sup>1</sup>H NMR (CDCl<sub>3</sub>):  $\delta$  = 6.64–6.54 (m, 3 H), 3.58 (s, 3 H), 3.47 (s, 3 H), 2.46 (t,  $J$  = 7.6 Hz, 2 H), 2.14 (t,  $J$  = 7.1 Hz, 2 H), 1.55–1.44 (m, 4 H), 0.82 (s, 9 H), 0.00 (s, 6 H).

<sup>13</sup>C NMR (CDCl<sub>3</sub>):  $\delta$  = 174.2, 149.9, 142.7, 133.4, 121.8, 120.6, 109.1, 54.7, 51.5, 34.1, 30.2, 29.6, 26.2, 24.9, 18.9, –3.8.

ESI-MS:  $m/z$  = 353 [M + H]<sup>+</sup>, 375 [M + Na]<sup>+</sup>, 391 [M + K]<sup>+</sup>.

Anal. Calcd for C<sub>19</sub>H<sub>32</sub>O<sub>4</sub>Si: C, 64.73; H, 9.15. Found: C, 64.81; H, 9.22.

**5-[2-(*tert*-Butyldimethylsilyloxy)-3-methoxyphenyl]pentan-1-ol (8)**

Compound **7** (4.0 g, 11.0 mmol) was dissolved in anhyd THF (10 mL) and the soln was cooled using an ice-bath. LAH (0.4 g, 11.0 mmol) was added slowly and the mixture stirred at r.t. for 4 h under an Ar atm. After completion of the reaction (TLC), the mixture was cooled to 0–5 °C and quenched with 1 N NaOH (10 mL). The resulting white precipitate was filtered through Celite and the filtrate was dried over anhyd Na<sub>2</sub>SO<sub>4</sub> and evaporated. The crude residue was purified by chromatography (hexane–EtOAc, 7:3) to give product **8**.

Colorless viscous oil; yield: 3.35 g (91%);  $R_f$  = 0.31 (hexane–EtOAc, 7:3).

IR (CHCl<sub>3</sub>): 2953, 2930, 1720, 1465, 1250, 1082 cm<sup>-1</sup>.

<sup>1</sup>H NMR (CDCl<sub>3</sub>):  $\delta$  = 6.68–6.48 (m, 3 H), 3.58 (s, 3 H), 3.46 (t,  $J$  = 6.4 Hz, 2 H), 2.45 (t,  $J$  = 7.3 Hz, 2 H), 1.43–1.13 (m, 6 H), 0.82 (s, 9 H), 0.00 (s, 6 H).

<sup>13</sup>C NMR (CDCl<sub>3</sub>):  $\delta$  = 149.9, 142.7, 133.9, 121.9, 120.6, 109.0, 62.9, 54.7, 32.8, 30.0, 29.1, 26.2, 25.8, 18.9, –3.8.

ESI-MS:  $m/z$  = 325 [M + H]<sup>+</sup>, 347 [M + Na]<sup>+</sup>, 363 [M + K]<sup>+</sup>.

Anal. Calcd for C<sub>18</sub>H<sub>32</sub>O<sub>3</sub>Si: C, 66.62; H, 9.94. Found: C, 66.73; H, 9.88.

**5-[2-(*tert*-Butyldimethylsilyloxy)-3-methoxyphenyl]pentyl 4-Methylbenzenesulfonate (9)**

Compound **8** (3.0 g, 9.2 mmol) in anhyd CH<sub>2</sub>Cl<sub>2</sub> (10 mL) was treated with Et<sub>3</sub>N (1.0 mL), TsCl (1.74 g, 9.2 mmol) and DMAP (cat.) and the resulting mixture stirred at r.t. for 2 h. After completion of the reaction (TLC), the reaction mixture was quenched with brine (10 mL) and extracted with CH<sub>2</sub>Cl<sub>2</sub> (3  $\times$  50 mL). The combined organic layer was dried over anhyd Na<sub>2</sub>SO<sub>4</sub> and evaporated to give a crude residue which was purified by chromatography (hexane–EtOAc, 9:1) to furnish product **9**.

Colorless oil; yield: 4.11 g (93%);  $R_f$  = 0.50 (hexane–EtOAc, 7:3).

IR (CHCl<sub>3</sub>): 3013, 2920, 1720, 1432, 1389, 1208, 1065 cm<sup>-1</sup>.

<sup>1</sup>H NMR (CDCl<sub>3</sub>):  $\delta$  = 7.71 (d,  $J$  = 8.0 Hz, 2 H), 7.60 (d,  $J$  = 8.0 Hz, 2 H), 6.63–6.51 (m, 3 H), 3.83 (t,  $J$  = 6.3 Hz, 2 H), 3.57 (s, 3 H), 2.39 (t,  $J$  = 6.9 Hz, 2 H), 2.27 (s, 3 H), 1.47–1.19 (m, 6 H), 0.81 (s, 9 H), 0.00 (s, 6 H).

<sup>13</sup>C NMR (CDCl<sub>3</sub>):  $\delta$  = 149.9, 147.0, 144.8, 142.7, 141.6, 133.4, 130.4, 127.0, 121.9, 120.7, 109.2, 70.7, 54.7, 30.3, 29.4, 28.8, 26.2, 25.3, 21.8, 18.9, –3.7.

ESI-MS:  $m/z$  = 479 [M + H]<sup>+</sup>, 501 [M + Na]<sup>+</sup>, 517 [M + K]<sup>+</sup>.

Anal. Calcd for C<sub>25</sub>H<sub>38</sub>O<sub>5</sub>SSi: C, 62.72; H, 8.00. Found: C, 62.67; H, 8.12.

***tert*-Butyl(2-methoxy-6-pentylphenoxy)dimethylsilane (10)**

Compound **9** (4.0 g, 8.3 mmol) was dissolved in anhyd THF (10 mL) and cooled in ice-bath. LAH (0.3 g, 8.3 mmol) was added slowly and the reaction mixture stirred at r.t. for 4 h under an Ar atm. After completion of the reaction (TLC), the mixture was cooled to 0–5 °C and quenched with 1 N NaOH (10 mL). The resulting white precipitate was filtered through Celite, the filtrate dried over anhyd Na<sub>2</sub>SO<sub>4</sub> and evaporated to give a crude residue which was purified by chromatography (hexane–EtOAc, 9:1) to furnish product **10**.

Colorless oil; yield: 2.4 g (95%);  $R_f$  = 0.83 (hexane–EtOAc, 7:3).

IR (CHCl<sub>3</sub>): 3019, 2839, 1585, 1486, 1261, 1099 cm<sup>-1</sup>.

<sup>1</sup>H NMR (CDCl<sub>3</sub>):  $\delta$  = 6.94–6.74 (m, 2 H), 3.84 (s, 3 H), 2.68 (t,  $J$  = 7.8 Hz, 3 H), 1.65 (t,  $J$  = 7.3 Hz, 1 H), 1.42 (t,  $J$  = 7.4 Hz, 3 H), 1.08 (s, 9 H), 0.96 (t,  $J$  = 6.9 Hz, 3 H), 0.25 (s, 6 H).

<sup>13</sup>C NMR (CDCl<sub>3</sub>):  $\delta$  = 149.9, 142.7, 134.3, 129.9, 121.9, 120.5, 108.9, 32.0, 30.6, 30.0, 26.2, 22.7, 19.0, 14.1, –3.4.

ESI-MS:  $m/z$  = 309 [M + H]<sup>+</sup>, 331 [M + Na]<sup>+</sup>, 347 [M + K]<sup>+</sup>.

Anal. Calcd for C<sub>18</sub>H<sub>32</sub>O<sub>2</sub>Si: C, 70.07; H, 10.45. Found: C, 70.18; H, 10.58.

**2-Methoxy-6-pentylphenol (11)**

Compound **10** (1.0 g, 3.2 mmol) was dissolved in anhyd DMF (2 mL) and the soln was cooled in an ice-bath. LiOH (220 mg, 9.6 mmol) was added slowly and the mixture stirred at r.t. for 4 h under an Ar atm. After completion (TLC), the reaction mixture was extracted with EtOAc (3  $\times$  20 mL). The combined organic layer was washed with brine (20 mL), dried over anhyd Na<sub>2</sub>SO<sub>4</sub> and evaporated to give a crude residue. Purification by chromatography (hexane–EtOAc, 7:3) gave phenol **11** (0.5 g, 80%) as a colorless viscous oil.<sup>7a</sup>

**2-Methoxy-6-pentyl-1,4-benzoquinone (Primin) (1)**

In a flame-dried flask purged with O<sub>2</sub>, phenol **11** (388 mg, 2 mmol) was dissolved in anhyd DMF (3 mL), salcomine (64 mg, 0.2 mmol) was added, and the reaction mixture was stirred vigorously for 6 h (TLC). The reaction mixture was extracted with EtOAc (3  $\times$  50 mL) and the combined organic layer washed with brine (10 mL), dried over anhyd Na<sub>2</sub>SO<sub>4</sub> and then evaporated to give a crude residue. Purification by chromatography (hexane–EtOAc, 6:4) gave primin (**1**)

as a yellow solid; yield: 336 mg (81%); mp 61–62 °C (Lit.<sup>7a</sup> mp 62–63 °C).

#### 5-(2-Hydroxy-3-methoxyphenyl)pentanoic Acid (12)

Ester **7** (704 mg, 2 mmol) was dissolved in 5% KOH in MeOH–H<sub>2</sub>O (12 mL, 3:1) and the resulting soln heated at reflux for 3 h under an N<sub>2</sub> atm (TLC). The reaction mixture was acidified with 1 N HCl (10 mL) and then extracted with EtOAc (3 × 20 mL). The crude residue was purified by chromatography (hexane–EtOAc, 6:4) to give acid **12** as a white solid; yield: 246 mg (55%); mp 124–125 °C (Lit.<sup>7b</sup> mp 125–126 °C).

#### 5-(5-Methoxy-3,6-dioxocyclohexa-1,4-dien-1-yl)pentanoic Acid (Primin Acid) (2)

In a flame-dried flask purged with O<sub>2</sub>, phenol **12** (224 mg, 1 mmol) was dissolved in anhyd DMF (3 mL), salcomine (32 mg, 0.1 mmol) was added, and the reaction mixture was stirred vigorously for 7 h (TLC). The reaction mixture was extracted with EtOAc (3 × 50 mL) and the combined organic layer washed with brine (5 mL), dried over anhyd Na<sub>2</sub>SO<sub>4</sub> and evaporated to give a crude residue. Purification by chromatography (hexane–EtOAc, 4:6) gave primin acid (**2**) as a yellow solid; yield: 168 mg (71%); mp 95–97 °C (Lit.<sup>7b</sup> mp 98 °C).

**Supporting Information** for this article is available online at <http://www.thieme-connect.com/ejournals/toc/synthesis>.

#### Acknowledgment

The authors are grateful to Dr. Ganesh Pandey, FNA, Head, Division of Organic Chemistry for support and encouragement. T.K. is grateful to the Council of Scientific and Industrial Research, New Delhi, India for the award of a Senior Research Fellowship.

#### References

- (1) Gunatilaka, A. A. L.; Berger, J. M.; Evans, R.; Miller, J. S.; Wisse, J. H.; Neddermann, K. M.; Bursuker, I.; Kingston, D. G. I. *J. Nat. Prod.* **2001**, *64*, 2.
- (2) (a) Schildknecht, H.; Schmidt, H. Z. *Naturforsch., B* **1967**, *22b*, 287. (b) Bloch, B.; Karrer, P. *Vjschr. Naturforsch. Ges.* **1927**, *72*, 1; *Chem. Abstr.* **1928**, *22*: 2784.

- (3) (a) Marini-Bettolo, G. B.; Monache, F. D.; da Lima, O. G.; Coelho, S. B. *Gazz. Chim. Ital.* **1971**, *101*, 41. (b) Bernays, E.; Lupi, A.; Bettolo, R. M.; Mastrofrancesco, C.; Tagliatesta, P. *Experientia* **1984**, *40*, 1010.
- (4) Pongcharoen, W.; Rukachaisirikul, V.; Phongpaichit, S.; Sakayaroj, J. *Chem. Pharm. Bull.* **2007**, *55*, 1404.
- (5) Tasdemir, D.; Brun, R.; Yardley, V.; Franzblau, S. G.; Rüedi, P. *Chem. Biodivers.* **2006**, *3*, 1230; and references cited therein.
- (6) (a) Carlsen, B. C.; Menné, T.; Johansen, J. D. *Contact Dermatitis* **2008**, *59*, 96. (b) Bonamonte, D.; Filotico, R.; Mastrandrea, V.; Foti, C.; Angelini, G. *Contact Dermatitis* **2008**, *59*, 174. (c) Fortina, A. B.; Piaserico, S.; Larese, F.; Recchia, G. P.; Corradin, M. T.; Gennaro, F.; Carrabba, E.; Peserico, A. *Contact Dermatitis* **2001**, *44*, 283.
- (7) (a) Bieber, L. W.; Chiappeta, A. D. A.; Souza, M. A. D. M.; Generino, M.; Neto, P. R. *J. Nat. Prod.* **1990**, *53*, 706. (b) Mabic, S.; Vaysse, L.; Benezra, C.; Lepoittevin, J.-P. *Synthesis* **1999**, 1127. (c) Davis, C. J.; Hurst, T. E.; Jacob, A. M.; Moody, C. J. *J. Org. Chem.* **2005**, *70*, 4414. (d) Jacob, A. M.; Moody, C. J. *Tetrahedron Lett.* **2005**, *46*, 8823.
- (8) (a) Bhattacharya, A. K.; Sharma, R. P. *Heterocycles* **1999**, *51*, 1681. (b) Bhattacharya, A. K.; Jain, D. C.; Sharma, R. P.; Roy, R.; McPhail, A. T. *Tetrahedron* **1997**, *53*, 14975. (c) Bhattacharya, A. K.; Pal, M.; Jain, D. C.; Joshi, B. S.; Roy, R.; Rychlewska, U.; Sharma, R. P. *Tetrahedron* **2003**, *59*, 2871. (d) Bhattacharya, A. K.; Pathak, A. K.; Sharma, R. P. *Mendeleev Commun.* **2007**, *17*, 27. (e) Bhattacharya, A. K.; Kaur, T. *Synlett* **2007**, 745; and references cited therein. (f) Bhattacharya, A. K.; Rana, K. C.; Mujahid, M.; Sehar, I.; Saxena, A. K. *Bioorg. Med. Chem. Lett.* **2009**, *19*, 5590. (g) Bhattacharya, A. K.; Kaur, T. unpublished results.
- (9) (a) Johnson, W. S.; Werthemann, L.; Bartlett, W. R.; Brocksom, T. J.; Li, T.-T.; Faulkner, D. J.; Petersen, M. R. *J. Am. Chem. Soc.* **1970**, *92*, 741. (b) Ziegler, F. E. *Chem. Rev.* **1988**, *88*, 1423. (c) Meza-Avina, M. E.; Ordonez, M.; Fernandez-Zertuche, M.; Rodriguez-Fragoso, L.; Reyes-Esparza, J.; de los Rios-Corsino, A. A. M. *Bioorg. Med. Chem.* **2005**, *13*, 6521.
- (10) Corey, E. J.; Venkateswarlu, A. *J. Am. Chem. Soc.* **1972**, *94*, 6190.
- (11) Lauchli, R.; Shea, K. J. *Org. Lett.* **2006**, *8*, 5287.
- (12) Ankala, S. V.; Fenteany, G. *Tetrahedron Lett.* **2002**, *43*, 4729.